



**XVI International Conference
on Chemical Reactors**

CHEMREACTOR-16

ABSTRACTS



**Berlin, Germany
December 1-5, 2003**

Boreskov Institute of Catalysis of the Siberian Branch of Russian Academy of Sciences,
Novosibirsk, Russia

DECHEMA (Society for Chemical Engineering and Biotechnology), Germany

Ministry of Industry, Science and Technologies of the Russian Federation

Russian Scientific and Cultural Center in Berlin

European Federation on Chemical Engineering

Scientific Council on Catalysis RAS

Russian Center of International Scientific and Cultural Cooperation of Ministry of Foreign Affairs RF

**XVI International Conference
on Chemical Reactors
CHEMREACTOR-16**

Berlin, Germany
December 1-5, 2003

ABSTRACTS

Novosibirsk, 2003

International Center for Catalysis and Kinetics
Russian Academy of Sciences
Boreskov Institute of Catalysis
28/40, Leninsky pr., Ekaterinburg, 620014, Russia
Tel: +7 (373) 236-3000
Fax: +7 (373) 236-3001
E-mail: info@icck.ru
Website: www.icck.ru

International Conference on Catalysis Kinetics (ICCK-2003)

July 1-5, 2003
Boreskov Institute of Catalysis

Abstracts

INTERNATIONAL SCIENTIFIC COMMITTEE

Mikhail G. Slinko, Honour Chairman	State Research Center "Karpov NIPCI", Moscow, Russia
Valentin N. Parmon, Chairman	Boreskov Institute of Catalysis, Novosibirsk, Russia
Gerhart Eigenberger, Vice-Chairman	Stuttgart University, Germany
David Agar	University of Dortmund, Germany
Manfred Baerns	Institute for Applied Chemistry Berlin-Adlershof, Berlin, Germany
Boris N. Chetverushkin	Institute for Mathematical Modelling RAS, Moscow, Russia
Mike P. Duduković	Washington University, St. Louis, USA
Gerhard Emig	University of Erlangen, Germany
Pio Forzatti	Technical University of Milan, Milan, Italy
Gilbert F. Froment	Texas A&M University, USA
Sergei S. Ivanchev	St. Petersburg Department of the Boreskov Institute of Catalysis, Russia
Valerii A. Kirillov	Boreskov Institute of Catalysis, Novosibirsk, Russia
Miloš Marek	Prague Institute of Chemical Technology, Prague, Czech Republic
Dmitrii Yu. Murzin	Abo Akademi University, Turku, Finland
Alexander V. Putilov	Ministry of Industry, Science and Technologies RF, Moscow, Russia
Albert Renken	Swiss Federal Institute of Technology, Lausanne, Switzerland
Kai Sundmacher	Max-Planck-Institute, Magdeburg, Germany
Robert Schlögl	Fritz-Haber-Institut der Max-Planck-Gesellschaft, Berlin, Germany
Andreas Seidel-Morgenstern	Max-Planck-Institute, Magdeburg, Germany
Gennadii F. Tereschenko	Russian Academy of Science, St. Peterburg, Russia

ORGANIZING COMMITTEE

Alexander S. Noskov, Chairman	Boreskov Institute of Catalysis, Novosibirsk, Russia
Willi Meier	DECHEMA, Germany
Victor A. Chumachenko	JSC «Katalizator», Novosibirsk, Russia
Svetlana A. Pokrovskaya	Boreskov Institute of Catalysis, Novosibirsk, Russia
Sergei I. Reshetnikov	Boreskov Institute of Catalysis, Novosibirsk, Russia
Andrei N. Zagoruiko	Boreskov Institute of Catalysis, Novosibirsk, Russia
Ilya A. Zolotarskii	Boreskov Institute of Catalysis, Novosibirsk, Russia
Tatiana V. Zamulina, Secretary	Boreskov Institute of Catalysis, Novosibirsk, Russia

INTERNATIONAL SCIENTIFIC COMMITTEE

State Academic Center "Korolev" RSCF, Moscow, Russia

Michael G. Baidy
Honorary Chairman

The organizers express their gratitude to

Samara University, Samara

Geoffrey B. Bignold
Vice-Chairman

University of Bremen, Germany

David A. J.

**Ministry of Industry, Science and Technologies
of the Russian Federation, Moscow, Russia**

Institute for Materials and Manufacturing RAS, Moscow, Russia

Mike

University of Bochum, Germany

Geoffrey B.

and

Technical University of Munich, Munich, Germany

The

JSC "Samara Catalyst Plant"

Samara Catalyst Plant, Samara

Geoffrey B.

Samara Catalyst Plant, Samara

Geoffrey B.

Samara Catalyst Plant, Samara

Geoffrey B.

for the financial support.

Samara Catalyst Plant, Samara

Geoffrey B.

ORGANIZING COMMITTEE

Samara Catalyst Plant, Samara

Geoffrey B.

PLENARY LECTURES

NEW WAYS OF PRODUCTION AND UTILIZATION OF N₂O

V.N. Parmon

Boriskov Institute of Catalysis, Novosibirsk, Russia

During the last decade a dramatic breakthrough has been achieved in heterogeneous selective oxidation processes since N₂O has been found to be an efficient alternative oxidant both in gaseous and liquid phases.

The presentation considers an extremely selective hydroxylation of benzene with N₂O over zeolite catalysts developed as AlphOx™ process for the large scale production of phenol, as well as some other promising applications of N₂O as selective oxidant in organic synthesis.

Development of new processes on the base of N₂O as a large scale oxidant gave an impetus to development of new cheap ways of the N₂O production. The presentation considers the newest process of the N₂O production *via* selective oxidation of ammonia over Bi-Mn-based catalysts.

AUTOTHERMAL REACTOR CONCEPTS FOR THE ENERGY-EFFICIENT COUPLING OF ENDO- AND EXOTHERMIC REACTIONS

Grigorios Kolios and Gerhart Eigenberger

Institut für Chemische Verfahrenstechnik

Universität Stuttgart, Germany

Many industrially important reactions like steam reforming or dehydrogenations are endothermic and require high temperatures for sufficient equilibrium conversion. The necessary heat of reaction is generally supplied by a combustion reaction but usually only about or less than half of the heat of combustion is transferred directly into the endothermic reaction. The rest has to be recovered from the hot effluents by a network of heat exchangers. This is the feasible state of the art if the reactor is part of a larger chemical plant.

Decentralized hydrogen production (e. g. for fuel cell applications) however requires reformer concepts with minimum excess heat production and an optimal heat integration of the endothermic and the exothermic reaction(s). This has led to the development of heat-integrated "autothermal" reactor concepts where the feed to and the effluents from the reactor are "cold" (i. e. at ambient temperature or just above the respective condensation temperature) and the hot temperature zone required for the reaction is kept completely inside the reactor. Such concepts will be of advantage also for other endothermic synthesis reactions if they result in well specified short contact time reaction conditions at high temperatures.

Previous reactor concepts of this kind had the disadvantage that either the heat recovery was weak or excessive peak temperatures well above the required synthesis temperature occurred. Excessive peak temperatures occurred in particular for the counter-current or reverse-flow coupling of exo- and endothermic reactions because both reaction zones tend to separate, leading to an uncontrolled run-away of the exothermic (combustion) reaction.

It will be shown that this separation and the resulting excessive temperature excursions can be avoided if, under counter-current or reverse-flow operation, the feed of combustion gas is locally distributed or if co-current heat exchange is applied for the exothermic and the endothermic reaction in the reaction zone.

The examples to be presented have been studied both experimentally and by simplified or detailed simulations. They comprise the steam reforming of methanol in a counter-current reactor with integrated feed evaporation and locally distributed burner gas feed, methane steam reforming with co-current heat exchange in the reaction zone and methane steam reforming with periodic flow reversal and distributed burner gas feed during the regeneration step. The experimental results show that a proper reactor design, ensuring good burner gas distribution and avoiding homogeneous back-ignition of the combustion reaction is crucial for a successful operation.

Acknowledgement: Support of this work through the Deutsche Forschungsgemeinschaft and through industrial partners is gratefully acknowledged.

Related literature:

- [1] Kolios, G., Frauhammer, J. and Eigenberger, G.: Autothermal fixed-bed reactor concepts. Chem. Eng. Sci. 55 (2000), 5945-5967
- [2] Kolios, G., Frauhammer, J. and Eigenberger, G.: A simplified procedure for the optimal design of autothermal reactors for endothermic high temperature reactions. Chem. Eng. Sci. 56 (2001), 351-357.
- [3] Kolios, G., Frauhammer, J. and Eigenberger, G.: Efficient reactor concepts for the coupling of endothermic and exothermic reactions. Chem. Eng. Sci. 57 (2002), 1505-1510.
- [4] Glöckler, B., Kolios, G. and Eigenberger, G.: Analysis of a novel reverse-flow reactor concept for autothermal methane steam reforming, Chem. Eng. Sci. 58 (2003).
- [5] Glöckler, B., Gritsch, A., Morillo, A., Kolios, G., and Eigenberger, G.: Auto-thermal reactor concepts for endothermic fixed-bed reactions. Trans. Inst. of Chem. Engineers, Part A (to be published).

DEVELOPMENT AND MODELLING OF MEMBRANE REACTORS

M. van Sint Annaland, U. Kürten, S.A.R.K. Deshmukh, J. Smit and J.A.M. Kuipers

Department of Science and Technology, Twente University, Enschede, The Netherlands

Abstract

In the quest for processes with higher product selectivities and overall process (separation) efficiencies and improved reactor controllability and safety, membrane reactors have been proposed. Membrane reactors achieve these improvements via the integration of reaction and separation in a single process unit. The reaction step can be improved through the integration of a separation step, as for example in membrane reactors for dehydrogenation reactions where hydrogen is withdrawn from the reaction mixture using perm-selective Pd-membranes thereby shifting the reaction equilibrium to the desired products. Alternatively, also the separation step can be improved due to the integration of a reaction step, as for instance in membrane reactors for the catalytic partial oxidation of methane using perm-selective dense perovskite membranes for the air separation, where the high consumption rate of oxygen at the permeate side helps increasing the chemical potential difference of oxygen across the membrane and hence the oxygen fluxes.

In this work the modelling and development of membrane reactors for partial oxidation systems will be addressed. Firstly, the benefits of controlled oxygen dosing via porous membranes to a packed catalyst bed (see Fig. 1a) are demonstrated and the effects of oxygen mass transfer limitations on the product selectivity are investigated. Then, it will be shown that with a membrane assisted fluidised bed mass (see Fig. 1b) heat transfer limitations can be effectively eliminated and almost isothermal conditions and plug-flow behaviour can be achieved simultaneously, thus yielding large improvements in conversion and selectivity. Finally, a new membrane reactor concept for the catalytic partial oxidation of methane with integrated air separation with oxygen perm-selective perovskite membranes (see Fig. 2) is discussed.

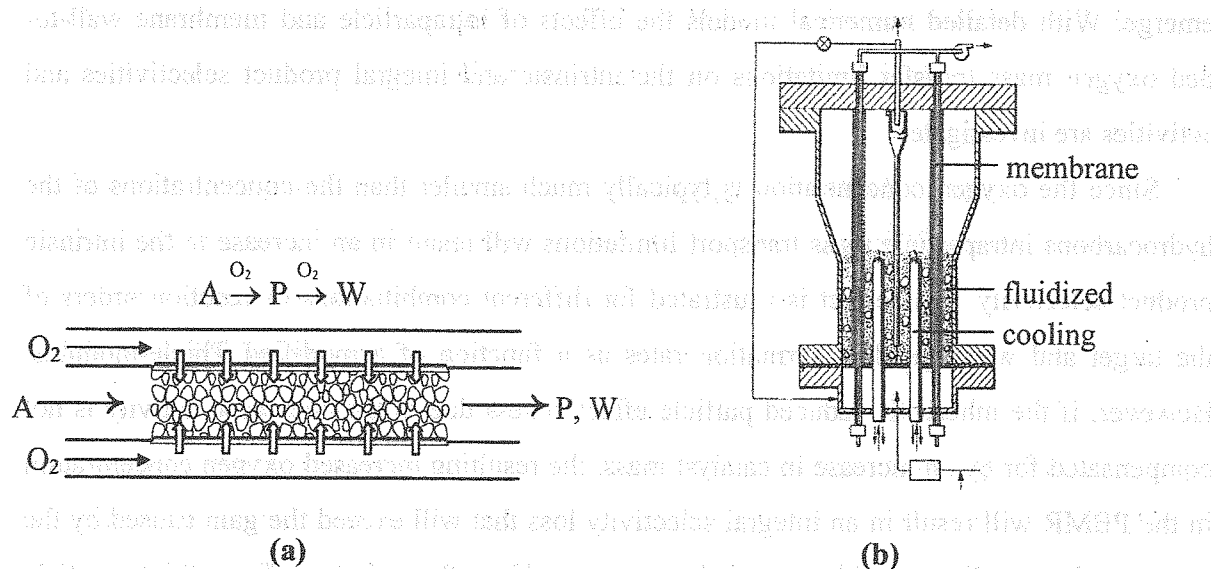


Fig. 1. Schematic representation of (a) a packed bed membrane reactor (PBMR) and (b) a membrane assisted fluidised bed reactor (MAFBR).

Packed bed membrane reactor

In partial oxidation systems in which the formation rate of the target (partially oxidised) product shows a lower dependency on the oxygen concentration than the formation rate of the waste (total oxidation) product, the product selectivity can be increased by reducing the oxygen concentration in the reactor. By distributive addition of oxygen to the reaction mixture along the axial coordinate of the reactor via porous membranes, high conversions can be achieved at a low local oxygen concentration level. Firstly, the potential yield improvements of packed bed membrane reactors (PBMR) will be identified by comparing the maximal product yield in a PBMR assuming a constant oxygen concentration level throughout the reactor with the optimal yield of a fixed bed reactor (FBR) with premixed oxygen feed, considering the partial oxidation system as a consecutive reaction scheme with power law reaction kinetics. The influence of the difference in oxygen reaction orders and the ratio of reaction rates of the consecutive and primary reaction will be shown. Furthermore, the optimal axial oxygen concentration profile in a PBMR with a given catalyst mass will be investigated. The ratio of premixed and distributed oxygen feeds is varied and the effect of different axial profiles for the oxygen distribution is compared.

For most industrially relevant partial oxidation systems a very strong decrease in the oxygen concentrations is required to achieve significant selectivity improvements. Since the reaction order in oxygen for the target product is typically smaller than unity, possible problems with the distribution of oxygen from the bulk of the gas phase to the centre of a catalyst particle, as well as from the membrane wall to the centreline of the packed bed may

emerge. With detailed numerical models the effects of intraparticle and membrane wall-to-bed oxygen mass transfer limitations on the intrinsic and integral product selectivities and activities are investigated.

Since the oxygen concentration is typically much smaller than the concentrations of the hydrocarbons intraparticle mass transport limitations will result in an increase in the intrinsic product selectivity. This effect is illustrated for different combinations of reaction orders of the target and waste product formation rates as a function of a modified Thiele-modulus. However, if the inherently reduced particle effectiveness due to the decreased activity is not compensated for by an increase in catalyst mass, the resulting increased oxygen concentration in the PBMR will result in an integral selectivity loss that will exceed the gain caused by the concentration gradients inside the catalyst particle. Nevertheless, the effect of intraparticle mass transport limitations on the integral product selectivity is not adverse, provided that the oxygen concentration is small compared to the concentrations of the hydrocarbons. In contrast, oxygen transport limitations from the membrane at the tube wall to the centre of the packed bed will decrease the intrinsic and integral product selectivities, especially at high values of the modified Thiele-modulus. Possible oxygen depletion in the centre of the packed bed even further decreases the product selectivity. Concluding, for maximal product selectivities the particle size should be chosen large enough that mass transport limitations from the membrane wall to the centre of the packed bed can be avoided and the possibly decreased catalyst activity due to intraparticle mass transport limitations should be compensated for by increasing the catalyst volume.

An important design criterion for industrial scale PBMRs is the maximum allowable pressure drop. To reduce the pressure drop typically relatively large particles are selected. Consequently, low aspect ratios of the tube-to-particle diameter, and thus a strong porosity profile near the membrane wall, are to be expected for industrial scale PBMRs. Due to the increased porosity near the wall the local catalyst concentration and thus the activity of the packed bed is decreased and the axial velocity is increased causing a by-pass flow. With a two-dimensional, pseudo-homogeneous reactor model the radial and axial concentration profiles and the local velocity field were calculated, while accounting for the influences due to the distributive feed via the membranes and the radial porosity profile. With these calculations it will be shown that the overall effect of the porosity profile on the conversion-selectivity plot is unexpectedly small. If the implementation of a radial porosity profile is not required by other considerations, e.g. for an accurate description of temperature effects, then the effect of the porosity profile can safely be neglected.

Membrane assisted fluidised bed reactor

By insertion of membranes in a gas-solid fluidised bed reactor employing very fine powders problems of mass and heat transfer limitations, both inside the particles and from the membrane walls to the emulsion phase, can be completely overcome. Due to the excellent heat and mass transfer characteristics of fluidised bed reactors almost isothermal operation can be achieved, even for reactions with a very high adiabatic temperature rise. With the insertion of membrane bundles in the fluidised bed not only the axial concentration profile can be optimised via distributive feeding of oxygen, but also the large effective axial dispersion – one of the main disadvantages of fluidised beds – can be effectively decreased via compartmentalisation of the fluidised bed. The addition of gas via the membranes improves the hydrodynamics of the two-phase system (reduction of macroscale circulation patterns) even further decreasing the axial dispersion. Moreover, by insertion of the membrane bundles in a suitable configuration the bubble growth can be impeded, strongly enhancing the bubble-to-emulsion phase mass transfer and thereby reducing reactant by-pass via rapidly rising large bubbles. Thus, in the membrane assisted fluidised bed reactor (MAFBR) not only the concentration profiles can be optimised via distributive feeding, also the hydrodynamic behaviour of the fluidised bed is strongly improved.

Firstly, experimental results will be shown demonstrating that the air permeation through small ceramic porous membranes is not effected by the hydrodynamics and properties of the fluidised bed. Then, the experiments to study the influence of the presence of membrane bundles and the effect of gas addition via the membranes on the local heat transfer coefficient between the tube and the fluidised bed (determined by measuring the temperature drop over the cooling tubes inside the fluidised bed) and on the effective axial dispersion (determined from steady state concentration profiles of a tracer gas) will be discussed. The experimental results clearly show that the axial dispersion can indeed be very strongly decreased with horizontal membrane bundles and gas addition via the membranes, while simultaneously maintaining excellent heat transfer characteristics. Finally, the reactor concept will be demonstrated for the partial oxidation of methanol to formaldehyde. In conventional reactors the methanol concentration is restricted to below about 10% because of explosion limits and heat transfer limitations. With experimental results it will be shown that with the MAFBR higher product selectivities can be achieved at much higher methanol concentrations (up to about 25-30 %) at almost full conversion without any problems regarding explosion limits or heat removal.

Reverse flow catalytic membrane reactor

In Gas-To-Liquid (GTL) processes the partial oxidation of methane (POM) is combined with the Fischer-Tropsch reaction to produce liquid fuels. GTL-processes have a great potential as alternative to conventional oil and coal processing. However, an important part of the investment costs of a conventional GTL-plant is related to cryogenic air separation. These costs could be substantially reduced by separating air with recently developed oxygen permeable perovskite membranes, which typically require similar temperatures as the POM reaction for sufficiently large oxygen fluxes. Integration of these membranes in the POM reactor seems very attractive because oxygen reacts at the membrane surface resulting in high driving forces over the membrane increasing the oxygen permeation.

Because the POM-reaction is only slightly exothermic, the natural gas and air feeds have to be preheated to high temperatures to obtain high synthesis gas yields, which will be shown with an adiabatic thermodynamic analysis. Since the Fischer-Tropsch reaction is carried out at much lower temperatures, recuperative heat exchange is essential for an air-based POM process. Since external heat transfer at elevated temperatures is very expensive, the recuperative heat exchange is preferably carried out inside the reactor, which can be achieved with the reverse flow concept. To combine the POM reaction, air separation and regenerative heat exchange in a single apparatus, a novel multi-functional reactor, the reverse flow catalytic membrane reactor (RFCMR) is proposed. To create the reverse flow behaviour a small amount of methane is combusted at the air side and to keep the centre of the reactor isothermal some steam is injected. With model simulations the theoretical feasibility of the new reactor concept is demonstrated, showing that high overall syngas yields can be achieved with very high energy efficiencies.

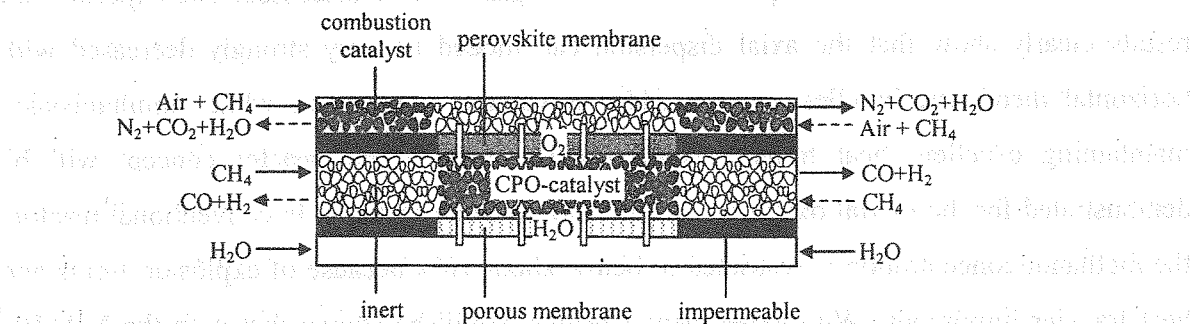


Fig. 2. Schematic representation of the Reverse Flow Catalytic Membrane Reactor (RFCMR)

NMR IMAGING: A POWERFUL TOOLKIT FOR CATALYTIC RESEARCH

I.V. Koptyug

International Tomography Center, Novosibirsk 630090, Russia

Fax: +7 3832 331399, e-mail: koptyug@tomo.nsc.ru

The nuclear magnetic resonance imaging (MRI) technique is well known for its ability to visualize the internal structure of various liquid-containing objects, from humans to prewetted rock cores and fiber-reinforced car tires [1-3]. It is of paramount importance, however, that image contrast in MRI is governed not only by the structural characteristics of an object under study, but also by a broad range of its other properties and the processes within it. Furthermore, one can purposefully adjust the image contrast in MRI depending on the main goal of a particular study so that the desired information can be obtained. It is one of the aims of this presentation to demonstrate that MRI is not a single research tool, but rather a sophisticated and versatile toolkit which can provide unique and diverse information on the reactor structure and functional behavior and their interrelation.

The spatial resolution of the MRI technique is of the order of 10-100 μm , which is clearly not high enough to visualize the geometry of the individual pores even for many macroporous materials. However, it is adequate for studying the geometry at the reactor level, e.g., of the void space in packed beds. This can be done, for instance, by filling the porous space of the bed with a fluid which gives an observable NMR signal. A three-dimensional (3D) MRI experiment then yields the 3D structure of the bed in a digital form (Fig. 1), which can then be processed statistically or used directly in model calculations. It is essential that the same experimental arrangement can be used to study transport of the fluid

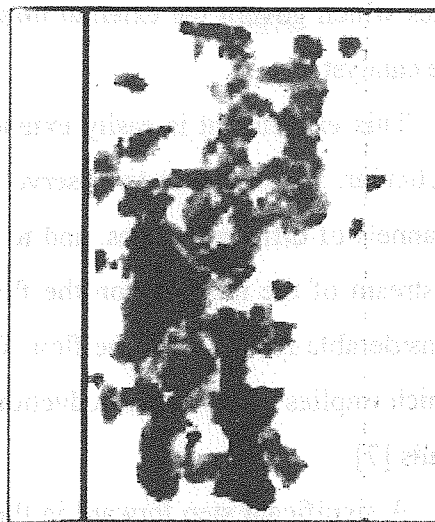


Fig. 1. A three-dimensional image of a cluster of fine alumina particles (200 μm , partially saturated with vaseline oil) which fill out the voids of a porous bed comprised of larger (5 mm) alumina beads. The latter do not contain any liquid and are thus invisible to MRI.

within the bed if one just turns on the fluid flow (*vide infra*). Furthermore, in most MRI experiments the structural information about the object under study is obtained along with other information such as transport properties, chemical composition, etc., which is useful for establishing the structure-function relationship. At the same time, the information can be obtained with spatial resolution, i.e. without averaging over the entire (possibly inhomogeneous) structure of the reactor.

The functioning of chemical reactors is governed by various types of mass transport processes within them, including molecular diffusion, flow and hydrodynamic dispersion. MRI provides a whole range of approaches for studying these and other types of mass transport in model chemical reactors [2]. Using one of the tools from the MRI toolkit (the so-called phase method [2,4,5]), we have obtained the spatial maps of all three velocity components of water inflowing into the transport channels of a monolithic catalyst for its entire cross-section and at various distances from its inflow edge [6,7]. This experiment has yielded a detailed picture of the branching and rearrangement of the flow and has revealed the presence of reverse flow in those regions where the main stream is deflected. The maps clearly show the establishment of the developed laminar flow along the channels. More importantly, the results contain the complete information about the flow field directly linked to the flow geometry. This means that MRI is able to provide the information about shear rates which govern the external mass transport of the flowing fluid with the porous walls of the catalyst.

This experiment is easily extended to the studies of structure-transport relationships. In particular, it allowed us to observe the differences in the flow fields for monoliths with the channels of different shapes, and to directly visualize the effect of flow distributors installed upstream of the monolith on the flow pattern within the monolith channels. In particular, a considerable reduction of the flow shear rates is observed when a flow distributor is present, which implies a substantial reduction of the mass transfer between the fluid and the monolith walls [7].

A significant step forward in the development of such applications is our first successful application of MRI to study the flow of proton-containing gases (propane, butane, acetylene) in pipes and channels, including the channels of monolithic catalysts [6-8]. While the sensitivity and resolution for MRI of gases is lower as compared to liquids, the experiment can still be used to visualize flow patterns in the channels wider than 1 mm, while the utilization of elevated gas pressures could improve the spatial resolution of the experiment.

We have shown that other MRI-based flow imaging techniques (e.g., flow tagging [2,5]) are also applicable to gases [8].

The MRI techniques that are used to visualize the flow patterns can be used to study the filtration processes, e.g., filtration of a liquid through a packed bed, but only in those cases when the characteristic pore sizes are much larger than the spatial resolution limit. This approach was used to study a flow of water through a bed of 3.2 mm solid glass beads (Fig. 2). Once again, since the experiment yields the velocity maps which also visualize the bed geometry, it is reasonably straightforward to correlate the flow pattern with the bed structure. In particular, higher flow velocities are apparent near the bed walls where higher bed porosity is expected.

This approach, however, is not practical for beds with much smaller pore sizes and for gases. Nevertheless, the MRI toolkit has a different tool for the studies of filtration processes. It is based on the detection of the so-called average propagator $P(R, \Delta)$ – the probability density for a molecule

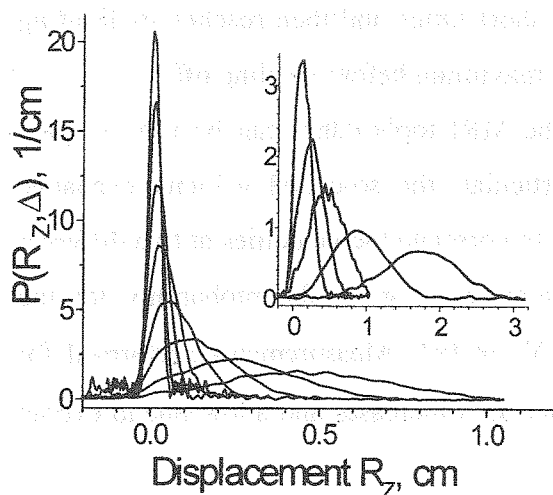


Fig. 3. The average propagator for the axial displacements of butane gas flowing through a cylindrical bed (21 mm in diameter) comprised of solid glass beads (3.2 mm) measured for the observation time values of $\Delta=1$ ms, 2 ms, 5 ms, 10 ms, 20 ms, 40 ms, 80 ms, 150 ms (inset - $\Delta=40$ ms, 80 ms, 150 ms, 300 ms, 600 ms).

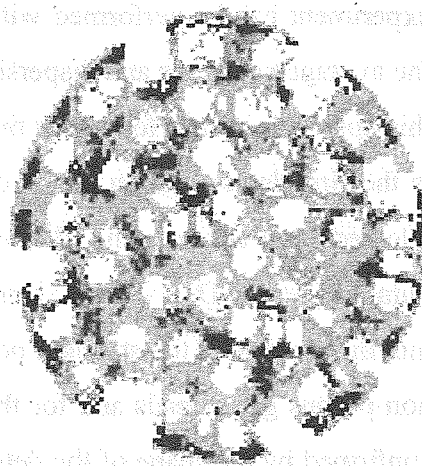


Fig. 2 Flow velocity map for filtration of water through a cylindrical bed 22 mm in diameter comprised of solid glass beads. Darker shades of gray represent higher axial velocities, white regions correspond to the beads invisible to MRI.

to travel over a distance R during a selected travel time Δ as a function of this distance [9]. The important point is that the displacements of the molecules are measured directly and within the bed, while many traditional approaches use tracers and the detection is performed downstream of the bed. The direction in which the displacements are measured can be chosen at will. The measurements can thus yield the average velocity of the fluid in the bed (U) and both axial (D_{\parallel}) and transverse (D_{\perp}) dispersion coefficients (i.e., both parallel and normal to the pressure gradient). The

experiment can be performed with a coarse spatial resolution, which allows one to compare the average velocities and dispersion coefficients for different parts of the granular bed. While this approach is used for a long time to study the filtration of liquids, our recent work [7,8,10] is the first demonstration that it can be applied to the studies of gases as well (Fig. 3). This allowed us to compare the filtration of liquid (water) and gas (butane) in terms of the Peclet number ($Pe=Ud/D$, d – grain diameter) and to demonstrate that for water the exchange of the moving fluid with the stagnant pools is an important dispersion mechanism even for beds of non-porous glass beads and for the stationary regime of the filtration process. This is further confirmed by the shape of the detected propagators which exhibit a pronounced peak at small displacement values which corresponds to water molecules characterized by a reduced mobility as compared to the rest of the ensemble. The amplitude of this peak decreases as the observation time increases, which gives the direct confirmation of the exchange of water molecules between the stagnant and the moving liquid and provides the means to measure the characteristic time of exchange. In the case of gases, the stagnant pools are evident only when the bed is comprised of porous grains. Furthermore, the measurements of the dispersion coefficients as a function of the observation time are helpful in revealing the two mechanisms responsible for the dispersion effects in the limit of short and long observation times, respectively. The interplay of the coherent (short time limit) and non-coherent (long time limit) transport mechanisms leads to the characteristic behavior of $D_{||}$ and D_{\perp} as functions of the observation time. The former grows rapidly at short times and then reaches its limiting value asymptotically, while the latter goes through a maximum before leveling off.

There are much more sophisticated tools in the MRI toolkit that can be used to gain further details about the filtration process. In particular, the so-called velocity exchange spectroscopy (VEXSY) experiment [11] allows one to correlate the velocities at two different instants in time. The resulting two-dimensional propagator gives the probability for the molecule to have velocity V_0 at $t=0$ and velocity V_{Δ} at $t=\Delta$. Measurements performed for various values of Δ demonstrate the loss of coherence as Δ increases and allow one to extract the characteristic correlation time [10].

We have further extended the average propagator technique and applied it to study the gravity driven filtration of 80-200 alumina particles through a bed of 4-5 mm alumina spheres [10]. Preliminary results have shown that despite a “discrete” nature of the filtration of individual particles at low flow rates, the experiment can be successfully employed to study such processes. A representative propagator is shown in Fig. 4. The results show that the

average filtration velocity goes through a maximum as the flow rate is increased. The initial increase is attributed to the intensification of the convective flow of air due to the increase in the amount of freely falling solids in a straight vertical section of a tube between the supply funnel and the granular bed and the resulting increase in the initial velocity of solids (confirmed experimentally) when they enter the granular bed. The decrease of the average filtration velocity at higher flow rates was found to be due to the partial flooding of the porous bed with the granular material. The filtration of gas-solids suspensions is important in chemical engineering and catalytic applications, and we believe that similar studies can be performed with cyclone separators, pneumatic transport and suppression of dust, fluidized bed reactors, etc.

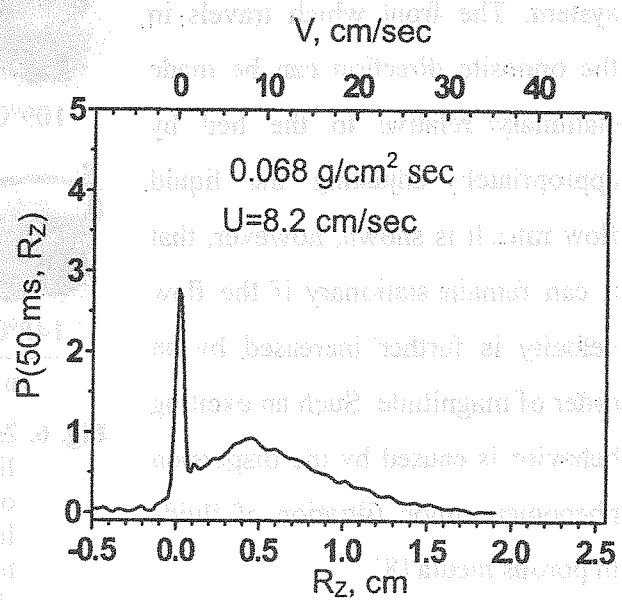


Fig. 4. Average propagator for the gravity driven filtration of solid particles through a bed of 4-5 mm alumina beads. Solids flow rates and the average filtration velocities are indicated in the figure.

An important problem in chemical engineering and catalysis is the influence of mass and heat transport on a chemical reaction, and in particular the possible coupling of the transport processes with the chemical transformation. These issues are directly related to the efficiency of large-scale reactors and the safety of their operation. One of the striking examples of the coupling of mass transport and a chemical reaction is the Belousov-Zhabotinsky (BZ) oscillator. We have employed the MRI technique to study the propagation of chemical waves in the BZ reaction carried out in model porous media (Fig. 5) [10]. The reduction of the wave front velocity is shown to be related to the reduction of the effective diffusivity in porous media as compared to bulk liquids. For given concentrations of the key reactants, a critical pore size value exists below which the propagation of concentration wave fronts is not observed. The most interesting behavior is found when the reaction mixture flows in a porous medium. The measured velocity of the downstream propagating front is much larger than the sum of the average flow



Fig. 5. Propagation of concentration waves in the BZ reaction carried out in a bed of 0.5 mm solid glass beads.

system. The front which travels in the opposite direction can be made stationary relative to the bed by appropriately adjusting the liquid flow rate. It is shown, however, that it can remain stationary if the flow velocity is further increased by an order of magnitude. Such an exciting behavior is caused by the dispersion phenomena upon filtration of fluids in porous media [8].

Heterogeneous catalytic hydrogenation is one of the model

reactions widely used in the studies aimed at a better understanding and the optimization of large-scale catalytic processes, and is also of practical importance for chemical industry. We have employed a combination of NMR imaging (Fig. 6) and spectroscopy to visualize the processes in an operating single catalyst pellet [10,12,13] or in a granular catalyst bed. During the experiments, the catalyst (1% Pd/ γ -Al₂O₃) is residing inside the rf coil of the NMR instrument, and the H₂ gas and the liquid reactant (α -methylstyrene) preheated to 68-80 °C are supplied to the reaction volume. The catalyst temperature can be as high as 170-190 °C due to the exothermic nature of the reaction. A slice-selective spin-echo sequence was used to obtain 2D images of the liquid distribution with the spatial resolution of 230×140 μm^2 (pellet) or 230×310 μm^2 (bed) within a 2 mm slice. To reduce the T₁ times of the liquids, the catalyst was impregnated with manganese. This allowed us to acquire the 2D images in 34 s and to obtain a detailed picture of the redistribution of the liquid phase within the pellet or the bed in the course of the reaction. These studies have revealed the existence of the oscillating regimes of the process caused by the oscillations of the catalyst temperature and directly demonstrated the existence of the coupling of mass and heat transport with the chemical reaction itself.

In order to determine the composition of the liquid phase with spatial resolution, free induction decays were phase encoded along one or two spatial coordinates within a vertical slice of a cylindrical catalyst bed. Despite a substantial linewidth, the spatially resolved NMR spectra clearly indicate the increase in the relative amount of product (cumene) towards the lower (downstream) edge of the catalyst bed. We have shown earlier [12] that substantial line

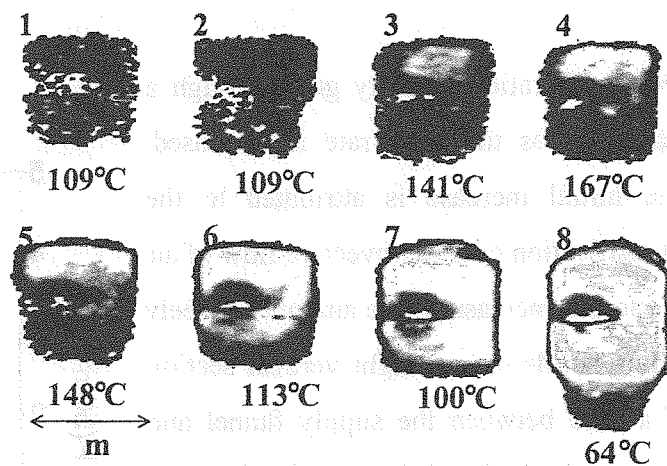


Fig. 6. 2D images demonstrating the redistribution of the liquid phase inside the catalyst pellet in the course of AMS hydrogenation. AMS is supplied as a liquid to the top of the pellet. The pellet temperature is indicated for each image. Lighter shades of gray correspond to higher liquid contents, while white areas correspond to regions where signal is below the noise level.

broadening and distortions in the NMR spectra of liquids permeating porous solids can be somewhat reduced if the NMR spectra are detected with spatial resolution. Our latest results show that the linewidths are further reduced at elevated temperatures (ca. 800 Hz at 20 °C; ca. 300 Hz at 130 °C). Note that these preliminary spectroscopic experiments were performed under highly unfavorable conditions, i.e., with the catalyst impregnated with paramagnetic manganese. Without it the lines should be appreciably narrower, and an accurate quantification of the mixture composition throughout the catalyst pellet or bed should be possible.

The MRI toolkit is so large that it is impossible even to simply list all the tools available, and only some of them are presented here. Some other possible applications that can be useful for catalysis and related disciplines are the drying of porous materials [14-16] (including contact drying, external mass transfer across the fluid/solid interface), adsorption [14,16,17] (including sorption of water vapor and adsorption of gases by various porous sorbents), and the *in situ* visualization of supported catalyst preparation [18].

The results presented above are intended to demonstrate that the MRI toolkit is useful for establishing the structure-transport-chemistry interrelation in an operating chemical reactor, with various aspects of its performance studied under the same experimental conditions or even in the same experimental run. We hope that the work reported will help to further develop and promote the chemical engineering and catalytic applications of the MRI technique.

This work was supported by RFBR (grant # 02-03-32770), SB RAS (Intergation grants #41 and #166), and the Russian President's program of support of the leading scientific schools (grant # NSch-2298.2003.3).

References

1. I.V. Koptug, R.Z. Sagdeev. *Russ. Chem. Rev.*, **71**, 593 (2002).
2. I.V. Koptug, R.Z. Sagdeev. *Russ. Chem. Rev.*, **71**, 789 (2002).
3. I.V. Koptug, R.Z. Sagdeev. *Russ. Chem. Rev.*, **72**, 183 (2003).
4. A. Caprihan, S.A. Altobelli, E. Benitez-Read. *J. Magn. Reson.*, **90**, 71 (1990).
5. E. Fukushima. *Annu. Rev. Fluid Mech.*, **31**, 95 (1999).
6. I.V. Koptug, S.A. Altobelli, E. Fukushima, A.V. Matveev, R.Z. Sagdeev. *J. Magn. Reson.*, **147**, 36 (2000).
7. I.V. Koptug, L.Yu. Ilyina, A.V. Matveev, R.Z. Sagdeev, V.N. Parmon, S.A. Altobelli. *Catal. Today*, **69**, 385 (2001).
8. I.V. Koptug, A.V. Matveev, S.A. Altobelli. *Appl. Magn. Reson.*, **22**, 187 (2002).
9. P.T. Callaghan. *Principles of Nuclear Magnetic Resonance microscopy*. Clarendon Press, Oxford, 1991.

10. I.V. Koptug, A.A. Lysova, A.V. Matveev, L.Yu. Ilyina, R.Z. Sagdeev, V.N. Parmon. *Magn. Reson. Imaging*, **21**, 337 (2003).
11. S.-I Han, S. Stapf, B. Blumich. *J. Magn. Reson.*, **146**, 169 (2000).
12. I.V. Koptug, A.V. Kulikov, A.A. Lysova, V.A. Kirillov, V.N. Parmon, R.Z. Sagdeev. *J. Amer. Chem. Soc.*, **124**, 9684 (2002).
13. I.V. Koptug, A.V. Kulikov, A.A. Lysova, V.A. Kirillov, V.N. Parmon, R.Z. Sagdeev. *Chem. Sust. Dev.*, **11**, 109 (2003).
14. I.V. Koptug, R.Z. Sagdeev, L.Yu. Khitrina, V.N. Parmon. *Appl. Magn. Reson.*, **18**, 13 (2000).
15. I.V. Koptug, S.I. Kabanikhin, K.T. Isakov, V.B. Fenelonov, L.Yu. Khitrina, R.Z. Sagdeev, V.N. Parmon. *Chem. Engng Sci.*, **55**, 1559 (2000).
16. I.V. Koptug, L.Yu. Khitrina, V.N. Parmon, R.Z. Sagdeev. *Magn. Reson. Imaging*, **19**, 531 (2001).
17. I.V. Koptug, L.Yu. Khitrina, Yu.I. Aristov, M.M. Tokarev, K.T. Isakov, V.N. Parmon, R.Z. Sagdeev. *J. Phys. Chem. B*, **104**, 1695 (2000).
18. L.Yu. Khitrina, I.V. Koptug, N.A. Pakhomov, R.Z. Sagdeev, V.N. Parmon. *J. Phys. Chem. B*, **104**, 1966 (2000).

4 MAIN OBJECTIVES FOR THE FUTURE OF CHEMICAL AND PROCESS ENGINEERING MAINLY CONCERNED BY THE SCIENCE AND TECHNOLOGIES OF NEW MATERIALS PRODUCTION

Pr. Jean-Claude CHARPENTIER

President of the European Federation of Chemical Engineering

Department of Chemical Engineering/CNRS

Ecole Supérieure de Chimie, Physique et Electronique de Lyon

BP.2077

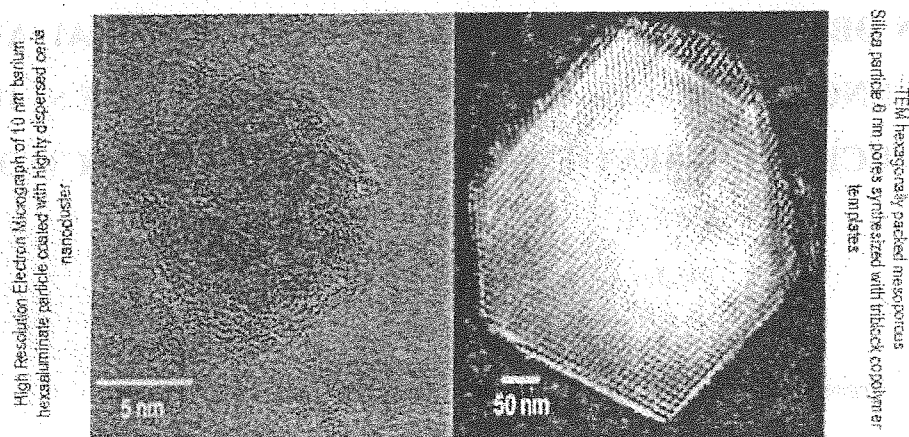
69616 VILLEURBANNE Cedex – France

E-mail: charpentier@cpe.fr, tel.: +33 4 72 43 17 02, fax: + 33 4 72 43 1670

Today the Chemical and Process Engineering especially involving Chemical Reactor Engineering has to answer to the changing needs of the chemical and related process industries such as petroleum, petrochemical, bituminous, pharmaceutical and health, agro and food, environment, iron and steel, building materials, paints, glass, surfactants, electronics, cosmetic and perfume ..., and to meet market demands. So being a key to survival in globalisation of trade and competition, the evolution of chemical engineering is thus necessary. And to satisfy both, the market requirements for specific end-use properties of the products manufactured in (bio) chemical reactors and the social and the resource-saving and environmental constraints of the industrial-scale processes and technologies, it is shown that a necessary progress is coming via a multidisciplinary and time and length multiscale approach.

In such a frame the future for the science and technologies of new materials can be summarized by four main objectives :

1. A total multiscale control of the process (or the procedure) to increase selectivity and productivity i.e, nanotailoring of materials with controlled structure : opportunities for molecular engineering in catalysis (figure) [1] or increase selectivity and productivity by supplying the process with a local "informed" flux of energy or materials.



Perspective (Y. J. Ying, MIT, AIChE Journal -2000) Nanostructural Tailoring : Opportunities for Molecular Engineering in Catalysis

Figure 1. Nanotailoring of materials with controlled structure. [1]

2. A design of novel equipment based on scientific principles and new operation modes and methods of production : process intensification in chemical reactors in using multifunctional technologies that couple or uncouple elementary processes (transfer – reaction - separation) such as in catalytic distillation reactors, or reaction and crystallization equipment, or crystallization and distillation equipment, or membrane technologies, and use of non-traditional structured packing. **Process intensification concern also the use of new operation modes** such as unsteady or cyclic operations, extreme high temperature and pressure technologies and supercritical media. The reduction in the size and in the number of equipment units leads to reduced investment costs and significant energy recovery or savings. Furthermore, improved product selectivity leads to a reduction in raw material consumption and hence, operating costs. Globally process intensification through multifunctional reactors and new operation modes permits 10-20% significant reduction in both investment and plant operating costs [2].

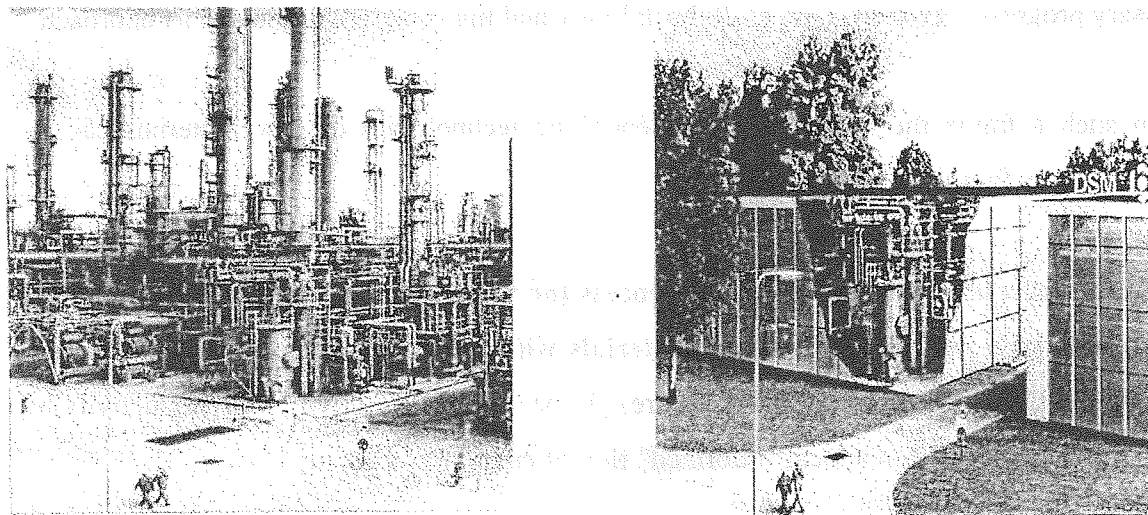


Figure 2. One vision of how a future plant employing process intensification may look (right) vs. a conventional plant (left) [2]

Process intensification involves also the use of micro-engineering and micro-technologies. The miniaturisation of chemical analytical services in micro-total analysis system with micro-reaction technology promises to yield a wide range of novel devices for reaction kinetic and micro-mechanism studies, and on-line monitoring of production systems, or for high-throughput screening experiments for rapid catalyst screening.

3. A formulation or a product design and engineering : manufacturing end-use properties. This involves the development of multidisciplinary and multiscale product-oriented engineering with a special emphasis on complex fluids and solid technology. I have called it the "Génie du triplé Processus moléculaire – Produit – Précédé (3P Engineering)". Indeed the quality and properties of emulsified or past like and solid products is determined at the micro-and nano scale level. Therefore to be able to design and control the product quality [3] and make the leap from the nano-level to the process level, chemical and process engineering involved with structured material have to face many challenges in fundamentals (structure-activity relationships on molecular level, interfacial phenomena i.e, equilibria, kinetics ..), in product design (nucleation growth, internal structure, additives..), in process integration (simulation and design tools based on population balance) and in process control (sensors and dynamic models).

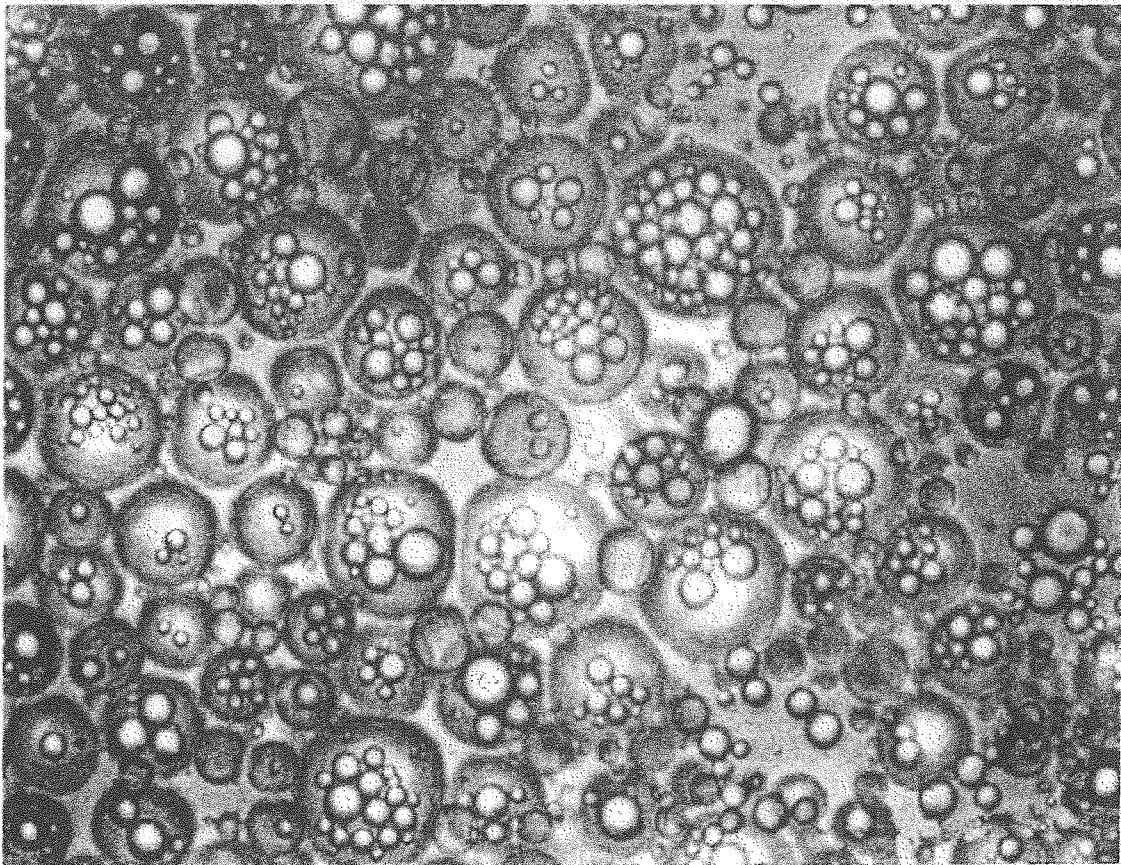


Figure 3. Multiple W/O/W emulsion manufactured by partial-phase soluinversion technology (Gohla, [3])

4. A implementation of the multiscale and multidisciplinary computational chemical engineering modelling and simulation to real-life situations : from the molecule to the overall complex production scale into the entire production site. Through the interplay of molecular theory, simulation, and experimental measurements evolves a better quantitative understanding of structure-property relations, which, when compled to macroscopic chemical engineering science, can form a basis for new materials and process design. Computer Aided Process Engineering European Programs such as CAPE OPEN or Global CAPE OPEN aim expanding and developing interface specification standards to insure interoperability of CAPE software components. And a standardization body CAPE OPEN laboratories Network has been established to maintain and disseminate the software standards and to ensure that software tools used by the process industries reach a level of interoperability that will help ensure growth and competitiveness.

In a context of society and market demands versus technology development it is clear that the future for the science and technologies of new materials production is heading in these four directions and requires the integrated approach presented as the 3P Engineering [4]. Moreover, chemical and process engineering will also be increasingly involved and concerned with the application of Life Cycle Assessment to new material design and production and its use but also to the plant and the equipment together with the associated services. This

concerns sustainability (environmental protection, security, societal demands, and business leading to better conversion and selectivity of raw material and energy for consumer desired product quality), regardless of the industries which use these technologies of new material production.

References

1. Ying, J. Y, "Nanostructure tailoring : opportunities for molecular engineering in catalysis". AIChE Journal, 2000, 46, 10, pp 1902 – 1906,
2. Stankiewicz, A.I. Moulijn, J.A., Process Intensification, transforming chemical engineering, Chem.Eng.Prog. 2000, 96, n° 1, pp 22-34,
3. Gohia, S.H, "Simple and multiple lipidic systems in cosmetic formulation" 3rd world Congress on Emulsions, 2002, Theme 4, 290, 24-27th September, Lyon – France
4. Charpentier J.C. "Market demand versus technological development : the future of chemical engineering" International Journal of Chemical Reactor Engineering, 2003, 1, A14.ppl.30.

KEY-NOTE LECTURES

REDACTED INFORMATION



Hydrogen production for fuel cells in mobile applications

L. Kiwi-Minsker

*Laboratory of Chemical Reaction Engineering, Swiss Federal Institute of Technology,
CH-1015 Lausanne, e-mail: liubov.kiwi-minsker@epfl.ch*

Mobility, being defined as displacement of people and goods, is increasing during the last decades. For any sustainable society mobility should be safe, environmentally clean and economic. Vehicles can be run either by connecting them to a continuous supply of energy, or by storing energy on board. Fuel cells convert chemical energy into electrical energy with a high efficiency and low emission of pollutants. Fuel cell powered electric cars using hydrogen-rich gas present a low-emission alternative to gasoline internal combustion engines. Fuel cells (FCs) offer significant environmental benefits over competing technologies and hence the environment is a strong driving force behind the development of FC systems for transport applications. Moreover, fuel cells are not limited in their efficiency by the restrictions of the Carnot cycle. However, fuel cells in mobile applications require safe and efficient hydrogen storage by physical or chemical means, or the production of hydrogen on-board.

Hydrogen is gaseous at room temperature and atmospheric pressure, and 4 kg of hydrogen occupies a volume of 45 m³ under normal conditions. This corresponds to a balloon of 5 m diameter, being not a practical solution for a vehicle. The high-pressure containers are more compact, but present significant disadvantages: the fuel would be available at a pressure dropping from 450 bar to zero overpressure, so additional pressure control is essential. High-pressure vessels create a considerable risk — the compression itself is the most dangerous and complicated part.

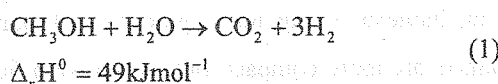
Another approach for hydrogen storage is to use adsorption of hydrogen on light and reasonably cheap materials of high surface area, like nanostructured graphite. Interesting results have been published on the hydrogen storage in carbon nanotubes, but whether a hydrogen-storage material will emerge from it, remains an open question. The amount of adsorbed hydrogen is proportional to the specific surface area of the carbon nanotube material and limited to about 2 mass% for carbons.

Many metals and alloys are capable of reversibly absorbing large amounts of hydrogen via hydride formation. Reversible hydrogen-storage capacities approaching 3 mass% at room temperature have been reported. Some of the lightest elements in the periodic table, for example lithium, boron, sodium and aluminium, form stable and

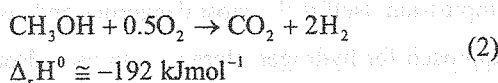
ionic compounds with hydrogen. The hydrogen content reaches values of up to 18 mass% for LiBH_4 , but such compounds desorb the hydrogen only at temperatures from 80 °C up to 600 °C, and the reversibility of the reaction is not fully proven.

Taking into account these results, it is scientifically interesting and challenging to continue research on the hydrogen storage using well-characterized materials, but alternative approach of producing hydrogen on-board has to be considered and developed. There are several "primary fuels" as potential hydrogen sources for proton exchange membrane fuel cells (PEMFC) used in automotive propulsion as methane (natural gas), liquefied gas, gasoline, alcohols. Due to their high storage density, liquid fuels are the most attractive for mobile application. Except steam-reforming of alcohols, all processes for generating hydrogen from these fuels require water-gas shift reactors of significant size. This occurs because the higher operating temperatures used lead to unacceptably large amounts of CO. All processes require low- or zero-sulfur fuels, and add to the fuel cost.

Methanol is considered to be safer than the currently used petrol with respect to ignition temperature, and it can be produced from renewable sources. Moreover, steam reforming (1) offers the highest attainable hydrogen concentration in the product gas (75%):

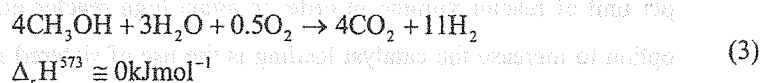


For comparison, product gas from partial oxidation has only 35-45% of hydrogen:



Lower hydrogen percentages adversely affect cell performance. Moreover, the high exothermicity of reaction (2) drastically lowers the efficiency of the process since waste heat is generated and temperature control of the reactor may be complicated. From another side, pure steam-reforming suffers from poor transient operation. Therefore, combination of partial oxidation with steam-reforming of methanol appears the leading candidate for on-board generation of hydrogen. Oxidative steam reforming of methanol (OSRM) is based on the combination of an exothermic oxidation and an endothermic reforming of methanol carried out in the

same reactor. At 300°C an autothermic reaction for the following composition of the reactant feed is attained:



Reactors for this process operate autothermally, i.e. without any external heating or cooling when reached the reaction temperature, with hydrogen content in the product gas of 73% with oxygen in the feed or 65% if air is used. For fast start-up or transient response, the methanol/oxygen ratio can be varied. The main difficulty in carrying out the OSRM is due to the much faster methanol oxidation compared to the reforming reaction. As a consequence, heat is generated mostly at the reactor entrance, whereas the heat consumption occurs in the middle and rear of the reactor. In conventional reactors with low axial and radial heat conductivity, pronounced axial temperature profiles are developed. They are characterized by “hot spots” at the reactor entrance and “cold spots” near the reactor outlet. The high temperatures damage the catalyst and the low temperature diminishes the reforming rate leading to poor reactor performances. Therefore, temperature control in the reactor is crucial.

Metal based catalysts with high thermal conductivity can help to integrate the exothermic combustion of methanol and the endothermic steam reforming. The beneficial effect of improved heat transfer was demonstrated for the OSRM using either a conductive material, or the micro geometry of a monolith. Microstructured catalytic reactors have some unique characteristics that classical reactors cannot achieve, like short dynamic response times, narrow residence time distribution and large heat exchange capacity.

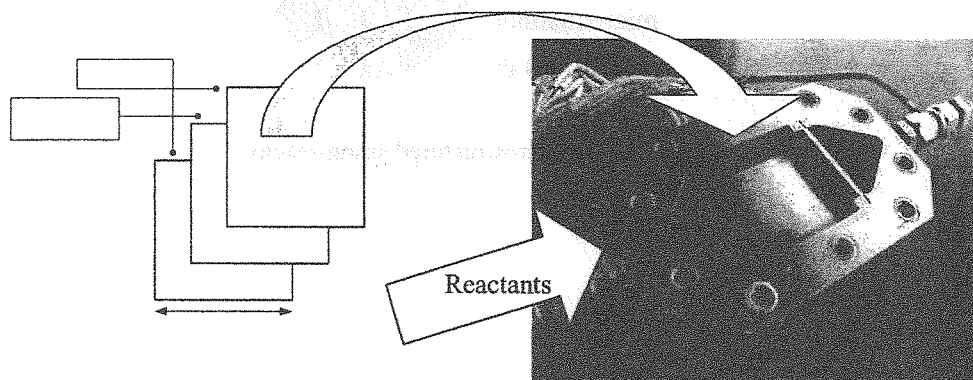


Figure 1: Scheme of the microreactor used for the SRM kinetic measurements

To profit from these advantages, one has to introduce sufficient fraction of catalyst per unit of reactor volume in order to attain high reactor efficiency. One promising option to increase the catalyst loading is the use of sintered metal fiber (SMF) plates as catalyst support. SMF consist of metal filaments (\varnothing 2-30 μm) and provide uniform 3D open structures with porosity up to 90%. Ten SMF plates and metal foils were stacked together in housing (Fig.1) to form the microstructured reactor. Pressure drop remained low with high catalyst loading up to 25 mass%. Catalytic activity was investigated for a copper based catalyst in the SRM for the production of hydrogen.

Another microstructured reactor, designed as catalytically active wires placed in parallel into a tube, which we call "string-reactor" (see Fig.2), was developed for the OSRM to produce hydrogen in autothermal mode. The heat generated during methanol oxidation at the reactor entrance is axially transferred to the reactor zone of the endothermic steam-reforming. The brass metal wires (Cu/Zn = 4/1) were used as precursors for the preparation of string-catalysts. High methanol conversion in the OSRM together with CO_2 -selectivity of 99% and H_2 -selectivity of 60% were obtained and results will be presented in details.

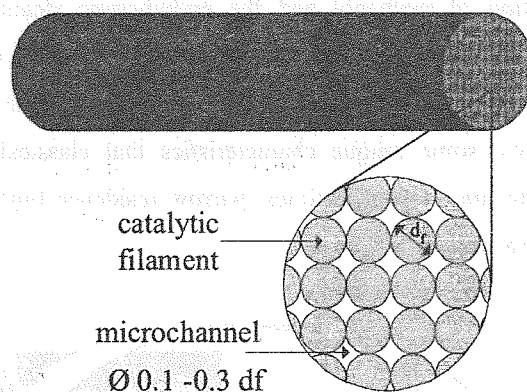


Figure 2: The microstructured string-reactor.

AN APPROACH TOWARD THE UTILIZATION OF RENEWABLE FEEDSTOCKS: CO₂ SELECTIVE REDUCTION; ALCOHOLS INTO MOTOR FUEL CONVERSION

M.V. Tsodikov, I.I. Moiseev

*A.V. Topchiev Institute of Petrochemical Synthesis, RAS,
Leninsky Prospekt 29, 119991 Moscow GSP-1, Russia,*

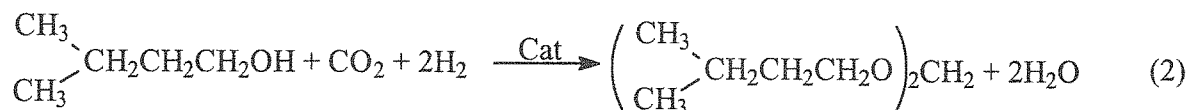
*N.S. Kurnakov Institute of General and Inorganic Chemistry, RAS,
Leninsky Prospekt 31, 119991 Moscow GSP-1, Russia,*

Carbon dioxide is both an abundant anthropogenic generated waste material and a source of bound carbon. Ethanol and its lower homologues can be produced via biomass fermentation. In this paper reactions of CO₂ and alcohols catalysed by intermetallics will be discussed.

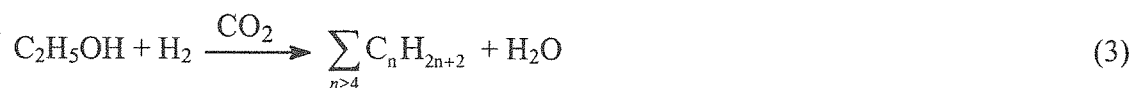
CO₂ was found to undergo reduction by hydrogen giving rise to CO and methane under 20-350°C in the presence of TiFe_{0,95}Zr_{0,03}Mo_{0,02}. A catalytic combination of hydride phase [TiFe_{0,95}Zr_{0,03}Mo_{0,02}]H_{0,36} and Pt/Al₂O₃ was shown to yield 99% CO under the conversion of CO₂ close to 60% at 350°C and 10-50 at. Cyclohexane reacts with CO₂ in the presence of TiFe_{0,95}Zr_{0,03}Mo_{0,02} and Pt/Al₂O₃ at 430°C and 15 at according to the equation (1):



Intermetallic TiFe_{0,95}Zr_{0,03}Mo_{0,02} modified with Cu catalysed reductive reaction of CO₂ with 3-methylbutanol-1 giving rise to diisopentylformal according to the equation (2):

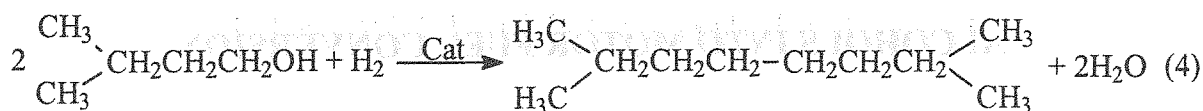


Formation of mixture consisted of linear and branched hydrocarbons was observed while ethanol was treated with CO₂/H₂ mixture in the presence of TiFe_{0,95}Zr_{0,03}Mo_{0,02} and Pt/Al₂O₃ composition according to the equation (3):

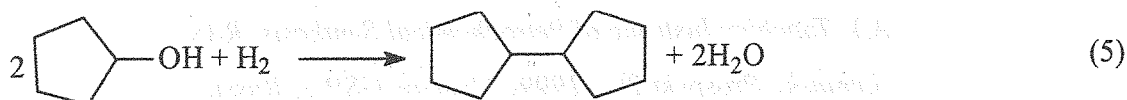


Reductive dehydration of an alcohol, a reaction in which alcohol molecule undergoes dehydration and condensation giving rise to a saturated hydrocarbon, has been found to take

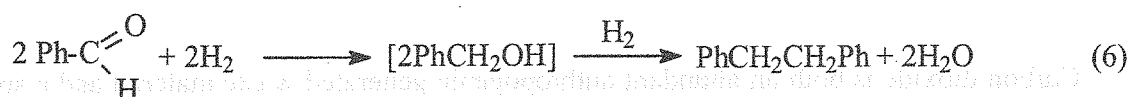
place in the case of other alcohols as well. The number of C atoms in the product molecule is at least doubled in comparison to the starting alcohol, e.g., equation (4):



Reduced melted iron catalyst converted cyclopentanol at 250°C to dicyclopentyl (see Eq. 5):



Analogously, benzaldehyde was found to undergo reduction giving rise to 1,2-diphenylethane possibly *via* intermediate benzyl alcohol formation (see Eq. 6):



Mechanistic aspects of the above mentioned and related reactions are discussed.

References

1. M.V.Tsodikov, V.Ya.Kugel, E.V.Slivinskii, F.A.Yandieva, V.P.Mordovin, I.I.Moiseev. *Rus. Chem. Bull., Int. Ed.*, 2001, v. 50, No 7, p. 1201-1207.
2. M.V.Tsodikov, V.Ya.Kugel, F.A.Yandieva, E.V.Slivinskii, I.I.Moiseev, G.Colón, M.C.Hidalgo, and J.A.Navio, *Studies in Surface Sciences and Catalysts*, 2001, v. 138, p. 239.
3. G.A.Kliger, L.S.Glebov, M.V.Tsodikov, V.Ya.Kugel, F.A.Yandieva, V.G.Zaikin, A.I.Mikaya, E.V.Slivinskii, N.A.Plate, A.E.Gekhman, I.I.Moiseev. *Kinetics and Catalysis (Rus.)*, in press, 2003.

**NEW MULTIPHASE FIXED-BED TECHNOLOGIES. COMPARATIVE
ANALYSIS OF INDUSTRIAL PROCESSES (EXPERIENCE OF
DEVELOPMENT AND INDUSTRIAL IMPLEMENTATION)**

L.B. Datsevich, D.A. Mukhortov*

University of Bayreuth, Germany (Bayreuth), Germany

**FSUF RSC "Applied Chemistry" (St. Petersburg), Russia*

Proceeding from the analysis of chemico-physical processes in existing gas-liquid fixed-bed reactors, two new technologies for gas-liquid reactions on a fixed-bed catalyst are developed. In the first technology worked out in the Russian Scientific Center "Applied Chemistry", the process is carried out under conditions of the gravitational liquid film flow over the catalyst surface and liquid recycling. In the second process - presaturated one-liquid-flow technology (POLF technology) [L.B. Datsevich, D.A. Mukhortov, Process for hydrogenation of organic compounds, Russian patent 2083540, to Datsevich], the reaction is brought about without the presence of the gaseous phase – only the liquid phase is fed into the reactor, but this liquid is preliminarily saturated with the gas in a special highly intensive device before the reactor. These new technologies allow carrying out reactions with high productivity and process safety at low energy input in the reactor. The comparative analysis of the existing three-phase fixed-bed technologies destined for exothermic reactions is given. Some approaches to scale-up and industrial realisation of these processes are considered. Keywords. Multiphase reactions, Fixed-bed (stationary) catalyst, Trickle bed reactors (TBR), Bubble column reactors (BC), presaturated one-liquid-flow (POLF) technology, Mass transfer

ANALYSIS OF POLITICAL PROCESSES (EXHIBIT 1) IN THE STATE OF TEXAS

1. Introduction

The purpose of this study is to analyze the political processes in the State of Texas, focusing on the legislative branch.

The legislative branch of the State of Texas is composed of the Texas House of Representatives and the Texas Senate. The House has 90 members, and the Senate has 24 members. The legislative process begins with the introduction of a bill by a member of the House or Senate. The bill is then assigned to a committee for review. After the committee has finished its work, the bill is reported back to the chamber. The chamber then debates the bill and votes on it. If the bill passes, it goes to the other chamber for review. If the other chamber also passes the bill, it goes to the Governor for signature. If the Governor signs the bill, it becomes law. If the Governor vetoes the bill, the legislature can override the veto with a two-thirds majority vote in both chambers.

ORAL PRESENTATIONS

SECTION I.

**PHYSICO-CHEMICAL AND MATHEMATICAL BASES OF
PROCESSES OCCURRING ON CATALYSTS SURFACE**

ORAL PRESENTATIONS

SECTION I

PHYSICO-CHEMICAL AND MATHEMATICAL ASPECTS OF
POLYMERIZATION OF VINYL MONOMERS

KINETICS OF NO_x REDUCTION OVER Ag/ALUMINA BY A HIGHER HYDROCARBON IN EXCESS OF OXYGEN

F. Klingstedt, K. Eränen, K. Arve, J. Wärnä, L.-E. Lindfors and D.Yu. Murzin

*Laboratory of Industrial Chemistry, Process Chemistry Centre, Åbo Akademi University,
Biskopsgatan 8, FIN-20500 Turku/Åbo, Finland*

Introduction

During the last ten years, improved fuel economy in vehicles, has become a dominating factor when developing engines, due to the concern of the growing CO₂ greenhouse emissions. A perfect example of efficient fuel economy is demonstrated by the common-rail turbo diesel engine, which operates under highly lean-burn conditions. These oxygen rich conditions, however, make the conventional three-way catalysts unsuitable for the reduction of NO_x emissions. In this paper we have investigated the application of a silver-alumina catalyst for selective catalytic reduction of NO_x using hydrocarbons (HC-SCR). Since HC-SCR is based on the use of unburned hydrocarbons together with added hydrocarbons it is of highest interest to study the reaction kinetics in order to optimise the process conditions in the engine and the catalytic converter. The present study is devoted to experiments with simulated diesel exhaust mixtures, where the concentration of the reactants were varied and the results were mathematically treated to determine orders in NO, HC and O₂.

Experiments and results

A 2 wt.% Ag/alumina catalyst was prepared by impregnation of a commercial alumina support (LaRoche Industries Inc.) with a 0.022 M silver nitrate solution of high purity. The experimental data for the kinetic study was obtained in activity runs, where the Ag/alumina particles (250-500 μm, 0.4 g) were tested in a quartz micro reactor.

Different sizes of particles and variations in the bed length were investigated to elucidate the impact of mass-transfer limitations. The internal mass-transfer resistance over the Ag/alumina was tested using particle sizes of 1.0-1.41 mm, 0.250-0.500 mm and 0.09-0.180 mm with equal mass of the bed and the results are presented in Figure 1. The external mass transfer experiments were carried out using three different lengths of the Ag/alumina

OP-I-1

bed: 0.35, 0.7 and 1.05 cm. The results confirmed, that there are no internal and external mass transfer limitations over the Ag/alumina catalyst.

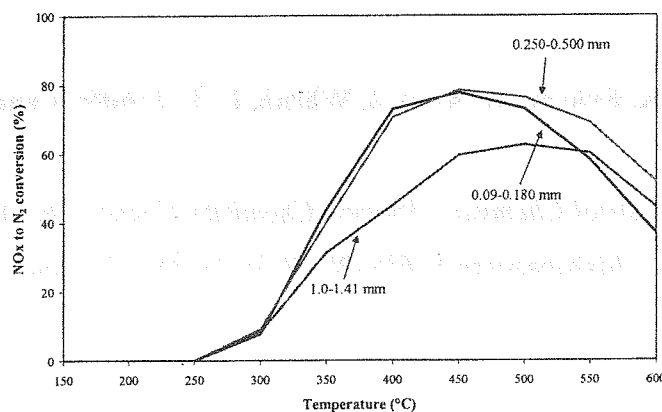
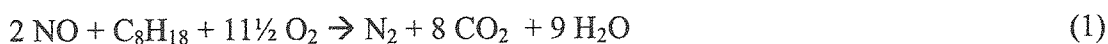


Figure 1. Effect of particle size on the conversion of NO_x over Ag/alumina. Catalyst mass = 0.4 g, C₁/NO = 6 (octane as reductant) and GHSV = 60 000 h⁻¹.

Kinetic tests were thus carried out in the absence of internal and external mass transfer limitations. A temperature window of 150-550 °C with sampling at steady state conditions (GHSV = 60 000 h⁻¹ and 550 ml/min) was used for the catalytic activity runs. Orders in NO, HC and O₂ were determined by variation in the concentrations of the involved reactants (NO: 250-1000 ppm, octane: 134-750 ppm and O₂: 1-12 vol. %). Oxygen was led separately into the reactor in order to avoid reaction between NO and O₂ before entering the catalyst bed. The concentrations of N₂, CO₂, CO and O₂ were determined using a GC (HP 6890). More details on general experimental procedure as well as on analysis are provided in [1].

The reaction was assumed to follow the simplified reaction scheme:



A phenomenological power-law kinetic model of exponential order was set up for the reactions:

$$r_1 = k_1 x_{\text{NO}}^{m_1} x_{\text{OCT}}^{n_1} x_{\text{O}_2}^{o_1}; r_2 = k_2 x_{\text{OCT}}^{m_2} x_{\text{O}_2}^{o_2}; r_3 = k_3 x_{\text{OCT}}^{m_3} x_{\text{O}_2}^{o_3}; r_4 = k_4 x_{\text{CO}} x_{\text{O}_2}^{0.5} \quad (5)$$

where k are rate constants, m, n, o-reaction orders.

The rate constants and reaction orders were estimated with simplex and Levenberg-Marquardt methods implemented in the software ModEst 6.0 (ProfMath, Helsinki). The concept of a plug flow reactor was applied

$$\frac{dx_i}{dz} = \frac{m_{cat}}{n} r(x_i) \quad (6)$$

where z is length coordinate in reactor, m_{cat} catalyst mass, x -molar fraction.

The mass balances were solved with the backward difference method during the parameter estimation procedure. The results obtained are presented in Table 1 (for the main reaction) and Figure 2.

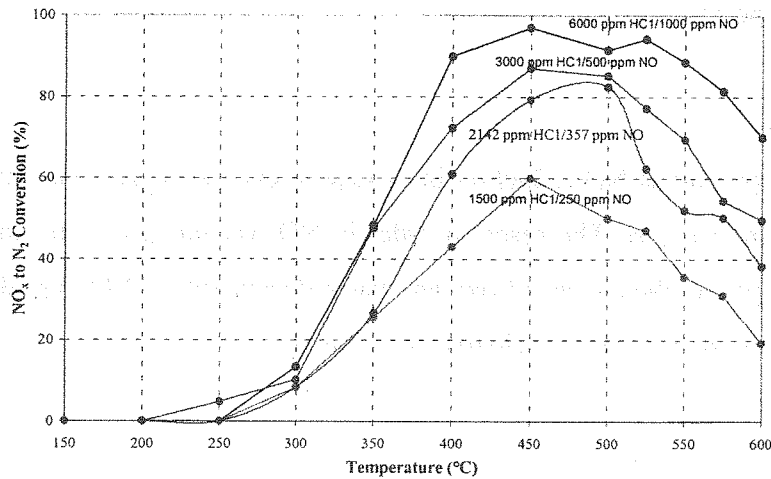


Figure 2. Activity test over Ag/alumina with varying concentration of octane and NO but having $HC_1/NO = 6$ and $GHSV = 60\ 000\ h^{-1}$.

Table 1. Reaction orders of NO, octane and O_2 at different temperatures.

Temperature (°C)	NO	octane	O_2
300	~ 0	1.7	1.0
350	~ 0	1.9	1.3
400	~ 0	1.9	1.1
450	~ 0	1.4	0.88
500	0.07	1.3	0.60
550	0.26	1.2	0.25

The reaction order close to zero order in NO was calculated between 300 and 500 °C and at the final temperature of 550 °C it increased to 0.26, indicating that the reaction rate is almost independent of the concentration of NO. The strong dependence of the NO_x conversion on the hydrocarbon concentration is clearly seen, as the order varies from 1.9 at low temperatures to 1.2 at the highest temperature. In oxygen, on the other hand, there is a high order at low temperatures, which gradually decreases to 0.25 at 550 °C.

Experimental data suggests that octane reactivity dominates the rate of NO reduction. The mechanistic explanation for observed kinetics could be that in the rate-determining step

OP-I-1

octane reacts with the aid of predominantly oxygen over the Ag/alumina catalyst to form an oxygenated hydrocarbon (via H-abstraction). Although the influence of NO is not manifested kinetically, meaning that the coverage of adsorbed NO or nitrates (nitrites) is small, the presence of NO is vital to create active intermediates for the reactions to proceed, as octane does not transform totally in the absence of NO in the gas feed. An alternative explanation, which could account for zero order in NO is that the surface is almost completely covered by NO_x containing species.

Conclusions

Kinetics of continuous NO reduction by octane in excess oxygen was investigated over a 2 wt.% Ag/alumina catalyst. The reaction order in NO was equal to zero, indicating that the rate of NO reduction in the excess of oxygen was independent on NO partial pressure. At the same time reaction orders in octane clearly exceed unity.

References

- [1] K. Eränen, L.-E.Lindfors, F. Klingstedt, D.Yu.Murzin, Continuous reduction of NO_x with octane over a silver/alumina catalyst in oxygen-rich exhaust gases: combined heterogeneous and surface mediated homogeneous reactions, *Journal of Catalysis*, 2003, 219, 25

THEORETICAL STUDIES ON MULTIFUNCTIONAL CATALYSTS WITH INTEGRATED ADSORPTION SITES

Wulf Dietrich, Marcus Grünewald, David W. Agar

Chair of Reaction Engineering (Prof. D. W. Agar),

Department of Biochemical and Chemical Engineering, University of Dortmund,

Emil-Figge-Str. 66, D-44227 Dortmund, Germany

Fax: +49(231) 755-2698, Email: wulf.dietrich@bci.uni-dortmund.de

Introduction

The integration of multiple process functions in multifunctional reactors, e.g. heterogeneous catalysed reactions and separation processes, has been recently intensively investigated as a promising tool for process intensification [1]. Whenever more than one functionality has to be incorporated in a reactor the spatial distribution of the functionalities becomes an important parameter for the optimisation of the reactor performance. So far the distribution of the functionalities in multifunctional reactors has been optimised primarily on the reactor scale, e.g. spatial distribution of adsorbent and catalyst particles along a fixed bed. However, the inter-and intra-particle mass transfer can pose a serious constraint for the utilisation of the synergy potential offered by multifunctional reactors, especially for very fast reactions. If the integration of the functionalities is extended to the particle level, i.e. multifunctional catalyst particles with an integrated secondary functionality, the mass transfer between the different functional sites can be intensified significantly. Furthermore, microstructuring offers an additional degree of freedom for the design of a multifunctional reactor as the functionalities can be arranged in a structured way inside the particles and thus provides a tool for the deliberate manipulation of intra-particle concentration and temperature profiles. The optimal distribution of a single and two different catalytic activities in a particle has been derived earlier for steady-state conditions [3], [5]. Here we focus on multifunctional catalysts with integrated adsorption sites for the conversion enhancement of equilibrium limited reversible reactions. Due to the inherent unsteady-state nature of adsorption processes a theoretical analysis of these multifunctional catalysts has to be carried out based on a dynamic process model.

Modelling

A two phase dispersion model with internal pore diffusion describing the dynamic behaviour of a fixed bed adsorptive reactor with multifunctional catalyst particles has been developed. The spatial distribution of the functionalities inside the multifunctional catalyst particle was mathematically described according to the volume fraction of each functionality, whereby all possible particle structures could be accounted for. The model was implemented in Aspen Custom Modeler® with a modular model structure and solved using orthogonal collocation on finite elements for the discretisation of the spatial domain, whereas the finite elements were allocated on the radial axis of the particle in such a manner so as to obtain a volume equivalent grid.

The adsorption process was assumed to be mass transfer limited only and the reactor was considered to be isothermal. We considered catalyst and adsorbent sites in the multifunctional particle to have the same properties as for the separate particles. Particle size and structure were averaged for all particles (multifunctional and conventional) in order to permit a direct comparison of different particle and reactor configurations.

Simulation Results

Simulation studies were carried out for two test systems of industrial significance – Claus process and watergas shift reaction – in the first case a product is adsorbed and in the latter a reactant is desorbed, both resulting in a conversion enhancement of the equilibrium reaction according to Le Chatelier's law.

Table 1. Test reaction systems for multifunctional catalysts

Reaction system	Adsorbate	Adsorbent	Catalyst	T [°C]	p [bar]
Claus process [4] $2 \text{H}_2\text{S} + \text{SO}_2 \rightleftharpoons \frac{3}{n} \text{S}_n + 2 \text{H}_2\text{O}$	H ₂ O	Zeolite 3A	$\gamma\text{-Al}_2\text{O}_3$	250	1
Watergas shift reaction [2] $\text{CO} + \text{H}_2\text{O} \rightleftharpoons \text{CO}_2 + \text{H}_2$	H ₂ O	Zeolite 3A	Cu/ZnO/Al ₂ O ₃	250	1

Using the parameter values reported in the literature, particle size and reaction rate were augmented to investigate the influence of the ratio of reaction rate and internal diffusion as well as the ratio of convective and intra-particle mass transfer on the performance of multifunctional catalysts. The performance was quantified using the cycle time prior to the breakthrough point of unconverted reactant for a given reactor volume compared to a conventional adsorptive reactor.

The anticipated intensification of the mass transfer between catalyst and adsorbent was confirmed by the simulation results for both reaction systems. With increasing diffusional resistance the advantage of multifunctional catalysts compared to conventional adsorptive

reactors was more pronounced, too. While an increased reaction rate with respect to the internal mass transfer rate restricts the reaction zone to a region close to the particle surface and thus restricts the utilisation of the particle core leading to a poorer performance enhancement of multifunctional catalysts. Figure 1 gives a summary of the simulation results.

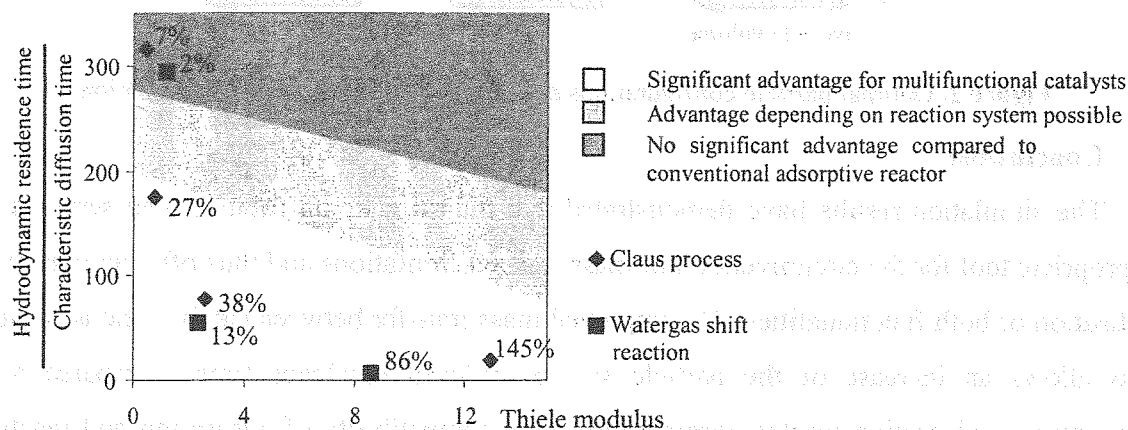


Figure 1. Cycle time enhancement by multifunctional catalysts depending on the mass transfer resistance

Furthermore, a discrete optimisation of the particle structure for a given average volume fraction of catalytic and adsorptive functionalities was carried out for both test reaction systems under different conditions (Figure 2). By means of this procedure the ratio of reaction and internal mass transfer rates (Thiele modulus) was identified to be the main factor influencing the optimal particle structure.

As long as the intrinsic reaction rate is the limiting step, the catalyst activity can be maximised if the catalyst volume fraction is increased towards the particle surface, since this exposes the catalyst to the highest reaction driving force.

The higher the Thiele modulus the more favourable an arrangement with a lower catalyst and a higher adsorbent volume fraction close to the particle surface. This reduces the catalytic activity close to the surface and thus extends the reaction zone further into the core of the particle. By means of the structured arrangement of the functionalities inside the particles the mass transfer rate between the sites with different functionalities can be harmonised with both the reaction and adsorption rate and thus the utilisation of the particle maximised. The same particle structure was found to be optimal for the conversion enhancement both by adsorption of a reaction product and by desorption of a reactant. For all cases particle structures with zones containing overlapping functionalities were superior to arrangements with separate catalyst and adsorbent shells due to the more intimate spatial integration in the mixed zones.

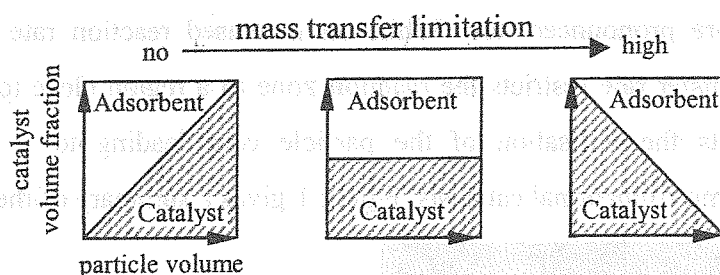


Figure 2. Optimal particle configurations depending on the mass transfer limitation

Conclusions

The simulation results have demonstrated that multifunctional catalysts can serve as an appropriate tool for the circumvention of mass transfer limitations and thus offer an improved utilisation of both functionalities. The improved mass transfer between catalyst and adsorbent also allows an increase of the particle size or reduced residence times compared to a conventional adsorptive reactor configuration. The compatibility of adsorption and reaction rates which is a crucial criterion for the feasibility of adsorptive reactors [4] is facilitated by multifunctional catalysts. However, if the mass transfer between the different functionalities is not limiting, the benefit of multifunctional catalysts will be not sufficient to compensate the more complex manufacturing process. The performance enhancement found for a single reversible reaction suggests similar or even higher improvements for more complex reaction schemes, e.g. increased selectivity for consecutive side reactions, and holds promise for further investigations of multifunctional catalysts with integrated adsorption sites.

References

- [1] Agar, D. W., Chem. Eng. Sci. 54 (1999), 1299-1305.
- [2] Amadeo, N. E., Laborde, M. A., Int. J. Hydrogen Energy 20 (1995), 949-956.
- [3] Ardiles, D. R., Scelza, O. A., Castro, A. A., Coll. Czechoslov. Chem. Commun. 50 (1985), 726-737.
- [4] Elsner, M. P., Dittrich, C., Agar, D. W., Chem. Eng. Sci. 57 (2002), 1607-1619.
- [5] Morbidelli, M., Servida, A., Varma, A., Ind. Eng. Chem. Fundam. 21 (1982), 278-284.

TRANSIENT KINETICS OF V/Ti-OXIDES REDUCTION BY TOLUENE

D.A. Bulushev*, E.A. Ivanov, S.I. Reshetnikov, L. Kiwi-Minsker* and A. Renken*

*Swiss Federal Institute of Technology, LGRC-EPFL, CH-1015 Lausanne, Switzerland

Boreskov Institute of Catalysis, 630090, Pr. Acad. Lavrentieva 5, Novosibirsk, 630090, Russia

Reshet@catalysis.nsk.su

Cyclic reduction and re-oxidation of the catalyst is one of the ways to reach an improved performance in hydrocarbon partial oxidation reactions. The physical basis is the ability to regulate the concentration of adsorbed species by reaction conditions. This way of the reactor operation can allow formation of more active or selective state of the catalyst, which is not formed in steady-state conditions. Benzaldehyde (BA) and benzoic acid are valuable products of toluene partial oxidation over vanadia/titania catalysts. It was found [1,2] that during toluene interaction with a V/Ti-oxide catalysts containing potassium BA is formed for a long time with a very high selectivity while CO₂ is evolved only during the first moments of the reaction.

The aim of this work is the investigation of the kinetics of the toluene interaction with pre-oxidised V/Ti-oxide catalysts with different vanadia content. This step is important for the heterogeneous oxidation of toluene taking place via a Mars - Van Krevelen mechanism.

Catalyst preparation. TiO₂ (Aldrich) with anatase structure was used as a support. It contained 0.2 wt.% of potassium as was determined by atomic emission spectroscopy. Monolayer catalysts with 0.27, 0.47 and 0.57 wt.% V content were prepared by 2-, 5- and 10-steps of VOCl₃ vapour deposition on the surface of TiO₂, respectively, hydroxylation and drying (grafting technique). The catalysts were dried and calcined in air at 723 K during 120 min. The BET specific surface area was equal to 9 m²/g. The amount of vanadium corresponds to 0.35, 0.62, 0.75 monolayers (ML), respectively. The monolayer is taken to be equal to 10 V-atom nm⁻² [3].

Set-up and procedure. An experimental set-up used for the transient response study has been described in [1]. The catalyst (1 g) was loaded to a fixed bed reactor of i.d. 6 mm. Before every experiment the catalyst was pre-treated in oxidative atmosphere (20 vol.% O₂ in Ar) at 673 for 30 min. Then, the flow was switched to Ar, cooling was performed to the reaction

OP-I-3

temperature and a 2 vol.% toluene/Ar mixture (1 ml/s) was introduced into the reactor. Products were analysed by a quadrupole mass spectrometer and gas-chromatograph.

Kinetic model and results. The kinetic model is based on the following results and assumptions [1-4]: (1) BA and CO₂ are formed mainly on different active sites, nucleophilic (O²⁻) and electrophilic (O⁺) oxygen, respectively; (2) The ratio of these active sites is not dependent on the temperature; (3) Adsorbed benzoates and other coke-like species are formed on the surface of vanadia/titania during the toluene interaction; (4) Diffusion of oxygen from the bulk is not important in the studied temperature range.

The kinetic scheme with the minimal amount of steps describing responses of toluene and reaction products was chosen. It includes following steps:

	<i>Kinetic steps</i>	<i>Rate of reactions</i>
1)	$C_6H_5CH_3 + 2 [YO] \rightarrow 2 [Y] + C_6H_5CHO + H_2O,$	$R_1 = k_1 C_T [YO]^m,$
2)	$2 C_6H_5CHO + 3 [YO] \rightarrow 2 [YC_6H_5COO] + [Y] + H_2O,$	$R_2 = k_2 C_{BA} [YO],$
3)	$C_6H_5CH_3 + 18 [ZO] \rightarrow 18 [Z] + 7 CO_2 + 4 H_2O,$	$R_3 = k_3 C_T [ZO]^k,$
4)	$C_6H_5CH_3 + [ZO] \rightarrow [ZOC_7H_8],$	$R_4 = k_4 C_T [ZO],$
5)	$[ZOC_7H_8] + 17 [ZO] \rightarrow 18 [Z] + 7 CO_2 + 4 H_2O,$	$R_5 = k_5 [ZOC_7H_8] [ZO].$

Toluene interacts with nucleophilic oxygen sites (YO) of the catalyst with the BA formation in the first step. BA interacts with the same oxygen sites forming benzoate (step 2). Toluene can be adsorbed with the ring parallel to the surface on a group of ZO sites. Electrophilic oxygen in these sites provides fast formation of CO₂ by fission of the aromatic ring in adsorbed toluene (step 3). Toluene may also adsorb on a single ZO site (step 4). In that case it interacts with electrophilic oxygen of other ZO sites forming the total oxidation products (step 5). A continuous stirred tank reactor approach was used for mathematical modelling.

The main products of the toluene interaction with the pre-oxidised vanadia/titania catalyst in the temperature range 523-633K are BA, CO₂, CO and H₂O. The transient behaviour of CO is similar to CO₂, but CO concentration was 5-6 times less. Hence, it was not taken into account.

Figs. 1a and 1b demonstrate the BA and CO₂ evolution, obtained during the toluene interaction with the pre-oxidised vanadia/titania catalyst (0.75 ML V/TiO₂) at different temperatures. The response curves presented in figures indicate that the dynamics of the CO₂ and BA formation is different. The CO₂ formation declines quickly, while BA is formed for a

long time. This was explained by participation of different oxygen species in partial and total oxidation [1]. Except of gaseous products the coke-like species are formed on the catalyst surface. This follows from the balance calculations as well as from the oxygen introduction experiments after the toluene interaction. CO_2 , CO и H_2O were found in products of the oxygen interaction, but BA was never observed. It is seen that the calculated responses of BA and CO_2 at different temperatures correspond to the experimental data (Fig. 1).

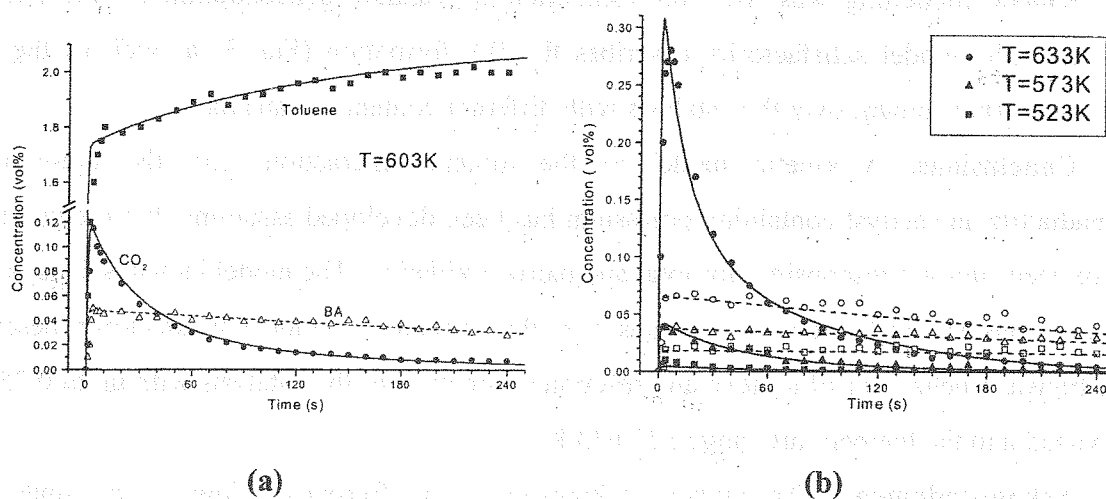


Fig. 1. Toluene interaction with the pre-oxidised 0.75 ML V/TiO₂ catalyst at different temperatures. Benzaldehyde (light points) and CO_2 (dark points). Points – experiments, lines – modelling.

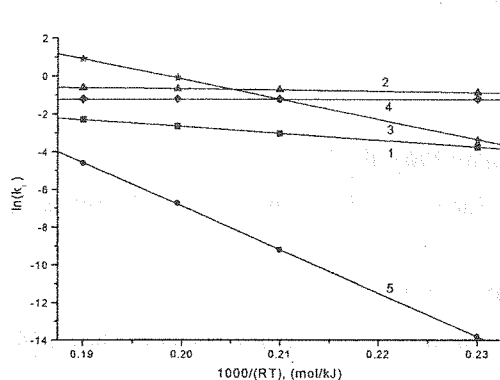


Fig. 2. Arrhenius plots for the rate constants.

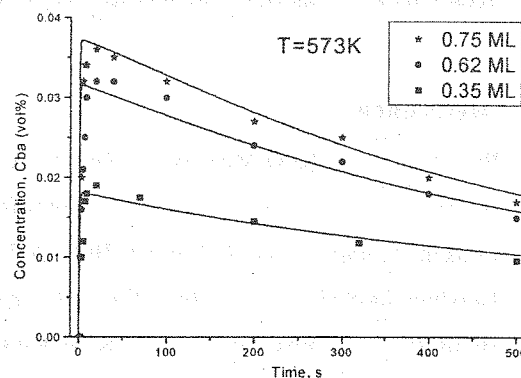


Fig. 3. Dependences of the benzaldehyde formation on time after the switch of the Ar flow to the 2 vol.% toluene/Ar mixture over the pre-oxidised V/Ti-oxide catalysts at 573 K. Coverage of titania by vanadia in monolayers is shown. Points – experiments, lines – modelling.

Fig. 2 demonstrates the calculated dependence of the $\ln k_i$ on temperature. The rate constants fit nicely the Arrhenius plots. The step 5 has the lowest rate constant and higher activation energy. Hence this step contributes to the CO_2 formation more strongly at high temperature.

OP-I-3

Dynamics of the BA formation are compared during the toluene interaction with the pre-oxidised catalysts containing different vanadia concentrations (0.35, 0.62 and 0.75 ML) (Fig. 3). Maleic anhydride and benzoic acid have never been found in products. BA formation increases with the vanadia content. No gaseous products were detected during toluene interaction with pure titania support. These data point out that the vanadia species in a monolayer are active in the BA formation.

Kinetic modelling was used for estimation of vanadia concentration in YO and ZO species. The model satisfactorily describes the BA formation (Fig. 3) as well as the CO₂ formation (not shown) over the catalysts with different content of vanadia.

Conclusions. A kinetic model of the toluene interaction with the pre-oxidised vanadia/titania catalyst containing potassium has been developed assuming that the two types of oxygen sites are responsible for total and partial oxidation. The model includes 5 steps. The kinetic constants and activation energies were determined. The model satisfactorily describes the transient behaviour of toluene and reaction products over the catalysts with up to 0.75 ML of vanadia in the temperature range 523-633 K.

Acknowledgment. The authors acknowledge the European Commission under the INCO-Copernicus Program for the financial support. The work of E.A. Ivanov and S.I. Reshetnikov has been supported by RFBR (Grant N 98-03-32395).

References:

1. Bulushev, D. A.; Kiwi-Minsker, L.; Renken, A. *Catal. Today* **2000**, *61*, 271.
2. Bulushev, D. A.; Kiwi-Minsker, L.; Zaikovskii, V. I.; Lapina, O. B.; Ivanov, A. A.; Reshetnikov, S. I.; Renken, A. *Appl. Catal. A: General* **2000**, *202*, 243.
3. Grzybowska-Swierkosz, B. *Appl. Catal. A: General* **1997**, *157*, 263.
4. Bulushev, D. A.; Reshetnikov, S. I.; Kiwi-Minsker, L.; Renken, A. *Appl. Catal. A: General* **2001**, *220*, 31.

STUDIES ON THE KINETICS OF CARBON DIOXIDE ABSORPTION WITH IMMOBILISED AMINES

X. Zhang, S. Schubert, M. Grünewald, D.W. Agar

Chair of Reaction Engineering,

Department of Biochemical and Chemical Engineering, University of Dortmund

Emil-Figge-Str. 66, D-44227 Dortmund, Germany

Fax: +49(231) 755-2698, Email: xiaohui.zhang@bci.uni-dortmund.de

Introduction

Blends of primary or secondary amines with tertiary amines, such as methyldiethanolamine (MDEA), are frequently used for the removal of CO₂ from gas mixtures [1]. These 'activated' amine solutions are advantageous, since they combine the high absorptive capacity of the tertiary amines with the high absorption rates achievable with primary or secondary amines. However, the acceleration of CO₂ absorption via the rapid formation of carbamates with primary or secondary amines is usually only required locally within the absorption column. In other parts of the absorption process homogeneous activating additives can give rise to undesirable side-effects, such as increased corrosion or higher energy demands for regeneration. It would thus seem to be preferable to immobilise the activators on a solid carrier, which would ideally also serve as a packing material, within the absorption column. In this way one could localise the activators in those parts of the absorption process where they are needed and exclude them elsewhere.

The formation of carbamate would then take place as a kind of chemical adsorption process through the reaction of CO₂ with the immobilised primary or secondary amines. The activators are regenerated 'in-situ' and continuously by the reaction between the flowing aqueous MDEA phase and the carbamate releasing bicarbonate into the solution (Figure 1).

Orientating Experiments

The positive effect of immobilised activators on the absorption behaviour was demonstrated by means of preliminary batch experiments in an aerated stirred tank reactor [2]. For the experiments an adsorber resin functionalised with benzyl amine (BA) groups (Lewatit VP OC 1065, Bayer AG) was chosen as the immobilised activator material. These resin particles are spherical with a diameter of 0.5-1 mm and have a density of 1.092 kg/m³.

OP-I-4

The concentration of BA groups was determined by titration with 0.1 m HCl to 0.33 mol/l Lewatit.

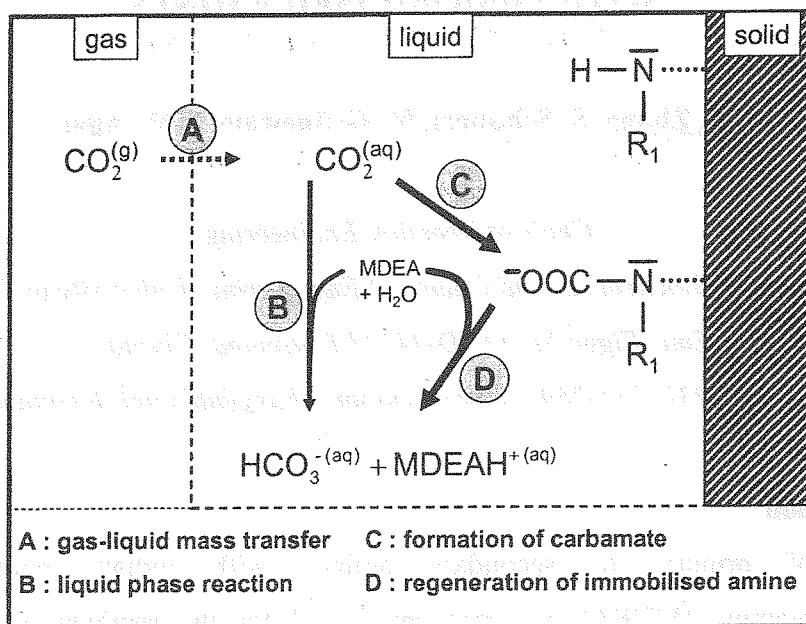


Figure 1. Schematic reaction mechanism for immobilised activators

As discussed in previous paper [2] immobilised activators similarly enhance the absorption of CO_2 into an aqueous MDEA solution as an equivalent quantity of liquid activators (diethanolamine). Further experiments related to the regeneration process have demonstrated that CO_2 loaded immobilised activator can be regenerated with MDEA (0.5 M) solution and afterwards shows the same absorption behaviour like fresh material.

Kinetic Measurements

To quantify the different mass transfer and reaction processes occurring in the three-phase system (see figure 1) and to locate possible rate-limiting steps additional experiments were carried out in a gas-liquid twin CSTR contactor and a liquid/solid fixed-bed column.

a) Gas-liquid twin CSTR

The experiments in a gas-liquid twin CSTR contactor were carried out to determine the reaction kinetic of dissolved CO_2 and amines immobilised on suspended resin. Furthermore it should be investigated whether the immobilised amines enhance the absorption of CO_2 into an aqueous MDEA solution for this kind of gas-liquid contactor or not. The used gas-liquid twin CSTR contactor (total volume 1.091 l, liquid volume 0.5 l) offers the advantage that no analysis of the liquid phase is required because the pressure decrease is the determining factor for the evaluation of the unknown parameters. In each experiment a certain amount of CO_2 was rapidly injected into the reactor and the pressure decrease caused by absorption and reaction was recorded. From this record, the reaction kinetic of the dissolved CO_2 and the

suspended immobilised amines was estimated by using a mathematical model based on the film theory, which was then implemented into Aspen Custom Modeler.

The absorption experiments with an aqueous MDEA solution and suspended immobilised amines showed that for this kind of gas-liquid contactor no enhancement of the absorption rate by the immobilised activators occurs. Based on the mathematical model it can be demonstrated, that the gas-liquid mass transfer is the rate-limiting step in this system. According to the film theory, it can be reasoned, that in contrast to their liquid counterparts the suspended immobilised activators don't enhance the reaction rate of CO₂ within the film and therefore don't favourably influence the absorption.

b) Liquid-solid fixed bed

In order to measure the kinetic parameter of the adsorption of CO₂ dissolved in water with the immobilised activator and the kinetic parameter of the regeneration of loaded immobilised activators with an aqueous MDEA solution a fix-bed reactor was set up. The diameter of the reactor was 20 mm and the height was 100 mm. It was packed with 34.5 ml Lewatit.

In the first preparatory step of the experiment for the determination of the adsorption parameter CO₂ was bubbled in distilled water in a tank in order to saturate the liquid. Then the water with dissolved CO₂ was fed to the fixed bed column at different flow rates. An electric conductivity detector was used to record the change of CO₂ concentration at the exit of the reactor. Due to the difficulty to calculate CO₂ concentration in liquid phase from the conductivity signal a new analytical method has been developed for the determination of CO₂ solved in water. Samples with 8 ml CO₂-water and 1ml NaOH (to freeze CO₂ in water) were taken at the exit of the reactor along the time. Then the probe was injected in the bottle of sulphuric acid. CO₂ injected by the probe was driven out and carried away by constant helium gas flow to TCD (thermal conductivity detector). This method was calibrated by NaCO₃ solution at different concentration.

For the determination of the regeneration parameters aqueous MDEA solutions with different concentrations were fed into the loaded fixed bed column. Samples were also taken at the exit and analysed as described above.

References

- [1] A.L. Kohl, R.B Nielsen, *Gas Purification*, Houston: Gulf Publishing Company, 1997.
- [2] S. Schubert, M. Grünwald, D. W. Agar, *Chem. Eng. Sci.* 2001, 56, 6211-6216.

**TURBULENT AND STRIPES WAVE PATTERNS
CAUSED BY LIMITED CO_{ADS} DIFFUSION
DURING CO OXIDATION OVER Pd(110) AND Pt(100):
STATISTICAL LATTICE MODELS**

V.I. Elokhin, E.I. Latkin, A.V. Matveev, V.V. Gorodetskii

Boreskov Institute of Catalysis SB RAS

Prosp. Akad. Lavrentieva, 5, 630090, Novosibirsk, Russia

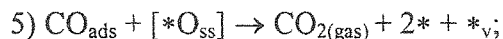
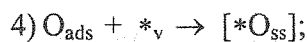
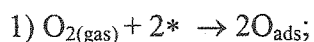
Fax: (+7-3832) 34 30 56, E-mail: elokhin@catalysis.nsk.su

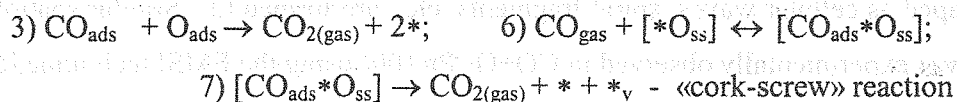
The complex dynamic behavior in oxidation reaction over platinum metals (bistability, oscillations, surface autowaves, etc.) can be directed by the structure of the reaction mechanism, specifically by the laws of physicochemical processes in the «reaction medium - catalyst» system. The most popular factors used to interpret the critical effects are the following [1]: i) phase transformations on the catalyst surface, including the formation and decomposition of surface and subsurface oxides during the reaction (e.g., Pd(110)), ii) structural phase transitions of the surface and its reconstruction due to the influence of the reaction media (e.g., Pt(100)).

In our opinion, the imitation (or statistical) simulation based on the Monte-Carlo technique is the most efficient tool for describing the spatio-temporal dynamics of the behaviour of adsorbates on the real catalytic surface, whose structure can change during the reaction. Recently the statistical lattice models for imitating the oscillatory and autowave dynamics in the adsorbed layer during CO oxidation over Pd(110) [2] and Pt(100) [3] single crystals, differing by the structural properties of catalytic surfaces, has been studied.

The aim of this contribution is to study the influence of surface diffusion intensity on the shapes of surface concentration waves obtained in simulations. Let us restrict our consideration by CO oxidation reaction over Pd(110) (similar results has been obtained by simulation of CO+O₂/Pt(100)).

Detailed mechanism of this reaction has been established by means of FEM, TPR and XPS studies [4]:





Let us briefly describe the algorithms used in simulations. The model catalyst surface was represented by the square lattice $N \times N$ ($N = 400 - 1600$) with periodic boundary conditions. States of the lattice cells are determined according to the rules prescribed by the detailed reaction mechanisms used in the cases under study. So-called Monte Carlo step (MCS) consisting from $N \times N$ elementary actions was used as a time unit. During the MCS each cell is tested on the average once. By elementary action it is meant a trial to change a state of the randomly chosen centre in such a manner, as it will with the substances taking part in the elementary processes (steps) constitute the detailed reaction mechanism. The probability of the particular process w_i is determined by a ratio between the rate coefficients, therewith the rate coefficients for the adsorption processes are multiplied by the relevant partial pressures. The values of the rate coefficients of the elementary processes used in simulations could be found in [2,3]. During the MCS after each of $N \times N$ trial to carry out one of the elementary action the inner cycle of CO_{ads} diffusion has been arranged (usually $M = 50-100$ attempts of diffusion). The diffusion is necessary for the spatio-temporal processes synchronization occurring on the different regions of the model surface. The reaction rate and surface coverages were calculated after each MCS as a number of CO_2 molecules formed (or the number of cells in the corresponding state) divided by the total number of the lattice cells N^2 .

In both cases [2,3] the synchronous oscillations of the reaction rate and surface coverages are exhibited within the range of the suggested model parameters under the conditions very close to the experimental observations – e.g., Fig 1 [2]. These oscillations are accompanied by the autowave behaviour of surface phases and adsorbate coverages, Fig. 2 [2]. The intensity of CO_2 formation in the CO_{ads} layer is low, inside oxygen island it is intermediate and the highest intensity of CO_2 formation is related to a narrow zone between the moving O_{ads} island and surrounding CO_{ads} layer («reaction zone», characterised by the elevated concentration of the free active centres). The presence of the narrow reaction zone was found experimentally by means of the field ion probe-hole microscopy technique with 5 \AA resolution [5]. The important role of the diffusion rate and of the lattice size on the synchronisation and stabilisation of surface oscillations has been demonstrated. Particularly, in the case of Pt(100), the decrease of the diffusion intensity (parameter M) from 100 to 30 leads to the irregular oscillations and to the turbulent patterns on the model surface – in this case the mobile islands

of O_{ads} shaped as cellular waves, spiral fragments, etc., are formed [3]. Similar spatiotemporal behavior was experimentally observed in $CO+O_2/Pt(100)$ using the EMSI technique [6].

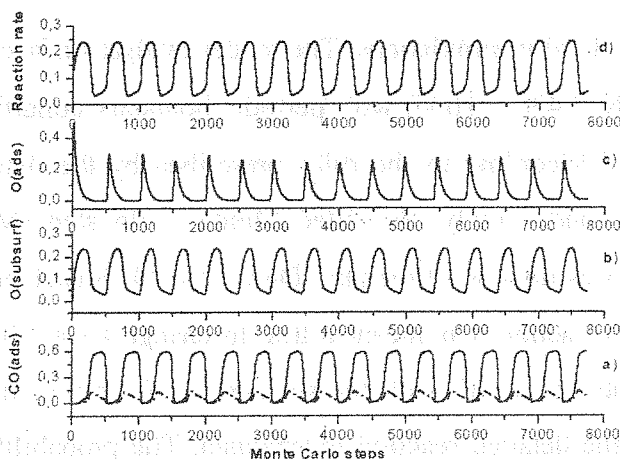


Fig. 1. Dynamics of changes in the surface coverages CO_{ads} (solid line) $[CO_{ads} * O_{ss}]$ (dash-dotted line) (a), $[*O_{ss}]$ (b), O_{ads} (c), R (d) - for CO oxidation over $Pd(110)$. $N = 768$, $M = 50$. The values of the rate constants of steps (s^{-1}) (see scheme): $k_1=1$, $k_2=1$, $k_2=0.2$, $k_3=inf$, $k_4=0.03$, $k_5=0.01$, $k_6=1$, $k_6=0.5$, $k_7=0.02$. The partial pressures of reagents (CO and O_2) are included in the rate constants of adsorption (k_1 , k_2 , k_6).

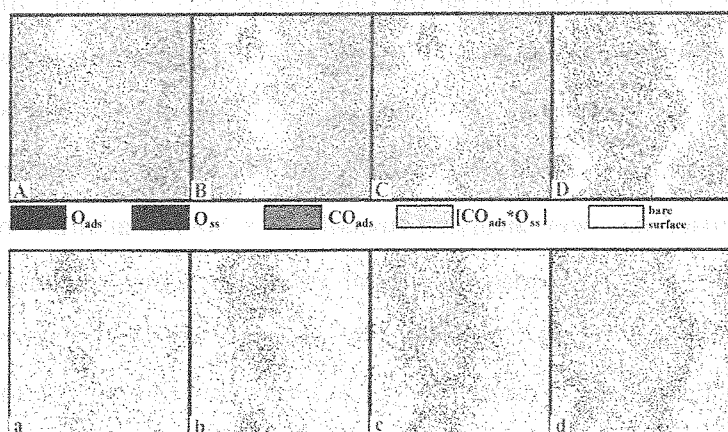


Fig. 2. The distribution of different adsorbates (see designations) over the surface (A-D) and the intensity of CO_2 formation (a-d) at the moment when the coverages change on the $Pd(110)$ surface. The grey scale reflects the reaction rate intensity (a-d). The lattice size $N = 768$, diffusion intensity parameter $M = 50$.

Let us study the influence of diffusion intensity M on the shape of the surface waves in the case shown in the Fig. 2. Increase of M up to value $M = 100$ doesn't change the oscillatory and wave dynamics, but decreasing M to value $M = 20$ drastically changes both the shape of oscillations and the spatiotemporal behavior of simulated surface waves. Period and amplitude of oscillations decrease considerably, the dynamic behavior of reaction rate and surface coverages demonstrate the intermittence. During these oscillations oxygen is always present on the surface in the form of turbulent spatiotemporal structures (Fig. 3a). Step-by-step decrease of oxygen partial pressure (remember, that the values for O_2 and CO adsorption coefficients, k_1 , k_2 , and k_6 , can be treated as product of the impingement rate ($k_i \times P_i$) and of the sticking coefficient (S_i)) leads to the gradual thinning of oxygen travelling waves (Fig. 3b-e). At low values of k_1 (Fig. 3d-f) the long and thin oxygen stripe (or worm-like) patterns are formed on the simulated surface, and the clear tendency of turbulent patterns to combine into spirals disappeared at $k_1 < 0.8$. The amplitude of oscillations diminished with decreasing of

k_1 . At last, at $k_1 = 0.71$, the oxygen stripe wave vanishes slowly from the surface and the system transform to the low reactive state.

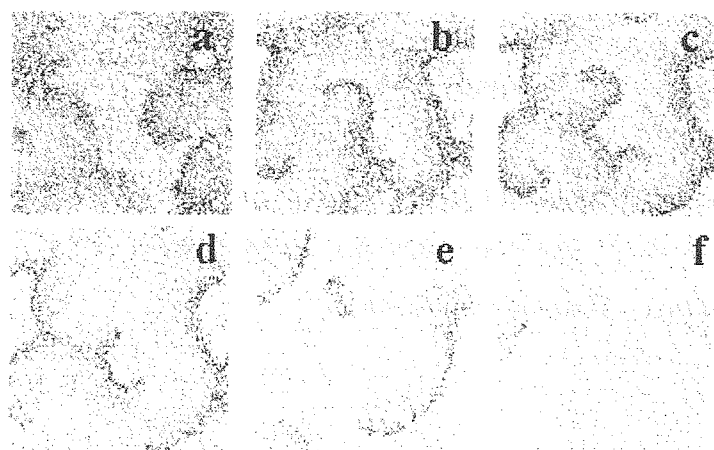


Fig. 3. Typical snapshots of the adsorbate distribution over the surface ($N = 1000$) at step-by-step reducing of k_1 in the case of restricted diffusion intensity of CO_{ads} ($M=20$). The designations of adsorbate are the same as for Fig. 2(A-D). The values of partial pressure of oxygen (i.e., k_1) are the following: 1 (a), 0.9 (b), 0.85 (c), 0.8 (d), 0.73 (e), 0.71 (f).

The reverse increasing of k_1 leads to hysteresis in oscillatory behaviour. The oscillation appears only at $k_1 = 0.85$ via very fast “surface explosion” (Fig. 4a-h).

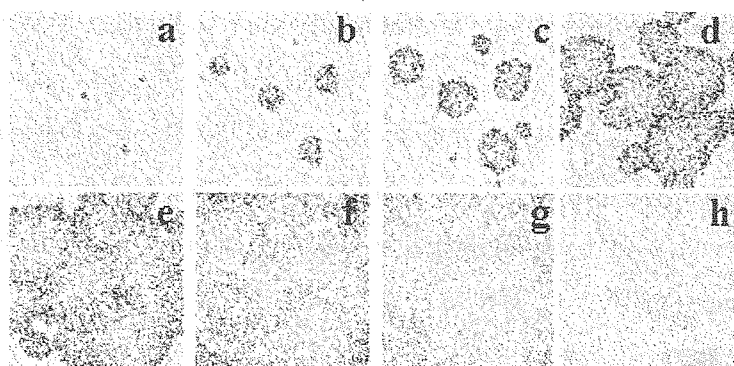


Fig. 4. The snapshots illustrating the rise of oscillations at inverse step-by-step increasing of k_1 . The designations of adsorbate are the same as for Fig. 2(A-D). The difference between the frames is 5 MC steps.

Thus, the possibility for the appearance of the target and turbulent patterns, spiral and stripe waves on the surface in the cases under study has been shown. The results obtained make possible to interpret the surface processes on the atomic scale.

Acknowledgement. This work was supported by Russian Fund for Basic Research (RFBR Grants # 02-03-32568 and # 03-03-89013) and partly by NWO Grant # 047.015.002.

References

- [1] G. Ertl. *Surface Sci.*, 1994, **299/300**, 742-754, and references therein.
- [2] E.I. Latkin, V.I. Elokhin, A.V. Matveev, V.V. Gorodetskii. *J. Molec. Catal. A, Chem.*, 2000, **158**, 161-166.
- [3] E.I. Latkin, V.I. Elokhin, V.V. Gorodetskii. *J. Molec. Catal. A, Chem.*, 2001, **166**, 23-30.
- [4] V.V. Gorodetskii, A.V. Matveev, A.V. Kalinkin, B.E. Niewenhuys. *Chem. for Sustain. Dev.*, 2003, **11**, 67-74.
- [5] V.V. Gorodetskii, W. Drachsel. *Appl. Catal. A: General*, 1999, **188**, 267-275.
- [6] J. Lauterbach, G. Bonilla, T.D. Fletcher. *Chem. Eng. Sci.*, 1999, **54**, 4501-4512.

KINETIC MODELING OF *meta*-XYLENE ISOMERIZATION OVER USY ZEOLITE IN A RISER SIMULATOR

Abduljelil Ilyas and Sulaiman Al-Khattaf*

Department of Chemical Engineering, King Fahd University of Petroleum & Minerals,

Dhahran 31261, Saudi Arabia. Tel.: +966-3-8601429; fax: +966-3- 8604234

*E-mail address: skhattaf@kfupm.edu.sa

Introduction

The kinetic study of catalytic isomerization of xylenes has been investigated by several workers [1-4]. However, in many of these studies, fixed bed reactors are often utilized for the reaction. Many difficulties are encountered in using the fixed bed reactor for this reaction owing to its complex nature. Temperature and/or concentration gradients usually occur within the flowing phase of the catalyst bed coupled with irregular coking of the catalyst, which often affect the values of kinetic parameters reported from such studies. Differential reactors and pulsed micro reactors have been applied to reduce the gradient difficulties, but analytical problems due to low conversion levels have been identified and as such minimization of the bulk phase gradient may not be assured [1].

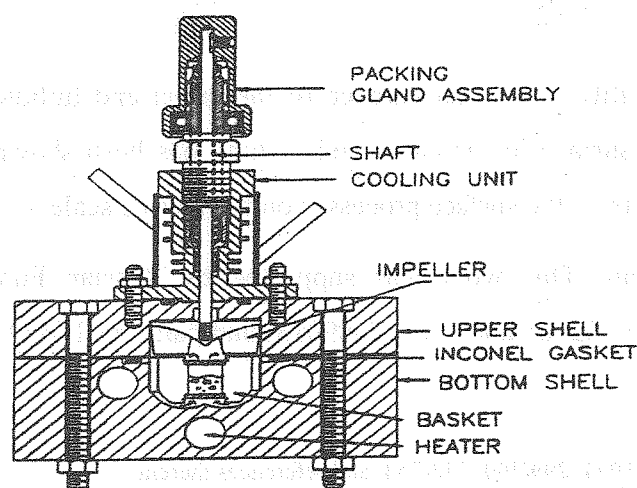


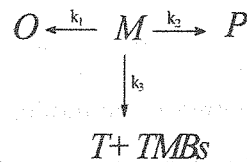
Fig. 1. Schematic diagram of the Riser Simulator

In this work, the Riser Simulator (Fig. 1): a novel bench scale equipment which is operated as a batch, well mixed fluidized bed reactor was employed as a tool in investigating xylene isomerization over USY zeolite catalyst under different reaction times and

temperatures. This reactor was invented by de Lasa [5] to overcome the technical problems of the standard micro-activity test (MAT), and to our knowledge the xylene isomerization reaction has not been reported in the open literature to have been carried out in such a reactor. USY zeolite was chosen for the study since only a few kinetic studies reporting the kinetic parameters for the various reaction paths during xylenes isomerization reaction over USY zeolite is available [2].

Model Development

According to the distribution of products observed in the present study, we proposed a sequence reaction scheme, in which an irreversible reaction path is assumed for both the isomerization and disproportionation reaction. This is due to the low experimental conversions (<15%) obtained, with the implication that the rate of reverse reactions are negligible in comparison with forward reactions. In addition, we also suggested that the disproportionation products: toluene and trimethylbenzenes are mainly from the meta-xylene feed considering that the yield of both para and ortho-xylenes has a maximum value of 4wt %. These assumptions are reasonable given that the ratio of M/P and M/O is always very high (90/4). A further assumption is that the reactor operates under an isothermal condition [5]. Therefore, the proposed reaction scheme is as follows:



Where M = m-xylene, O = o-xylene, P = p-xylene, $T + TMBs$ = disproportionation products

In order to estimate the kinetics parameters, the differential equations describing the reaction for a first order isomerization [3,4] and disproportionation [3] reactions were derived as follows:

$$-\frac{V}{W_c} \frac{dy_m}{dt} = \left[k_{01} \exp\left(\frac{-E_1}{R} \left[\frac{1}{T} - \frac{1}{T_0}\right]\right) + k_{02} \exp\left(\frac{-E_2}{R} \left[\frac{1}{T} - \frac{1}{T_0}\right]\right) + k_{03} \exp\left(\frac{-E_3}{R} \left[\frac{1}{T} - \frac{1}{T_0}\right]\right) \right] \exp(-\alpha t^{0.5}) y_m \quad (1)$$

$$\frac{V}{W_c} \frac{dy_p}{dt} = k_{02} \exp\left(\frac{-E_2}{R} \left[\frac{1}{T} - \frac{1}{T_0}\right]\right) \exp(-\alpha t^{0.5}) y_m \quad (2)$$

$$\frac{V}{W_c} \frac{dy_o}{dt} = k_{01} \exp\left(\frac{-E_1}{R} \left[\frac{1}{T} - \frac{1}{T_0}\right]\right) \exp(-\alpha t^{0.5}) y_m \quad (3)$$

$$\frac{V}{W_c} \frac{dy_d}{dt} = k_{03} \exp\left(\frac{-E_3}{R} \left[\frac{1}{T} - \frac{1}{T_0}\right]\right) \exp(-\alpha t^{0.5}) y_m \quad (4)$$

OP-I-6

In the above equations, the mass fraction of any species i , is related to its concentration as follows: $C_i = \frac{y_i W_{hc}}{MW_i V}$, where W_{hc} is the mass of the reactant feed (0.16×10^{-3} kg), V is the volume of the reactor (50×10^{-6} m³), MW_i is the molecular weight of species i (Kg/Kmole), t is the reaction time (sec), W_c is weight of catalyst (Kgcatal), k_{oi} is the pre-exponential factors in m³/(kg cat.sec), E_i apparent activation energies (KJ/mole). $\varphi = \exp(-\alpha t^{0.5})$ represents catalyst deactivation function with a constant, α used by previous researchers [6], T_o is the average reaction temperature introduced for re-parameterization of kinetic constants [7].

A computer program in a MATLAB package was developed using the classical fourth order Runge-Kutta method of fixed interval size in order to determine the model parameters in eqs (1)-(4). The values of the kinetic constants and activation energies obtained with their corresponding 95% confidence limits (nonlinear hypothesis), are presented in Table 1. These values were found to compare favorably with those reported by Gendy [2] over a similar catalyst.

TABLE 1. Estimated kinetics parameters

	$k_{01} \times 10^3$	E_1	$k_{02} \times 10^3$	E_2	$k_{03} \times 10^3$	E_3	α	r^2
	0.48	10.4	0.45	10.9	0.03	13.1	0.48	0.99
95% CFL	0.19	2.4	0.18	2.7	0.01	3.4	0.18	

Fig. 2-5 shows the comparison between the model predictions and the experimental data at various temperatures. As observed in these plots the model predictions compare favourably with the obtained experimental data for the various conditions, indicating that the model can be used to accurately represent the experimental data following the assumptions made.

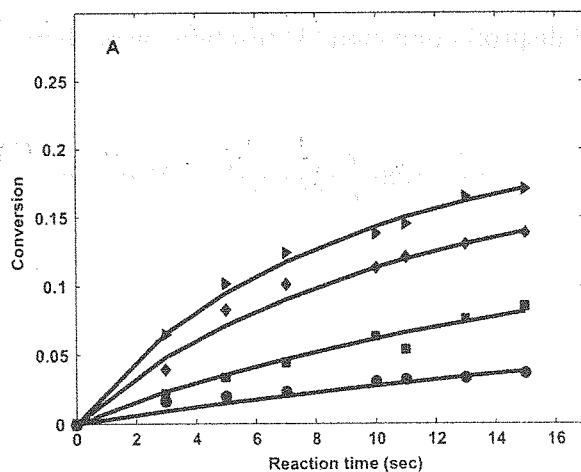


Fig. 2. Comparison between experimental results and model prediction for conversion
 (●) 350°C (■) 400°C (◆) 450°C (▶) 475°C

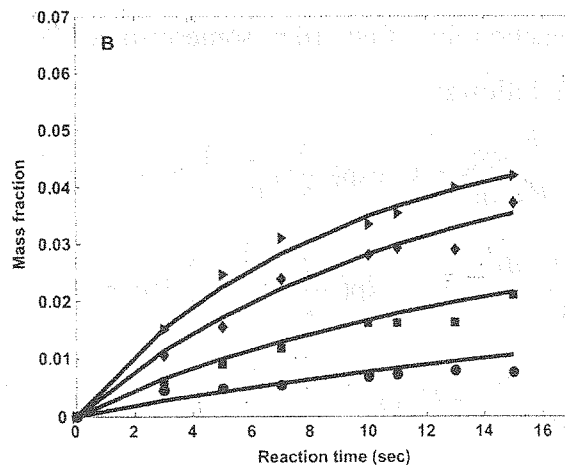


Fig. 3. Comparison between experimental results and model prediction for p-xylene
 (●) 350°C (■) 400°C (◆) 450°C (▶) 475°C

Conclusion

1. The gas phase meta-xylene isomerization and disproportionation reactions are initiated over USY zeolite catalyst using the Riser Simulator under different reaction conditions.
2. The apparent activation energies for the isomerization of m-xylene to o-xylene and m-xylene to p-xylene are closely identical with an average value of 10.7 Kcal/mol. This can be explained due to the similarity of both reactions, as both involve the 1, 2 methyl shift of adjacent methyl group along the benzene ring [3].
3. While, the apparent activation energy for disproportionation is higher (13.1 Kcal/mol) than that of isomerization. This is in agreement with the well established fact that the energy required to move out a methyl group during disproportionation reaction should be higher than the intramolecular methyl transfer during isomerization by magnitudes of 3 to 4 kcal/mol [8].
4. The quantitative agreement of the obtained kinetic parameters with those earlier reported in the literature, and the close comparison between the model predictions and the obtained experimental data indicate that the Riser Simulator and associated modeling techniques can be used as an effective tool in the investigation of the kinetics of meta-xylene isomerization.

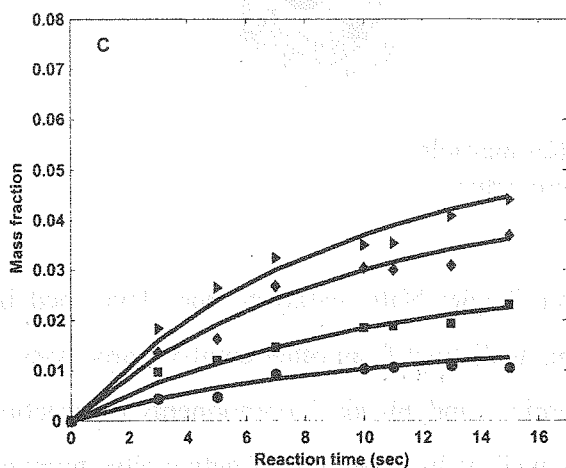


Fig. 4. Comparison between experimental results and model prediction for o-xylene
 (●) 350°C (■) 400°C (◆) 450°C (▶) 475°C

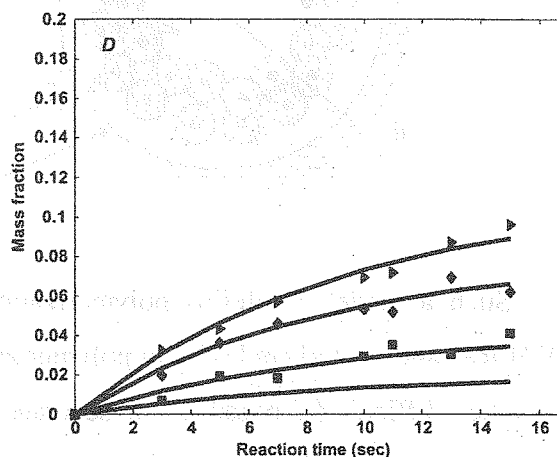


Fig. 5. Comparison between experimental results and model prediction for T + TMBs
 (●) 350°C (■) 400°C (◆) 450°C (▶) 475°C

References

- [1] Y.H. Ma, Savage L.A., *AIChE J.* 33 (1987) 1233.
- [2] T.S. Gendy, K.C. Pratt, *Chem. Eng. Sci.* 37 (1982) 37.
- [3] K.L. Hanson, A.J. Engel, *AIChE J.*, 13 (1967) 260.
- [4] A. Cortés, A. Corma, *J. Catal.*, 51(1978), 338.
- [5] H.I. de Lasa, U.S. Patent 5, 102 (1992) 628.
- [6] A., Corma, F. Llopis, J.B. Monton, *J. Catal.*, 140 (1993) 384.
- [7] A.K. Agarwal, M.L. Brisk, *Ind. Eng. Chem. Proc. Des. Dev.*, 24 (1985) 203.
- [8] A. Corma, E. Sastre, *J. Catal.*, 129 (1991) 177.

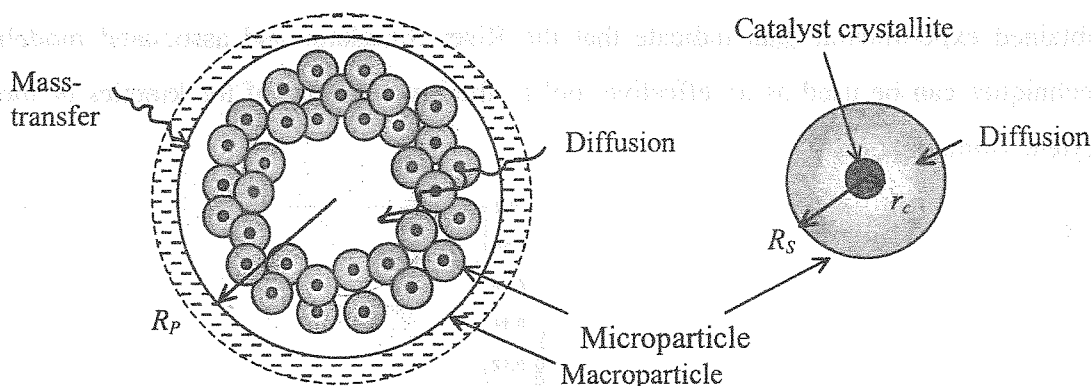
ABOUT MECHANISM AND MODEL OF DEACTIVATION OF ZIEGLER-NATTA POLYMERIZATION CATALYSTS

N.M. Ostrovskii, F. Kenig

AD Hemijska Industrija – HIPOL, Odžaci, Yugoslavia

Fax: 381 25 / 743-191, E-mail: ostrovski@hipol.com

Polymerization processes are unsteady-state by their nature, because of the reaction rate changes with time. The catalyst has to be part of product, since the polymer “grows” on the catalyst surface. Figuratively, growing polymer particle can be imaged as a pomegranate fruit, where the fruit (macroparticle) include grains (microparticles), with seeds (catalyst crystallites):



Such a model of olefins polymerization on Ziegler-Natta catalysts was developed by W.H.Ray and coworkers [1-3]. In polymerization, as distinct from other catalytic processes, it is rather difficult (if possible) to separate chemical and physical components of reaction dynamics. It determines by particle growing, as well as by changing of active sites number. The latter happens due to the formation of active sites under the influence of cocatalyst, and their transformation during the reaction. These processes proceed with approximately the same rates, and therefore also cannot be separated.

That is why there are not many investigations in literature on deactivation of polymerization catalysts [4]. In most cases, the matter concerns “resultant dynamics” of process within the limits of residence time in reactor. Such an approach is justified because of “one-use” operation of catalyst in polymerization processes.

Nevertheless, from the catalyst development and process technology points of view, it is very important to understand the reasons of dynamic behavior, their mechanisms and comparative effect. Most authors agree in opinion, that the main reason for the observed decrease of catalyst activity, is its poisoning by ethylaluminum dichloride (AlEt_2Cl_2), which is the product of catalyst (TiCl_3 , TiCl_4) interaction with cocatalyst (AlEt_2Cl , AlEt_3).



As a result, the gradual elimination of chlorine from the catalyst takes place. Ambrož et al. [5] have drawn attention to this phenomenon as far back as 60-th. Authors of [6] come to a similar conclusion on the base of recent investigations using modern technique of "surface science". It was established in [5], that chlorine loss reach 50% of total chlorine in TiCl_3 , and therefore could not be removed from the surface layers of the catalyst crystal only, but have to "touch" the bulk. Thus, the matters can concerns mobility of chlorine in the lattice of TiCl_3 or TiCl_4 , similarly to oxygen mobility in oxides or carbon in carbides. These processes in solid phase are quite slow, (formally are similar to diffusion), and can determine the distinctive process dynamics.

In this work, we try to estimate parameters of such "diffusion" and their effect on reaction rate dynamics in propylene polymerization.

Simple evaluation

Rate of polymerization usually expressed as [1-5]:

$$R_p = k_p C_Z C_m \quad (2)$$

Since in reaction (1) AlEtCl_2 is a product of cocatalyst action and is in adsorption equilibrium [4], the rate of deactivation will be proportional to concentration of AlEt_2Cl . The compensation of dechlorinated centers one can consider as a diffusion flux in the catalyst crystallite from bulk to surface:

$$\frac{dC_Z}{dt} = -k_d^1 C_Z C_A + D_C S \left. \frac{dC_V}{dr} \right|_{r=r_c} \quad (3)$$

Since C_A const, then $k_d = k_d^1 C_A$. The specific surface of crystallite S , depending of their form, can be written as $S = (1.5 \div 3)/r_c$. The diffusion flux can be approximately expressed as:

$$D_C S \left. \frac{dC_V}{dr} \right|_{r=r_c} \approx \beta (\bar{C}_V - C_Z), \quad \beta \approx (1.5 \div 3)^2 D_C / r_c^2 \quad (4)$$

After substituting these formulas in (3) and its integration, we are able to describe the experimental data of [5], fig. 1-a.

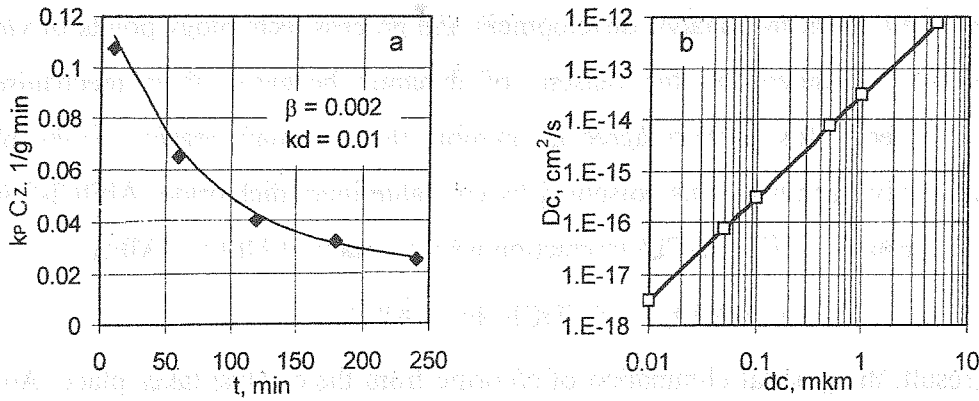


Fig. 1. Variation of polymerization rate ($k_p C_Z$) with time.

(a): Points – experiments of [5]; lines – model prediction, eq. (3).

(b): Correlation of D_c and d_c at $k_d = 0.01$.

Since β is proportional to D_c / d_c^2 , where $d_c = 2 r_c$, then a lot of combination of D_c and d_c are probable, presented in fig. 1-b. The d_c of industrial catalysts is usually within the values $0.01 \div 0.1 \mu\text{m}$ (after shattering with the onset of polymerization).

Then diffusivity $D_c = 10^{-17} \div 10^{-15} \text{ cm}^2/\text{s}$, that is typical for diffusion in solids [7].

Bulk diffusion

In presented experiments the reaction rate does not measured during initial 10 min, thus the initial period of rate increasing is not detected and is leaved out of account in eq. (3). For complete simulation of dynamics it is necessary to write the equation for potential centers in crystallite bulk (equation of chlorine mobility):

$$\frac{\partial C_V}{\partial t} = D_C \frac{\partial^2 C_V}{\partial r^2}, \quad r = 0: \frac{dC_V}{dr} = 0, \quad r = r_c: D_C S \frac{dC_V}{dr} = -k_A^1 C_S C_A \quad (5)$$

$$\frac{dC_Z}{dt} = k_A^1 C_S C_A - k_d^1 C_Z C_A, \quad C_S = C_V(r = r_c) \quad (6)$$

The solution of (5) at $r = r_c$ have to be in form:

$$C_S(t) = C_V(r_c, t) = \sum_{n=1}^{\infty} A_n \exp\left(-\frac{\mu_n^2 D_C}{r_c^2} t\right) \quad (7)$$

μ_n are roots of characteristic equation $\text{ctg } \mu_n = \mu_n D_C / k_A r_c^2$,

$$A_n = 2 \sin \mu_n \cos \mu_n / (\mu_n + \sin \mu_n \cos \mu_n).$$

Substituting (7) in (6) and integrating we obtain:

$$C_Z(t) = k_A \sum_{n=1}^{\infty} \frac{A_n}{k_d - \beta_n} \left(\exp(-\beta_n t) - \exp(-k_d t) \right), \quad \beta_n = \frac{\mu_n^2 D_C}{r_c^2} \quad (8)$$

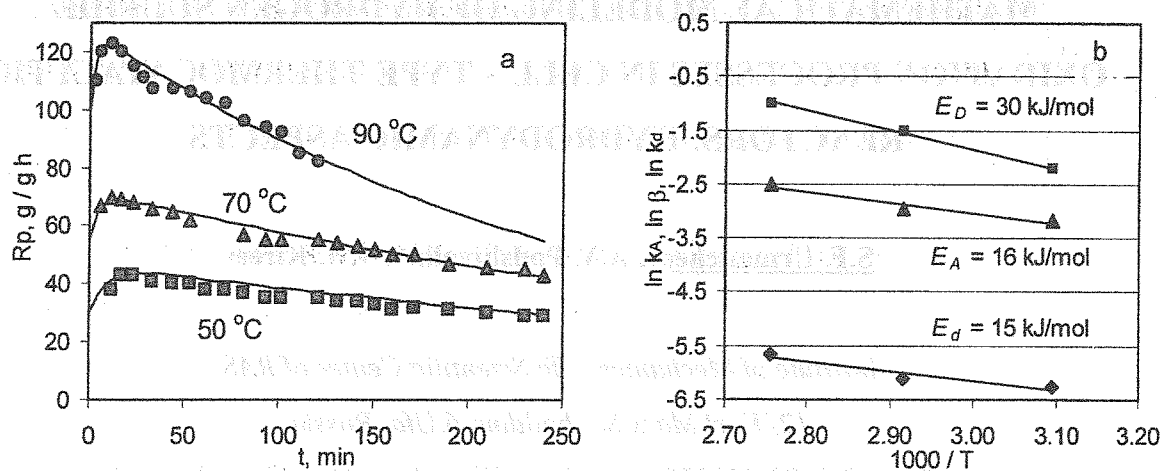


Fig. 2. Dynamics of propylene polymerization rate on catalyst $\text{TiCl}_3 + \text{AlEt}_2\text{Cl}$.

(a): Points – experimental of [8]; lines – model prediction, eqs. (2,8).

(b): Calculations of E_D , E_A , and E_d .

System (2,8) provides the qualitative and quantitative simulation of typical dynamics of polymerization rate (fig. 2). The following estimations were obtained:

$$D_C = (2 \div 7) 10^{-17} \text{ cm}^2/\text{s}, k_A = 0.04 \div 0.08 \text{ 1/min}, k_d = (1.9 \div 3.5) 10^{-3} \text{ 1/min.}$$

Activation energies (fig. 2-b): Of reaction – $E_P \approx 29$ kJ/mol; diffusion – $E_D \approx 30$ kJ/mol;

catalyst activation ($k_A' C_S C_A$) – $E_A \approx 16$ kJ/mol;

catalyst deactivation ($k_d' C_Z C_A$) – $E_d \approx 15$ kJ/mol.

Nomenclature

R_p , k_p – polymerization rate and its constant; C_Z , C_V – concentration of potential active centers on surface and in catalyst bulk; C_m , C_A – concentrations of monomer and alkylaluminum chloride; D_c – diffusivity of chlorine in catalyst; r_c , d_c – radius and diameter of catalyst crystallite; k_A , k_d – constants of catalyst activation and deactivation.

References

1. Nagel E.J., Kirillov V.A., Ray W.H. – Ind. Eng. Chem. Prod. Des. Dev., 1980, **19**, 372-379.
2. Debbling J.A., Ray W.H. – Ind. Eng. Chem. Res., 1995, **34**, 3466-3480.
3. Skomorokhov V.B., Zakharov V.A., Kirillov V.A. – Macromol. Chem. Phys., 1996, **197**, 1615-1631.
4. Yoon J.-S., Ray W.H. – Ind. Eng. Chem. Res., 1987, **26**, 415-422.
5. Ambrož J., Osecký P., Mejzlik J., Hamřik O. – J. Polymer. Sci. Part C, 1967, No 16, 423-430.
6. Magni E., Malizia F., Somorjai G.A. – Polypropylene – past, present and future: The challenge continues, Montell Italia S.p.A., October 1998, p. 175-203.
7. Ovsicer O.Yu., Sokolovskii V.D. – Catal. Lett., 1991, **8**, 379-384; 1993, **17**, 239-244.
8. Choi K.Y., Ray W.H. – J. Appl. Polymer Sci., 1985, **30**, 1065-1081.

**MATHEMATICAL MODELING OF HYDROGEN SULFIDE
OXIDATION PROCESSES IN CELL – TYPE THERMOCATALYTIC
REACTORS: HYDRODYNAMIC ASPECTS**

S.F. Urmancheev, A.V. Podshivalin*, V.N. Kireev

Institute of Mechanics, Ufa Scientific Center of RAS,

12, Karl Marx St., building 6, Ufa, Russia,

fax: +7-3472-230878; e-mail: said@anrb.ru, kireev@anrb.ru

**Institute of Petroleum Refining and Petrochemistry,*

12, Inicativnaya St., Ufa, Russia,

fax: +7-3472-422471; e-mail: podshivalin@anrb.ru

1. Introduction

It is very important for the environment protection to improve refining of the tail gases. The hydrogen sulfide is a widely – spread pollutant. Nowadays, the industrial oxidation of concentrated hydrogen sulfide is carried out according to Claus-method. The efficiency of a two-stage Claus-process is about 90-92%. Therefore, the hydrogen sulfide left in tail gases requires further utilization. This problem can be solved by means of a honeycomb monolithic catalyst.

In this paper the mathematical model of catalyst oxidation of hydrogen sulfide is presented. Honeycomb catalyst behaves according to an ideal displacement scheme. Modeling of hydrogen sulfide conversion with a detailed consideration of wall mass-transfer and flow structure has been made. A corresponding computer code was applied to obtain numerical results with their further comparison with the experimental data of laboratory investigations.

2. Based equations

Since the block catalyst consists of channels located regularly and separated by baffles of solid catalyst material and their number over the block cross section is very large for the procedure of space averaging, a multiphase media approach is considered for modeling purposes (Nigmatulin, [1]).

In this context the flow of reacting multicomponent gas in porous medium of channel structure is considered. The equations derived on the base of conservation laws of mass,

molar, momentum and energy are given taking into account the kinetics of chemical oxidation.

Mass balance equation of gas mixture:

$$\frac{\partial \rho_1^0}{\partial t} + \frac{\partial \rho_1^0 v_1}{\partial x} = 0. \quad 1)$$

Mass balance equation of reacting component (e. g. hydrogen sulfide):

$$\frac{\partial \alpha_1 \rho_1^0}{\partial t} + \frac{\partial \alpha_1 \rho_1^0 v_1}{\partial x} = -J. \quad 2)$$

Momentum of gas mixture:

$$\frac{\partial \rho_1^0 v_1}{\partial t} + \frac{\partial \rho_1^0 v_1^2}{\partial x} = -\frac{\partial P}{\partial x} - F. \quad 3)$$

Energy balance for gas:

$$\frac{\partial \rho_1^0 T_1}{\partial t} + \frac{\partial \rho_1^0 v_1 T_1}{\partial x} = -\frac{P}{C_{v1}} \frac{\partial v_1}{\partial x} + \frac{1}{C_{v1}} F v_1 - \frac{1}{\alpha_1 C_{v1}} Q. \quad 4)$$

Energy balance for solid phase (catalyst):

$$\frac{\partial \rho_2^0 T_2}{\partial t} = \frac{Q}{\alpha_2 C_2} + \frac{\lambda_2}{\alpha_2 C_2} \frac{\partial^2 T_2}{\partial x^2} + \frac{JQ}{\alpha_2 C_2}. \quad 5)$$

The system of equations (1) – (5) must be closed. Assuming the ideal gas equation as the closing relation, we get to:

$$P = \rho_1^0 R_g T_1.$$

The friction force in porous medium of channel structure can be expressed as:

$$F = 8a_f^{-2} \mu \alpha_2 v_1.$$

The expression for the heat transfer rate is assumed to be:

$$Q = S \lambda_1 Nu (T_2 - T_1) / a_q.$$

Nusselt number will be determined according to the empirical expression of Chudnovsky [1] describing heat exchange at Reynolds numbers typical for the process under consideration.

The partial pressures of gas components may be written as

$$P_i = c_i P, \quad (i=1, \dots, n)$$

where $P_1 = P_{H_2S}$, $P_2 = P_{O_2}$, etc., $n =$ quantity of gas components and $P = \sum_{i=1}^n P_i$.

The problem mathematical definition may lead to an equation of convective diffusion for concentration $c(t, x, y)$ of some reagent at gas laminar flow in the channel with rigid walls.

As a result of the solving of equation of convective diffusion we have estimation for concentration near walls:

$$c_s(x, a/2) = c_0 - \frac{Aa}{2\beta^{1/3}} \int_0^x \frac{J_s(c_s)}{(x-\chi)} d\chi,$$

where $A = \Gamma(4/3)\Gamma^{-1}(2/3)\Gamma^{-1}(1/3)6^{1/3}$ - combination of gamma-functions, $\beta = a^2V/2D$.

With this estimation we improved based 1-D equations and defined adequate values of conversion of hydrogen sulfide.

3. Kinetic model of hydrogen sulfide catalytic oxidation

Based on the work of Alkhazov and Amirgulyan [2], let us consider the reaction mechanism for catalytic oxidation of hydrogen sulfide, the reaction is assumed to occur through the interaction between H_2S molecule adsorbed on center Z_1 and oxygen molecule adsorbed dissociatively on center Z_2 .

The overall reaction rate can be represented as follows:

$$W = K \frac{P_{H_2S}}{1 + b_1 P_{H_2S} + b_2 P_{H_2O}} \frac{P_{O_2}^{0.5}}{1 + b_3 P_{O_2}^{0.5}},$$

where the various kinetic coefficients were calculated from experimental data and are equal to:

$$K = 4.19 \cdot 10^2 \cdot \exp(-21.4/RT) \text{ mol} \cdot \text{KPa}^{-1.5} / (\text{m}^3 \cdot \text{s}),$$

$$b_1 = 0.149 \cdot \exp(5.24/RT) \text{ KPa}^{-1},$$

$$b_2 = 1.67 \cdot 10^{-8} \cdot \exp(3.56/RT) \text{ KPa}^{-1},$$

$$b_3 = 8.35 \cdot 10^{-3} \cdot \exp(22.9/RT) \text{ KPa}^{-0.5}.$$

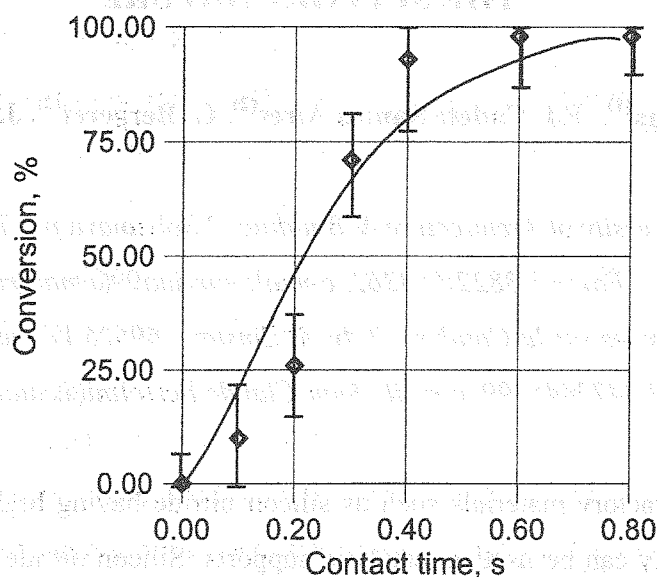
Based on elementary geometric considerations, a formula for recalculation was derived:

$$J = SW/S_0.$$

4. Comparison with experimental data

As a result of the experiments, contact time and reaction temperatures have been determined, which provide for practically complete conversion of hydrogen sulfide into elemental sulfur (with a measurable limit of 98%). Sulfur itself did not react. Therefore, the process was selective. The found optimum contact time ranges from 0.6 s to 0.8 s, the corresponding temperature values varying from 490 K to 510 K. The contact time in the experiments was regulated by a given initial velocity of the flow. Picture compares calculated

and experimental data for dependence of hydrogen sulfide conversion (relative to the initial concentration) on the contact time.



Comparison of calculated and experimental results for hydrogen sulfide conversion versus gas-catalyst contact time

Based on the comparison of the results, one can arrive at a conclusion that the developed mathematical model describes adequately the process of hydrogen sulfide catalytic oxidation to elemental sulfur using block catalyst. Thus, based on the presented model one can make design and optimization calculations for above types of commercial reactors. One should take into account the effect of flow acceleration in the channels, which may cause turbulence and loss of advantages of block catalysts. This fact suggests the necessity of limiting the length of catalyst blocks at a given channel cross section and using the clearances between rows of blocks located one after another.

References

1. R. I. Nigmatulin, *Dynamics of Multiphase Media*, vol. 1, Hemisphere, Washington, 1990
2. T. G. Alkhazov and N. S. Amirgulyan, *Catalytic Oxidation of Sulfide over Iron Oxides*, *Kinetika i kataliz*, vol. 23, pp. 1130–1134, 1982 (in Russian).

TOTAL OXIDATION OF METHANE OVER Pd CATALYSTS SUPPORTED ON SILICON NITRIDE. INFLUENCE OF THE SUPPORT NATURE

I.A. Kurzina⁽¹⁾, F.J. Cadete Santos Aires⁽²⁾, G. Bergeret⁽²⁾, J.C. Bertolini⁽²⁾

⁽¹⁾ Tomsk State University of Architecture & Building, 2 Solyanaya pl., Tomsk 634003, Russia.

Fax: +7(3822)653362, e-mail: kurzina99@mail.ru

⁽²⁾ Institut de Recherches sur la Catalyse, 2 Av. A. Einstein, 69626 Villeurbanne Cedex, France.

Fax: +33 472445399, e-mail: Jean-Claude.Bertolini@catalyse.cnrs.fr

Non-oxide refractory materials such as silicon nitride having high thermal stability and thermal conductivity can be used as catalytic supports. Silicon nitride with different specific area and crystallinity: amorphous silicon nitride, amorphous silicon nitride annealed at 1450°C and α -Si₃N₄ were chosen as the supports for Pd catalysts. A strong influence of the phase composition and the crystalline state of supports on the catalytic properties in the total oxidation of methane of the Pd catalysts was found. The activity of Pd catalysts increases with the α -Si₃N₄ content of the support.

Highly dispersed main group metals oxides such as Al₂O₃, SiO₂ and silica-alumina are generally used as catalyst supports. However, the structural stability of such catalysts for the highly exothermic reactions working at high temperature is not sufficient. In order to improve the stability of catalysts, other materials having high thermal stability and high thermal conductivity should be employed as supports. Among the non-oxide ceramics, silicon nitride is a promising candidate for high temperature applications [1] owing to its advantageous properties, like rather high thermal conductivity, high hardness and strength, excellent creep, oxidation and corrosion resistance, as well as its low density. Amorphous silicon nitride powder with much higher specific area (66 m²/g) than crystalline α or β Si₃N₄ offers a priori considerable advantages and can be used as a support for Pd catalysts. Moreover, one can expect to produce the silicon nitride powder with the 80-90% crystalline phase content by direct annealing under nitrogen flow at 1420-1500°C [2] of the amorphous powders keeping a reasonable specific area with changes in the chemical composition, the α/β ratio and the microstructure.

In order to investigate the influence of the phase-structural state of silicon nitride on the catalytic properties of Pd, three kinds of silicon nitride were used as supports in this work: amorphous silicon nitride (SiN-am); amorphous silicon nitride annealed at 1450°C for 2h under nitrogen flow (SiN-annl) and α -Si₃N₄. The catalytic properties of the resulting systems toward the total oxidation of methane were compared.

Experimental

The Pd catalysts were prepared by impregnation of the silicon nitride supports with adequate amounts of Pd(II) bis acetylacetonate [Pd(C₅H₇O₂)₂] dissolved in toluene [3]. The total oxidation of methane over Pd catalysts was carried out between 25°C and 650°C in a flow tubular quartz reactor with a stationary layer of catalyst. The products were analyzed by mass-spectrometry. Methane conversion versus temperature was measured for two states of the samples: state 1- as prepared catalysts and state 2 - samples after the heating for 3h at 650°C in the presence of the reagents mixture. The phase composition, the chemical state and the morphology of the silicon nitrides supports and the supported Pd catalysts were checked by XRD, XPS and TEM.

Results and discussion

The XRD analysis was used in combination with TEM and XPS analyses to determine the composition and the structure of silicon nitride supports. The SiN-am support had greater specific surface area - 66 m²/gas compared to the α -Si₃N₄ (7 m²/g) and contains a larger amount of surface oxygen (22% of the Si_{2p} XPS signal). The SiN-am powder was mainly amorphous with a crystalline fraction about 10 wt% containing the α -phase and

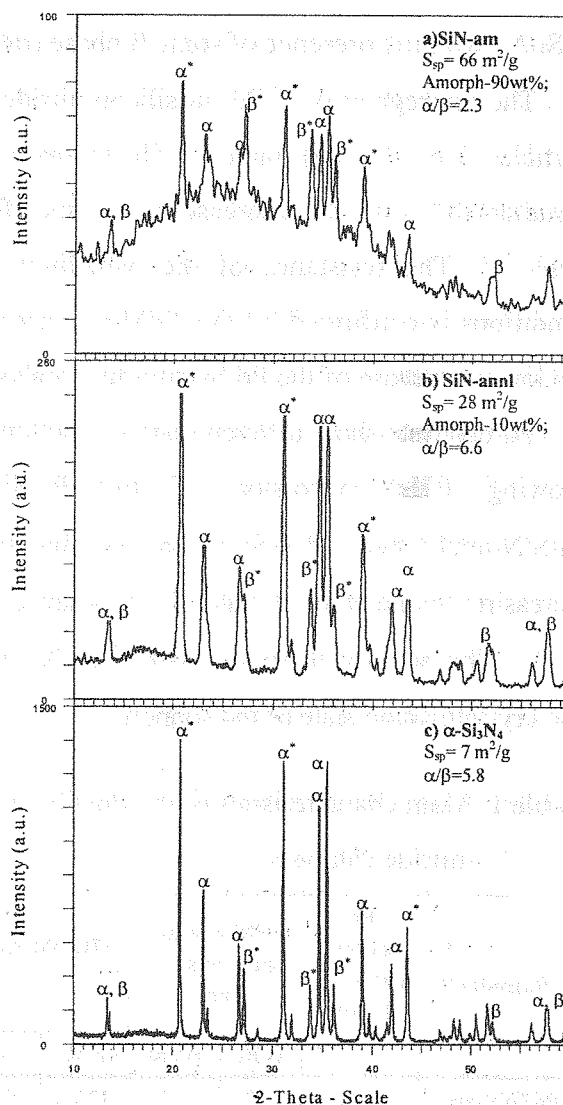


Fig. 1. X-ray diffraction pattern and the main properties of the amorphous silicon nitride (a); annealed silicon nitride (b) and α -Si₃N₄ (c) supports. The lines noted with * were used for the calculation of α/β ratio

β -phases (fig.1a) with a α/β ratio of 2.3. The amorphous silicon nitride support consisted of uniform (~30 nm), spherical particles with very few of silicon nitride crystals.

After treatment at 1450° C under nitrogen flow, the crystalline fraction became very high (90 wt%) and the α/β ratio increased to 6.6 (fig. 1b). Crystallization is associated with grain coarsening as it is shown by changes of the specific area and also by TEM measurements. The specific surface area decreased from 66 to 28 m²/g. The support annealing in nitrogen flow leads to a significant decrease of the surface oxygen content to 6 at% determined by XPS. Among the α -Si₃N₄ crystals some whiskers with β -phase structure were observed.

The α -Si₃N₄ support was found to be a very well crystalline material containing mainly α -Si₃N₄ with the presence of some β phase (ratio $\alpha/\beta=5.8$) (fig 1c).

The impregnation of Pd on silicon nitride supports leads to the formation of small metal particles (2.6 - 5.6 nm) (table 1). The increase of the Pd particles size for as prepared catalysts simultaneous with the decrease of the specific surface areas of the supports was observed (table 1). The resistance of the palladium metallic particles to sintering under reaction conditions is confirmed by the TEM average particle size measured after reaction as well as the lower decrease of the Pd/Si ratio for catalysts after reaction (table 1).

Pd catalysts show different catalytic activity for the total oxidation of methane. The curves showing CH₄ conversion of the Pd/SiN-am, Pd/SiN-annl and Pd/ α -Si₃N₄ as a function of increasing temperature at states 1 and 2 are given in fig. 2. The activity increases with α -Si₃N₄ content and crystallization state of the support.

Table 1. Main characteristics of the Pd/silicon nitride catalysts

Samples	Pd content (wt%) \pm 0.008	TEM average particle size (nm)		BE Pd 3d _{5/2} , eV	
		B.R.	Af.R.	B.R.	Af.R.
Pd/SiN-am	0.44	2.9	3.2	335.3	337.0
Pd/SiN-annl	0.42	3.2	3.6	335.9	337.3
Pd/ α -Si ₃ N ₄	0.49	4.3	5.8	335.9	337.3

BE-Binding energy; B.R.-catalyst before reaction; Af.R.-catalyst after reaction

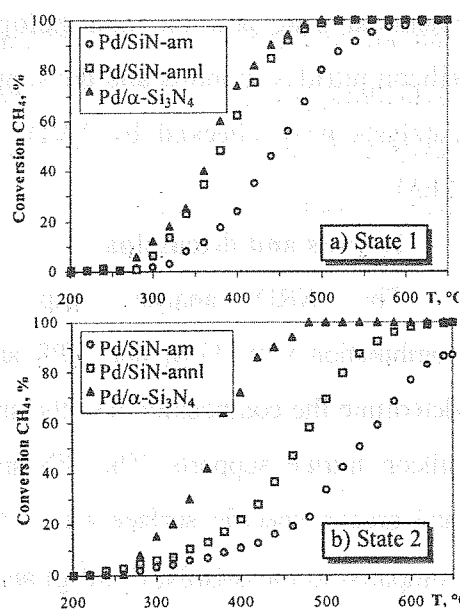


Fig. 2. Methane conversion over Pd/SiN-am; Pd/SiN-annl; Pd/ α -Si₃N₄ catalysts according to their « states » of reaction

The activity of Pd/ α -Si₃N₄ is very stable with state 2 similar to state 1. Pd/SiN-annl catalyst exhibits a catalytic behavior quite comparable to the Pd/ α -Si₃N₄ in state 1; the light-off temperature (at half-conversion) is quite the same, near 350-370°C. However, after aging at 650°C under the gas mixture (state 2), a significant decrease of activity is observed (fig 2 (b)) and the light-off temperature increases from 370° to 470°C. Pd/SiN-am catalyst is less active compared with Pd/SiN-annl and Pd/ α -Si₃N₄ samples. Moreover the activity decreases under reaction conditions; the conversion of methane in state 2 does not reach 100%.

The Si 2p and O 1s XPS peaks changed in shape and intensity after reaction for Pd/SiN-am, indicating that oxidation of the silicon nitride support has occurred. The oxygen content doubled after reaction. It was not observed any strong oxidation for the Pd/SiN-annl and Pd/ α -Si₃N₄. However, Pd particles covered by an amorphous thick layer were observed in some regions of the Pd/SiN-annl catalyst after reaction (fig. 3).

The catalytic difference of the Pd catalysts can be explained with respect to the properties of the Pd particles. The binding energy of Pd 3d XPS peak of Pd/SiN-annl and Pd/ α -Si₃N₄ is higher than for Pd/SiN-am (table 1). The line shape of both the Pd 3d XPS peaks and the corresponding Auger spectrum is quite comparable to that obtained for a reduced Pd⁰ state as measured for a massive palladium sample [4]. The higher value of Pd 3d_{5/2} (336.1 eV) instead of 335.3-335.4 eV for Pd metal was also found for Pd(0.75%)/ α -Si₃N₄ catalyst and it is quite higher than for Pd deposited on Al₂O₃ [3]. This can be related to a modification of the electronic properties of the Pd particle due to specific interaction between Pd metal and α -Si₃N₄ phase. The decrease of the activity can be explained by the recovering of the Pd particles (fig. 3) due to the presence of amorphous fraction in the support which can be easier oxidized and mobile at high temperature with the presence of oxygen. In conclusion, Pd/ α -Si₃N₄ was found to be active and stable under reaction conditions, in the absence of amorphous fraction.

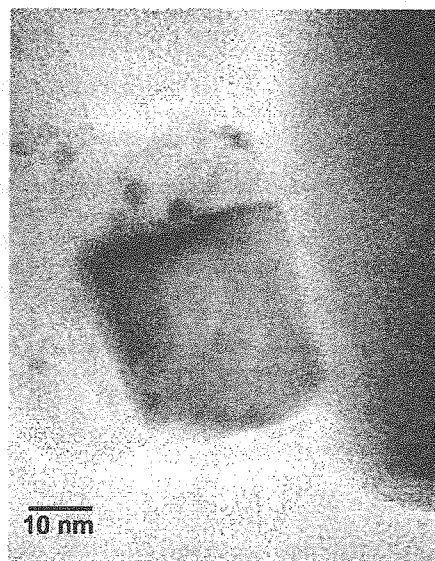


Fig. 3. TEM pictures of Pd/SiN-annl catalyst after reaction

References

- [1] W. Dressler, R. Riedel Int. J. of Reflectory Metals & Hard Material 15 (1997) 13-47.
- [2] J. Szépyölgyi, I. Tóth, T. Székely. Proc. ISPC-9, V.11, Pugnochiuso, Italy, 1989, 727-732.
- [3] C. Méthivier, J. Massardier, J.C. Bertolini. Applied Catalysis A :General 182 (1999) 337-344.
- [4] M. Brun, A. Berthet, J.C. Bertolini, J. Eletron Spectrosc. Related Phenom. 104 (1999) 55.

REACTIVITY OF TSEFLAR™-TREATED GIBBSITE IN THE REHYDRATION PROCESS UNDER MILD CONDITIONS

**L.A. Isupova, Yu.Yu. Tanashev, I.V. Kharina, E.M. Moroz, G.S. Litvak,
N.N. Boldyreva, E.A. Paukshtis, E.B. Burgina, A.A. Budneva, A.N. Shmakov,
N.A. Rudina, V.Yu. Kruglyakov, V.N. Parmon**

Boriskov Institute of Catalysis SB RAS, Novosibirsk

Thermal activation of hydrargillite/gibbsite (HG) is known to be a method for production of highly reactive state of $Al_2O_3 \cdot xH_2O$. Rehydration of this product is a basis of a number of wasteless/low-waste technological lines used for manufacturing the pseudoboehmite-structured hydroxide with the skipped reprecipitation stage which requiring a large consumption of feedstocks and producing wastewater in a large amount.

The properties of the products of the thermal decomposition and their reactivity will depend considerably both on properties of the initial hydrargillite (including the particle size) and on conditions of the thermal decomposition process, viz. the decomposition temperature, heating rate, HG bed thickness, residence time in the hot zone, hardening rate, water partial pressure etc., which determine the defect structure of an oxide phase formed and, hence, its physicochemical properties.

Few methods for the implementation of the thermal decomposition process were developed. These are:

1. Thermal decomposition in the flue gas backflow at high temperatures;
2. Thermal decomposition in the flue gas backflow at moderate temperatures and certain steam pressure – TCA;
3. Thermal decomposition in the fluidized bed of a catalyst or solid heat carrier – TDP;
4. Thermal decomposition in a thin bed in flowing flue gases.

Thermal decomposition of hydrargillite using a TSEFLAR™ installation [1] is a new way to implement the thermal decomposition process which allows a combination of a fixed decomposition temperature, thin bed, fast heating, hardening, short contact times and steam pressure. In addition, a more pure product -CTA HG- is obtaining of not contaminated by incomplete burning products or by the carrier.

Specific features of the TSEFLAR™ process of the HG thermal decomposition necessitated to investigate the conditions of the formation of the active product (CTA HG), its nature and physicochemical properties including its reactivity to the rehydration reactions.

Experimental

The product from the Pikalev Silica Complex was used as initial HG. The initial moisture content was 9 wt %, impurities: 0.22% of Na_2O ; the fraction composition: 8% of the 0–38 μm fraction, 10% of the 38–53 μm fraction, 55% of the 63–106 μm fraction, 27% of larger than the 106 μm fraction; $S_{\text{specific}}=2-5 \text{ m}^2/\text{g}$. The product was subjected to the thermal decomposition at the varied main process parameters: the initial HG wetness, rotation speed (0.5 to 1.7 s), temperature (350 to 600°C), feeding rate (5 to 40 kg/h), dispersion state (with and without sifting) and steam pressure (up to 100 torr).

The samples were characterized using such techniques as XRD (including the mode with the synchrotron radiation-SR), DTA, BET, IRS, EM, and NMR. Solubility of the samples was determined in acid and base media.

Results and discussion

The CTA HG product composition

The phase composition of the CTA HG products is considerably affected mainly by the TSEFLARTM plate temperature, pre-drying temperature and contact time (or feeding rate) but practically independent of the plate rotation speed. For example, the XRD data show that the rise of the plate temperature from 330 to 600°C results in the decrease in the HG proportion in the CTA product while the content of the X-ray amorphous component increases and boehmite is detected. Almost the whole product formed upon the treatment at 530 – 580°C is X-ray amorphous. Table 1 shows the characteristics and preparation conditions of some CTA HG products.

The DTA data demonstrate a non-uniformity of even the high-temperature (fully X-ray amorphous) CTA HG product; it seems to comprise both an “oxide” and “hydroxide” constituents. The effects, a broadened endoeffect below 800°C accompanied by a monotone weight decrease and an exoeffect at 820°C at no weight change, seen in DTA curves of CTA HG samples indicate the presence of not only a disordered oxide phase and chemisorbed water but also disordered hydroxide phases (Fig. 1). The IRS data argue in favor of this conclusion; and the same is with the SR-data on the phase composition which allow, due to a higher sensitivity, a χ -like phase of alumina and afps of hydrargillite and boehmite to be detected in the high-temperature CTA HG sample (Fig. 2).

From the IRS data, the CTA HG products also comprise χ -like alumina along with weakly bonded/molecular water (removed on heating at 100°C) and structurally disordered hydroxides. That is seen from a poorly resolved IR absorption data at the region of stretching vibrations of bound hydroxides. Therefore, the X-ray amorphous CTA HG product seems to contain a considerable quantity of structurally disordered hydroxides in its “hydroxide” constituent and chemisorbed water in its “oxide” constituent. The IRS data show also the

presence of carbonate species in the CTA products which may form due to an interaction of the active oxide species produced during the thermal decomposition with carbon dioxide, which present in the ambient.

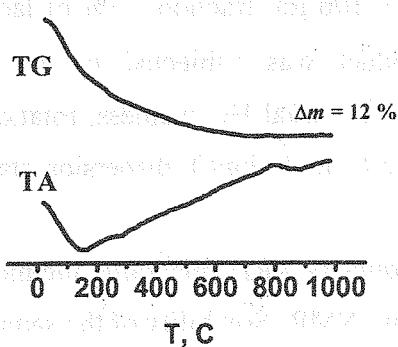


Fig. 1. Thermogram of gibbsite treated with TSEFLAR™ at 580 °C

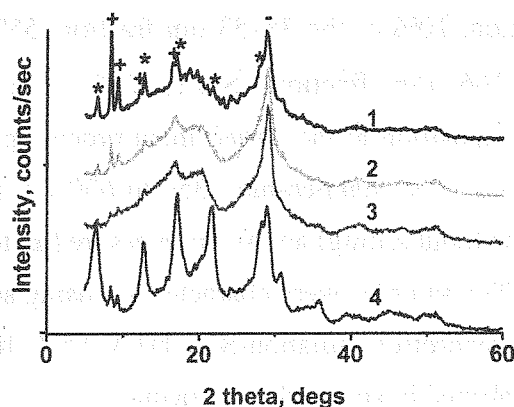


Fig. 2. The samples' phase composition according to the Synchrotron XRD versus the preparation conditions: 1- TCA+MT, 2 CTA-580, 3-CTA-580+MT, 4-3+hydration in an ammonia solution at pH 10 during 2 h. (*-Boehmite, - gibbsite, - χ -like alumina)

The increase in the content of the amorphous oxide component in the products also is favored at longer contact times (lower rates of the HG consumption by TSEFLAR™), while a pre-drying of the samples at 180°C results naturally in a higher content of boehmite in the product.

Therefore, low temperatures (below 400°C), high consumption rates (15 – 20 kg/h), pre-heating of HG at the temperature not higher than 100°C will cause an increase in the content of an “amorphous hydroxide” component, including amorphous HG, in the CTA products, and *vice versa*, high temperatures (above 500°C), the small particle size and low consumption rates (lower than 10 kg/h) will allow a fully X-ray amorphous “hydroxide”-free products to be obtained, in which aluminum atoms form a kind of the χ -oxide phase in its close proximity (from the IRS data).

The surface area of the CTA HG products

The treating of HG with TSEFLAR™ results in a considerable increase in the surface area of the samples depending on the conditions of thermal decomposition. The surface area increases upon the elevation of the decomposition temperature but decreases upon the elevation of the pre-drying temperature. For example, if the CTA HG temperature is in the range of 470-545°C, S_{specific} increases up to 180 m²/g in the sample pre-heated to 140°C but up to 250 m²/g in the sample not subjected to pre-heating. It is interesting that the surface area is considerably lower when being determined at room temperature than that after the pretreatment at 300°C. This is an evidence of the inaccessibility of some part of the adsorbate surface due to the presence of chemisorbed water and/or specific morphological arrangement of the particles.

Morphology of CTA HG products

The particle aggregates are practically not varied in size after treating HG with TSEFLAR™ (from the EM data and the data obtained by Coulter). The electron microscopic studies reveal that the particles formed during HG treating with TSEFLAR™ at 470 and 575°C are a pseudomorphose to the initial HG (Fig. 3). These are almost regularly shaped (truncated hexagon or distorted rectangular in the projection) coarse (1–1.5 μm) particles with the slightly broken surface. Sometimes fine acicular particles of ca. 70 to 100 Å in size are seen at the particle edges. Elongated spots – slit-like pores – can be observed in some individual particles. There are also shapeless aggregates of lamellar microporous particles of 0.5–2 μm in size in the samples.

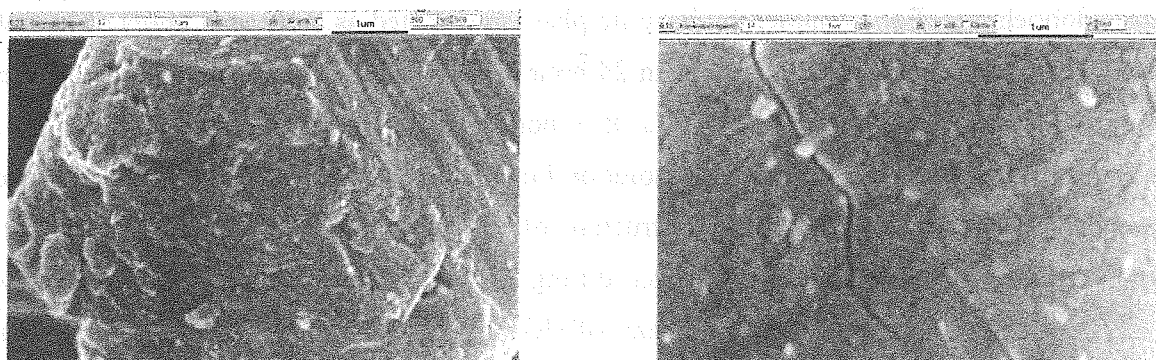


Fig. 3. Photomicrography of gibbsite treated with TSWFLAR™ at 580 °C (different magnifications).

Preservation of the layered HG structure in the products of the TSEFLAR™ thermodecomposition indicates feasibility of the dehydration stage without a concomitant rearrangement of the oxygen sublattice because the layered structure of the CTA product (as argued for by the presence of the HG pseudomorphose) is not characteristic of the formed product with the composition close to $\text{Al}_2\text{O}_3 \cdot x\text{H}_2\text{O}$ (the oxide product). However, the formed structure differs from the initial one since all the layers are porous and splitted. Therefore, the CTA product seems to be in a non-equilibrium metastable state of oxide phase and, for this reason, possesses a higher energy capacity and a higher reactivity. When the temperature of the HG treatment is elevated to above 600°C, the formation of an oxide crystal lattice is not excluded in the CTA product. Hence, some temperature range may be identified for the formation of the active CTA product with the transitional non-equilibrium layered structure of the hydroxide type which is dehydrated in more or less extent; this is the range between 330 and 600°C.

Reactivity of the CTA HG products

Depending on the preparation conditions, different solubilities are characteristic of the CTA HG samples (Table 1). For example, the solubility in an alkaline ammonia solution at 20°C increases with the elevation of the decomposition temperature and, *visse versa*, decreases

if the samples are disintegrated. The solubility in acid solutions varies antipathetically to that in the alkaline solutions. The water solubility is rather low for all the samples; the solution formed showing an alkali reaction (pH 10-11). It is interesting that the TCA HG sample is the one most soluble in the ammonia solution and least soluble in water that indicates its acidic properties (that may be accounted for by higher temperatures of the sample preparation or by a lower steam partial pressure), while the CTA HG product is more alkaline.

A longer hydration of the samples in an alkaline medium and water produces pseudoboehmite first (Fig. 2) and then, at even longer exposure, bayerite. The hydration during a week results in formation of almost one-phase bayerite from both TCA HG and CTA HG. However, there is a considerable difference in the maximal quantity of the formed pseudoboehmite. For example, the bayerite phase is detected as early as 5 hours of hydration of the CTA HG product in water but in 24 hours (when the pseudoboehmite content reaches ca. 50%) of hydration of the TCA HG. It is not excluded that rehydration of the CTA HG products skips the stage of their redissolution but by the reaction Solid+Liquid. This process may be favored due to the layered structure of the products. One can also notice that no formation of pseudoboehmite is detected during 24 hours in an acidic medium (at otherwise identical conditions) and, again, exposure of HG or pseudoboehmite (reprecipitation) in acid or alkali aqueous solutions does not cause any changes in the phase composition of the samples.

Thus, CTA HG products at the temperature range of 330 to 580°C are the ones with a transitional non-equilibrated layered hydroxide structure with partly lost hydroxide groups. The structure does not correspond to the produced chemical composition and, therefore, reveals a higher reactivity. Such a system is already readily hydrated at room temperature in water and aqueous ammonia to form eventually the stable bayerite-like hydroxide structure. In an acid solution at room temperature, the product does not undergo any phase transitions even if exposed for a week; that may happen due to formation of a dense hydroxide film on the particle surface.

Acknowledgements. The work is financially supported by Presidium of SB RAS, the Ministry of Science and Technology of the Russian Federation and the Ministry of Education of the Russian Federation.

References

1. V. I. Pinakov, O. I. Stoyanovsky, A. A. Pikarevsky et al. // Proc. XVI Conf. on Chemical Reactors "CHEMREACTOR-16", Kazan (Russia), 17-20 June 2003. P.193.

Table 1. Some properties of the CTA Gibbsite products

Sample/ Chemical composition	Disperga- tion	Phases, % (X-Ray)	TA					Solubility		
			Humidity, %	Am.	Al(OH) ₃ Gibbsite	AlOOH boemite	AlOOH, Pseudoboe- mite.	NH ₄ OH, pH 10, 20 °C, 60 min	H ₂ SO ₄ * 40 °C, 1 min	H ₂ O** 25 °C, 120 min
Gibbsite Al ₂ O ₃ * 3.53H ₂ O	no	Gib-92 Boe-8	38.25	no	77	26.6	0.4	no	-	no
CTA-380 Al ₂ O ₃ * 1.68H ₂ O	no	Am-65 Boe-15 Gib-20	22.75	44.3	39	16.7	0	1.9	1.2	0.02
CTA-380 Al ₂ O ₃ * 1.85H ₂ O	dezi	Am82 Boe-3 Gib-15	24,5	36,97	44,7	18,33	0	1	11.5	0.025
CTA-580 Al ₂ O ₃ * 0.79H ₂ O	no	Am	12	81.13	5.71	8.33	4.77	2.2	2	0.02
CTA-580 Al ₂ O ₃ * 0.95H ₂ O	dezi	Am-95 Boe-3 Gib-2	16,5	83,5	4,84	11,66	0	1.4	3.9	0.025
TCA (for comparision) Al ₂ O ₃ * 0.79H ₂ O	dezi	Am-95 Gib-5	12	76	11	13	0	3	2	0.01

* Samples solubility in sulfur acid (1:1) during heating, up to 80 °C (full solubility)

** water pH rises up to 10-11

***IN-SITU* THERMOGRAPHY TO STUDY SURFACE TEMPERATURE OF NICKEL CATALYST DURING CATALYTIC REACTION OF PROPANE OXIDATION**

A.Yu. Gladky, V.V. Ustugov, A.I. Nizovskii, V.N. Parmon, V.I. Bukhtiyarov

Boriskov Institute of Catalysis SB RAS

Pr. Akad. Lavrentieva, 5, Novosibirsk 630090, Russia

A proper design of chemical reactors has to rely on many characteristics of a chemical process. One of such characteristics is a temperature of a catalyst surface. However, the use of thermocouples for the detection of a catalyst temperature is widely spread, in the case of strongly exothermic or strongly endothermic reactions, a correct measuring the catalyst temperature is of considerable difficulty. This is even more difficult in case of highly dispersed catalysts.

The method of thermography makes it possible to measure the temperature of working catalysts in a wide temperature range and in the micrometer scale. Although, this method requires a specific design of the reactor (fig.1), which has to have an optical window, it permits one to exclude possible side thermal effects due to a material of a thermocouple.

We tested the method of thermography in the reaction of propane oxidation over a nickel catalyst. Fig. 2 shows a series of micro-thermographs recorded during the propane oxidation over a nickel foil at the gas temperature 750°C, pressure 1 torr, and propane/oxygen ratio 9/1. As it is seen, such technique allows the detection of temperature non-uniformity of working catalysts.

A possible mathematical treatment of visual experimental data is discussed.

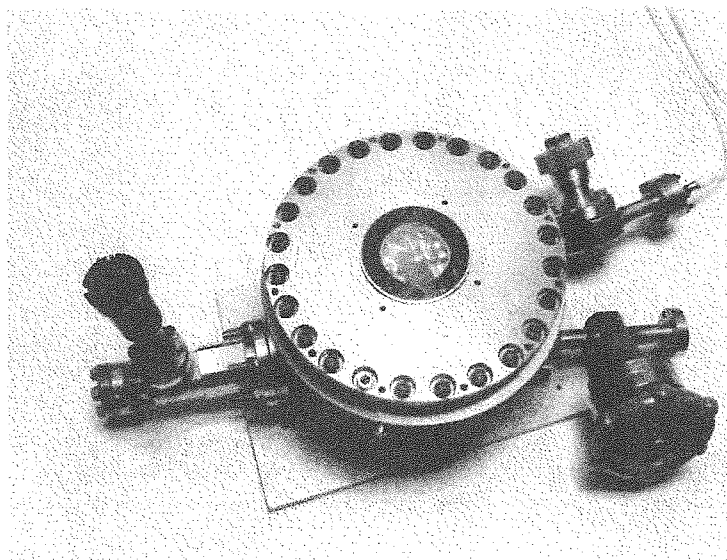


Figure 1. Thermography reactor.

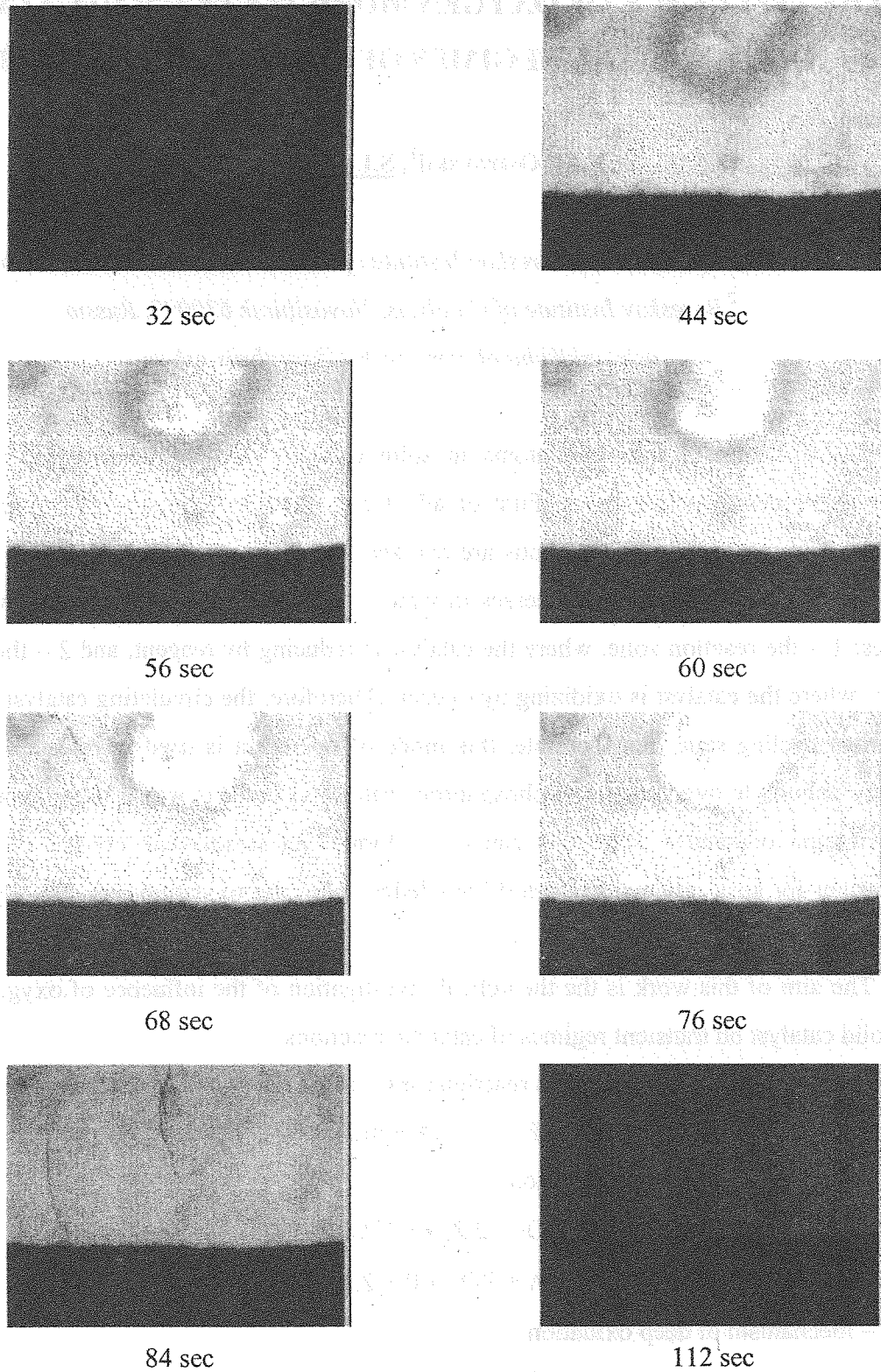


Figure 2. Evolution of surface temperature of a nickel foil during oscillatory oxidation of propane. Propane/oxygen ratio is 9/1. A frame size is 500x750 μm .

THE INFLUENCE OF OXYGEN MOBILITY IN SOLID CATALYST ON TRANSIENT REGIMES OF CATALYTIC REACTION

N.M. Ostrovskii¹, S.I. Reshetnikov²

¹ Omsk Department of Boreskov Institute of Catalysis, Omsk 644040, Russia

² Boreskov Institute of Catalysis, Novosibirsk 630090, Russia

ostrovski@hipol.com, reshet@catalysis.nsk.su

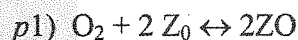
The diffusion of ions and atoms in solid catalysts can influence significantly on a catalytic processes performance. First of all, it concern with diffusion of oxygen in metal oxides. The most oxidation reactions are realized with the presence of oxygen in gas phase. Nevertheless, there are some processes in which the operation is preferable in two separate zones: 1 – the reaction zone, where the catalyst is reducing by reagent, and 2 – the oxidation zone, where the catalyst is oxidizing by oxygen. Therefore, the circulating catalyst works in a transient cycling state. For example, this mode of operation is used in butane oxidation to maleic anhydride over vanadium-phosphorous catalysts [1]. This way of operation can allow a formation of catalyst state that cannot be formed in steady-state conditions. The most important for such processes is detail knowledge about the oxidation-reduction dynamics of catalyst surface.

The aim of this work is the theoretical investigation of the influence of oxygen mobility in solid catalyst on transient regimes of catalytic reactions.

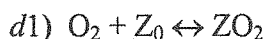
Let consider the following two reaction runs – of partial and deep oxidation:



– mechanism of partial oxidation:

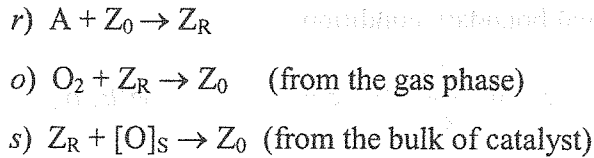


– mechanism of deep oxidation:

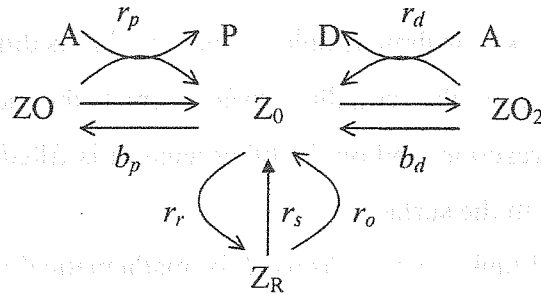


– mechanism of the active sites (Z_0) blocking and reduction:

¹ Present address: AD Chemical Industry – HIPOL, Odžaci, Yugoslavia



This mechanism can be represented by the following schematic diagram:



The rates of steps of this oxidation-reduction mechanism can be define using mass-action law:

$$r_p = k_p (b_p Y_O)^{1/2} Y_A \theta_o; \quad r_d = k_d b_d Y_O Y_A \theta_o;$$

$$r_r = k_r Y_A \theta_o; \quad r_o = k_o Y_O \theta_R; \quad r_s = k_s \theta_R \sigma_S.$$

where Y_A, Y_O are molar portions of A and O_2 ; θ_o, θ_R are portions of oxidized and reduced sites; σ_S is the oxidation level of catalyst surface; k_i is reaction rate constants; b_i is equilibrium constants of adsorption.

It should be note, that the stage (s) is named «reaction» only formally, since actually, this is the substitution of surfaces oxygen vacancy by oxygen from the catalyst bulk.

From the normalization condition, one can obtain the equation for concentration of sites at the beginning of process:

$$\theta_o^o = 1 / [1 + (b_p Y_O)^{1/2} + b_d Y_O], \quad \theta_R = 1 - \theta_o / \theta_o^o$$

The diffusion in crystalline lattice of metal oxides occurs due to displacement point defects. This process can proceeds by different mechanisms depending on type of the defect: exchange atom crystalline structure with its vacancy, simultaneous cycling replacement several atoms and others [2].

Let us define the «oxidation level» of crystallite (σ) as the relation of oxygen concentration in crystalline lattice to its maximal concentration. The oxidation level of catalyst surface (σ_S) depends on diffusion of oxygen ions in catalyst crystallite. For modeling of diffusion in metal oxides the following differential equation can be used [3]:

$$\frac{\partial \sigma}{\partial \tau} = \frac{1}{\varphi^2} \frac{\partial^2 \sigma}{\partial \xi^2} \quad (1)$$

OP-I-12

with the initial and boundary conditions:

$$t = 0: \sigma = 1; \quad \xi = 0: \frac{d\sigma}{d\xi} = 0, \quad \xi = 1: \frac{d\sigma}{d\xi} = -\phi^2 \theta_R \sigma_S \quad (2)$$

Here $S_c = 1/L$ is specific surface of crystallite, cm^2/cm^3 ; $\phi^2 = L^2 k_s / D$ is the analogue of Thiele modulus; D is diffusion coefficient of oxygen, cm^2/s ; L is the half-thickness of catalyst crystallite, cm ; $\tau = k_s t$ is dimensionless time; $\xi = l/L$ is dimensionless coordinate.

The boundary condition on the crystallite surface depicts the fact, that surface oxygen on the one hand, is spend in reaction, and on the other hand, it is filled up owing to diffusion of oxygen ions from the bulk to the surface.

The continuous stirred tank reactor was used for mathematical modelling. The results are presented in Figs. 1-4.

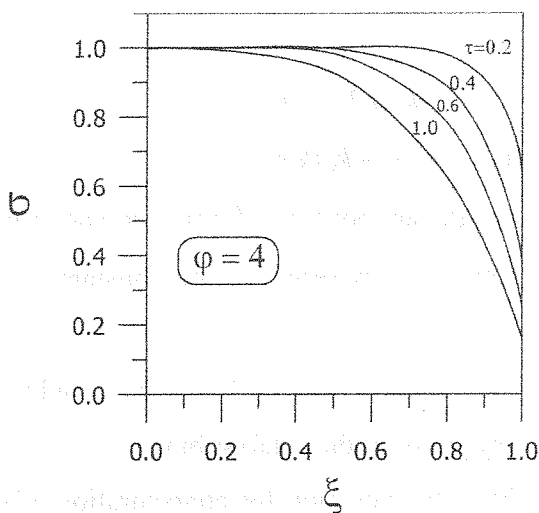


Fig. 1. Profiles of oxidation level of crystallite along its depth (ξ).

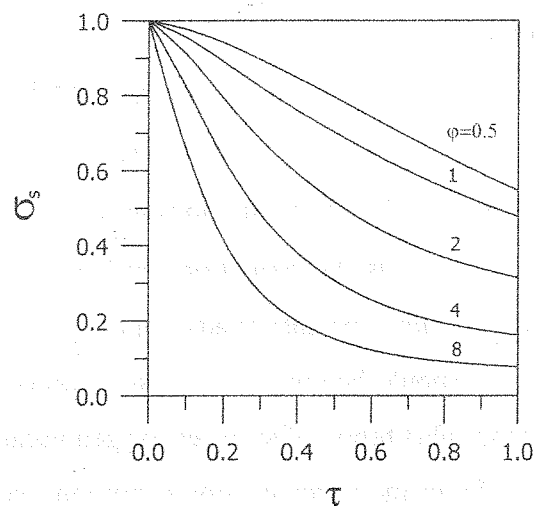


Fig. 2. Dependences of oxidation of crystallite surface on time (τ).

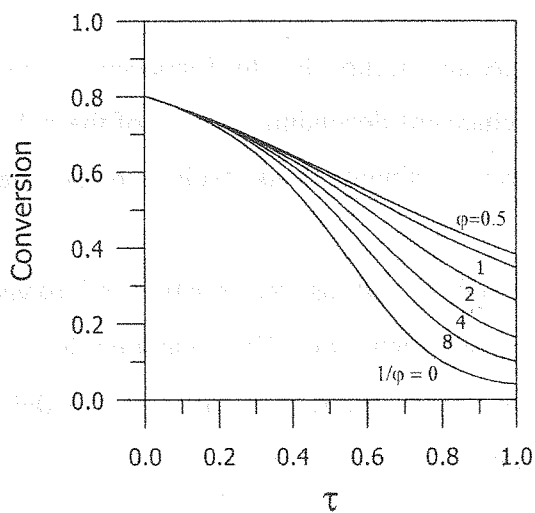


Fig. 3. Dependences of reagent conversion on dimensionless time (τ).

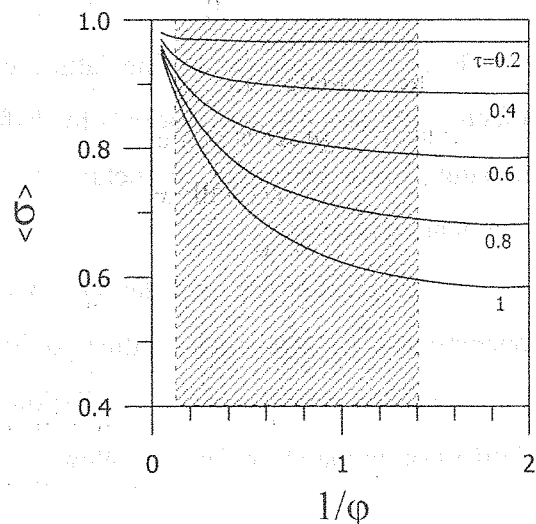


Fig. 4. Dependences of the average oxidation of crystallite on Thiele modulus (ϕ).

Fig. 1 shows dependence of oxidation level of crystallite along the crystallite depth at different time. At the initial moment, the only oxygen from subsurface catalyst layers takes part in surface oxidation, and then the oxygen from the bulk is diffused. As we can see from (1-2), the rate of diffusion and consequently the oxidation level of the catalyst surface (σ_s) are defined by Thiele modulus (φ). With increasing of φ (the diffusion coefficient is decreased) the oxidation level of the catalyst surface is decreased (Fig. 2). Therefore, the conversion of reagent (X) is also decreased (Fig. 3). The conversion in our case is calculated by equation:

$$X = D_a \theta_o / (1 + D_a \theta_o)$$

where $D_a = a \tau_r [k_d b_d Y_O + k_p (b_p Y_O)^{1/2} + k_r]$.

Fig. 4 demonstrates the dependence of the average oxidation of crystallite, defined as:

$$\langle \sigma \rangle = \int_0^1 \sigma(t, \xi) d\xi$$

versus Thiele modulus at different time. It is seen that there are two regions of φ in which the diffusion of oxygen in solid catalyst do not effect the transient regime of catalytic reaction.

At $\varphi > 8$ ($1/\varphi < 0.125$) there is not influence owing to low oxygen mobility and at $\varphi < 0.7$ ($1/\varphi > 1.4$) the oxygen mobility is faster in comparison with the rate of reaction.

Taking into account that $\varphi^2 = L^2 k_s / D$, one can obtain the estimation of the diffusion coefficient. Let suppose, that the size of crystallite is approximately equal to the size of the catalyst pore $L = 5$ nm, and the rate of oxygen interaction with active sites equals $4 \cdot 10^{-3} \text{ s}^{-1}$. Then we obtain the interval of oxygen mobility ($D = 10^{-17} - 10^{-15} \text{ cm}^2/\text{s}$) where diffusion influences the transient regimes of catalytic reaction. This value of D is in a good agreement with diffusion coefficients of oxygen in some metal oxides [2].

References:

1. Contractor R.M., Sleight A.E. Catal. Today 1987, 1, 587.
2. Kofstad P. Nonstoichiometry, diffusion and electrical conductivity in binary metal oxides. Willey-Interscience, New-York, 1972.
3. Ostrovskii N.M. Kinetic of catalyst deactivation. Moskva, Nauka, 2001 (in Russian).

PHOSPHATE-PROMOTED SILVER CATALYSTS FOR THE ETHYLENE GLYCOL OXIDATION

A. Knyazev, O. Magaev*, O. Vodyankina*,

S. Koscheev**, A. Boronin**, A. Titkov**, A. Salanov**, L. Kurina**

Institute of Petroleum Chemistry SB RAS, Russia, Tomsk, av. Akademicheskii, 3,

fax: (3822)258457, e-mail: kas854@mail.ru

**Tomsk State University, Tomsk, Russia*

***Boreskov Institute of Catalysis SB RAS, Novosibirsk, Russia*

Silver is widely used catalyst for the processes of ethylene epoxidation, synthesis of formaldehyde, glyoxal etc. For increasing the selectivity promoting substances of different nature are added to the Ag catalyst. Phosphorous content compounds are used as promoters increasing selectivity of the silver catalyst of the ethylene glycol oxidation process, [1]. Mechanism of the P-content promoter action introduced in silver catalyst is not practically investigated so far. Recently at the studying of the processes carrying out on the Ag foil surface under the action of P-content promoter we have proposed that addition of the promoter on the Ag surface leads to the formation of mobile Ag clusters distributed in the phosphate matrix [2]. It has been shown that this system is very stable under the action of high temperature and reaction mixtures of the ethylene glycol oxidation process.

The aim of the present work is to study the catalytic activity of P-content Ag catalysts and also to investigate the formation mechanism of an active silver surface under the influence of reduced reaction conditions by following methods: XPS, AES, and SEM.

The investigated sample is an electrolytic Ag crystal which is promoted by the phosphorous acid solution. Catalytic activity of the samples has been studied on the flow catalytic device with the fix-bed reactor. P-content silver catalysts are more effective in contrast to the unpromoted sample (Fig. 1). Comparison of our results with catalytic data obtained by Deng J. et al [1] showed that the investigated samples of Ag/P catalyst are more effective in glyoxal synthesis. It is worth while to note that general behaviour of the obtained dependencies is also similar to Deng's one.

Glyoxal yield as a function of the oxygen-content in the reaction mixture has a non linear character. Moreover, maximum of the glyoxal yield for the P-content Ag catalyst shifts to the higher partial oxygen pressure in the reaction mixture (Fig. 1).

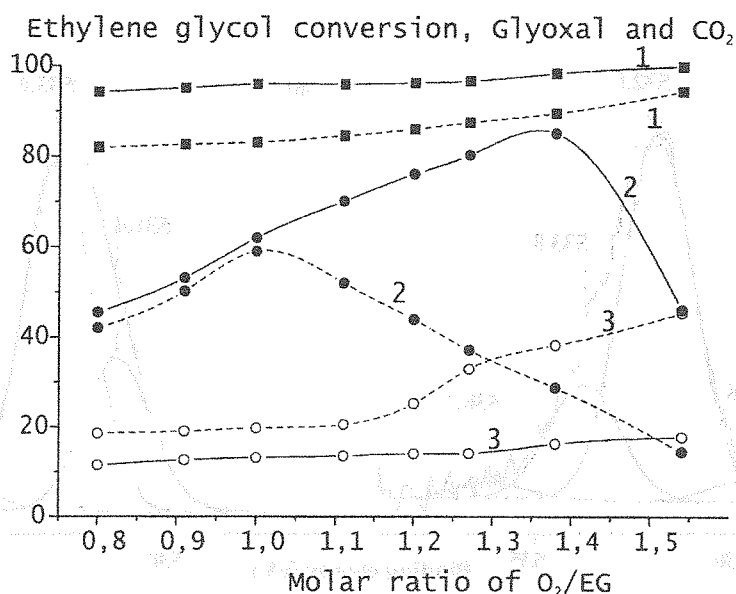


Fig. 1. Catalytic activity of the initial and P-doped Ag catalysts in the ethylene glycol oxidation process.

Curves are indexed in the following order: (1) Ethylene glycol conversion, (2) glyoxal yield, (3) CO₂ yield.

Composition of the reaction mixture is O₂/EG/N₂/H₂O = 1 / 1 / 30 / 3.4, T = 833 K.

Dotted lines – Ag catalyst, solid lines – Ag/P.

CO₂ yield for P-promoted catalyst is significantly lower compared to unpromoted Ag sample. It's clear from XPS investigations (Fig. 2b) that the P-content layer being formed on the Ag surface prevents the appearance of Ag₂O centres which take part in the deep oxidation of ethylene glycol (Fig. 1, curves 3) [3].

Before the action of the reaction mixture O1s spectra obtained from the surfaces of both the initial Ag catalyst and P-content sample are presented in Fig.2. On the initial Ag sample we observed a few different oxygen forms (Fig.2a). O1s peaks with BE of 532.0 and 533.8 eV may be associated with oxygen centres of subsurface type located in defects of crystalline Ag lattice [4-7]. Oxygen peak characterized by BE = 529.8 eV is related to the oxide-like oxygen structure [8, 9]. O1s peak with BE = 536.2 eV is related to the presence of the water and oxygen molecules included in micropores and defects of the polycrystalline Ag sample.

The treatment of the Ag surface by phosphorous acid leads to the appearance of two new oxygen states characterized by BE = 531.4 and 533.2 eV (Fig. 2.b). Taking into account the data presented in Ref [10] those oxygen forms might be associated with both bridging oxygen of Ag-O-P, P-O-P-groups and terminal oxygen of P=O group correspondingly. O1s peak with

BE = 535.1 eV might be related to water molecules included in the structure of phosphorous acid on the Ag surface. The annealing of P-doped Ag sample at 923 K in air leads to the polymerization of the promoter, because the intensity of O1s peak with BE = 531.4 eV increases.

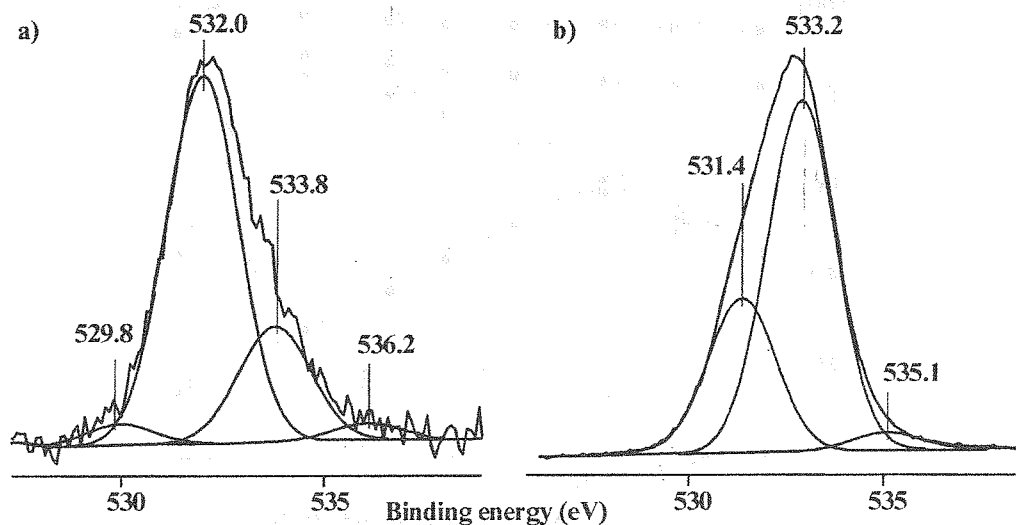


Fig. 2. O1s spectra of Ag samples before the action of the reaction mixture (a) initial Ag catalyst, (b) P-doped Ag catalyst after the drying at 473 K for 60 min.

Silver phosphate salt was used as the basic material for the modelling of the influence of reaction conditions on the P-content Ag catalyst. It is shown that $AgPO_3$ composition (Fig. 3a) is similar to the chemical composition of the surface layers of the real P-promoted Ag catalyst.

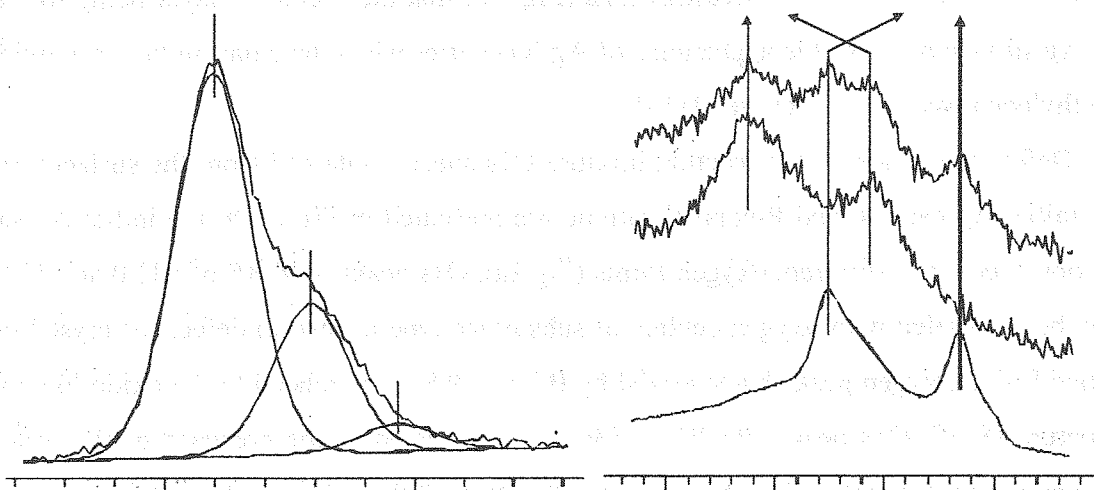


Fig. 3. O1s (a) and Auger Ag-NMM spectra (b) obtained from the surface: clean Ag foil (1), silver phosphate before (2) and after (3) the treatment by reduced reaction mixture.

According to the Auger spectra of Ag-MNN the treatment of silver phosphate by reduction atmosphere (H_2) at the temperature region of 473-723 K leads to the formation of

the metal Ag clusters on the sample surface. The annealing of the investigated pattern at 723 K in vacuum leads to the diffusion of Ag clusters from the surface into the bulk. As a result of the high temperature action the metal Ag particles are surrounded by matrix of phosphate salt.

It is proposed that a similar process occurs on the surface of P-promoted Ag catalyst under the action of the reaction mixture of the ethylene glycol oxidation process. Active centres participating in the selective ethylene glycol oxidation into glyoxal are formed on the Ag clusters located along the promoter layer. The high stability of the active surface of P-content Ag catalyst under the temperature action is related to the matrix of phosphate salt which is an obstacle for the sintering of the Ag clusters.

This fact has been established by SEM data obtained at the detailed studying of the morphology of the surfaces of the investigated samples during all stages of the promoting process before and after the action of different reaction mixtures.

Acknowledgements

This work was supported by Russian Ministry of Education under grant E02-5.0-340 and Grant of President of Russian Federation №YD-243.2003.03.

References

1. Deng J.F., Wang J., Xu. X. // *Catalysis Letters*. 1996. V.36. P.207.
2. Knyazev A.S., Boronin A.I., Vodyankina O.V., Koscheev S.V., Kurina L.N. // *Kinetika i Kataliz* 2003 (in press).
3. Vodyankina O.V., Kurina L.N., Boronin A.I., Salanov A.N. // *Stud. Surf. Sci. Catal.* 2000. V.130B. P.1775.
4. Lefferts L van Ommen., J.G., Ross J.R.H. // *Appl. Catal.* 1986. V.23. P.385.
5. Boronin A.I., Koscheev S.V., Malakhov V.F., Zhidomirov G.M. // *Catal.Lett.* 1997. V.47. P.111.
6. Boronin A.I., Koscheev S.V., Zhidomirov G.M. // *J. Electr. Spectr.* 1998. V.96. P.43.
7. Nagy A., Mestl G. // *Applied Catalysis A: General*. 1999. V.188. P.337.
8. Bao X., Muhler M., Schedel-Niedrig Th., Schlögl R. // *Phys.Rev.B*. 1996. V.54. P.2249.
9. Boronin A.I., Koscheev S.V., Murzakhmetov K.T., Avdeev V.I., Zhidomirov G.M. // *Applied Surf. Sci.* 2000. V.165. P.9.
10. Moulder J.F., Stickle W.F., Sobol P.E. et al., (Ed. by J. Chastain), *Handbook of X-ray photoelectron spectroscopy*, Perkin-Elmer Corporation, Physical Electronics Division, Eden Prairie, Minnesota, 1992, 261 p.

**A NOVEL SPECTRAL APPROACH TO THE STUDY OF DIFFUSION
OF INDIVIDUAL COMPONENTS IN GASEOUS MIXTURES
INVOLVED IN CATALYTIC REACTIONS OR GAS SEPARATION
ON ZEOLITES**

V.B. Kazansky, N.A. Sokolova

*Zelinsky Institute of Organic Chemistry of Russian Academy of Sciences Leninsky prospect
47, Moscow 1179, Russia. Fax: 7(095)135-53-28. E-mail: vbk@ioc.ac.ru*

Most of industrial catalytic processes utilize high surface microporous catalysts. Therefore, the corresponding reactions are at least in some extent diffusion limited. The similar is also true for separation of gaseous mixtures by adsorption on zeolites or other microporous materials. In this connection, investigation of diffusion of gases inside micro-meso- and macropores of adsorbents and catalysts attracts attention of different research groups around the world [1]. Unfortunately, the majority of such works is devoted to the study of diffusion of individual gases whereas for catalysis and separation processes one needs information on diffusion of ingredients of gaseous mixtures. Indeed, even in monomolecular catalytic reactions the initial and the final products form the mixtures where both components are diffusing in the opposite directions either from the surrounding gas inside micropores to the active sites of a catalyst or outside from the internal micropores. In the similar way separation of gaseous mixtures via adsorption by zeolites or other microporous adsorbents also deals with codiffusion or counterdiffusion of gaseous components inside and outside micro- meso- and macropores of the corresponding adsorbents.

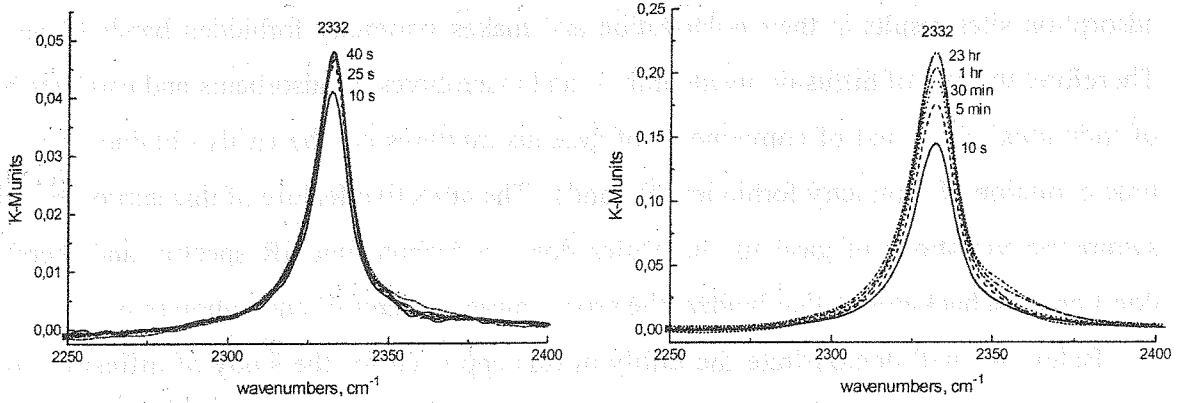
Unfortunately, information on diffusion of individual components in gaseous mixtures could not be delivered by such well - known and widely used techniques as gravimetry, pressure drop measurements or pressure response method, which provide information only on the average effective diffusivity. Therefore, below we suggest a new spectral approach to the study of transport of individual components of gaseous mixtures in microporous materials that can be used both for catalytic reactions and gas separation. This approach is based on development upon adsorption of symmetrical molecules of the symmetry forbidden IR bands that are absent in the spectra of gaseous molecules. However, such bands are gradually developing upon diffusion - controlled adsorption since interaction of the molecules with

adsorption sites results in their polarization and makes symmetry forbidden bands IR active. Therefore, the rate of diffusion inside micro- and macropores of adsorbents and catalysts both of individual gases and of components of gaseous mixtures can be easily obtained from the time evolution of symmetry forbidden IR bands. The attractive feature of this approach is that symmetric vibrations of gaseous molecules don't contribute into IR spectra, and therefore don't create a background that hinders the proper measurements of adsorption rates.

Below we will demonstrate the utility of this approach for the study of diffusion inside micro - and macropores of different zeolites of individual components of the nitrogen - oxygen or light paraffins - hydrogen mixtures. These examples could be considered as models of industrial nitrogen - oxygen separation or hydroisomerization and cracking of light paraffins. The obtained results demonstrated that diffusion of the individual components of the above - mentioned gaseous mixtures inside micropores of zeolites is by about two orders of magnitude more slow than of the corresponding individual gases. It was also demonstrated that such transport limitations are connected with counterdiffusion of components inside macropores whereas even for NaA the diffusion limitations inside the micropores are less important.

Our experiments were carried out at room temperature for the mixtures of the above - mentioned gases of different composition. DRIFT spectra of adsorbed gases were measured with the "Nicolet Impact" spectrophotometer equipped with a home - made diffuse reflectance attachment. All of the spectra were transformed into Kubelka - Munk units whereas the backgrounds created by zeolites were subtracted. The zeolites under the study included NaA, NaZSM-5, HZSM-5 and NaLSX. Before spectral measurements they were either pressed into the very thin pellets or crashed after pressing into grains with dimensions of 0.5-1 mm. In the latter case DRIFT measurements were carried out at the bottom of the zeolite layers with the thickness of about 1 cm. Before spectral measurements the samples were evacuated for 4 hours at 673 K.

Development of DRIFT N=N stretching bands resulting from adsorption on NaLSX of pure nitrogen at atmospheric pressure is shown in Fig. 1 (a), whereas the similar results for nitrogen adsorption from air in Fig. 1 (b). The difference between the rates of nitrogen adsorption in both cases is quite impressive: nitrogen adsorption from air is about two orders of magnitude more slow than of pure nitrogen indicating a very strong retarding influence of oxygen on diffusion of nitrogen inside micro- and macropores of the zeolite.



(a)

Fig.1

(b)

To discriminate whether such transport limitations occur inside micro-, meso- or macropores, we compared diffusion – limited adsorption of nitrogen from air by the thick zeolite layers and the thin pellets. The corresponding results for kinetics of nitrogen adsorption by NaLSX in the I/I_{max} versus square root of time coordinates are presented in Fig. 2. Since dimensions of micropores inside zeolite grains and pellet are certainly the same, the slower nitrogen adsorption by the thicker layer of the zeolite grains definitely

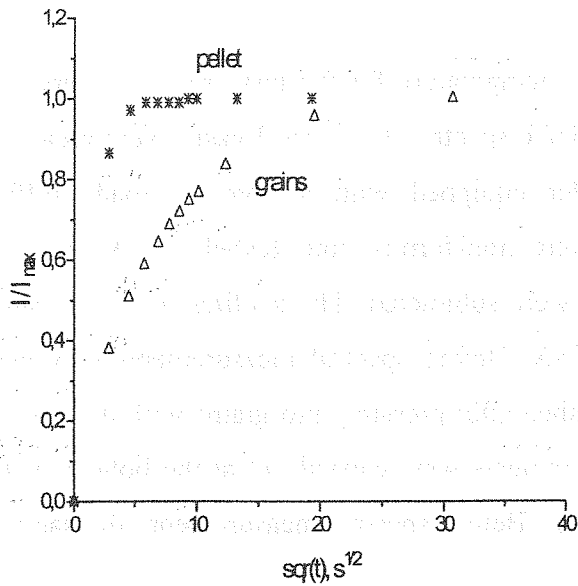


Fig.2

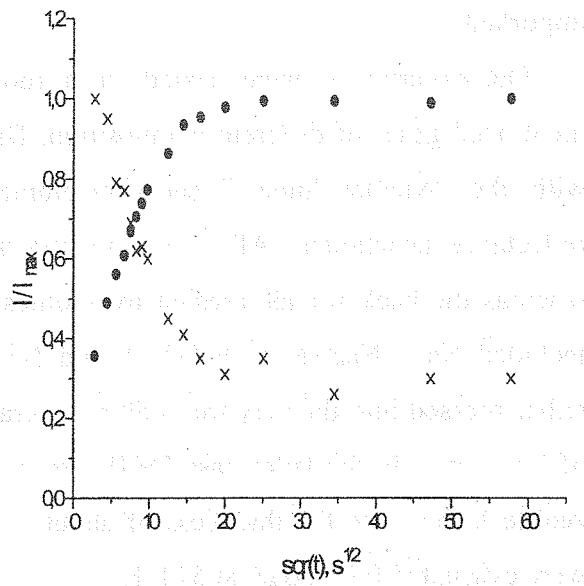


Fig.3

indicates that transport limitations are connected with counterdiffusion of nitrogen and oxygen inside meso- or macropores rather than inside micropores of the zeolite microcrystals.

Despite of the very high diffusivity of hydrogen, it also very strongly retards nitrogen diffusion in the zeolite macropores. This is illustrated by Fig. 3, where kinetic of hydrogen and nitrogen adsorption by CaA from the same 1:1 H₂ – N₂ mixture at room temperature and

atmospheric pressure is presented in the similar $1/t$ versus square root of time coordinates as in Fig. 2.

We also studied the diffusion – limited adsorption by ZSM-5 of hydrogen mixtures with light paraffins as the models for their hydrocracking or hydroisomerization. The obtained results also indicated the similar strong retarding influence of hydrogen on the diffusion – limited adsorption of light paraffins. Similar to the diffusion – limited adsorption of nitrogen from hydrogen - nitrogen mixtures, adsorption of H_2 – RH mixtures also starts with the very fast diffusion of hydrogen inside HZSM-5 micropores followed by the much slower subsequent adsorption of paraffins that in mixture with hydrogen is also about hundred times slower than for the individual substances.

Thus, the results of the present study demonstrated that diffusion of individual components of gaseous mixtures inside the pores of adsorbents and catalysts is very different from diffusion of pure gases. Diffusion of gaseous mixtures inside the pores of microporous materials is also very different from diffusion in gaseous mixtures outside the pores. Therefore, modeling of diffusion in porous materials requires special measurements, whereas utilization for this purpose of diffusion coefficients of pure gases or of their mixtures outside the pores is impossible.

References

1. J.Karger, D.M.Rutheven, "Diffusion in Zeolites and other Microporous Materials", John Wiley and Sons Inc., New York 1992.

SECTION II.
PROCESSES IN CHEMICAL REACTORS

SECTION II
PRINCIPLES OF CHEMICAL REACTIONS

DIRECT GAS-PHASE EPOXIDATION OF PROPENE WITH NITROUS OXIDE OVER MODIFIED SILICA-SUPPORTED FeO_x CATALYST

E. Ananieva, A. Reitzmann, B. Kraushaar-Czarnetzki

Institute for Chemical Process Engineering CVT, University of Karlsruhe, Germany

Kaiserstr.12, 76131 Karlsruhe; Phone: ++49-721-4266, Fax: -6118;

e-mail: Ekaterina.Ananieva@ciw.uni-karlsruhe.de

Introduction:

Propylene oxide (PO) is one of most important intermediates in the chemical industry. It was produced 5 million metric tons in 2000. The world wide growth rate of PO-production is 5 % per year [1]. The major amount of this, more than 95%, is synthesised by multiple-stage production routes. The large quantity of waste-products and the inevitable formation of a coupling product are substantial drawbacks of these industrial processes. Recently, considerable scientific effort has been invested to avoid these disadvantages and to eventually discover alternative economically more favorable manufacturing processes. Most of these new processes were conducted in the gas phase involving the direct epoxidation of propylene with different oxidants like O₂, H₂O₂, H₂/O₂ and N₂O. Some of these, for example the process using H₂O₂ (Degussa AG), have been planned to realise on an industrial scale.

The other interesting oxidant is N₂O. It is used for the production of phenol [2], for the oxidation of cumene and for the epoxidation of propene [3]. These examples prove the feasibility of the reaction with N₂O. It is apparent that these oxidation reactions are a type of vinyloxydation and only double bonds were attacked. In the present work, a direkt epoxidation of propene to propylene oxide in the gas phase with N₂O is presented. The aim has been to study the reaction network and to understand the course of the reaction. It is known that apart from PO several other substances like acetone or propanal, acrolein and CO₂ are produced in parallel by-reactions. As yet, it remains unknown wich conditions of operation and catalyst preparation (acid-base-properties) do have an influence on the product distribution.

Experimental:

The measurements were conducted in an integral isothermal fixed bed reactor (15 mm i. d.).

The reaction products were analysed quantitatively using a gas chromatograph 3800 from

OP-II-1

Varian. For the carbon balance was used after the total oxidation a CO_2 -binos. Usually, propene to N_2O ratios 1 to 15 were used. The concentration of propene was kept at 1 % all the time. The reaction temperature was varied between 350 and 520 °C. The total flow (GHSV) was set to 2, 4, and 10 $\text{l/h} \cdot \text{g}_{\text{AMCat}}$. (AMCat- =activ mass of catalyst)

As a catalyst for the direct propene epoxidation with N_2O , a Na-promoted FeOx/SiO_2 -type, was demonstrated in the work of Duma and Hönike [3]. The catalyst used in our study were based on the materials reported by Hönike and Duma [3], but we extensively modified the receipes. A special elaborate methode for the iron impregnation was used. By a pre-treatment of the catalysts in vacuum it is possible to avoid large amounts physically adsorbend water in the catalysts. This should lead to a homogeneous dispersion of the active components.

The support used was a silica gel from Merk (average pore diameter 60 Å, BET surface of 370 m^2/g). This support was impregnated by incipient wetness method with solution of Fe(III)-acetylacetonate in toluene. The iron loading (active component) of the prepared catalysts was 300 ppm. Alkaline ions (Na^+ and Cs^+ as promoter) were impregnated by the same methode as the iron-ions. The alkaline loadings were varied between 300 and 6000 ppm. Thereby, it is possible to change the acid-base-properties. Especially, the influence of the catalyst properties on the reaction pathway was investigated. Some of catalyst samples were shaped by extrusion with LUDOX (AS-40) from Du Pont and later ground and sieved to obtain 0,315 – 0,500 mm particles. All samples were calcined after every treatment like impregnation and extrusion at 600 °C (in air).

Results:

By different amounts of promoter (Na ion) an influence of the acid-base-properties on the formation of propylene oxide was observed. Figure 1 shows the selectivity (S) to propylene oxide versus conversion (X). The measurements were conducted at different values of GHSV (2, 4 and 10 $\text{l/h} \cdot \text{g}_{\text{AMCat}}$). The catalyst deactivated very fast. Therefore, only the values from the initial point of time (time-on-stream = TOS = 100 min), where the carbon balance is valid exactly, were taken into account. As can be seen, the degree of propylene oxide selectivity decreases with increasing Na ion content of the catalyst. The catalyst with a small concentration of Na ions is more active and more selective than the other catalysts, $X_{\text{Max}} = 20\%$ und $S(\text{PO})_{\text{Max}} = 40\%$. The maximum value of the selectivity to propanal was 20 %. At conversions below 10 %, the differences in PO formation between the catalysts with 300 (Δ) and 600 ppm Na ions (*) are negligible; S(PO) in both cases amounts to 40 %. On the catalyst

with the maximum amount of Na ions (6000 ppm) (\blacktriangle), only little propylene oxide was produced.

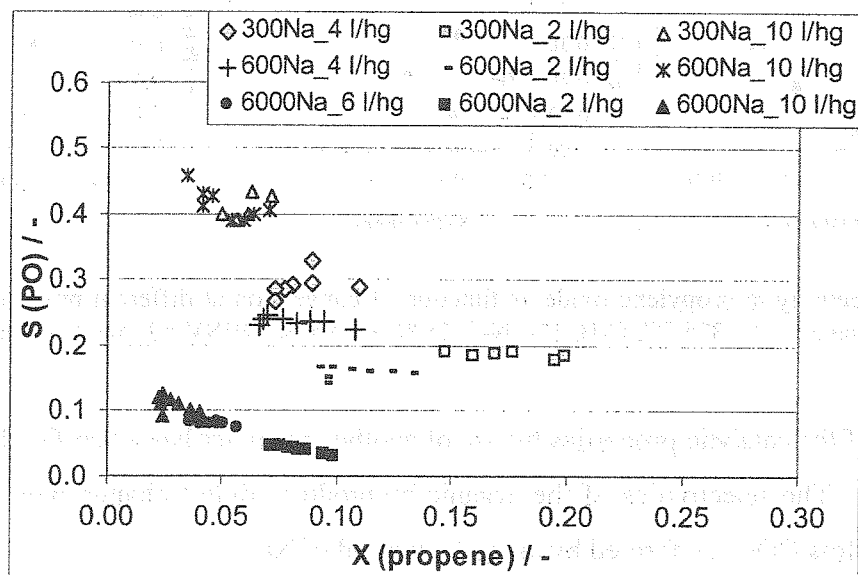


Figure 1: Selectivity to propylene oxide as function of conversion at different gas hourly space velocities and Na amounts. Reaction parameters: $T = 375\text{ }^{\circ}\text{C}$, C_3H_6 1%, N_2O 15 %, He 84 %

The selectivities to acrolein and CO_2 reach values of 30 %, both. The values were increased by around 66 % compared with the catalysts with 300 and 600 ppm sodium ions. Thereby, more coke was produced and the selectivity to propanal ($S = 5\%$) decreases to around 50 %. The variation of the properties of the catalyst has no influence on the acetone formation.

The propylene oxide can form only on the non-acidic catalyst. Surprisingly, we observe a decrease in PO selectivity when the amount of Na ions is increased.

As can be observed, the catalyst with 300 ppm Na ion is more suitable for the PO-formation than the other catalyst with higher concentrations of Na. Further, the influence of the type of alkaline was investigated by the impregnation with a cesium salt. The results obtained with the different promoter ions on the catalyst are presented in figure 2. The amount of alkali ions was kept unchanged for better comparability (300 ppm). It should be noted that the 3 plots refer to 3 different TOS. A severe catalyst deactivation can be clearly observed. The catalyst with Cs ion is more active and more selective. With Cs, it is possible to achieve a selectivity to PO of more than 50 % at conversions levels below 5 % and $S(\text{PO})$ of 20 % at conversions levels of 20 %. The other catalyst has a selectivity to PO of only 25 % at conversions levels of 2 % and $S = 5\%$ at conversion levels of 12 %.

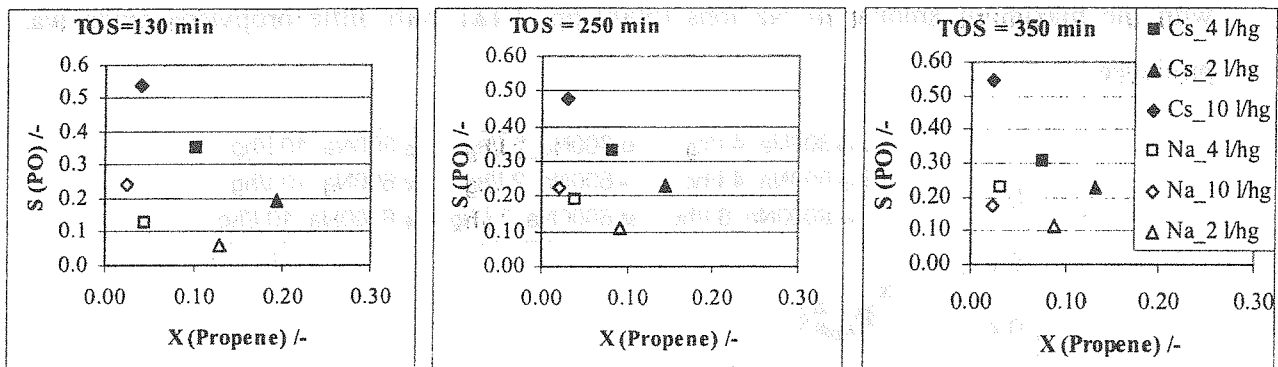


Figure 2: Selectivity to propylene oxide as function of conversion at different promoter Cs and Na. Reaction parameters: T = 375 °C, C₃H₆ 1%, N₂O 15 %, He 84 %, GHSV =2; 4 and 10 l/hg_{AMCat}.

The change of the catalytic properties by use of another promoter has a beneficial effect on the PO formation. The selectivities of the organic by-products didn't change with changing the promoter but less CO₂ was formed by using Cs instead of Na.

References:

[1] Th. Haas, W. Hofen, G. Thiele, DGMK-Tagungbericht 2001, pp. 127-130
 [2] A. Reitzmann, M. Häfele, G. Emig; Chemical Engineering Vol. 3, 1996, pp. 63-79
 [3] V. Duma, D. Hönike, Journal of Catalysis 191, 2000, pp. 93-104

OSCILLATION THEORY: EXPERIMENTAL CONFIRMATION AND CONTRADICTIONS BETWEEN THE THIELE / ZELDOVICH MODEL AND EXPERIMENTAL DATA IN LIQUID-PHASE REACTIONS

Leonid B. Datsevich

LS CVT University of Bayreuth Universitaetsstr.30, D-95447 Bayreuth, Germany

Tel.: ++49 921 55 74 32, ++49 1511 16 14 019

Fax: ++49 921 55 74 34

E-mail: Ldatsevich@web.de, datsevich@ledahim.com

The conventional description of multiphase reactions on a catalyst particle is based on the Thiele / Zeldovich model [1], proceeding from the assumptions that mass and heat transfer is carried out exclusively by the molecular mechanism (Fick's and Fourier's laws).

This model allows one to obtain the concentration and temperature profiles, the temperature difference between the centre and the surface of the catalyst particle (Prater's equation [2]) as well as the reaction rate and the heat flux from the catalyst surface as a function of the particle size, the concentration(s) on the outer particle surface, the effective diffusion coefficient(s) and the thermal conductivity.

Absolutely a new model, the oscillation theory, was recently developed [3-5]. According to this theory, under some conditions in liquid / liquid-gas reactions, the oscillatory motion of liquid should take place in pores due to the formation of gas or gas-vapor bubbles. The velocity of liquid motion can reach values of 10 m/s and even much higher. Due to such forced alternating motion of liquid, the reaction runs with the considerably higher rate than predicted by Thiele / Zeldovich model and there is a very strong influence of the reaction on the external mass transfer of reacting compounds to the catalyst surface.

Under conditions of intensive oscillations, the equation for the reaction rate on a single catalyst particle can be expressed as $r_{obs} \sim (r_{true}(C_s))^{1/2}$ where $r_{true}(C_s)$ is the reaction rate without intraparticle diffusion limitation.

In this paper, main notions of the oscillation theory are given. The oscillation behaviour (oscillatory motion of liquid in catalyst pores and capillaries, catalyst destruction by cavitations in pores) will be demonstrated in several experiments during the presentation. The

following experimental data that contradict to the conventional models and theories are discussed:

1. The heat flux from the catalyst surface in experiments of hydrogenation of 1-octene to n-octane is about 80 times more than the heat flux estimated by the Thiele model.
2. The temperature difference between the centre of the particle and its surface directly measured at hydrogenation of 1-octene to n-octane is four to nine times more than the maximum possible difference defined by Prauter's equation.
3. The reaction rate observed in hydrogenation reactions of 1-octene, acetone, 2,4/2,6-dinitrotoluene, furfural and hydrogen peroxide decomposition has absolutely different dependence than the reaction rate predicted by the Thiele model.
4. There is a very strong influence of the chemical reaction on external mass transfer in hydrogenation reactions (1-octene, acetone and furfural) as well as in reactions with gas production (hydrogen peroxide decomposition, leaching process at activation of Ni-Al catalyst).
5. There is a hysteresis in hydrogenation reaction of 2,4-dinitrotoluene [6].

The directions of the process intensification and catalyst improvement, which follow from the oscillation theory, are discussed in [3,4]. The first experimental results of the process enhancement according to the theory are presented.

References:

- [1] C.N. Satterfield, Mass Transfer in Heterogeneous Catalysis, MIT Press, Cambridge, 1970.
- [2] C.D. Prauter, The temperature produced by heat of reaction in the interior porous particle, Chem. Eng. Sci. 8 (1958) 284-286.
- [3] L.B. Datsevich, Oscillations in pores of a catalyst particle in exothermic liquid (liquid-gas) reactions. Analysis of heat processes and their influence on chemical conversion, mass and heat transfer, Appl. Catal. A 250 (2003) 125-141.
- [4] L.B. Datsevich, Alternating motion of liquid in catalyst pores in a liquid / liquid-gas reaction with heat or gas production, Catal. Today 79-80 (2003) 341-348.
- [5] L.B. Datsevich, Some theoretical aspects of catalyst behaviour in a catalyst particle at liquid (liquid-gas) reactions with gas production: oscillation motion in the catalyst pores, Appl. Catal. A 247/1 (2003) 101-111.
- [6] Rajashekharam M.V., Jaganathan R. & Chaudhari R.V., A trickle-bed reactor model for hydrogenation of 2,4 dinitrotoluene: experimental verification. Chem. Eng. Sci. 53 (1998) 787-805.

STUDY OF VISBREAKING OF ATMOSPHERIC RESIDUE DERIVED FROM WAXY CRUDE OIL

M.A. Edreder* and S.M. Eldabah

***Email :** mahdred@hotmail.com , **Fax :** 0218-21-4836820, 0218-4830031

Petroleum Research center -Tripoli- Libya , BOX: 6431

Keywords: Visbreaking, Stability, Thermal Cracking, Residue, Coil Reactor,soaker.

Abstract

Visbreaking is a mild thermal cracking process with the principal objective to reduce the viscosity and pour point of residual fuel oil and heavy crude oil. Other main benefits of this process include an increase in the production of more valuable distillate products and a corresponding decrease in the production of less valuable residual fuel oil. The aim of this paper is to study the effect of cracking temperature and residence time on the yield and stability of visbroken products. For the purpose of realizing the said objectives, a pilot plant set-up consisting a coil reactor and a soaker drum was utilized. The experimental work was performed on atmospheric residue (340°C) derived from waxy crude oil. Feedstock and visbroken products were characterized for their physico-chemical properties such as specific gravity, viscosity, pour point, asphaltene and CCR. Cracking temperature, residence time and conversion were correlated using simplified kinetic model.

A MODEL OF MULTIFUNCTIONAL REACTOR FOR PARTIAL OXIDATION OF METHANE TO METHANOL

Kafarov V., Dallos C.

*Chemical Engineering Department, Universidad Industrial de Santander,
Bucaramanga, Colombia,*

Tel: (57) –(097)- 6344746, Fax (57) –(097)-66344684, E-mail: kafarov@uis.edu.co.

The problem

Costs of many industrial chemical processes are unfavourably influenced by the equilibrium limitations of the involved reactions. This influence is expressed in high additional costs for the separation of non-converted reactants from the reactor outlet product and their recycling to the reactor inlet. In conventional industrial processes of the methanol syntheses, the desired product must be separated from the reactor outlet mixture by condensation. The heat-transfer coefficients in condensers are reduced by the presence of the inert non-converted reactants, increasing the required cooling area. The flows through the reactor are increased because the non-condensed gases are recycled to the reactor. Due to this recycling, the pressure drop over the reactor and the condensers is increased and so the energy required for the compression of the recycle stream. Long reactor lengths are required because in the reactor the equilibrium is approached and consequently reaction rates are reduced, increasing again the pressure drop and the energy demand. Additional energy is required for cooling and heating over again the non-converted gaseous reactants in and after the condensing section [1-2].

Partial oxidation of methane

The direct partial oxidation of methane to methanol is one of the most promising routes of natural gas conversion into more easily transportable fuels and valuable chemicals [3-6]. The process may be accomplished with both catalytic and homogeneous conditions. In the last case high pressures exceeding 50 atm are necessary for appropriate product yield.

Being an exothermic reaction, the direct conversion of methane to methanol would be superior to the conventional industrial process for the production of methanol via syngas by steam reforming of methane in terms of energy efficiency. Technoeconomic evaluation has

demonstrated that, giving over 70% methanol selectivity at 8–15% methane conversion, the direct process is able to compete with the indirect one. Unfortunately, most of the reported methanol selectivity shaves not broken through 70%, while methane conversions were always below 5% when high methanol selectivity was obtained. The gas phase partial oxidation of methane is operated by a free radical mechanism, which is extremely hard to control. Therefore, it is expected that the participation of catalyst would improve methanol selectivity and yield. But until now, the catalytic reaction has not produced yields of methanol plus formaldehyde better than those reported gas phase process, except for a few good reports.

Process intensification

Process intensification is the strategy of making significant reductions in the size of a chemical plant in order to achieve a given production objective. Innovations in catalytic reactors, which constitute the heart of such process technologies, are often the preferred starting point. The integration of chemical reaction and physical separation in one single unit often leads to a significant reduction in investment and operating costs. The economic benefit may be caused by a reduction of raw material use, diminution of recycle streams by higher rates of conversion, improvements in selectivity and/or energy integration [7-9].

A very interesting type of application is a multifunctional reactor, in which fine adsorbent trickles through the fixed bed of catalyst remove selectively in-situ one or more of the products from the reaction zone. In case of the methanol synthesis from syngas, this led to conversions significantly exceeding the equilibrium conversions under given conditions [1, 10].

A reactor's model for intensification of partial oxidation of methane

In this work we will formulate a steady-state model for a reactor that intensifies reactions by adsorption, and discuss the influence of various process parameters on the behaviour of the reactor. We apply our model to the case of the partial oxidation of methane to methanol with a silica-alumina powder as the methanol adsorbent. The parameter identification of the adsorbent was developed using the method proposed by the authors in previous works [11-13].

The purpose of the present computational study was to analyse the effects of various operating parameters, such as temperature, residence time, adsorbent parameters and reactive input ratio on the CH_3OH formation.

To obtain the reactor model, we simulated the adsorption processes on the adsorbent, the homogeneous or heterogeneous phase reactions, and also optimized the conversion of the reaction. Likewise, we worked varying the configuration of the equipment, the physical characteristic and the method of supply of the adsorbent and the conditions of pressure, temperature and feed input.

The characteristics of designed equipment depend in great measure of the kinetic path chosen for the reaction. This can include the choice of a catalyst for the partial oxidation of methane, the selection of the partial oxidation of the methane with O_2 at high or low temperature, or any other path.

The computations were made on Pentium IV PC using GAMS with solver CONOP. It was shown that these reactors could achieve high conversion of methane to methanol, despite the unfavourable thermodynamics equilibrium. So the particle use of this model opens new possibility for process intensification of one of the most important industrial processes, the methanol syntheses.

References

1. A. Stankiewicz. "Reactive separations for process intensification: an industrial perspective". *Chemical Engineering and Processing*, 42 (2003), 137-144.
2. K. Roel Westerterp, Michal Kuczynski, Charles H. M. Kamphuis. "Synthesis of Methanol in a Reactor System with Interstage Product Removal". *Ind. Eng. Chem. Res.*, Vol. 28, No. 6, 1989.
3. Qijian Zhang, Dehua He., Jinlu Li, Boqing Xu, Yu Liang, Qiming Zhu. "Comparatively high yield methanol production from gas phase partial oxidation of methane". *Applied Catalysis A: General*, 224 (2002), 201-207
4. Tetsuya Takemoto, Dehua He, Yonghong Teng, Kenji Tabata, Eiji Suzuki. "The optimization of methanol yield in direct selective oxidation of methane with O_2 and NO in the presence of Cu-ZnO/ Al_2O_3 ". *Journal of Molecular Catalysis A: Chemical*, 179 (2002), 279-286.
5. Neil R. Foster. "Direct catalytic oxidation of methanol to methanol - a review". *Applied Catalysis*, 19 (1985), 1-11.
6. G.A. Foulds, B.F. Gray. "Homogeneous gas-phase partial oxidation of methane to methanol and formaldehyde". *Fuel Processing Technology*, 42 (1995), 129-150.
7. G. Schembecker, S. Tlatlik. "Process synthesis for reactive separations". *Chemical Engineering and Processing*, 42 (2003), 179-189.
8. Martin P. Elsner, Christoph Dittrich, David W. Agar. "Adsorptive reactors for enhancing equilibrium gas-phase reactions - two case studies". *Chemical Engineering Science*, 57 (2002), 1607-1619.
9. Y. Ding, E. Alpay. "Adsorption-enhanced steam-methane reforming". *Chemical Engineering Science*, 55 (2000), 3929-3940.
10. M. Kuczynski, M. H. Oyevaar, R. T. Pieters, K. R. Westerterp. "Methanol synthesis in a countercurrent gas-solid-solid trickle flow reactor. An experimental study". *Chemical Engineering Science*, Vol. 42 (1987), No. 8, 1887-1898.
11. Viatcheslav Kafarov, Carlos Dallos. "Mathematical method for analysis of dynamic processes in chemical reactors." *Chemical Engineering Science*, Vol. 54 (1999), 4669-4678.
12. Viatcheslav Kafarov, Carlos Dallos. "New method for computer aided analysis of steady state multiplicity of catalytic processes". *Computers and Chemical Engineering*, Vol. 22 (1998), S659-S662.
13. Viatcheslav Kafarov, Carlos Dallos. "Computer aided method for construction of kinetic models of chemical reactions, based on application of Chebyshev-Hermite polynomials". *Computers and Chemical Engineering*, Vol. 22 (1998), S663-S666.

SYSTEMATIC MODELLING AND NONLINEAR ANALYSIS OF MEMBRANE REACTORS

Michael Mangold^a, Fan Zhang^a, and Achim Kienle^{a,b}

*a*Max-Planck-Institut für Dynamik komplexer technischer Systeme, Sandtorstraße 1,
39106 Magdeburg, Germany

*b*Otto-von-Guericke-Universität Magdeburg, Lehrstuhl für Automatisierungstechnik und
Modellbildung, Universitätsplatz 2, 39016 Magdeburg, Germany

1. Introduction

Membrane reactors are a comparatively new class of chemical processes that, in comparison with traditional reactor types, may offer advantages with respect to conversion, yield, and selectivity (Saracco et al. 2000). The two basic operation principles of membrane reactors are (a) selective product removal across the membrane and (b) side injection of reactants. In the first case, the membrane serves as a separating unit that shifts the reaction equilibrium of an equilibrium limited reaction to the product side and thereby enhances the conversion. In the second case, the distributed feeding of reactants can increase the yield of an intermediate product in a consecutive reaction. The potentials and limitations of membrane reactors are still subject to current research. This contribution addresses questions of the model based design of membrane reactors and outlines some nonlinear and dynamic phenomena occurring in membrane reactors. In the first part, a general framework for the systematic modelling of membrane is presented that underlies a tool for the computer assisted model development. The second part discusses the possibility of incomplete conversion in membrane reactors with selective product removal. The third part concerns the formation of spatiotemporal patterns in membrane reactors with side injection.

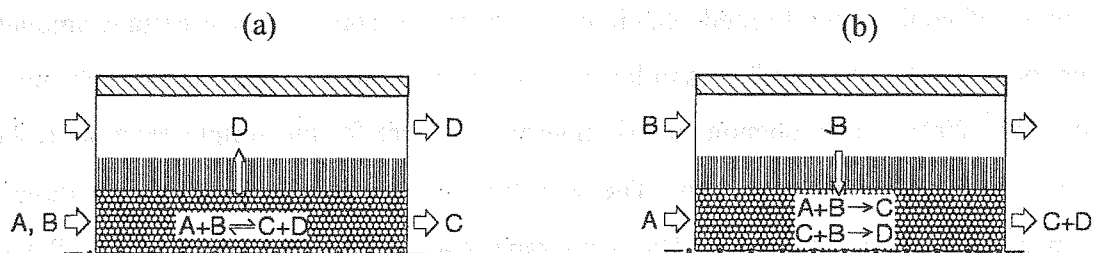


Figure 1. Basic schemes of membrane reactors; (a) selective removal of products to increase conversion; (b) side injection of a reactant to increase the yield of an intermediate product C

2. Systematic and computer assisted modelling of membrane reactors

The behaviour of membrane reactors depends on complex interacting processes like chemical reaction, mass transport through porous media, adsorption and surface diffusion effects. A realistic description of such a reactor requires detailed physical models whose development and implementation is a challenging and time consuming task. A computer tool is desirable that supports the model development process and relieves the model developer from algebraic manipulations and coding work. Such a tool has been developed for the modelling of membrane reactors with porous membranes and gaseous reactants (Mangold et al. 2003). The user of the tool no longer specifies his model in terms of algebraic and differential equations, but in terms of physical phenomena like 'mass transport according to the dusty gas model'. Based on the physical assumptions of the user, the computer tool generates the underlying balance equations including consistent boundary conditions and converts them to simulation code. In the future, the tool is going to be extended to electrochemical reactors and fuel cells.

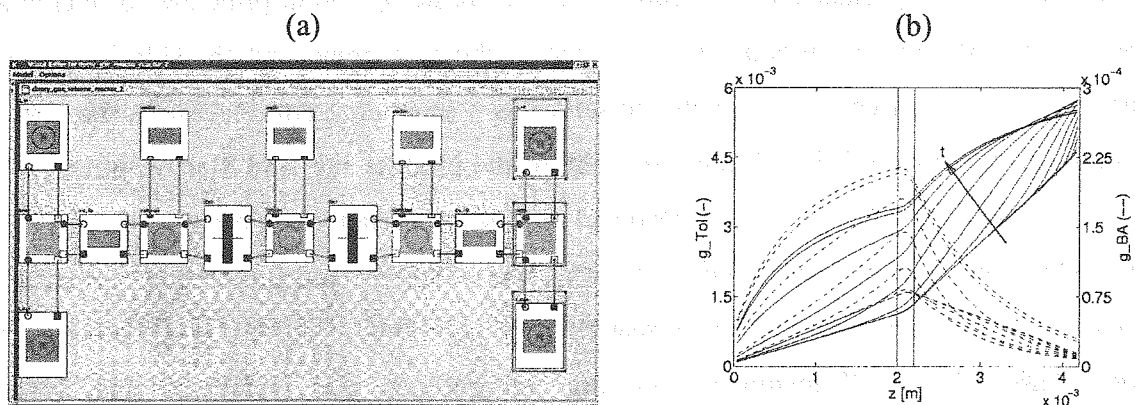


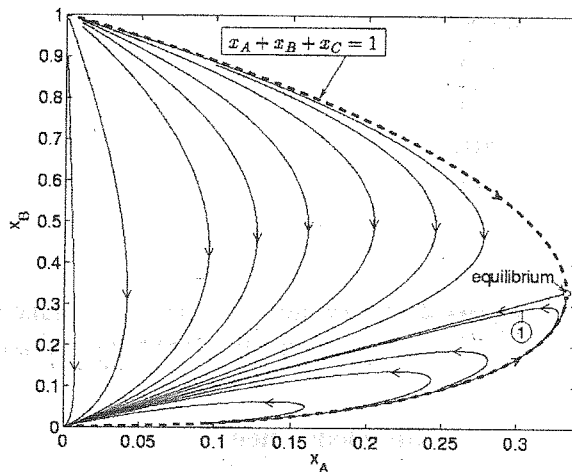
Figure 2. Implementation of a dynamic spatially distributed membrane reactor model in ProMoT; (a) screenshot showing the structured model; (b) result of a dynamic simulation: response of concentration profiles to a pressure change.

3. Conversion of equilibrium reactions

The product removal across a permeable selective membrane aims at increasing the conversion of equilibrium limited reactions. However, in some cases a certain amount of conversion cannot be exceeded, similar to azeotropic points in distillation (Huang and Sundmacher, 2003). This phenomenon is investigated here for the simple example reaction $2A \rightleftharpoons B + C$ under isothermal conditions. The mass transport through the membrane is described by a linear driving force approach. The membrane is assumed to be permeable for B and C , but impermeable for A . Concentrations of the products B and C on the sweep gas side are neglected. Despite those favourable conditions, the conversion of A remains incomplete, if the

mixture consists totally of the three reactants, the steady state composition always tending to an equilibrium point shown in Fig.3. The reason for that behaviour can be seen in the changing flow rate along the reactor coordinate. Adding an inert that cannot penetrate the membrane can circumvent the point of incomplete conversion.

Figure 3. Steady state profiles for the equilibrium reaction $2A \rightleftharpoons B + C$ in a phase diagram. Despite the selective permeability of the membrane to B and C , total conversion of A cannot always be achieved.



4. Pattern formation due to side injections

Nekhamkina et al. (2000) pointed out the analogy between the dynamic behaviour of a classical CSTR and the steady state behaviour of a plug flow membrane reactor with side injections, constant flow rate, and a non-selective membrane. In this contribution, a detailed reaction mechanism for the selective oxidation of ethane from (Klose et al., 2003) is used to demonstrate that the spatiotemporal patterns found by Nekhamkina et al. (2000) for simple model reactions may occur for partial oxidations of hydrocarbons in membrane reactors. Furthermore, the analysis is extended to reactor models with variable flow rate and the limiting case of a chemical reaction in equilibrium due to an infinite reaction rate. It is shown that the assumption of reaction equilibrium can cause discontinuous patterns (Fig. 4 a). Under dynamic conditions, those discontinuities can arise as a response to small disturbances around an unstable steady state (Fig. 4 b). The disturbances lead to gradually sharpening inhomogeneities in the temperature and concentration profiles that finally end in vertical temperature and concentration fronts. In this sense, the discontinuities are similar to shock waves in hyperbolic systems. However, the source of the discontinuities is not a nonlinear wave propagation velocity, but a singularity on the left-hand side of the balance equations.

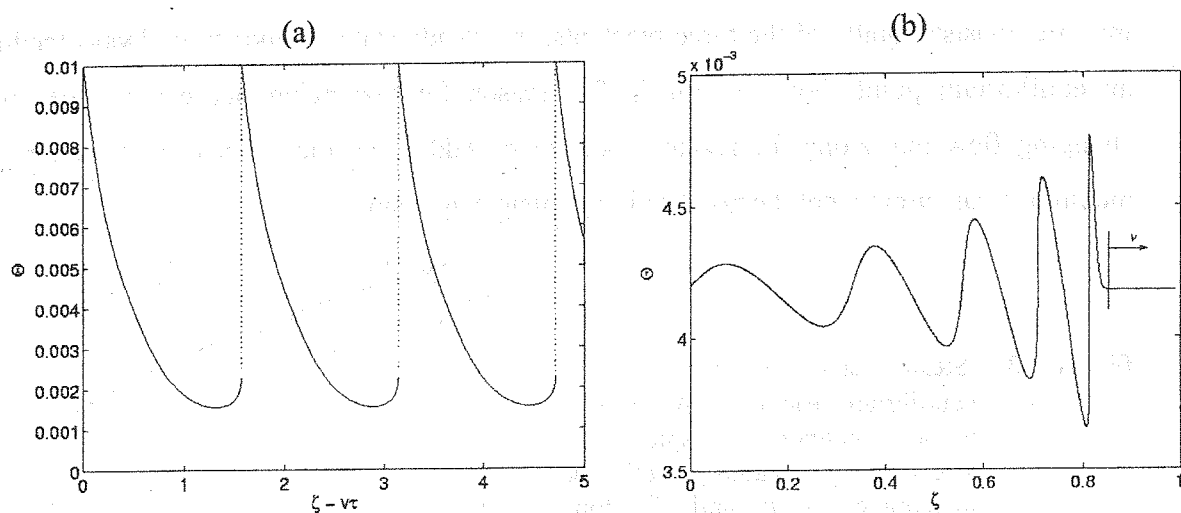


Figure 4. Pattern formation in a membrane reactor with equilibrium reaction $A \Delta B$; (a) discontinuous periodic solution; (b) transient space profile during the evolution of a discontinuous pattern.

Acknowledgement

The financial support by the Deutsche Forschungsgemeinschaft in the framework of the joint research project 447 “Membrane Supported Reaction Engineering” is gratefully acknowledged.

References

1. Huang, Y., Schlünder, E.U., and Sundmacher, K. (2003). Mass transfer effects on the residue curve maps for membrane reactors. *Proceedings of ISMR3-CCRE18, Bath 27-29 August 2003*, 175-176.
2. Klose, F., M. Joshi, C. Hamel, A. Seidel-Morgenstern (2003). Selective oxidation of ethane over a $VO_x/\gamma-Al_2O_3$ catalyst – investigation of the reaction network. *Applied Catalysis A – General*, submitted.
3. Mangold, M., Ginkel, M., Gilles, E.D. (2003). A model library for membrane reactors implemented in the process modelling tool ProMoT. *Computers and Chemical Engineering*, in press.
4. Nekhamkina, O., Rubinstein, B., Sheintuch, M. (2000). Spatiotemporal patterns in thermokinetic models of cross-flow reactors. *AIChE Journal*, 46, 1632-1640.
5. Saracco, G., Neomagus, H., Versteeg, G., and van Swaaij, W. (2000). High-temperature membrane reactors: Potentials and problems. *Chemical Engineering Science*, 54, 1997-2007

POSSIBILITIES FOR OPTIMIZATION OF TECHNOLOGICAL MODES FOR ETHYLENE POLYMERIZATION IN AUTOCLAVE AND TUBULAR REACTORS

Ju.N. Kondratiev*, S.S. Ivanchev**

* *Central R&D Institute of Complex Automation, Moscow, Russia*

** *St-Petersburg Department of the Boreskov Institute of Catalysis
of the Siberian Branch of the Russian Academy of Sciences*

14, prospect Dobrolubova, 197198, St-Petersburg, Russia

Fax +7 812 2330002, Email: ivanchev@SM2270.spb.edu

Results of the experimental studies on high pressure ethylene polymerization at industrial autoclave and tubular reactors are considered using various peroxides and their mixtures with oxygen as initiators.

A possibility for the process improvement providing the increase of conversion, productivity and versatility of the obtained polyethylene brands is demonstrated.

According to the experimental data for the processes performed in single- and two-zone mixing mode reactors the initiator consumption, temperature profile stability and possibilities for rapid control over the process are analyzed depending on the type of the used peroxides or their complex mixtures.

The kinetic features of the applied initiating systems are shown to be capable of considerably affecting the technical and economic characteristics of the process and versatility of the produced polyethylene brands.

Peculiarities of ethylene polymerizations in tubular reactors using the initiators either individually (stepwise initiation) or in a complex (mixed) initiation modes are revealed and considered.

The heating agent used in the reactors is shown to retard the polymerization rate growth under certain initiation conditions.

The limitations to the optimum concentration of primary radicals yielded by the initiator degradation are defined in accordance with the requirements to the obtained polymer quality and initiation efficiency.

In the case of complex initiation the polymerization rate profile along the tubular reactor zones is considered with the comparative analysis of the activation energy of the initiators in the areas of maximum rates.

MATHEMATICAL MODELING OF NONLINEAR PHENOMENA DURING THE REACTION OF CO OXIDATION OVER Pt-GROUP CATALYSTS

E.S. Kurkina, N.L. Semendyaeva

*Moscow State University, Department of Computational Mathematics and Cybernetics,
Moscow 119992, Russia*

Tel.: +7 095 939 4079, Fax: +7 095 939 2596, E-mail: elena.kurkina@cs.msu.su

In the present study, the $\text{CO}+\text{O}_2$ reaction over Pt-group metals including the Langmuir-Hinshelwood mechanism of CO oxidation and metal oxide formation and removal (TSM reaction scheme) is considered.

Mathematical models of various space scales are constructed and investigated in order to explain different types of experimentally observed oscillations in the rate of CO_2 production, spatiotemporal pattern formation and chemical wave propagation. Both stochastic and deterministic approaches are suggested.

A microscopic stochastic model describes the dynamic behaviour of a small scale lattice-gas $\text{CO}+\text{O}_2$ reaction model on an atomic space scale. A mesoscopic stochastic simulations is a Markovian process of elementary reaction steps over a spatially homogeneous cell of surface of mesoscopic size. The corresponding deterministic limits of stochastic models for large particle numbers represent mean-field rate equations (MF) for one single surface cell or mean-field reaction-diffusion equations (RDE) for several cells.

By means of a numerical bifurcation analysis of developed deterministic models and stochastic simulations the fluctuation-induced transitions, kinetic oscillations, reaction rate propagation are investigated. The effect of internal fluctuations, diffusion length and cell size is considered.

HYDROGENOLYSIS OF ORGANOHALOGEN COMPOUNDS OVER BIMETALLIC SUPPORTED CATALYSTS

V.I. Simagina, I.V. Stoyanova, A.G. Gentsler, E.S. Tayban, O.V. Netskina

Boreskov Institute of Catalysis, Pr. Acad. Lavrentieva, 5, 630090, Novosibirsk, Russia

The disposal of organic wastes containing halogen has become a major environmental problem, because most of them are toxic and thermally stable accumulate in surroundings for the long periods of time. Catalytic hydrodehalogenation, also called hydrogenolysis, with heterogeneous catalysts is recognized as a facile and efficient procedure. However, the practical application of catalysts to the hydrodechlorination of organic halides is always accompanied by the problem of the deactivation of the catalysts due to hydrogen chloride formed as by-product in the reaction. For practical use, the development of catalysts that maintain their catalytic activity for a prolonged time is an essential problem.

The aim of this work was designing and investigation the catalytic system with enhanced resistance to corrosion giving, at the same time to the catalyst both high activity and stability.

In this sense this problem was decided

- (i) at employment of bimetallic catalysts (the changing physicochemical characteristics of the metal atom are modified of a second metal)
- (ii) change the properties of the supports (doping Na species on the catalyst surface) using phase – transfer agent

Monometallic and bimetallic supported catalysts, which contain Pd with Pt, Fe, Ni or Co were prepared by precipitation of metals from their solution of corresponding metal salts with following low-temperature reduction by NaBH_4 . We used a carbonaceous material, called "Sibunit", as the support. Activity and stability of the catalysts was investigated in reactions of the liquid phase hydrodechlorination of chlorobenzene and hexachlorobenzene.

In our study liquid-phase hydrodechlorination of hexachlorobenzene carried out in the presence phase – transfer (PT) agent. Using PT agents leads to considerable increasing the rate of hydrodechlorination (table 1) and allows carrying out reaction under mild condition at hydrogen atmospheric pressure and 50°C . As phase – transfer agents we used alkylammonium salts. From results (table 1) follows that the highest activity of catalytic system we obtained in the presence of tetramethylammonium chloride. The role of phase

OP-II-8

transfer is not clearly. We suggest that strong alkaline media quickly removes HCl produced in reaction adsorbed on the surface of catalysts. Its possible, as result Phase-Transfer agent transfers OH anion (alkali) from aqueous phase to surface of catalyst, so allowing a faster regeneration of the catalyst surface [1].

Table 1. Conversion hexachlorobenzene in the presence of alkylammonium salts; catalyst $\text{Ni}_{95}\text{Pd}_5/\text{C}$; $\text{S}(\text{C-Cl})/\text{Cat}$ ratio, 10:1; $T=50^\circ\text{C}$, 50% KOH; $p_{\text{H}_2}=1$ atm; solvent, isopropanol-toluene, 4:7 (15 ml)

PT agent	Conversion hexachlorobenzene to benzene after 90 min
$(\text{C}_8\text{H}_{17})_3\text{N}^+\text{CH}_3\text{Cl}^-$ (Aliquat 336)	74
$(\text{CH}_3)_4\text{N}^+\text{Cl}^-$	100
$(\text{C}_2\text{H}_5)_4\text{N}^+\text{Cl}^-$	35
$(\text{C}_2\text{H}_5)_3\text{N}^+\text{OH}^-$	42
—	20

Transition metals supported on various materials are used commonly as hydrodechlorination catalysts. It was determinate the activity of monometallic catalysts in chlorobenzene hydrodechlorination. Obtained results permitted to build the following order of transition metal with regards to the decreasing activity $\text{Pd}/\text{C} > \text{Ni}/\text{C} > \text{Co}/\text{C} > \text{Ti}/\text{C} > \text{Fe}/\text{C}$. It was shown that Pd is the most efficient metal for hydrodechlorination.

These results according to literature data followed that successful dechlorination of polychlorinated compounds by using Ni catalysts requires severe reaction condition – high temperature and high hydrogen pressure Pd catalysts permitting successful dechlorination of polychlorinated aromatic compounds under mild condition are not feasible for large-scale application because of its high cost. Designing a cheaper but selective catalyst to convert organohalogen compounds into useful products with using bimetallic Pd-Ni/C catalysts appears to be possible.

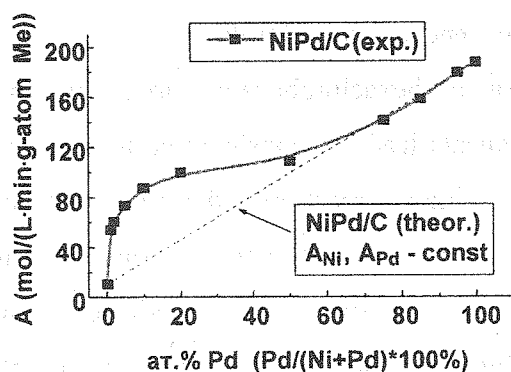


Fig. 1. Activity of nanodispersed $\text{Pd}_x\text{Ni}_y/\text{C}$ catalysts (reducing NaBH_4) in the hydrodechlorination of chlorobenzene depending on Pd concentration (at%)

Fig. 1. shows the dependence of the bimetallic catalysts activity and mixture of monometallic catalysts on Pd concentration. From these results following that activity of bimetallic catalysts shows nonadditive effect relative to the mixtures of Pd and Ni catalysts at Pd content as from 1 to 40%.

For understanding of the reason lead to increasing of activity bimetallic Pd-Ni catalysts we preparing several of bimetallic catalysts from metalloorganic precursor and carefully investigated them. Here we see results of characterization of catalytic samples be chemical analysis X-ray diffraction and analytical electronic microscopy. Using analytical electronic microscopy allows to determinate of metal surface concentration. The data follows that outmost surface of catalysts is enriched in Pd. Thus it was found that In Pd-Ni alloys Pd has a strong tendency to migrate at the surface. Such surface segregation of bimetallic alloy open the way to new generation of catalysts with «tuned» surface, highly concentrated in the active component for given reaction, in our case Pd and in this case we have economic benefit [2].

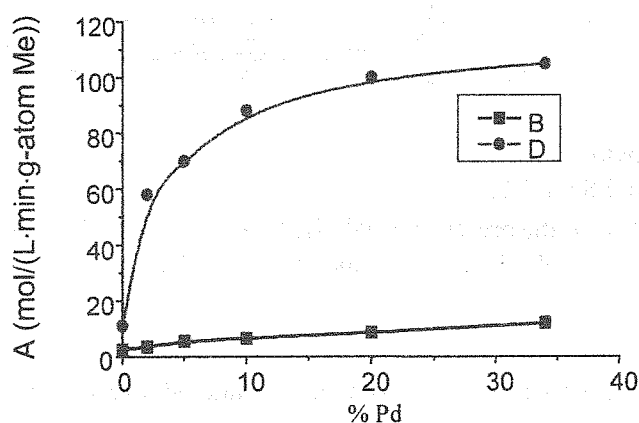


Fig. 2. Dependence of the Activity of bimetallic NiPd/C catalysts on Pd concentration
 B – catalyst by H_2 from metalloorganic compounds
 D – catalyst reduced by $NaBH_4$ at $20^\circ C$ from metal chloride

The dependence (Fig. 2) demonstrate that catalysts prepared from metal salts and reduce by $NaBH_4$ higher active than catalysts prepared from metalloorganic compounds and reduce by hydrogen in the hydrodechlorination of hexachlorobenzene. These data can indicate that sodium addition increased catalytic activity. From results obtained with X-ray Photoelectron Spectroscopy and XRD study follows that hydrogen chloride formed during reaction can be neutralized by sodium supported on catalyst surface (from $NaBH_4$). Indeed formation $NaCl$ was detected by XRD and XPS. We suggest it is very impotent at the beginning of reaction and sodium adsorbed onto the carbon keeps the metals particles clean of chloride ions allowing the reaction to proceed up to high hexachlorobenzene conversion. These results according to literature data about increasing catalytic activity with modification supports by Na [3].

Prepared bimetallic catalysts shows activity in hydrodechlorination environmentally problematic compounds such as polychlorobiphenyls. Sovtol-10 is a common commercial biphenyl pollutant mixture that contain a fraction of environmentally persistent tetra-, penta- and hexachlorinated biphenyl and therefore is an especially significant mixture for reductive dechlorination. Figure 3 shows the chromatomass spectroscopy of commercial Sovtol-10 before and after reaction over bimetallic PdNi catalyst. We can see high conversion polychlorinated biphenyl to biphenyl can be achieved.

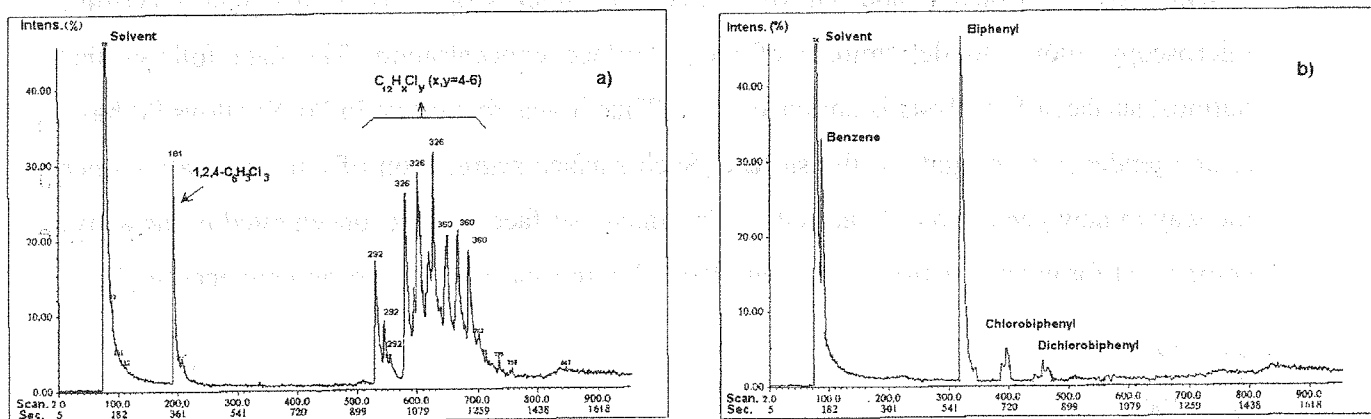


Fig. 3. Hydrodechlorination of Commercial Sovtol-10

a) The initial solution of dielectric liquid Sovtol-10

b) The same solution after 3 hour reaction in the presence of Pd₂Ni₉₈/C at 50 °C and 10 atm H₂. (It was determinate that mixture of polychlorobiphenyls contained 54 wt.% Cl and 46 wt.%(C+H).

According to these results it could be possible to design active and stable catalysts, catalytic processes for dechlorination of hydrogen of environmentally problematic compounds without production of any waste.

References

- [1] C.A. Marques, O. Rogozhnikova, M. Selva, P.Tundo, J. Mol. Cat., A. Chem., 1995, 96, 301
- [2] V. Simagina, V. Likholobov, G. Bergeret, M.T. Gimenez, A. Renouprez, Catalytic Appl. Cat. B:Environ., 2003, 40, 293.
- [3] F.J. Urbano, J.M. Martines, J. Mol. Cat., A. Chem., 2001, 173, 329.

PHASE-TRANSFER CATALYSIS: SPECIFICITY OF CONDUCTING OF HYDROCARBONS OXIDATION REACTIONS

Z.P. Pai

Boriskov Institute of Catalysis SB RAS
Russia, 630090, Novosibirsk, Akad. Lavrentiev Prosp., 5
Fax: (383) 2 34 30 56; E-mail: zpai@catalysis.nsk.su

In the present work the influence of variety of factors concerned with the modes of mixing of biphasic liquid media (*organic phase-liquid phase*) effecting upon the proceeding of the reactions of organic substrates oxidation in the phase-transfer conditions was studied. Realization of these researches was stimulated by the contradiction of the data obtained by us and other researchers, for example [1-3], when conducting reactions of cycloolefins, alcohols and unsaturated fatty acids oxidation with the 30 % hydrogen peroxide in the presence of catalysts based on the peroxopolyoxometallates in combination with quaternary ammonium cations – phase-transfer catalysts.

Mixing of two liquid phases was carried out in two ways: by the blending of liquids in a vessel by means of magnetic stirrer and by the shaking of the reactor of “catalytic duck” type fixed on the rocker.

Analysis of obtained results carried out with the assumption that, starting from the some frequencies of mixing or shaking, reaction proceeds in the kinetic region. The surface area of the phase separation border was determined by the value of product yield.

It was established experimentally that in the case of execution of the mixing by means of the magnetic stirrer at sufficiently high swiftness in addition to the target product the number of products formed as a result of side reactions present in the reaction mixture. The emerging of these products is accounted for the cavitation processes conditioned by the high speed of the activator rotation in the reaction mixture. Characteristic dimensions of the emulsified substrate species was defined at which the drastic decrease of the oxidation reactions selectivity is observed.

This work was supported by the RFBR grant №01-03-32862 and the FASTP Contract №41.015.1.2455.

References

1. C. Venturello and M. Gambaro, *J. Org. Chem.*, 1991, **56**, 20, 5924-5931.
2. Y. Ishii, K. Yamawaki, T. Ura, et al., *J. Org. Chem.*, 1988, **53**, 20, 3587.
3. Bi ying-li, Zhou Mei-juan, Hu Hong-yu, et al. *React. Kinet. Catal. Lett.*, 2001, **72**, 1, 73.

**THE CAUSE AND QUANTITATIVE DESCRIPTION
OF CATALYST DEACTIVATION
IN THE ETHYLENE OXIDE HYDRATION PROCESS**

**V.F. Shvets, R.A. Kozlovskiy, I.A. Kozlovskiy, M.G. Makarov,
J.P. Suchkov, A.V. Koustov**

*D. Mendeleev University of Chemical Technology of Russia,
Miusskaya Sq. 9, 125047 Moscow, Russia, fax: +7(095)973-31-36*

shvets@muctr.edu.ru

The ethylene glycol, producing by hydration of the ethylene oxide, is one of the main products of the basic organic synthesis with more than 15 billion t/a capacity in the world. Main disadvantages of conventional technology are: 1) Noncatalytic reaction; 2) The large excess of water ($H_2O:C_2H_4O = 15\div 20$ mol) that results to significant energy consumption during Ethylene Glycol separation.

The reason of water excess is low selectivity of noncatalytic reaction concerning Ethylene Glycol (Fig 1):

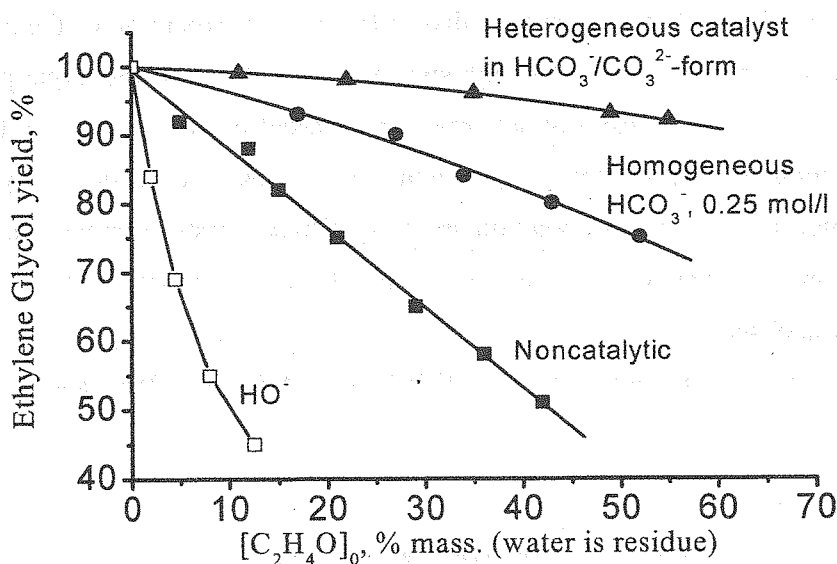
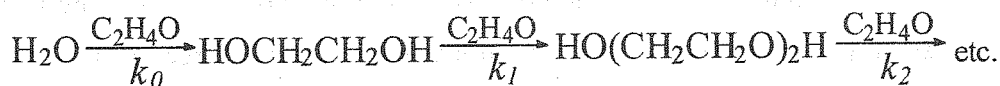


Fig. 1. Influence of catalyst type and Ethylene Oxide/Water ratio on Ethylene Glycol yield.

Recently it has been revealed that the salt forms of ion-exchanging resins may be used as selective heterogeneous catalysts [1]. These catalysts allow to sufficiently increasing the Ethylene Oxide concentration in the initial water solution without reducing selectivity and thus obtaining the high concentration of Ethylene Glycol in the reaction mixture and saving energy during separation of the product. That is why the problem to build the model for the reactor of catalytic hydration is really crucial. This model has been recently reported on ChemReactor-15 [2] but it allows describing the process in the case when catalyst properties are known.

The aim of the present investigation was to build the model for behavior of the catalyst along time to predict the catalyst lifetime and correcting the process to obtain highest activity and selectivity. The typical behavior of the catalyst activity along the time is represented on fig. 2.

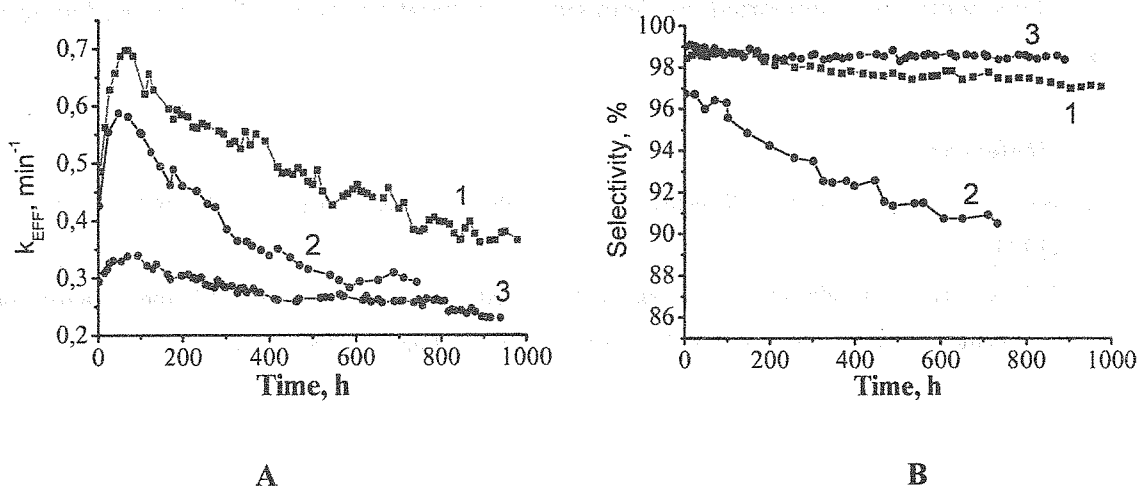


Fig. 2. Behavior of the catalyst along the time in the tube continuous reactor:

A) Pseudo first order rate constant, min^{-1} ;

B) Selectivity concerning Ethylene Glycol, %.

Experimental conditions:

1 - 105°C ; $[\text{EO}]_0 = 12\%$; 2 - 105°C ; $[\text{EO}]_0 = 20\%$; 3 - 95°C ; $[\text{EO}]_0 = 12\%$.

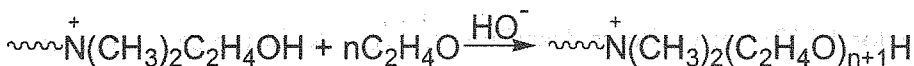
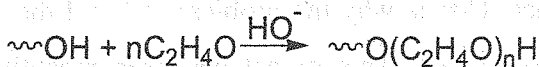
It was found that during the functioning catalyst decreases its activity due to two processes: swelling of the catalyst and loss of the active centers of the ion-exchanging resin. Basing on numerous experiments we have elaborated the mathematical model for continuous tube fixed-bed catalytic reactor for Ethylene Oxide hydration making following main assumptions:

1. The loss of the exchange capacity of catalyst is being explained by Hoffmann cleavage reaction:





2. The swelling of the catalyst is being explained by polyoxyethylation of its functional groups:



This model allow describe adequately the product distribution and predict state of catalyst (volume and capacity) vs. time. Reactor simulation gave one of the possibilities of replacing of conventional noncatalytic reactor with catalytic one, that allow to obtain of 40% Glycol stream instead of 14% and hence to exclude 4-units evaporation installation and to save about 1.4 t of high pressure steam per 1 t of Glycol.

This work was supported by Ministry of Education of the Russian Federation, grant 203.02.03.004.

References

1. Shvets V.F., Makarov M.G., Koustov A.V., and others, Russian Patent, PCT/RU99/00087, WO99/12876, (1999)
2. V.F. Shvets, I.A. Kozlovsky, A.V. Koustov, M.G. Makarov, R.A. Kozlovskiy, XV International Conference on Chemical Reactors Chemreactor-15, Helsinki, Finland, June 5-8, 2001, c 102

**APPLICATION OF NON-STATIONARY HEAT CONDITIONS
FOR RUNNING HIGH-EXOTHERMICAL CHEMICAL SYNTHESIS
IN DEVELOPMENT OF INDUSTRIAL-SCALE REACTORS**

D.S. Pashkevich

FSUE RSC "Applied Chemistry", 14 Dobrolubov ave., St.-Petersburg, Russia

e-mail: pds@peterlink.ru

A concept of stationary and non-stationary heat conditions for running exothermal chemical reactions was introduced in chemical macro-kinetics by D.A.Frank-Kamenetsky/1/. According to /1/, if the rate of heat evolution in a volume is above the rate of heat removal, such heat conditions for running exothermal reaction is called non-stationary. Under conditions $ER^{-1}T_0^{-1} \gg 1$, $E(T_{\max} - T_0)R^{-1}T_0^{-2} \gg 1$ an exothermal process runs under combustion regime when wave localization of the reaction zone able to self-propagation is observed.

Non-stationary heat conditions are widely used in special engineering and power technology for fuel combustion. Stationary conditions when all evolving heat is removed from a reacting system in the reaction zone are conventionally applied in chemical industry. This is due to that under non-stationary heat conditions the temperature in a reactor at commercially valuable output may be too high for provision thermal stability of products.

But synthesis of a number of substances which are in demand by industry is possible and expedient to carry out under non-stationary heat conditions: under conditions of combustion or heat explosion, because equipment arrangement of these processes is rather easy and a high reaction rate, realized in a high-temperature process, allows creature of apparatus of high specific output. It is of great importance for high-exothermal reactions in media of low effective heat conductivity.

For processes running under conditions of self-propagating heat wave a number of parameters determining their effective application is typical:

- preliminary mixing components to avoid diffusion regime of combustion and influencing the composition of products;
- method of initiation of a high-temperature self-propagating reaction zone which provide safe start-up of the reactor;
- rate of flame propagation which influences the industrial reactor output;

OP-II-11

- maximal temperature in the wave that determines the rate of chemical reactions and composition of wave synthesis products;
- concentration limits of flame propagation which determine process stability;
- rate of cooling the products outside the reaction zone that affects their composition.

In addition a factor of great importance that determines the construction and operating conditions of a wave reactor is phase state of initial substances.

There are examples of successful design of wave reactors for such phase systems as gas-solid body, gas-gas, solid body - solid body and gas-liquid. Application of non-stationary heat conditions for systems of liquid-liquid is inexpedient because in this case it is rather easy to provide intense heat removal from the reaction zone.

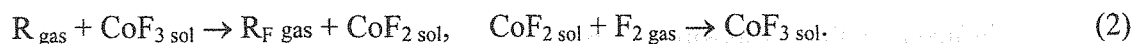
The process of industrial production of sulfur hexafluoride SF₆ from elements has been implemented in a gas-liquid system under combustion conditions:



On the basis of thermodynamic calculation it has been shown that the maximal SF₆ output is observed at a temperature up to 1000-1200K at fluorine excess. An industrial-scale reactor for this process was designed as an inclined pipe which most cross section was filled with liquid sulfur at a temperature of 150-200°C.

Fluorine was fed into a pipe segment free of sulfur at the pipe end where a stationary diffusion combustion jet of evaporating sulfur in fluorine was formed without initiation. Sulfur hexafluoride yield (up to 95%) was maximized by choosing the temperature of diffusion flame. For that a height of gas segment in the reactor and the reactor slope towards horizontal plane as well as fluorine discharge rate were changing. In Russia there were constructed two large production of sulfur hexafluoride: 500 ton facility at JSC "Halogen" and 450 tons facility at JSC "Kirovo-Chepetsky Khimichesky Kombinat".

A number of processes of fluorination of hydrocarbons with CoF₃ was implemented in a gas-solid body phase system under combustion conditions. In these processes a gaseous substance is fed on a fixed bed of CoF₃ in which a following wave of filtration combustion is formed where fluorination of raw material occurs and CoF₂ is formed, the latter is regenerated in the same reactor also under conditions of following wave of filtration combustion:

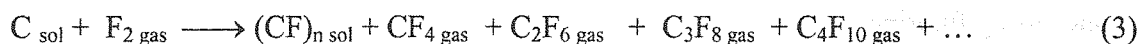


Initiation of filtration combustion was realized by setting CoF₃ powder initial temperature of about 100°C. It made possible to avoid a slip of raw material through the combustion wave along the frozen layer of the reactor wall. The maximal wave temperature, at which

destruction of carbon skeleton of substances to be fluorinated is small, was 450-500°C. The wave velocity was from 0.5 to 5 at a gas velocity of from 20 to 200 mm·min⁻¹.

Filtration combustion conditions have been applied for synthesis units of annual output of 10 tons for C₃F₈ production from C₃F₆ at Experimental plant of RSC "Applied Chemistry" (EP RSC AC) and for a production unit of annual capacity of 25 tons at JSC "Halogen" as well as for a unit of perfluorodecalin C₁₀F₁₈ production of annual output of 2 tons at EP RSC AC.

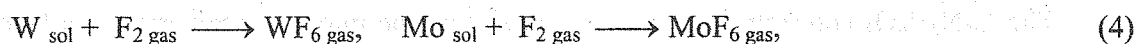
One more large-scale development in the field of application of combustion conditions in a high-exothermal system of gas-solid is a technology to produce CF₄ from elements:



For CF₄ production there was designed a reactor with a graphite fixed bed in which graphite fluorination was carried out in inverse wave of filtration combustion. In order to avoid formation of undesired admixtures according to equation (4) and to provide safe start up of the reactor, initiation of synthesis wave is realized by burning a propane-butane mixture in fluorine flow by means of an injector of a special construction. After formation of the high-temperature reaction zone, feeding the propane-butane mixture is stopped and CF₄ synthesis is carrying out. The reaction heat is removed by means of heat radiation of the reaction zone towards the cooled injector. The fluorine flow rate is chosen in such a way that to avoid conditions of film boiling of heat carrier in the injector and overheating the reaction zone (not more than 2000K) which may result in fluoroolefines formation.

A facility of tetrafluoromethane CF₄ annual output of 600 tons according to this method has been made at FSUE "Angarsky Electrolysis chemical combine".

Synthesis in inverse wave of filtration combustion was also used in production of hexafluorides of tungsten and molybdenum:



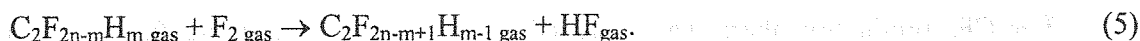
where fluorine was blowing through a fixed powder bed of the mentioned metals. At that, inverse wave of filtration combustion is formed without any initiation. The sole products at the wave temperature of 1000-1500K are WF₆ and MoF₆. Production of WF₆ of annual output of 50 tons has been established at JSC "Halogen".

Production facilities for PF₅ and IF₅ from elements of annual output of 10 tons have been created at EP RSC AC. There were used shelf reactors in which fluorine was blowing above the powder bed of the substance to be fluorinated. The yield of by-products was minimized by choice of a temperature in the reaction zone.

A very interesting example of application of non-stationary heat conditions in a gas-solid phase system is SF₄ production from elements (1) in a falling bed reactor under conditions of

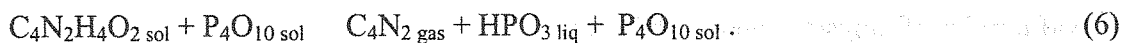
heat explosion. In this reactor, fluorine and a mixture of sulfur and CaF₂ powder (the latter was used as a heat ballast) were fed into the upper part of a vertical pipe where sulfur was evaporating and fluorinating in the freely falling powder bed under conditions close to adiabatic. At a maximal temperature in the reactor zone of 1400-1800K the yield of SF₄ reached 80%. An industrial-experimental scale reactor for SF₄ production by the proposed method of annual output of 10 tons has been made at EP RSC AC.

An example of application of combustion process as a synthesis conditions for a gas-gas reaction system is production of more high-fluorinated ethanes from less high-fluorinated ones using fluorine:



It has been determined that at preliminary mixing reagents and at a fluorine concentration below 30 vol.% (T_{max}~1000K) the carbon skeleton of fluoroethanes is stable. For this process there was designed an efficient reactor of a "tunnel burner" type with premixing of components, flame stabilization and initiation of process by means of a heated reactor wall. This method has been successfully tested in an experimental-industrial unit at SIA "Energomash" for C₂F₅H production from C₂F₄H₂. The C₂F₅H selectivity reached 90%.

As an example of industrial implementation of wave synthesis in a solid-solid phase system one may consider a number of processes to produce nitriles of carbonic acids by dehydration of respective amides with phosphorus pentoxide. A process to produce C₄N₂ by the proposed method under conditions of stationary self-propagating heat wave in a thick (about hundreds mm) bed and at conditions of non-stationary wave in a thin (about some mm) bed at a sufficient exceed of P₄O₁₀ in the mixture has been implemented at EP RSC AC:



The C₄N₂H₄O₂ concentration was chosen so that the maximal temperature in heat wave would not exceed 400°C, the wave velocity in this case was 400 mm·h⁻¹. The wave process initiation was realized by heating the reactor wall. The C₄N₂ yield reached 50% from the theoretical one. The facility output was about 1 ton of dicyanoacetylene per year.

Thus, it may be asserted that at present non-stationary heat conditions of high-exothermal synthesis (or combustion conditions) have found application in production of a whole number of commercially valuable products including large-tonnage ones.

References

1. D.A.Frank-Kamenetsky. Diffusion and heat transfer in chemical kinetics. M.: Nauka. 1967. 491 pp.

**APPLICATION OF NON-STATIONARY BED OF SOLID PHASE
FOR A REACTOR DEVELOPMENT FOR HIGH-EXOTHERMAL
PROCESSES USING ELEMENTAL FLUORINE IN
A GAS-SOLID SYSTEM**

**D.S. Pashkevich, Yu.I. Alekseev, D.A. Moukhortov, V.B. Petrov, V.S. Asovich,
G.G. Shelopin**

*FSUE RSC "Applied Chemistry", 14 Dobrolubov ave., St.-Petersburg, Russia
e-mail: pds@peterlink.ru*

Processes of fluorination with elemental fluorine are characterized by very high heat evolution. Thus, for example, in carbon fluorination to produce CF_4 the heat efficiency is 932 kJ/mol. Therefore one of the most important tasks in development of a reactor for such processes is removal of evolving heat from the reaction zone in order to provide stability of compounds to be synthesized.

It is well known that a gas-solid phase system is distinguished by a low ($0.01-0.1 \text{ W m}^{-2} \text{ K}^{-1}$) effective heat conductivity. Therefore unsteady-state heat conditions of running an exothermal reaction are realized in a reactor with a representative size of about hundreds millimeters with a fixed powder bed, through which fluorine is blowing. Here a filtration combustion wave with a maximal temperature up to 2000K is formed. That is why application of unsteady-state heat conditions to produce thermodynamically stable compounds is mostly effective in creation of large-tonnage facilities.

Steady-state heat conditions make possible to obtain a temperature in the synthesis zone at which substances produced are stable. But for processes using fluorine it is ineffective to develop a reactor with a fixed powder bed running under steady-state heat conditions because the reactor diameter in dependence on the reaction heat effect should make a value from tenth to some millimeters.

In order to develop a high-efficient reactor it is expedient to apply a moving (agitated) powder bed. Intensity of heat transfer to the reactor wall in such a system is much more higher than in a fixed bed. Therefore it is possible to provide steady-state heat conditions of running a reaction in a reactor non-continuous for solid phase.

Besides, application of a dynamic powder bed allows development of a reactor continuous for solid phase. In this case a powder to be fluorinated, which is in excess regarding stoichiometry, can play a role of a heat capacity by means of which the necessary temperature in the reaction zone is obtained without heat exchange with the reactor walls. Regeneration of reaction heat is realized outside the reactor and the cooled powder is recycled.

There are known different types of powder dynamic beds used in industrial equipment: vibro-revolving bed, gas-dust flow, fluidized bed, beds agitated by a spiral-screw auger and inside a rotating horizontal cylinder.

The authors have carried out a number of experimental and calculation works on application of different types of continuous and non-continuous regarding solid phase reactors with unsteady-state powder bed for high-exothermal fluorination processes using elemental fluorine.

Graphite fluorination in fluidized bed to produce a mixture of CF_4 , C_2F_6 , C_3F_8 , C_4F_{10} may be considered as an example of implementation of high-exothermal synthesis under steady-state heat conditions in a reactor non-continuous regarding solid phase with a dynamic powder bed.

It is known that in interaction of fluorine and graphite at a temperature above $1000^\circ C$ the almost sole reaction product is tetrafluoromethane and at a temperature below $500^\circ C$ the sole product is fluorographite, a condensed compound. For synthesis of a mixture of gaseous perfluorocarbons, among which compounds containing more than one carbon atom are of the greatest interest, it is necessary to remove reaction heat and keep the temperature within a range $550-700^\circ C$.

A laboratory reactor in a shape of thick-walled pipe with inside diameter of 12mm and 0.5m length has been made. Intensive heat removal from the reaction zone was realized by fluidization of a graphite beds with a mixture of argon and fluorine, the content of the latter was varied from 20 to 40 vol%. The mass flow of the gaseous mixture was chosen in such a way that the bed of classified graphite with a particle size of below 0.24 mm would expand to the full reactor length at gas blowing.

By means of temperature measurements in the reaction channel it has been shown that at heat transfer coefficient a from the fluidized bed to the reaction wall of about $500 W m^{-2} K^{-1}$ in the reaction volume it is possible to obtain isotropic temperature distribution that proves the existence of steady-state heat conditions of the synthesis. At a temperature about $600^\circ C$ in the reaction mixture there was observed the greatest quantity of perfluoroalkanes with the number

of carbon atoms more than one. An average composition of products at this temperature is approximately as follows: CF₄-30wt.%, C₃F₆-25wt.%, C₃F₈-15wt.%, C₄F₁₀-30wt.%. Thus, application of fluidized graphite bed has allowed formation of steady-state heat conditions of synthesis and achievement of a commercially valuable yield of C₂F₆, C₃F₈, C₄F₁₀.

In order to obtain gaseous fluorinated organic compounds there are often used solid higher fluorides of metals of transient valency, named as fluorine carrier, in particular CoF₃ as a fluorinating agent. Processes of CoF₃ fluorination are high-exothermic, so the heat effect of hexafluoroethane synthesis from ethylene is 1384kJ/mole. Conventionally for such processes there was used a column type equipment with a steady-state powder bed operating under conditions of following wave of filtration combustion. Such reactors were distinguished by low specific output due to low intensity of heat removal from the reaction zone and due to difficulty to scale-up the process from a laboratory model to industrial implementation.

CoF₃ powder has a tendency to caking and bridging, therefore application of fluidized bed in this case is inexpedient. It was proposed to use a horizontal rotating cylinder as a reactor for fluorination of gaseous compounds with cobalt trifluoride. The calculation have shown that at a filling degree with CoF₃ powder below 3.14 rad the heat transfer coefficient α reaches a value of 400-430 W m⁻² K⁻¹. The experiments carried out on a pilot reactor, a steel cylinder with inside diameter of 208mm and of 0.17m length have shown that at using cobalt difluoride the experimental values of α differ from the calculated ones and make a value from 100 to 300 W m⁻² K⁻¹ at varied rotational speed from 0.1 s⁻¹ to 1.5 s⁻¹. The calculation showed that at such a value of α the maximal admissible diameter of a reactor (a rotating cylinder) operating under steady-state heat conditions would be about 0.5m. The output of such a reactor at its length of 1 m in case of pentafluoroethane production from ethylene will be approximately 500 tons per annum that is by some orders of magnitude higher than that of a reactor of the same volume with a stationary bed of cobalt trifluoride.

A reactor for graphite fluorination with fluorine in a gas-dust flow in order to obtain CF₄, C₂F₆, C₃F₈, C₄F₁₀ is an example of implementation of a reactor non-continuous on solid phase with a dynamic powder bed and with reaction heat regeneration in a remote heat exchanger.

In order to conduct the fluorination process investigation there was developed a reactor system named "circuit". Such a reactor consists of a vertical lifting part, where moving solid particles upwards is realized at the expense of their carrying along by gas flow, a bunker-separator and a downtake part, where particles are moving downward in dense bed at the expense of gravity. In the gas-dust flow, where dispersed material plays the role of a heat carrier, the heat transfer coefficient from the reacting gas to particles, moving together with

OP-II-12

the gas, is about $1000 \text{ W m}^{-2} \text{ K}^{-1}$ while that from the flow to the reaction walls is about $200 \text{ W m}^{-2} \text{ K}^{-1}$.

The experiments carried out in a laboratory circuit, which lifting part was a pipe with inside diameter of 9 mm and 1200mm length, have shown that at a mass flow of fluorine of 20mg/s and 4 g/s for graphite respectively at heating the gas-dust flow from 520 to 580°C the composition of fluorination products is as follows: : CF_4 -31wt.%, C_3F_6 -25wt.%, C_3F_8 -13wt.%, C_4F_{10} -31wt.%. These results correspond to the results obtained under isothermal conditions in fluidized bed.

A reactor with a free falling bed is a reactor continuous on solid phase with a dynamic powder bed. This reactor is a vertical pipe, fluorine and solid material to be fluorinated are fed into the top part of the pipe by means of a screw. Solid and gaseous products are removed from the bottom. The reaction heat is absorbed by the solid phase which in excess in the process. Heat exchange with the reactor wall is negligible in comparison with heat evolution.

Application of such a reactor has been implemented in sulfur tetrafluoride production. The reactor was a vertical pipe with inside diameter of 60mm and 1 m height, a mixture of sulfur and calcium difluoride (the latter was used as a heat capacity) was fed into the top part as well as fluorine. Worked out CaF_2 was removed from receiver, arranged in the bottom , by means of a screw, then it was cooled and used for preparation of a fresh mixture of CaF_2 and sulfur. At sulfur concentration in fluorite of 7.5wt.% the yield of sulfur tetrafluoride reached 80% from the theoretical one at a reactor output of 10 tons per annum.

Thus, application of equipment with non-stationary powder bed either continuous or non-continuous on solid phase may allow development of effective industrial reactors for a wide range of high-exothermal reactions in a gas-solid system.

NEURAL NETWORKS AND FUZZY LOGIC FOR PREDICTION OF CATALYSTS DEACTIVATION DURING HYDROTREATMENT OF DEASPHALTED VACUUM BOTTOMS IN INDUSTRIAL REACTOR

F.Y. Jiménez¹, V.V. Kafarov¹ and M. Núñez²

¹*Chemical Engineering Department, Universidad Industrial de Santander, A.A. 678, Bucaramanga, Colombia,*

e-mail: kafarov@uis.edu.co, FAX 57 -76-350540

²*Instituto Colombiano del Petróleo (ICP), Piedecuesta, Colombia.*

Introduction

A set of catalysts for the hydrotreating of deasphalted vacuum bottoms has been investigated as fresh catalysts and after aging in an industrial reactor during a typical commercial run. Several structural parameters have been varied in the catalysts series. In particular, pore size, surface area, porosity, pellet size and active metals loading were changed to investigate the role of this parameters in this process [1].

Fresh and aged samples were analyzed by a variety of techniques, which include atomic adsorption in order to determinate the contents of retained Ni, V and Mo, allowing for a comparative analysis of the different samples according to the capacity to retain metals (catalytic activity). The analysis of this data and the influence of textural and chemical parameters of fresh catalysts on catalytic activity is the purpose of this investigation. The physicochemical characteristics measured for some catalysts are observed in *Table 1*.

On the other hand, today it is impossible to design a theory to predict the capacity to retain metals in quantitative form and based on strict laws of heterogeneous catalysis, because of the complex hierarchic organization of the heterogeneous catalytic systems. Furthermore, a lot of information accumulated in the literature is presented in descriptive form or has a high uncertainty level. To solve this problem the authors present a new methodology based on the following investigation stages:

In the **first stage** we make an evaluation of the uncertainty of the experimental data collected in the industrial reactor by means of the Hotelling's T^2 distribution. In the **second stage** we propose a methodology on the basis of Brandon's method, which provides a mathematical model adapted to predict the activity with high precision. The Brandon's

OP-II-13

Method uses a weight factor for each variable and is proposed to find these weight factors using Neural Networks. In the **third stage** we propose the application of Fuzzy Logic and Artificial Neural Networks to select the different alternatives, after which it is possible to take decisions on the optimum composition and the structure of the catalyst.

Table 1. Physicochemical characteristics of some catalysts

No. Catalyst	Activity: % metals (y)	Porosity % x1	Area mc/g x2	Pore Size (Å) x3	Equiv. diam. (mm) x4	% Nickel x5	% Molybdenum x6
1	35	53.3	157	85	1.555	2.12	11
2	45	58	255	69	1.857	3.93	13.33
3	66	66	150	146	1.873	3.14	10.66
4	69	62.6	176	113	1.292	2.67	9.3
5	100	75.9	146	233	2.2	1.96	8
6	116	69.7	187	141	1.381	2	6
7	124	65.5	144	140	0.879	3.14	10.66
8	133	71.9	224	133	2.057	0.6	11.5
9	150	67	187	131	0.801	1.56	5.9
10	165	68.9	200	128	1.292	2.3	10
11	188	70.6	260	116	0.922	0	2.8

Hotelling's T^2 distribution

The comparison of catalysts was accomplished according to the maximum capacity to retain metals (catalytic activity). Classification and comparison of twenty-four hydrodemetallation catalysts with sufficient reliability were achieved by means of application of Hotelling's T^2 test.

Brandon's method and Neural Network

The second stage of the investigation was the selection or design of an optimum catalyst. With the intention of interrelating simultaneously the principal parameters of catalysts (porosity, superficial area, pore diameter, size, metals content, etc.) with its activity, it was proposed to apply the combination of Neural Networks and the Brandon's method, which provides a mathematical model capable of predicting the activity with a small error.

We obtain the model for the hydrodemetalization process using Brandon's method in combination with Neural Networks. In this method the regression equation is written in the form

$$\hat{y} = af_1(x_1)f_2(x_2)\dots f_j(x_j)\dots f_k(x_k); \quad (1)$$

here $f_j(x_j)$ is a function of the variable x_j . The order of factors x_1, x_2, \dots, x_k in equality (1) is not indifferent for the accuracy in the elaboration of the results of observations: the greater the influence on "y" of the parameter " x_j ", the smaller must be the order of the index "j". The aspect of the functions " f_j " is chosen by means of empirical regression lines, and the influence on "y", through the use of a methodology with Neural Networks.

Fuzzy logic

Under the conditions of hydrotreatment process, the models for the prediction of catalytic activity frequently requires applications of those data that can not be expressed in quantitative form but as descriptive verbal characters; that means that it is necessary to work with ideas, relationships and diffuse expressions of the natural language. For this reason, the decision processes on models would have to be provided with fuzzy logic applications and representations, in order to select the different alternatives and to take decisions about the optimum composition and the structure of the catalyst.

It is assumed that the activity in the catalyst is determined by some combination of its physicochemical properties (superficial area, porosity, pore diameter, equivalent diameter, initial Nickel % and initial Molybdenum %). After a broad bibliographic search, the possible variation ranges of each parameter were obtained, a properly vocabulary and the belonging functions were defined, a verbal description of process was made, and fuzzy relationships among the parameters and among parameters and activity were built.

As a result, it was obtained a properly fuzzy model with high representation of activity of the deasphalted vacuum bottoms hydrotreatment process. The equations of the activity in function of the specified parameters confirm that the retention of metals is associated with an optimum porosity, high superficial area, pore diameter and a small equivalent diameter.

Conclusions

It was built a final activity equation in function of porosity, superficial area, pore diameter, equivalent diameter, Ni % and Mo % using Brandon's method, and assigning through a Neural Networks methodology the priority or importance of the selected

parameters. The obtained model presents a real physical sense and activity forecast very near to the experimental data. Likewise, they were obtained other models by classic statistics, with Neural Network, and it was developed a precise fuzzy model to predict the catalytic activity on the basis of textural and chemical characteristics of hydrotreatment catalysts.

According to the present comparison we may infer that the ideal catalyst should have a combination of:

1. High initial activity, given by the active metal loading and surface area in the proper pore range (e.g. $> 100\text{\AA}$).
2. Homogeneous distribution of metal deposition to assure a uniform utilization of the catalyst. Increasing pore size and reducing pellet size, which minimizes the diffusional limitations, achieve this.

The latter condition will also impact catalyst life, since a catalyst with small pore size will quickly deactivate.

References

1. Núñez M., Kafarov V., Pachón Z., Resasco D. "Deactivation of Ni-Mo/Al₂O₃ catalysts aged in a commercial reactor during hydrotreating of deasphalted vacuum residuum". *Applied Catalysis A. General* 5057 (2000), 1-11.
2. Jiménez F., Kafarov V., Núñez M. "Selección de catalizadores óptimos para procesos químicos industriales en condiciones de incertidumbre". In: *Vías para el diseño de plantas químicas en condiciones de incertidumbre*, Cuba, 2000.
3. Newson E. "Catalyst Deactivation Due to Pore-Plugging by Reaction Products". *Ind. Eng. Chem. Process. Des. Develop.*, Vol. 14, No 1, 1975, 27-33.
4. Staenek V. "The effect of liquid flow distribution on catalytic hydrogenation of cyclohexene in adiabatic trickle-bed reactors". *Chemical Engineering Science*. Vol. 37, No 9, 1982, 1283-1288.
5. Tanoubi P. "Simulation de la désactivation d'un catalyseur d'hydrodémétallisation à géométrie ouverte". *Revue de l'Institut Français du Pétrole*. Vol. 46, No 3, Mai-Jun 1991, 389-405.
6. Marincovic R. "Deactivation of Industrial Hydrotreating Catalyst for middle petroleum fractions processing". *Applied Catalyst A: General*, 107 (1994), 133.
7. Pereira C. "Metal Deposition in Hydrotreating Catalysts. 1. A Regular Perturbation Solution Approach". *Ind. Eng. Chem. Res.* 1990, Vol. 29 No 4, 512-519.
8. Pereira C. "Modeling of Hydrodemetalation Catalysts", *Ind. Eng. Chem. Res.*, Vol. 28, No 4, 1989, 22-27.
9. Le Page J.F. *Applied Heterogeneous Catalysis. Design, manufacture and use of solid catalysis*. Editions Technip, 1987.

FUNDAMENTALS OF CHEMICAL REACTIONS IN SUPERCRITICAL WATER AND THEIRS PRINCIPAL APPLICATIONS

Vladimir Anikeev, Anna Yermakova

Boreshkov Institute of Catalysis, SB RAS, Novosibirsk, Russia

E-mail: anik@catalysis.nsk.su, Fax: +7 383 239 74 47

Oxidation and decomposition chemical reactions in supercritical water (SCW) are used to wastewater processing, conversion of hazardous substances, destruction of toxic wastes, environmentally benign processes by temperature and pressure close to the critical point of water. High conversion degree of the most organic compounds is reached in the oxidation and decomposition chemical reactions in SCW. To understand how supercritical water affects the rate and selectivity of chemical reactions, one need to know the critical parameters of the mixture and how they change with reaction time. Though the chemical processes in SCW are very effective for the processing different kind of wastes, there are problems related to this technology.

FUNDAMENTALS

Thermodynamic and kinetic models of chemical transformations in supercritical fluids (SCF) have been created. Phase diagrams of complex mixtures are investigated and their critical parameters have been found. Effect of density on the rate of chemical reaction is studied by means of experiments and modeling. 2-propanol dehydration and aliphatic nitrocompounds decomposition and oxidation reactions in SCW have been selected for the experimental investigations of fundamental rules.

The mechanisms of 2-propanol dehydration and propene hydration reactions in SCW, appropriate to the acid-catalyzed mechanism have been proposed [1]. It was shown that the rate of direct and reverse reactions is directly proportional to the concentration of appropriate reagents and H_3O^+ ions playing a role of the homogeneous catalyst. It was shown also, that the sharp growth of H_3O^+ concentration in SCW with the increase of its density/pressure correlates unequivocally with the experimental dependencies of the pseudo-first order rate constants of reactions from the above named parameters.

Kinetic of nitromethane (NM), nitroethane (NE) and 1-nitropropane (NP) decomposition and oxidation in SCW near the critical point has been studied using a flow reactor as a first step in the development of technology for the treatment and processing of wastes from manufacture of commercial explosive substances containing nitrogenous compounds.

Experimental data on the decomposition of aliphatic nitrocompounds (RNO_2) in SCW showed that the apparent rate constants, calculated on the assumption of the first order reaction, increased exponentially with increasing pressure at constant temperature. It was shown that the rate of the named aliphatic nitrocompounds decomposition reactions in SCW decreased with increasing number of carbon atoms. And vice versa, the rate of oxidation reactions increased with increasing number of carbon atoms.

Effect of pressure on the decomposition rate of NM, NE and NP in SCW was investigated at constant temperature, Fig 1.

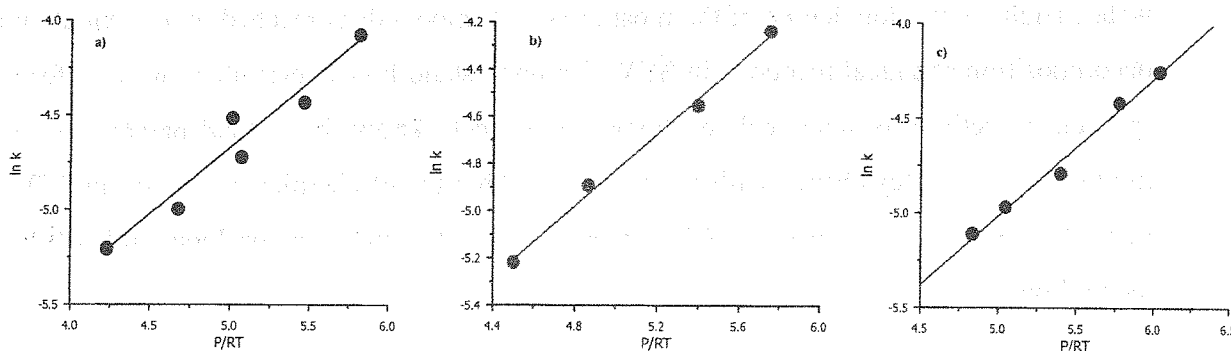


Fig. 1. (a, b, c) presents the dependencies of $\ln k_{obs}$ on (P/RT) at constant temperature for NM, NE and NP, respectively.

These primary data were processed by means of equation below:

$$k_{obs} = k_0 \exp\left(\frac{-\Delta\bar{V}^\ddagger P}{RT}\right) \quad (1)$$

The difference between the partial molar volumes (PMV) of transition state (TS) and reagent (RNO_2) $\Delta\bar{V}^\ddagger = \bar{V}_{TS} - \bar{V}_{RNO_2}$ is an activation volume. Note that $\Delta\bar{V}^\ddagger$ value in (1) does not depend on pressure. The results are presented in Table.

Reagent	$\Delta\bar{V}^\ddagger$, cm^3/mol	$k_0 \times 10^4$, $1/c$
NM	$-702,6 \pm 31,1$	$2,792 \pm 0,305$
NE	$-763,3 \pm 19,3$	$1,765 \pm 0,196$
NP	$-730,8 \pm 23,9$	$1,407 \pm 0,123$

The calculated values of activation volumes in the reactions of NM, NE and NP decomposition in SCW were similar that allowed suggestion on the same nature of the activation complexes in all three cases. The apparent rate constants of aliphatic

nitrocompounds decomposition in SCW decreased almost linearly in the order $NM > NE > NP$.

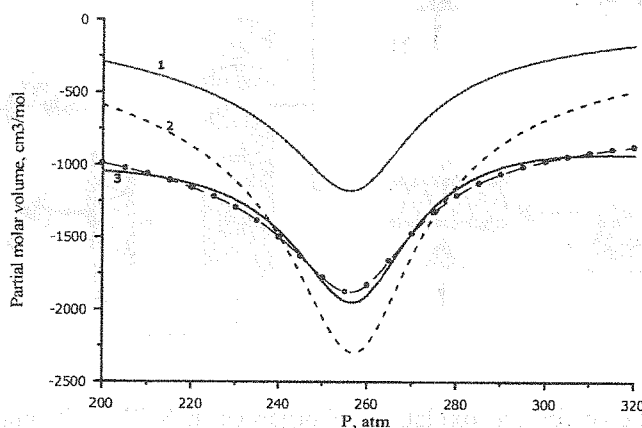
The transition state theory has been applied to simulate the data obtained. In the framework of the transition state theory, the main stage of RNO_2 decomposition is the formation of TS which exists in equilibrium with initial RNO_2 :



To calculate the partial molar volumes of TS and reagent which is the partial derivation of the mixture volume with respect to number of moles:

$$V_j = \left(\frac{\partial(nV_m)}{\partial n_j} \right)_{T,P,n_i, i \neq j}$$

the Redlich-Kwong-Soave (RKS) equation of state with binary interaction coefficients k_{ij} and c_{ij} has been used.



The pressure dependence of PMV: curve 1 – NM-SCW, at $k_{ij} = -0.3$, $c_{ij} = 0.3$; curve 2 – TS, “experimental”; curve 3 – TS, calculation at $k_{ij} = -0.5346$, $c_{ij} = 0.5240$; 4 – TS, calculation at variable k_{ij} и c_{ij} . $T = 665$ K

Fig. 2 shows that the pressure dependence of TS PMV calculated using variable with pressure k_{ij} and c_{ij} agrees well with “experimental” dependence. Meanwhile, when the pressure dependence of TS PMV was calculated using constant k_{ij} and c_{ij} values, respective mean-square deviation attained 25%.

Thus, the application of transition state theory allows quite correct modeling of the pressure effect on the rate constant of the studied chemical reactions in SCW. It proves experimental fact on the independence of activation volume on pressure. The natures of initial

nitro-compounds and TS differ only by the character of solvent-reagent interactions. This phenomenon can be successfully modeled by the RKS equation of state.

APPLICATION

Supercritical water oxidation (SCWO) technologies are generally used to oxidize the organics, destruction hazardous and non-hazardous wastes and treat wastewater streams.

The technological scheme for the oxidation of organic impurities in SCW has been proposed, Fig.2, in this work. Mathematical models of all apparatuses in the scheme (heat exchangers, chemical reactor, separator) consider specific properties of chemical processes realized in supercritical water (change of heat capacity, enthalpy and critical parameters of mixture with pressure, temperature and composition). Non-ideal thermodynamic methods have been used to calculate the properties of two phase multi- component mixtures.

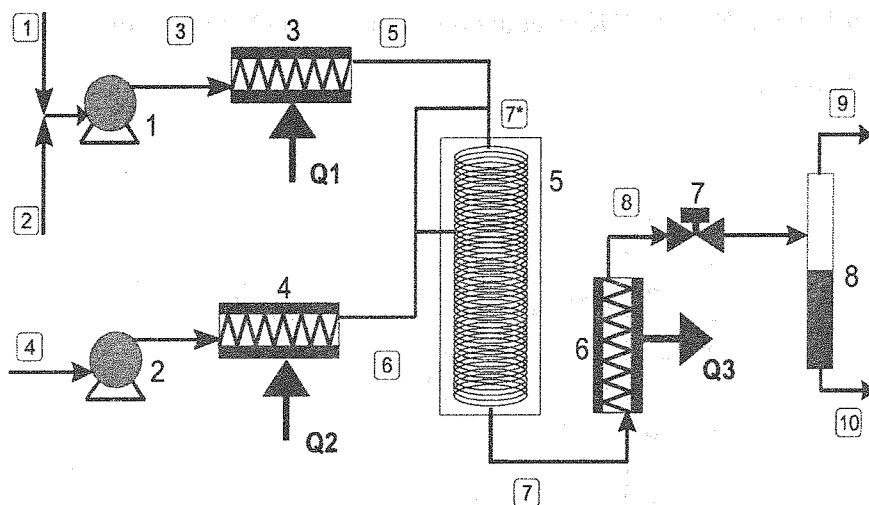


Fig. 2. Principal scheme for the oxidation of organics in SCW. 1,2- pump; 3,4 – heat exchanger, 5- reactor, 6-cooler; 7- back pressure regulator; 8-separator

Detailed numerical analysis and optimization of the proposed scheme for the oxidation of acetic acid by oxygen in SCW have carried out. Calculation results formed the basis of the pilot plant.

References

1. V.I. Anikeev, A. Yermakova. The influence of the density of supercritical water on the rate constant for the dehydration of isopropanol. Russian J. Physical Chemistry, 2003, 77, 2, p.211-214.
2. A. Yermakova, V.I. Anikeev. Calculation of spinodali line and critical point of a mixture. Theoretical Fundamentals of Chemical Engineering. (Russian). 2000, v.34, 1, p.57-64.
3. V.Anikeev, A.Yermakova. Binary interaction coefficient in the RCS equation of state. Theoretical Foundation of Chemical Technology. (Russian). 1998, 32, 508-514.

MODELING OF GAS-LIQUID REACTORS TAKING INTO ACCOUNT THE LIMITATION OF LIQUID REACTANT DIFFUSION TO THE INTERPHASE IN PROCESSES OF MASS-TRANSFER WITH CHEMICAL REACTION

I.V. Kuchin, A.V. Kravtsov, E.F. Stefoglo

Coal and Coal Chemistry Institute, Rukavishnikov, 21, Kemerovo, 650610, Russia

Fax: 7-3842- 21-18-38; E-mail: Stefoglo@yandex.ru

As followed from numerous works [1]-[5] and others sources, for describing of chemical reaction influence on mass-transfer in many cases it is enough to use the simplified models, the most prevailing of them is a stagnant film model. It should be noted that also in the network of the film model some aspects of mass-transfer with chemical reaction seem to be studied insufficiently. Among such cases is the first-order irreversible reaction.

Let us consider two fluid phase system. Initially a phase I (gas phase) contains compound A_1 and a phase II (liquid phase) contains compound A_2 . Gas A_1 is absorbed by a liquid where it reacts irreversibly with reactive species A_2 according to the following chemical reaction:

$$\nu_1 A_1 + \nu_2 A_2 \rightarrow \nu_3 A_3.$$

Let us write a mass balance for compound A_i in a differential volume of the liquid boundary layer, where diffusion and the first-order chemical reaction take place:

$$D_i d^2 c_i(x)/dx^2 + \nu_i k c_1(x) = 0 \quad (1)$$

The boundary conditions are:

$$x = 0, \quad c_1(x) = c_1^*, \quad dc_2(x)/dx = 0, \quad dc_3(x)/dx = 0 \quad (2)$$

$$x = \delta, \quad c_1(x) = c_{1b}, \quad c_2(x) = c_{2b}, \quad c_3(x) = c_{3b} \quad (3)$$

These equations were written in assumption that concentration of compound A_2 is over zero along the all thickness of the film. But the reacting compounds supply into the film due to molecular diffusion only, so a deficit of liquid reactant in the film in fact can take place. In such conditions eqs.(1)-(3) are no longer be used for describing of process going.

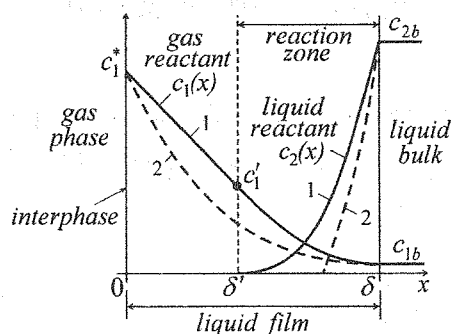


Fig. 1. The scheme of concentrations distribution in the film of liquid.

1 - diffusion limitation of A_2 is taken into account;
2 - diffusion limitation of A_2 is not taken into account.

In Fig. 1 the typical profiles of concentrations $c_1(x)$ and $c_2(x)$ which can be obtained by solution of eq(1) are showed as dashed lines. The curve $c_2(x)$ intersects the axis x and concentration becomes negative. That fact testifies that eqs.(1)-(3) can not be used in these conditions. The solid lines in Fig. 1 are the actual profiles $c_1(x)$ and $c_2(x)$ obtained with taking into account the diffusion limitation of A_2 in film. Let us write mathematical equations describing the concentrations behavior in this case.

On the interval $0 < x < \delta'$ $c_2(x) = 0$, chemical reaction does not take place, so the profile $c_1(x)$ is a straight line going through the points c_1^* and c_1' (where c_1' - a certain concentration value to be found later):

$$c_1(x) = c_1^* + x(c_1' - c_1^*)/\delta' \quad (4)$$

On the interval $\delta' < x < \delta$ mass balance for compound A_1 is:

$$D_1 d^2 c_1(x)/dx^2 + v_1 k c_1(x) = 0 \quad (5)$$

$$\text{The boundary conditions: } x = \delta' \quad c_1(x) = c_1'; \quad x = \delta, \quad c_1(x) = c_{1b} \quad (6)$$

An equation for concentration of A_1 in the bulk of phase II can be found from the equality of diffusion rate of A_1 from the film to the bulk of phase II and the rate of A_1 consumption on reaction in the bulk:

$$c_{1b} = \frac{1}{\lambda \delta (\beta - 1)} \frac{c_1' - c_{1b} \text{ch}[\lambda(\delta - \delta')]}{\text{sh}[\lambda(\delta - \delta')]}, \text{ where } \beta = \varepsilon_{II}(a\delta), \lambda = \sqrt{-v_1 k / D_1} = Ha/\delta \quad (7)$$

To obtain unknown values of δ' and c_1' we write the following equations:

$$\frac{c_1' - c_1^*}{\delta'} = \frac{\lambda(c_{1b} - c_1' \text{ch}[\lambda(\delta - \delta')])}{\text{sh}[\lambda(\delta - \delta')]} \quad (8) \quad c_{2b} + \frac{v_2 D_1}{v_1 D_2} \left[c_1' - c_{1b} + (\delta - \delta') \left(\frac{c_1' - c_1^*}{\delta'} \right) \right] = 0 \quad (9)$$

Eq.(8) is written from the equality of gradients $dc_1(x)/dx$ to the right and to the left sides of the point $x = \delta'$. The equality of gradients must be an obligatory condition since a flow of A_1 intersecting the boundary $x = \delta'$ is the same to both sides of boundary. Eq.(9) is based on the fact that at the point $x = \delta'$ concentration $c_2(x)$ is equal to zero.

In the table 1 the expressions for the main magnitudes characterizing the process are presented for two different cases. The profiles of concentrations in the film of liquid can be calculated by solving a set of equations (7)-(9) and substituting obtained values of δ' , c_{1b} and c_1' to expressions for $c_1(x)$ and $c_2(x)$ (see table 1).

As can be obtained from system (7)-(9) diffusion limitation of A_2 does not take place in the film and the dependencies found by means of solution of eq.(1) can be used, if values of parameter Z exceed values calculated by the following expression:

$$Z = \frac{1 - Ha/\text{sh}Ha}{\text{ch}Ha[1 + Ha(\beta - 1)\text{th}Ha]} + \frac{Ha}{\text{th}Ha} - 1 \quad (10)$$

Since parameter $\beta = \varepsilon_{II}/(a\delta)$ has a weak influence on the form of curve $Z(Ha)$ calculated by eq(10) it can be used the following simplified equation obtained from (10) at $\beta \rightarrow \infty$:

$$Z = Ha/\text{th}Ha - 1 \tag{11}$$

Table 1.

	A case when diffusion limitation of liquid reactant A_2 does not occur in the film	A case when diffusion limitation of liquid reactant A_2 occurs in the film
Concentration of A_1 in the film	$c_1(x) = \frac{c_{1b} \text{sh}(\lambda x) + c_1^* \text{sh}(\lambda(\delta - x))}{\text{sh}(\lambda\delta)}$	$c_1(x) = c_1^* + \frac{c_1' - c_1^*}{\delta'} x \text{ at } 0 < x < \delta'$ $c_1(x) = \frac{c_{1b} \text{sh}[\lambda(x - \delta')] + c_1' \text{sh}[\lambda(\delta - x)]}{\text{sh}[\lambda(\delta - \delta')]} \text{ at } \delta' < x < \delta$
Concentration of A_2 in the film	$c_2(x) = c_{2b} \left[1 + \frac{v_2 D_1}{v_1 D_2} \frac{c_1(x) - c_{1b}}{c_{2b}} \times \left(\frac{\delta - x}{c_1(x) - c_{1b}} \left[\frac{dc_1(x)}{dx} \right]_{x=0} + 1 \right) \right]$	$c_2(x) = c_{2b} + \frac{v_2 D_1}{v_1 D_2} \left[c_1(x) - c_{1b} + (\delta - x) \left(\frac{dc_1(x)}{dx} \right)_{x=\delta'} \right]$
Concentration of A_1 in the bulk of phase II	$\bar{c}_{1b} = \frac{1}{1 + \text{Hath}(Ha)(\beta - 1)}$	Can be found by means of solution of equations set (7)-(9)
Enhancement factor	$E = \frac{Ha}{\text{th}Ha} \left(\frac{1 - \bar{c}_{1b}/\text{ch}Ha}{1 - \bar{c}_{1b}} \right)$	$E = 1 + \frac{Z}{1 - \bar{c}_{1b}}$
Efficiency	$\eta = \frac{1}{Ha\beta} \left[\frac{\text{th}(Ha) + Ha(\beta - 1)}{1 + \text{Hath}(Ha)(\beta - 1)} \right]$	$\eta = \frac{1 - \bar{c}_{1b} + Z}{Ha^2 \beta}$

It can be seen from Fig. 2 that decreasing of parameter Z value and increasing of Ha value lead to the process passing in the region of compound A_2 limitation. This fact has a simple physical explanation since decreasing of Z value means decreasing the diffusion ability of A_2 as an increasing of Ha implies more intensive consumption of A_2 on reaction.

The dependences of apparent process rate (rate of gas diffusion into liquid phase) on fraction of liquid film ($1/\beta$) at different relations of diffusion abilities of gas and liquid components are shown in Fig. 3. In the case of low values of gas diffusion coefficient the gas concentration in the film reaches zero, the reaction passes in the film within limits of gas penetration into liquid phase. In the bulk of liquid phase reaction does not occur, so to increase the apparent rate of process it is necessary to raise the film fraction (line 1,2 in Fig. 3). Therefore such type of processes must be carried out in packed columns, tray

columns, high agitated reactors and other units with developed specific interphase area and high fraction of the film in liquid phase.

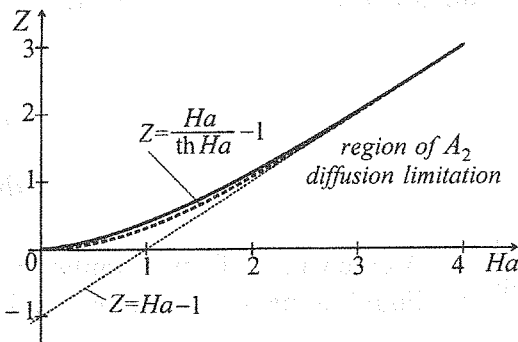
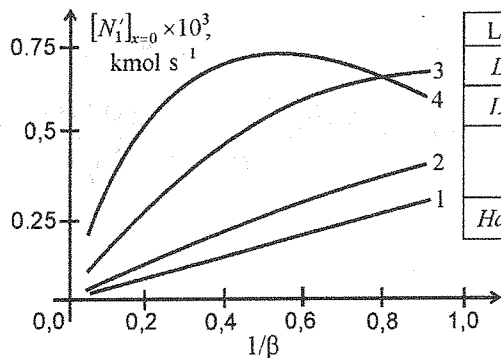


Fig. 2. Dependence of Z on Ha calculated by eq.(10) and indicating at boundary of A₂ diffusion limitation region.
Solid line – calculated by eq.(10), β = 2;
Dashed line – calculated by eq.(11), β → ∞.



Line number →	1	2	3	4
$D_1 \times 10^9, m^2 s^{-1}$	0.5	2	10	30
$D_2 \times 10^9, m^2 s^{-1}$	1.5	1	1	0.5
$Z = \frac{v_1 D_2 c_{2b}}{v_2 D_1 c_1^*}$	5	0.833	0.167	0.028
$Ha = \delta \sqrt{-v_1 k / D_1}$	4.743	2.372	1.061	0.612

$\delta = 1.5 \times 10^{-3} m; v_1 = v_2 = -1;$
 $k = 5 \times 10^{-3} s^{-1}; c_1^* = 0.3 kmol m^{-3};$
 $c_{2b} = 0.5 kmol m^{-3}.$

Fig. 3. The apparent process rate as a function of liquid film fraction (1/β).

If diffusion ability of liquid reactant is much more than gas component, the liquid reactant does not reach interphase, while diffusing through the film it becomes depleted due to consumption on reaction. In this case reaction goes both in the bulk of liquid phase and in the part of film from the side of bulk see (Fig. 1). A total volume V_r , where reaction takes place, diminishes with increasing of the film fraction $1/\beta$, since a volume of bulk decreases. At high values of $1/\beta$ it can lead to decreasing of apparent rate of process (line 4 in Fig. 3). The elevation of process rate at low values of $1/\beta$ is explained by growth of gas component concentration in the bulk of liquid phase. For such system the reactors with moderate content of liquid film are the best. Any additional supply of energy into the system in such conditions is useless.

References

1. Astarita, G. Mass Transfer with Chemical Reaction, Elsevier, Amsterdam, 1967.
2. Doraiswamy, L. K., & Sharma, M. M.(1984). Heterogeneous reactions. Analysis, examples, and reactor design. In *Fluid-fluid-solid reactions*, Vol.2. New York: Wiley.
3. Hikita, H., & Asai, S. (1964). Gas absorption with (m, n)th order irreversible chemical reaction. *International Chemical Engineering*, 4, 332.
4. Roizard, C. & Wild, G. (2002). Mass transfer with chemical reaction: the slow reaction regime revisited. *Chemical Engineering Science*, 57, 3479-3484.
5. van Swaaij, W. P. M., & Versteeg, G. F. (1992). Mass transfer with complex reversible reactions in gas-liquid system: An overview *Chemical Engineering Science*, 47, 3181-3195.

FUNDAMENTALS OF THE INFLUENCE OF GAS DISSOLVED CONCENTRATION IN REACTION MEDIUM ON PERFORMANCE OF GAS-LIQUID PROCESSES ON SUSPENDED CATALYST

E.F. Stefoglo, I.V. Kuchin, O.P. Zhukova

Institute of Coal and Coal Chemistry, Rukavishnikov, 21, 650610, Russia

Fax: 7-3842- 21-18-38; E-mail: Stefoglo@yandex.ru

Let us consider a gas-liquid reaction on a suspended catalyst in a continuous stirred vessel. Neglecting the liquid-solid mass-transfer and interparticle resistance the material balance equations take the form:

- for the gas phase:
$$V_G \frac{dC_{HG}}{dt} = Q_G (C_{HG}^{in} - C_{HG}^{out}) - V_L \beta_{G-L} (C_H^* - C_{HL}) \quad (1)$$

Assuming that the behavior of a gas phase can be described according to the law of ideal gases $p_{H_2} V_G = nRT$, $p_{H_2} = C_{HG} RT$, and Henry law $p_{H_2} = C_H^* H$, we obtain

$$C_{HG}^{in} = C_{H_0}^* H_e / RT_{R_0}, \quad C_{HG} = C_H^* H_M / RT_{R_0} \quad (2)$$

Here: H - Henry's constant for a solution mixture (suspension), which can be empirically expressed as $H_M = H_e^{1-x} H_p^x$, H_e and H_p are Henry's constants determined experimentally for the initial solution of hydrogenated substance and for reaction products, respectively. By substitution (2) in (1) then differentiating on T_R taking into account that C_H^* , H and T_R function of t the new mathematical model of general continuous or batch type of stirred reactor can be presented in the dimensionless form:

- for gas phase (pressure change or corresponding equilibrium value of C_H^*):

$$\begin{aligned} \frac{d\bar{C}_H^*}{dt} = \frac{1}{\theta_G} \left(\frac{H_0}{H_e^{1-x} H_p^x} \bar{T}_R - \bar{C}_H^* \right) - \frac{V R \bar{T}_R T_{R_0}}{H_e^{1-x} H_p^x} (\bar{C}_H^* - \bar{C}_H) + \frac{\bar{C}_H^* d\bar{T}_R}{\bar{T}_R dt} - \\ - \bar{C}_H^* \left[\pm \frac{dT_R}{dt} \frac{1}{RT^2 T_{R_0}} [Q_e(1-X) + Q_p X] + \frac{dX}{dt} \ln \frac{H_p}{H_e} \right] \end{aligned} \quad (3)$$

In eq.(3) the sign "plus" is used when $H_{e,p} = H_{e,p0} \exp(-Q_{e,p}/RT)$ and in this case the gas solubility in educt and product solution is lowered with the temperature. When "minus" is used then $H_{e,p} = H_{e,p0} \exp(+Q_{e,p}/RT)$ the solubility grows with the temperature.

- for gas dissolved in suspension:

$$d\bar{C}_{HL}/dt = 1/\theta_L (\bar{C}_{HL}^{in} - \bar{C}_{HL}) - (\bar{C}_H^* - \bar{C}_H) - r \quad (4)$$

- for reaction mixture temperature:

- for liquid compound:

$$d\bar{C}_L/dt = 1/\theta_L (1 - \bar{C}_L) - r \quad (5)$$

$$\frac{d\bar{T}_R}{dt} = \frac{1}{\theta_G} \frac{V_G \rho_G C_{PG} (\bar{T}_{G0} - \bar{T}_R)}{V_R \rho_R C_{PR}} + \frac{1}{\theta_L} \frac{V_L \rho_L C_{PL} (\bar{T}_{L0} - \bar{T}_R)}{V_R \rho_R C_{PR}} - \frac{r C_{L0} (-\Delta H_R)}{\rho_R C_{PR} T_{R0}} - \frac{(\bar{C}_H^* - \bar{C}_H) C_{H0}^* (-\Delta H_S)}{\rho_R C_{PR} T_{R0}} - \frac{UF(\bar{T}_R - \bar{T}_C)}{\beta_{G-L} V_R \rho_R C_{PR}} \quad (6)$$

Here $\bar{C}_H^* = C_H^* / C_{H0}^*$, $\bar{C}_{HL} = C_{HL} / C_{H0}^*$, $\bar{C}_L = C_L / C_{L0}$, $Q = C_{H0}^* / C_{L0}$, $X_L = (C_{L0} - C_L) / C_{L0}$, $V = V_L / V$, $\gamma = RT_{R0} / H_M$, $M_{n,m} = k_0 \exp(-E / RT_{R0} \bar{T}_R) C_{cat} (C_{H0}^*)^{n-1} (C_{L0})^m / \beta_{GL}$, $t = \beta_{G-L} \tau$, τ - time, $r = M_{n,m} \bar{C}_{HL}^n \bar{C}_L^m = dx/dt$, $\theta_L = V_L \beta_{GL} / Q_L$, $\theta_G = V_G \beta_{GL} / Q_G$, $\theta_C = V_C \beta_{GL} / Q_C$.

Initial conditions:

$$1. t = 0, C_H^* = 1, \bar{C}_{HL} = 0, \bar{C}_L = 1, \bar{T}_R = 1, \bar{T}_C = T_C / T_{R0} \quad (7)$$

$$2. t = 0, C_H^* = 1, \bar{C}_{HL} = 1, \bar{C}_L = 1, \bar{T}_R = 1, \bar{T}_C = T_C / T_{R0} \quad (8)$$

This model accounts for temperatures influences on gas pressure, physic-chemical properties of reaction mixture and consequently simultaneously on the gas content in liquid during the reaction pass.

Let us consider the adiabatic process for the first order reaction with respect to both gas and liquid components is considered. In the case when the solubility grows with temperature and conversion of educt substance we have some different situation (Fig.1) In the first case the solubility rises both with temperature and educt conversion (dotted line *a*) or with the changing of the mixture properties that do not effect the solubility, but the Henry's law constant is a function of the temperature and in this case the solubility also grows (*b*). The other case when the temperature does not influence the solubility, but only conversion changes and increases the gas content in reaction mixture (*c*). Finally, H_M is independent from conversion and temperature, but due to temperature rising the reaction rate goes up and \bar{C}_{HL} value also becomes minimum value through the acceleration of the reaction rate and by this increasing gas consumption. In the work also two cases are considered: 1) gas solubility in product solution is greater than in educt solution $H_e / H_p > 1$, and 2) gas solubility in product solution is less than in educt solution $H_e / H_p < 1$ and other examples. Thus now it is possible to develop more precisely the gas-liquid-solid reactors with different kind of gas temperature absorption law with the temperature and reaction composition change.

The hydrogen solubility found experimentally rises with temperature batch for liquid α -methylstyrene (α -MS) and cumene. Fig. 2 shows the comparison of the experimental data of α -MS hydrogenation to cumene and those which were calculated from the model (3)-(5) for a liquid batch reactor ($\theta_L \rightarrow \infty$) at initial pressure value $P_{H_2} = 2$ bar and $T = 60$ °C, $C_{Pd} = 0,005$ kg/m³ under nonisobaric isothermal condition utilizing the obtained dependence of $H_{\alpha-MS} = 4.45 \times 10^6 \exp(628/T)$, $H_{cum} = 4.06 \times 10^6 \exp(597/T)$, m³Pa/kmol. Kinetic of reaction is found zero order with respect to liquid components and *L-H* according to hydrogen.

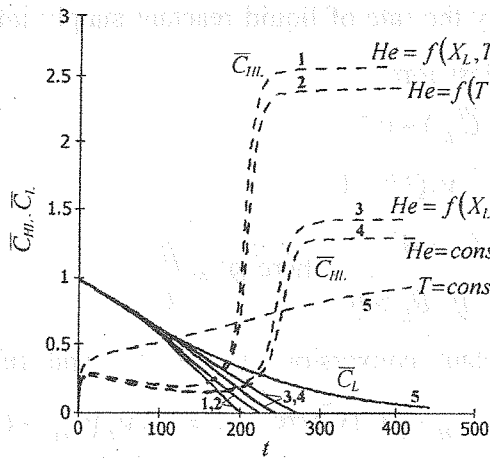


Fig. 1. Comparison of the C_{HL} and C_L dependencies from (1)-(6) during the reaction in a liquid batch reactor for different laws of gas reactant dissolution; $\theta_G = 10$, $M = 1$, $Q = 0.005$.

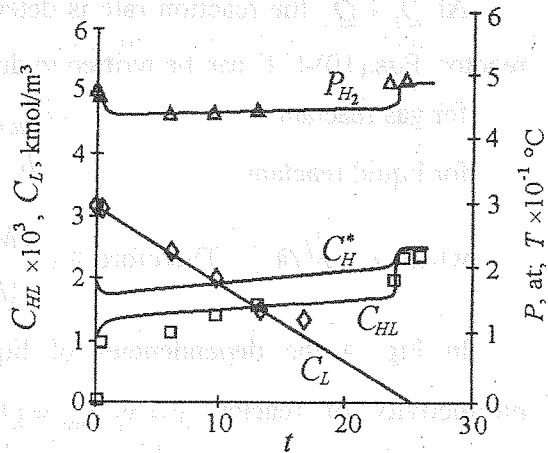


Fig. 2. Comparison calculated from the model (1)-(6) and experimental data for α -methylstyrene hydrogenation in a batch reactor of 1 l.

The kinetics of hydrogenation of ethyl ether of para-nitrobenzoic acid (EEpNBA) was investigated earlier by Stefoglo (1981). Reaction of EEpNBA hydrogenation has Langmuir-Hinshelwood mechanism with respect to both gas and liquid components, so a rate equation is:

$$r = kC_{cat} K_H C_{HL} / (1 + K_H C_{HL}) \cdot K_L C_L / (1 + K_L C_L), \text{ kmol}/(\text{m}^3 \text{ s}) \quad (9)$$

The values of kinetic constants k , K_H , K_L are:

$$k = 1.544 \cdot 10^{11} \cdot \exp(-9833.33/T), \text{ kmol}/(\text{kg}_{Pd} \text{ s}); \quad K_H = 5.38 \cdot 10^{-9} \cdot \exp(8000/T), \text{ m}^3/\text{kmol};$$

$$K_L = 8.186 \cdot 10^{-4} \cdot \exp(3032.5/T), \text{ m}^3/\text{kmol}; \quad K_p = 0.025 \cdot \exp(2400/T), \text{ m}^3/\text{kmol}.$$

It has been found the catalyst concentration influence on gas content in the suspension at different temperatures, pressures and chemical composition (conversion) during the reaction.

In Fig 3 the experimental and calculated data according to model (1)-(5) on EEpNBA hydrogenation are presented.

Liquid and gas continuous reactor

Let us consider the continuous for gas and liquid reactor operating under the isothermal isobaric conditions and the reaction rate equation is $r = -kC_{cat}C_{HL}$ (reaction of the type $v_1H_2 + v_2L \rightarrow v_3P$), influence of educt conversion on hydrogen concentration in suspension is neglected ($H = H_e = H_p$). Then mathematical model of process (eqs. (4)-(5)) for steady state conditions takes the form:

$$\text{for gas reactant} \quad -Q_L/V_L C_{HL} + \beta(C_H^* - C_{HL}) - v_1 r = 0 \quad (10)$$

$$\text{for liquid reactant} \quad Q_L/V_L (C_{Lo} - C_L) - v_2 r = 0 \quad (11),$$

$$\text{where } r = \begin{cases} kC_{cat}C_{HL} & \text{if } Q_L > Q_L^* \\ Q_L C_{Lo} / (v_2 V_L) & \text{if } Q_L < Q_L^* \end{cases}, \quad \text{here } Q_L^* - \text{volumetric flow rate of liquid, [m}^3/\text{s] such that } Q_L^* C_{Lo} / (v_2 V_L) = kC_{cat}C_{HL}$$

At $Q_L < Q_L^*$ the reaction rate is determined by the rate of liquid reactant supply into the reactor. Eqs.(10)-(11) can be written in dimensionless form:

for gas reactant
$$-\bar{C}_{HL}/\theta_L + (1 - \bar{C}_{HL}) - v_1 \bar{r} = 0 \tag{12}$$

for liquid reactant
$$(1 - \bar{C}_L)/\theta_L - v_2 Q \bar{r} = 0 \tag{13},$$

where $\bar{r} = r/\beta C_H^*$. Therefore $\bar{r} = \begin{cases} M\bar{C}_{HL} & \text{if } \theta_L < \theta_L^* \\ 1/(v_2\theta_L Q) & \text{if } \theta_L > \theta_L^* \end{cases}$, here $\theta_L^* = \frac{\beta V_L}{Q_L}$.

In Fig. 4 the dependencies of liquid reactant conversion $X_L = 1 - \bar{C}_L$ and relative productivity of reactor $\bar{y} = y/y_{max} = Q_L C_P / (v_3 k C_H^* V_L)$ (where $C_P = v_3/v_2 (C_{Lo} - C_L)$ - concentration of product in liquid phase, kmol/m³) on dimensionless parameters M and θ_L are presented. In the region *abcde* the reaction rate r , kmol/(m³ s) is equal $kC_{cat}C_{HL}$, in region *cdf* the reaction rate is determined by the rate of liquid reactant supply into the reactor, so $r = Q_L C_{Lo} / (v_2 V_L)$, kmol/(m³ s). The values of dimensionless parameters M and θ_L^* which belong to the boundary of regions *abcde* and *cdf* (i.e. lie on a projection of surfaces intersection curve *cd* (Fig. 4)) are described by the equation $\theta_L^* = (1 + v_1 M + \sqrt{(1 + v_1 M)^2 + 4v_2 Q M}) / (2v_2 Q M)$. The values M and θ_L^* correspond to conditions which ensure both a full liquid reactant conversion and the maximum possible at given value M productivity of the continuous stirred tank reactor. So these conditions are optimum for reactor operation.

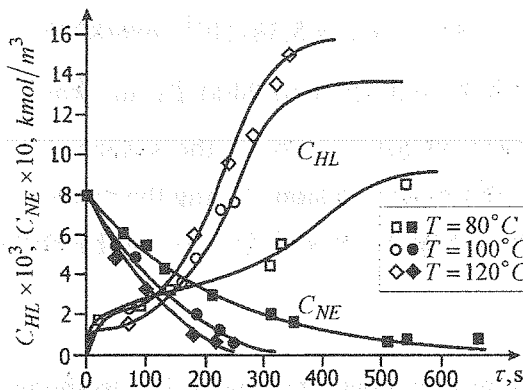


Fig. 3. Time dependencies of components concentrations at different temperatures, $C_{cat} = 0.083 \text{ kg}_{pd}/\text{m}^3$.

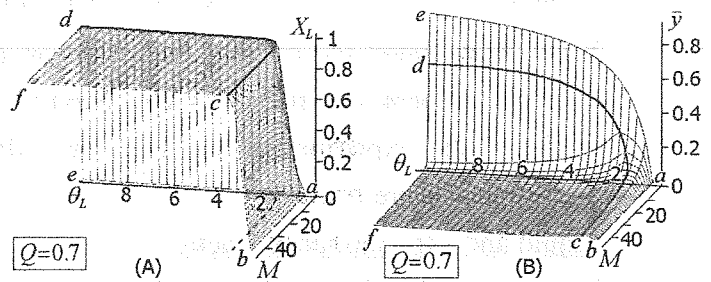


Fig. 4. Dependence of liquid reactant conversion (A) and relative performance of the continuous stirred reactor (B) on the process parameters M and θ_L in continuous stirred reactor ($M = kC_{cat}/\beta$, $\theta_L = \beta V_L / Q_L$, $Q = C_H^* / C_{Lo}$).

References

1. Stefoglo, E.F., Charpentier J.C., Midoux N. (1981). Etude experimentale de la reaction d'hydrogenation de l'alpha-methylstyrene sur palladium supporte en suspension en presence d'une resistance au transfert de matiere gaz-liquide. Entropie. 101, 51-59.

SECTION III.
NEW TYPES OF CHEMICAL
PROCESSES AND REACTORS

SECTION III
NEW TYPE OF CHEMICAL
REACTORS - RIG REACTORS

PULSED COMPRESSION REACTOR CONCEPT FOR SYNTHESIS GAS PRODUCTION

M. Glouchenkov, A. Kronberg, M. van Sint Annaland, J.A.M. Kuipers

Faculty of Science and Technology, University of Twente, The Netherlands

Introduction

Production of synthesis gas by steam reforming or by partial oxidation involves rather high temperatures of 800 – 1400 °C. The required heating of the feed and recovering of thermal energy of the product entail high capital and operating costs. These costs are associated with reactors, heat exchangers, furnaces, compressors, heat recovery boilers and turbines, which are made of very expensive high-temperature, scale-resistant alloys that can resist corrosion and withstand the effects of elevated temperatures and pressures. As a result the available synthesis gas based processes for the production of synthetic fuels are currently not economically attractive (Lange and Tijm, 1996).

A fundamentally new chemical reactor concept, namely the free piston pulsed compression reactor (Glouchenkov 1997, 1999), permits a breakthrough in synthesis gas production in terms of energy efficiency, capital costs, and portability. The novel reactor principle is totally opposite to the current trends in improvement of the existing technologies. Instead of developing better catalysts and decreasing the process temperature, in this new reactor no catalysts is required and the reactions occur at very high temperatures of 1500 – 3000 °C. Via integration of all process steps in a single unit significant improvements in the reactor performance are achieved.

Reactor concept

The basic idea of the reactor is schematically shown in Figure 1. The reactor consists of a double-ended cylinder and a free piston, which divides the cylinder into two compression-reaction chambers. The cylinder has inlet and outlet ports in its wall for feeding the reactants and exhaust of the reaction products. The free piston reciprocates with a very high frequency (up to 400 Hz) compressing in turn the feed gas, until it reacts, in the lower and upper chamber. The reciprocation is maintained by the reaction itself in case of exothermic reactions. An essential feature of the reactor is that the piston-cylinder assembly has no

sealing rings. Gas leakage through the annular piston-cylinder clearance is prevented by using contactless labyrinth seals. A relatively small gas leakage is even desired to provide gas lubrication (gas bearings), i.e. to prevent any contact of the piston with the cylinder wall by means of self-centering and self-alignment of the piston in the cylinder.

The use of the free, gas lubricated piston, makes it possible to achieve very high compression ratios (the ratios of the volumes before and after compression) and frequencies of the piston oscillation. The resulted very short duration of the extreme conditions prevents a significant heat exchange between the hot, compressed gas and the reactor walls.

Therefore unique combinations of pressures and temperatures from several hundreds to

several thousands of bars and up to several thousands of K can be obtained. These conditions are far beyond the feasible operation window in steady state chemical reactors. The achieved pressures and temperatures are ideal for almost instantaneous completion of many industrially important chemical reactions. The high frequency of the piston oscillation results in very high space velocities, i.e. ratio of volume throughput to reactor volume (millions per hour). Huge rates of temperature and pressure change (up to 10^7 K/s, 10^7 bar/s) afford an excellent way of "freezing" the high temperature products and producing a better yield in case of equilibrium reactions. Gas compression in the reactor can be adjusted depending on the desired conditions and is not determined by the mechanical restrictions as in conventional piston devices.

The free piston behaves like a pendulum swinging between two gas springs. Compensation of the inevitable energy losses due to friction and gas leakage is only required. These energy losses are very much smaller than the losses in the conventional processes. The reactor comprises the entire processing train: gas compression, heating of the reactants, reaction itself, cooling of products and utilization of the released reaction energy. The reactor is ideally suited for synthesis gas production by partial oxidation of various hydrocarbon feedstocks. Furthermore, the pulsed compression reactor technology may be very interesting for conducting of a great variety of other industrially important chemical reactions, as was proven experimentally using single-shot ballistic piston machines (Ryabinin, 1961).

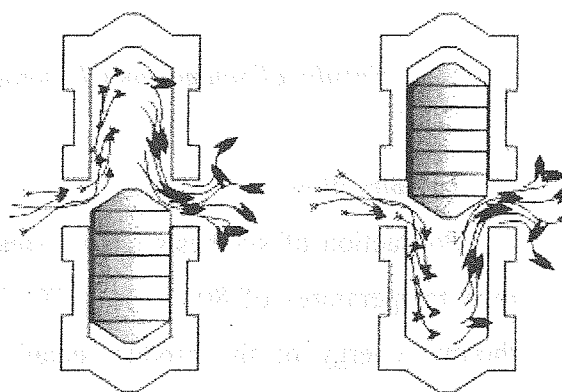


Figure 1. Operating principle of the pulsed compression reactor.

Experiments and results

Experiments without reactions. Firstly, the basic reactor performance was studied without chemical reactions using two reactors of 105 mm and 70 mm height, both with an inside diameter of 60 mm and many pistons of different density, dimensions and shape. In these experiments, compressed air was injected into the lower chambers either continuously through developed throttles or momentarily using developed fast acting valves.

The experiments showed that the reactors can easily be started-up using either of the two start up systems and operate smoothly without wear of the piston and cylinder walls. The reactors demonstrated a unique performance in terms of the achieved combinations of compression, frequency, temperature and pressure: compression ratio 5 – 45, piston frequency 50 – 200 Hz; piston speed 5 – 30 m/s; piston acceleration $(1 - 12) \times 10^3$ g. The maximum pressure and temperature observed in these conditions were 200 bar and 1360 K respectively. Such combinations are unique even for the state-of-the-art internal combustion engines and other known piston-compression machines whereas the values of these parameters can easily be increased several times in the developed reactors (Glouchenkov et al., 2002).

Experiments with reactions. To demonstrate the technical feasibility of the new reactor concept two reactors for carrying out chemical reactions – one with a single working chamber and a second with two working chambers as shown in Fig 1 - have been designed, manufactured and tested. The inner diameter of the both reactors was 60 mm. Six pistons of different shape and dimension were used for each reactor.

The experiments were conducted with methane/air, propane/air and ethyl ether/air mixtures. In most of the experiments propane/air mixtures were used; concentration of propane in the feed gas varied from 0.8 to 20 vol % (fuel/air equivalence ratio $\phi = 0.2 - 6.0$).

At first the conditions required for the reactions were studied in experiments without gas flow through the reactors. The occurrence of the reactions manifested through a significant increase of the maximum pressures (20 – 200 bar) compared to that at similar conditions but only with air.

The measurements showed unique pressures and reaction rates. Figure 2 shows the influence of propane on the pressure change in the single chamber reactor. It demonstrates in particular the capabilities of the pulsed compression reactors: extremely short reaction times (of about 10 μ s) and huge rates of pressure and temperature change. None of the available chemical reactors can provide these operating conditions.

Figure 3 shows an example of the pressure change during continuous operation of the reactor with single working chamber.

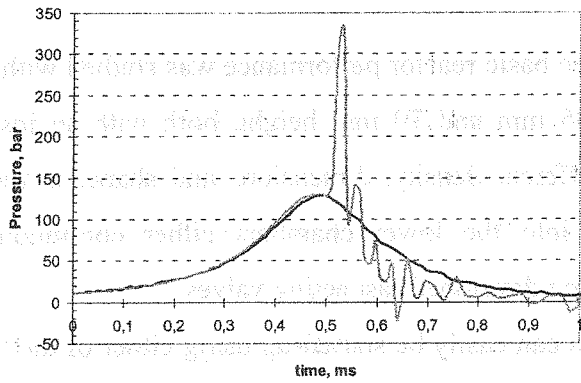


Figure 2. Influence of propane on the pressure change in the single-chamber reactor; dark blue line – without propane, purple line – with propane ($\phi = 0.63$).

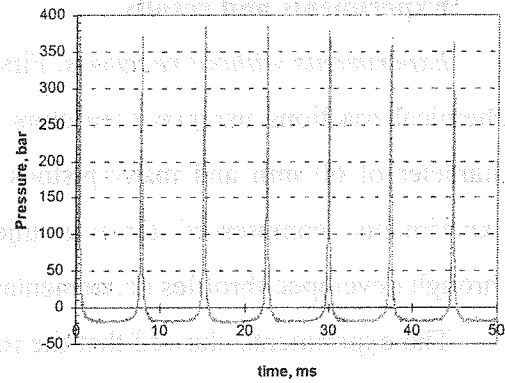


Figure 3. Pressure change in the single-chamber reactor during continuous syngas production: $\phi = 3.6$.

The analysis of the product composition revealed a significant yield of synthesis gas.

Conclusions

A new free piston pulsed compression reactor was developed. Experiments have shown its feasibility for economic synthesis gas production. Operation of the pulsed compression reactor is optimal in terms of energy efficiency. No other reactors integrate so many functions and allow so high pressures and temperatures, so high quenching rates and so high space velocities.

Furthermore, additional experiments have shown that the reactor permits reaction of propane and oxygen in a very wide concentration range (beyond the inflammability range). This finding may reveal new processes for e.g. manufacturing of carbon black, carbon-based nanoparticles (nanodiamonds, fullerenes) or direct oxidation of natural gas to formaldehyde, methanol, and higher alcohols.

References

1. Glouchenkov, M. Y. *Russian Pat.*, No 2097121, 29.01; No 2115467, 02.12, 1997.
2. Glouchenkov, M. Y. *Russian Pat.*, No 2142844, 05.04, 1999.
3. Glouchenkov, M., Kronberg, A., Veringa, H. *Chem Eng Trans.* 2002, 2, 983.
4. Lange, J.-P., Tijm, P.J.A. *Chem Engng Sci.*, 1996, 51, 2379.
5. Ryabinin, Y.N. *Gases at High Densities and Temperatures*, Pergamon Press, N.Y., 1961.

**OPTIMIZED OXIDANT DOSING
IN PACKED-BED MEMBRANE REACTORS
FOR THE CATALYTIC OXIDATION OF HYDROCARBONS**

**Frank Klose^{1,1}, Christof Hamel¹, Milind Joshi²,
Akos Tota², Andreas Seidel-Morgenstern^{1,2}**

¹*Max-Planck-Institut für Dynamik komplexer technischer Systeme, Sandtorstraße 1,
D-39106 Magdeburg, Germany*

²*Otto-von-Guericke-Universität Magdeburg, Lehrstuhl für Chemische Verfahrenstechnik,
Postfach 4120, D-39016 Magdeburg, Germany*

Catalytic oxidation of hydrocarbons can be described as a network of parallel and consecutive reactions via olefins and oxygenates as intermediates to carbon dioxide and water as the thermodynamically stable final products. Thus, the maximum possible yield of the intermediates is limited by the reaction kinetics itself. On the other hand, olefins and oxygenates belong to the most important base chemicals. For this reason there is a large interest in research and industry to develop economically feasible processes for their production. Thereby the strategy in maximizing the yields of the desired intermediates is twofold: first, the identification of more effective catalysts like the new Te-Mo-V-Nb-O catalysts [i, ii] and second, the improvement of the reactor design. Membrane reactors which are capable to lower oxygen partial pressure inside the catalyst bed are promising candidates in this field [iii - v].

The aim of our research is the systematic investigation of the potential of packed-bed membrane reactors in the catalytic oxidation of hydrocarbons including the evaluation of different types of catalysts and the derivation of the reaction network with the corresponding kinetic equations. The oxidation of ethane was chosen as a model reaction because of its challenges and the current intensive and broad research (e.g. [vi]). From the comparatively low yields normally obtained in classical fixed-bed reactors one can expect significant differences between fixed-bed and membrane reactors.

¹ Corresponding author,
phone: +49-391-6110 321/310, fax: +49-391-6110 532/152,
e-mail: klose@mpi-magdeburg.mpg.de

From the literature it is known, that supported reducible transition metal oxide catalyst are active even at temperatures less than 700 °C [vii, viii]. This group is primarily represented by the vanadium oxides, often mixed with other metal oxides. Iron and chromium compounds are also known as active catalysts [ix, x]. For this reason various γ -alumina supported catalysts containing oxides of V, Cr and Fe were compared. All catalysts were prepared by impregnation of the support particles ($d = 1.8 \text{ mm}$) with solutions of acetylacetonates of the metals in acetone followed by calcination at 700 °C for 4 h. The BET surface areas of all samples were comparable ($\sim 170 \text{ m}^2/\text{g}$) and the average pore size diameters ($\sim 10 \text{ nm}$), too.

Figure 1 shows a comparison of the different catalyst samples with respect to catalyst temperature and oxygen supply observed in a classical fixed-bed reactor (FBR, $d = 15 \text{ mm}$, $l = 30 \text{ mm}$). With increasing temperature and oxygen supply conversion increases and selectivity shifts from ethylene formation to deep oxidation. This shift is quite rapid for the Cr and Fe containing catalysts but much more moderate for the $\text{VO}_x/\gamma\text{-Al}_2\text{O}_3$ sample. For this reason the latter was selected as the preferred catalyst for the subsequent membrane reactor studies. Wall and gas phase reactions were not observed during these experiments.

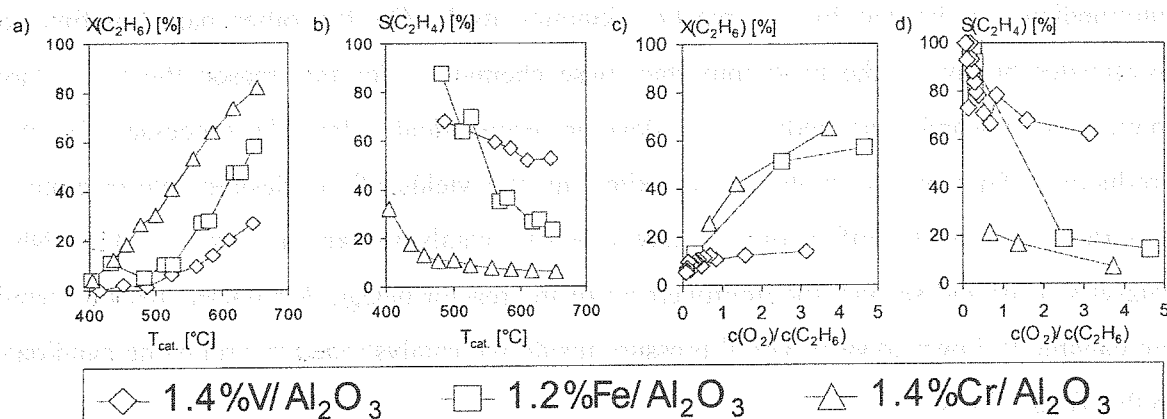


Fig. 1: Comparison of the catalysts in ethane oxidation

(FBR, 3.1 g catalyst, GHSV = 38000 h⁻¹, balance is N₂)

a) and b) - 0.7 % ethane, 2.5 % O₂, c) and d) - 0.7 % ethane, T_{cat} = 590 °C

From the FBR experiments including additional studies on ethylene and CO oxidation a reaction network was proposed (Fig. 2) and kinetic parameters were estimated. Ethylene formation from ethane (1) could be described by Mars van Krevelen mechanism. The CO_x forming reactions from the hydrocarbons (2-4) were fitted best by Langmuir Hinshelwood equations assuming non-competitive adsorption of reactants. Finally, CO oxidation to CO₂ can be described by a Langmuir Hinshelwood equation with competitive adsorption of CO

and oxygen. Kinetic parameters and parity plots are reported in [xi]. This kinetic model fits all experiments performed with oxygen to hydrocarbon ratios from 0.2 to 100.

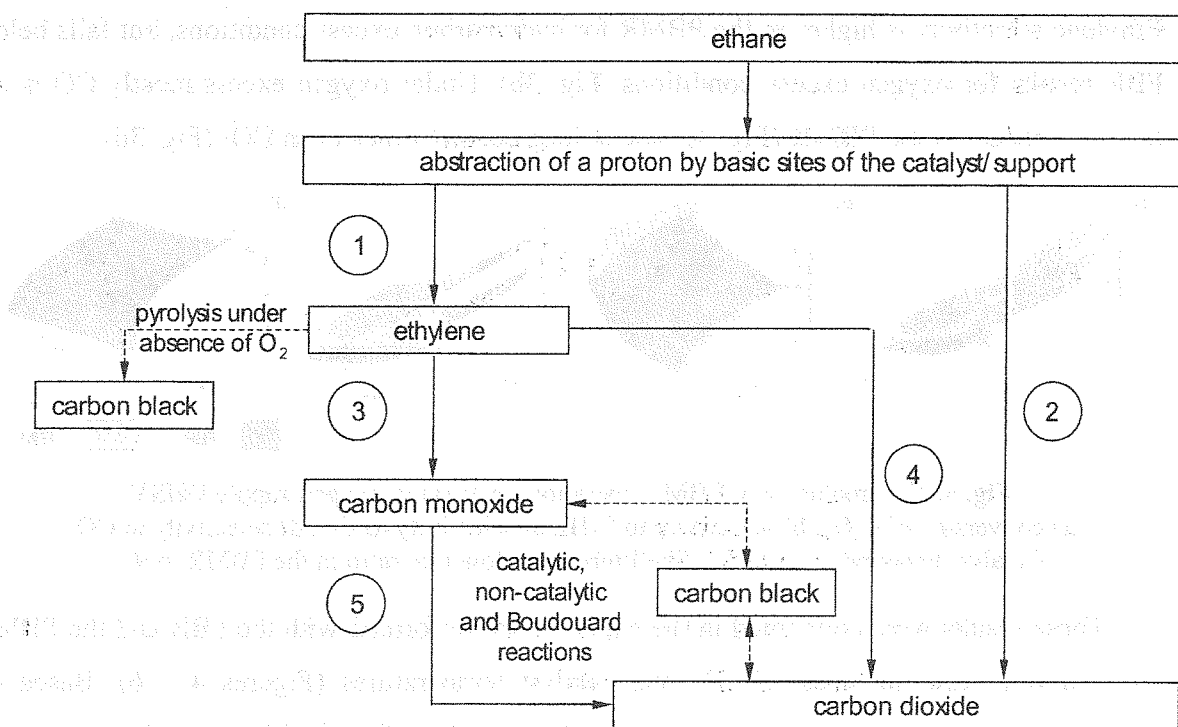


Fig. 2. The proposed reaction network for ethane oxidation

The results from kinetic measurements were used to investigate a packed-bed membrane reactor (PBMR) in comparison to the FBR theoretically and experimentally. The ceramic composite membrane for the PBMR was provided by Inocermic (Hermsdorf, Germany). It consisted of a mechanically stable α -Al₂O₃ support (average pore diameter: 3 μ m) on which three more α -Al₂O₃ layers (pore diameters: 1 μ m, 0.2 μ m, 60 nm; thickness of all: 25 μ m) and finally one γ -Al₂O₃ layer (pore diameter: 6 nm; thickness: 2 μ m) were deposited. The whole membrane tube had a length of 300 mm, an inner diameter of 7 mm and a wall thickness of 1.5 mm. Both ends of the membrane were vitrified, leaving in the centre of the membrane a permeable zone of 60 mm length. The membrane was filled with the VO_x/ γ -Al₂O₃ catalyst described above, and was used as an oxidant distributor in the PBMR. The PBMR was operated in dead-end configuration, so that all the feed inserted on the shell side was pressed via the membrane into the catalyst bed. Shell to tube side feed ratio was adjusted at 9 : 1. FBR and PBMR were compared on the basis of identical overall GHSV. For the simulation of the two reactors 1D and 2D models (pseudo-homogeneous, non-isothermal) were implemented in FEMLAB™ including modified Navier Stokes equations for calculation of the fluid velocity field.

Figure 3 shows 1D simulation results for both reactors at 590 °C as a function of oxygen supply and GHSV. Conversion is found to be higher in the PBMR (Fig. 3a) in general. Ethylene selectivity is higher in the PBMR for hydrocarbon excess conditions, but falls below FBR results for oxygen excess conditions (Fig. 3b). Under oxygen excess mostly CO is the favored product in the PBMR (Fig. 3c) and at long contact times even CO₂ (Fig. 3d).

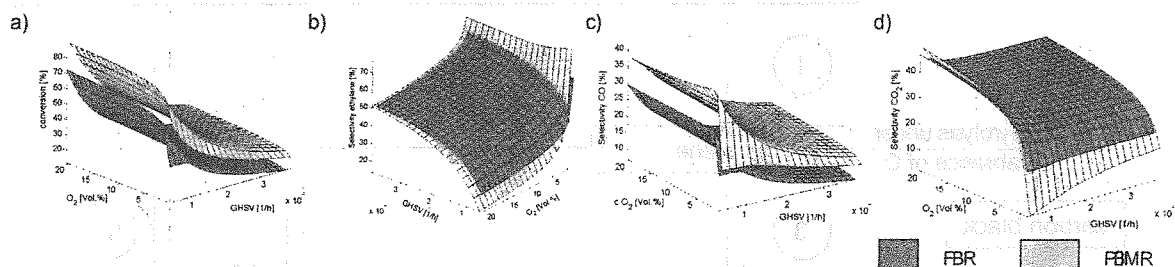


Fig. 3. 1D simulation of PBMR operation for varying oxygen supply GHSV, a) conversion of C₂H₆, b) selectivity to C₂H₄, c) selectivity to CO, d) selectivity to CO₂. Catalyst temperature: 590 °C, Shell/tube side flow rate ratio in the PBMR = 9 : 1.

These results were confirmed in the experiments performed with the FBR and the PBMR with varying feed mixtures, GHSV and catalyst temperatures (Figures 4 – 6). Based on analysis of all the data, three attractive operation modes of packed-bed membrane reactors were identified. These are selective oxidation mode (hydrocarbon excess, long contact times, high temperatures), CO favoring mode (oxygen excess, short contact times, moderate temperatures) and finally, deep oxidation mode (oxygen excess, long contact times, high temperatures). Each of the Figures 4 – 6 represents a typical experimental example of every operation mode. From FBR experiments with the blank support it can be concluded, that also in the PBMR wall and side reactions can be neglected.

The different operation modes of the PBMR can be explained by the interaction of changed concentration and contact time profiles compared to the conventional FBR. [xii, xiii]. Further, it can be concluded that the operation of packed-bed membrane reactors can be optimized for the formation of different products in the reaction network.

Fig. 4. Comparison of FBR and PBMR in selective oxidation mode, a) ethane conversion, b) ethylene selectivity, c) ethylene yield. Experimental conditions: 0.7 % C₂H₆, O₂ concentration and GHSV are given in the legend. Balance is N₂. Shell/tube side flow rate ratio in the PBMR = 9 : 1.

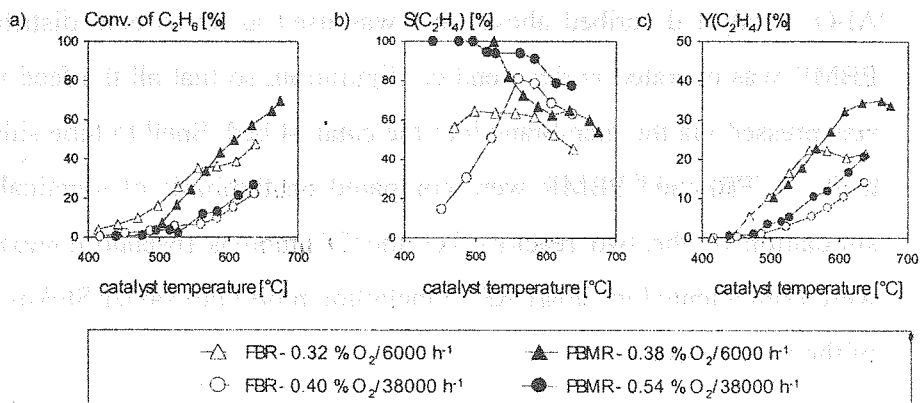


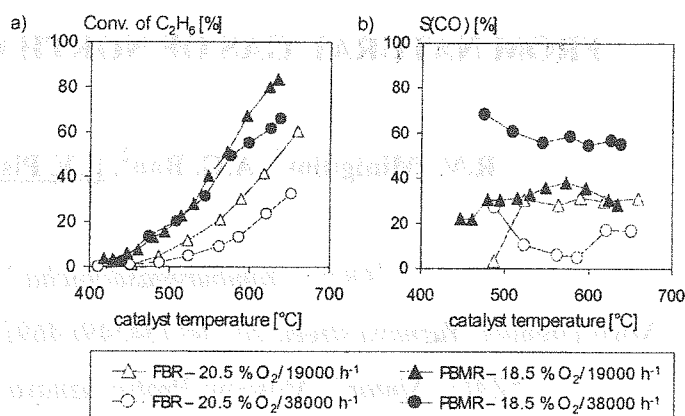
Fig. 5. Comparison

FBR and PBMR
in CO favoring mode,
a) ethane conversion,
b) CO selectivity

Experimental
conditions: 0.7 %
C₂H₆, O₂ concentration
and GHSV are given in
the legend.

Balance is N₂.

Shell/tube side flow
rate ratio in the
PBMR = 9 : 1

**Fig. 6.** Comparison of

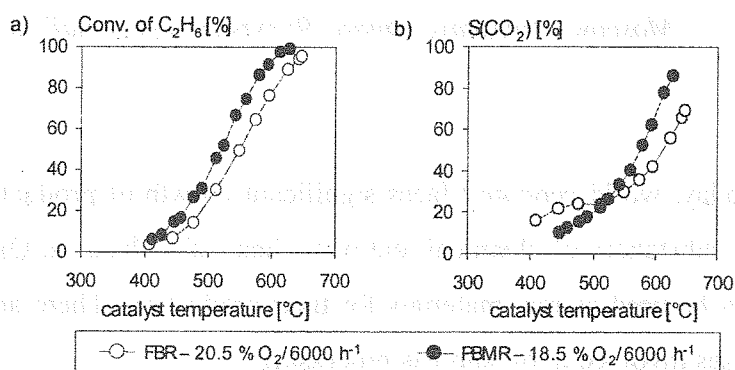
FBR and PBMR
in deep oxidation
mode,

a) ethane conversion,
b) CO₂ selectivity

Experimental
conditions: 0.7 %
C₂H₆, O₂ concentration
and GHSV are given in
the legend.

Balance is N₂.

Shell/tube side flow
rate ratio in the
PBMR = 9 : 1



References:

- [i] P. Botella, J.M. López Nieto, B. Solsona, A. Mifsud, F. Márquez, J. Catal. 209 (2002) 445-455
- [ii] J.M.M. Millet, H. Roussel, A. Pigamo, J.L. Dubois, J.C. Jumas, Appl. Catal. A – Gen. 232 (2002), 77-92
- [iii] J. G. Sanchez-Macano, T. T. Tsotsis, Catalytic Membranes and Membrane Reactors, Wiley-VCH, Weinheim, 2002
- [iv] K. K. Sirkar, P. V. Shanbhag, A. S. Kovvali, Ind. Chem. Eng. 38 (1999), 3715-3737
- [v] J. Coronas and J. Santamaría, Catal. Today, 51 3-4 (1999), 377-389
- [vi] F. Cavani, F. Trifirò, Catal. Today, 51 (1999), 561-580
- [vii] M. A. Banares, Catal. Today, 51 (1999), 319-348
- [viii] F. Cavani, F. Trifirò, Catal. Today, 51 (1999), 561-580
- [ix] J. E. Miller, M. M. Gonzales, L. Evans, A. G. Sault, C. Zhang, R. Rao, G. Whitwell, A. Maiti, D. King-Smith, Appl. Catal. A 2341 (2002), 281-292
- [x] M. Loukah, G. Coudurier, C. Jacques, J. C. Vedrine, M. Z. Ruíz, Microporous Materials 4 (1995), 345-358
- [xi] F. Klose, M. Joshi, Ch. Hamel, A. Seidel-Morgenstern, Selective Oxidation of Ethane over a VO_x/γ-Al₂O₃ Catalyst - Investigation of the Reaction Network, Appl. Catal. A.- Gen., submitted 2003
- [xii] F. Klose, T. Wolff, S. Thomas, A. Seidel-Morgenstern, Appl. Catal. A.- Gen., in press
- [xiii] F. Klose, T. Wolff, S. Thomas, A. Seidel-Morgenstern, Catal. Today, 82 (2003), 25-40

NOVEL INDUSTRIAL PROCESS OF METHANOL PRODUCTION FROM NATURAL GAS OF NORTH GAS FIELDS

R.M. Minigulov¹, A.G. Ban², E.V. Pisarenko³

¹OOO "Yamburggasdobicha"

Novii Urengoi, Yuznaya street, 2a; tel (34549) 46919; fax (34549) 45515

²ZAO "Sintop", Moscow, Profsoyuznaya street, 23;

Ban.Sintop@abb.ru; tel. (7095) 234-02-81

³Mendeleyev University of Chemical Technology

Moscow, Muisskaya square, 9; evpisarenko@mail.ru; (7095) 978-65-89

Today, world economy faces significant growth of productive capacity for the synthesis of key substances of chemical and petrochemical industries. Oil, gas condensate and natural gas can be used as raw materials for their production. There are more than 100 commercial processes involved in oil and gas processing.

In 80-90's of the last century, a steady increase in hydrocarbon fuel price, which resulted in increase in production cost of many petrochemical products, was observed. Now it becomes obvious that reconsideration of the development strategy of chemical and petrochemical industry of industrialized countries is necessary. Natural gas becomes widely used and it can substitute for oil and gas condensate. The process of natural gas processing on industrial scale is carried out through the stages of steam and dry reforming of methane. These reactions are endothermic and require significant energy consumptions. The price of syngas production is rather high and comes to 60-70 % of desired product price. At the following stages of methanol production, syngas is converted over low temperature promoted copper-zinc catalysts to desired product according to chemical technological scheme with recycle of unreacted syngas. The volumetric flow rate of recycled syngas exceeds by 5-8 times the one of fresh syngas entering catalytic reactor of the methanol synthesis. To reduce the methanol price, ICI company suggests to produce methanol without syngas recycle at gas fields only if the strata pressure of natural gas exceeds 7.0 MPa. However, such a technology of methanol production is not efficient for gas fields with middle and low pressures of natural gas.

New chemical technological scheme of methanol production from natural gas without any recycle of synthesis gas was developed after dedicated experiments at the laboratory and pilot plants for three years.

First, vast laboratory experimental study on the mechanism and kinetics of the reactions of steam and dry methane reforming to synthesis gas was carried out in flow-circulating reactor in the range of temperatures of 600-850 °C and volumetric flow rates of 500-10000 hr⁻¹. Concentrations of initial reactants such as methane, water, oxygen, carbon dioxide were varied at the reactor inlet while concentrations of carbon oxide, carbon dioxide, methane and hydrogen were analyzed at the reactor outlet. Total of 240 kinetic experiments were performed. Kinetic model comprising 32 kinetic constants based on 12-step mechanism of the reaction of steam and dry methane reforming was derived. Due to experimental results, kinetic constants were estimated by least square method and kinetic model was checked for adequacy by Bartlett criterion.

Then 7-step mechanism of syngas conversion to methanol was proposed. Kinetic model of the reaction comprising 22 kinetic constants was constructed. Kinetic experiments were carried out in both flow circulating reactor and flow single-row reactor in range of temperatures of 180-270 °C, pressures of 3.0-7.0 MPa and volumetric flow rates of reactants of 500-5000 hr⁻¹. Concentrations of CO, CO₂, methanol, N₂ in gas flow were analyzed. Sixty kinetic experiments were performed. Kinetic model constants were determined by least square method. The model adequacy to experimental results was proved by Hagao criterion.

To study the reaction of methanol production from syngas, experiments were carried out at the pilot plant. The reaction heat removal was performed by boiling heat carrier. The reactor model was developed and its macrokinetic parameters were estimated due to experimental results. Three and four reactor schemes of methanol production providing 75-90 % of syngas conversion and high quality of methanol produced were calculated. Methanol content in the reaction products exceeded 95 %, the rest was water and trace amounts of organic reaction products. The results of simulation of the reaction of methanol synthesis from syngas were confirmed by pilot plant experiments.

Mathematical models of different units of chemical technological equipment of the process of natural gas conversion to methanol were developed. For example, the reactor unit of methane conversion to synthesis gas and the reactor unit of syngas conversion to methanol with steam loop of the reaction heat utilization should be pointed out. The whole model of chemical technological scheme of the process developed was suggested. Due to this model, material and heat flows of the process concerned were determined, the design parameters of

OP-III-3

different apparatuses and the regimes of their operation were calculated. It was shown that steam generated in catalytic reactor units of methane conversion to syngas and of syngas conversion to methanol could be used as actuating fluid in steam turbines. Considerable quantity of heat and electrical energy generated in those turbines are quite enough to supply industrial installation working in North regions.

Carbon dioxide being a by-product of catalytic methanol synthesis is extracted from effluent gases with methanol and is then directed to the unit of methane conversion. The given ratio of hydrogen to carbon monoxide in synthesis gas can be reached by regulating CO_2 volumetric flow rate. The recycle of CO_2 allows one to increase in productivity of industrial installation of methanol production from natural gas up to 30 %.

The technology of natural gas conversion to methanol providing 70 thousand tons of methanol per year in North regions of Russian Federation has been developed. Due to the fact the methanol content in raw methanol produced is 95-98 % mass, it can be used directly for the needs of gas producing plants. High quality of methanol produced makes it possible to turn down the use of energy and metal consuming rectification unit of methanol concentration process. Methanol can be used as an inhibitor of hydrate blocks formation in gas industry, and as a raw material for DME and motor fuel productions in petrochemical industry. Another major advantage of the technology developed is the implementation of the methanol synthesis in the reactor unit with variable pressure that allows one to reduce energy consumption by 20-30 %. Economic estimates show that the payback period for the given installation is less than 4.5 years.

References:

1. Pisarenko V.N., Abaskuliev J.A., Chernomirdin A.V., Kachalov V.V., Brezgin B.E. Method of preparing methanol. RU patent № 2152378, 28.04.99.
2. Pisarenko V.N., Abaskuliev J.A., Ban A.G. Method of preparing methanol. RU patent № 2202531, 10.08.01
3. Pisarenko V.N., Abaskuliev J.A., Ban A.G. Method of preparing methanol. RU patent № 2203214, 28.12.2001

CELLULAR AUTOMATA METHOD AS A TOOL FOR COMPUTER-AIDED STUDY OF PROCESSES IN CHEMICAL REACTORS

A.V. Dimaki, E.V. Shilko, S.G. Psakhie

Institute of Strength Physics and Materials Science SB RAS,

av. Akademicheskii 2/1, 634021, Tomsk, Russia,

fax: +7-3822-25-95-76, e-mail: dav@usgroups.com

Development of the computing technique opens the wide possibilities for developing of the numerical and mathematical models to study even intricate physicochemical processes and phenomena. Now the computer-aided simulation is a powerful tool, which allows reducing the expenses of time and efforts as well as getting a new type of information source about the investigated processes.

The fundamentals of the computer simulation are methods of studied object description, which can be conditionally divided in two basic groups. Methods, which consider the simulated object as a continuous media, are related to the first group. In this case, the task solution is introduced as a solution of one (or several) differential equation.

Methods, which consider the simulated object as a system of associated discrete elements, are related to the second group. In this approach the solution is a space-time distribution of elements' parameters.

One of the most perspective approaches, which allows researching the wide range of processes and objects, is a cellular automata conception. This approach is oriented on the computer study of the processes in solid media on the base of such fundamental properties of substance as evolution and self-organization. Cellular automata conception allows both the numerical computations and analytic study of the common rules of the system behavior with different type and intensity of dynamic external actions.

For developing of the model of the processes in chemical reactors it is very important to know the features of the reaction kinetics and physicochemical properties of agents. On the base of this information the selection of equations, describing the simulated media, is performed (gas-dynamic equations, equation of thermal conductivity, mechanical equations an so on). Also, it is impossible to select the most significant properties of studied media, which will become the properties of cellular automaton. Thus, the built model is characterized by the vector of automaton parameters

$$\bar{Z} = (z_0, z_1, \dots, z_n) \quad (1)$$

and by the set of equations linking the automaton parameters and its space-time coordinates together.

$$\bar{F} = (f_0(\bar{Z}, x, y, z, t), f_1(\bar{Z}, x, y, z, t), \dots, f_m(\bar{Z}, x, y, z, t)) \quad (2)$$

On the base of equations (1) and (2), the set of automata switching rules is built:

$$\bar{X} = (X_0(\bar{Z}, \bar{F}), X_1(\bar{Z}, \bar{F}), \dots, X_k(\bar{Z}, \bar{F})) \quad (3)$$

On the base of above-stated, let us list the fundamental features of cellular automata models:

- discrete coordinates
- discrete time
- discrete conditions of automata
- presence of the set of automata switching rules

At that, the state of whole system is fully defined by the values of parameters of every cell.

As the example, illustrating the cellular automata conception application, the model of exothermal chemical reaction propagation in heterogeneous media is built. For the first time the description of the exothermal process front propagation in chemically active media was realized by Zeldovitch and Frank-Kamenetskii in 1938. In the frame of this approach the solution of reactionary-diffusive equation is found:

$$c_p \rho \frac{\delta T}{\delta t} = \lambda \frac{\delta^2 T}{\delta t^2} + q \rho \frac{\delta f(u)}{\delta t} \quad (4)$$

On the base of cellular automata approach the propagation of such reaction can be presented as a propagation of wave of bistable cellular automata states switching.

Usually, the distributed active media, which consists of bistable cellular automata, in approximation of continuous media, is described by the next equation:

$$\frac{\delta u}{\delta t} = f(u) + D, \quad (5)$$

where D – some coefficient of transfer.

The generalized solution of this differential equation for reaction front velocity is

$$C_0 = \sqrt{\frac{1}{2} \cdot \frac{q_0}{c} \cdot \frac{D_0}{u_1 u_2 u_3} \cdot \gamma (1 - \gamma / \gamma_{\max})^2 (u_1 + u_3 - 2u_2)}, \quad (6)$$

where γ - porous rate of medium, γ_{\max} – critical porous rate, u_1, u_2, u_3 – model parameters of automata switching.

This approach allows getting very good compliance of obtained results with the experimental data concerning such parameters as the reaction front velocity and the temperature in reaction front.

During the study of complex media with specific internal structure the necessity of developing explicit assignment of the start structure of simulated region is arising very often. The developed model based on the cellular automata method allows building the 2D-structure of the simulated region and the field of temperature in simulated region (Fig.1).

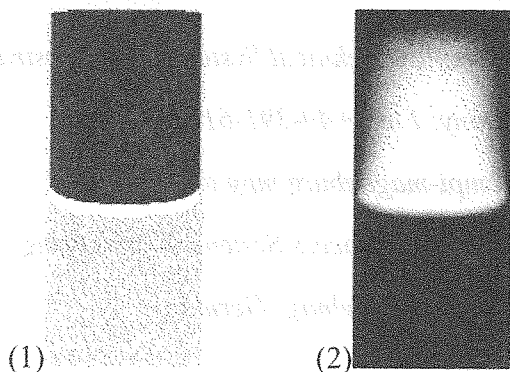


Fig. 1. Structure (1) and field of temperature (2), obtained by simulation on the base of the cellular automata method.

The velocity of reaction front propagation and the temperature inside the reaction front are in good compliance with experimental data.

A wide row of methods of initiation and setting of the order of chemical reaction processing needs the defined conditions of mechanical loading to the reacting media. For example, there are detonation-initiated SHS reactions and reactions in solid phase under shear deformation. To build the models of such reactions it is necessary to explicitly take into account the mechanical stress in solid medium and the intermixing and fragmentation of agent particles. In these models it is very perspective to use the movable cellular automata method (MCA). This method allows to explicitly take into account the mechanical loadings and the destruction processes in reacting media. Usage of the MCA method allows performing the simulation of SHS reaction under shock-wave compact with explicitly taking into account the destruction of agent particles.

Thus, using the cellular automata conception for simulation of processes in chemical reactors is very perspective. The cellular automata conception allows both performing the analytical solution of the task of velocity of reaction front propagation description and building the numerical schemes on the base of discrete representation of solid medium. The results, which are obtained with this method, are in good compliance with experimental data. The development of the cellular automata approach – movable cellular automata method – allows to explicitly take into account the mechanical properties of the media and the presence of mechanical loading and destruction.

EXPERIMENTAL STUDY ON ELECTROCHEMICAL MEMBRANE REACTOR FOR *n*-BUTANE PARTIAL OXIDATION

Yinmei Ye^a, Liisa Rihko-Struckmann^a, Barbara Munder^a, Kai Sundmacher^{a,b,*}

^{a,*} Max Planck Institute for Dynamics of Complex Technical Systems, Sandtorstrasse 1,

D-39106 Magdeburg, Germany; Fax: +49-391-6110353;

E-mail: sundmacher@mpi-magdeburg.mpg.de.

^b Otto von Guericke University Magdeburg, Process Systems Engineering,

Universitätsplatz 2, D-39106 Magdeburg, Germany

Introduction

The interest in the application of membrane reactors for the partial oxidation processes has been grown in the last years [1, 2]. With the help of membranes one can achieve a better distribution of oxygen along the catalyst bed, reduce the average oxygen concentration and in such a way increase the selectivity toward the desired partially oxidized products.

Recently, the partial oxidation of hydrocarbons using dense ceramic membrane has been widely investigated, for example, partial oxidation of methane to synthesis gas and selective oxidation of ethane using oxygen ion conductive membrane [3, 4], oxidative coupling of methane into ethylene and ethane using proton-conducting membrane [5] or mixed ion-electron conductive membrane [6]. To our knowledge, the butane oxidation to maleic anhydride (MA) using dense membrane has not been reported.

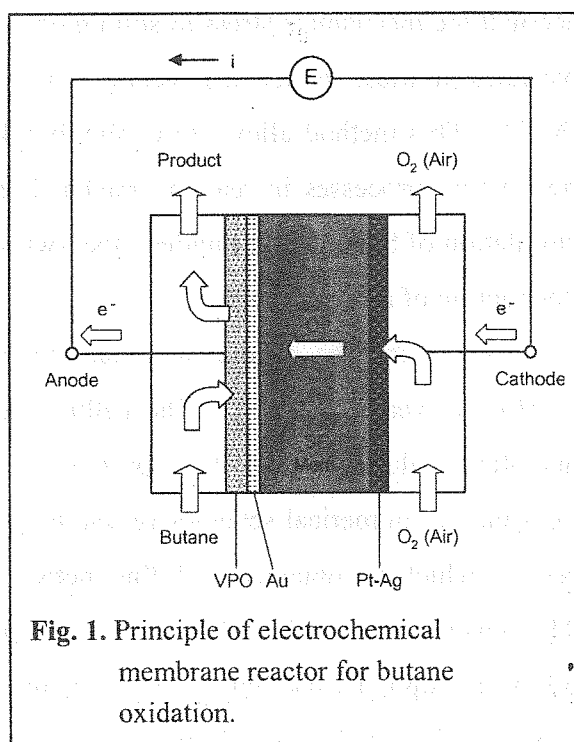
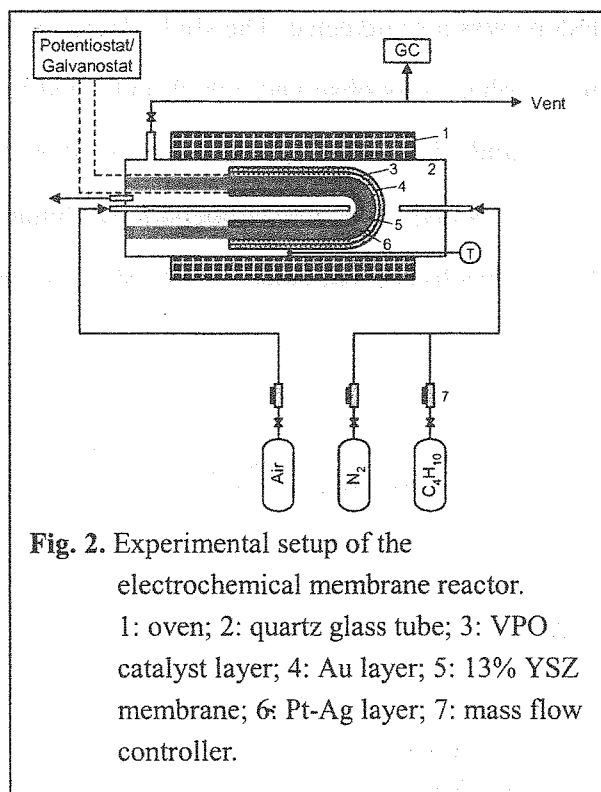


Fig. 1. Principle of electrochemical membrane reactor for butane oxidation.

In this contribution, the feasibility of the partial oxidation of n-butane to MA using oxygen ion conducting membranes in an electrochemical reactor will be demonstrated experimentally. The working principle of such a reactor is shown in Figure 1. Oxygen is reduced to oxygen ions at the cathode and transferred through the membrane to the anode, on which the active oxygen species react with n-butane or discharge to form gaseous oxygen. The advantage of this reactor is that butane oxidation and oxygen separation can be carried out simultaneously on each surface of the reactor and butane flammability concentration is not limiting the process. The oxygen flux transferred across the membrane can be controlled by the electric potential or current externally applied between the two electrodes.

Experimental

The experimental setup is shown in Figure 2. 13 mol% yttria stabilized zirconia (YSZ) was chosen as the membrane material due to its relative high oxygen ion conductivity at low temperature and its stability under reducing atmosphere. The membrane reactor was fixed inside a quartz glass tube that was installed in an oven. The cathode was a mixture of silver and platinum paste. On the anode side, a gold layer was used as the current collector and a vanadium phosphorous oxide (VPO) layer was used as the catalyst. n-Butane with N_2 was introduced into the hermetic isolated anodic chamber between the membrane reactor and the quartz tube. The total flow rate of the gas mixture was 17.5 ml/min with n-butane concentration of 0.6 mol%. Air was introduced into the cathode chamber. In order to decrease the mass transfer limitation at the cathode, the flow rate of air was fixed at 40 ml/min. The current (0 - 50 mA)



between the anode and the cathode was controlled by a galvanostat. The terminal voltage between the two electrodes was measured simultaneously. The butane oxidation was carried out in the temperature range from 730 to 773 K. The reactants and the products were analyzed

with an on-line gas chromatograph with TCD and FID detectors using five columns with two 6-way valves.

Results

The oxygen amount of transport through the membrane by applied current was determined in oxygen pumping experiments. The catalyst performance has been investigated as a function of time. The effects of current density and temperature on the catalyst performance have been studied as well. As example, the catalyst performance over time and the effect of the applied current are illustrated in this abstract.

Dynamic behaviour of catalyst performance

The catalyst performance with respect to time was investigated at different current densities. Figure 3 illustrates the dynamic behaviour of catalyst performance in the electrochemical membrane reactor at current density 2.65 mA/cm². The catalyst performance with other measured current densities was qualitatively similar in butane partial oxidation to MA. The main products were MA, CO and CO₂ with H₂O. Additionally, small amount of butene was also detected. The slight decrease in MA selectivity and butane conversion after the initial phase was observed, which indicated the deactivation of the catalyst. The deactivation was mainly due to the gradual reduction of the catalyst and carbon deposition on the anode side. At quasi-steady state, the conversions of butane and pumped oxygen were 15 - 16% and 47 - 50% respectively. The selectivity of MA was about 39%, and the selectivity ratio of CO₂ to CO was 1.5 - 1.7.

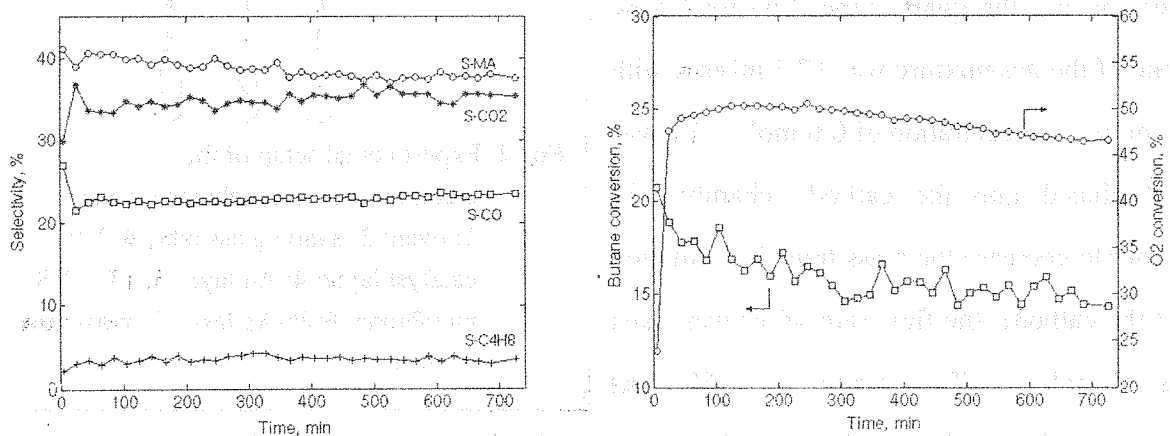


Fig. 3. Dynamic behavior of catalyst performance for butane oxidation in the electrochemical membrane reactor.

Effect of current density

The effect of the applied current density on butane partial oxidation in the electrochemical membrane reactor is shown in Figure 4. The conversions of butane and the pumped oxygen increased with the applied current density, and MA selectivity and MA yield were enhanced as well. The increase in MA yield as a function of current density was mainly due to the higher conversion of butane.

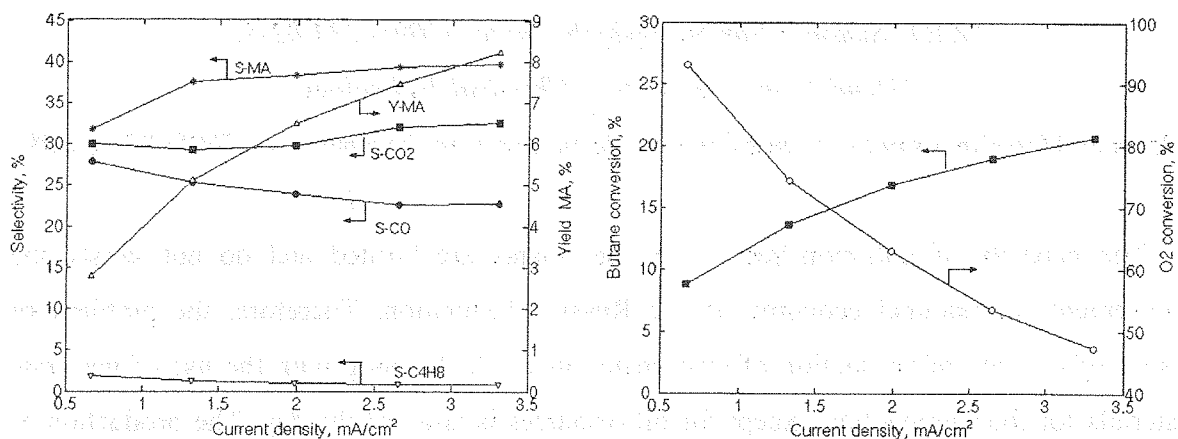


Fig. 4. Effect of applied current density on butane oxidation in the electrochemical membrane reactor.

References

- [1] Mallada, R.; Menéndez, M.; Santamaria, J., *Catal. Today*, **2000**, *56*, 191.
- [2] Stoukides, M., *Catal. Rev. Sci. Eng.*, **2000**, *42*, 1.
- [3] Satoshi, H.; Ryuji, S.; Takashi H.; Kunio S.; Kazuhisa M.; Katsuomi T.; Masaki K.; Junji N.; Toshio U., *J. Electrochem. Soc.*, **2000**, *147*, 839.
- [4] Hamakawa, S.; Sato, K.; Hayakawa, T.; York, A. P. E.; Tsunoda, T.; Suzuki, K.; Shimizu, M.; Takehira, K., *J. Electrochem. Soc.*, **1997**, *144*, 1.
- [5] Langguth, J.; Dittmeyer, R.; Hofmann, H.; Tomandl, G., *Appl. Catal. A: General*, **1997**, *158*, 287.
- [6] ten Elshof, J.E.; Bouwmeester, H.J.M.; Verweij H., *Appl. Catal. A: General*, **1995**, *130*, 195.

NOVEL INDUSTRIAL PROCESS OF HIGH-OCTANE OXYGENATED MOTOR FUEL PRODUCTION FROM NATURAL GAS

R.M. Minigulov¹, A.G. Ban², E.V. Pisarenko³, V.N. Pisarenko³

¹OOO "Yamburggasdobicha", Novii Urengoi, Yuznaya street, 2a;

tel (34549) 46919; fax (34549) 45515

²ZAO "Sintop"; Ban.Sintop@abb.ru; tel. (7095) 234-02-81

³Mendeleyev University of Chemical Technology

Moscow, Muisskaya square, 9; pvn@muctr.edu.ru; evpisarenko@mail.ru; (7095) 978-65-89

The capacity of pollution-free motor fuel plants are limited and do not satisfy the requirements of national economy of the Russian Federation. Therefore, the problem of raising of the rate of production of oxygenated motor fuels along with the use of new raw materials for their production except for oil resources is issue of the day. The production of oxygenated diesel fuels is practically lacking despite the fact that their use as fuel for heavy transport - diesel-locomotive shunters, riverboats, and trucks would allow one to reduce exhaust gas emissions, such as CO, CO₂, NO₂ in environment and to improve ecological situation in many cities and industrial regions of the Russian Federation. The objective of present research was to develop new catalysts for processing of natural gas of low-yield and low-pressure wells to pollution-free oxygenated motor fuels and high purity DME used in cosmetic and fragrance industry. DME being the component of diesel fuels, that is containing 5 – 10 % mass. of water, has its market price of 180\$ per ton of product while its prime cost is of 110 \$ per ton of product. DME with water content of 0.01 % mass. purified of water and organic compounds has its market price over 500\$ per ton of product because it can be widely used in cosmetic and fragrance industries. Due to azeotrope absence in given system, the additional DME purification is not expensive and promise significant profits to the industrial plants.

Vast experimental research on directed catalyst selection for DME synthesis from syngas and methanol was carried out. Catalysts for DME production from syngas providing high conversion of initial reactants and high quality of desired product in the range of temperatures of 170-210 °C, pressures of 3.0-7.0 MPa were selected. Catalysts for DME production from methanol in combined reactive rectification apparatuses operating at temperatures of 110-

150°C were selected as well. The use of such a low temperature catalysts for DME production allows one to solve the problem of high quality DME synthesis in combined reactive rectification apparatuses while simultaneous purification of side-product such as water from oxygen containing compounds to be used further in production technological cycle.

Due to experimental data obtained in laboratory and pilot reactors, kinetic models of the reactions studied, reactor models and models of different reactor units were developed. Design parameters of chemical technological equipment and the regimes of their operation were calculated according to the models. The process of methanol dehydration was implemented at low temperatures in combined reactive rectification apparatuses to reach high conversion of initial reactants while low energy and raw material consumption.

Novel technology of natural gas processing to DME to be used as fuel by one-pass process of syngas conversion in a reactor unit consisting of two packed reactors in series has been developed. Initial reactant conversion in the reactor unit exceeded 80 % while 20-30 % decreases in energy consumption compared to traditional technologies.

Novel technology of natural gas conversion to high purity DME to be used for cosmetic and fragrance industries implemented in combined reactive rectification system with additional water purification from oxygen containing compounds has been developed. The process developed is energy-saving and is characterized by significant reductions in raw material consumption compared to traditional technologies. Ecological parameters of the processes concerned meet all federal Russian standards.

References:

1. Pisarenko V.N., Abaskuliev J.A., Chernomirdin A.V., Kachalov V.V., Brezgin B.E. Method of preparing methanol. RU patent № 2152378, 28.04.99.
2. Pisarenko V.N., Abaskuliev J.A., Kosunov O.A. Method of preparing methanol. RU Patent №2188790, 07.08.01

NOVEL PROCESS OF COMPLEX PROCESSING OF PRODUCED WATER OF GAS FIELDS

R.M. Minigulov¹, A.G. Ban², E.V. Pisarenko³, V.N. Pisarenko³

¹ OOO "Yamburggasdobicha" Novii Urengoi, Yuznaya street, 2a;

tel (34549) 46919; fax (34549) 45515

² ZAO "Sintop" Moscow, Profsoyuznaya street, 23;

Ban.Sintop@abb.ru; tel. (7095) 234-02-81

³ Mendeleev University of Chemical Technology Moscow, Muisskaya square, 9

The processes of utilization of secondary sources of raw materials and energy, in particular, the process of complex processing of produced waters of gas condensate fields are of great importance for the development of highly profitable plants of the production and processing of natural gas.

The content of hydrocarbons of gas condensate, methanol, iodine, bromine and cations of salts of (Co, Ni, Ba, Ag, Zn) in produced waters varies with the type of gas condensate field and methods of its development. Now, the extraction of valuable chemical organic and inorganic products from produced waters that can be used further for different technological purposes have a great potential.

Special requirements exist regarding the quality of purified water that has to contain less than 40 ppm hydrocarbons. This value was standardized by international agreement in 1993. Discharges of produced water containing more than 100 ppm hydrocarbons into seas or other reservoirs are determined as oil pollution. Installations for produced water purification in the US coastal areas have in average 29 ppm hydrocarbons in purified water while the maximum monthly average value is 42 ppm. It should be mentioned that these values could slightly differ depending on the region of the US coast. Apparently, methods of produced water purification near the coast are different from that at sea gas producing platforms where large-scale industrial equipment cannot be used. The platform load is about 1 ton of purified water/m².

In 1995, Americal oil Institute recommended some methods for purification of produced waters of gas and oilfields. Among them, we mention the following:

1. coal adsorption purification from hydrocarbons, acids and bases;

2. floatation purification from volatile hydrocarbons, benzole, toluene, phenol, naphthalene;
3. membrane filtration from fine-dispersed suspended substances and emulsions of hydrocarbons;
4. destruction of volatile and non-volatile organic compounds by UV radiation;
5. oxidation of hydrocarbons, hydrogen sulfide, acids and bases by ozone and hydrogen peroxide;
6. biological purification from hydrocarbons, organic compounds and hydrogen sulfide.

The only three first methods of produced water purification mentioned above, have practical significance for gas producing plants in the North regions of the Russian Federation. New process of produced water processing at gas condensate fields with significant methane amounts has been developed. The process specifies the four-stage processing.

At the first stage, combined processes are performed in one membrane block, such as precipitation of fine dispersed solid particles (mainly quartz and iron oxides) and separation of hydrocarbon and water phases in liquid membranes. Mass transfer processes of separation of different substances in liquid membranes were investigated on the laboratory scale. Chemical compositions of liquid membranes providing efficient separation of hydrocarbons from water-in-methanol mixture were determined. Mathematical model of given mass transfer unit was developed, its design parameters and operating regimes were calculated. Mass flows of hydrocarbons and water-in-methanol mixture were determined.

At the second stage of the process, water-in-methanol mixture is directed to the membrane unit where separation of produced water from surface-active materials, corrosion inhibitors and soluble substances with significant molecular weight takes place. Mathematical model of membrane unit was developed based on experimental results. Due to the model, the membrane unit design and operating regimes were calculated.

At the third stage of the process, the permeate flow from membrane unit goes to the rectification column after which the distillate with methanol content more than 95% mass. is supplied to the consumer – gas producing plant. The bottom product is directed to the unit of additional purification. Due to the results of laboratory experiments, the equations of vapor-liquid equilibrium for binary mixtures were determined.

At the fourth stage of the process, the bottom product of the rectification column feeds the installation of membrane separation where the concentrate with increased content of salts and hydrocarbons is taken out of the installation and the permeate flow - purified water with total content of impurities of less than 60 ppm as technical water is supplied to the consumer.

OP-III-7

According to experimental results, the mathematical model of the membrane unit was constructed and the regimes of its operation were determined.

The flow of side products such as the hydrocarbon flow of the second stage and the bottom aqueous flow of rectification column of the fourth stage could serve as initial raw materials for hydrocarbon motor fuel and iodine productions.

Hydrocarbon flow of the second stage feed the stabilization column and is then directed to the fractionation column where flow separation in pentane-hexane fraction, benzene fraction and kerosene-gas-oil fraction occurs. Pentane-hexane fraction is taken to the adiabatic catalytic reactor in which it is converted to benzene-isomerize hydrocarbons at temperatures of 240-290 °C. Benzene fraction is converted to high-octane hydrocarbon motor fuels by reforming process. Kerosene-gas-oil hydrocarbons are used as the components of liquid membranes.

Aqueous flows of the forth process stage with iodine content of more than 20 mg/l is directed to the installation of iodine production by means of desorption method. The installation consists of the unit of concentration of sodium and potassium iodides in raw materials, adsorption-desorption aggregate with recycling sorbent and the unit of chlorine and chloride water production by electrolytic method, the units of drilling water, acid and chloride supply and the unit of sulfur combustion. Desired product contained 99 % of iodine and 0.8 % of water. The ration of iodine extraction exceeded 92 %. Laboratory experiments of different process stages of iodine production were carried out. Mathematical models of different units and models of the whole chemical technological scheme were developed. Design parameters of apparatuses were determined and operating regimes were calculated. The adequacy of the models of some apparatuses and the model of the whole chemical technological scheme was checked at the pilot plant producing 1.0 kg of iodine per hour.

Based on the results of the process study of produced waters processing of gas and gas/condensate fields, the profitability of the technology developed for practical use in the North regions of the Russian Federation have been demonstrated.

CHEMICAL PROCESSES INVESTIGATION BY AEROSOL NANOCATALYSIS TECHNOLOGY

I.M. Glikina

Severodonetsk Technological Institute Eastern-Ukrainian National University,

59-a, Sovetskiy avenue, Severodonetsk, Lugansk region, 93400, Ukraine

Tel.: (06452)34028 E-mail: glikin@sdtcom.lg.ua

Present is a transfer of science and technique to micro- and nanoscale. This way is called nanochemistry, which can divide to nanocatalysis and nanotechnology. Aerosol catalysis technology is one of the ways of them. It consists of heterogeneous catalysis on nanosized particles without carrier. Deep and partial organic and inorganic compounds oxidation, oxidehydrochlorination, oxidative coupling of methane, industrial and municipal wastes treatment with different aggregate states were carried out by this technology. One of the main conditions of aerosol catalysis technology with fluidized bed (ACFB) and with vibrating bed (ACVB) is mechanical and chemical catalyst activation in situ. The catalytic processes is realized on ultradispersed catalyst particles with 10^{-8} - 10^{-9} meter particle size. It was placed by experiment. Mechanical and chemical activation and catalyst particle size result in change surface property and it lead to increase catalyst activity in 5-6 times compare with traditional (catalyst concentration is changed from 10 to 0,0001 g/m³ by transfer from ACFB to ACVB).

New method of kinetic characteristic investigation of heterogeneous and catalytic reaction was created. It's simple, laborious less and reproduce ACFB condition method. It consists of reactor with vibrating bed of inert materials, which created mechanical and chemical activation and catalyst aerosol. If we use this method, than decrease laboratory reaction volume in 50-250 times, simplify organization and management of experiment, make possibility manage mechanical and chemical activation intensity [1].

Experimental data for deep oxidation of methane and also its mixture with hydrogen and ammonia are shown special influence to reaction rate. Dependence reaction rate from components concentration can be resulted with empirical equation, such as (1):

$$W = k * C_{CH_4} * C_{H_2}^n * C_{NH_3}^m \quad (1)$$

by $C_{CH_4}=2,4-11,2\%vol.$, $C_{H_2}=24-26\%vol.$, $C_{NH_3}=0,3-0,34\%vol.$

OP-III-8

where W – reaction rate, mol/sec; C_{CH_4} , C_{H_2} , C_{NH_3} – methane, hydrogen and ammonia concentration respectively, g/m^3 ; k – rate constant; n , m – reaction order by component hydrogen and ammonia respectively.

It suggest, that the aerosol nanocatalysis process goes in diffusion field. The activation energy of deep oxidation of methane on Fe_2O_3 catalyst at 600-750⁰C is up to 20 kJ/mol. Influence particle size of inert materials (quartz sand) to reaction rate is shown oh Figure for this processes.

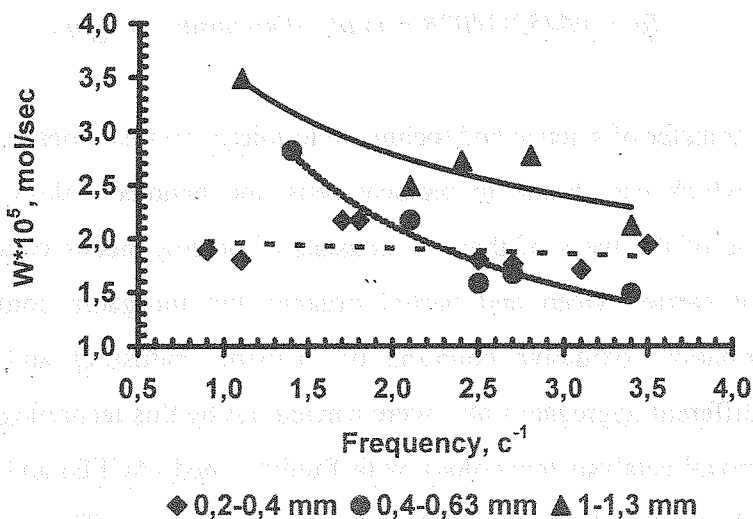


Fig. Dependence reaction rate of deep oxidation of methane from particle size of inert material.

In order to investigation aerosol nanocatalysis processes you need obtain influence the main parameters, such as quantity and type of catalyst and inert materials, particle size of inert materials, mechanical and chemical activation intensivity, temperature and concentration regime and also analytic control off-gas.

Reference

1. I.M. Glikina, V.S. Novickiy, N.F. Tyupalo. M.A. Glikin / Aerosol nanocatalysis investigation in vibrating bed // Chemical industry of Ukraine, N3, 2003, P. 24-29.

SIMULATION OF CATALYTIC DEHYDROGENATION PROCESS IN A FIXED BED CONTAINING MOVING FINE SOLID PARTICLES

L.V. Barysheva, N.A. Chumakova, D.A. Stepanov, V.M. Khanaev

Boriskov Institute of Catalysis SB RAS, 630090, Novosibirsk, Russia

E-mail: barysheva@catalysis.nsk.su

Usage of moving solid particles as a heat carrier in a fixed catalyst bed seems to have definite advantages for highly endo- and exothermic processes, because moving particles provides additional heat supply/removal to the reaction zone. Introduce to the reaction gas mixture of fine solid particles brings controlled increase of the heat capacity of gas-solid flow. Simultaneously a heat conditions in fixed bed are changed too. The aim of this research is a development of a mathematical model for the simulation of unsteady states in plug flow reactor with granular catalyst bed with and without the filtration of fine solid particles.

Let consider the catalytic dehydrogenation of *i*-butane in lab-scale reactor of 150 cm³ volume. The reaction



is endothermic and reversible. The feed gas mixture is of a complex composition and consists of *i*-butane, hydrogen and water vapor. The concentrations distribution over the bed length is described by the equation:

$$U_g \cdot \frac{\partial C}{\partial z} = -R \cdot w \quad (2)$$

Kinetic data of the reaction over the Pt/Sn-catalyst are taken from [1].

Mathematical model looks as follows:

heat balance for the gas phase:

$$\begin{aligned} \phi \cdot \varepsilon \cdot C_{p_g} \cdot \rho_g \cdot \frac{\partial T_g}{\partial t} + C_{p_g} \cdot \rho_g \cdot U_g \cdot \frac{\partial T_g}{\partial z} = \\ = \alpha_{pg} \cdot S_p \cdot (T_p - T_g) + \alpha_{gc} \cdot S_c \cdot (T_c - T_g), \end{aligned} \quad (3)$$

heat balance for the fine particle phase:

$$\begin{aligned} (1 - \phi) \cdot \varepsilon \cdot C_{p_p} \cdot \rho_p \cdot \frac{\partial T_p}{\partial t} + C_{p_p} \cdot \rho_p \cdot (1 - \phi) \cdot \varepsilon \cdot U_p \cdot \frac{\partial T_p}{\partial z} = \\ = \alpha_{pg} \cdot S_p \cdot (T_g - T_p) + \alpha_{pc} \cdot S_c \cdot (T_c - T_p), \end{aligned} \quad (4)$$

heat balance for the catalyst phase:

$$(1 - \varepsilon) \cdot C_p \cdot \rho_c \cdot \frac{\partial T_c}{\partial t} = \lambda_c \cdot \frac{\partial^2 T_c}{\partial z^2} + \alpha_{pc} \cdot S_c \cdot (T_p - T_c) + \alpha_{gc} \cdot S_c \cdot (T_g - T_c) - R \cdot w \cdot \Delta H + \alpha_w \cdot S_w \cdot (T_w - T_c), \quad (5)$$

heat balance on the reactor wall:

$$\alpha_w \cdot S_w \cdot (T_w - T_c) = \alpha_a \cdot S_a \cdot (T_a - T_w). \quad (6)$$

Boundary conditions:

$$z = 0: \quad C = C_0, \quad T_p = T_{p0}, \quad T_g = T_{g0}, \quad T_{p0} = \text{const},$$

$$\lambda_c \cdot \frac{\partial T_c}{\partial z} = \alpha_{gc} \cdot (T_c - T_g) + \alpha_{pc} \cdot (T_c - T_p), \quad (7)$$

$$z = L: \quad \frac{\partial T_c}{\partial z} = 0. \quad (8)$$

Initial conditions:

$$t = 0: \quad T_p = T_c = T_g = T^0.$$

We use the following notation:

T – temperature, K; C – vector of concentration; U_g – superficial gas flow velocity, $\text{m} \cdot \text{s}^{-1}$; U_p – particles flow velocity, $\text{m} \cdot \text{s}^{-1}$; S – specific surface area, m^2 ; w – load of catalyst, $\text{kg} \cdot \text{m}^{-3}$; z – axial coordinate, m; α – heat exchange coefficient, $\text{kJ} \cdot \text{s}^{-1} \cdot \text{m}^{-2} \cdot \text{K}^{-1}$; ε – the fixed bed porosity; ϕ – the gas fraction in the velocity; λ_c – heat conductivity of fixed bed, $\text{kJ} \cdot \text{s}^{-1} \cdot \text{m}^{-1} \cdot \text{K}^{-1}$; ρ – density, $\text{kg} \cdot \text{m}^{-3}$.

Indexes: p – particles, g – gas, c – catalyst, w – wall, a – air.

It is possible to consider a simplified model. For instance, the heat capacity of the catalyst is much higher compared to the other phases, and consequently we can consider the reduced model with vanished terms

$$\frac{\partial T_c}{\partial t} = 0 \quad \text{and} \quad \frac{\partial T_p}{\partial t} = 0$$

The next simplification is based on the assumption that the temperatures of gas and fine solid particles are rather closed to each other. Therefore the equations (3) and (4) can be rewritten in the form of a single equation.

Thus, an unsteady mathematical model of the process of catalytic dehydrogenation in the fixed-bed reactor with moving fine particles as a heat carrier is developed and its simplified cases are considered. The simulation of the process dynamics is performed and the influence of different parameter is studied.

References

1. Lyu Kam Lok, H.A. Gaidai, B.S. Gudkov, S.L. Kiperman, S.B. Kogan. Study of kinetics and mechanism of isobutane dehydrogenation over the Pt/Sn-catalysts. Kin. and Cat. 1986, V. XXVII, No.6, P.1365-1377 (in Russian).

DESIGN OF CATALYSTS AND CATALYTIC BURNERS FOR FUEL CELL POWER PLANT REFORMER

**Z.R. Ismagilov^{1*}, M.A. Kerzhentsev¹, V.A. Sazonov¹, L.T. Tsykoza¹, N.V. Shikina¹,
V.V. Kuznetsov¹, V.A. Ushakov¹, S.V. Mishanin², N.G. Kozhukhar²,
G. Russo³, O. Deutschmann⁴**

¹ *Boreskov Institute of Catalysis, Pr. Ak. Lavrentieva, 5, Novosibirsk, 630090, Russia*

² *Russian Federal Nuclear Center All-Russian Research Institute of Experimental Physics,
Pr. Mira, 37, Sarov, 607190, Russia*

³ *Instituto di Richerche sulla Combustione, Piazzale V. Tecchio, 80125, Naples, Italy*

⁴ *University of Heidelberg, Im Neuenheimer Feld, 368, Heidelberg, 69120, Germany.*

Fuel Cell Power Plants (FC PP) are very attractive novel energy generating systems, which keep environment clean and provide saving of energy resources. The initial fuel for use in FC PP is natural gas or methane. Natural gas is subjected to the catalytic reforming in the Power Plant fuel conditioning system, where it is converted into a hydrogen-rich gas mixture used in an FC stack for electrochemical reaction of hydrogen oxidation.

A functioning FC stack produces a gas mixture (the anode gas), which contains a certain amount of combustible components, such as hydrogen, carbon monoxide, and methane residue. This mixture is also burned, in order to obtain heat required for the PP internal consumption, thus increasing the PP efficiency.

Usually, flame combustion is used in the fuel processing system to provide heat for endothermic steam reforming reactions of natural gas. However, the use of flame burners in the reformers results in overheating of the walls of heat absorbing elements of the reformer reactor, thus reducing considerably the reformer service life. Another serious drawback of flame combustion is formation of NO_x and products of incomplete combustion: CO, HCOH, and soot.

The alternative to flame combustion is flameless catalytic combustion. This process has received increasing attention in the last decades for numerous applications due to its potential

* Corresponding author. E-mail: zri@catalysis.nsk.su

OP-III-10

for reducing pollutant emissions, most notably nitrogen oxides. It also provides possibility to burn low calorific fuels, such as anode gases, under stable regimes and with high efficiency.

A schematic representation of the proposed concept of a catalytic burner installed in the fuel cell power plant is shown in Fig. 1.

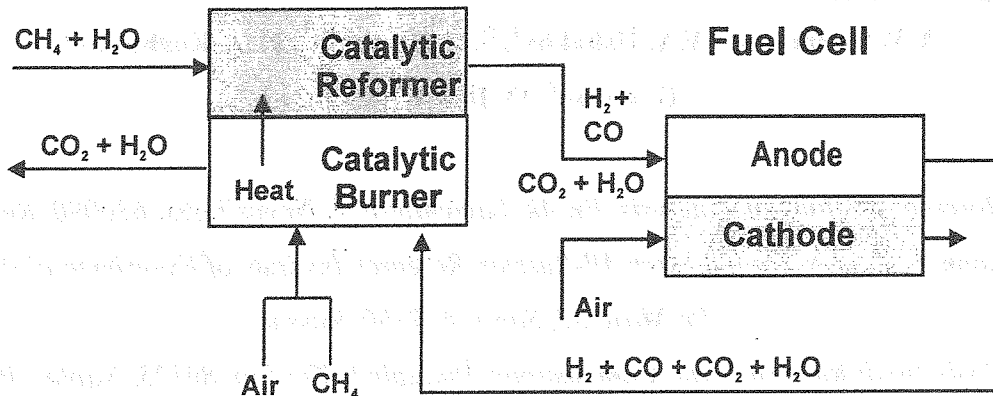


Fig. 1. Schematic representation of a catalytic burner combined with a fuel cell power plant

The main goals of the presented work are:

- ◆ development of highly effective stable catalysts operating at high temperatures 900-1200°C;
- ◆ characterization and testing of the catalysts;
- ◆ design and fabrication of the reformer with a prototype catalytic burner;
- ◆ testing of the reformer with a prototype catalytic burner.

Noble metals initiate combustion processes at rather low temperatures, however their application at elevated temperatures is limited due to volatilization, sintering and deactivation. Therefore the research was concentrated mainly on supported oxide systems.

The catalyst supports also must satisfy the requirements of catalytic fuel combustion processes by specific surface area, mechanical strength and especially by thermal stability for durable operation. Aluminas modified by Mg, Ce and La oxides were shown as good candidates.

Thermally stable manganese-containing supported catalysts have been developed. These catalysts retain the initial activity in methane oxidation up to 1000°C, and further increase of thermal stability of the catalysts (up to 1100-1300°C) can be achieved by catalyst doping with modifying agents (La, Ce and Mg oxides). The stability of these catalysts can be explained by the formation of solid solutions at 900°C or hexaaluminates at 1100-1200°C due to interaction of manganese oxide with the catalyst support.

A series of Mn containing oxide catalysts on spherical (1.4-1.8 mm) γ - Al_2O_3 or $(\gamma+\chi)$ - Al_2O_3 , pure or doped with La, Ce and Mg oxides were prepared. The content of Mn (calculated as MnO_2) was varied in the range 4-10 wt.%. The catalysts were characterized by chemical analysis, XRD, BET surface area and activity measurements in methane oxidation (Fig. 2).

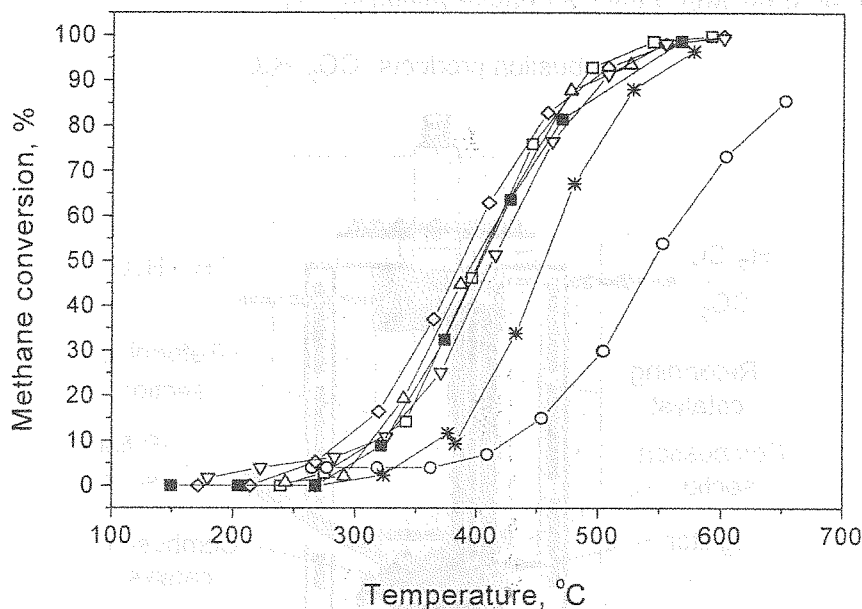


Fig. 2. Activity of Mn-Al-O catalysts in methane oxidation measured in a flow setup at $V=1000 \text{ h}^{-1}$:
 \square - 5%Mn/ γ - Al_2O_3 ; \diamond - 5%Mn/ $(\gamma+\chi)$ - Al_2O_3 ; \circ - 5%Mn/ $(\gamma+\chi)$ - Al_2O_3 (Commercial);
 Δ - 5%Mn/ $(\gamma+\chi)$ - Al_2O_3 +MgO; ∇ - 5%Mn/ $(\gamma+\chi)$ - Al_2O_3 +MgO+ La_2O_3 ;
 $*$ - 5% Mn/ $(\gamma+\chi)$ - Al_2O_3 +MgO+ CeO_2 ; \blacksquare - 10%Mn/ γ - Al_2O_3

A batch of Mn-Mg-La-Al-O catalyst was prepared for further testing in a model reformer with a catalytic burner.

The testing of this catalyst in a prototype pilot catalytic burner under realistic conditions of natural gas combustion at high temperature ca. 1200°C and low excess oxygen $\alpha = 1.0$ - 1.15 also proved that this catalyst could be efficiently used in catalytic burners for fuel cell power plant reformers (Table 1)

Table 1.

Results of testing Mg-La-Al-O in catalytic combustion of natural gas in a pilot burner

Conditions of testing			Composition of combustion products, vol.%				
α^*	$T_1, ^\circ\text{C}$	$T_2, ^\circ\text{C}$	H_2	CO	CH_4	CO_2	O_2
1.00	1204	1002	0.0100	0.0017	0.0090	11.46	0.06
1.06	1199	987	0	0.0069	0	10.12	1.24
1.15	1135	1003	0	0	0	10.34	2.67

OP-III-10

Catalyst loading is 220 cm^3 , natural gas flow rate 50 l/h, α is coefficient of air excess,

T_1 is temperature at the bottom of the catalyst bed, T_2 is the temperature in the middle of the bed

A pilot reformer for methane steam reforming was designed and fabricated for testing in the composition of the pilot Fuel Cell Power Plant (Fig. 3).

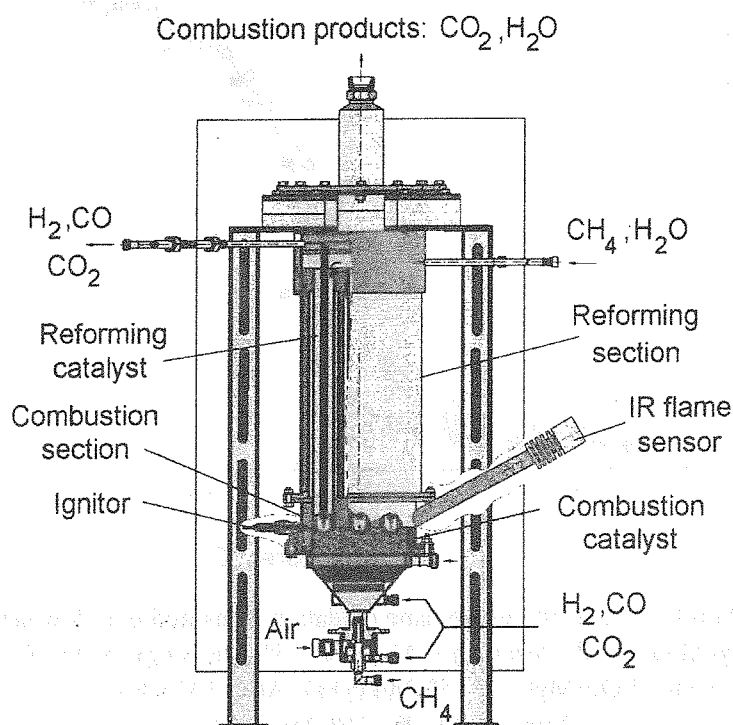


Fig. 3. The drawing of the pilot catalytic reformer with a catalytic burner.

The reformer contains a catalytic reforming unit in the heat insulated casing with a catalytic burner located below. The reformer section consists of 7 tubular modules containing $\text{Ni}/\text{Al}_2\text{O}_3$ catalyst for methane reforming. Each module consists of three concentric tubes of original design.

The long-term tests of the pilot reformer with a catalytic burner working both with methane and the mixture of natural gas and anode gases showed that the parameters of the catalytic burner are stable. The unit is recommended for industrial application.

Acknowledgements: To the International Science and Technology Center for support of this work in frame of ISTC project # 16 78, to the INTAS-0180 and NWO.

FLUIDIC BUS SYSTEM FOR CHEMICAL PROCESS ENGINEERING IN THE LABORATORY AND FOR SMALL-SCALE PRODUCTION

A. Müller, V. Cominos, V. Hessel, B. Horn, J. Schürer, A. Ziogas,

Institut für Mikrotechnik Mainz GmbH, e-mail: muellera@imm-mainz.de,

K. Jähnisch, Institut für Angewandte Chemie Berlin-Adlershof e.V.,

V. Grosser, V. Hillmann, K. A. Jam,

Fraunhofer Institut für Zuverlässigkeit und Mikrointegration,

A. Bazzanella, Dechema e.V.,

G. Rinke, M. Kraut, Forschungszentrum Karlsruhe GmbH

Within the framework of a BMBF-funded project, a consortium consisting of a number of German companies and research institutes developed a standardized system for the combination of micro devices and laboratory equipment of various suppliers thus leading to the build up of chemical plants.

Although a number of micro devices and process equipment like valves, pumps, etc. are currently on the market, only a limited number of applications have been reported so far which combine micro reactors from the same or even different suppliers. Aside from problems with capacity differences, one key limitation of these devices is that they use different kinds of interfaces which hamper their direct connection. Standardized interfaces would allow the execution of complex chemical processes. Through the collaboration of the above-mentioned five project partners in a BMBF-funded strategic project [1, 2] and with the advice of an industrial board, a so-called *backbone interface* has been developed based on the bus concept where the flow is passed through a central spine (Figure 1). Such a "microplant" is seen as an alternative or a supplement to the miniplant approach in plant engineering. Similar to this technology a closed loop set-up with a refeeding of side products is realized if unit operations for product separation can be integrated. At the present state of development this demands the integration of conventional miniplant glassware, for example, by the installation of a distillation column into the microplant set-up. Such a combination is feasible because the flow rates of a microplant are similar to typical flow rates of miniplant separation units.

Microplant components can also be looked at as a supplement to miniplant components if one has to deal with highly exothermic reactions or high-pressure environments. Due to their low internal volume, micro devices withstand large internal pressures. In such a way, a

OP-III-11

pressurized subregion of a plant can be kept at high pressure using micro devices (appropriate control equipment exist) whereas the rest of the plant is kept under low pressure using miniplant equipment. Similar examples [3, 4] exist for very fast and/or highly exothermic reactions or reactions in the explosive regime (unthinkable with standard glassware).

In the presented contribution, a combination of miniplant and microplant equipment is used as a production facility for fine chemicals. This approach differs from the usual application of a miniplant as a mediator between laboratory-scale and pilot plant-scale operation.

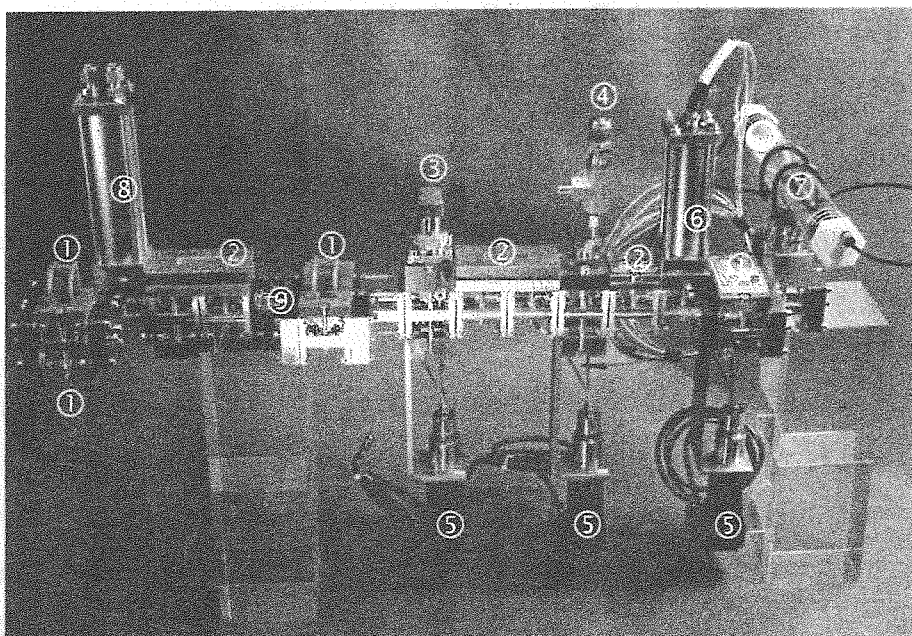


Figure 1 Example of a microplant based upon the modular fluidic backbone.

- (① heat exchanger, ② mixer, ③ valve, ④ safety valve, ⑤ pump,
⑥ heated residence-time module, ⑦ mixer-settler extractor,
⑧ heated mixer-tube reactor, ⑨ thermal decoupler)

The modular backbone presented here allows both commercial and demonstration-type micro devices to be coupled in all three dimensions in a flexible and easy manner. Its construction leads to compact systems with low internal volume of 35.3 to 950.0 mm³ (per backbone element) which can be operated up to 300°C and 100 bar, being only limited by the physical properties of the gaskets used (e.g. steel, graphite, Viton, Kalrez). By exchanging tubes and borings of various diameters, a large range of volume flows is accessible. For liquid-phase processes, volume flows of up to 32 l/h at a pressure loss of 150 mbar (per spine unit) can be realised and extended to 1000 l/h (30 mbar) by use of special adapters, thereby enabling pilot-plant operation. The backbone interface has the additional advantage of being

able to incorporate within its body sensors such as those developed within the Match-X consortium [5, 6] and of performing as a platform for commercially available valves and mass flow controllers. Such a backbone consists of single standardised elements each incorporating a number of pipes and housing parts and will also be equipped with internal trace heating for the fluidic channels. Figure 2 gives a comparison between a fluidic/mechanical backbone element and its archetype a human vertebra.

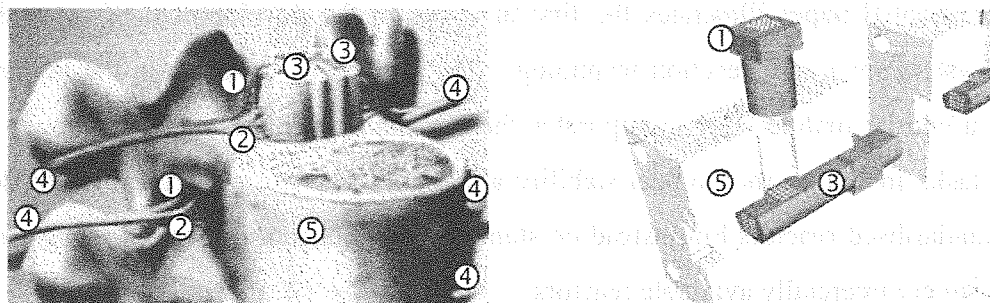


Figure 2 Archetype human vertebra (① sensor nerves, ② motoric nerves, ③ spinal cord, ④ spinal nerves, ⑤ bone structure) and backbone element as electro-mechanical equivalent to a spinal cord (① sensor signals, ③ signal bus, ⑤ mechanical support)

The performance of the backbone shall be examined using several case study reactions. Among them are advanced multi-step reactions in organo-metallic boron chemistry (l), fast and exothermic sulphonation of alkyl-substituted aromatics (g/l), and catalytic investigations on ethylene oxide synthesis (g). Starting from the direct connection between a few micro devices, entire set-ups shall be built based upon a 'plug and produce' plant assembly systematic.

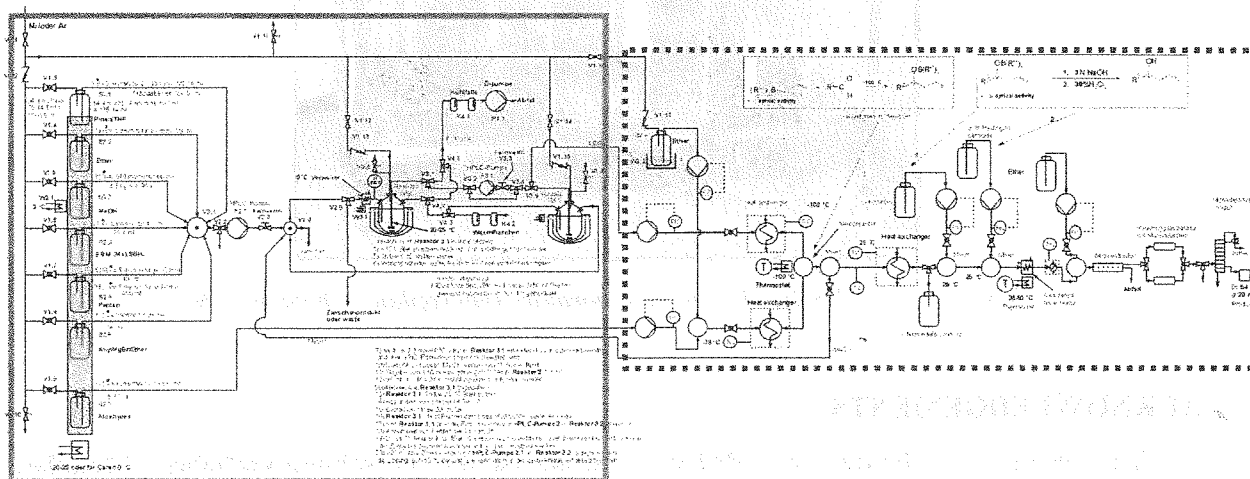


Figure 3 Flowsheet of case study involving organoborane synthesis split into two sections – one to be run in a miniplant, the other in a microplant (hatched line)

OP-III-11

In Figure 4 it is demonstrated that the microplant setup in Figure 3 exhibits a larger complexity than the miniplant setup but it nevertheless consumes a much smaller package volume of the plant setup. During the experiments the microplant concept will also be assessed by measuring abilities like seal reliability and thermal cross-talk between parallel fluidic channels.

CONCLUSIONS

The presented paper illustrates the first attempts in the development of a standardised modular system for micro reaction technology. The concept is based upon the human spine which in a similar manner also incorporates the simultaneous handling of a number of very different tasks including mechanical stability and signal transmission. The system does not rely on standardised reactors but instead on standardised connections thus allowing the use of non-uniform commercially available reactors.

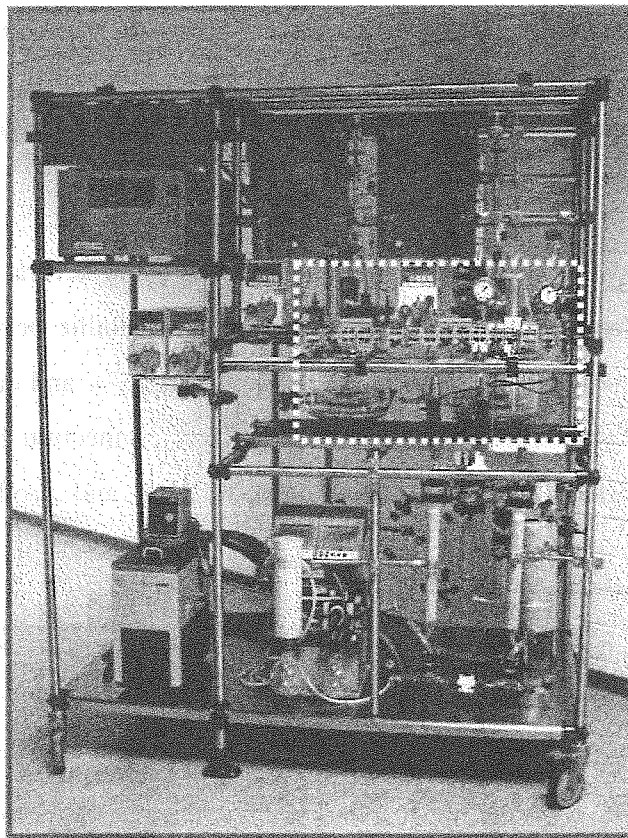


Figure 4 Realization in the laboratory (microplant = hatched line)

ACKNOWLEDGEMENTS

The project is funded by BMBF ("Strategisches Forschungsvorhaben Modulare Mikroverfahrenstechnik μ VT", Förderungskennzeichen 16SV1459).

REFERENCES

- [1] G. Rinke¹, M. Kraut¹, V. Großer², V. Hillmann², A. Müller³, B. Horn³, K. Jähnisch⁴, A. Bazzanella⁵,
¹Forschungszentrum Karlsruhe GmbH, ²Fraunhofer Institut für Zuverlässigkeit und Mikrointegration, 13355
 Berlin, Germany, ³Institut für Mikrotechnik Mainz GmbH, ⁴Institut für Angewandte Chemie Berlin-
 Adlershof e.V., ⁵Dechema e.V., *Modular Micro Process Engineering and Applications*, International
 Conference on Microreaction Technology 7 (IMRET), Proceedings, September 7 - 10, Lausanne, Schweiz
- [2] A. Müller, V. Cominos, K. Drese, V. Hessel, B. Horn, H. Löwe, A. Ziogas, Institut für Mikrotechnik Mainz
 GmbH; K. Jähnisch, Institut für Angewandte Chemie Berlin-Adlershof e.V., V. Grosser, V. Hillmann, K. A.
 Jam, Fraunhofer Institut für Zuverlässigkeit und Mikrointegration, G. Rinke, Forschungszentrum Karlsruhe
 GmbH, A. Bazzanella, Dechema e.V., *Fluidic Bus System for Chemical Micro Process Engineering*,
 Abstracts of the lecture groups, Achema 2003, Frankfurt/M., Germany, 19-24 May 2003
- [3] Kestenbaum, H., Lange de Olivera, A., Schmidt, W., Schüth, H., Ehrfeld, W., Gebauer, K., Löwe, H.,
 Richter, T.; *Silver-catalyzed oxidation of ethylene to ethylene oxide in a microreaction system*, Ind. Eng.
 Chem. Res. 41, 4 (2000) 710-719
- [4] Hagendorf, U., Janicke, M., Schüth, F., Schubert, K., Fichtner, M., *A Pt/Al₂O₃ Coated Microstructured
 Reactor/Heat Exchanger for the Controlled H₂/O₂-reaction in the Explosion Regime*, in Ehrfeld, W.,
 Rinbard, J.H., Wegeng, R.S. (Eds.), *Process Miniaturization: 2nd International Conference on Microreaction
 Technology*, Topical Conference Reprints, AIChE, New York, USA, 1998
- [5] Amiri Jam, K.; Hillmann, V.; Großer, V.; Michel, B.: *Design, fabrication and test of electrical modules with
 several assembly layers*, at MicroTec2003, Munich, Germany, 13.-15. Oct. 2003.
- [6] Großer, V., et al.: *Microfabrication of modular MEMS - Assembly and Reliability*, at DTIP 2002, Cannes
 Mandelieu, 5 - 8 May 2002

NUMERICAL SIMULATION OF FLOW DISTURBANCES INDUCED BY BOUNCY FORCE IN A HORIZONTAL REACTOR

N.Yu. Romanvukha, A.G. Churbanov, N.G. Churbanova, B.N. Chetverushkin

Institute for Mathematical Modelling, Russian Academy of Science

Miusskaya sq. 4A, 125047, Moscow, Russia, e-mail: rona@imamod.ru

The work is supported by the projects 03-01-00544 and 02-01-00700 of Russian Foundation for Basic Researches

Introduction. Compressible viscous gas flows characterized by strong density variations at essentially subsonic medium motion are observed in various industrial applications including the flows in different chemical reactors. In this article we study the flow disturbances resulting from the interaction between the main flow and buoyancy-induced secondary flows in horizontal chemical reactor for syngas production.

The considered reactor is a cylindrical tube with the gas flow (Methane/Oxygen/Argon mixture) in the channel. The inlet gas flow is preheated up to the temperatures 500-800K, and the platinum nets, attached to the walls up to - 1000K - 1200K. The contact times of the gas flow with the catalytic surface are short enough - at about several milliseconds. The dynamical processes are characterised by low Mach numbers (0.01-0.1), large Reynolds numbers (500-1000), and strong temperature gradients in the boundary layer. The influence of two primary governing parameters - the Reynolds number and the Grashof number on the flow in the channel was numerically investigated.

Mathematical method. The method is based on the two-scale pressure splitting developed in the frame of Low-Mach Number (LMN) approximation introduced in the work (Rehm and Baaum,1978). Pressure $p(t,x)$ is decomposed into a volume-averaged part $\bar{p}(t)$ which has thermodynamic sense and depends on time only and a dynamic fluctuation $p_d(t,x)$ varying both in space and time so that in dimensionless form: $p(t,\bar{x}) = \bar{p}(t) + \gamma M^2 p_d(t,\bar{x})$,

$$\int_{\Omega} p_d(t,\bar{x}) dV = 0 \text{ where } \Omega \text{ is the problem domain.}$$

This two - scale splitting of the pressure allows to avoid any singularities in the governing equations as Mach number M vanishes. It should be noted that in contrast to LMN approximation we solve the full Navier-Stocks equations without any reductions or

preconditioning. That allows to apply the unified code to numerical simulation of quite different types of viscous flows (Churbanov and Pavlov, 1998).

The governing equations in the dimensionless formulation are presented by the following mass, momentum and energy conservation equations with equation of state for perfect gas and additional integral restriction closing the system in correct way:

$$\frac{\partial \rho}{\partial t} + \text{div}(\rho \bar{v}) = 0,$$

$$\frac{\partial \rho v_i}{\partial t} + \text{div}(\rho v_i \bar{v}) + \text{grad}_i p_d = \frac{2}{\text{Re}} \left(\text{DIV}_i(\mu \dot{S}) - \frac{1}{3} \text{grad}_i(\mu \text{div} \bar{v}) \right) + \frac{Gr}{\text{Re}^2} \frac{\rho e_i}{r_T},$$

$$\frac{\partial \rho T}{\partial t} + \text{div}(\rho \bar{v} T) = \frac{1}{\text{Re} \cdot \text{Pr}} (\text{div}(\lambda \text{grad} T)) + (\gamma - 1) \left(\frac{1}{\gamma} \frac{\partial \bar{p}}{\partial t} + M^2 \frac{\partial p_d}{\partial t} \right) + (\gamma - 1) M^2 \left((\bar{v} \cdot \text{grad} p_d) + \frac{J_{dis}}{\text{Re}} \right)$$

$$J_{dis} = 2\mu \left(\dot{S} - \frac{1}{3} (\text{div} \bar{v})^2 \right), \quad \rho = p/T, \quad p = \bar{p} + \gamma M^2 p_d, \quad \int_{\Omega} p_d dV = 0,$$

Here $\gamma = c_p / (R - c_p)$, ρ, c_p and T are density, heat capacity and temperature, μ and λ are dynamic viscosity and thermal conductivity, S is the stress tensor. Re, Pr, Gr, M are Reynolds, Prandtl, Grashoff and Mach numbers defined by the following relations:

$$Re = \rho_{ref} v_{ref} L_{ref} / \mu_{ref}, \quad Pr = \mu_{ref} c_{p,ref} / \lambda_{ref}, \quad Gr = -g \rho_{ref}^2 L_{ref}^3 \Delta T / \mu_{ref}^2 T_{ref},$$

Here $\rho_{ref}, \mu_{ref}, c_{p,ref}, v_{ref}, T_{ref}$ are the referenced values of density, viscosity, specific heat, velocity and temperature, $\Delta T = T_{hot} - T_{cold}$ is difference between maximum and minimum temperature in the computational domain, $r_T = \Delta T / T_{cold}$.

The Douglas-Rachford - type operator-splitting technique (very close to SIMPLEC and the other pressure correction methods) has been adopted along with the finite-difference approach to construct discrete equations on the MAC-type staggered grid. The continuity and the energy equations are fully implicit and the momentum equation is splitted into two parts, that allows to compute the pressure and velocity components independently.

Numerical simulation. Predictions have been performed in the 2D Cartesian formulation. The computational domain is the rectangular $14H$ in horizontal x direction and $1H$ in vertical y direction, $H = 0.01m$, u and v are velocity components.

Boundary conditions:

inflow: the left boundary is the inlet with the Poiseuille velocity profile and fixed temperature, $u = V_0 \ 6 y(1-y) V_0 = 0.5m/s, v=0, T=T_0=500K$.

outflow: the right boundary is the outlet with the simplest open boundary conditions.

rigid walls: the upper and lower boundaries are thermally-insulated rigid walls with heated segments of a fixed temperature and unit length located at the unit distance from the inlet, $u = v = 0, \frac{\partial T}{\partial y} = 0, 0 < x < H, 2H < x < 14H, T = 1200K$ for $H < x < 2H$.

Normalization procedure was performed via the channel width H , mean velocity V_0 and viscosity taken at the reference value of the temperature $T_0 = 300K, T_{hot}=1200K, T_{cold}=300K$. The fine grid 300×180 , uniform for the vertical co-ordinate y and non-uniform for the horizontal co-ordinate x with minimal spacing 0.01 along the heated segments with stretching to the inlet and outlet has been employed.

Numerical results. It is well-known that in mixed convection problems there are the two primary governing parameters - the Reynolds number Re , defining forced convection, and the Grashoff number Gr , defining buoyancy force. The ratio Gr/Re^2 standing as a factor at the buoyancy term in momentum equation governs the flow regimes in horizontal channels with heated parts on the walls (Jensen et al,1991 and Kleijn and Hoogendoorn, 1991). At low values of the parameter the channel flow is undisturbed whereas at high enough values, recirculation zones appear due to strong free convection effects. These recirculation zones essentially disturb the flow structure and lead to different negative effects.

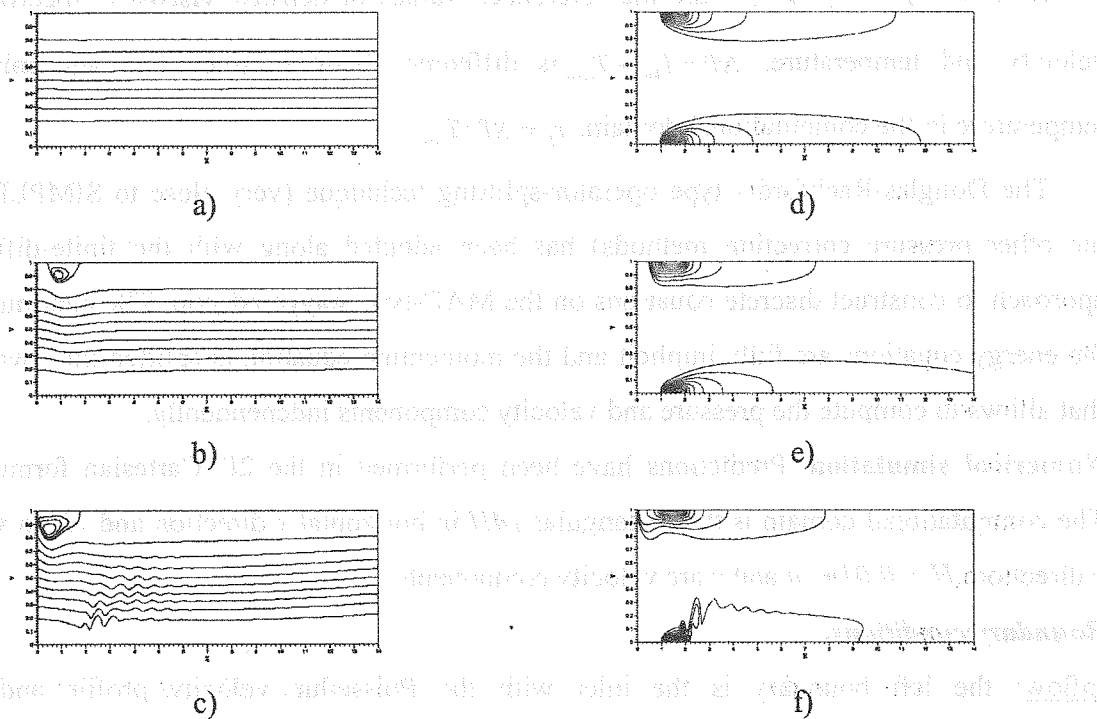


Fig. 1. The flow structure changes as a function of Gr/Re^2 .

For the considered reactor with $Re=500$ there were conducted predictions with different values of Gr/Re^2 . It was found that in a small enough range of this governing parameter

Gr/Re^2 the heat and fluid flow in the channel can be changed greatly. Fig. 1 presents the stream lines and isotherms corresponding to different values of the governing parameter Gr/Re^2 . At the Fig.1a, Fig.1d there are depicted streamlines and isotherms, respectively, for the steady-state regime at $Gr/Re^2 = 1$. It is easy to see that the channel flow is very closed to the developed Poiseuille flow and the temperature field is practically symmetric with respect to the midline. For $Gr/Re^2 = 10$ the flow structure becomes more complicated (see Fig. 1b and Fig. 1e) - a recirculation zone appears in the vicinity of the leading edge of the upper heated segment. As a consequence, the temperature field (Fig. 1e) lost its symmetry. This regime is steady-state, too. The further increasing of the governing parameter up to $Gr/Re^2 = 40$ leads to stability losses. Fig. 1c and Fig.1f demonstrate instantaneous flow pattern and temperature field respectively for the oscillatory regime. The next Fig. 2 presents time-history for the maximal modules of the horizontal velocity. It is easy to see, that after some transitional stage there is an oscillatory flow regime in the channel.

It should be noted, that this oscillatory regime has been obtained with the fixed Poiseuille profile at the inlet located very close to the heated segment.

A more correct in the physical sense formulation of the boundary conditions for this situation requires additional investigations.

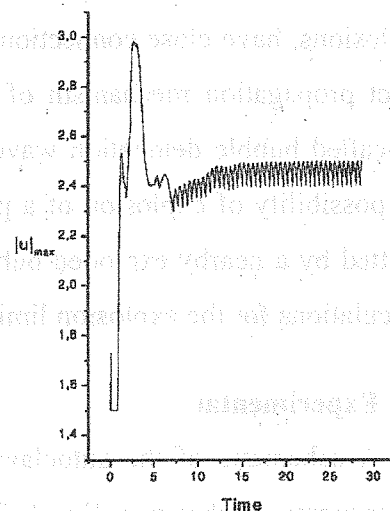


Fig. 2. Oscillatory behaviour for the maximal modules of the horizontal velocity

References

1. Churbanov, A.G. and A.N.Pavlov, 1998. A pressure-based algorithm to solve the full Navier-Stokes equations at low Mach number. In: Computational Fluid Dynamics 98, Eds. K.D. Papailiou et al, Vol.1, pp.894-899. Wiley, Chichester.
2. Churbanov, A.G., 2001. A unified algorithm to predict compressible and incompressible flows. In: ECCOMAS Computational Fluid Dynamics Conf., September 4-7, Swansea, Wales, UK, CD-Rom Proceedings.
3. Garbey, M., B. Chetverushkin, N. Romanyukha, D. Tromeur-Dervout, 2001, Mathematical modelling of methane oxidation in a fast contact chemical reactor. Transactions of French-Russian Inst., Vol. 2, pp.127-140, Moscow, Science.
4. Jensen, K.F., E.O. Einset and D.I. Fotiadis, 1991. Flow phenomena in chemical vapor deposition of thin films. Annual. Rev. Fluid Mech., 23, pp.197-232.
5. Kleijn, C.R. and C.J. Hoogendoorn, 1991. A study of 2 and 3D transport phenomena in horizontal chemical vapor deposition reactors, Chemical Engrg. Sci. 46, pp.321-334.
6. Rehm, R.G. and H R. Baum, 1978. The equations of motion for thermally driven buoyant flows NBS J. Res.83, 297-308.

SOME SAFETY ASPECTS OF A BUBBLY MEDIUM INSIDE CHEMICAL REACTOR

K. Mitropetros, P.A. Fomin, H. Hieronymus

Federal Institute for Materials Research and Testing (BAM), Unter den Eichen 87, D-12205

Berlin, Germany; e-mail: Konstantinos.Mitropetros@bam.de; fax: +49-30-81 04 12 27

Introduction

Common processes in the chemical industry involve an organic liquid containing oxidizer bubbles. Wave phenomena in these systems, connected with shock induced bubble explosions, have close connection with the performance and safety of chemical reactors. The exact propagation mechanism of self-sustaining waves in chemically active bubbly liquids (so-called bubble detonation waves) is still not adequately investigated. In the present work the possibility of explosion of a pre-compressed bubble due to interaction with shock wave, emitted by a nearby exploded bubble has been experimentally and theoretically investigated. Calculations for the explosion limits of single bubbles are also presented.

Experimental

A schematic of the autoclave, which was used for the experiments, is shown in Fig. 1. The autoclave has the form of a vertical cylindrical tube of 100 mm inner diameter and 1 070 mm length. The bubble generator is installed at its bottom. The autoclave contains four holes of 100 mm diameter, in two of which the windows for the optical measurements are installed. In the other two holes the adapters for the pressure measurements are installed. The following positions are denoted in Fig. 1: (1) gas inlet, (2) gas outlet, (3) exploding wire, (4 - 7) pressure sensor positions, (8) liquid outlet and (9) gas inlet for the bubbles.

A shock wave in the liquid is generated by a gas detonation of the explosive acetylene-oxygen gas mixture above it. The liquid phase consisted of pure cyclohexane. The initial pressure of the mixture was 1 bar. All experiments were performed at room temperature.

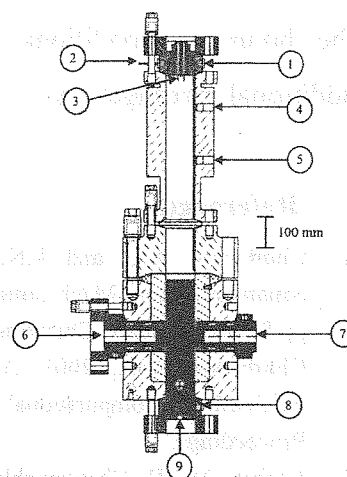


Fig. 1. Schematic of the autoclave

Results and discussion

The shock wave that was generated in the liquid by the impact of the detonation in the gas phase, was used to compress and consequently ignite the bubbles. In Fig. 2, oxygen bubbles in cyclohexane under shock wave impact are presented. Time zero corresponds to the moment when the shock wave enters the observation window. The incident shock wave can be observed on the frame at $t = 8 \mu\text{s}$. After the shock wave passage, bubble compression follows. During this phase also jet penetration through the bubble can occur (e.g. see bubble No. 3). As a result of the bubble compression, ignition in some of the bubbles was observed (e.g. see Fig. 2, $33 \mu\text{s}$).

It was observed that shock waves emitted by exploding bubbles were able to trigger bubble ignition of nearby compressed bubbles. For example, the bubble No. 2 ignition was initiated by the overlapping of two shock waves from nearby bubble explosions (Fig. 2, $35 \mu\text{s}$). Then the shock wave of this explosion ignited the bubble No. 4 (Fig. 2, $40 \mu\text{s}$).

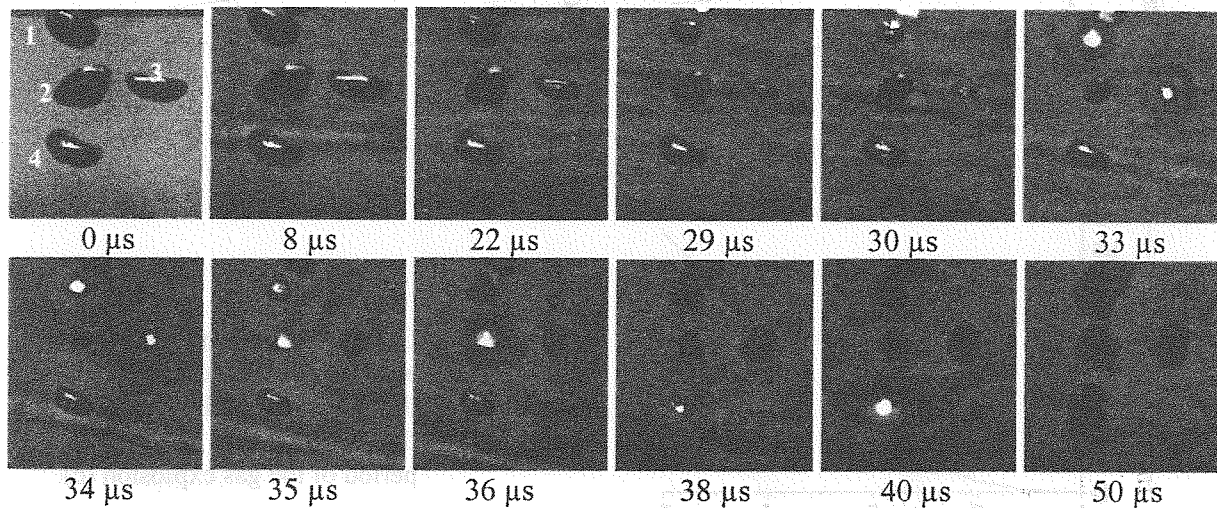


Fig. 2. Bubble ignition from the incident wave or from nearby bubble explosion. Initial equivalent diameter of the bubbles No. 1-4: 3.7 mm, 4.1 mm, 3.6 mm and 3.6 mm respectively.

A possible explanation of this kind of bubble ignition is the following. The fact that the gas phase of the bubble is compressed means that the acoustical impedance is higher than the initial one in the bubble. Based on the experimental measurements of the bubble radius before the second shock wave impact, it is calculated that the increase of the acoustical impedance of the gas is about two orders of magnitude. The impact of the shock wave on the already compressed bubble, creates a new shock wave in the gas inside it that result into ignition.

In Fig. 3 a calculation for the pressure (a) and the temperature (b) behind such a shock wave inside the bubble, as well as the induction period of the gas explosion (c), is presented. For the calculation, the following scenario was assumed. An incident shock wave of 40 bar

OP-III-13

impacts two bubbles. The first bubble ignites when it reaches the radius, R_{ign} . The explosion pressure, P_{ign} , inside the first bubble was calculated by the model described in [1] to be $5 \cdot 10^3$ bar. The bubble explosion emitted in the liquid a secondary shock wave, P_{SSW} , which has an amplitude initially equal to P_{ign} . The P_{SSW} as a function of the distance from the center of the exploded bubble, L , can be described by the known equation for spherical acoustical waves: $P_{SSW} = P_{ign} \cdot (R_{ign}/L)$. At the time when this shock wave impacts the second bubble, it is assumed that its internal pressure is equal to the pressure of the incident shock wave, 40 bar. The calculated temperature inside the bubble at that time is then 585 K.

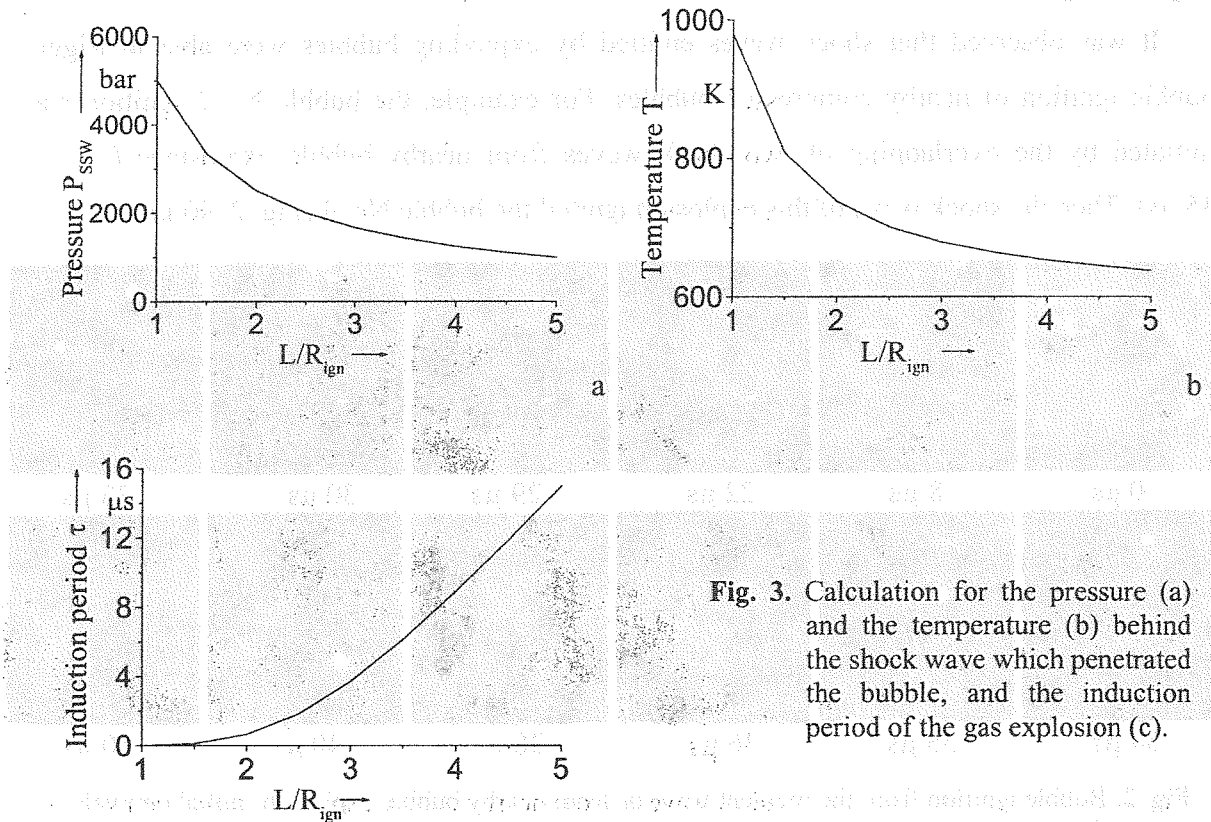


Fig. 3. Calculation for the pressure (a) and the temperature (b) behind the shock wave which penetrated the bubble, and the induction period of the gas explosion (c).

From Fig. 3 it can be seen that, provided the two interacting bubbles are close enough, the shock wave that penetrates the second bubble can ignite it. It can also be seen from this calculation that the pressure at the front of the shock wave and the temperature increase behind it, can be high enough to result into an induction period for the ignition, less than the time necessary for the bubble to change its radius (i.e. a few μs). This explains the "instantaneous" ignition that was observed in the experiments. For example, if the distance between the center of the first bubble and the surface of the second bubble, L/r_{ign} , is less than 2, the induction period is less than $0.65 \mu s$, i.e. the second bubble is ignited practically instantaneously.

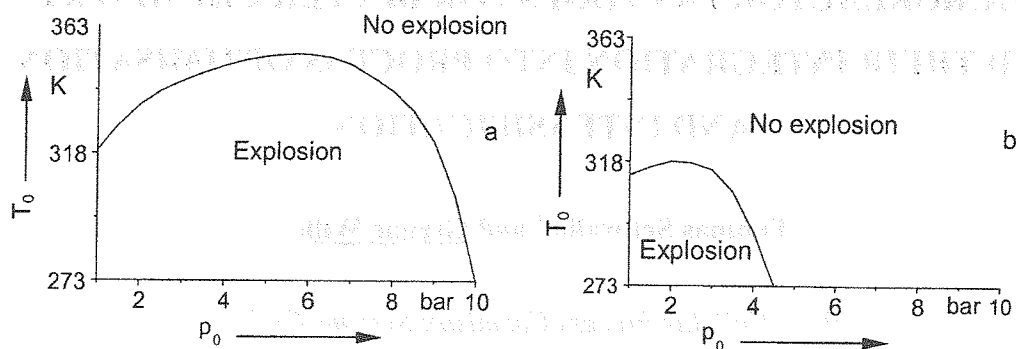


Fig. 4. Calculated explosion limits of a single bubble at different initial temperatures, pressures and amplitudes of shock waves (40 bar (a) and 20 bar (b)).

In Fig. 4 the calculated explosion limits of a single bubble under one shock wave impact are presented. The calculation is made at different initial temperatures, pressures and amplitudes of incident shock waves. It was assumed that if the duration of the first bubble compression is less than the induction period of the gas explosion, the bubble does not explode. From Fig. 4 it can be seen that for a certain amplitude of incident shock wave, a combination of initial temperature and pressure exist, above which no bubble explosion takes place.

Conclusions

It was shown by experimental observations and by theoretical calculations that the explosion of bubbles can ignite nearby compressing bubbles. This fact indicates that an automatic process of synchronization of bubble explosions is possible. This behavior could help us to understand better the exact mechanism of self-sustaining waves inside bubbly media.

Calculations show that in order to prevent bubble explosions inside a chemical reactor, the operating conditions (temperature and pressure) should be above a certain limit.

Reference

1. P.A. Fomin, K.S. Mitropetros, H. Hieronymus. Modeling of detonation processes in chemically active bubble systems at normal and elevated initial pressures. *Journal of Loss Prevention in the Process Industries*, 2003, 16, pp. 323-331.

MICROREACTORS AS TOOLS FOR BETTER CHEMISTRY AND THEIR INTEGRATION INTO PROCESS OPTIMISATION AND INTENSIFICATION

Thomas Schwalbe* and Gregor Wille

CPC – Cellular Process Chemistry Systems GmbH

Hanauer Landstrasse 526/G58, 60343 Frankfurt, Germany

Tel.: 0049 (0)69 4109 2320, Fax: 0049 (0)69 4109 2322, E-mail: info@cpc-net.com

Abstract

The standard CYTOS microreactor was demonstrated to match or even to improve many liquid/liquid reaction's yields. Highly exothermic reactions were conducted under practically isothermic conditions at 0°C or higher. Examples are given for nitration reactions, lithium halide exchanges, acylations and Grignard reactions. Improved safety features and cost cutting effects for cooling turned the microreactor into a powerful synthesis tool for broadband applications. The microreactor is incorporated in automatically operating systems for inline infrared analysis. This instrument enables a rapid access to reaction optimisation based on microreaction technology, including their well known benefits (e.g. reduced scale up problems) without analytical bottleneck.

1. Introduction

Catering to today's chemical markets imposes radically changed organisational capabilities on those involved in chemistry. Shorter product life spans and increasingly tight specifications are accompanied by ever increasing demands for higher and more specific functionality of chemical entities such as faster approach to the markets. One of the crucial points in this process lies in the repetitive adaptation of chemistries to increasing batch sizes, the scale-up process. Synthesis in microreactors provide a variety of advantages, especially the opportunity to avoid scale-up problems by the so-called numbering-up process. This permits an direct transfer of processes from bench to production.

2. Technology and Results

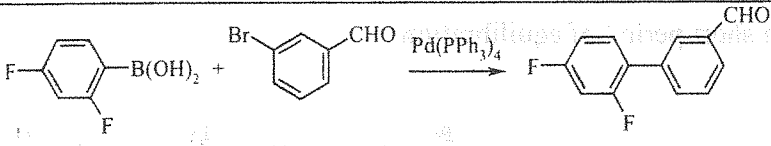
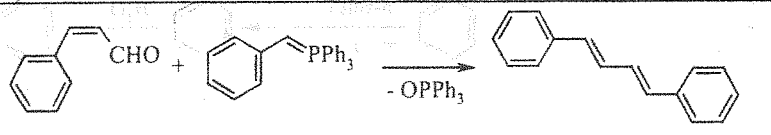
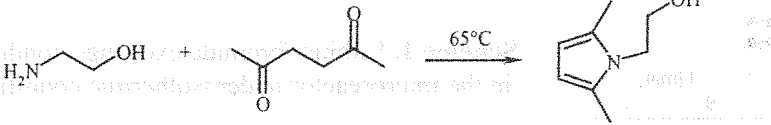
2.1. General

Standard microreaction systems refer to chemists' demands in research and process development. Chemical technology from our company is based on the CYTOS standard microreactor for multipurpose applications. Aiming at a high added value in pharmaceutical synthesis in the standard microreactor is especially designed for a wide range of reaction conditions in liquid/liquid phase synthesis. The broad-bend applicability of the microreactor

* Correspondence author: Dr. Thomas Schwalbe

was proven in a variety of organic syntheses (also see lit. [1]). A choice of selected examples is given in Table 1 ranging from single bond formation, double bond formation to heteroaromatic synthesis (for more examples see lit. [2]). Continuous reactions in microreactors were found to proceed with higher or at least similar yields and conversion rates than described for their conventional counterpart [3].

Table 1. Selected example reactions in the CYTOS microreactor.

	Yield [%] Conventional 63 microreactor 88
	Yield [%] Conventional 61, [7a] microreactor 67
	Yield [%] Conventional 74, [7b] microreactor 98 Throughput 136 g/h

The CYTOS microreactor (Figure 1a) is part of an integrated CYTOS Lab System fully equipped with periphery as displayed in Figure 1b and 1c. The modular structure of the microreactor in combination with the residence time units (RTU) permits fast and easy modification according to residence time requirements. Since the instrument is designed for product sampling after each RTU the maximum configuration (microreactor and three RTUs) provides 47 min as the maximum residence time (flow rate 2×0.5 ml/min) whereas working on maximum flow rate and using only the microreactor results in a residence time of 8 seconds. The effect to the reaction yield depending on a varying number of RTUs is demonstrated in section 2.3.

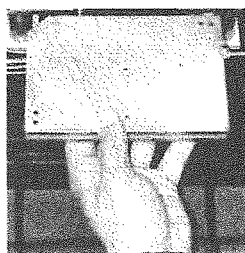


Fig. 1a. CYTOS microreactor.

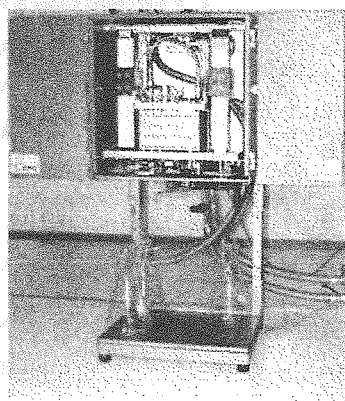


Fig. 1b. CYTOS Lab System (CLS).

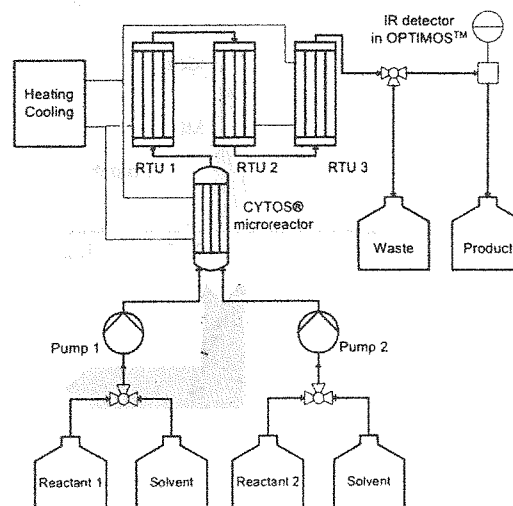


Fig 1c. Flow diagram of the CLS including the ReactIR cell for inline analysis (OPTIMOS).

2.2. Comparison of heat absorbing microreactor vs. flask

With respect to considerable expenses for cooling it seems appropriate to watch out for reaction systems with enhanced heat absorption capabilities due to their inner architecture. Figure 2 outlines the temperature characteristic of the microreactor (inner volume 2 ml, surface to volume ratio 95) compared to a 100 ml flask (surface to volume ratio 1) in an cryogenic lithium/bromide exchange experiment. Since the inner temperature of the vessel rises up close to the boiling point of the solvent (THF), the cooling system of the microreactor keeps it strictly to 0°C after a short period of equilibration.

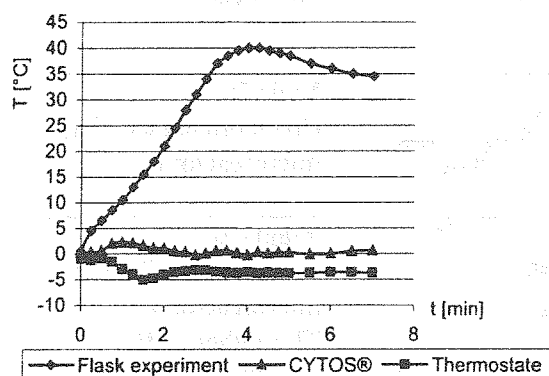
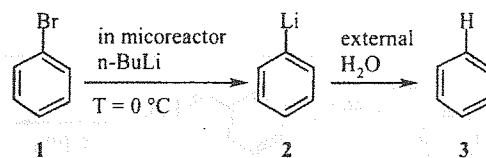


Figure 2. Temperature growth in the microreactor and 100 ml flask (ice cooling) for the lithium/bromide exchange.



Scheme 1. Lithium/bromide exchange conducted in the microreactor under isothermic conditions.

Yield: quantitative, total flow rate: 5 ml/min, volume microreactor 2 ml, residence time: 24 s, conc. BuLi 2.5 M.

Efficient temperature control also has a positive effect on chemoselectivity. Basically, microreactors provide a more narrow temperature distribution than in batch vessels (Figure 2). For a hypothetical reaction $A \rightarrow B$ additionally creating the undesired side product C an improved product profiles is expected upon running the synthesis in microreactor. Fine-tuning of the temperature will keep the energy supply below the activation level for transition state C'. This consideration was subject of verification in an nitration experiment.

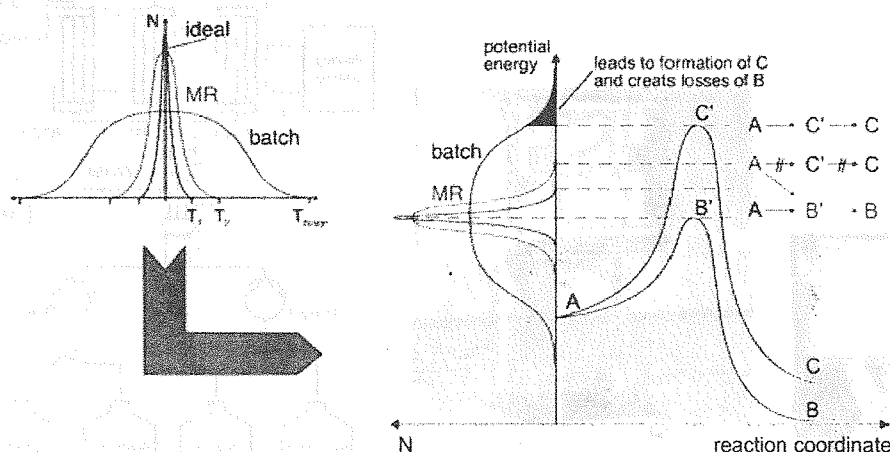


Figure 3. Effect of temperature distribution in microreactor and batch vessel on side reactions.

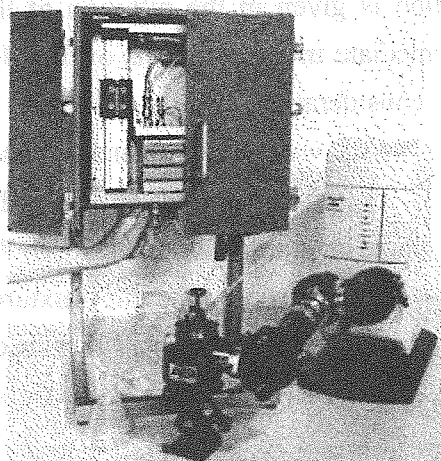


Figure 4. OPTIMOS

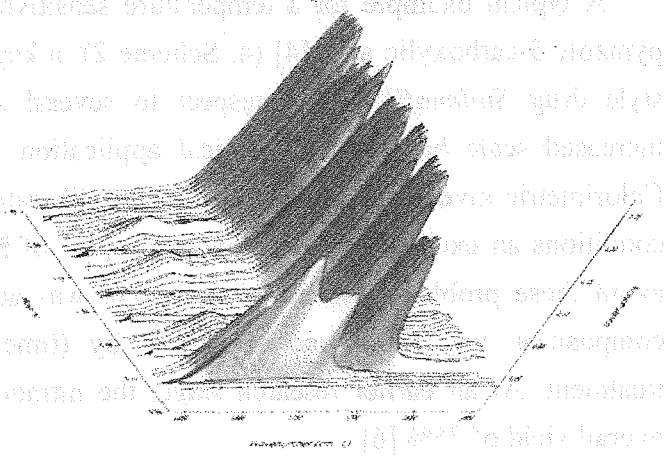
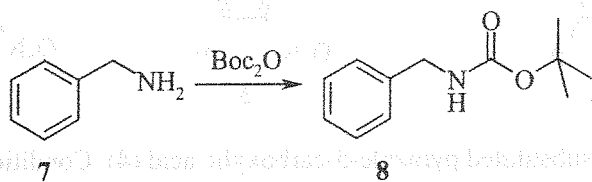
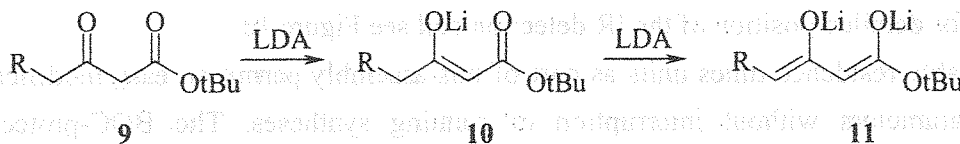


Figure 5. ReactIR[®] diagram of the formation of 8 (leftovers of Boc₂O at 1800-1750 cm⁻¹).

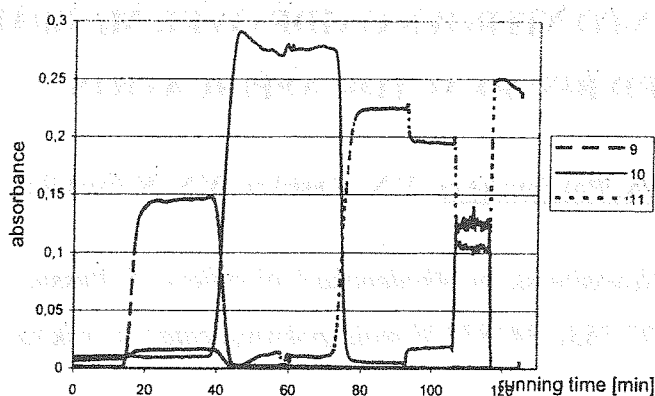


Scheme 3. Boc-protection of benzylamine (7).

The major advantages of the microreaction technology in terms of heat absorption become clear in cryogenic reactions. Scheme 4 outlines the two step deprotonation of acetoacetate tert-butylester (9) with lithiumdiisopropylamide (LDA) to give intermediate 10 and 11, respectively (compound 11 was quenched outside the microreactor with various electrophiles). The formation of the two lithiated intermediates was clearly monitored by inline infrared spectroscopy (Figure 6). Upon using two equivalents of LDA individual conversion levels were addressed by adjusting certain residence times. Since the yield of product 11 dropped down by more than 50% and significant amounts of intermediate 10 left untouched upon 0.4 min of residence time, maximum conversion was achieved after 19 min (T = -10°C for all experiments).



Scheme 4. Two step deprotonation of acetoacetate tert-butylester (1) with LDA, T = -10°C, R = alkyl.



Running time [min]	Residence time [min]
85	15
100	5
110	0,4
120	19

Figure 6. Absorbance of starting material (9) at 1721 cm^{-1} and products (10 and 11) at 1655 cm^{-1} and 1610 cm^{-1} , respectively. The residence time was modified by changing the number of RTUs in use after 85, 100, 110 and 120 min of experimental running time.

3. Conclusion

Chemistry in microreactors today covers a full set-up of tools for advanced organic synthesis. It enables the scientist in R & D to apply high-tech continuous chemistry in up-to-date multipurpose microreactors. Encouraging results from heat absorbing experiments make the technology attractive for hazardous reagents and conditions which appeared unacceptable for large scale synthesis so far.

References and notes

1. S.J. Haswell, R.J. Middleton, B. O'Sullivan, V. Skelton, P. Watts, P. Styring, *Chem. Comm.* 2001, 391.
2. T. Schwalbe, V. Autze, G. Wille *CHIMIA* 56, (2002) 636-646.
3. All experiments were carried out in the CYTOS[®] microreaction system, *EP 0116024-A2*, 2001, for more information see our website www.cpc-net.com.
4. a) A. S. Bell, D. Brown, N. K. Terrett, *EP 0 463 756 A*, 1991; b) S. Kunio, J. Isegawa, M. Fukuda, M. Ohki *Chem. Pharm. Bull.* 32, (1984) 1568; c) V. Papesch, R. M. Dodson *J. Org. Chem.* 30, 1965, 199.
5. J. D. Dale, P. J. Dunn, C. Golightly, M. L. Hughes, P. C. Levett, A. K. Pearce, P. M. Searle, G. Ward, A. S. Wood *Organic Process Research & Development* 4, (2000) 17.
6. In the meantime the yield was increased up to 96% by intensive development efforts, see [5].
7. a) L. F. Fietze, Th. Eicher, 'Reactions and synthesis in the organic chemistry laboratory', University Science Books, Herndon, USA, 1986; b) P. Buu-Hoi Ng, *J. Org. Chem.* 20, (1955) 639.

AMMONIA OXIDATION INTO NITROUS OXIDE OVER Mn/Bi/Al CATALYST. FLUIDIZED BED REACTOR APPLICATION

A.S. Noskov, I.A. Zolotarskii, S.A. Pokrovskaya, V.N. Kashkin, V.N. Korotkikh

Boreskov Institute of Catalysis, Novosibirsk, pr. Akademika Lavrentieva, 5, Russia
Phone: 007-3832-344491; fax: 007-3832-341878, E-mail: pokrov@catalysis.nsk.su

Application of nitrous oxide as a mild oxidant to produce bulk chemicals raises the development of high capacity and safe technologies for nitrous oxide on purpose production [1]. R&D performed by Solutia Inc. and Boreskov Institute of Catalysis prove that nitrous oxide manufacturing via selective ammonia oxidation over Mn/Bi/ α -Al₂O₃ catalysts is an attractive route [2,3].

Recently, results of piloting a tubular reactor for ammonia oxidation into nitrous oxide have been published [4]. The present work deals with a development of a fluidized bed reactor for the same purpose.

1. Fluidized bed reactor piloting

Catalyst batches with different activity levels were applied for fluidized bed tests. The intrinsic properties of batch samples measured in a bench scale setup were found to be close to ones for a macrospherical catalyst. Nitrous oxide selectivity reaches 88-89 %, including the conditions with high inlet concentrations of ammonia, up to 44-46%, the selectivity to nitrogen oxide does not exceed 0.4%.

Experimental fluidized bed studies were carried out in several setups equipped by reactors with inner diameter of 1.6", 2.5" and 2.8". Interphase mass transfer rate was varied by installing or removing internal screens. Effects of temperature, interphase mass transfer and inlet feed composition, as well as catalyst stability were studied with operation conditions given in Table 1.

Table 1. Operation conditions

Gas velocity	0.15- 0.45 ft/sec	
Temperature	330-380 °C	
Pressure	15-30 psig	
Inlet concentrations:	ammonia	17 - 51% vol
	oxygen	17 - 55% vol
	water	0 - 33% vol
	nitrogen	balance

Test studies in the 1.6" and 2.5" ID reactors were carried out in the Solutia Research Center in cooperation with employees of the company.

Figure 1 shows examples of experimental data. Screens removal results in the higher mass transfer resistance followed by an evident decrease of the apparent catalyst activity. Notordinary rise of N₂O selectivity with increasing mass transfer resistance is caused by specific features of process kinetics [4].

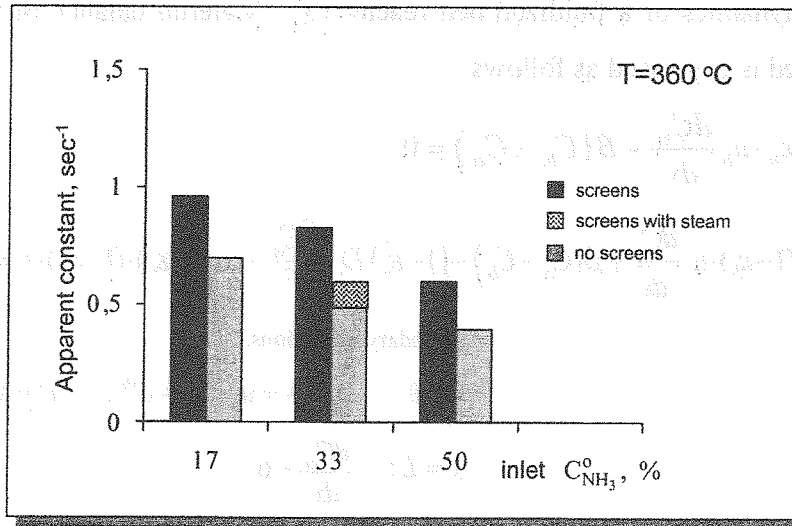


Fig 1a. Effect of interphase mass transfer rate and inlet ammonia concentration on catalyst activity.

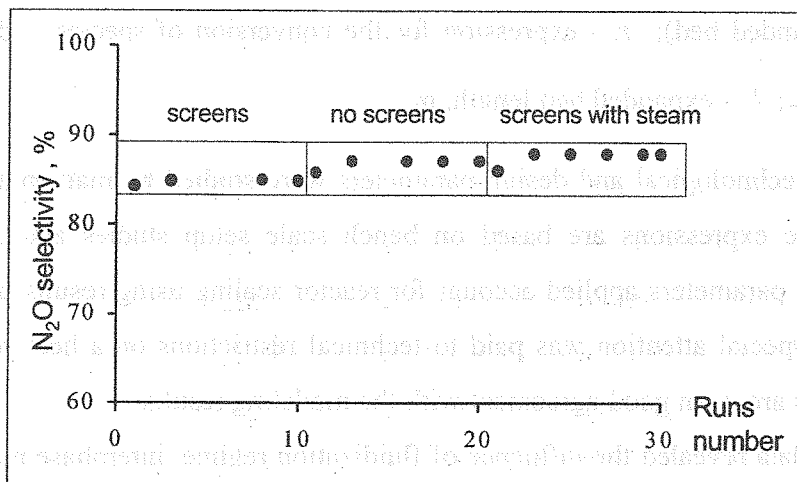


Fig. 1b. Effect of interphase mass transfer rate and steam on N₂O selectivity.

T = 360 °C, inlet ammonia concentration 33 %.

A number of runs with the same pressure, contact time, inlet gas composition shows minor temperature effect on N₂O selectivity in the range of 330-370°C. The selectivity to nitrous oxide of 84-88% is reached at the ammonia conversion of 90 – 99.5%.

Catalyst stability was checked by two ways – direct stability tests and the comparison of intrinsic properties of a fresh and used catalyst. Catalyst activity and N₂O selectivity did not change during whole period of pilot testing.

2. Reactor modeling

Two-phase model taking into account gas axial dispersion in the dense phase is used to describe hydrodynamics of a fluidized bed reactor [5]. Material balance of the species *i* in the expanded bed is expressed as follows:

$$\varepsilon_b \cdot u_b \frac{dC_{bi}}{dx} + \beta(C_{bi} - C_{ei}) = 0$$

$$(1 - \varepsilon_b) \cdot u_e \frac{dC_{ei}}{dx} + \beta(C_{ei} - C_{bi}) - (1 - \varepsilon_b) D_z \frac{d^2 C_{ei}}{dx^2} - \alpha \cdot (1 - \varepsilon_b) \cdot (1 - \varepsilon_d) \cdot r_i = 0$$

Boundary conditions:

$$x = 0: \quad D_z \frac{dC_{ei}}{dx} = u_e(C_{ei} - C_{ei}^0), \quad C_i(0) = C_i^0,$$

$$x = L: \quad \frac{dC_{ei}}{dx} = 0,$$

where u_b, u_e - gas velocity in bubble and dense phase, m/s; C_{bi}, C_{ei} - concentration of the species *i* in bubble and dense phase, mole/m³; β - mass transfer coefficient, s⁻¹ (per unit volume of expanded bed); r_i - expression for the conversion of species *i* due to chemical reaction, $\frac{\text{mole}}{\text{m}^3 \text{ cat} \cdot \text{s}}$; L - expanded bed length, m.

Effects of technological and design parameters were studied by mathematical modeling. The kinetic rate expressions are based on bench scale setup studies and are proprietary. Hydrodynamics parameters applied account for reactor scaling using results of the cold flow studies [6]. A special attention was paid to technical restrictions on a heat removal system. Pilot test results are in a good agreement with the modeling results.

Modeling data revealed the influence of fluidization regime, interphase mass transfer and gas axial dispersion on the reactor size and performance. The high inlet ammonia concentration, up to 45 %, was found to be achieved for operation of a large-scale fluidized bed reactor. Mass transfer limitations and gas axial dispersion influence moderately on the reactor performance. Calculated N₂O selectivity rises with an increase of mass transfer resistance and gas axial dispersion.

As a result, feasible variants of large-scale reactors were chosen for further economical evaluation.

3. Summary

N₂O selectivity up to 86-88% is achieved in pilot fluidized bed reactors with 98-99.5% ammonia conversion. Both activity and selectivity were stable within pilot tests.

Slightly lower conversion with the same level of selectivity is expected in the commercial reactor according to mathematical modeling results.

Application of a fluidized bed reactor in comparison to a tubular one enables to enhance catalyst productivity and maximum single train capacity due to much higher concentrated feed. Inlet ammonia concentration is 7-8% vol. (corresponding adiabatic temperature rise ca 600 °C) for the tubular reactor and 30 – 45 % vol. (corresponding adiabatic temperature rise 2400-3600 °C) for the fluidized bed reactor.

Acknowledgements

The authors are gratefully acknowledged:

- ◆ to the Solutia Incorporated for financial support of these studies;
- ◆ to colleagues from Boreskov Institute of Catalysis E.M.Slavinskaya, V.V.Mokrinskii, A.S. Ivanova and I.A.Polukhina for preparation and characterization of catalyst batches.

References

1. A.K. Uriarte, M.A. Rodkin, M.J. Gross, A.S. Kharitonov, G.I. Panov, In Proc. 3rd Intern. Congress on Oxidation Catalysis, R.K. Grasselli, S.T. Oyama, A.M. Gaffney and J.E.Lyons, Stud. Surf. Sci. Catal., Elsevier Science B.V., 110 (1997) 857-864.
2. V.V. Mokrinskii, E.M. Slavinskaya, A.S. Noskov, I.A. Zolotarsky, PCT Int. Appl. WO 9825698 (1998), priority: RU 96-96123343.
3. A.K.Uriarte, In Proc. 12th Intern. Congress on Catalysis, A.Corna, F.V.Melo, S.Mendioroz and J.L.G.Fierro, Stud. Surf. Sci. Catal., Elsevier Science B.V., 130 (2000), 743-748.
4. A.S. Noskov, I.A. Zolotarskii, S.A.Pokrovskaya, V.N. Korotkikh, E.M.Slavinskaya, V.V.Mokrinskii, V.N.Kashkin, Chem. Eng. J, 91 (2003), 235-242.
5. H.T.Bi, N.Ellis, I.A.Abba, J.R.Grace, CES, 55 (2000) 4789-4825.
6. V.N. Kashkin, V.S. Lakhmostov, I.A. Zolotarskii, A.S. Noskov, J.J. Zhou, Chem. Eng. J., 91 (1998), p.215-218.

**PERFORMANCE OF SELECTIVE CATALYTIC EXOTHERMIC
REACTIONS IN THE "REVERSED HEAT WAVE" MODE:
A WAY TO IMPROVE SELECTIVITY**

Andrey N. Zagoruiko

Boriskov Institute of Catalysis, pr.Lavrentieva, 5, Novosibirsk, 630090, Russia

Phone +7-3832-344491, fax +7-3832-341878, e-mail: zagor@catalysis.nsk.su

Improvement of selectivity and aim product yield in complex reaction systems, such as partial oxidation reactions, is one of the major problems in catalytic reaction engineering and also one of the main challenges in the unsteady-state catalysis area.

One of the most prospective approaches for solution of the problem is application of forced feed composition cycling (FFCC) in the packed catalyst bed, meaning periodical alteration of reactor feed between oxidation and reduction mixtures up to the limit case of periodical separate feeding of oxidant and reductant. Such approach may provide enhancement of selectivity as it was shown for numerous reaction systems (see overview in [1]). At the same time, in most cases the observed results relate to isothermal laboratory reactors and do not take into account the possible heat effects of reactions and related unsteady-state phenomena in the adiabatic catalyst bed, therefore, these results cannot give direct answer on possible efficiency of FFCC in process conditions. Moreover, account of interaction between all these effects may give additional possibilities for development of new catalytic processes.

Let us consider the simplest model reaction scheme, typical for partial oxidation catalytic reaction:



where A and B are initial reagents (A – reductant, B - oxidant), C – partial oxidation product (aim product), D – complete oxidation product (undesired by-product), [B], [] – oxidized and reduced sites at the catalyst surface respectively. Let us also propose that all reactions are irreversible and exothermic, that activation energy for complete oxidation reaction (2) is

higher than that for reaction (2), and that reaction rates kinetic equations corresponds to mass-action law.

This model system was analyzed by means of numerical simulation using the standard unsteady-state model of the packed catalyst bed [2], accounting for occurrence of reactions (1-3), heat/mass transfer between gas and catalyst and heat conductivity of the catalyst bed framework. Both steady-state (with continuous feeding of both components) and FFCC unsteady-state (with periodical separate feeding of oxidant and reductant) regimes were simulated. Steady-state simulation was used as a basis for comparance. Kinetic parameters were chosen arbitrary to provide maximum steady-state yield of aim product C at the level of ~20%.

First, the FFCC regime during feeding of reductant stream into preliminary oxidized and preheated catalyst bed was simulated. In this case the heat and concentration waves are moving in direction co-current with the gas flow. Interaction of heat emission in the reaction zone with heat exchange between gas and catalyst (both tending to increase catalyst temperature) leads to overheating of the catalyst bed and, thus, low selectivity in respect to aim product C. Moreover, formed C may interact with adsorbed B giving complete oxidation product D in the outlet bed area resulting in further decrease of selectivity and yield of aim product (sometimes practically to zero).

The second and much more interesting mode of FFCC process operation is shown in Fig.1. The reductant stream is fed into preliminary oxidized bed, but in this case only some small part of the bed (in the outlet area) is preheated to reaction temperature. Reaction heat emission in this part of the bed tends to heat the catalyst, while heat exchange is directed conversely. If the gas velocity (and, thus, the intensity of heat exchange) is low enough, then heat conductivity may provide movement of the heat and concentration waves in direction counter-current to the direction of gas flow. Such regime ("reversed heat wave") is characterized by some unusual properties. First of all, there is no catalyst overheating and catalyst temperature during the whole cycle is kept at moderate level (even in case of highly concentrated inlet stream), being beneficial for high selectivity achievement. Surface concentration of adsorbed oxidant in the area of maximum reaction rates is low enough and it gives additional gain in selectivity. Finally, the formed aim product will not react to complete oxidation products in the outlet part of the bed, because the catalyst surface here is already free of adsorbed oxidant.

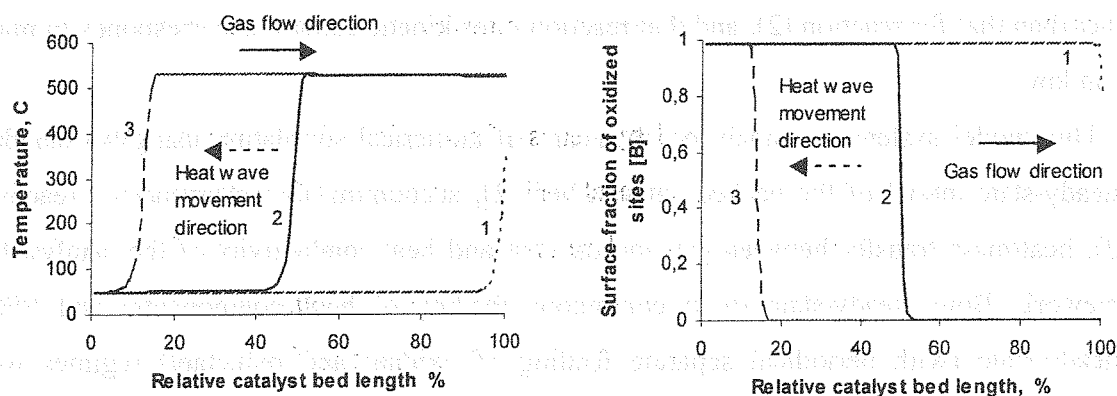


Fig. 1. Evolution of catalyst temperature (left) and surface composition (right) profiles versus catalyst bed length in FFCC/reversed heat wave regime. (1,2,3 – cycle start, middle and end)

As a result, the “FFCC/reversed heat wave” regime compared to steady-state provide much higher product C yield and relative catalyst productivity.

Of course, the actual gain and selectivity and aim product yield for the real processes will depend upon real reaction kinetics and other parameters. Nevertheless, it may be summarized that “forced feed composition cycling/reversed heat wave” process operation mode may become a new way for development of highly-efficient catalytic processes for oxidative dehydrogenation, selective oxidation, selective hydrogenation and other selective exothermic reactions [3].

References

1. P.L.Silveston. *Composition modulation of catalytic reactors*. Gordon and Breach Science Publishers, 1998.
2. Yu.Sh.Matros. *Catalytic processes under unsteady-state conditions*. Elsevier Science Publishers, 1988, Amsterdam - New York.
3. A.N.Zagoruiko, V.N.Tomilov. Russian patent application No.2002134060, 2002.

METHANOL DECOMPOSITION ON Pd(111) STUDIED BY HIGH-PRESSURE SFG AND XPS SPECTROSCOPY

G. Rupprechter, M. Morkel, M. Borasio, H.-J. Freund

Fritz-Haber-Institut der Max-Planck-Gesellschaft,

Faradayweg 4-6, D-14195 Berlin, Germany

rupprechter@fhi-berlin.mpg.de Fax +49 30 8413 4105

V.V. Kaichev, I.P. Prosvirin, V.I. Bukhtiyarov

Borekov Institute of Catalysis of SB RAS, Lavrentieva ave. 5, Novosibirsk 630090, Russia

vib@catalysis.nsk.su Fax +7 3832 343056

Methanol decomposition was studied from 10^{-6} -0.1 mbar and 300-550 K by sum frequency generation (SFG) and X-ray photoelectron spectroscopy (XPS). The experiments were carried out in two UHV-high pressure cells specially designed for in-situ studies. CO and carbonaceous deposits were detected as decomposition products and monitored via their vibrational and photoemission characteristics. The formation of carbon deposits by cleavage of the methanolic C-O bond was found to be strongly dependent on temperature and methanol pressure.

Corresponding experiments with CO did not produce any carbon. This rules out CO originating from methanol dehydrogenation as source of carbonaceous species and suggests that C-O bond scission must occur via CH_xO intermediates. Methanol decomposition at pressures up to 15 mbar and temperatures up to 550 K, followed by gas chromatography, did not produce measurable decomposition products, showing the fast carbon poisoning under catalytic reaction conditions. The mechanism of C-O bond cleavage is discussed.

1. Introduction

Methanol decomposition on noble metals has been the subject of many surface science studies under ultrahigh vacuum (e.g. [1,2] and references therein). Catalytic decomposition into CO and H_2 may provide a source of hydrogen but catalyst deactivation by carbon deposits seriously limits this process. Consequently, one important aspect is the probability of the methanolic C-O bond cleavage, producing carbon or carbonaceous species (CH_x ; $x = 0-3$). Previous reports on Pd(111) suggested that C-O bond scission requires near monolayer

methanol coverage [1] or surface defects [2]. Another question concerns the origin of CH_x species because they may either originate from C-O bond scission within methanol or from a consecutive dissociation of the dehydrogenation product CO.

We have studied methanol decomposition and CO dissociation on well-annealed and defect-rich Pd(111), combining vibrational sum frequency generation (SFG) and X-ray photoelectron spectroscopy (XPS). Pd model catalysts were exposed to low (1×10^{-6} mbar) as well as high (0.1 mbar) methanol pressures between 300 and 550 K, monitoring the time- and temperature-dependent evolution of carbonaceous species. Methanol decomposition on Pd(111) at pressures up to 15 mbar and temperatures up to 550 K was also followed by gas chromatography.

2. Experimental

The experiments were carried out in two UHV chambers, both equipped with high-pressure reaction cells for *in-situ* studies (SFG: [3]; VG ESCALAB "high-pressure" electron spectrometer [4, 5]). Well-annealed (perfect "p") and ion-bombarded (defect-rich "d") Pd(111) were prepared as described in [4]. Methanol (p.a.) was purified by freeze-thaw cycles while CO (purity $\geq 99.997\%$) was cleaned using a liquid nitrogen cold trap and a carbonyl absorber.

3. Results and Discussion

Fig. 1 shows SFG and XPS C1s spectra acquired after exposing well-annealed ("p") Pd(111) to 10^{-6} mbar methanol for 90 minutes (time-dependent evolution not shown here). The SFG spectrum (300 K; Fig. 1a) displays the C-O stretching region revealing a peak at 1915 cm^{-1} indicating ca. 0.5 ML hollow/bridge bonded CO originating from CH_3OH decomposition. In the corresponding XPS spectrum (Fig. 1b) two peaks can be identified and attributed to adsorbed CO and CH_xO (285.6 eV; ~ 0.5 ML) and to carbon or carbonaceous species (CH_x ; 283.8 eV). The amount of carbonaceous species is ~ 0.15 ML which is apparently too low to induce significant changes in the SFG spectrum.

Increasing the temperature or CH_3OH pressure increased the amount of carbonaceous deposits, as shown in Fig. 1b (10^{-6} mbar/400 K: ca. 0.3 ML; 0.1 mbar/300 K: ca. 1 ML). Apparently, under catalytic reaction conditions in the mbar range, even on a well-annealed Pd(111) surface a significant amount of CH_x can be observed. A very similar result was obtained for CH_3OH decomposition on defect-rich Pd(111) indicating that C-O bond scission was not considerably enhanced by surface defects.

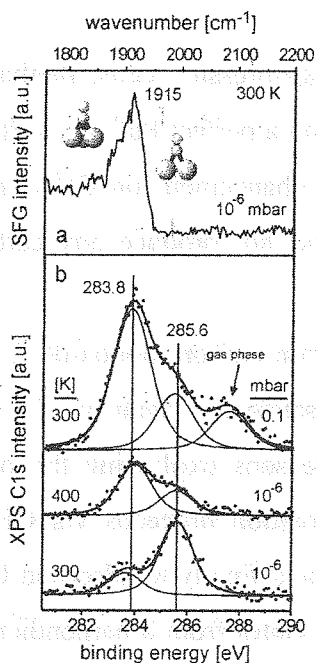


Figure 1. SFG (a) and XPS C1s (b) spectra of CH_3OH decomposition; see text.

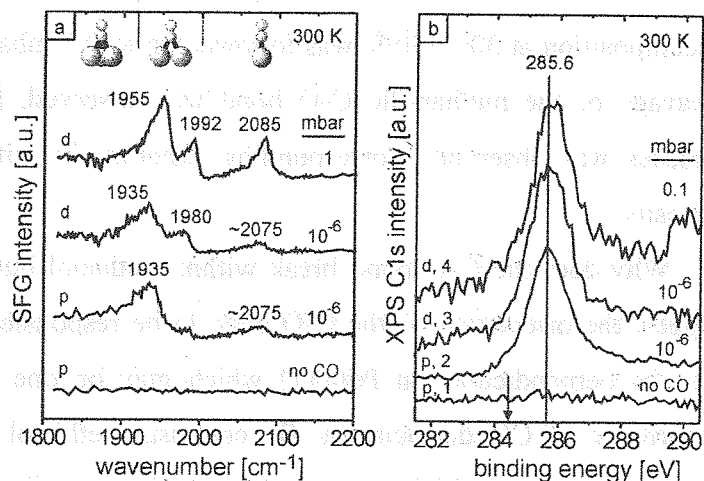


Figure 2. SFG (a) and XPS C1s (b) spectra measured during CO adsorption at 300 K.

In order to identify the origin of the carbon deposits, experiments were also carried out with CO. Fig. 2a shows SFG spectra of CO adsorbed on perfect “p” and defect-rich “d” Pd(111) at 300 K. Comparison of “p” and “d” SFG spectra at 10^{-6} mbar CO (Fig. 2a) evidences that ion sputtering gave rise to an additional feature at 1980 cm^{-1} which is due to CO bridge bonded to defects [4]. The two common features at 1935 cm^{-1} and $\sim 2075\text{ cm}^{-1}$ originate from CO on bridge and on-top sites on (111) terraces, respectively. Raising the CO pressure to 1 mbar mainly increased the on-top CO intensity.

C1s core-level spectra at 10^{-6} mbar CO are very similar for “p” and “d” surfaces exhibiting a single peak at $\sim 285.6\text{ eV}$ (Fig. 2b, traces 2,3). According to our previous SFG/XPS study [4], the C1s peak corresponds to bridge and/or three-fold hollow CO at a coverage of $\sim 0.5\text{ ML}$. On the sputtered (“d”) surface the C1s binding energy is slightly higher (285.8 eV) due to the contribution of CO adsorbed on sputtering-induced defects such as steps, kinks or vacancies. However, most importantly, carbon deposits (amorphous, graphitic, etc.), which typically appear at $\sim 284.5\text{ eV}$ (marked by an arrow in-Fig. 2), were not detected on both surfaces. Thus, CO can be excluded as source of carbon deposits during methanol decomposition.

4. Conclusions

By combining SFG and XPS spectroscopy with suitable high-pressure cells, methanol decomposition at 300-550 K was followed up to 0.1 mbar. Even on a perfect Pd(111) surface cleavage of the methanolic C-O bond was observed, and no enhancement on defect-rich surfaces was observed. Corresponding experiments with CO did not produce any carbon deposits.

Why does the C-O bond break within methanol but not within carbon monoxide? We suggest the orientation of the C-O bond to be responsible, as discussed in detail in [6]. CO adsorbs perpendicular on Pd(111) which may be one of the reasons explaining the non-occurrence of CO dissociation. By contrast, methanol decomposition proceeds via CH₃O (methoxy) groups, which are stepwise dehydrogenated to CH_xO and finally to adsorbed CO. This route includes adsorption geometries where the C-O axis deviates from a perpendicular orientation. For instance, a methoxy CH₃O group bonded to the surface via the oxygen atom has to turn over in order to produce CO bonded via the carbon atom. Consequently, C-O bond cleavage during methanol decomposition presumably proceeds via CH_xO intermediates including a tilted C-O bond. The fast formation of surface CH_x species leads to a rapid self-poisoning of methanol decomposition in the mbar pressure range.

Acknowledgments

MM acknowledges support from the German Science Foundation. VVK is grateful for a DAAD fellowship. VIB is indebted to the Russian Science Support Foundation supporting this work.

References

- [1] J.-J. Chen, Z.-C. Jiang, Y. Zhou, B.R. Chakraborty, N. Winograd, *Surf. Sci.* 328 (1995) 248.
- [2] M. Mavrikakis, M. Barteau, *J. Molec. Catal. A* 131 (1998) 135.
- [3] G. Rupprechter, *Phys. Chem. Chem. Phys.* 3 (2001) 4621.
- [4] V.V. Kaichev, I.P. Prosvirin, V.I. Bukhtiyarov, H. Unterhalt, G. Rupprechter, H.-J. Freund, *J. Phys. Chem. B.* 107 (2003) 3522.
- [5] R.W. Joyner, M.W. Roberts, K. Yates, *Surf. Sci.* 87 (1979) 501.
- [6] V.V. Kaichev, M. Morkel, H. Unterhalt, I.P. Prosvirin, V.I. Bukhtiyarov, G. Rupprechter, H.-J. Freund, *Surface Science*, submitted.

DETOXICATION OF A CHLORINATED ORGANIC COMPOUNDS IN A MEMBRANE SEPARATED REACTOR IN AN AQUEOUS MEDIA

S.M. Kulikov

*University of the West Indies, Cave Hill Campus, POB 64, Bridgetown, Barbados,
kulikov@uwichill.edu.bb (2003-10-2004-03 on leave, Karl-Winnacker Institute
Der DECHEMA e.V, 60486, Theodor-Heuss-Allee 25, Frankfurt/M, Germany,
smkulikov@hotmail.com)*

Chlorinated organic compounds (COC) are widely spread in the environment and are very dangerous because of their high toxicity and persistency to the biodegradation. Removal of the chlorine atoms usually converts them into less toxic and biodegradable substances. One of the promising methods of a chlorine removal is an electrochemical reduction, which converts polychlorinated organic compounds into non toxic chloride ions and hydrocarbons. Such an electrolytic reduction should be done in a separated electrochemical cell to avoid anodic oxidation into by-products, which can be even more dangerous than starting materials.

In this study self-designed two compartment electrochemical reactor has been used. Reactor material is Teflon, counter electrode is platinum net, working electrode carbon cloth and Zn-modified carbon cloth. Convenient three-electrode scheme has been used with double junction standard calomel electrode (SCE) as a reference. The anodic and the cathodic compartments were separated by the cation exchange membrane. As a solvent mixture of a methanol and water with sodium sulphate as a supporting electrolyte has been used. The reactor dimensions are 15x15x5 cm with useful electrodes and membrane area about 30 square cm. Reactor can be used either in continuous flow or in flow circulation modes with an electrolytes rates 5-500 mL/min. As a model substrates dichlorobenzene and pentachlorophenol in the range of starting concentrations 1 mmol/L - 10 μ mol/L were used.. In a potentiostatic mode potentials -1.8V, -2.0V and -2.2V were applied for the time period 1-6 hrs with a current 100-10 mA. In a galvanostatic mode current of 50 mA has been applied.

In the end of each experiment solutions from the cathodic compartment were analysed with the chloride-selective electrode, and, after extraction with organic solvent (chloroform, n-hexane and benzene were used) GC-MS analysis has been carried out. In all experiment at least partial reductive dechlorination has been detected which was confirmed both by increasing of chlorine ions concentration in solution and the detection of a less chlorinated products by the GC-MS analysis. Conversion as high as 85% was reached in some experiments with average current efficiencies 5-20%.

Author express his gratitude to the Alexander von Humboldt Foundation for the financial assistance.

THE COMPUTING EXPERIMENT AND OPTIMIZATION OF CATALYTIC PROCESSES

S.A. Mustafina, S.I. Spivak

Sterlitamak State Pedagogic Institute, Sterlitamak

Institute of Petrochemistry and Catalysis

of Ufa Scientific Center of Russian Academy of Sciences, Ufa

At the present time overwhelming part of processes is realized with the help of catalyst, therefore the effectiveness of the whole technological scheme is essentially depends on how effectively the catalytic process passes. This fact defines the significance of the problem of creation of reliable optimally controlled catalytic reactor.

Let's consider the kinetic model of the reaction of oligomerisation of α -methylstyrene with the catalyst «Tseokar-10». Experimental data were obtained U.M.Djemilev with co-authors. The oligomerisation reaction attracts our attention by the fact that reaction products of the mentioned reaction are valuable petrochemical raw material. So, for instance, saturated cyclic dimer – 1,1,3-trimethyl-3-phenylindan is of interest in the capacity of lubricant or insulating material, which is stable to γ -radiolysis of reactive fuel. The products 4-methyl-2,4-diphenylpenten-1 и 4-methyl-2,4-diphenylpenten-2 are used as solvents of varnishes, dielectric liquid, base of lubricating oil, plasticizer of rubbers.

The equations of material balance of process of reaction of oligomerisation of α -methylstyrene in the presence of catalyst "Tseokar-10" are presented by the following way:

$$\frac{dx_i}{dt} = \frac{F_i - x_i F_N}{N} \quad (1)$$

$$\frac{dN}{dt} = F_N$$

with the initial conditions $t = 0$: $x_i = x_i^0$, $N = 1$ (2)

Taking into account the matrix of stoichiometric coefficients the right parts of (1) may be presented as:

$$\begin{aligned}
 F_1 &= -2w_1 - 2w_2 - 2w_3 - w_6 - w_7 - w_8 \\
 F_2 &= w_1 - w_4 - w_6 - w_9 \\
 F_3 &= w_2 - w_5 - w_7 + w_9 \\
 F_4 &= w_3 + w_4 + w_5 - w_8 \\
 F_5 &= w_6 + w_7 + w_8 \\
 F_N &= -w_1 - w_2 - w_3 - w_6 - w_7 - w_8
 \end{aligned} \tag{3}$$

While solving the problems of such a kind we should distinguish 2 stages of optimization: theoretical and technological optimization of reactor. Let's consider the problem of theoretical optimization. On the whole this stage is purposed to the elucidation of extreme properties (characteristics) of chemical production. The important particularity of this stage is abstracting from the possible hardware realization of obtained answer.

The problem of optimization of catalytic process of oligomerisation of α -methylstyrene, which mathematical description is given by the equations (1), (3), with initial conditions (2) is set as the problem of finding the optimal temperature conditions (settings) in the reactor $T(t)$, on condition that the concentration of products of the reaction A_i , $i=2..4$ on leaving the apparatus is maximum.

Let's consider the general case when the limitations are imposed on the choice of optimal value of the temperature.

$$T_1 \leq T \leq T_2$$

There are no any assumptions concerning the sizes of the reactor. Therefore particularities of variants with given and unknown value of size are marked in solution of the problem.

The problem is solved with the help of maximum principle of Pontryagin[1]. According to the general procedure of using the principle of maximum the optimal temperature in each section of the reactor is found from condition of maximum for function H .

$$H(\varphi(t), x(t), T_{opt}(t)) = -\frac{\varphi_0}{N} \sum_{i=2}^4 (F_i - x_i F_N) + \sum_{i=1}^5 \varphi_i \frac{F_i - x_i F_N}{N} + \varphi_6 F_N$$

Here functions $\varphi_0, \dots, \varphi_6$ satisfy the system of equations, named conjugate:

$$\frac{d\varphi_i}{dt} = -\frac{\partial H}{\partial x_i}, \quad i=0..6 \tag{4}$$

with boundary conditions on $\varphi_i(\tau_k)$, $i=1..6$

Thus, determination of optimal temperature conditions is reduced to the problem of integration of the systems of differential equations of process (1), (3) and conjugate system

for auxiliary functions (4) with boundary conditions, given on the both end points of an interval of integration, i.e. to the solving of the boundary problem. But solving such problems becomes complicated by the fact that it is difficult to expect analytical results for the systems of large dimension (more than 3 equations). Moreover, this problem can also occasionally appear for the systems of smaller dimension if right parts of equations of the model have got fractional polynomial type [2]. Hereupon to define the general integrals of systems of equations describing variable $x_i(t)$ or $\varphi_i(t)$ for any t becomes impossible. Therefore the numerical methods of integration of systems data have to be used.

For numerical solving of the set boundary problem can be used some methods: reduction the boundary problem to the problem of minimization of function of finite number variables; linear interpolation with auxiliary step; linear interpolation without auxiliary step; gradual approximations in the space of equations.

On the base of the available experimental data and mathematical description of the process of oligomerisation of α -methylstyrene the inverse kinetic problem was solved and numerical values of kinetic constants of the process were determined.

When the problem of the theoretical stage is solved the choice of a technological scheme is accomplished, i.e. selection of the optimal, constructive and operating conditions of reactor: isometric sizes, forms, locations of centers, pressures, concentrations etc.

But as a rule phase variables must lie in the certain limits in the catalytic reactor. For example, overheat (superheat) of catalyst above determined temperature causes the reduction of its activity. Then in mathematical formulation a problem of optimization of a process is reduced to the finding the extreme of the certain functional from the large number of variables, on the variation range of them different kind of restrictions are imposed in the form of the system of partial differential equations and systems of algebraic inequalities.

The example of such problem can be a process of hydrogenisation of pinene in tubular reactor. The practical application of α -pinene is highly various. Since ancient times α -pinene (the turpentine) has been used as a solvent of varnishes and paints. α -pinene serves as the initial raw material to obtain the camphene, which is applied in industrial production of synthetic camphor, using for the necessities of medicine and military technology (the production of gun-powder). Besides, α -pinene is a universal initial compound for obtaining of medicinal preparations (terpinhydrate and terpineol), preservatives for pharmaceutical and cosmetic preparations, aromatic substances.

On basis of analysis of experimental data the two-stage scheme of conversions of the process of hydrogenisation of α -pinene on nickel-silicate catalyst is proposed: irreversible stage of interaction of α -pinene with hydrogen with a formation of the cis-pinane and reversible stage of an isomerisation of the α -pinene. As an isomer of the α -pinene averaged analogue between dipentene and α -terpinene is chosen. Calculation of process is possible by means of mathematical description for two technological variants: in reactor with a heat removal and in the adiabatic reactor (in this case heat transmission coefficient α_x in the equation of heat balance is equal to zero, and the equation is struck off the system of equations).

All variables, describing the technological process, are divided into two groups: phase variable, which define the condition of the process, but don't yield to the direct (immediate) influence, controlling parameters (controls) – the variables, defining the operating regime (mode of operation), which we can change, influencing hereby on the course of process. For chemical processes phase variables are a concentrations of components, temperature, pressure, number (quantity, amount) of adsorbed on a catalyst materials. In the capacity of controlling parameter it is possible to choose the quantity of catalyst, geometric sizes of reactor, the load on reactor, the input temperature and the composition of reactionary mixture.

Permissible values both managements and phase variable are usually restricted by technological limits. Taking into consideration the safety of catalyst or technological equipment the rising of the temperature in reactor above the certain limit, for example, is undesirable.

Different kind of restrictions, imposed on variables, complicate the solving of problems of optimization. It may turn out that criterion of optimization not at all has the extreme in analytical sense, and its maximum or minimum value is reached when one or several variables are fixed on limit values.

The penalty function method is usually used the for solving the problems with restrictions on phase variables.

For calculation of optimum mode of operation of tubular flow fixed-bed catalytic reactor the maximum output of pinane is chosen as a criterion of optimization (G_2 , kg/h).

Controlling parameters are: 1) pressure in reactor (P , atm); 2) input temperature (T , °C); 3) consumption of a fluid stream (pinene) at the inlet of reactor (L , l/h); 4) consumption of a gas flow (the hydrogen) at the inlet (G , m³/h).

References

1. Mustafina S.A., Spivak S.I. // The Bashkir Chemical Journal, in Russian, 1999, T.6, №1.
2. Iremadze E.O., Mustafina S.A., Spivak S.I. // Mathematical Modeling, in Russian, 2000, T.12, №3.

SECTION IV.
CHEMICAL REACTORS FOR SOLVING THE FUEL
AND ENERGY PRODUCTION PROBLEMS

SECTION IV.
CHEMICAL REACTORS FOR SOLVING THE FUEL
AND ENERGY PRODUCTION PROBLEMS

THE FORMATION AND CONTROL OF NO_x EMISSIONS

A.A. Omer

High Technical Institute, Sirt, Libya (Sirte)

Ammar Almaraid S. Omer High Technical Institute P.O.Box 733 Sirte, Libya

FAX:00218-54-64790 TEL:00218-54-66210 E-mail : abany2003@hotmail.com

The formation and emission of nitrogen oxides in stationary combustion plants need to be controlled. Stationary combustion sources contribution is expected to grow to 75% by the year 2005. Recently, it has been determined that additional control development is needed to maintain NO_x air quality. Current NO_x control applications employ combustion process modification to suppress the formation of both thermal and fuel NO_x. Current and future process modification technology is directed at hardware changes on existing units or on new units of conventional design. This paper covers a wide range of subject , including method of energy savings readily applicable to existing combustion systems, structural considerations for energy savings in designing new system.

Keywords: NO_x emission, gas combustion, energy saving.

CATALYTIC HEATING ELEMENTS OF 0.75 kW POWER**A.V. Kulikov, B.N. Lukyanov, N.A. Kuzin, L.G. Simonova, V.A. Kirillov***Boreskov Institute of Catalysis, Prosp. Akad. Lavrentieva, 5**630090 Novosibirsk, Russia**e-mail: lukjanov@catalysis.nsk.su; fax: 34 11 87*

Oxidation of propane-butane mixtures in catalytic heat generating elements (CHGE) is one of the most effective and ecologically safe methods of heat generating in the autonomous residential heat supplying. A element and its environment are heated due to the catalytic combustion that is the fuel oxidation with air oxygen on the catalyst surface. The optimal heat capacity of one CHGE in the domestic convector is usually not higher than 750 W. Based on the experimental investigations performed at the Institute of Catalysis, state enterprises "Kometa" and "Izmeritel", we have developed and manufactured catalytic heat generating elements of 0.75 kW power (CHGE -0.75), which were utilized in a series of gas catalytic convectors "Uyut" ("Comfort") [1-3].

The aim of the present work was to develop a new construction and a technology for manufacturing of catalytic heat generating elements of 0.75 kW power with the use of different glass tissue and charged catalysts as well as determination of their life time provided that the elements cost will be reduced (1.5 to 2 times) and its ecological parameters preserve (waste: $\text{CO} \leq 5$ ppm, no traces of NO_x).

Catalytic Heat Generating Elements of 0.75 kW Power

Fig. 1 schematically shows the pre-production model of CHGE -0.75 supplied with a separate countercurrent feeding of reagents. The model operates as follows: a hydrocarbon gas flow is supplied to a gas-distribution tube (GDT) to be distributed along its length and directed into the catalyst bed through a number of perforation holes. Atmospheric oxygen passes to the reaction zone (catalyst bed), situated outside the gas-distributing tube, due to free convection and diffusion in the porous medium. The process of catalytic oxidation proceeds both inside the catalyst bed and on its surface. Water (steam) and carbonic acid are the reaction products.

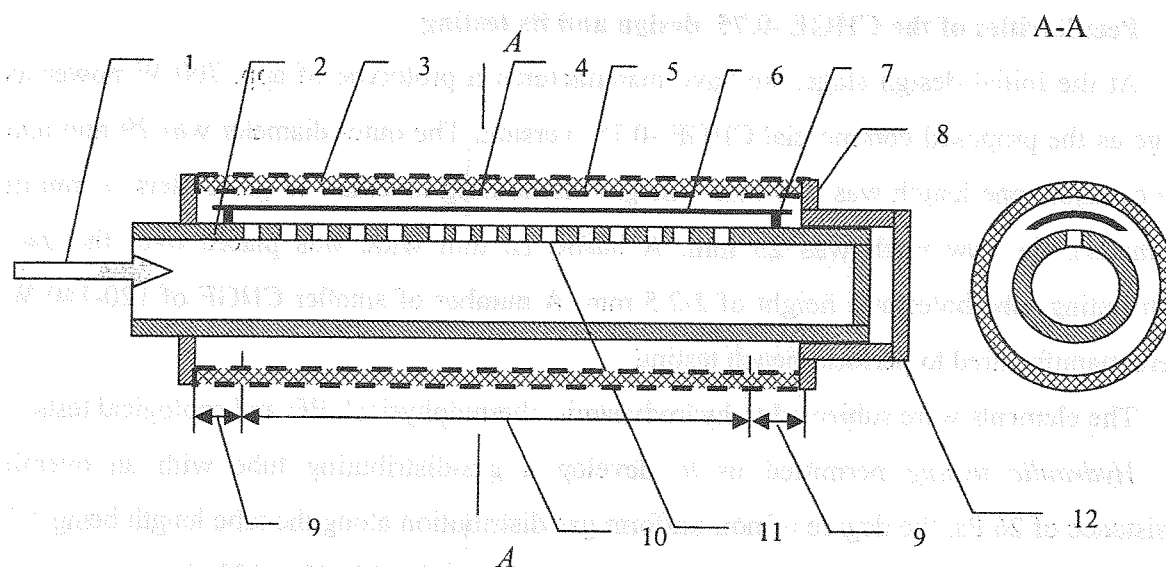


Fig. 1: Schematic of the pre-production CHGE -0.75. Designations: gas inlet (1), gas-distributing tube (2), outer cylinder made of a stainless steel grid (3), inner cylinder made of stainless steel grid (4), catalyst (5), baffle (6), embedding (7), back end wall (8), end wall (9), catalyst zone (10) (stable temperature zone); gas outlet (11), temperature compensator (12).

Catalysts and their testing

Two catalyst types were tested: glass tissue catalysts and granular catalysts (granular diameter is 0.25 – 1 mm). The catalysts were tested as a part of the CHGE -0.75. To prepare glass tissue supports, we used Al-Na-Si commercial glass tissues (Polotsk plant "Steklovolokno"). After leaching, the tissue predominantly contains silica (> 98 % SiO₂) and sodium admixtures (<0.2%), which provides their high thermal stability. The glass tissue was impregnated with a (NH₄)₂[PtCl₆] solution, washed with deionized water, dried at 110°C, calcined in air at 300°C, and reduced in a hydrogen flow at 300°C for 2 h. The platinum concentration was varied from 0.03 to 0.2 wt.%. Two charged catalyst were tested at a time: Pt/Al₂O₃ (Pt 0.1 wt.%) prepared at the Institute of Catalysis and M-0-3 (Ce 2 wt.%, Pt 0.01 wt.% supported on Al₂O₃, prepared at IOCE, Alma-Ata. As a support we used Al₂O₃ formed by 0.25-1 mm granules.

When CHGE -0.75 were tested at a design mode, glass tissue catalyst KO (0.06 wt.% Pt) exhibited long operation ($\tau = 3504$ hours). At abnormal conditions (severe conditions), the time of deactivation of glass tissue catalysts reduced to 1592-1968 hours.

Testing of the charged catalysts at the design operation conditions has shown that the catalyst life is rather long (> 6000 h) and its activity preserves constant. Besides, their thermal stability is higher than that of the glass tissue catalysts if the catalyst surface temperature increases by 100-150°C from the design temperature.

Peculiarities of the CHGE -0.75 design and its testing

At the initial design stage, we have manufactured a prototype of app. 700 W power as large as the proposed commercial CHGE -0.75 version. The outer diameter was 29 mm and the catalyst zone length was 360 mm. The gas-distributing tube had 15 gas outlets (1 mm in diameter), the row pitch was 23 mm. A baffle 12 mm wide was placed over the gas-distributing tube holes at a height of 2-2.5 mm. A number of smaller CHGE of 120-140 W were manufactured to perform bench testing.

The elements were subjected to hydrodynamic, thermophysical, life and ecological tests.

Hydraulic testing permitted us to develop a gas-distributing tube with an overall resistance of 26 Pa, the degree of non-uniform gas distribution along the tube length being 1.7 %. *Thermophysical testing* permitted us to determine the optimal baffle width, its arrangement in the CHGE and the temperature compensator design, which provided almost isothermal temperature distribution over the catalyst bed surface. *Life and ecological tests* provided information on the service life of the element upon its high stable operation. For the design operation mode, the concentration of CO in waste gases was <2-4 ppm during the testing period.

Thus, the developed CHE-0.75 kW is characterized by long life and low cost (2-4 times lower than the existing CHGE).

References

1. V.A. Kirillov, N.A. Kuzin, V.A. Kuzmin, A.V. Kulikov, G.A. Kirillov. Catalytic Heat Generating Element. Russian Federation Patent No 2062402, 1996.
2. B.N. Lukyanov, N.A. Kuzin, V.A. Kirillov, A.V. Kulikov, A.B. Shigarov, M.M. Danilova. Ecologically safe method of hydrocarbon gases oxidation on catalytic heat generating elements. Chemistry for Sustainable Development, No 9, 667-677, 2001.
3. V.A. Kirillov, N.A. Kuzin, I.A. Onufriev, A.I. Popov, A.N. Melnik, Catalytic Gas Convector. Russian Federation Patent No 2181463, 2002.

**SYNTHESIS GAS CONVERSION INTO HYDROCARBONS
(GASOLINE RANGE) OVER BIFUNCTIONAL ZEOLITE-
CONTAINING CATALYST: EXPERIMENTAL STUDY AND
MATHEMATICAL MODELLING**

V.M. Mysov^a, S.I. Reshetnikov^b, V.G. Stepanov^a, K.G. Ione^a

^a*Scientific - Engineering Centre «Zeosit», Pr. Acad. Lavrentieva 5,*

Novosibirsk, 630090, Russia

zeosit@batman.sm.nsc.ru, Fax: (007-383-2) 39-62-51

^b*Boreskov Institute of Catalysis, Pr. Acad. Lavrentieva 5, Novosibirsk, 630090, Russia*

Reshet@catalysis.nsk.su

Synthesis gas transformation into liquid hydrocarbons attracts much attention as an alternative way to produce motor fuels [1-3]. During the recent decades, a great number of scientific, pilot and industrial investigations have been made to examine various versions of the process of natural gas conversion to gasoline via synthesis gas. The bifunctional catalysts composed of metallic oxides ($\text{ZnO-Cr}_2\text{O}_3$) and ZSM-5 zeolite were first proposed for use in the transformation of synthesis gas to liquid hydrocarbons by Chang, Lang and Silvestri [4].

The effectiveness of liquid hydrocarbons production from synthesis gas depends on a great number of technological parameters such as the feeding gas composition, the temperature in the reactor, the circulation rate (the molar ratio of the recycle and feeding gases), the reaction mixture and the catalyst contact time etc. All these parameters are interrelated so that changing one of them causes changing the others. It results in a change in the reactor productivity as well as in the overall transformation of the carbon contained in the fed synthesis gas to the target products thus modifying the economic indices of the process as a whole.

The subject of this report is to analyse how the technological parameters of the process using a bifunctional zeolite-containing catalyst affect the catalyst selectivity and productivity with regard to liquid hydrocarbons.

ZSM-5 and Beta zeolites were prepared via hydrothermal synthesis. To prepare the bifunctional catalysts, the powders of both zeolite and metallic components were

OP-IV-3

homogenised in a mortar in the desired proportion followed by pressing, crushing and sieving. The particle fractions of 0.25-0.5 mm and of 3-4 mm were used in the reaction.

The process of synthesis gas conversion to hydrocarbons (gasoline range) was investigated experimentally in the temperature range 320 - 400°C, at pressures 40 - 80 atm, GHSV = 500 - 20000 h⁻¹, ratio H₂/CO = 2 - 10.

The reaction products were analysed in three gas chromatographs equipped with integrators. H₂, CO, CO₂, N₂ and CH₄ were analysed in a thermal conductivity detector (TCD) with an activated carbon column. Methanol, DME, and water were analysed with a TCD using a column filled with chromosorb-102. The gaseous hydrocarbons were analysed with a TCD using a column packed with Al₂O₃. The liquid hydrocarbons were analysed in a TCD using a 3-m-long column with Benton-34/SP-1200 on 100/120 Supelcoport or with a flame ionisation detector (FID) with a 50-m-long capillary column. The identification of products was conducted by GC-MS.

The influence of the catalyst composition on the products distribution and the process productivity with regard to the liquid hydrocarbons has been examined already [5]; now we turn to how the pressure, temperature, and molar ratio H₂/CO in the reactor input affect the C₅₊ productivity of the process.

Fig. 1 shows how C₅₊ productivity depends on GHSV for various H₂/CO molar ratios in the reactor input. It can be seen that as the syngas space velocity grows, the conversion towards C₅₊ hydrocarbons increases, while the intensity of the conversion growth decreases following the increase of H₂/CO molar ratio in the reactor input.

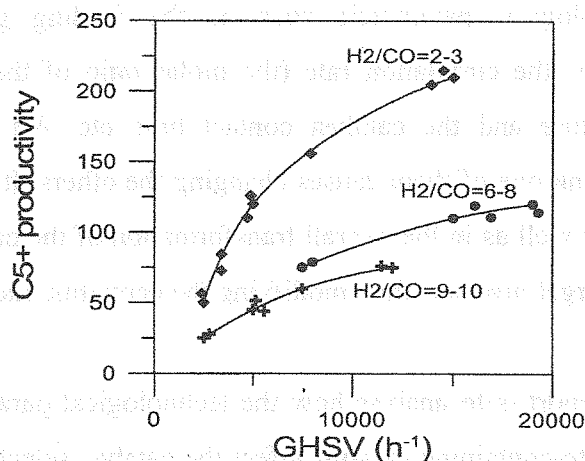


Fig. 1. Dependence of C₅₊ productivity (g/L Cat/h) on GHSV. P=80 atm, T=380°C.

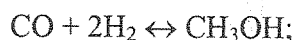
It can be seen from Table 1 that when the pressure and temperature grow the C₅₊ productivity increases.

Table 1. Dependence of C₅₊ productivity (relative units) on pressure and temperature

Temperature, °C	Pressure, atm		
	40	60	80
320	<1	<1	1
340	1	1.2	1.6
360	1.1	2.2	3.7
380	1.3	3.3	4.2
400	2.2	5.0	5.9

Mathematical modelling has been developed for the process flow sheet with the unreacted gas recycling. To simulate the process of hydrocarbons synthesis in a fixed-bed reactor, the one-dimension plug flow model was taken. To calculate the gas-liquid balance in the separator, we used a program based on the Gibbs energy technique for the reaction components. The following overall reactions were taken in consideration:

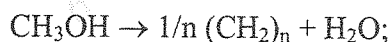
methanol synthesis:



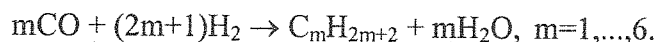
water-gas-shift reaction:



methanol conversion to hydrocarbons (gasoline range):



paraffins synthesis:



Here the $1/n (\text{CH}_2)_n$ is the hydrocarbons of the gasoline range C₅₊.

To model the reaction of methanol synthesis and the water-gas-shift reaction, we used the kinetic equations from [6]. The kinetic equation for methanol conversion into hydrocarbons was developed under the assumption that hydrocarbons were synthesized from methanol according to the Chang scheme modified by Voltz and Wise [3]. The scheme implies the direct conversion of methanol and dimethyl ether to olefins and their subsequent conversion to hydrocarbons. The reaction rate and activation energy constants calculation was based on experimental data obtained through using a laboratory isothermal flow reactor.

The reactor productivity depends on the gas composition at the reactor inlet. According to the gas stream recycling scheme, the light hydrocarbons are accumulated as well as hydrogen and the inert gases contained in the feed gas (N₂, CH₄). The concentration of hydrogen at the recycle depends on how much the CO/H₂/CO₂ mixture deviates from the stoichiometric composition for the reaction, the latter being defined by the so-called *module*: $f = (\text{H}_2 - \text{CO}_2)/(\text{CO} + \text{CO}_2)$. To prevent accumulation of the inert in the recycle gas, part of the

OP-IV-3

recycle stream is removed from the recycle loop as a purge gas. The ratio of the purge gas to the feeding gas, α , is one of the most economically significant parameters defining the carbon transformation to target products. On the one hand, increasing this parameter causes a more reactive mixture to be established at the recycle, thus increasing the productivity of each m^3 of the catalyst; on the other hand, an increase in the purge gases volume decreases the degree of carbon transformation to the hydrocarbons.

At Fig. 2, the dependences of the module value and catalyst productivity versus the quotient α are shown at various gas GHSV values. Since hydrogen is deficient in the feed gas ($\text{CO}=24\%$, $\text{H}_2=67\%$, $\text{CO}_2=8\%$, $\text{CH}_4=0.5\%$, $\text{N}_2=0.5\%$), its concentration gets smaller at the recycle when the purge gas volume decreases. A low hydrogen concentration at the reactor

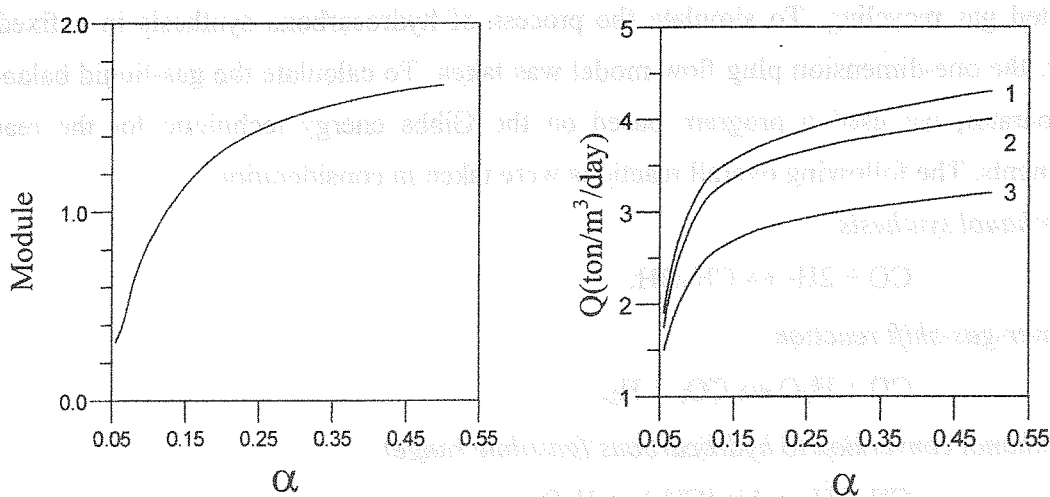


Fig. 2. Dependence of the module value and catalyst productivity vs. the molar ratio α of the purge gas to the feeding gas at: GHSV = 23000 h^{-1} (curve 1), 18000 h^{-1} (2), 9000 h^{-1} (3).

inlet results in decreasing the rate of hydrocarbons formation. The figure demonstrates the productivity decrease with decreasing the purge gas volume. The decrease is especially sharp for $\alpha < 0.1$. It is caused both by decrease in the quantity of the gasoline range hydrocarbons being formed and by accumulation of essential amounts of the carbon-containing components as well as of inert gases contained in the feed gas.

References

1. K. Fujimoto, Y. Kudo and H. Tominaga, *J. Catal.* 87, 136-143 (1984).
2. F. Simard, A. Mahay, A. Ravella, G. Jean and H. de Lasa, *Ind. Eng. Chem. Res.* 1991, 30, 1448-1455.
3. C.D.Chang, Hydrocarbons from methanol. *Catal. Rev.-Sci. Eng.*, 25 (1983) 1-117.
4. C.D.Chang, W.H. Lang and A.J. Silvestri, *J. Catal.* 56, 268 (1978).
5. V.M.Mysov, K.G.Ione and A.V.Toktarev. In "Natural Gas Conversion V" (A.Parmaliana et al. eds.), *Stud. Surf. Sci. Catal.*, Amsterdam, 119 (1998), 533-538.
6. V.M.Pomerancev, I.P.Muchlenov, D.G.Trober. Methanol synthesis in fluidized bed reactor. *J. Appl. Chem.*, 36 (1963) 754-762 (in russian).

OPTIMIZATION OF THE REACTOR INTENDED FOR HYDROGEN AND BOEHMITE PRODUCTION FROM WATER-SUSPENDED ALUMINIUM POWDER

V.K. Ikonnikov, A.V. Bersh, V.Yu. Rijkin

FSUE Russian Scientific Center «Applied Chemistry»

197198, 14, Dobrolubov ave., St. Petersburg, Russia

N.N. Jukov, O.A. Trubachev,

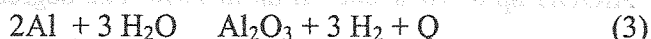
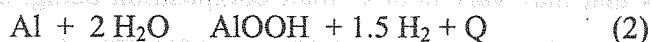
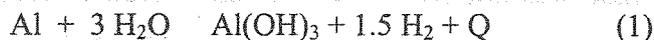
JSC «Firm RIKOM SPb»

195273, 63 (off.308), Piskarevsky ave., St. Petersburg, Russia

The main issue of the work was to develop a reactor intended to produce hydrogen and to synthesize aluminum hydroxide (boehmite) basing on aluminum oxidation with water. To achieve the goal we studied experimentally some macro-kinetic regularities of superfine aluminum powder oxidation with liquid water.

The size of aluminum powder species has a dramatic impact both on their properties and reactivity. It is established that superdispersed powder (SDP) is actively oxidized by water even at 320K resulting in oxide/hydroxide phase and hydrogen.

Aluminum oxidation with water follows one of the reactions shown below:



In our study we made use of superdispersed aluminum powders ACD-4 and ACD-6. The problems to be solved in our research were as follows:

- to assess both the completeness and the rate of the aluminum oxidation process at various Al/H₂O ratios in reactors of various design and construction,
- to determine the composition and dispersivity of solid oxidation products; and
- to determine the water temperature range for boehmite formation.

Both the phase composition and the size of crystal products formed in the process of aluminum oxidation with water were determined through X-ray phase analysis (RFA) with the help of DRON-3 diffractometer (CuK α -emission) and using external standards. The

OP-IV-4

granulometric composition of the powders was determined through conductometry at a laboratory set-up equipped with Koulter sensor (TA-2).

Two different methods were applied to estimate the volume of the released hydrogen:

- reasoning from the knowledge of the reactor volume and pressure, temperature and amounts of liquid phase, temperature and pressure of the saturated water vapour;
- reasoning from the pressure and temperature in the hydrogen accumulating tank, its volume being known.

At the 1st stage of this our study we used a reactor of volume 225 cm³, its internal diameter being 43 mm. The mass of the aluminum powder under study varied within the range 5 – 30 g, the “water : Al” ratio varied from 1:1 to 6:1 (by mass). The rate of the reactor heating was about ~ 5°C/min, till the wall temperature reached 520K. The oxidation reaction was substantially increasing in velocity starting at T = 320...330K.

For ACD-6 the average rate of aluminum oxidation ($dm/d\tau$) was about ~ 0.018 g/s within the water temperature range 330K-510K. It rose to 0.039g/s at T ≥ 510K and P=20.0 MPa. The final degree of aluminum oxidation (φ) was as high as $\varphi = 0.95 - 1.0$.

For ACD-4 within the water temperature range 330K-510K the rate of aluminum oxidation ($dm/d\tau$) was about ~ 0,008 g/s, and $dm/d\tau = 0,017\tau/c$ at $T_{H_2O} \sim 550K$. The degree of aluminum oxidation (φ) was $\varphi = 0.95 - 1,0$.

The analysis of ACD-6 и ACD-4 oxidation products has revealed that their general oxidation degrees, as well as their product chemical and phase composition depended on “H₂O : Al” ratio. When the ratio was low (H₂O : Al < 2) the oxidation resulted in powder including solid agglomerates that may vary in size, their composition being: α -Al₂O₃ up to 80...90% by mass, θ -Al₂O₃, AlOOH up to 10%, and Al up to 10%. The degree of aluminum oxidation was steadily growing (up to 1) with the “H₂O : Al” ratio (up to 5), as this took place the number of the agglomerates fell to zero, and the percentage of boehmite in the powder reached 100%. In the most of our experiments according to the X-ray analysis the boehmite crystal size was 600...900 Å. The average median size of the particles was 14-15 mcm, being 3 times as great as that of initial species.

The second set of experiments was conducted with a cylindrical reactor of volume 3.5l, internal diameter 100mm, and 500mm in length. The reactor was charged with suspension containing 150-200 g of ACD-4 or ACD-6 aluminum powder and 750-1200 cm³ of distilled water.

The reactor was being heated at rate $\sim 4^{\circ}\text{C}/\text{min}$ till the water temperature reached 520K, after that the heating was switched off. When the temperature of the water-Al suspension exceeded 340-350K its further growth was due to the heat released in Al oxidation process, the temperature gradient being $\sim 25^{\circ}\text{C}/\text{min}$ for ACD-4 and $\sim 60^{\circ}\text{C}/\text{min}$ for ACD-6. The average velocity of aluminum powder oxidation grew considerably as against the small reactor: within the temperature range $T=200\div 260^{\circ}\text{C}$ it achieved 0.3g for ACD-4 and 1.1g for ACD-6. The temperature of 340K and the maximal velocity of ACD-6 oxidation (3g/s) was achieved at $\text{H}_2\text{O}:\text{Al} = 5:1$. The oxidation product was a superdispersed powder consisting of 100% boehmite, its crystal size was $600\text{\AA} \div 900\text{\AA}$, and the particle size was $1\div 20\text{mcm}$, the average size being 14 mcm. In this reactor the total period of oxidation after achievement of $T=70^{\circ}\text{C}$ was 600s for 200g of ACD-4 aluminum, and 300s for ACD-6.

Therefore, the obtained results have testified that the autoclave method of boehmite manufacture does not allow high velocity of Al oxidation and, consequently, it cannot provide high rate of hydrogen release.

To accelerate the hydrothermal oxidation of aluminum and boehmite (aluminum oxide) formation we chose to heat the water suspension to the needed temperature $T=550\text{-}590\text{K}$. With this in mind we prepared aluminum powder suspension in water with their ratio (1: 5 \div 6) and sprayed it into a water-charged reactor preliminary heated to the required $T=570\div 590\text{K}$.

The experimental flow-through reactor was made of a tube sized 76x10mm, its total volume being 3l. The reactor was heated with outward nichrome spiral of total capacity 3 kW, and insulated. Two connecting pipes were provided at its top; the sprayer was inserted into the central axially located pipe, the second pipe served to withdraw hydrogen. The bottom was conical and a hole in its center was provided to withdraw boehmite suspension.

Aluminum-water suspension with pre-assigned $\text{H}_2\text{O}:\text{Al}$ ratio was prepared in a special mixer under continuous stirring and fed into the reactor with the help of a high-pressure plunger pump (up to 40.0 MPa). The suspension flow adjustment within the range 5-33 cm^3 was provided with the help of the plunger pump.

The experimental development of the aluminum powder (ACD-6) oxidation process in the flow reactor at continuous operation resulted in determination of the required work parameters that may provide the maximal velocity of aluminum oxidation:

- nominal temperature of the reactor housing preliminary heating is 600 – 620K;
- “ $\text{H}_2\text{O} : \text{Al}$ ” ratio is 6.5-8.0;
- the velocity of the Al/water suspension heating up to $300^{\circ}\text{C}/\text{s}$ was provided through atomization of the spray;

OP-IV-4

— the velocity of the vapour-hydrogen mixture withdrawal has to provide the constant temperature in the reactor 580-600K;

— the minimal time period needed for complete the oxidation of ACD-6 aluminum at $T_{\text{work}} = 580\text{K} \div 600\text{K}$ is 80 ÷ 100 s.

Every 80-100s, that is at regular intervals granting complete oxidation of aluminum and formation of aluminum hydroxide (in the form of boehmite – AlOOH) the boehmite suspension has to be withdrawn through the bottom connecting pipe in such amounts that at least 500cm^3 of water would still remain in the reactor.

The developed design of the flow-through reactor of volume 3l provided 100% oxidation of the aluminum and the manufacture both of the best quality boehmite powder and pure hydrogen (~100% purity) in the continuous process, when the suspension flow involved $30\text{ cm}^3/\text{s}$ of water, and 4 g/s of Al. The hydrogen humidity was controlled through its drying with silica gel. When the work parameters were constant the boehmite crystal sizes were practically unchanged (800 – 900 Å), the average median size of the particles was about ~5µm.

**APPRAISAL OF Pt-CATALYSTS AND PREDICTION
OF DEVELOPMENT WORK DUTY IN INDUSTRIAL
TECHNOLOGY OF REFORMING OF BENZINE USING
NON-STATIONARY KINETIC MODEL**

A.V. Kravtsov, E.D. Ivanchina, S.A. Galushin, D.S. Poluboyartsev

Tomsk Polytechnic University, Chemical technological department,

Lenin ave. 30, Tomsk, 634034, Russia,

Fax: +7(3822)563435, E-mail: ied@zmail.ru

Processing of hydrocarbon raw materials is characterized by multi component composition of raw materials, variety of simultaneous reactions with very discriminate rates, bifunctional nature of applied catalyst and strong catalytic stimulation by means of activation and deactivation effects.

The principle physicochemical components aggregating in complicated feed was based in model kinetic construction of gasoline processing [1, 2]. Detailed mechanism registration of feed components interaction (reagent and admixture) with catalyst is of fundamental importance in mathematical model creation. It makes mathematical model invariant to feed stock changes. At the same time, the main reasons of Pt-contacts deactivation (ageing, chlorine and sulfur poisoning, coking) was marked out and mechanism of each processes was mathematically described. The reasons and mechanism of deactivation can be related to different active catalyst center, catalyst with different chemical composition, unused and regenerated catalyst. These processes can be called selective deactivation for bifunctional catalyst. Investigation of detailed deactivation mechanism give the opportunity to forecast duration and operating practices of process work cycles, and ,what is very essentially, operating practices change with feed stock changes. In particular, non-stationary kinetics predetermines catalysts choice for concrete processes on basis of model, which adequately describes real process. As a whole, the structure of intelligence computing system is showed in the picture.

Practical propositions of hydrocarbon raw materials processing theory were used for improvement of industrial processes, operation enhancement of commercial plant of gasoline and aromatic hydrocarbons making. Computing system on basis of non-stationary kinetics

OP-IV-5

model allows to get results in practically important directions: catalyst testing, optimization of catalyst activity level, forecasting of catalyst activity level in work cycle, complex gasoline technology, compounding of finished blend.

Forecasting computer technique allows to determining catalysts activity level using chromatographic analysis data of raw material and stable catalysate. Catalyst activity level is divided into initial, current and optimal. Quantification of current catalyst activity level is raw materials aromatization speed.

$$W = k_0 \cdot e^{-\frac{E}{RT}} \cdot f(C)$$

E – measure of intermolecular energy content, which is essential for reaction passing probability. Current catalyst activity level is calculated through aromatic hydrocarbons going out. It reflects operating practices of plant regime on the current moment and composition of feed stock. Processing rate (second factor) and composition of feed stock (third factor) influence on current catalyst activity level. Characteristics of current activity level (different mark) were calculated for models and showed, that regeneration and catalyst configuration regimes during after regeneration period influence on work cycle duration. Optimal catalyst activity level is completely defined by measure of reaction passing probability. It is expressed by a formula:

$$k_0 = A \cdot e^{\frac{\Delta S}{R}}$$

A – measure of molecular collisions frequency. It is defined by number and power of active centers. S – probability or entropy of molecular collisions.

It is necessary in manufactured condition to maintain required proportion between target reforming and balance of formation and hydrogenising structure, which is determined by proportions of active acid and metallic sites. Selective admixture «poisoning» (water and chlorine) surveys give the opportunity to choose processing regime, which can provide reactor with maximum performance (maximum performance is in terms of octane-tonns), that is optimal catalysts activity. In that case toxic substances become gas promoters.

Activity catalyst forecasting during service cycle and overall service life period, which is accomplished on the model, allow to evaluate catalyst capabilities, deactivation speed depending on volume and quality of feed stock.

Thus, using pursued researches we can get the following conclusions:

1. Catalyst selection depends on peculiarity of technology and hydrocarbon composition of feed stock. Objective appraisal of catalyst application effectiveness (different commercial mark) and operating conditions is possible only by direct methods of analysis by way of real potential Pt-contact with using non-stationary kinetic model.
2. Using model for calculating of current catalyst activity level admits to correct operating practices and determine source of deleterious influence on catalyst (admixture in raw materials, changing of raw materials composition, presence of non-stoichiometric components in raw materials).
3. Dependence of active metals dispersion during reduction is determined by chlorine concentration and temperature. It has extremal nature. At that with using «Activity» program quantitative assessment of carbon burning regime, refacing and is very important.
4. Carbon deposition the active sites depends on equilibrium hydrogenation-polymerization reaction. Optimal activity of Pt-contacts can be calculated by value of thermodynamic and kinetic parameters depending on catalyst mark and catalyst operating regime.
5. Prediction of regeneration and replacement catalyst data is determined by process rigidity and composition of feed stock. It is calculated using «Prognoz» program.

References

1. Kravtsov A.V., Ivanchina E.D. Computer forecasting and optimization of benzine processing. – Tomsk: STT, 2000. – 192 p.
2. Kravtsov A.V., Ivanchina E.D., Averin S.N., Dyakonova L.V. Computer forecasting of catalytic reforming process of gasoline fraction. – Chemical technology of fuels and lubricants, №6, 2001. – p. 11.

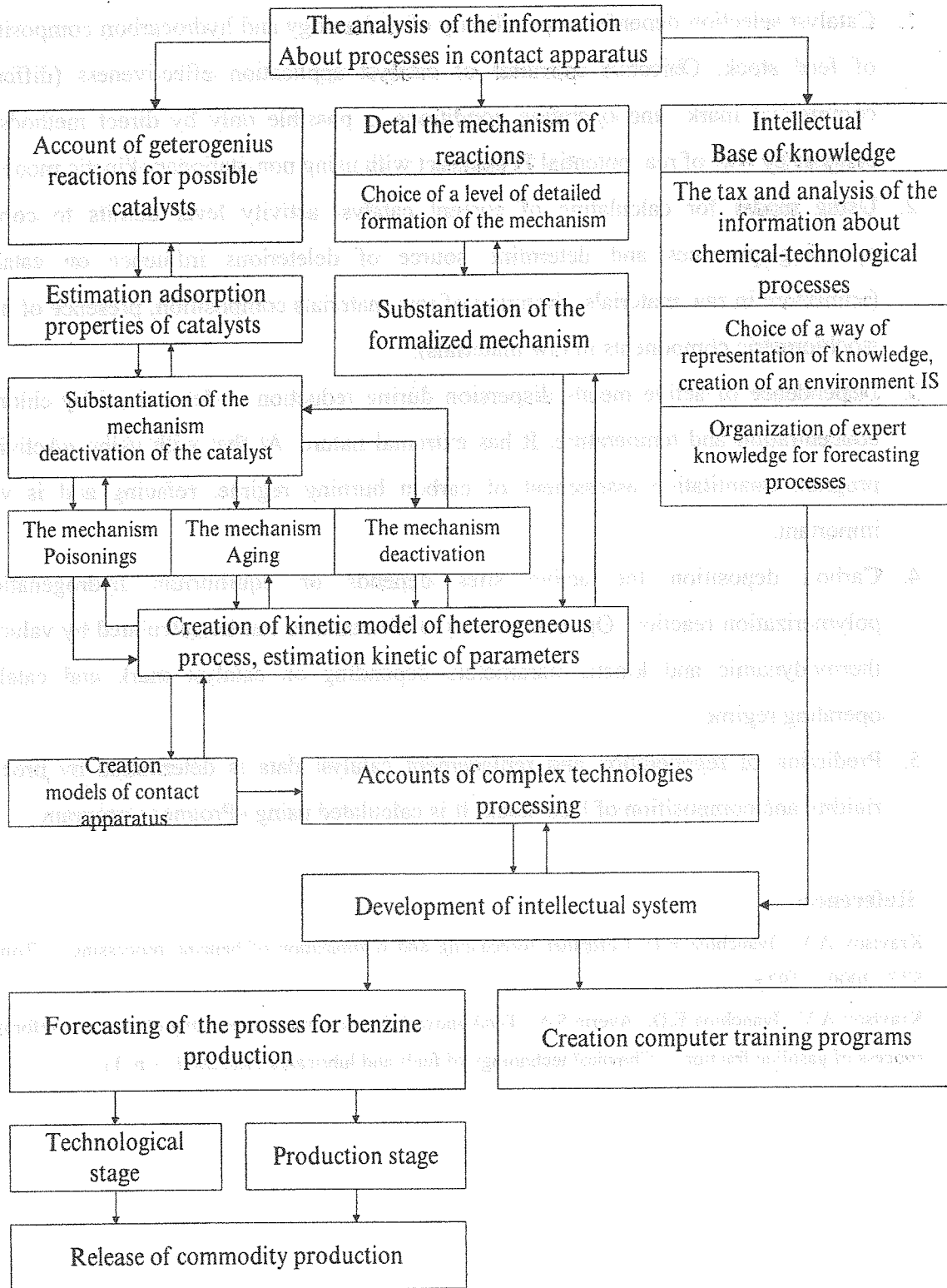


Fig. 1 Basic development cycles and applications IS at chemical-technological processes

SECTION V.
WASTE DETOXICATION AND PROCESSING

SECTION V.
WASTE IDENTIFICATION AND PROFILING



EFFICIENCY OF HEAT RECOVERY VERSUS MAXIMUM CATALYST TEMPERATURE IN A REVERSE-FLOW COMBUSTION OF METHANE

Krzysztof Gosiewski

Institute of Chemistry and Environmental Protection,

Pedagogical University of Czestochowa,

ul. Armii Krajowej 13/15, 42-201 Czestochowa, Poland

E-mail address: gosiew@cidg.net.pl

Abstract

Methane has global warming potential (GWP) several times higher than that of CO₂. Furthermore, it is emitted from a host of sources and thus produces a substantial contribution to overall global warming (the estimated share of CH₄ is around 19 %). Large quantities of methane are exhausted to the atmosphere with coal-mine ventilation air with very low CH₄ content (0.1 – 1 vol.%). The global emission of methane from this source is estimated at, roughly, 15 Mt/year. Apart from the environmental impact this leads to considerable energy losses, as methane is a fuel in its own right. Unfortunately, the concentration of methane in ventilation air is too low to support homogeneous combustion. Thus, the only viable option is catalytic oxidation in an autothermal reverse-flow reactor fitted with an energy withdrawal system to recover the heat from the hottest parts of the catalytic bed. Extensive simulations reveal that, for CH₄ concentrations in the feed air below 1 vol.%, the efficient heat recovery from the reactor becomes fairly complex. The average flowrate of ventilation air emitted from a single shaft is about 700,000 m³(STP)/h; if we assume that the energy recovery remains a viable alternative as long as CH₄ concentration exceeds 0.4 vol.%, the heat flux generated due to the oxidation would be almost 28 MW (and even about 70 MW at peak methane concentrations). Such quantities of energy cannot be utilized as low-quality heat, and the sole practical solution is the production of high-pressure steam, which can further be used to generate electricity. In order to find the efficient heat recovery method from a reverse-flow methane combustor a number of simulations based on mathematical model of the process were performed. The simulations were carried out for two different types of catalyst. Initially, the catalyst used was that based on MnO₂ but it occurred, that maximum temperature approaching 1000 °C in the catalyst bed could be dangerous for safe catalyst work. Then, in order to ensure lower maximum temperatures within the catalytic bed (and thus, additionally to avoid the homogeneous combustion in the gas phase) the other catalyst was used with palladium as an active component. The simulations are regarded as a preliminary analysis of the process. Consequently, the exact values of the parameters characterizing the steam produced are not specified (these parameters determine, in turn, steam temperatures in the various parts of the installation). However, since the boilers usually produce superheated steam at a pressure of about 4 MPa or higher, we can tentatively assume that the system should guarantee the generation of steam of at least such quality. In such a system the low-temperature section includes a water heater (economizer), while the high-temperature part incorporates a steam superheater. The evaporators operate at intermediate temperatures.

The economizer is commonly fed with treated water at a temperature slightly above 373 K (100 °C), although present-day boilers enable the cooling of the gas to about 333 K (60 °C) by utilizing a part of the heat in the water treatment plant. The steam produced usually has a temperature of about 723 K (450 °C). These assumptions result in the following conditions: incorporating the various elements of the boiler into the heat withdrawal system and, simultaneously, providing sufficiently high temperature difference between the heating medium (gas from the reactor) and the medium that consumes heat (water and steam) requires that the gas temperature at the inlet to the boiler system should be at least 823 K (550 °C), and that the gas itself should not be cooled below 333 K. These conditions lead to approximate temperatures characterizing the heat withdrawal system. Obviously, the higher the gas temperature at the boiler inlet the better. Too high gas temperatures in the reactor lead to yet another group of problems (among others, too large a contribution of the homogeneous combustion resulting in rapid catalyst destruction).

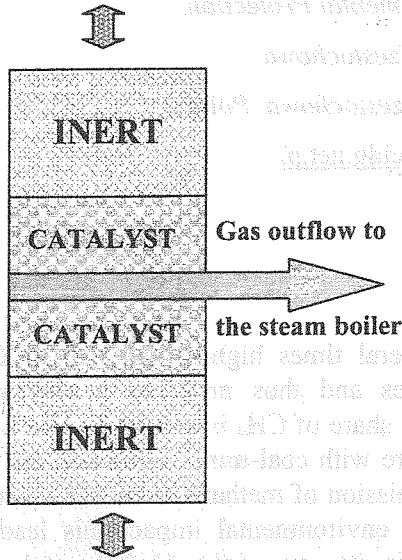


Fig. 1 Schematic diagram of a reverse-flow reactor with heat recovery by the hot gas withdrawal

In general, the heat of reaction can be withdrawn in either of the two ways. In a method termed “central cooling” the whole gas stream flows through the heat exchanger. On the other hand, the technique of “hot gas withdrawal” (Fig. 1) is based on feeding the boiler with a part of the hot gas withdrawn from the central part of the reactor, which is then discharged to the atmosphere. The simulations revealed that hot gas withdrawal would enable higher efficiency of the heat recovery than “central cooling”, so in present study only this method is analyzed. A drawback of the hot gas withdrawal is that a part of the gas stream passes only through a half of the catalyst bed, whereupon it leaves the system without participating in the reaction occurring in the second half. Effective conversion of the reactor about 90% can be obtained, however. On the other hand the temperature of the gas withdrawn from central part is high enough, that some additional fixed catalyst bed located on this side stream allows obtainment of nearly full methane conversion. Thus incomplete conversion is not a real problem when this solution is applied.

The mathematical model used for simulations is a one-dimensional in space, two phase model, both for heat and for mass transfer. It takes into account the effective thermal conductivity in the solid phase and dispersion in the gas phase.

Energy balance for the gas

$$0 = -n_g c_{p,g} \frac{\partial T_g}{\partial z} + \varepsilon \frac{n_g c_{p,g} d_p}{Pe_g} \frac{\partial^2 T_g}{\partial z^2} + \alpha S (T_c - T_g) - \Delta H r_{\text{hom}} \quad (1)$$

Energy balance for the catalyst

$$\rho_b c_k \frac{\partial T_c}{\partial t} = \lambda_{eff} \frac{\partial^2 T_c}{\partial z^2} + \alpha S (T_g - T_c) + \rho_b \eta r_{CH_4} (-\Delta H) - \frac{4}{D_r} h_{surr} (T_c - T_{surr}) \quad (2)$$

Molar balance of CH₄ in the gas phase

$$\varepsilon \rho_g \frac{\partial y_{CH_4}^g}{\partial t} = \varepsilon \rho_g D_{eff} \frac{\partial^2 y_{CH_4}^g}{\partial z^2} - n_g \frac{\partial y_{CH_4}^g}{\partial z} + \beta S (y_{CH_4}^s - y_{CH_4}^g) - \varepsilon r_{hom} \quad (3)$$

Algebraic equation describing mass transport from the bulk gas to the catalyst surface

$$y_{CH_4}^s = \frac{\rho_b \eta r_{CH_4}}{\beta S} + y_{CH_4}^g \quad (4)$$

with appropriate initial and boundary conditions.

The kinetic equations, used for both examined catalysts were obtained from the Boreskov Institute of Catalysis in Novosibirsk.

The simulations revealed, that there is a visible contradiction between efficiency of heat recovery aimed to high-pressure steam production and maximum temperature in the bed.

The heat recovery coefficient is shown in Fig. 2, while maximum temperatures in the bed in Fig. 3, as a function of inlet methane concentration to the reactor.

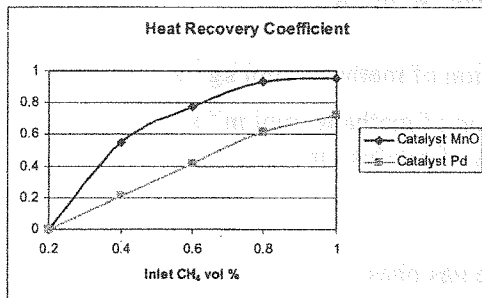


Fig. 2 Heat recovery coefficient as a function of inlet methane concentration.

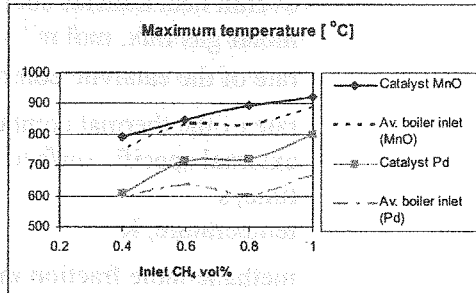


Fig. 3 Maximum temperatures as a function of inlet methane concentration (solid lines). Average inlet temperature to the boiler shown by the dashed lines

Input data for simulations were selected as for pilot plant processing 30 000 m³ (STP) of ventilation air. There is a lot of degree of freedom when selecting the process parameters, since one can assume various combinations of inert and catalyst section length, apparent gas velocity in the reactor, size and shape of the catalyst and inert filling, various reversal times and many others. In the case presented the parameters were selected that way to obtain lowest possible temperatures in the catalyst bed, in order to avoid the catalyst destruction mainly due to appearance of homogeneous combustion in the gas phase. One should be aware, however, that this aim is inconsistent with very high efficiency of the heat recovery, since the lower temperature the lower heat recovery coefficient.

On the one hand this conclusion seems to be obvious, while hot gas withdrawn is always cooled down to the same target temperature. In our case it was 333 K (60 °C). On the other hand, however, this effect could have been compensated by higher flowrate of the hot gas withdrawn in these cases when the gas has lower temperature. Unfortunately such compensation is not sufficient enough. For MnO₂ catalyst and 1 vol% of CH₄ 29% of hot gas could be withdrawn without danger of the reactor extinction, while for the same methane concentration this amount could be enlarged only to maximum 34% while Pd catalyst is used (an optimal value is about 30%). As one can see in Fig. 3 in these case decrease of average inlet temperature to the boiler exceeds 200 K.

Conclusion

Design of the reverse-flow combustor from the point of view of the heat recovery efficiency and maximum temperature in the bed is a matter of compromise. High heat recovery coefficient demands high gas temperature at the boiler inlet. On the other hand high catalyst temperature promotes homogeneous gas phase combustion what could result in the catalyst destruction.

Acknowledgements

This work was supported by the European Union Grant (Contract No. ICA2-CT-2000-10035).

Notation

c_k	heat capacity of the catalyst, J kg ⁻¹ K ⁻¹
$c_{p, g}$	heat capacity of the gas, J mol ⁻¹ K ⁻¹
D_r	reactor diameter, m
D_{eff}	effective mass dispersion coefficient, m ² s ⁻¹
D_e	effective diffusion coefficient, m ² s ⁻¹
h_{surr}	overall heat transfer coefficient, W m ⁻² K ⁻¹
n_g	molar gas flux, mol m ⁻² s ⁻¹
r_{CH_4}	rate of the catalytic combustion of methane, mol kg ⁻¹ s ⁻¹
r_{hom}	rate of the thermal combustion of methane, mol m ⁻³ s ⁻¹
S	external specific surface area of catalyst, m ² m ⁻³
t	time, s
T	temperature, K
$y_{CH_4}^g$	methane mole fraction in the gas phase
$y_{CH_4}^s$	methane mole fraction on the catalyst surface
z	axial coordinate along the bed, m

Greek letters

α	heat transfer coefficient, W m ⁻² K ⁻¹
β	mass transfer coefficient, mol m ⁻² s ⁻¹
ΔH	heat of reaction, J mol ⁻¹
ε	void fraction
η	effectiveness factor of the pellet
λ_{eff}	effective thermal conductivity, W m ⁻¹ K ⁻¹
ρ_b	bulk density of the bed, kg m ⁻³
ρ_g	molar gas density, mol m ⁻³

MODELLING OF IN DUCT DESULFURIZATION REACTORS

Garea A., Irabien A.

Dpto. Ingeniería Química y Química Inorgánica, Universidad de Cantabria

*✉: ETSIT, Avda. de los Castros s/n 39005 Santander, Spain

☎: +34 942 20 15 88, ☎: +34 942 20 15 91, ✉: gareaa@unican.es

1. Introduction

Related to the control of acid rain, new regulations must be taken into account to control the emission of SO₂ and NO_x. A simple, Gas-Solid technology to be applied to sulfur dioxide control is based on the injection of a basic reagent, mainly calcium hydroxide, in the duct in order to capture the pollutants.

The modelling of "in duct" reactors for desulphurization processes at low temperatures was performed using models based on the gas-solid kinetics and based on non-linear empirical models obtained from the fitting of experimental results using neural network analysis. A comparison between both procedures is given in the paper.

2. Experimental data

The prediction of the SO₂ removal efficiency was performed from data obtained in an entrained flow reactor at pilot scale which is described elsewhere [1, 2]. The operational parameters of the in-duct injection process are the Calcium to Sulfur molar ratio (Ca/S), and the residence time that determines the contact period between gas and solid phases in the flow reactor (or duct). Pilot plant data covered the intervals of Ca/S 1.5-18 (molar basis) and residence times 0.3-4 seconds. The influence of other variables in the gas-solid reaction was also considered in the experimental planning: relative humidity 50-70%, SO₂ inlet concentration 1000-2000 ppmv, and temperature 50-70°C.

3. Modelling and results

At a microscopic level, the modelling of the gas-solid reaction that takes place in the in-duct reactor was based on the application of the shrinking core / grain equations to any single particle at any axial position along the reactor with the corresponding boundary conditions. The extent of reaction for a given grain was calculated from the shrinking radius with time.

The overall reaction rate included the terms of surface reaction and diffusional mass transfer resistance in the product layer of the grain. The intergrain mass transfer resistance was considered negligible, checked in previous studies [3]. The estimation of parameters, product layer diffusivity and kinetic constant, was based on the criteria of least square minimization related to the experimental data of SO₂ concentration in the gas phase along the reactor. The obtained results indicated that the controlling step is the diffusional resistance in

the grain product layer. Figure 1 (a) shows some experimental and simulation results as representative.

As a non-linear empirical modelling approach, a neural network was used for the prediction of the SO₂ removal efficiency in the in-duct desulfurization reactor. The process variables are the elements of the input layer and the experimental SO₂ concentration values at any axial position along the reactor are the output – target values [4]. The predicted profiles of SO₂ concentration along the reactor at different residence times are shown in Figure 1 (b), that indicates a better prediction for higher efficiency levels of SO₂ removal in comparison to the mechanistical approach (see Figure 1 (a)).

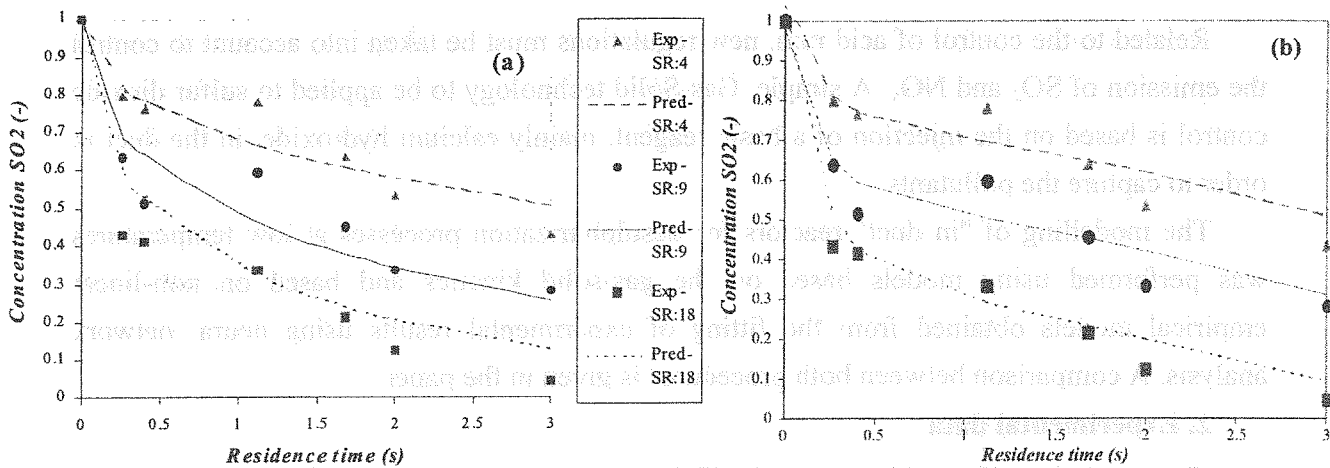


Figure 1. Experimental and simulation results of dimensionless SO₂ concentration along the reactor, at different Ca/S molar ratios (SR). Conditions: 60% relative humidity, 1000 ppmv SO₂ inlet conc., 60 °C.

Acknowledgements

This research has been financially supported by Ministry of Science and Technology of Spain (Project No. PPQ2000-0251).

References

[1] Marques, J.A., A. Garea, A. Irabien, 14th International Congress of Chemical and Process Engineering, CHISA, vol.1, pp.45, 2000.
 [2] Marques, J.A., A. Garea, A. Irabien, 11th International Conference on Coal Science, DOE/NETL-2001/1153.
 [3] Garea, A., J.A. Marques, T.L. Hechavarría, A. Irabien, European Symposium on Computer Aided Process Engineering-11, pp. 147-152, 2001.
 [4] Garea, A., J.A. Marques, J.A. Irabien, 17th International Symposium on Chemical Engineering, ISCRE 17, 2002.

FLUIDIZED BED REACTOR FOR FLUORIDE REMOVAL

R. Aldaco, A. Irabien

Dpto. Ingeniería Química y Química Inorgánica, Universidad de Cantabria

*✉: *ETSIT, Avda. de los Castros s/n 39005 Santander, Spain*

☎: +34 942 20 15 79, ☎: +34 942 20 15 91, ✉: *aldacor@unican.es*

1. Introduction

The conventional method for fluoride removal from industrial wastewater generally involves a chemical precipitation process [1],[2],[3]. Of the various treatment methods employed to remove fluoride, hydroxide precipitation is the most common treatment technology. Fluoride is removed by adding alkali such as lime or hydrated lime to adjust the wastewater pH to the point where the fluoride exhibits a minimum solubility. Then the precipitated fluoride is removed by a proper solid-liquid separation technique such as sedimentation and filtration. The conventional fluoride removal process generates huge amounts of a water rich sludge, which has to be disposed off with increasing costs. Due to the high water content and the low quality of the sludge, reuse of fluoride is not an economical option [4].

In recent times, it has developed several processes for fluoride removal from wastewaters. An alternative is to apply controlled crystallization in a fluidized bed reactor instead of conventional precipitation.

The aim of this work is to study the recovery of fluoride in a fluidized bed reactor in viable technically conditions.

2. Process and System description

The process is based on the crystallization of calcium fluoride upon seed grains in a fluidized bed (Figure 1). The reactor consists of a vessel partially filled with suitable seed material (in this case sand) in which water is pumped in an upward direction through the reactor and at such a velocity that the pellet bed is kept in the fluidized state.

Reaction is induced by the addition of calcium reagent. The fluoride covered grains are removed from

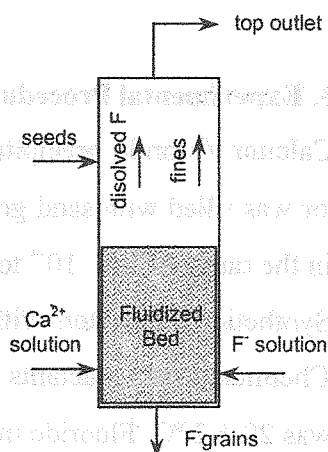


Figure 1. Schematic representation of the fluidized bed.

the bottom of the bed and replaced intermittently by fresh seed grains.

Simultaneously to the precipitation upon the grains (heterogeneous nucleation), two unwanted processes occur: nucleation in the liquid phase (homogeneous and secondary nucleation) and abrasion of the mineral layer in the bed. Both processes lead to small particles (referred to as “fines”), which leave the bed at the top and form, together with the remaining fluoride in solution, the fraction of the fluoride that is not recovered in the reactor [5].

Heterogeneous primary nucleation may occur so the calcium fluoride precipitation takes place upon the sand surface. For this purpose, significantly lower supersaturations may require [7]. In practice, a small primary nucleation happens at a fluoride concentration of 100-200 mg·l⁻¹ F⁻ [4].

Recycle ratio is required to obtain a fluoride concentration to prevent primary nucleation. In addition, another recycle is necessary in order to obtain the appropriate calcium dosage. Figure 2 shows the fluidized bed reactor circulation system.

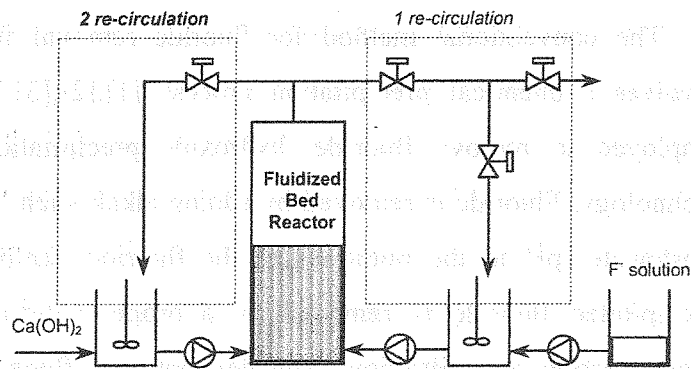


Figure 2. The pellet reactor circulation system

The efficiency of fluoride removal was calculated by measuring the concentration of both fines and dissolved fluoride in the outlet stream. The dimensionless conversion (X), fines fraction (X_F) and efficiency (precipitated fluoride upon sand) (X_R) are defined as:

$$X = \frac{W_{F,dis in} - W_{F,dis out}}{W_{F,inf l}} \quad X_F = \frac{W_{F,fines}}{W_{F,inf l}} \quad X_R + X_F = X \quad (1)$$

3. Experimental Procedure

Calcium fluoride precipitation was conducted in continuous fluidized bed reactor. The reactor was filled with sand grains up to a height of 0.20 ± 0.01 m. The sand grains had sizes within the range of 1.5 · 10⁻⁴ to 3 · 10⁻⁴ m.

Synthetic wastewaters with a fluoride content of 300-2,000 mg·l⁻¹ are treated.

Chemical grade reactants and demineralized were used. The temperature in the fluidized bed was 20 ± 2 °C. Fluoride in outlet streams was measured by specific fluoride ion electrode. Experiments and experimental conditions are listed in Table 1.

Table 1. Experimental conditions.

Exp No.	$C_{F,in}$ (mg·l ⁻¹)	(Ca/F) _{in} (-)	$C_{F,in}$ reactor (mg·l ⁻¹)	$F_{F,in}$ (ml·min ⁻¹)	$F_{Ca,in}$ (ml·min ⁻¹)	$F_{recir, F}$ (ml·min ⁻¹)	$F_{recir, Ca}$ (ml·min ⁻¹)	SV (m ³ ·h ⁻¹)
SR1.1	300	1.1	150	250	250	-	-	30
1R1.1	2,000	1.1	136	34	200	266	-	30
2R1.1	2,000	1.1	136	34	200	266	200	30

4. Results and discussion

Figure 3 presents the effect of the inlet fluoride concentration (F_{in}) on the fines generation. From figure it is possible to prove that a high local supersaturation favors the homogeneous nucleation and therefore the generation of fines [4],[5], [6],[7],[8].

Fluoride concentrations higher than 150 mg/l imply about 20% of fines. In practice, it has been worked with a fluoride concentration smaller that 150 mg/l.

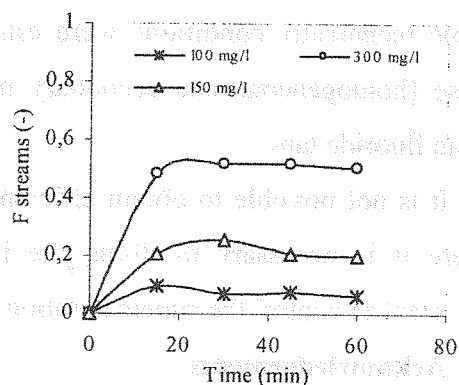


Figure 3. Dimensionless fines generation in the fluidized bed as a function of supersaturation.

Figure 4 shows the dimensionless fluoride streams defined by eq. (1) as a function of the time in the fluidized bed.

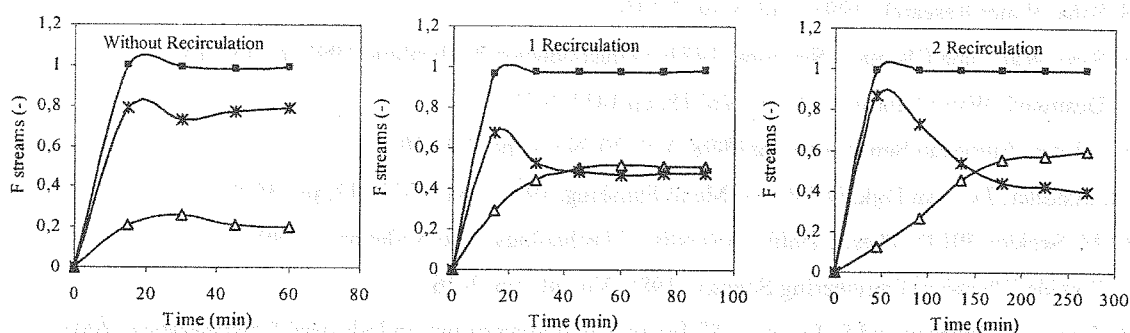


Figure 4. Dimensionless fluoride streams in the fluidized bed as a function of time. ■ = conversion (X), Δ = fines (X_F), * = efficiency (X_R)

The conversion of the process (X) is the same in all the studied case for Ca/F molar ratio equal to 1.1. However, the fines fraction (X_F) and therefore, the efficiency (X_R) of the process is different. In stationary-steady, with 1 and 2 recirculations, the fluoride removal efficiencies are 48% and 39% respectively, while without recirculation the efficiency is around 80%.

The local supersaturation ratio is significantly higher in fluoride dilution tank due the recycled calcium excess. This is proposed to be the cause of the homogeneous nucleation and

greater degree of fines formation. In addition, the recycled fines could be the reason of an additional fines formation by secondary nucleation, and therefore, the heterogeneous nucleation in the reactor is lower than without recirculation.

5. Conclusions

High global supersaturation level decreased the fluoride removal efficiency due to the formation of fines.

The main processes concerning the precipitation of calcium fluoride in a fluidized bed in viable technically conditions were established. Fines are produced by nucleation in liquid phase (homogeneous and secondary nucleation and molecular growth) at the reactor and dilute fluoride tank.

It is not possible to obtain efficiencies bigger than 40% in viable technically conditions where it is necessary to dilute the influent through recirculation. In this sense is very important to control the supersaturation at the system.

Acknowledgements

This research has been financially supported by Ministry of Science and Technology of Spain (Project No. PPQ2000-0251). We would like to thank Head Office of Research of Spain (Grant No. FPI2000-4858).

References

- [1] S. Saha. Water Research, 1993, Vol. 8, pp 7-1350
- [2] S. Sato. Water and Chemical Sessions: 14TH Semiconductor Publication, 1995. pp 131-152
- [3] F. Desmond. Water Research , 1984. Vol 18, pp 1411-1419
- [4] A. Giesen. European Semiconductor, 1998. Vol. 20. No. 4, pp. 103-105
- [5] M. Schöller, J.C. van Dijk, D. Wilms. Metal Finishing, 1991, Vol 89, No 11, pp. 46-50
- [6] M.M. Seckler. PH.D. Thesis, Delft University of Technology, The Netherlands, 1994
- [7] J. Garside. Chemical Engineering Science, 1985, Vol. 40, pp. 3-26
- [8] A. Lewis, K. Petersen and S. Lacour. 15th International Symposium on Industrial Crystallization, 2002

KINETIC STUDY OF DIRECT DECOMPOSITION OF NITRIC OXIDE OVER COPPER ION-EXCHANGED ZSM-5 ZEOLITE

Fakhry Seyedeyn-Azad and Dong-ke Zhang*

Chem Eng. Dept., University of Isfahan, Isfahan, Iran

**School of Chem. Eng., Curtin University of Technology, G.P.O. Box U1987,
Western Australia, 6845, Perth, Australia*

Abstract

Kinetic study of Nitric Oxide (NO) decomposition over copper ion-exchanged ZSM-5 zeolite was investigated in a packed bed tubular reactor. The catalyst was prepared from Na-ZSM-5 zeolite synthesized using template free method. The synthesized zeolite was ion-exchanged with ammonium nitrate. The obtained solid phase was calcined to remove ammonia from the zeolite lattice prior being ion-exchanged with copper ions.

The catalyst was tested for the direct decomposition of NO over a temperature range of 250-650 °C in order to determine the temperature at which the maximum conversion occurs. A relatively high conversion was achieved over the catalyst and the maximum NO conversion into N₂ occurred at 400-450 °C. The kinetic studies were performed at 350, 450 and 550 °C to examine the reaction mechanisms close to the temperature with the maximum NO conversion, and at both sides of that temperature where the NO conversions into N₂ decrease.

The reaction order of NO and the rate constant, at 350, 450 and 550 °C were obtained. The orders of NO concentration in the reaction rate were 1.05, 1.13 and 1.63 at 350, 450 and 550 °C respectively. The order of NO in the reaction rate was very close to 1 at 350 °C whereas at 450 and 550 °C derivation from the first order was observed.

It was concluded that the reaction mechanisms at the both sides of the most effective temperatures were different. The general form of the reaction rate reported in the literature was confirmed for temperatures greater than the most effective temperature and a new reaction mechanism and a new reaction rate were proposed, which showed that the dependence of NO decomposition was first order in NO concentration in the absence of oxygen and the reciprocal of the rate increased linearly with the oxygen concentration when oxygen was present.

ORANGO SILICON POISONING OF Pt/ γ -Al₂O₃ CATALYST IN TOTAL OXIDATION OF VOC

M. Rahmani^{a,b}, N. Cruise^c, M. Sohrabi^a, O. Augustsson^c, M. Sanati^b

^a Chemical Engineering Department, Amir-Kabir University of Technology, Tehran, Iran

^b School of Biosciences and Process Technology, Växjö University, SE-351 95, Växjö, Sweden

Email: Mohammad.Rahmani@ibp.vxu.se, Fax: +46-470-70 8756

^c Perstorp Catalysts, Perstorp AB, SE-284 80, Perstorp, Sweden

1. Introduction

Supported noble metals catalysts are used widely in air pollution control system. A major limitation imposed on the reliable operation and useful lifetime of such catalysts is their susceptibility to poisoning by a very small amount of poison compounds in the feed. Poisoning of Pt/ γ -Al₂O₃ by organo silicones has been reported in total oxidation of volatile organic compounds [1-3] and catalytic sensing elements for detecting flammable gas [4,5]. Present work examines the influence of HexaMethylDisilOxane (HMDSO) as a poison precursor on the activity of Pt/ γ -Al₂O₃ catalyst, during total oxidation of EtAc as a VOC model compound. HMDSO was selected as a poison precursor because it is a monomer of other silicon oils and EtAc is one of the most frequently encountered VOC in different industries while its complete oxidation is difficult. A series of fast deactivation experiments with high level of poison concentration have been performed and the residual activities have been measured.

2. Experimental

1.1. Reactor setup

The experimental setup includes a parallel feed arrangement, a micro-injection pump (from ALiTEA), a vaporizer, a preheater and a small fixed bed reactor. Two sample points just before the reactor inlet and after the reactor outlet were provided for online analyzing.

The Fixed bed was stainless steel tube reactor with 36 mm internal diameter and 180 mm height equipped with an electrical mantel. Two total hydrocarbon analyzers (from Brenath Atomic, model 3006) were used to measure the inlet and outlet hydrocarbon concentrations.

CO and CO₂ in the product stream were measured simultaneously using an IR analyzer (Fuji Electronic, model ZRF).

1.2. Material

High purity γ -alumina extrudate from SASOL were used as the catalyst supports. Pure EtAc, 98.8%, and pure HexaMethylDisilOxane (HMDSO), 98+% supplied by Sigma Aldrich.

1.3. Catalyst

The catalysts were prepared by the using the impregnation method. The support is an alumina extrudate with a surface area in the range of 95-135 m²/g and a diameter of 3 mm and length approx. 12 mm. After impregnation and careful washing, pellets are dried and then calcined at 500 °C and reduction step with hydrogen at 300 – 500 °C. The target Pt loading on the catalyst was 900 ppm.

1.4. Activity measurements

Activities of the fresh catalysts were measured using 60 ml catalyst, at 4 steady-state temperatures, 250,300,325 and 350 °C. The gas hourly space velocity (GHSV) was set at 11500 h⁻¹, equal to 11.5 lit/min fresh air containing 420 ppm EtAc.

1.5. Fast deactivation experiments

Fast deactivation experiments were performed using 60 ml catalyst. Inlet temperature was 350 °C and the gas hourly space velocity was set at 11500 h⁻¹. A solution of 4.8 vol% HMDSO in EtAc has been injected into the hot air stream in vaporizer. In each experiment EtAc first was introduced to the reactor until steady-state conversion and temperature were achieved. The feed was then switched to HMDSO+EtAc. Deactivation continued for 10 h. The heating and poison injection then stopped and reactor cooled to room temperature for 14 h in a fresh air stream (11.5 lit/min). After this period the temperature of reactor increased to 350 °C to check the residual activity.

3. Result and discussion

Activity measurements on fresh catalyst showed more than 99.4% EtAc conversion at 350°C. Figure 1, shows the conversion of EtAc to CO₂ for 10h deactivation. The catalyst lost its activity very quickly during first 5 hours of experiments. The change in activity is very rapid especially at the first minutes of deactivation. After 30 minutes, while the EtAc conversion

OP-V-5

was high the CO_2 yield had decreased to about 50%. It has been identified that, EtAc has been undergone some kind of partial oxidation reactions. After 5 hours the CO_2 yield remained almost unchanged at 25%. Following to the deactivation period for 10h, catalyst

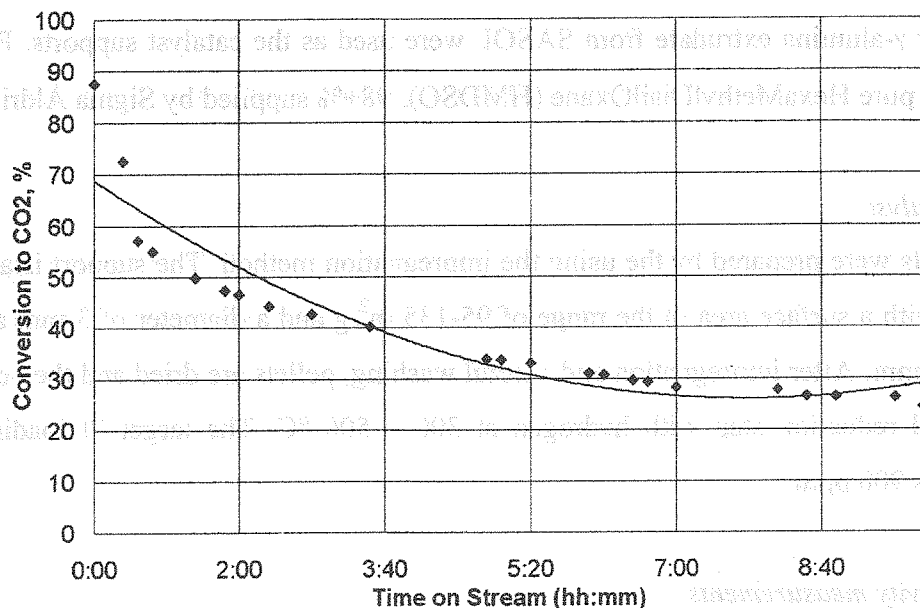


Figure 1 Deactivation of Pt/γ-Al₂O₃ catalyst by HMDSO during total oxidation of EtAc. Inlet temperature 350°C, VOC concentration, 420 ppm, GHSV, 11500 h⁻¹.

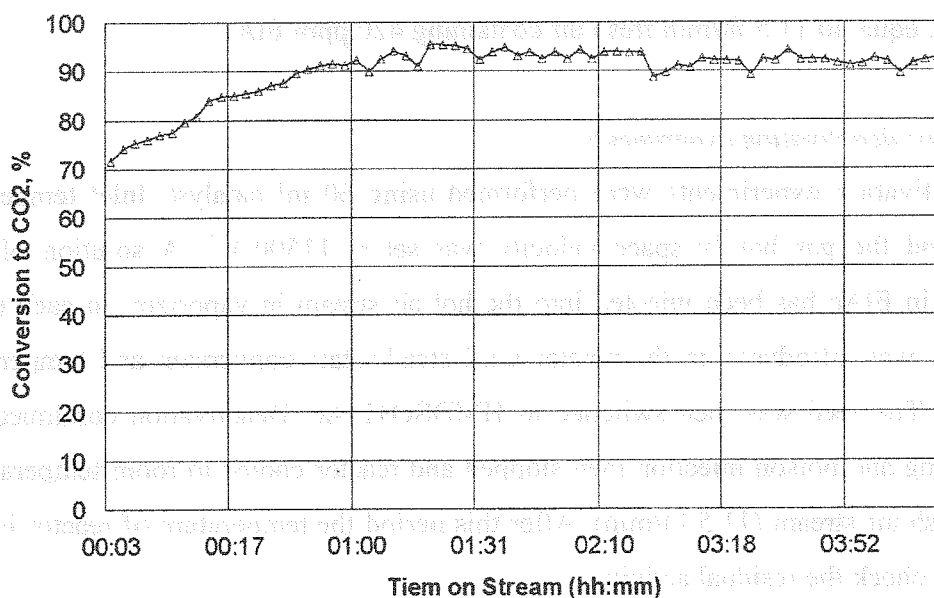


Figure 2 Regeneration of fast deactivated Pt/γ-Al₂O₃ catalyst after 14 h exposing to fresh air (11.5 l/min). Inlet temperature 350°C, GHSV 11500 h⁻¹, EtAc concentration 420 ppm.

was cooled down for 14 hours in a fresh air stream. The first data point after this period, showed about 71% conversion to CO_2 , at 350 °C. That means catalyst has recovered about 45% of its initial activity after removing the poison from feed stream. Figure 2, shows the

trend of recovery in the second cycle of experiment. These figures indicate, fast deactivation of Pt/ γ -Al₂O₃ by HMDSO in total oxidation of EtAc is reversible. It was thought Si species deposited in form of organo material, which during the poison exposure saturated the catalyst surface. The activity loss is related to pore blockage by these large organosilicon molecules. FTIR analysis of deactivated samples [8] proves the existence of Si-R on the catalyst surface.

4. Conclusion

The presence of HMDSO during total oxidation of EtAc represents a serious poisoning of Pt/ γ -Al₂O₃ catalyst. Removing the poison from feed, and increasing the inlet reactor temperature to the condition of poisoning or higher makes almost total recovery. The oxidation of organo silicon compounds leads to deposition of organo-Si residue on the surface of the catalyst. These species masks the active sites of the catalyst, which then becomes inaccessible to the reactant, that is the so-called non-selective poisoning and leads to deactivation of the catalyst.

5. Acknowledgements

The authors would like to acknowledge the financial support from Perstorp AB.

6. References

- [1] Gentry, S. J., Jones, A., Poisoning of Catalytic Oxidations I. The Effect of Silicon Vapour on the Gas Phase Oxidation of Methane, Propane, Carbon Monoxide and Hydrogen over Platinum and Palladium Catalysts, *J. Appl. Chem. Biotechnol.* 28, 727 (1978)
- [2] Cullis, C.F., and Willatt, B.M., The Inhibition of Hydrocarbon Oxidation over Supported Precious Metal Catalysts, *J. Catal.* 86, 187 (1984).
- [3] Libanati, C., Ullenius, D.A., and Pereira, C.J., Silica Deactivation of Bead VOC Catalysts, *Appl. Catal. B* 15, 21 (1998).
- [4] Colin, L., Cassuto, A., Ehrhardt, J.J., Ruiz-Lopez, M.F., and Jamois, D., Adsorption and Decomposition of Hexamethyldisiloxane on Platinum: An XPS, UPS and TDS Study.
- [5] Ehrhardt, J.J., Colin, L., and Jamois, D., Poisoning of Platinum Surfaces by Hexamethyldisiloxane (HMDS): Application to Catalytic Methane Sensors, *Sensors and Actuators B* 40, 117 (1997).
- [6] M. Rahmani, M. Sohrabi, O. Augustsson, and M. Sanati, Simulated Pilot Deactivation of Pt/ γ -Al₂O₃ Catalyst: Deactivation by HMDSO in the VOC Total Oxidation, *Proceeding of 53rd Canadian Chemical Engineering Conference*, Hamilton, Canada, 2003.

CO₂ REFORMING OF CH₄ TO SYNGAS (CO/H₂) USING Ni-WC/Al₂O₃ & Ni-CaO/Al₂O₃ CATALYSTS FOR JAMBI GAS FIELD UTILISATION

A. Hanif¹⁾, T. Suhartanto¹⁾ and M.L.H. Green²⁾

¹⁾Pertamina Upstream, 14th Fl. Kwarnas, Jl. Merdeka Timur No.6, Jakarta, Indonesia.

²⁾Wolfson Catalysis Centre, ICL, University of Oxford, South Parks Road, Oxford, U.K

Introduction

The consumption of fossil fuels is set to increase in the immediate future, although alternatives to crude oil will be necessary, since oil depletion is predicted for around 2020. Natural gas is one of the best alternatives, being both cleaner to the environment and available in vast deposits in many areas of the globe. One natural gas reserve is found amongst Indonesia's 16,000 islands, at Jambi, Sumatra (Fig. 1). This is interesting because it is composed predominantly of CO₂ (see Table 1). This stranded field still was undeveloped due to unutilised high CO₂ content. An alternative strategy would be to convert the natural gas mixture to synthesis gas (CO + H₂) by mixture the dry reforming of methane with carbon dioxide and steam reforming of methane using H₂O; the synthesis gas can then be used for the production of a wide variety of chemicals and fuels using gas-to-liquids technology (GTL), e.g. Shell's SMDS.

This has three major advantages compared with the LNG route: i) less separation stages

will be needed; ii) dry reforming is an effective way of incorporating CO₂ in the products, which will eventually end up, for example, as fuel powering an engine; and iii) the cost of gas injection to underground reservoir will be lower, since there will be much less CO₂ remaining after the reforming process. In this study, it will be shown that unpromoted and promoted nickel catalysts are active and stable for methane dry reforming to synthesis gas with high CO₂ content natural gas feedstocks, such as those found at West Jambi Gas Field.

Table 1. Dry composition of the Natuna natural gas field.

Compositions	mol. %
CO ₂	40
CH ₄ + C ₂ + hydrocarbons	59
H ₂ S/ Impurities	0.2
N ₂	0.8



Fig. 1. The location of Jambi gas field in Indonesia.

Experimental

Catalysts were synthesised using the wet impregnation method outlined in detail before and catalyst testing was carried out in a quartz microreactor with on-line product analysis via a Hewlett-Packard 5880A G.C.

Results and Discussion

2% nickel on γ -alumina, WO_3 doped 2% nickel on γ -alumina and CaO doped 8% nickel on magnesia were tested for methane dry reforming, and the results and reaction conditions are shown in Figure 2. It can be seen that all three of the catalysts were stable for the duration of the reactions (approx. 80 h). In addition the reactant conversions and product distributions were very high, close to those predicted by thermodynamic equilibrium; when the reactor temperature was increased, higher conversions and selectivities were achieved as predicted. No coke formation was observed on any of the post-reforming catalysts, indicating that under the conditions used, with excess CO_2 , coke formation may not be a significant problem (as is the case for steam reforming with excess H_2O), although this observation does not exclude very slow coke formation, causing reactor downtime after a period of weeks or months. However, previous work has shown that the addition of WO_3 or alkaline-earth metal oxides, e.g. CaO, to nickel leads to more active, more coke resistant and more stable catalyst materials. Therefore, if long term coke formation is occurring these doped catalysts may be the solution.

Therefore, the application of methane dry reforming for the utilisation of high CO_2 content gas fields is likely to become much more important in the future, and the nickel catalysts tested here appear to be excellent candidates; they are cheaper than the noble metals and more stable than the transition metal carbides, which have also been shown to be active and coke resistant for methane dry reforming and steam reforming.

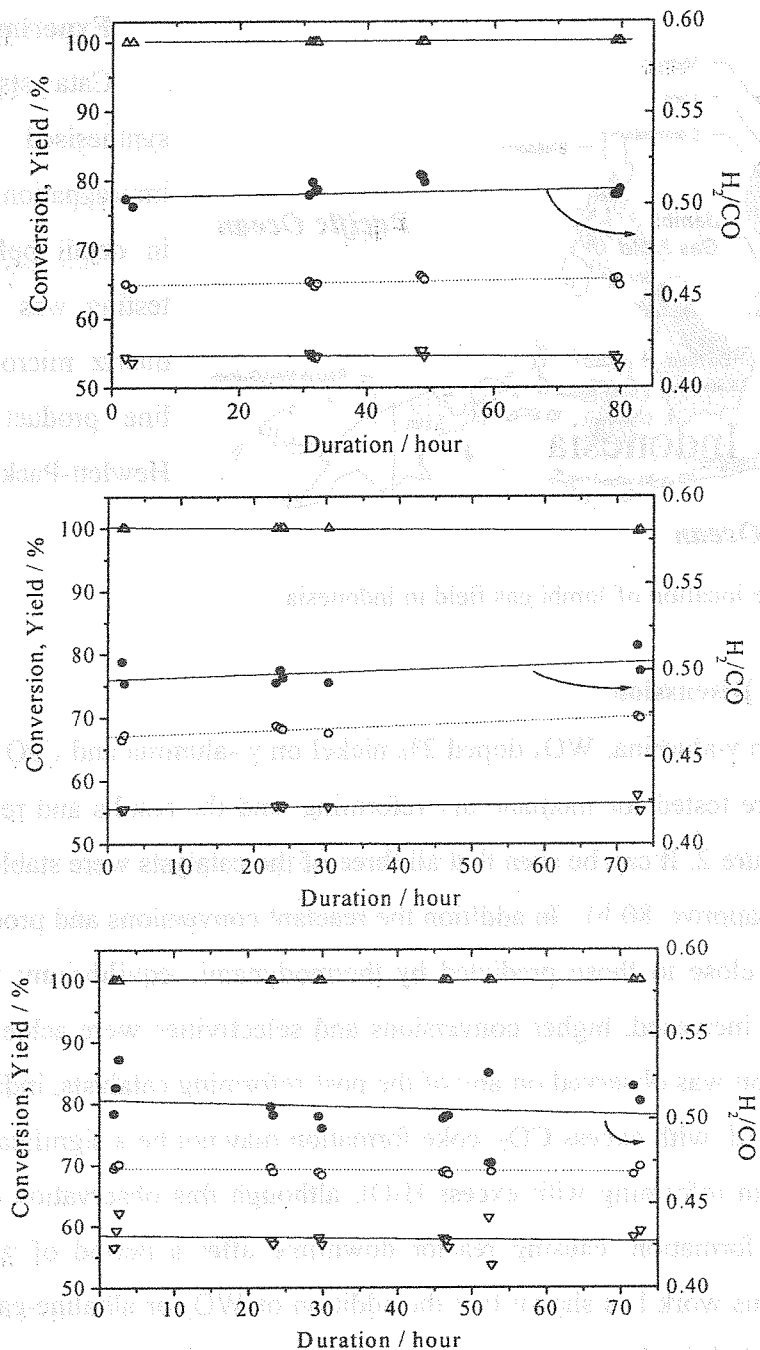


Fig. 2. Methane dry reforming over a) Ni₂Al, b) Ni₂W₂Al, and c) Ni₈Ca₂Mg (CO₂/CH₄ = 2.9, 1123 K, 1 atm., 105 mg catalyst); ∇: C[CO₂]; Δ: C[CH₄]; o: Y[CO]; and ●: H₂/CO.

References

1. A.T. Ashcroft, et al., Nature, 352 (1991) 225;
2. J.R. Røstrup-Nielsen, Cat.Sci.Tech., 5(1994)1.
3. A.P.E. York, et al., Cat. Let. Vol.71, (2001)1;
4. T-C. Xiao, et al, Chem. Phys. 4(18), (2002) 4549
5. A. Hanif, Chem. Mat., 14(3), (2002) 1009.

EFFECT OF SULFUR REMOVAL CATALYST GRANULES PROPERTIES ON THE COMMERCIAL-SCALE BED MACROKINETICS

V.L. Hartmann

JSC Novomoskovsk institute of nitrogen industry

301650, Novomoskovsk, Tula region, Kirov str., 11, niap_sm@novomoskovsk.ru

At present fine natural gas purification from H₂S and small amounts of other sulphur compounds occurs via its irreversible reaction with granules of high surface area zinc oxide



The process is usually carried out at operating pressure within the range of 1 ÷ 45 atm, temperatures within the range of 260 ÷ 395°C and space velocities within the range of 600 ÷ 2000 h⁻¹. The integral average total content of sulfur amounts now at different plants from 0 up to 40 ppm, and maximal reaches up to 50 ppm. Maximum permissible sulfur content in the purified gas varies within the range of 0.1 ÷ 0.5 ppm.

Two key features distinguishing sulfur absorption from steady catalytic processes are:

1) basic nonstationarity

Each reaction (1) run, in addition to realization of objective – sulfur removal from a gas phase, – irreversibly reduces protective action of an absorbent bed.

2) Multilevel structure

Reaction fronts in gas and solid phases simultaneously and interdependently move through the bed, granules and particles of ZnO. Hydrogen sulphide diffuses through granule pores to a surface of particles aggregates, then through intercrystalline gaps (flat dislocations) in primary particles sulfur reaches crystallites surfaces, whence its diffusion into a crystallite begins. Oxygen, first as atoms, and through pores as part of H₂O, makes the same path in the opposite direction.

It has been shown in [1], that the adjoint problem of modelling the reaction between minor admixture of H₂S in gas and the bed of porous granules of ZnO (accepting first order of reaction rate with respect to H₂S content) can be separated into two independent ones: the expression for local reaction rate in the absorbent bed is determined by the analysis of absorbed sulfur front movement through a granule in a quasistationary approximation within

the framework of shrinking core model (fig. 1), and then used in the sulfur fronts movement problem through gas phase and absorbent bed. It should be noted, that the second problem in the simplest case is reduced to the set of two differential partial equations of hyperbolic type with nonlinear right members.

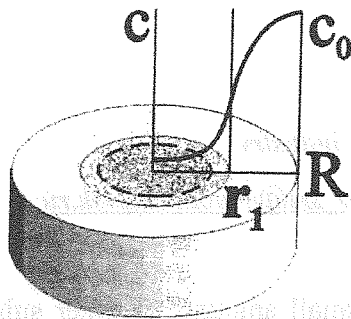


Fig. 1. Distribution of sulfur admixture in pores of partially sulphurated granule. c – H_2S content in gas phase inside a granule; c_0 – H_2S content in gas phase at a granule surface; R – granule radius; r_1 – core radius.

On the one hand, it was found that this problem has the solution in quadratures. On the other hand, it turns out to be possible to introduce a variable efficiency factor of reaction inside a granule, related to pore-diffusion resistance in its pores. The pattern of this factor dependence on the local value of ZnO to ZnS conversion level, namely, its approximate constancy over a wide range of conversion level values, allows to use Bohart-Hinshelwood model [2, 3] to analyse and predict sulfur absorbers operation.

In this model the set of equations describing an absorbent bed behaviour has the explicit analytical solution, and for such important process variables as the rate $\bar{\alpha}$ of use of an overall sulfur pick-up of loading and a time t_{br} of loading run before breakthrough of maximum permissible content of hydrogen sulphide at the unit outlet, as well as for some others, simple analytical expressions were obtained:

$$\bar{\alpha} = 1 - \frac{V}{Q} \ln \left(\frac{c_0}{c_1} - 1 \right),$$

$$t_{np} = \frac{P_0}{\bar{\alpha} V},$$

characteristic width of absorbed sulfur front

$$\Delta x = 4uQ^{-1} = 4LVQ^{-1},$$

where \bar{c}_0 – the integral average inlet gas sulfur content; c_0 – the instantaneous inlet sulfur gas sulfur content; V – space velocity; Q – dynamic characteristic of absorbent; P_0 – overall sulfur pick-up per unit bed volume; L – bed length. For the most of known up-to-date sulfur removal catalysts (except 1 - 2 brands), Q values (at NTP) amount to $7500 \div 8000 \text{ h}^{-1}$ (7800 h^{-1} for

NIAP-02-05 [4]). Then for a sulfur removal unit of 1360 tonnes per day ammonia plant ($V = 600 \text{ h}^{-1}$) the absorbed sulfur front width Δx (height of mass transfer zone) amounts to $\approx 30\%$

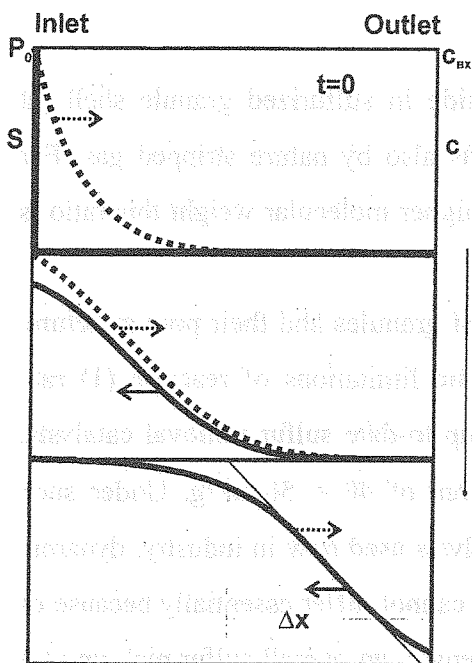


Fig. 2. Sulfur distribution profiles in absorbent bed.

of the total absorbent bed length. The rate of the absorbed sulfur front movement for such a unit under usual up-to-date conditions has the order of magnitude of millimeters per day.

It needs to be emphasized, that thus obtained estimations of sulfur removal catalyst run and the rate of use of the bed overall sulfur pick-up are inferior.

Distribution profiles (fronts) of sulfur in a gas flow and absorbent bed are shown on fig. 2.

The described above approach to prediction of sulfur absorption unit operation has been approved when calculating the costeffective loading of the sulfur removal unit together with the specialists of JSC "Metafraks" (Gubakha) and ICI Syntetix

during its realization for the methanol M-750 plant [5].

Taking into account the structure of local reaction (1) rate under the conditions of a pore-diffusion resistance in a granule, and also characteristic values of such parameters of an absorbent as the ratio of fresh and sulphurated absorbent diffusivities and characteristic ZnS front width in a granule, allows to receive approximate expression for such basic integrated process variable of the apparatus of a sulfur absorption, as the rate $\bar{\alpha}$ of use of the loading overall sulfur pick-up, containing, in addition to above mentioned parameters, an effective size R of absorbent granules, an effective diffusivity $D_s^{*(1)}$ (at normal pressure) of hydrogen sulphide in sulfurized granule shell and operating pressure P (atm) in the sulfur absorber:

$$\bar{\alpha} \approx 1 - \frac{R^2 V^{(1)}}{10 D_s^{*(1)}} \left(1 + \frac{0.22}{\sqrt{P}} \right) \ln \left(\frac{c_0}{c_1} - 1 \right) \quad (2)$$

The effective diffusivity in a porous solid essentially depends on parameters of the pore structure. When zinc oxide is converted to sulphide then molar volume increases almost 1.7 folds and it results in appreciable decrease of porosity. Dependence between porosity θ_0 of a fresh absorbent and θ_s – of sulfurized one, can be seen from the following expression

$$1 - \theta_s = 4.2(1 - \theta_0)S$$

where S – sulfur pick-up (per unit mass). Using values $\theta_o = 0.5$ and $S = 0.32$ (typical ones for up-to-date absorbents), we receive $\theta_s = 0.32$. At $\theta_o = 0.26$ $\theta_s = 0$, i.e. pores are completely closed, and the granule does not absorb any more.

Value of an effective diffusivity of hydrogen sulphide in sulfurized granule shell (at normal pressure), in addition to a pore structure, depends also by nature stripped gas. For methane it is 1.3 times less than for H_2 , and for gases of higher molecular weight this ratio is even greater.

Thus, unit dynamics is mainly determined by a size of granules and their pore structure. Certainly, it can take place only in the absence of kinetic limitations of reaction (1) rate which is ensured with the production techniques of the up-to-date sulfur removal catalysts, permitting to obtain active zinc oxide with a surface area of $40 \div 50 \text{ m}^2/\text{g}$. Under such condition which is met by the most of sulfur removal catalysts used now in industry, dynamic characteristics of absorbents from different manufacturers cannot differ essentially because of the restrictions superimposed by necessary mechanical strength, an overall sulfur pick-up of a bed unit volume and pressure drop across the absorbent bed, especially at low pressures.

On the other hand, if the value of effective diffusivity is obtained through data interpretation of H_2S sorbtion by ZnO granules, the expression (2) allows to estimate dynamic properties of an absorbent in certain range of granule sizes and operating conditions.

References

1. Hartmann V.L., Danzig G.A., Kondrashchenko T.A., Grigor'eva T.P. // Studies of catalysts for ammonia production: Tr. GIAP-M., 1985. - pp 85 - 95.
2. Bohart G.S., Adams E.Q, J. Am. Chem. Soc., 42, 523 (1920).
3. Danby C.J., Davoud J.G., Everett D.H., Hinshelwood C.N, Lodge R.M.//J. Chem. Soc. - 1946. - pp 918-934.
4. TU 113-03-2002-86.
5. Daut V.A., Hartmann V.L., Konovalov S.J., Tararyshkin M.V., Obysov A.V., Beskov V.S., Golosman E.Z. // Khim. Prom. - 2000. - #10. - pp 507-511.

MODELLING OF H₂/D₂ EXCHANGE OVER Pd**H. Backman, K. Rahkamaa-Tolonen, J. Wärnä, T. Salmi, D.Yu. Murzin***Laboratory of Industrial Chemistry, Process Chemistry Center, Åbo Akademi, FIN-20500**Åbo, Finland, Fax: +358-2-2154479, E-mail: Henrik.Backman@abo.fi***Introduction**

The interaction of hydrogen with metal surfaces is a fundamental problem of surface science. Because of its apparent simplicity the investigation of hydrogen adsorption on metal surfaces has regained experimental interest with respect to both the dissociation behaviour and the atomic adsorption properties. In environmental catalysis, the main issue is to optimize catalytic converters to remove pollutants. A detailed understanding of the kinetic processes taking place simultaneously and interactively is therefore needed. Isotope-labelled reactants are therefore used to follow reaction pathways and to determine reaction mechanism. Steady-state isotopic transient kinetic analysis involves replacement of a reactant by its isotopically labelled counterpart in the form of a step or pulse input function. In the present work, deuterium step changes have been utilised to trace the hydrogen reaction pathways over Pd-alumina, as it eventually can help in developing a fundamental understanding of the role of hydrogen in the reduction of NO.

Experimental

The methods of preparation of the described catalyst and experimental setup have been reported by Rahkamaa-Tolonen et.al¹. The isotopic exchange between hydrogen and deuterium was studied using isotopic changes between 1% H₂/Ar and 1% D₂/Ar. A split of the product flow was taken through a capillary to a quadrupole mass spectrometer. Experiments with D₂ and H₂O were also performed to determine the deuterium exchange with hydrogen in water.

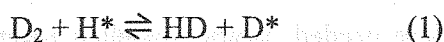
Result and discussion

In the experiment hydrogen was initially pre-adsorbed on the surface. When D₂-atoms reach the catalyst surface, the isotopic exchange takes place with adsorbed hydrogen atoms, and formation of HD was immediately observed. The production of water was observed in the first and last step of the experiment, which can be attributed to the reaction of chemisorbed H*-atoms and OH-groups present in the alumina support. Small amounts of HDO and D₂O

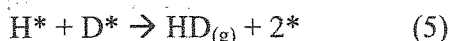
could be observed during the second stage of the experiment. To clarify the reaction mechanism for the isotope exchange between water and deuterium experiments were performed with H_2O and D_2 . Once water entered the reactor dissociation took place and the isotopic products HDO , D_2O and HD started to form.

The transient step-responses were described quantitatively with a dynamic plug flow model. Adsorption, surface reaction and desorption steps, as well as isotopic exchange steps were included in the model. The gas phase components and surface intermediates were described with separate mass balances. The kinetic parameters were determined with non-linear regression analysis. Several mechanistic models were tested taking into account the adsorption and dissociation of hydrogen. An adsorption-assisted-desorption mechanism for the H_2/D_2 -exchange was also included in the isotope exchange mechanism.

The mechanism best describing the H_2/D_2 reaction on Pd was a mechanism where reaction takes place between a molecule and a chemisorbed atom forming HD:



When more vacant sites are available, D_2 dissociates and react further with the H^* atoms according to the following reactionsⁱⁱ:



This result is in agreement with previous experiments, which demonstrated that hydrogen is adsorbed dissociatively on palladiumⁱⁱⁱ. The estimated equilibrium constant for the reaction $\text{H}_2 + \text{D}_2 \rightleftharpoons 2\text{HD}$ is 3.15 which is close to the theoretical equilibrium constant, 3.54^{iv} at 155°C .

Modelling and parameter estimation for the $\text{D}_2 + \text{H}_2\text{O}$ reaction was also done. In this reaction the adsorption-assisted-desorption between H_2^* and D_2 had to be taken into account to achieve a good fit to the experimental data. This could lead to the conclusion that adsorption-assisted-desorption only plays a minor role in the H_2/D_2 -exchange but have to be considered in the reaction between deuterium and water. The comparison between experimental data and modelled simulations for the H_2/D_2 -exchange is presented in Figure 1. Figure 2 displays the fit of the $\text{D}_2 + \text{H}_2\text{O}$ -reaction to the experimental data. As can be seen the proposed model is able to describe the transient behaviour of the system.

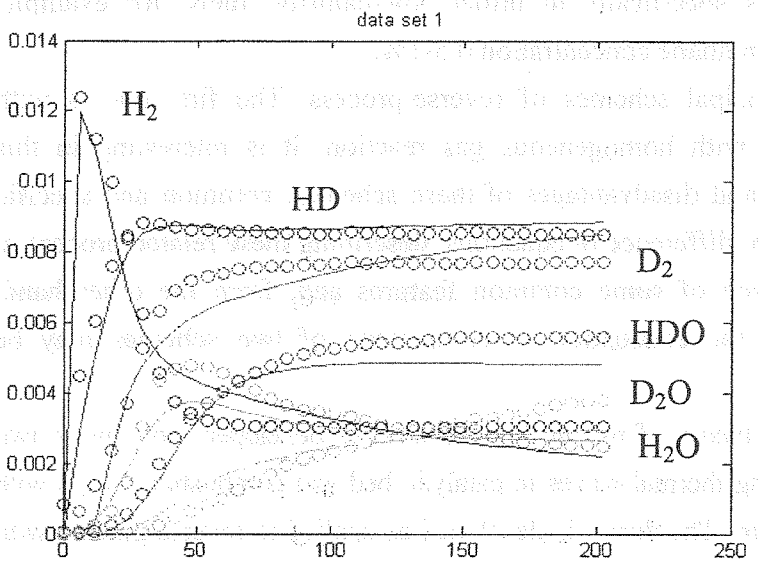
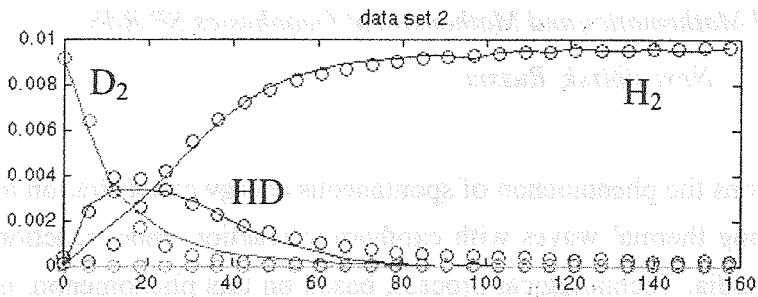
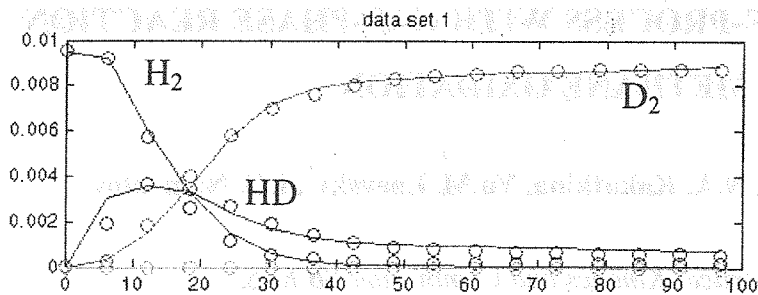


Figure 1. H₂/D₂-exchange on Pd/alumina. Comparison between experimental data (symbols) and calculations (curves). The degree of explanation is 99.3%.

Figure 2. D₂+H₂O on Pd/alumina. Comparison between experimental data (symbols) and calculations (curves). Degree of explanation ca 93%.

ⁱRahkamaa-Tolonen, K, Salmi, T., Murzin, D.Yu., Barreto Dillon, L., Karhu, H., Keiski R.L & Väyrynen, *J. of Cata.* 210(1), 17-29, 2002

ⁱⁱ Miyamoto, S-I., Sakka, T., Iwasaki, M., *Can. J. Chem.* 67, 857-861

ⁱⁱⁱ Miyazaki, E., 1980, *J. Catal.* 65, 84-94

^{iv} Bond, G.C. "Catalysis by Metals", Academic Press, London, 1962

ASPECTS OF REVERSE-PROCESS WITH GAS-PHASE REACTION FOR METHANE OXIDATION

V.S. Babkin, V.A. Bunev, N.A. Kakutkina, Yu.M. Laevsky¹, I.G. Namyatov

Institute of Chemical Kinetics and Combustion SB RAS,

¹*Institute of Computational Mathematics and Mathematical Geophysics SB RAS,*

Novosibirsk, Russia

There is under certain conditions the phenomenon of spontaneous energy concentration in chemical reaction zone of travelling thermal waves with exothermic reaction under reaction gas mixture filtration in porous media. Technological process, based on this phenomenon, is named reverse-process. It allows specifically to utilize low-calorific fuels, for example, venting gases of coal mines with methane concentration 0.5-1%.

There are possible two principal schemes of reverse-process. The first one is with catalytic reaction and the other with homogeneous gas reaction. It is interesting in this connection to reveal advantages and disadvantages of these schemes, common and specific features of the processes. Marginal difference in equations, describing these related processes, allows us to assume the existence of some common features and, from the other hand, specifics in the schemes. Thus the conception of comparison of two schemes may be informative and useful.

In this connection qualitative theory of hybrid thermal wave is developed, combining two types of wave processes – travelling thermal waves in catalytic bed and combustion waves with gas reaction in inert porous medium. The theory is developed as applied to reverse-process with operating parameters in transition region. In this region surface and volume reactions proceed simultaneously. The theory allows us to analyze an influence of controlling parameters on main characteristics of thermal wave, to predict regime transitions, to study unsteady-state effects. It is shown that theoretical and experimental results are in a good agreement.

Normal mode of reverse-process operating implies regular repetition of characteristics of temperature, concentration, and velocity fields. In other words, any disturbances, unsteady-state deviation in half-cycle of reverse-process have to be compensated in the following half-cycle. Otherwise one can expect failure of normal mode. In this connection the analysis of hydrodynamic, thermal-diffusion and gravitational flame instability has been done under filtration combustion with homogeneous gas reaction. There was shown the principal possibility of such types of instability in experiments. The analysis of parameters, determining flame front instability, has been carried out. It is assumed that in reverse-process some types of instability are compensated at changing of flow direction. As far as instability of wave front with catalytic reaction is concerned, there is not enough data on this question.

Optimal operating regimes of reverse-process depend on many factors. One of the most important among them is process thermal efficiency. It is determined by the value $\Delta T/\Delta T_{ad}$, where ΔT_{ad} is adiabatic heating-up. The theory of filtration combustion shows that thermal efficiency at equality of heat capacity fluxes of solid and gas phases tends to infinity. Of course this situation is not real, for example due to heat losses. It is darkly for the time present what is the reality at parameter values tending to the critical condition. Experiment shows that the combustion wave structure can change in these conditions.

In frame of conception of comparison of two reverse-process schemes it is interesting to compare global kinetic parameters for catalytic and homogeneous gas reactions. These parameters determine which of two schemes takes place in practice. The comparison of methane oxidation rates in catalytic and homogeneous gas reaction shows that rates are comparable at temperature close to 1000 K. At the same time appreciable scatter of data on global kinetic parameters for homogeneous gas reaction was displayed in data of different authors. Data analysis shows that the scatter of data is due to not only by error of measurement, but mainly by changing of global kinetic parameters at reaction path changing. In particular if initial temperature changes proportional to the distance (the model of reverse-process), then ignition temperature increases and ignition delay decreases at temperature gradient rise. The same tendency is observed under increasing of gas mixture flow rate. In other words, methane oxidation rates, determined for the same methane oxidation mechanism, with different temperature increasing ways, are different.

Taking into account this circumstance, values of global kinetic parameters were selected from the array of literature data based on the principle of maximum variety of chemical reaction conditions. Among them are isothermal and nonisothermal (with temperature gradient) conditions, conditions close to reverse-process (inverse problem of propagation of filtration combustion wave), laminar and turbulent flame conditions and others. As a result of such selection there was obtained the following expression for methane oxidation rate in a range of methane concentration 0.5-1.5 % and temperature range 800-2000K

$$W=1.2 \cdot 10^{10} [\text{CH}_4] \exp(-50000/RT), (\text{mol}/\text{cm}^3\text{s}).$$

The work was partially supported by EC Commission within the Program INCO Copernicus – 2 (contract ICA-2-CT-2000-10035)

References

1. V.S. Babkin, I. Wierzba, G.A. Karim. The phenomenon of energy concentration in combustion waves and its applications. Chem. Eng. J., 2003, v. 91, pp. 279-285.
2. Yu.M. Laevsky, V.S. Babkin, On the theory of traveling hybrid wave. Combust. Sci. and Tech., 2001, v. 164, pp. 129-144.
3. V.S. Babkin, Yu.M. Laevsky, Z.R. Ismagilov. Travelling waves of filtration combustion with homogeneous-heterogeneous reaction. Proc. of the 1st Intern. Conf. on Application of Porous Media. Eds: R. Bennacer and A.A.Mohammad, 2002, Jerba, Tunisia, pp. 643-654.
4. V.S. Babkin, V.A. Bunev, V.I. Gritzan. Problems of fire and explosion safety in context of sustainable development. J. Phys. IV France, 2002, v. 12, pp. 413-421.

**COMPLETE ABATEMENT OF ANILINE AND PHENOL IN
WASTEWATER IN THE PRESENCE OF CARBON CATALYSTS BY AIR
OXIDATION AND ADSORPTIVE-CATALYTIC OXIDATION IN
LIQUID PHASE**

N.M. Dobrynkin, M.V. Batygina & A.S. Noskov

Boreskov Institute of Catalysis of Siberian Branch of Russian Academy of Sciences,

Pr. Ak. Lavrentieva, 5, Novosibirsk-90, 630090, RUSSIA

Phone: (+7)-3832-34 44 91 Fax: (+ 7)-3832-341878, E-mail: dbn@catalysis.nsk.su

This paper is devoted to development of carbon catalysts and application of catalytic wet air oxidation for deep cleaning of polluted waters. According to experimental data graphitized carbon, Ru-CeO₂/carbon and Ru/carbon are the most highly-effective solid catalysts in catalytic wet air oxidation of aniline and phenol at elevated pressures and temperatures (T=160 – 200 °C, P_{total} = 1.0 - 3.0 MPa). Use of carbon both an adsorbent and the catalyst simultaneously let us [1] possibility to offer new purification processes of fluids by use carbon catalyst - adsorbent in a non-stationary mode. The method based on the adsorption of pollutants at a catalytically active porous material (CAPM) and regeneration of CAPM in medium of cleaned fluid in the same reactor in that a layer of CAPM by simultaneous rise of pressure and temperature. As CAPM we tested various types of commercial graphite-like materials Sibunit with different physico-chemical properties [2].

Introduction

The creation of systems for wastewater treatment and a reuse of water resources is one of technological priorities now. The most expedient way for the treatment of typical wastewater is the Catalytic Wet Air Oxidation (CWAO) - the oxidation in a liquid phase at the elevated temperatures and pressures with the use of specially designed solid catalysts. WAO of dissolved toxic substances is widely investigated in the presence of different catalysts and as a rule it is used for oxidation of pollutant's molecules into bio-degradable compounds. Thus the similar processes are usually carried out in steady conditions. Accordingly our previous data [2-5] graphite-like carbon and Ru/graphite-like carbon were shown to be effective as in the complete oxidation of the carbon chain of variety compounds, both in nitrogen- and sulfur-containing molecules.

Experimental

The experiments performed in a batch reactor [4] have shown a principal capability simultaneously to use CAPM as adsorbent and either as catalyst, or as a catalyst support for oxidation of aniline and phenol. Thus there is a capability to realize an adsorption, regeneration and oxidation, by means of combination of them carried out in solution of cleaned fluid. So for aniline and phenol adsorption on carbon catalysts at room temperature there is a decrease of concentrations of these substances on 74 % and 92% accordingly. The further temperature rise with simultaneous oxygen supply results in oxidation both of adsorbed and desorbed species on a surface of CAPM.

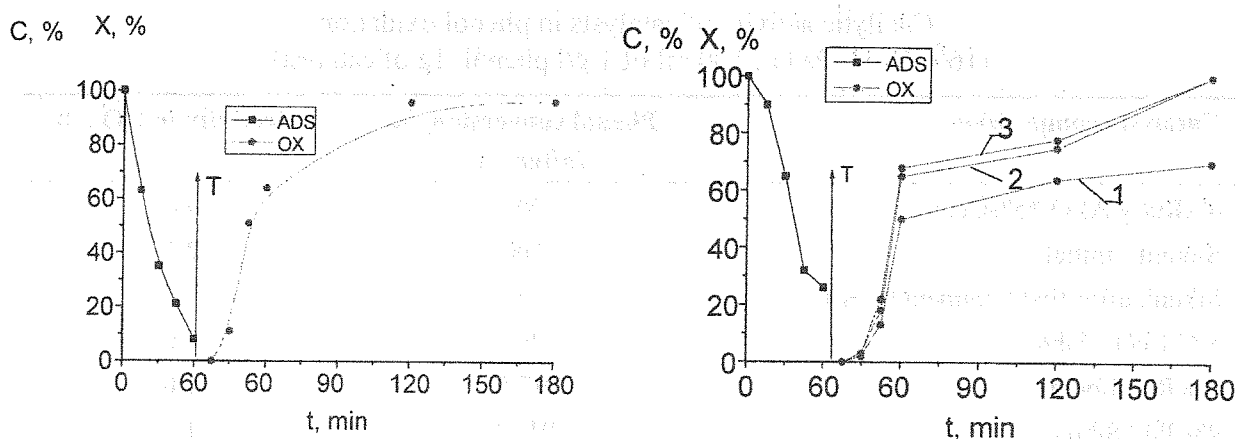


Fig. 1-2. The oxidation of phenol (Fig.1) and aniline (Fig. 2) on CAPM Sibunit-4 (1, 2, 3 – three recycle adsorptive – catalytic operations).

Periodic mode of operation:

Time: 0-60 min - mode of an adsorption,

60 min - increasing of the temperature and pressure, supply of oxygen,

60 - 180 min - the oxidation mode

At periodic realization of process it results in a 96.4% degree of cleaning of water solutions with initial concentration of aniline of 1.00 g/l. The further experiments have shown the activation of catalyst (the level of purification is achieved 99, 99 %) starting from the second cycle. The special methods of an activation of carbon catalyst allow: a) to decrease the reaction temperature from 200°C to 160°C, and b) to increase the activity of carbon up to values comparable with activity of Ru/carbon catalyst (Tables 1, 3). Full cleaning (more than 99, 99) is possible at continuous realization of process in unsteady conditions. The experimental results indicate that there is another way for mount to high level of cleaning solutions by use two-stage process. So, design of more active catalytic systems allow to oxidize aniline and phenol almost completely at 160 °C (Tables 2, 3) in wet air oxidation process, that is applicable for sharp abatement of pollutants concentration at first stage and use catalytic - adsorptive technique for further deep cleaning of the solutions at second stage.

Table 1

Catalytic activity of Sibunit-4 in Aniline and phenol wet air oxidation
(1 M Pa O₂, 100 ml of 1 g/l aniline, 1g catalyst)

Aniline oxidation				
Catalyst	Temperature, °C	Reaction time, h	Conversion, %	Selectivity to N ₂ , %
Sibunit - 4	200	3	40	100
Sibunit - 4 (activated)	160	3	56	90

Table 2

Catalytic activity of catalysts in phenol oxidation
(160 °C, 1MPa O₂, 100 ml of 1 g/l phenol, 1g of catalyst).

Catalysts composition	Phenol conversion, % (after 3 h)	Selectivity to CO ₂ , %
4%Ru/(γ-Al ₂ O ₃ *5%CeO ₂)	99	22
Sibunit - initial	100	2.3
Sibunit after first treatment by H ₂ O ₂	99	8
5 % CeO ₂ / Sibunit	99	1.0
5% Ru/ Sibunit	97.5	1.0
4% Pd / Sibunit	91-95	1.0
4.2% Pt/ Sibunit	100	19.6
5.3% Pt/ Sibunit	100	100
(0.5% Ru+ 5 % CeO ₂)/ Sibunit	100	53.3
(0.4% Ru+ 5 % CeO ₂)/ Sibunit	100	70.4
(0.5% Ru+ 3 % CeO ₂)/ Sibunit	100	60.8
(0.6% Ru+ 5 % CeO ₂)/ Sibunit	100	96.3
(0.3 % Ru +0.3 % Pt)/ Sibunit	100	64.3

Table 3.

Catalytic activity of Ru- supported catalysts in Aniline wet air oxidation
(1 M Pa O₂, 100 ml of 1 g/l aniline, 1g catalyst)

Catalyst	T, °C	Conversion, %	Selectivity to CO ₂ , %
5% Ru/Sibunit-4	200	71	13
5% Ru/Sibunit-4 (after H ₂ O ₂ activation)	160	78	31
4% Ru/γ-Al ₂ O ₃ +5%CeO ₂	200	75	53
4% Pd/ Sibunit	200	100	2
(0.4% Ru +5%CeO ₂)/Sibunit	160	98	100
(0.6% Ru +5%CeO ₂)/ Sibunit	160	98	49
(0.6% Ru +4%CeO ₂)/ Sibunit	160	99	66
(0.6% Ru +8%CeO ₂)/ Sibunit	160	99	69

Summary

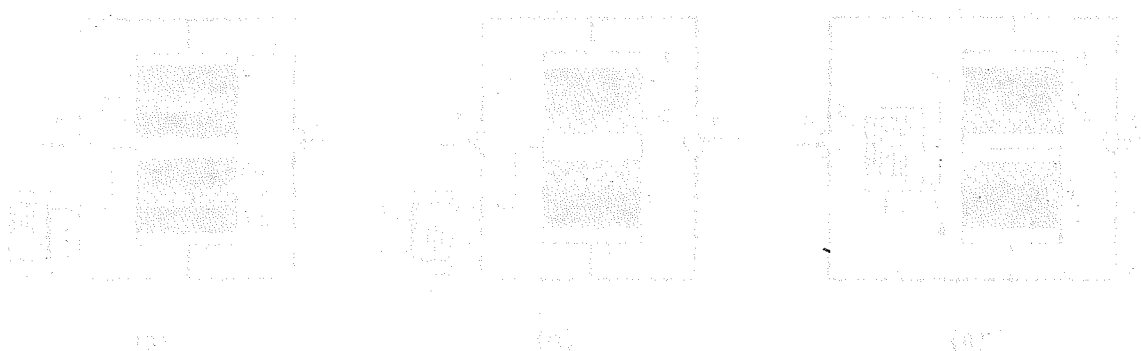
The described catalysts and method are solving the problem of development environmentally reliable method for fluids treatment and allow carrying out the adsorption of pollutants on carbon CAPM with following regeneration of the CAPM without the loss of adsorptive qualities. The experiments have shown a principal capability simultaneously to use carbon CAPM as adsorbent and either as catalyst, or as a catalyst support for oxidation of aniline and phenol in water solutions.

Acknowledgement

This study is financial supported partly by the INTAS within the project INTAS-00-129. The support is gratefully acknowledged. Special thanks are due to Viktor Korotkikh and Dmitrii Shljapin for technical assistance.

References:

- [1] Dobrynkin N.M., Noskov A.S., Batygina M.V. Method of Purification of Liquids and Device for Carrying It out. // Russian Patent № 2176618.
- [2]. Bal'zhinimaev B.S., Batygina M.V., Dobrynkin N.M., Likholobov V.A., Noskov A.S., et.al. Heterogeneous Catalytic Oxidation of Sodium Sulfide // 12TH INTERNATIONAL CONGRESS ON CATALYSIS, Recent Reports of the 12thICC, Granada, Spain, July 9–14, 2000. CD-ROM, RR035.
- [3] Batygina M. V., Dobrynkin N. M., Noskov A. S. Study of carbon catalysts in liquid phase oxidation of water contaminants by oxygen.// 15th International Congress of Chemical and Process Engineering CHISA 2002. Prague, Czech Republic, 25- 29 August 2002, -P1.68. P.203-204.
- [4] Batygina M.V., Dobrynkin N.M., and Noskov A.S. Advances Environ. Res. J., 2000, vol. 4, p.123-132.
- [5]. Dobrynkin N.M., Pestunova O.P., Batygina M.V., Noskov A.S., Parmon V.N. The study of aniline and phenol liquid phase oxidation in the presence of solid catalysts. // VI Conference "Mechanisms of Catalytic Reactions" (MCR-VI), Moscow, Russia, October 1-5, 2002.



THEORETICAL AND EXPERIMENTAL STUDY OF METHANE VENT-GASES UTILIZATION FOR HIGH-TEMPERATURE HEAT PRODUCTION IN UNSTEADY-STATE OPERATION

A.S. Noskov^{a)}, N.A. Chumakova^{a)}, O.P. Klenov^{a)}, P.G. Tsyrunnikov^{b)},
V.N. Korotkikh^{a)}, V.I. Drobyshevich^{c)}, L.V. Yausheva^{c)}

^{a)}*Boreshkov Institute of Catalysis, 630090 Novosibirsk, Russia,*

^{b)}*Omsk Department of Boreshkov Institute of Catalysis, 644040 Omsk, Russia,*

^{c)}*Institute of Computational Mathematics and Mathematical Geophysics,
630090 Novosibirsk, Russia*

First suggestion to use the periodic reversals of gaseous reaction mixture flow in a catalytic fixed bed with a view of high-temperature heat production was done in [1] (see Fig. 1a). The subsequent studies on the matter have brought to light a number of technical difficulties in the process realization. First of all, that concerns the periodic changes of the flow direction of the hot gaseous mixture in the heat-exchange apparatus – boiler-utilizer (position 5, Fig. 1a). The higher the maximal temperature in the catalytic fixed bed, the better is the heat utilization efficiency. Nevertheless, the industrial catalysts have a long service life only if they are used at temperatures below 800-850°C. That restricts the range of organic compounds concentrations in the reaction mixture to be processed with the aim of the reaction heat utilization without catalyst overheating. These problems demanded further development of the technique mentioned above. Some new results are presented in the report.

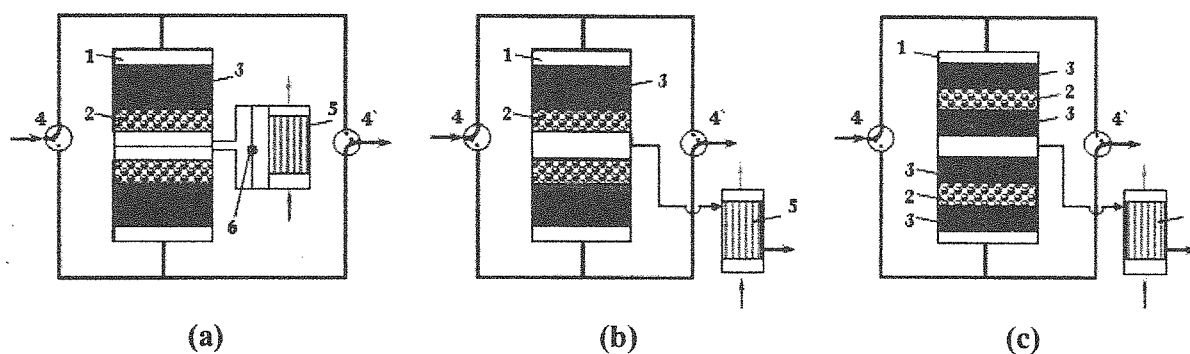


Figure 1. Reverse-process flowsheets with the reaction heat utilization: 1 – reactor, 2 – catalyst fixed bed, 3 – fixed bed of inert particles, 4 and 4' – valves, 5 – heat exchanger, 6 – by-pass with a flow regulator.

In the reverse-process corresponding to the scheme 2 (Fig. 1b), a part of the hot gas stream is directed from the high-temperature central zone of the reactor into a heat exchanger and after that passed to atmosphere. The rest stream goes through the reactor and the second catalyst fixed bed as in a conventional reverse-process. In contrast to the scheme 1 (Fig. 1a), in that case the stream route and the hot gas flow rate in the heat exchanger are invariable in time.

To avoid the catalyst being at rather high temperatures, we consider the scheme 3 shown in Fig. 1c. According to this scheme, the catalyst in the central part of the fixed beds is replaced with the inert material, while the smaller catalyst beds serve to activate the compounds oxidation process and operate at the temperatures up to 700°C. In the central fixed beds of inert material the homogeneous oxidation of organic compounds occurs and the temperature is 700-950°C.

In our study the theoretical analysis of the flow sheets 1b and 1c has been done by means of mathematical modeling under the assumptions of the well known two-phase mathematical model of the heat and mass transfer processes in a fixed bed of catalyst or inert material. Considering the scheme 1b we used the kinetic parameters of methane oxidation on the Pd catalyst. In the technological scheme 1c, the data of methane oxidation over the Mn-oxide catalyst were in service. Modeling of homogeneous methane oxidation in the central fixed beds of inert material was based on the kinetic data obtained by V.S. Salnikov.

In the report a detailed parametric survey of the influence of different control parameters on the heat utilization efficiency is presented. Namely, we considered inlet methane concentration (above 0.3 vol.%), catalyst and inert particles sizes, lengths of catalytic and inert fixed beds, gas flow velocity. The study of the process operation stability in dependence of inlet methane concentration and degree of the reaction heat utilization has been done.

The experimental study of catalytic oxidation of low-concentrated methane-air mixture in a pilot scale unit corresponding to the scheme 2 has shown the feasibility of the method developed. The experimental and theoretical results are in a good agreement.

The study was performed under financial support of European Commission in the framework of the programme INCO-2 (contract No. ICA2-CT-2000-10035) and aimed at utilizing the methane content of vent air from coal mines for high temperature energy production and simultaneously to convert the greenhouse methane to less harmful compounds.

Reference:

1. RU Patent No. 1160201, 1985.

The first part of the report is devoted to a description of the...
...the...
...the...
...the...
...the...

The second part of the report is devoted to a description of the...
...the...
...the...
...the...
...the...

The third part of the report is devoted to a description of the...
...the...
...the...
...the...
...the...

The fourth part of the report is devoted to a description of the...
...the...
...the...
...the...
...the...

The fifth part of the report is devoted to a description of the...
...the...
...the...
...the...
...the...

The sixth part of the report is devoted to a description of the...
...the...
...the...
...the...
...the...

The seventh part of the report is devoted to a description of the...
...the...
...the...
...the...
...the...

POSTER PRESENTATIONS

WOLFE MITTELSTADT



METHANOL DECOMPOSITION IN THE MICROREACTOR WITH DIRECT RESISTANCE HEATING AND A MASSIVE COPPER CATALYST

D.V. Andreev, L.L. Makarshin and V.N. Parmon

Borshkov Institute of Catalysis, Prosp. Ak. Lavrentieva, 5, 630090 Novosibirsk, Russia

fax: +7-3832-34-30-56; e-mail: makarshin@catalysis.nsk.su

Introduction

Microreactors are promising facilities for production of hydrogen to be used, for example, in fuel cells [1]. In conventional reactors for endothermic catalytic processes, heat is supplied to the catalyst bed from the heated reactor walls due to the heat radiation from the walls, convection and heat conductivity of the bed. There are obvious fundamental limitations on the maximal heat flux density under these conditions that cause insufficient energy release on the catalyst surface to complete the endothermic reaction [2].

Comparison between direct resistance and external heating

Experimental studies of the endothermic reaction of methanol dehydrogenation were aimed at comparison of the efficiency of direct resistance heating of the catalyst bed against the external heat supply. A thin quartz tube (1.4 mm internal diameter, 28 cm length) with a copper wire coil (1 mm diameter, 4.5 cm length, made from copper wire of 0.1 mm in diameter) as a catalyst in the inside was used as the reactor. Current leads were made of stainless steel. A cylindrical furnace was used for external heating of the quartz tube. The direct resistance heating was achieved by passing electric current through the copper coil. The temperature was controlled using a thermocouple mounted on the outer surface of the tube and, additionally, by measuring resistance of the heat-evolving copper coil. Reactants (a mixture of argon and methanol vapor, volume ratio 4:1) were fed at the flow rate of 5 ml/min. Concentration of hydrogen was measured by gas chromatograph.

The yield of hydrogen as a function of temperature during methanol dehydrogenation on the copper coil is shown in Fig. 1. The reaction is seen to start at a 50°C lower temperature in the case of direct heating by electric current passed through the coil than in the case of external heating, hysteresis being observed in the former case with hydrogen evolved in a

higher amount at the same temperature during cooling (Fig. 1). Therefore, the yield of hydrogen depends on the procedure used for the catalyst heating and cooling.

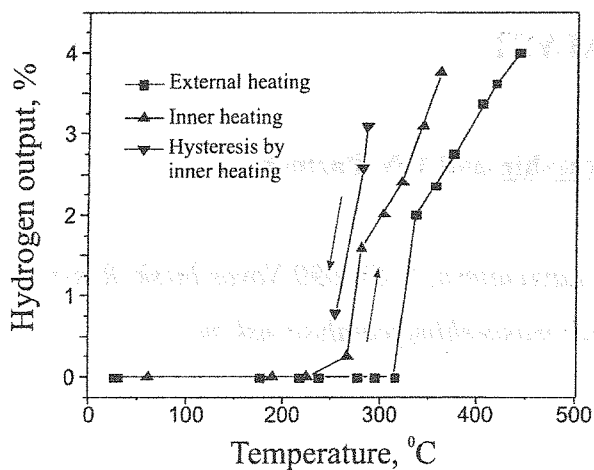


Fig. 1. The H_2 yield vs. temperature during methanol decomposition on the copper coil

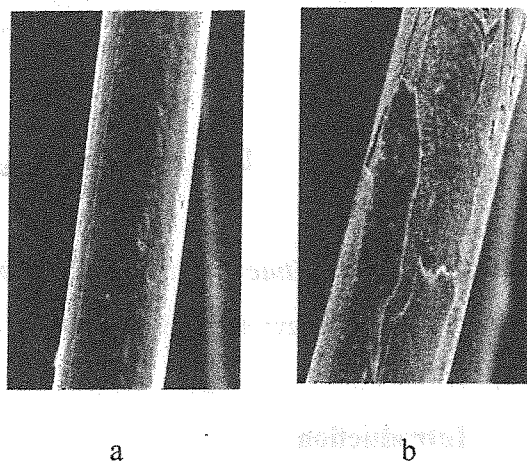


Fig. 2. SEM photos of external heated (a) and internal heated (b) copper wire.

It looks like the copper coil surface is modified on direct heating that favors the effective catalytic reaction. Microscopic studies (Fig.2) reveal that surface microcracks appear on the coil subjected to direct heating (b) but not on the coil heated by external furnace (a). Additional experimental data allow us to suppose that the defects are generated on the copper surface under the simultaneous action of the sharp temperature drop (coil – reaction mixture), electric current and the reaction products. The data obtained at alternating external and direct heating also indicate the higher efficiency of the direct heating due to modification of the copper surface in the course of the catalytic reaction. Notice that the copper coil modified this way behaves further as a more effective catalyst irrespectively of the method used for heating.

Methanol decomposition in steel tubular microreactor with monolithic copper catalyst

We studied thermal decomposition of methanol ($CH_3OH=2H_2+CO$) in tubular steel microreactor (100 mm long, i.d.=1 mm) with direct ohmic heating and monolithic copper as a catalyst. Four microreactor profiles with different relative surface/volume (S/V) ratio were used. **I.** Empty steel tube, $S/V=1$. **II.** Steel tube with copper wire (0.65 mm in diameter) inside, $S/V=1.91$. **III.** Steel tube with copper wire (0.95 mm in diameter) inside, $S/V=10.5$. **IV.** Steel tube with two nickel wire (each 0.5 mm in diameter) inside, $S/V=3.57$. Test runs of the microreactors were carried out with CH_3OH vapor-Ar mixture (1:4 molar ratio) in the temperature range of 170-450 °C and at the values of residence time 0.05-1 sec. The reaction

products – hydrogen and carbon monoxide was analyzed by chromatograph. No coke formation occurs.

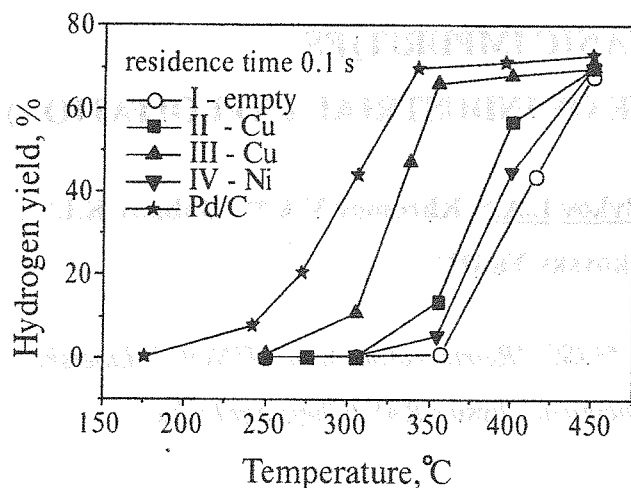


Fig. 3. H₂ yield vs. temperature for different microreactor profiles

The temperature dependencies of H₂ yield (Fig.3) indicate that increasing of S/V ratio provides more effective H₂ output at the same temperatures. Besides, the material of inner element of the microreactor plays an important role – profile II (Cu-wire) with less S/V ratio turns out to be more effective than profile IV (Ni-wire). In other words, despite the fact that specific surface of the monolithic copper is very low, its catalytic activity in the methanol conversion takes place. We also tested our microreactor with a conventional Pd/C catalyst without inner elements. One can see (Fig.3), that microreactor with massive copper catalyst with high S/V ratio, and consequently with high rates of heat and mass transfer, approaches effectiveness of the microreactor with dispersed Pd/C catalyst.

Conclusions

1) The endothermic methanol dehydrogenation catalyzed by copper metal is more efficient at the direct resistance heating of the catalyst than at the external convective heating.

2) The direct heating modifies the copper catalyst surface during methanol dehydrogenation that results in lowering of the reaction temperature and an increase in the hydrogen yield.

3) Described microreactor with massive copper catalyst with high S/V ratio and with direct ohmic heating provides high rates of heat and mass transfer. Such low cost sectional microreactors with the exchangeable inner elements are very promising in hydrogen production for various applications.

References

- [1] W. Wiese, B. Emonts, R. Peters. *J. Power Sources* **84** (1999) 187
- [2] Yu.I. Aristov, V.N. Parmon, V.I. Anikeev et al., *Thermochemical conversion of solar energy in solar catalytic reactors. New Horizons in Catalysis. Collected works of Institute of Catalysis, Novosibirsk 1985*, p.16.

CASSETTE REACTOR DESIGN WITH SILICA FIBER GLASS WOVEN CATALYSTS FOR PURIFICATION OF INDUSTRIAL GAS EXHAUSTS FROM ORGANIC IMPURITIES

(THREE YEARS EXPERIENCE OF INDUSTRIAL EXPLOITATION)

Barelko V.V.*, Prudnikov A.A.*, Bykov L.A.*, Khromov V.A.**, Bubnov K.I.**,
Manukovsky Yu.D****

**JSC "Chemphyst" (Chernogolovka), **JSC "Refrigerator plant STINOL" (Lipetsk),*

****Institute of Problem of Chemical Physics RAS (Chernogolovka)*

The process is organized with the catalysts on the base of silicate fiber glass woven materials (SiO_2 96 – 98 % mass) activated by noble metals (contents 0.05 – 0.2 % mass). The catalytic cartridge has a cassette design, so the cartridge may be easily installed in neutralizer or extracted from it.

The catalytic materials are produced in a form of rolls. Width of the catalytic band is 80 – 100 cm, mass of 1 m^2 – 500-1000 g. Woven structure of the catalysts may be produced with demands of customers: usual cloth, satin, grid etc.

We have an experience of the industrial exploitation of the gas purification systems. Almost three years the catalytic installation is continuously acting without changing catalytic cartridge on the Lipetsk refrigerator plant "STINOL" for neutralization of air exhausts from painting sets of the plant. Some characteristics of the process are as following :

- ◆ Air flow for purification – $10,000 \text{ m}^3/\text{h}$
- ◆ Inlet temperature – 350-400 C
- ◆ Impurities content (organic solvent) – $0.5-1 \text{ g}/\text{m}^3$
- ◆ Catalyst amount – $100-200 \text{ m}^2$
- ◆ Pt-content – 0.2% mass
- ◆ Catalytic cartridge – 7-10 layers, total width of the catalytic filter about 1 cm
- ◆ Level of purification – more than 90%

The catalytic material and the purification set are protected by the Russian patent:

Patent No 2171430, 27.07.2001 "Installation for catalytic purification of air exhausts from painting systems"

We propose the new systems for catalytic purification of industrial gas exhausts from organic impurities. These systems may be used, in particular, in machine-building, car-building, cable, furniture industries for neutralization of air flows from painting and covering by varnish installations.

Price of the catalytic cartridge is lower than all of traditional materials by 2-3 times

The proposed catalytic materials may be delivered to customers in any amounts during 1-2 months after signing of a contract.

CATALYTIC ACTIVATION OF FURNACE ATMOSPHERE FOR METALS AND ALLOYS GAS NITRIDING PROCESS

(8 years of development and exploitation of "catalytic nitriding")

V.Ya. Syropiatov and V.V. Barelko*

(NIITAvtoprom (Moscow), *Institute of Problem of Chemical Physics RAS (Chernogolovka),

JSC "Chemphyst" (Chernogolovka)

Introduction. A lot of machinery components during their exploitation are being exposed by increased load and intensive deterioration. For example, it refers to such very important machine elements as cylinder sleeve, crank-shafts of engines, transmission gears and other machinery systems and mechanisms. Nitriding is a well-known (a century history!) process of thermal chemical treatment of different metallic parts and elements for hardening of their surfaces by means of saturation by nitrogen of surface layer and forming nitride phases in it.

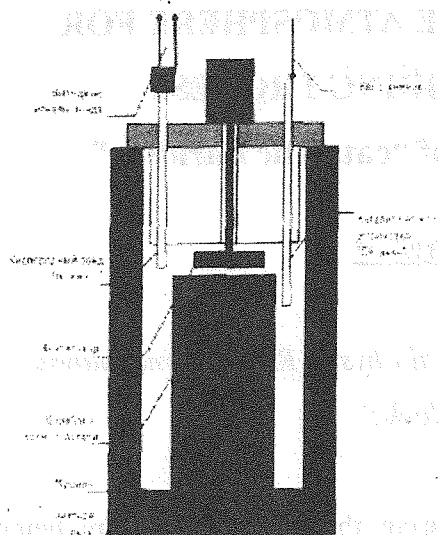
Eight years ago we created and are actively developing a new technology for metals and alloys nitriding following result of gaining maximum effective characteristics to metal components:

- Hardness and endurance
- High thermal and chemical resistance
- Adequate resistance to fatigue

A numerous scientific investigations and industrial implementation of the process (up to now seven Russian plants successfully use the technology) allow to elaborate "know-how" and regime parameters for nitriding treatment of different alloys and machine articles.

Main goal of the technology is a catalytic preparing of ammonia furnace atmosphere - "catalytic nitriding" method. The method uses catalytic action not for classic aim, i.e. for production of any final stable substance. A function of catalyst in "catalytic nitriding" process is to activate ammonia-oxygen atmosphere, to produce active, metastable particles (for example, radicals, ions, ions-radicals) in the medium. Mechanisms of the "catalytic nitriding" phenomenon demand special scientific investigations and discover a new possible direction in catalysis - chemical transformations in catalytically generated nonequilibrium gas media.

Technology & Equipment



The developed technology proved in actual practice the possibilities of the essential widening of the nitriding process possibilities and the receiving of unique parameters in treating metal articles by introduction into the traditional muffle-nitriding furnace a catalytic element being able to regulate the transformations of the nitriding ammonia-air furnace atmosphere at the "in situ" regime. JSC "Chemphyst" created special glass fiber woven catalysts doped by Pt, Pd, Rh and Cr for the "catalytic nitriding" process.

The process of "catalytic nitriding" uses a specially selected regime (a regime of "abortive catalysis"). The regime provides a furnace atmosphere with unusual characteristics allowing to realize a radical change both in regime itself and consuming parameters of end articles.

"Catalytic nitriding" technology doesn't require a major modification of technological equipment. It includes only catalytic devise and an oxygen sensor controlling O_2 contents in the muffle furnace. The catalytic material is placed in a special small reactor, which is installed on line of ammonia flow inside of nitriding furnace. With the help of these modifications it become possible to manage nitriding process efficiently and increase hardness and endurance of metal articles.

New nitriding process parameters and technological comparison. The new nitriding process have changed its character very strongly both in the regime parameters and qualities of the article treated:

- ◆ Alpha-solid solution range was very widened
- ◆ Control of the final nitrogen content in steel articles was realized in the range which is inaccessible under the traditional non-catalytic nitriding
- ◆ Corrosion resistance of structural steel was increased
- ◆ Hardness of the treated articles was increased to the depth more than 1 mm
- ◆ Decarbonizing process during the nitriding was strongly depressed
- ◆ Nitriding process was sufficiently accelerated simultaneously with the multiply decrease of the ammonia consumption

Some technological parameters of traditional, ion and catalytic nitriding have been compared and performed in below table:

	Traditional nitriding	Ion nitriding	Catalytic nitriding
Nitriding coating thickness, micron	100 - 150	100 - 150	до 250
Layer micro hardness, HV01	1200	1050	1050
Phase contents of surface zone	ϵ	γ'	γ'
Weakening temperature, °C	500	550	700
Additional technological operations	Degreasing	Ultrasonic cleaning	None

Fields of industrial application. The developed "catalytic nitriding" technology discover new possibilities of nitriding operations which cannot be realized in the traditional nitriding regimes:

- ◆ High-speed cutting steel nitriding
- ◆ Nitralloys nitriding
- ◆ Forming-tools nitriding
- ◆ Stainless steels nitriding
- ◆ Powder metallurgy articles nitriding
- ◆ Ti-alloys nitriding

Patent

Russian patent No 2109080, Bull. 11, 20.04.98

"Installation for gaseous low-temperature chemical-thermal treatment of steels and alloys

V.Siropiatov, V.Barelko, V.Zinchenko, L.Bikov

Publications

1. Zintchenko V.M., Syropiatov V.Y., Safonova O.N., Barelko V.V. New way in low-temperature chemical heat treatment of metals. Abstracts of the 10-th Congress of the International Federation for Heat Treatment and Surface Engineering. Brighton, UK, Sep. 1996, 12-13.
2. Zintchenko V.M., Syropiatov V.Y., Barelko V.V., Bykov L.A. Gas nitriding in catalytically prepared ammonia media. MITOM, 1997, No.7, 7-11. (in Russian).
3. Barelko V.V. New cellular catalyst systems on glass and metal body. In "Catalyst body and cellular catalyst structures". S Petersburg, 1995, Vol. 1, 118. (In Russian).

4. Syropiatov V.Y., Barelko V.V., Zintchenko V.M., Bykov L.A. Getero-catalitical activation of the ammonia with air furnace atmosphere as a new way in surface engineering of metals. Abstracts of the 2-nd International G.K. Boreskov Memorial Conference. Novosibirsk, 1997, 139-140. (in Russian).
5. Zintchenko V.M., Syropiatov V.Y., Barelko V.V., Bykov L.A. Gas nitriding in catalytically prepared ammonia media. Metal Science and Heat Treatment, CONSULTANTS BUREAU, New York, Jan. 1998, 23-28.
6. Syropiatov V.Y., Zintchenko V.M., Barelko V.V., Bykov L.A. New abilities of gas nitriding - reserves of a hundred-years old technologies. Nauka proizvodstvu, 1998, No. 1, 24-36. (in Russian).
7. Zintchenko V.M., Syropiatov V.Y. New abilities of the gas nitriding as a method for anticorrosive treatment of a machinery parts. Proceeding of 11-th Congress of the IFHT & SE, Florence, Italy, Oct. 1998. - Vol. 3, 9-17.
8. Syropiatov V.Y., Zintchenko V.M., Barelko V.V. Catalyst nitriding as a way for surface hardening of Ti and Ti alloys. Proceedings of the 4-th Russian Metallurgist Conference, Pensa, Sept. 1998, 21-24. (in Russian).
9. Syropiatov V.Y., Zintchenko V.M., Barelko V.V., Bykov L.A. Catalitical gas nitriding -new technology for low-temperature and low-deformation thermo-chemical treatment of gears. Proceedings of the International conference "Tribology of gears and bearings", CNIITMASH, Moscow, Oct. 1997. (in Russian).

HIGH SELECTIVE FIBER GLASS WOVEN CATALYSTS DOPED BY NOBLE METALS IN THE REACTIONS OF AROMATIC NITRO-COMPOUNDS REDUCTION

Chuntian Wu*, Victor Dorokhov*, Alexey Suknev**,
Bair Balzhinimaev** and Viktor Barelko*

**Institute of Problems of Chemical Physics RAS, Chernogolovka, 142432 Russia*

***Boreskov Institute of Catalysis, Siberian Branch RAS, Novosibirsk, 630090 Russia*

The features of liquid-phase hydrogenation of trinitrotoluene and trinitrobenzene over woven silica fiberglass (SFG) catalysts doped by Pt (Pt content 0,1 wt.%) were investigated. Specific surface area (SSA) of the catalysts was ranged from 1 to 15 m²/g. The traditional Pd/C powdered catalyst (Pd content 5 wt.%, SSA of 500 m²/g) was used as reference sample.

The SFG catalysts showed a higher specific activity than conventional Pd/C one. An unexpected finding for SFG catalysts was that hydrogenation rates of second and third nitro-groups in trinitrotoluene and trinitrobenzene were, respectively, by one and two orders of magnitude less than that of the first one. The selectivity effect was found to decrease with increasing of SSA for SFG catalysts and wasn't revealed at all for Pd/C sample.

Introduction. Recently the woven silica fiberglass (SFG) materials doped by platinum group metals were used as a catalyst in liquid-phase hydrogenation of nitro-aromatic hydrocarbons [1,2,4]. The nitrobenzene as a mono-functional aromatic nitro-compound was chosen in those studies. It was found that SFG catalysts show essentially higher specific activity compared with that of conventional powdered Pd/C catalyst. Physical-chemical studies of both silica fiberglass structure and the active sites location allowed to explain extremely high activity of SFG catalysts by specific origin and structure of the support as well as by ionic (clustered) state of metal in the bulk of glass fiber matrix [5-8]. The advantages of SFG materials in the processes of catalytic hydrogenation of aromatic nitro-compounds were protected by patent [3].

In this paper the study of features of nitro-aromatic hydrocarbons hydrogenation with SFG catalysts was extended on the reactions with multifunctional aromatic nitro-compounds, namely, trinitrotoluene and trinitrobenzene.

Experimental. Glass fiber woven material with an elementary fiber diameter of 7-9 microns was used as a carrier for SFG catalysts preparation. These woven materials are made from ordinary silicate glasses containing 55-98 wt.% of silica as well as alumina, magnesia, calcium oxide and boron oxide as residual components. In order to form specific structure of glass fiber matrix the leaching procedure of glass fiber supports in the acidic medium was performed as described elsewhere [5,6].

Platinum species was introduced into fiberglass matrix via ion exchange with aqueous solution of Pt-containing precursors followed by drying and calcination, which provides platinum content in the catalysts about 0,1 wt.%. SSA of the catalysts was varied from 1 m²/g (for silica fiberglass samples) to 15 m²/g (for aluminoborosilicate fiberglass samples). The Pd/C sample preparation procedure was close to that for commercial catalyst: carbon powder (AG-3, ARD) with the particle size of 100-200 μm, SSA of 500 m²/g and Pd content of 5 wt.%.

The experiments were carried out in the batch reactors (50-200 ml in volume) at 325 K and atmospheric pressure of hydrogen. The 1.5 g of the SFG catalyst (0.05 g of Pd/C) was loaded into solution of 1-3% trinitrotoluene (trinitrobenzene) in isopropanol. The reactor was continuously shaken with amplitude around 8-10 cm and frequency equal to 500 min⁻¹ that provided kinetic regime of reaction run. The reaction kinetics was measured via the hydrogen consumption rate in time. In parallel with hydrogen consumption measurements the reaction kinetics was monitored by periodic sampling of the reaction mixture followed by its chemical analysis to determine the concentration of the reagents and the products (nitroamines and amines). Volumetric measurements of H₂ consumed in combination with the chemical analysis of the reaction mixture provided correct description of the reaction kinetics.

Results and Discussion. Fig. 1 presents time dependencies of trinitrotoluene (TNT) conversion in the hydrogenation reaction over different catalysts (similar dependencies were also obtained for the reaction of trinitrobenzene reduction). The integral values of consumed hydrogen corresponding to complete stoichiometric reduction of one, two and all three nitro-groups, respectively, are denoted by the dotted lines.

The curve 1 describes the kinetics of TNT hydrogenation over SFG catalyst with SSA equal to 1 m²/g. One can see that rate of hydrogen consumption is strongly decreased after consumption of hydrogen volume corresponding to TNT conversion into dinitroaniline (i.e. at TNT conversion equal to 0.33). It can be proposed that after reduction of the first nitro-group (characteristic time is about 0.5 h) the hydrogenation process is retarded, so that the second

nitro-group is hydrogenated for more than 3 hrs; the hydrogenation of the third nitro-group proceeds considerably slower or doesn't happen at all.

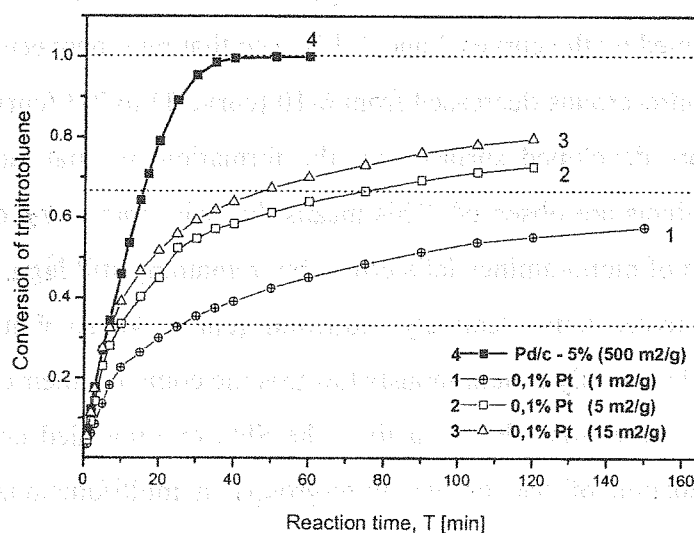


Figure 1. The dependence of trinitrotoluene conversion vs reaction time

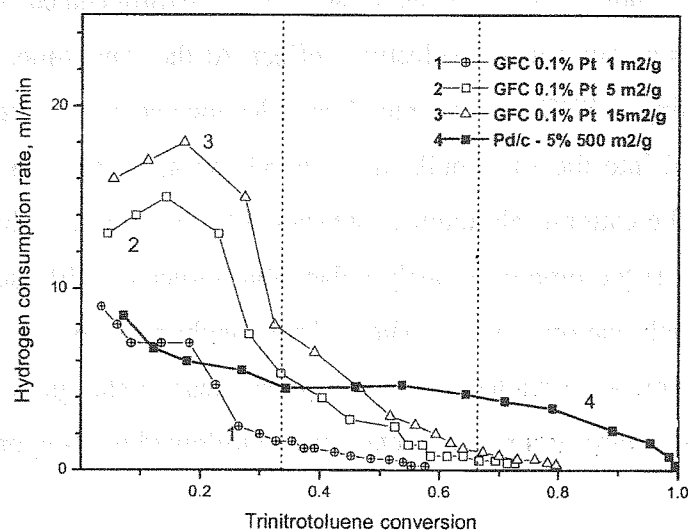


Figure 2. The dependence of hydrogen consumption rate on trinitrotoluene conversion

The proposed “stepwise” kinetic behavior becomes more pronounced if we express the data of Fig.1 as the dependence of hydrogen consumption rate vs trinitrotoluene conversion (Fig.2), i.e. reaction rate dependence vs hydrogen consumption. Again, the dotted lines mean the amount of hydrogen required for stoichiometric reduction of nitro-groups. It's seen that for SFG catalyst with SSA of $1 \text{ m}^2/\text{g}$ (curve 1) the reduction of the first nitro-group proceeds

with rates 6-10 times higher than that of the second nitro-group and more than two orders of magnitude higher than that of the third nitro-group.

The kinetic dependencies of TNT hydrogenation over SFG catalysts with SSA of 5 and 15 m²/g are presented by the curves 2 and 3. It's seen that ratio between hydrogenation rate of first and second nitro-groups decreased from 6-10 (curve 1) to 2-3 (curve 3). Note, in case of samples with more developed surface area the formation of small amounts of completely hydrogenated products are observed. This means that with increasing of SSA the selectivity towards formation of mono-amines falls down, but remaining still high. At the same time, the Pd/C sample catalyzes non-selectively reduction (curve 4), so that all nitro-groups are hydrogenated predominantly synchronously towards the complete their conversion to amines.

Thus, unlike conventional Pd/C catalyst, the SFG one revealed unusual performance in selective hydrogenation of one or two nitro-groups in multifunctional nitro-aromatics. At present we have no clear explanation of this phenomenon. Nevertheless, basing on our knowledge in SFG structure Pt state and its location, following reason of high selectivity can be proposed. In the case of TNT adsorption as a plane-ring complex on the surface of metal particles all nitro-groups seems to be equal and can be hydrogenated with comparable rates. As a result, there is no any specific selectivity effect. At the same time, there are two types of active sites coexisting in SFG catalyst: metal particles located on the external surface of fibers and Pt⁺² introduced into the fiber bulk (up to hundreds angstroms on depth). It was shown earlier [8] that i) the cationic platinum is substantially less active in hydrogenation reaction than metallic one; ii) the dipole or easily polarizable molecules diffuse fast into the bulk of glass fiber to reach cationic sites. Then, TNT anchoring by one nitro-group to Pt⁺² neighboring with metal particles (i.e. adsorption near metal-glass interface) results in interaction of second nitro-group with metal surface followed by its hydrogenation with active H-species.

So, unlike TNT ring (planar) adsorption, the anchoring via nitro-group (perpendicular) can lead to, mostly, mono- or di-amines. With increase in specific surface area of the support the contribution of "planar" reaction mechanism is also raised due to increasing of specific surface area of metal particles (Pt content in all SFG samples is the same). Therefore, the selectivity towards mono-amine formation should also decrease. Regarding Pd/C catalyst the first mechanism takes place only. As a result all nitro-groups are hydrogenated with comparable rates. Of course, this explanation is very preliminary and requires more detailed studies.

Conclusion. The main result is phenomenon of high selectivity in hydrogenation of multifunctional nitro-aromatics towards formation of dinitroanilines. Besides the fundamental issues, the obtained results open a technological possibility to produce aromatic nitro-amines using SFG materials by one-step catalytic process. Moreover, the SFG-assisted transformation of trinitrotoluene and trinitrobenzene may be applied as a new way for utilization of the explosives towards useful products.

Acknowledgements. Authors are very grateful to Polotsk (Byelorussia) fiberglass materials producer "Steklovolokno" for the help and providing of fiberglass woven materials.

The work is partially supported by NATO "Science for Peace" foundation (Project No SFP 971897).

References

1. Barelko, V., Dorokhov, V., et al., 1999, "Novel Prospects for Developing Liquid- and Gas-phase Catalytic Hydrogenation Processes Based on Fiberglass Woven Catalysts Doped with Palladium". 4th European Congress on Catalysis (EUROCAT-4), Italy, Book of Abstracts, P/II/290, p.828.
2. Dorokhov, V., Barelko, V., Bal'zhinimaev, B., Yuranov, I., 1999a, Novel Processes of Liquid Phase Reduction of Nitrobenzene to Aniline on the Fiberglass Pd-activated Catalysts. *Khimicheskaya promishlennost'* (in Russian), No.8, pp. 44-48.
3. Dorokhov V., Barelko V., Balzhinimaev B et al., 22.07.1999b, "Catalyst for hydrogenation of aromatic nitro-compounds". Patent of Russia No 2156654.
4. Dorokhov, V.G., Barelko, V.V., Balzhinimaev, B.S., 2000, A Novel Process of Liquid Phase Reduction of Nitrobenzene to Aniline on the Fiberglass Pd-activated Catalysts. Third International Symposium on Catalysis in Multiphase Reactors, May 2000, Naples, Book of Reports, pp.367-373.
5. Simonova, L.G., Barelko, V.V., Lapina, O.B., Paukshtis, E.A., Terskikh, V.V., Zaikovskii, V.I., Bal'zhinimaev, B.S., 2001a, Catalysts based on fiberglass supports: 1. Physicochemical properties of silica fiberglass supports. *Kinetics and Catalysis*, V. 42, No. 5, pp.693-702.
6. Simonova, L.G., Barelko, V.V., Paukshtis, E.A., Lapina, O.B., Terskikh, V.V., Zaikovskii, V.I., Bal'zhinimaev, B.S., 2001b, Catalysts based on fiberglass supports: 2. Physicochemical properties of alumina borosilicate fiberglass supports. *Kinetics and Catalysis*, V. 42, No. 6, pp.823-836.
7. Simonova, L.G., Barelko, V.V., Toktarev, A.V., Zaikovskii, V.I., Bukhtiyarov, V.I., Kaichev, V.V., Bal'zhinimaev, B.S., 2001c, Catalysts based on fiberglass supports: 3. Properties of supported metals (Pt and Pd) according to electron-microscopic and XPS data. *Kinetics and Catalysis*, V. 42, No. 6, pp.837-846.
8. Bal'zhinimaev, B.S., Barelko, V.V., Suknev, A.P., Paukshtis, E.A., Simonova, L.G., Goncharov, V.B., Kirillov, V.L., Toktarev, A.V., 2002, Catalysts based on fiberglass supports: 5. Absorption and catalytic properties of palladium catalysts based on a leached silica-fiberglass support in the selective hydrogenation of an ethylene-acetylene mixture. *Kinetics and Catalysis*, V. 43, No. 4, pp.542-549.

FLEXIBLE AUTOMATED PILOT PLANT FOR RESEARCHES OF CHEMICAL-TECHNOLOGICAL PROCESSES

V.V. Bogatov, R.M. Kasimov, E.M. Mamedov, K.A. Guseynov, I.U. Ibadzadeh

*Institute of chemical problems. Azerbaijan republic, Baku, 370143, 29 Husein Javid aven,
phone 994 39 41 59, E-mail: vbogatov@yahoo.com*

The automation of chemical experiment and instrumentations is the basic direction in creation of the modern equipment for the analysis and control of chemical-technological processes.

We developed automated universal chemical-technological pilot plant for research homogeneous and heterogeneous-catalytic processes, and also approbation of catalysts at high pressure. The plant contains two same reactors from corrosion-proof steel with two-section heating system, measuring-dozing devices executed on elements of jet engineering, and also device for cooling and separation of final products, devices of the control of temperature, pressure etc.

The system of automation of plant, is executed is based on personal computer IBM PC. Thus the modules ADAM of firm Advantech are applied for its interface to gauges and regulators.

Physical attachment of chromatography with the computer was carried out directly, through input-output circuit-board A-8111, or through the submodul ADC ACL-8113. Last has that advantage, that at high frequency of the manipulation to a target signal of at chromatography long enough time of the analysis does not result in high redundancy of the measuring information, entered into the computer.

For control of the magnetic valve of dump of liquid products, the signal system of an emergency and other operations applied the module of a 5-channel relay conclusion DC and isolated input I-7065B.

The information acting with gauges of chromatography, temperature, pressure of the charge of gas, liquid in separator of each of two reactors was entered into the computer.

For connection of these gauges to the computer was used of 12-bit analog and digital input-output circuit-board A-8111, and for jet gauges recording submission of gas and a liquid in system we used the module of input-output frequency of signals I-70-80/70-80D. At a

rejection of the measured charge from the given size the computer through a circuit-board of input-output gives out an adjusting signal on the module I-70-80/70-80D, by means of which the work of the step-by-step engine, thus stabilizing the given size of the charge of gas and liquid is adjusted. The creation of the similar automated system has allowed to get rid of a manual way of realization of experiment and essentially has facilitated a task of the operator who is carrying out its control.

Concerns to advantages of the described automated control system of pilot plant that being constructed with use of the means of dozing of a liquid and gas, and also technical and software of firms Octagon and Advantech it has the following advantage:

- ◆ Complete automation of measurements on a flow;
- ◆ Complete ecological safety of plant;
- ◆ High reliability of system determined by application of means with a time between failures of 100 000 hours and more;
- ◆ Simplicity of debugging of the working programs functioning in environment of Windows;
- ◆ Opportunity reconfiguration of system depending on technological task.

THE PARAMETRICAL ANALYSIS OF TURING'S TWO-DIMENSIONAL MODEL

V.I. Bykov, S.B. Tsybenova

Institute of Computing modeling, Krasnoyarsk, 660036, Russia, bykov@fvt.krasn.ru,

Krasnoyarsk State Technical University, Krasniyarsk, 660074, Russia, tsybenova@mail.ru

The distributed systems such as "reaction+diffusion" suppose multiplicity of steady states and self-oscillations. Interaction of the nonlinearity, nonsteady-state and to spatial heterogeneity leads to the big variety of possible dynamic behaviour of the distributed systems [1-4]. The parametrical analysis of such systems it is based on procedure linearization in a neighborhood of a homogeneous steady state. The mathematical model of Turing is represented by a system of two partial differential equations (PDE's),

$$\begin{aligned} \frac{\partial x_1}{\partial t} &= D_1 \left(\frac{\partial^2 x_1}{\partial \xi_1^2} + \frac{\partial^2 x_1}{\partial \xi_2^2} \right) + f_1(x_1, x_2), \\ \frac{\partial x_2}{\partial t} &= D_2 \left(\frac{\partial^2 x_2}{\partial \xi_1^2} + \frac{\partial^2 x_2}{\partial \xi_2^2} \right) + f_2(x_1, x_2), \end{aligned} \quad (1)$$

where x_1, x_2 are the concentrations of substances, D_1, D_2 are the diffusion coefficients, ξ_1, ξ_2 are the spatial variables, f_1, f_2 are nonlinear kinetic functions, t is the time.

The homogeneous spatial steady states x_1^*, x_2^* are defined from system of two nonlinear equations,

$$\begin{aligned} f_1(x_1^*, x_2^*) &= 0, \\ f_2(x_1^*, x_2^*) &= 0. \end{aligned}$$

After the procedure of linearization ($u_1 = x_1 - x_1^*, u_2 = x_2 - x_2^*$) the system of PDE's (1) are represented

$$\begin{aligned} \frac{\partial u_1}{\partial t} &= a_{11}u_1 + a_{12}u_2 + D_1 \left(\frac{\partial^2 u_1}{\partial \xi_1^2} + \frac{\partial^2 u_1}{\partial \xi_2^2} \right), \\ \frac{\partial u_2}{\partial t} &= a_{21}u_1 + a_{22}u_2 + D_2 \left(\frac{\partial^2 u_2}{\partial \xi_1^2} + \frac{\partial^2 u_2}{\partial \xi_2^2} \right), \end{aligned} \quad (2)$$

where $a_{ij} = \partial f_i(x_1^*, x_2^*) / \partial x_j$.

The solutions of system (2) in the local neighborhood of steady state x_1^*, x_2^* are founded,

$$u(t, \xi_1, \xi_2) = u(0, \xi_1, \xi_2) e^{\lambda t} e^{im \xi_1} e^{im_2 \xi_2}, \quad (3)$$

where n_1, n_2 are the frequencies of indignations of the solutions on the spatial variables ξ_1, ξ_2 .

The characteristic equation for system (2) looks as follows,

$$\lambda^2 - \sigma \lambda + \Delta = 0,$$

where

$$\sigma = a_{11} + a_{22} - (D_1 + D_2)(n_1^2 + n_2^2),$$

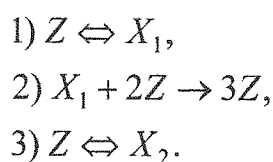
$$\Delta = a_{11}a_{22} - a_{12}a_{21} - (a_{11}D_1 + a_{22}D_2)(n_1^2 + n_2^2).$$

The coefficients of the characteristic equation ($\sigma = 0$) and ($\Delta = 0$) define exchange of stability of steady states and their multiplicity. At present paper the parametrical analysis of a homogeneous steady states are constructed the curves of local bifurcations in various planes of parameters. Influence the diffusion coefficients (D_1, D_2) on a kind of bifurcation curves ($\sigma = 0$) and ($\Delta = 0$) is determined.

The main calculations were carried out for kinetic dependence,

$$\begin{aligned} f_1(x_1, x_2) &= k_1 z - k_{-1} x_1 - k_2 x_1 z^2, \\ f_2(x_1, x_2) &= k_3 z - k_{-3} x_2, \end{aligned} \quad (4)$$

which are corresponded to the reactions on the catalyst surface. The scheme of reactions is,

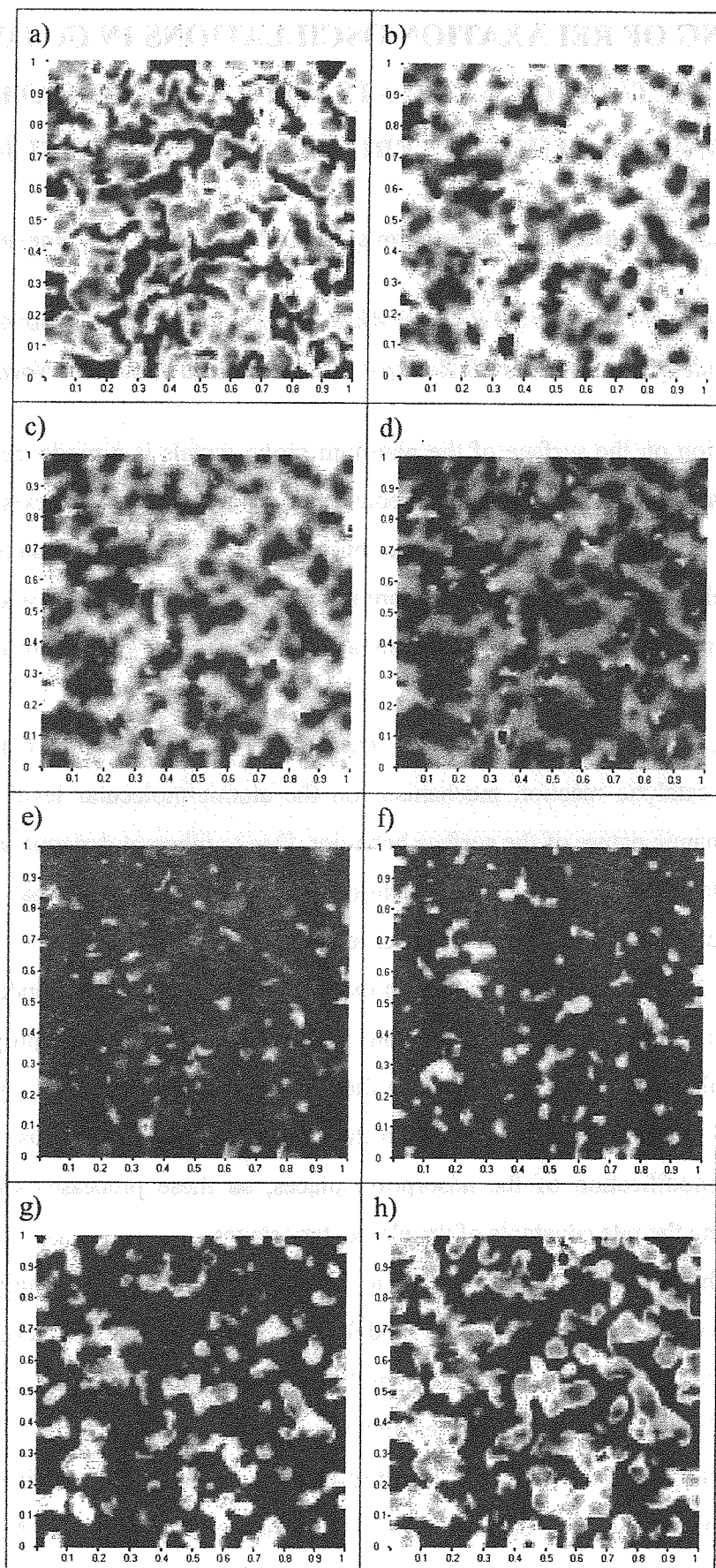


Nonlinear character of kinetics (4) leads to that the homogeneous steady state in the lumped system at presence of diffusion in the distributed system can lose stability. That is characterized by presence in the system (1) stable non-homogeneous solutions (диссипативных structures). These structures can be stable in time or periodically vary. That corresponds to autowaves on the catalyst surface. In this case adsorbed substances are self-organized in patterns, which periodically arise, grow, decrease and disappear. Such "blinking" intermediats on the catalyst surface leads to the complex dynamics of total rate of catalytic reaction. This macrocharacteristic essentially depends on parameters of nonlinear interaction intermediats and their diffusions on a microlevel.

The results of calculations of the system (1) with kinetic (4) are shown in Fig. 1(a) – $t_1 = 2000$, b) – $t_2 = 2050$, c) – $t_3 = 2100$, d) – $t_4 = 2150$, e) – $t_5 = 2200$, f) – $t_6 = 2250$, g) – $t_7 = 2300$, h) – $t_8 = 2350$). The values of parameters are $k_1 = 0.12$, $k_{-1} = 0.01$, $k_2 = 1$, $k_3 = 0.0032$, $k_{-3} = 0.002$, $D_1 = D_2 = 10^{-7}$. In this case the system (1) have got oscillations. Dark color shows degrees of a covering of substance X_1 (black tone corresponds $x_1 = 1$, white – $x_1 = 0$). The catalyst surface is characterized by essential heterogeneity, despite of presence of diffusion. Visually Fig. 1a–h are reminded the distributions intermediats on an active surface at modelling similar processes by Monte Carlo method.

References

1. V.I. Bykov, S.B. Tsybenova, M.G. Slinko, DAN. 2001. V. 380. №5. pp.649-651.
2. V.I. Bykov, S.B. Tsybenova, FGV. 2001. V. 37. №6. pp.22-29, (english translation in Combustion, Explosion, and Shock Waves, Vol. 37, №6, 2001, pp. 634 – 640).
3. V.I. Bykov, S.B. Tsybenova, Theoretical Foundations of Chemical Engineering. 2003. V. 37. №1. pp.650-662.
4. V.I. Bykov, S.B. Tsybenova, M.G. Slinko, DAN. 2003. V. 388. №6. pp.749-753.]
5. V.I. Bykov, S.B. Tsybenova, M.G. Slinko, DAN, 2001, Vol. 378, №2, pp.214-217, (english translation in Doklady Physical Chemistry, Vol.378, Nos. 1-3, 2001, pp. 134 – 137).
6. V.I. Bykov, S.B. Tsybenova, M.G. Slinko, DAN, 2001, Vol. 378, №3, pp.355-358, (english translation in Doklady Physical Chemistry, Vol.378, Nos. 1-3, 2001, pp.138-140).
7. V.I. Bykov, S.B. Tsybenova, Chemical Reactors (CHEMREACTOR-15), Helsinki, 2001, pp.256-258.
8. S.B. Tsybenova, Chemical Reactors (CHEMREACTOR-16), Kazan, 2003, pp.113-116.



MODELING OF RELAXATION OSCILLATIONS IN CO OXIDATION OVER METALLIC CATALYSTS WITH CONSIDERATION OF RECONSTRUCTIVE HETEROGENEITY OF THE SURFACE

E.A. Ivanova, N.A. Chumakova, G.A. Chumakov*, A.I. Boronin

Boreskov Institute of Catalysis SB RAS, Pr. Akad. Lavrentieva 5, 630090 Novosibirsk, Russia

**Sobolev Institute of Mathematics SB RAS, pr. Akad. Koptyuga 4, 630090 Novosibirsk, Russia*

CO oxidation on the surface of the platinum group metals is a model reaction whereby the main fundamental notions of heterogeneous catalysis are verified. The existence of critical phenomena in heterogeneous catalytic reactions, such as steady states multiplicity or self-oscillations, helps in determination of a more reliable reaction mechanism and permits better understanding the essence of physical-chemical processes in the system "reaction medium - catalyst".

Nowadays, it becomes obviously the trend has been towards the construction of a heterogeneous catalytic reaction mechanism on the atomic-molecular level by taking into account the dynamic nature of the surface behavior. Due to inherent dynamic variations of the catalyst surface under the reaction conditions, the critical phenomena and relaxation oscillations of catalytic reaction rate are observed.

Earlier the analysis of the CO oxidation mechanism on the Ir surface under conditions of ultrahigh vacuum was carried out taking into account the reconstructive properties of open planes on the platinum metals [1,2]. Due to these surface properties some oxygen atoms can reconstruct the surface and/or penetrate into the subsurface layers, and cause both structural and chemical modification of the adsorption places, so these processes are in charge of discrete changing the rate constants of the elementary stages.

Kinetic scheme and model suggested in [1,2] consist of 12 elementary stages and 5 differential equations, respectively. This model was found to be effective enough, permitted to describe experimental data and predict multiplicity of steady states, existence of critical phenomena and self-oscillations of the reaction rate.

However, the model obtained was found to be too complex for qualitative analysis of the reaction dynamics by means of methods of dynamical systems theory. Now we suggest another approach to theoretical study of the nonlinear kinetic models dynamics based on the distinction of slow and fast variables in the model [3,4]. So we can describe dynamics of the

original model on the basis of results, received for sub-models (some models of lower dimension).

This paper is devoted to the development of low-dimension kinetic models of CO oxidation on metallic catalyst surface and theoretical investigation of arising nonlinear phenomena in terms of the method proposed above.

We consider the conventional adsorption mechanism of catalytic CO oxidation:



where ZO and ZCO are intermediate compounds of oxygen and CO on the Ir surface, Z is an active center of Ir surface layer. Constants of the reaction stages rates depend on both the temperature and partial pressures of CO and O₂ as follows:

$$k_1 = k_{10}P_{\text{CO}}, \quad k_2 = k_{20}P_{\text{O}_2}, \quad k_{-1} = k_{-10}\exp(-E_1/(RT)), \quad k_3 = k_{30}\exp(-E_3/(RT)).$$

We can write a kinetic model after the mechanism (1)-(3), which describes changing of non-dimensional concentrations of CO (x) and oxygen (y) adsorbed on the surface under assumption that properties of the surface do not depend on x and y :

$$\begin{aligned} x' &= k_1(1-x-y) - k_{-1}x - k_3xy, \\ y' &= 2k_2(1-x-y)^2 - k_3xy. \end{aligned} \quad (4)$$

This model permits qualitative interpretation of the steady states multiplicity. The analysis of algebraic equations determining the steady states shows that there exist no more than three steady states with $0 < x, y < 1$ and $x+y < 1$. Moreover, the steady state $x_s=0, y_s=1$ is present for all values of model parameters, and it is unstable. From the Bendixon criterion we can conclude that in the model (4) there are no self-oscillations of reaction rate.

For description of self-oscillations observed in the experiment we suggest to change the model (4) taking into account possibility of the metallic surface modification in the course of reaction due to oxygen penetration.

At first, we suggest that under exceeding of adsorbed oxygen concentration over a critical value $y_c - \delta$, there occurs the surface modification and the reaction capability of oxygen is changing, so as the activation energy of stage (3) – the interaction between the adsorbed oxygen and CO – is sharply increasing. Thus, we introduce the dependence $E_3(y)$ and two additional parameters y_c and δ , which determine the location and width of the interval of adsorbed oxygen concentration y , where an increase of activation energy E_3 takes place (see Fig.1). The difference between the maximal and minimal E_3 values is determined from the experimental data.

Construction of bifurcation curves on the parametric plane (P_{CO} , P_{O_2}) permits us to separate areas of CO and O₂ partial pressures, for which there are self-oscillations and/or multiplicity of steady states in the model.

For instance, we obtained, that under decreasing temperature the maximal values of P_{CO} and P_{O_2} , for which self-oscillations exist, decrease too.

Under investigation of the model for different intervals changing the activation energy of CO₂ formation we received, that for big values of δ the increasing of $E_3(y)$ occurs rather slow, and there are no self-oscillations in the system for small P_{CO} and P_{O_2} values. Under decreasing δ for fixed P_{CO} and T values (for example, $P_{CO}=1.1 \cdot 10^7$ Torr, $T=500$ K) the width of P_{O_2} interval, where self-oscillations exist, firstly increase and then decrease. The amplitude and period of self-oscillations under decreasing δ increase (see Figs.2-3). Besides, the middle rate of CO₂ formation on the periodic solution is by an order greater than the reaction rate in the middle unstable steady state.

We study the influence of the parameter y_c value in the neighbourhood of which the change of the surface properties occurs, on the reaction dynamics. Numerical analysis of the model (4) for different y_c values has shown that for small y_c and fixed P_{CO} and T values, there are two intervals of oxygen partial pressure P_{O_2} where self-oscillations of the reaction rate can be observed. Note that under approach to one of the boundary of each interval the period of oscillations becomes unlimitedly great.

Thus, in this work we present method of analysis nonlinear dynamics in kinetic models of catalytic reactions with hierarchy of characteristic times. The conducted analysis of two-dimensional kinetic models of CO oxidation over Ir catalyst in framework of this method gives us foundation for the description of the complex dynamics in models of greater dimension.

1. V.I. Elokhin A.I. Boronin *Modelling of CO+O₂ reaction on Ir*. In: Mechanisms of adsorption and catalysis on clean metallic surfaces. Novosibirsk, Institute of Catalysis, 1989, pp.62-76. (in Russian)
2. A.I. Boronin, V.I. Elokhin *Dynamics of surface processes over iridium in carbon monoxide oxidation reaction*. Proceedings of the first Soviet-Chinese seminar on catalysis. Novosibirsk, Institute of Catalysis, 1991, pp. 5-20.
3. G.A. Chumakov, M.G. Slinko *Kinetic turbulence (chaos) of reaction rate for hydrogen oxidation over metallic catalysts*. – Dokl. Acad. Nauk USSR, 1982, Vol. 266, No. 5, pp. 1194-1198 (in Russian)
4. G.A. Chumakov, N.A. Chumakova *Relaxation Oscillations in a Kinetic Model of Catalytic Hydrogen Oxidation Involving a Chase on Canards*. – Chem. Eng. J., 2003, Vol. 91, No. 2-3, pp.151 – 158.

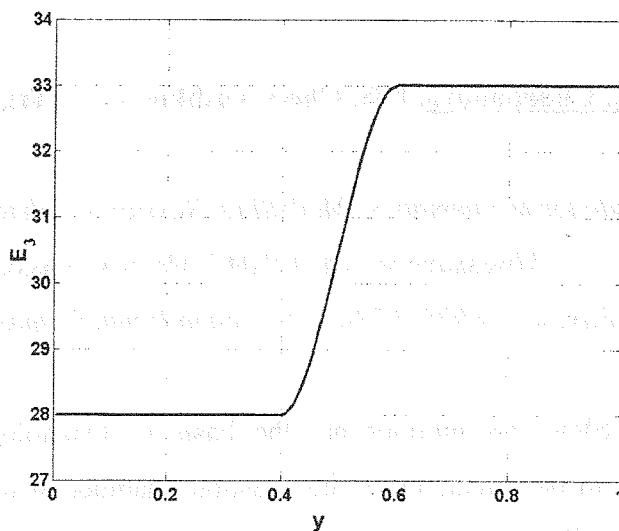


Fig. 1. Activation energy E_3 of the reaction stage (3) versus the oxygen concentration y for $\delta=0.1, y_c=0.5$.

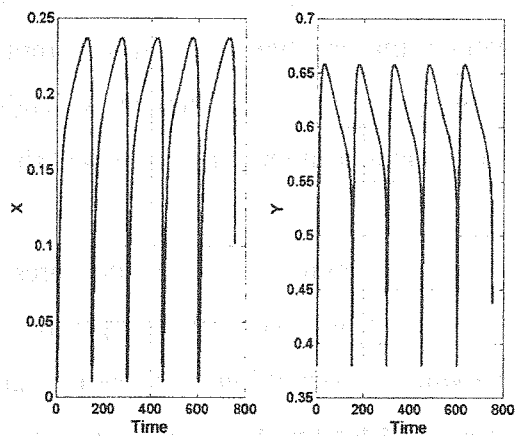


Fig. 2. Self-oscillation in the model (4) under $T=500$ K, $P_{CO}=1.1 \cdot 10^{-7}$ Torr, $P_{O_2}=8 \cdot 10^{-7}$ Torr, $\delta=0.1, y_c=0.5$.

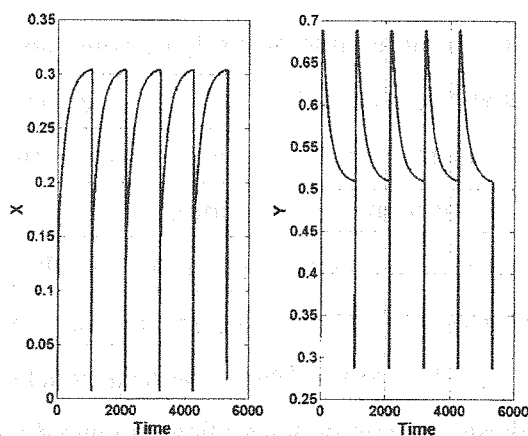


Fig. 3. Self-oscillation in the model (4) under $T=500$ K, $P_{CO}=1.1 \cdot 10^{-7}$ Torr, $P_{O_2}=8 \cdot 10^{-7}$ Torr, $\delta=0.01, y_c=0.5$.

SIMULATION OF GAS FLOWS AT LOW MACH NUMBER

N.G. Churbanova, B.N. Chetverushkin, M.A. Trapeznikova

Institute for Mathematical Modelling, Russian Academy of Science

Miusskaya sq. 4A, 125047, Moscow, Russia

Fax: ++7-(095)-973-07-23, e-mail: nata@imamod.ru

Introduction. Slow gas motions are the basis of technological processes in many industrial facilities, in particular, in the combustion chamber of a reciprocating engine, in chemical reactors etc. That is why numerical simulation of viscous compressible gas flows at low Mach number is of great practical interest.

However this simulation faces considerable difficulties. One of them is the Courant-Friedrichs-Levi time-step restriction when using explicit difference schemes. Unfortunately in this case even implicit methods do not lead to a success automatically. It is known that slightly compressible flows have some specific features that are typical for incompressible flows and reflect in decreasing the pressure-density coupling when Mach number M tends to 0 [1]. The mathematical model as well as the computational algorithm to be developed should take into account this uncoupling.

There are some approaches to this problem overcoming based on the pressure decomposition into a volume-average part and a dynamic part. While getting the dimensionless form of the governing equations employment of two different reference values for these two components allows to avoid singularities at M tending to 0 and to consider the limit case where M equals 0. Some authors include the decomposed pressure in so-called low-Mach-number approximation [2]-[4]. Development of the analogous pressure-based algorithm for solving the full Navier-Stokes equations is also known [5].

The present paper is devoted to implementation of this pressure splitting procedure for the quasi gas dynamical system of equations [6], [7] instead of the full Navier-Stokes equations. In order to avoid any loss of accuracy the authors employ not only the above model and pressure decomposition but they also develop a new implicit computational algorithm. One of important advantages of this algorithm is rather high efficiency of parallelization when adapting to parallel computers with distributed memory.

Mathematical model. It is known that in the case of slightly compressible gases the total pressure in every point of the domain oscillates at some average value which is constant for the whole domain. Its reference value is much greater than the average value of these oscillations. Generally while getting the dimensionless form of the governing equations the described average value of the pressure is used as the reference value of the total pressure. In consequence in the momentum equation the coefficient $1/M^2$ appears at the term $grad(P)$. When $M \rightarrow 0$ this coefficient leads to significant computational errors.

In order to get correctly the dimensionless form of the quasi gas dynamical equations in this paper by analogy with [5] it is suggested to decompose the original pressure into a sum of two components - the volume-average part \bar{p}^* depending on time only and the dynamic part Π^* which depends on time and on spatial variables. These terms have different reference values, what influences on their nondimensionalizing. As a reference value of \bar{p}^* some average value P_0 is taken, but Π^* is normalized by $\rho_0 V_0^2$ where ρ_0 and V_0 are reference values of the density and the velocity correspondently. Such normalization do not result in appearing coefficients of the type $1/M^2$,

$$P(t, x) = \bar{p}(t) + \gamma M^2 \Pi(t, x) \tag{1}$$

Since the additional variable is introduced the next integral relation is included in order to get the complete system of equations and to determine \bar{p} :

$$\bar{p} = \frac{1}{V_\Omega} \int p dx_1 dx_2 \tag{2}$$

or the equivalent relation:

$$\int_\Omega \Pi dx_1 dx_2 = 0$$

As a result the dimensionless system of quasi gas dynamical equations with the decomposed pressure can be written like this (for brevity the 1D case is presented):

$$\frac{\partial \rho}{\partial t} + \frac{\partial(\rho u)}{\partial x} = \frac{\gamma M^2}{Re} \frac{\partial \tau}{\partial x} \frac{\partial}{\partial x} (\rho u^2 + \Pi) \tag{3}$$

$$\begin{aligned} \frac{\partial(\rho u)}{\partial t} + \frac{\partial}{\partial x} (\rho u^2 + \Pi) &= \frac{\gamma M^2}{Re} \frac{\partial \tau}{\partial x} \frac{\partial}{\partial x} (\rho u^3 + 3\Pi u) + \\ &+ \frac{1}{Re} \frac{\partial \tau}{\partial x} \frac{\partial}{\partial x} (3\bar{p}u) \end{aligned} \tag{4}$$

$$\begin{aligned} & \frac{\partial}{\partial t}(\rho\varepsilon) + \gamma M^2(\gamma - 1) \frac{\partial}{\partial t} \frac{\rho u^2}{2} + \frac{\partial}{\partial x} u \left[\gamma M^2(\gamma - 1) \frac{\rho u^2}{2} + \rho\varepsilon + (\gamma - 1)P \right] = \\ & = \frac{\gamma M^2(\gamma - 1)}{\text{Re}} \frac{\partial \tau}{\partial x} \frac{\partial}{2 \partial x} \left[u^2 \left(\gamma M^2 \frac{\rho u^2}{2} + \frac{\rho\varepsilon}{\gamma - 1} + 2P \right) \right] + \quad (5) \\ & + \frac{1}{\text{Re}} \frac{\partial \tau}{\partial x} \frac{\partial}{2 \partial x} \left[\frac{P}{\rho} \left(\gamma M^2(\gamma - 1) \frac{\rho u^2}{2} + \rho\varepsilon + \bar{p}(\gamma - 1) + \gamma M^2(\gamma - 1)\Pi \right) \right] \end{aligned}$$

$$\rho = \frac{P}{T} \quad (6)$$

$$\varepsilon = \frac{T}{\gamma(\gamma - 1)M^2} \quad (7)$$

$$P = \bar{p}(t) + \gamma M^2 \Pi(x, t) \quad (8)$$

$$\int_{\Omega} \Pi(x, t) dx = 0 \quad (9)$$

where ρ is the density, P is the total pressure, \bar{p} and Π are the average and the dynamic components of the pressure, T is the temperature, ε is the inner energy, γ is the ratio of heat capacities, $\tau = \mu/P$, where μ is the viscosity coefficient.

Increment of the pressure. It should be noted that the equation of state (8) is solved in terms of the density which is evaluated from the pressure but not conversely. That is why one has to solve some special problem at every time level in order to obtain the pressure. For this purpose by analogy with [3] it is convenient to introduce so-called increments of the average and the dynamic components of the pressure:

$$\delta \bar{p} = \bar{p}^{n+1} - \bar{p}^n, \quad \delta \Pi = \Pi^{n+1} - \Pi^n \quad (10)$$

Using these increments we get the equation for the total pressure:

$$P^{n+1} + \delta \bar{p} + \gamma M^2 \delta \Pi \quad (11)$$

If to find some intermediate values of increments $(\delta \bar{p})^*$ and $(\delta \Pi)^*$ so that they comply with the relation:

$$P^{n+1} - P^n = (\delta \bar{p})^* + \gamma M^2 (\delta \Pi)^*, \quad (12)$$

then applying balance relations over the whole space one can obtain the final values of increments that appear to be equal to the next:

$$\delta \bar{p} + (\delta p)^* \frac{\gamma M^2}{V_{\Omega}} \int_{\Omega} (\delta \Pi)^* dx_1 dx_2 \quad V_{\Omega} = \int_{\Omega} dx_1 dx_2 \quad (13)$$

$$\delta \Pi = (\delta \Pi)^* - \frac{1}{V_{\Omega}} \int_{\Omega} (\delta \Pi)^* dx_1 dx_2 \quad (14)$$

The intermediate values of the pressure increments are found via the momentum and continuity equations of the initial system (3)-(9).

Test predictions. As a test for validation of the presented new approach the classical 2D problem of the isothermal lid-driven cavity flow was used. This problem is well studied and values of flow parameters for it were obtained in the paper [6] on the basis of high-accurate solutions of the Navier-Stokes equations. In our paper slightly compressible gases, that parameters are similar to parameters of incompressible fluid flows, are investigated. Therefore it was natural to compare results found in this work with benchmarks from [8].

The work is supported by the projects 02-01-00700, 03-01-00544 and MK-2423.2003.01 of Russian Foundation for Basic Researches

References

- [1]. M. Buffat. "Simulation of two- and three-dimensional internal subsonic flows using a finite element method", *Int. J. Numer. Methods Fluids*, **12**, 683-704 (1991).
- [2]. S. Paolucci. "On the filtering of sound from the Navier-Stokes equations." *Sandia National Laboratories Rep. SAND82-8257*, 1982.
- [3]. S. Paolucci and D.R. Chenoweth, "Transition to chaos in a differentially heated vertical cavity", *J. Fluid Mech.*, **201**, 379-410 (1989).
- [4]. R.G. Rehm and H.R. Baum, "The equations of motion for thermally driven, buoyant flows", *J. Res. Nat. Bur. Stand.*, **83**, 297-308 (1978).
- [5]. A.G. Churbanov and A.N. Pavlov, "A pressure-based algorithm to solve the full Navier-Stokes equations at low Mach Number", 894-899, CFD'98, Wiley, Chichester, 1998.
- [6]. T.G. Elizarova and B.N. Chetverushkin, "Kinetically coordinated difference schemes for modeling flows of a viscous heat-conducting gas", *J. Comp. Math. and Math. Phys.* U.K., No. 11, 64-75 (1988).
- [7]. B.N. Chetverushkin and N.G. Churbanova, "Simulation of gas flows at low Mach number", *Differentsialnye Uravneniya*, **34**, 988-992 (1998).
- [8]. V. Ghia, K.N. Ghia and C.T. Shin, "High-Re solutions for incompressible flow using the Navier-Stokes equations and a multi-grid method", *J. Comp. Phys.*, **48**, 387-411 (1982).
- [9]. M.A. Trapeznikova and N.G. Churbanova, "Simulation of multi-phase fluid filtration on parallel computers with distributed memory", 929-934, CFD'98, Wiley, Chichester, 1998.

THE CATALYTIC SYNTHESIS OF ACETONITRILE

S.I. Galanov^{1,2}, O.I. Sidorova¹, L.N. Kurina¹, A.K. Golovko²

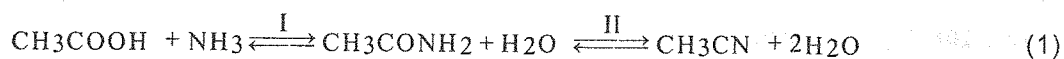
¹Tomsk State University, 36, Lenin Ave., 634050, Tomsk, Russia

E-mail: galanov@xf.tsu.tomsk.su

²Institute of petroleum chemistry, 3, Academichesky Ave., 634021, Tomsk, Russia

Acetonitrile is widely used in organic synthesis as an intermediate reagent, solvent, azeotropizer when separating the substances [1,2]. Acetonitrile is commercially produced as a by-product of acrylonitrile synthesis. Therefore the investigation and development of inexpensive and commercially convenient methods for Acetonitrile production represent an urgent problem. Developed are the methods for acetonitrile synthesis from ammonia and acetic acid [3,4], alcohols [5], paraffins and olefins [1,6]. Nevertheless, the syntheses from alcohols [5], paraffins and olefins [1,6] are characterized by an insufficient selectivity and low process efficiency. Acetonitrile synthesis from acetic acid is more promising due to low expenses for isolation and purification of the desired product.

The reaction of acetonitrile formation from acetic acid and ammonia occurs at several stages [3, 4]:



The calculation of thermodynamic functions and constant of equilibrium for stages I and II (scheme 1) has showed, that the reaction of acetamide formation from an acetic acid and ammonia (at temperatures 250 - 450°C) is weakly exothermal: $\Delta H_{av} = -2.18$ kJ/mol, $\Delta G = -(3.56 - 4.22)$ kJ/mol and a constant of equilibrium $K_p = 2.76 - 2.26$. The stage II - dehydration of acetamide is limited endothermal stage: $\Delta H_{av} = 84.37$ kJ/mol, $\Delta G < 0$ at temperature above 320°C. Thus, the rise of reactor temperature (the limitation is the thermal decomposition of acetic acid and products of reaction) or the change of loading on acetic acid (at the identical temperature) leads to the completeness of reaction ammonolysis of acetic acid. The increase in temperature of reactor is higher 400°C at ratio $\text{NH}_3:\text{CH}_3\text{COOH} = 1.5$ results to a high yield of acetonitrile at the big loading on acetic acid, the productivity on acetonitrile = $0.89 \text{ kg/dm}^3 \cdot \text{h}$. But in this case were observed: the decarboxylation of acetic acid to acetone and CO_2 ; formation of pitches and of the compaction products (CP) on a

surface of the catalyst with decrease in his activity. The decrease in temperature of reaction to 350 - 380°C leads to the decrease the amount of the compaction products (%CP) formed (from 0.19 at 400-450°C to 0.04% at 350-380 °C). In table 1 shows, that the decrease of reactor temperature to 380°C leads to high productivity on acetonitrile at the decrease in activity of the catalyst because of to formation of the compaction products. The production of high productivity on acetonitrile with the minimal formation of by-products at lower temperatures is more optimum.

Table 1. The influence of the reactant ration and temperature on process catalytic parameters

T, °C	Q, kg/dm ³ · h	Ration NH ₃ :CH ₃ COOH	K, %	S _{CH₃CN} , %	B _{CH₃CN} , %	P, kg/dm ³ · h	Mass amount of products / 1 kg of acetonitrile		
							CH ₃ COON H ₃	CH ₃ CON H ₂	other
350	1.02	1.5	88.5	62.2	55.1	0.384	0.39	0.99	-
350	1.02	2.0	92.1	74.6	68.7	0.479	0.22	0.53	-
350	1.02	3.0	92.0	86.1	79.2	0.552	0.19	0.25	-
350	1.02	4.0	92.2	89.2	82.2	0.573	0.18	0.19	-
360	0.49	2.0	100	99.3	99.4	0.333	-	-	0.010
360	0.58	2.0	99.2	99.4	98.7	0.391	0.02	-	0.009
360	0.67	2.0	99.2	99.5	98.5	0.451	0.02	-	0.007
360	1.02	1.5	88.6	86.6	76.7	0.535	0.28	0.25	-
360	1.02	2.0	89.6	88.8	79.5	0.554	0.25	0.20	-
360	1.02	3.0	92.9	93.4	86.8	0.605	0.15	0.11	-
360	1.02	4.0	100	96.1	96.1	0.670	-	0.06	-
380	1.02	1.5	99.5	95.5	95.0	0.662	0.01	0.07	-
380	1.02	2.0	99.5	97.0	97.0	0.676	0.01	0.04	-

The note: Q – loading on acetic acid, kg / dm³· h; K – conversion of acetic acid (%); S_{CH₃CN}, B_{CH₃CN} – selectivity and yield of acetonitrile (%); P – productivity on acetonitrile; other –basically acetone.

One of the parameters influencing the process of acetic acid ammonolysis may be varying the partial pressures of the reactants. The study of the influence of NH₃:CH₃COOH ratio on the process parameters demonstrated that at equal acid loads the increase in ratio leads to the increase in acetonitrile selectivity and yield despite of the reduction in contact time (table 1). This is connected with the reversibility of the reaction I (scheme 1), the increase in the partial pressure of ammonia shifts the equilibrium towards acetamide formation followed by acetonitrile formation (reaction II).

The study of $\gamma\text{-Al}_2\text{O}_3$ promoted by base - $\text{Ca}(\text{OH})_2$ and acid - H_3PO_4 shows that the increase in basicity of catalysts surface leads to the inhibition of stage II (scheme 1) in reaction of acetic acid ammonolysis. In this case the basic product of reaction is acetamide. The promotion of $\gamma\text{-Al}_2\text{O}_3$ by phosphoric acid results to the increase of selectivity and acetonitrile yield. Thus, the promotion of $\gamma\text{-Al}_2\text{O}_3$ by phosphoric acid leads to the acceleration of reaction of acetamide dehydration to acetonitrile.

The acetamide dehydration on $\gamma\text{-Al}_2\text{O}_3$ is accompanied by the reaction of acetamide hydrolysis to acetate of ammonium (table 2). The decrease in loading of acetamide or the rise in reactor temperature leads to the increase of productivity on acetonitrile and the reduce amount of acetate of ammonium formed.

Table 2. Influence of ammonia promotion on the catalyst of parameters of synthesis of acetonitrile reaction from acetamide

Catalyst	Reagents	T, °C	Loading on acetamide, kg/dm ³ ·h	K, %	B _{CH₃CN} , %	Productivity on acetonitrile, kg/dm ³ ·h	Mass amount of acetate of ammonium /1 kg of acetonitrile
$\gamma\text{-Al}_2\text{O}_3$	acetamide	360	1.05	79.7	68.1	0.489	0.157
			0.82	82.4	71.1	0.398	0.133
			0.58	90.7	80.7	0.319	0.104
		380	1.05	93.1	74.7	0.536	0.214
			0.82	97.2	87.9	0.492	0.081
			0.58	98.8	93.2	0.369	0.017
415	1.05	97.7	90.0	0.646	0.103		
$\gamma\text{-Al}_2\text{O}_3$	acetamide/ammonia =1:1.5	360	1.05	92.0	89.6	0.643	0.033
		380		98.3	97.7	0.701	0.007
6 mass % $\text{H}_3\text{PO}_4/\gamma\text{-Al}_2\text{O}_3$	acetamide/ammonia =1:1.5	360	1.05	100	99.5	0.714	-

The conversion of acetamide collaterally with ammonia leads to the increase of productivity on acetonitrile with the repressing of hydrolysis reaction. The effect of introduction of ammonia in a reactionary mix consists in competitive adsorption of ammonia and products of reaction on catalyst surface. The maximal productivity on acetonitrile at low temperatures is observed on $\gamma\text{-Al}_2\text{O}_3$ promoted by phosphoric acid catalyst (table 2), the acetate of ammonium in this case is not formed. The formation of percent of the compaction products (%CP) at the acetamide dehydration on $\gamma\text{-Al}_2\text{O}_3$ is equal 0.02, on $\gamma\text{-Al}_2\text{O}_3$ promoted by phosphoric acid catalyst the formation of the compaction products was not observed.

For reaction of the acetamide dehydration obtained the kinetic model, which is taking into account competitive adsorption of ammonia and products of reaction and reaction of acetamide hydrolysis.

$$w = k \cdot K_A \cdot p_A \left(\frac{1 + K_{NH_3} \cdot p_{NH_3} - K_{H_2O} \cdot (p_{H_2O})^{1/2}}{K_A \cdot p_A + K_{H_2O} \cdot p_{H_2O} + K_{NH_3} \cdot p_{NH_3}} \right) \quad (2)$$

The energy of activation for γ -Al₂O₃ and 6 % H₃PO₄/ γ -Al₂O₃ is equal 63.2 and 58.3 kJ/mol, accordingly.

Thus, for synthesis of acetonitrile from acetic acid and ammonia use two-reactor circuit with intermediate extraction of acetamide can be perspective. In the first reactor can be use the catalyst - γ -Al₂O₃ promoted by the base or production of acetamide with high selectivity at temperature 290-340 °C. In the second reactor on γ -Al₂O₃ promoted by acid to carry out of the acetamide dehydration to acetonitrile. It has led to: 1) the decrease of expenses on rectification of acetonitrile; 2) considerably to reduce formation of the compaction products, and to extend the catalyst life between regeneration; 3) to reduce of amount of circulating ammonia; 4) to increase the productivity on acetonitrile from unit of volume of the catalyst.

Reference

1. Hashimoto K., Morimoto K., Dodson S. // *Environ. Health Criteria.* – 1993, № 154. P. 1-110.
2. Pereushanu V., Korobya M., Muska G. *Production and Application of Hydrocarbons.* // Transl. from Romanian. V.G. Lipovich, G.L. Avrekh (Ed). Moscow: Khimiya. 1987. p. 288.
3. Vodolazhskiy S.V., Yakushkin M.I., Devecki A.V., Khvorov A.P. *Zhournal Organicheskoy Khimii.* 1988. Vol. 24 N 4. – P. 699.
4. USSR A.s.1321722, C 07 C 120/00. The method of reception of acetonitrile./Shepelev S.S., Ione K.G. bul. №25, 1987.
5. Pat. USA 2535082 (1950) Acetonitrile production/John E. Mahan.
6. Kovalenko T.I., Kovalenko V.I., Malook G.P., Dubchenko V.N. *Zhournal Prikladnoy Khimii.* 1972. N 8. – P. 1824-1827.

THE USE OF ETHANOL FOR COMBINED HEAT AND POWER STATIONS ON THE BASIS OF POLYMER ELECTROLYTE FUEL CELLS

Galvita V.^{a,b}, Sobyenin V.^b, Sundmacher K.^{a,c}

^a*Max-Planck-Institut fuer Dynamik Komplexer Technischer Systeme, Sandtorstrasse 1,
39106 Magdeburg, E-mail: galvita@mpi-magdeburg.mpg.de*

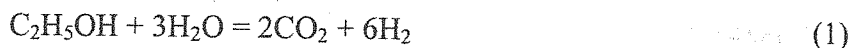
^b*Boreskov Institute of Catalysis, Lavrentieva ave 5, 630090 Novosibirsk, Russia*

^c*Otto-von-Guericke-Universitaet, Lehrstuhl fuer Systemverfahrenstechnik,
Universitaetsplatz 2, D-39106 Magdeburg*

Fuel cell technology holds the promise to produce electricity at local site from a wide range of fuels with high efficiency. Polymer electrolyte fuel cells are the most attractive type of fuel cell for stationary and mobile applications. This type of fuel cell operates on hydrogen, which has to be produced from different sources. Chemical storage of hydrogen in liquid fuels is considered to be one of the most advantageous way for supplying hydrogen to the polymer electrolyte fuel cell. A variety of liquid fuels, such as methanol, ethanol and hydrocarbons are suitable for this purpose.

Among liquid fuels, ethanol (EtOH) is a promising source of hydrogen while it is an easily accessible and non-polluting raw material which can be readily produced from renewable sources (biomass; bioethanol = aqueous solution containing ca. 12 wt.% ethanol).

The overall reaction of hydrogen production from ethanol corresponds to the formation of 6 mol of H₂ per mol of ethanol:



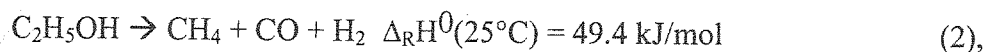
This reaction has to be carried out in more than three steps: (i) a high-temperature endothermic step (steam reforming), in which ethanol is converted to a gaseous mixture of H₂, CO, CO₂, CH₄ and unreacted H₂O (T>700°C); (ii) a subsequent, high and low temperature water gas shift reaction, in which CO is reacted with H₂O towards H₂ and CO₂ (T~200÷300°C). Because the shift reaction is equilibrium-limited, CO conversion is not complete and an additional step of CO removal (hydrogen-rich gas may contain only trace amounts of CO (<10 ppm) to avoid poisoning of the electrocatalyst of the fuel cell), (iii) selective CO oxidation (T~100÷200°C). In this case the fuel processor must consist of steam

reforming, WGS and selective CO oxidation reactors. This is the general concept of ethanol processing for fuel cell applications [1].

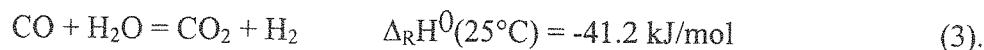
Fuel cell is extremely environmentally friendly energy generation with high efficiencies. Therefore they are particularly suitable for decentralized stationary energy supply close to the end user. The end user market is characterized by a demand for electricity and heat so that is suitable for energy provided by the combined generation of heat and power.

Fig. 1 illustrates the novel concepts of ethanol processing for combined heat and power stations on the basis of polymer electrolyte fuel cells.

The EtOH/H₂O feed is initially directed to the first reactor for decomposition of ethanol. This reactor contains bimetallic Cu-Pd supported CeO₂ catalyst and operates at temperatures 300-350°C. It produces a gaseous stream containing H₂, CO, CO₂, CH₄ and H₂O. There, CH₄, CO and H₂ are the primary products of the ethanol decomposition:



CO₂ is a secondary product and forms by the water-gas shift reaction [2, 3]:



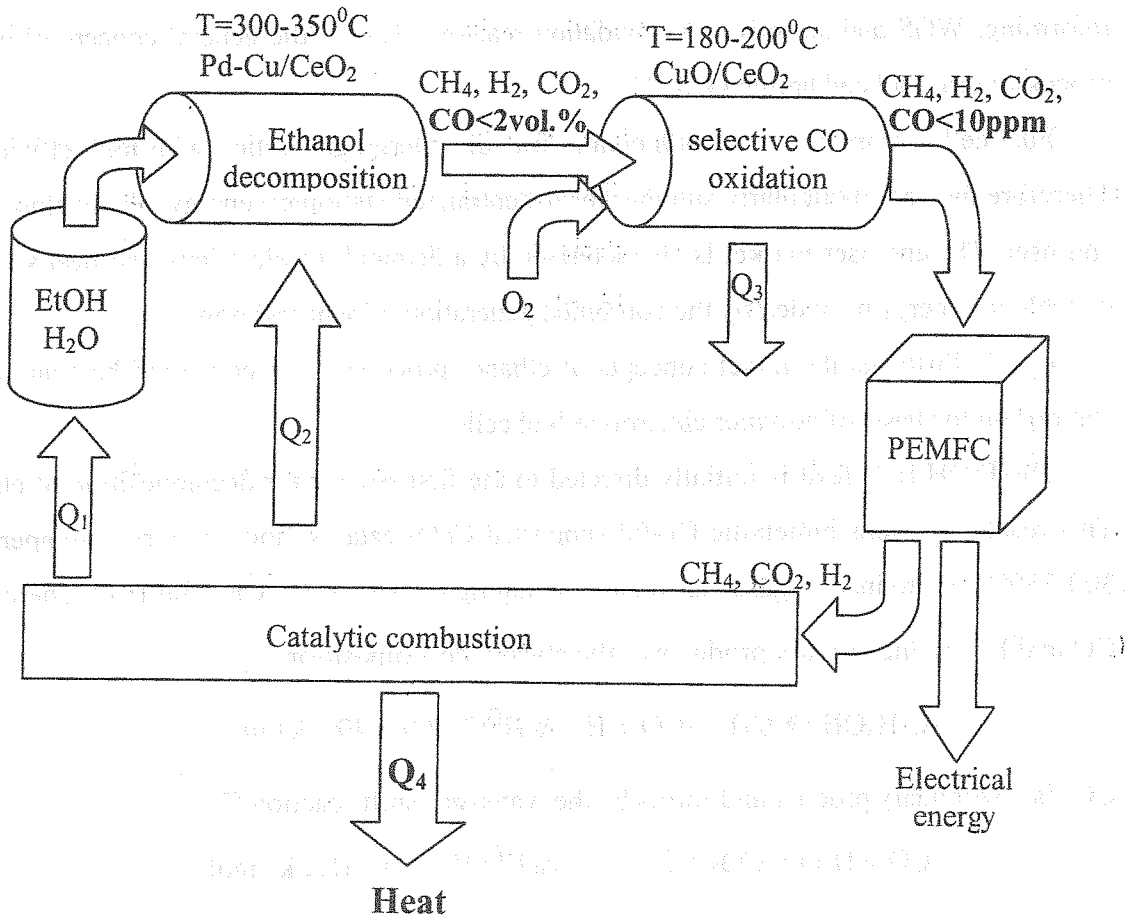
The use of bimetallic Cu-Pd catalyst supported on CeO₂ essentially promotes the water gas shift reaction (outlet concentration of CO is less than 1 vol.%) [4]. Moreover, the bimetallic catalyst showed higher activity and selectivity in ethanol decomposition reaction than the catalyst containing Pd only [4].

After cooling, the reactor outlet stream enters the selective CO oxidation reactors where the remaining CO is totally oxidized with the addition of small amounts of oxygen to CO₂. In this reactor we used CuO-CeO₂ catalyst which worked within temperature range of 180-200°C (residual CO ~10ppm) [5].

The CO-free, hydrogen-rich stream is then fed to the fuel cell, where hydrogen is electrochemically oxidized to H₂O with simultaneous production of electrical energy.

Methane and non-converted hydrogen after catalytic combustion are used for heating endothermic processes such as ethanol vaporization and decomposition, and heat supply to the end user.

In this work we present new approach to use ethanol for combined heat and power stations on the basis of polymer electrolyte fuel cells. Concept of ethanol processing is suggested.



References

1. Theophilos Ionnedes, Thermodynamic analysis of ethanol processor for fuel cell application, *J. Power Sources*, 92 (2001) 17.
2. V.V.Galvita, G.L.Semin, V.D.Belyaev, V.A.Semikolenov, P.Tsiakaras, V.A.Sobyanin, Synthesis gas production by steam reforming of ethanol, *Appl. Catal. A: General*, 220 (2001) 123.
3. Galvita, V.V., Belyaev, V.D., Semikolenov, V.A., Tsiakaras, P., Frumin, A.V. and Sobyanin, V.A.: Ethanol decomposition over Pd-based catalyst in the presence of steam, *React. Kinet. Catal. Lett.* 76 (2002) 343.
4. Galvita V., Sundmacher K., Production of hydrogen by reforming of bioethanol in a two-layer fixed bed reactor for fuel cell applications, International Conference Innovation in the Manufacture and Use of Hydrogen, October 15-17, Dresden, Germany
5. Snytnikov P.V., Galvita V.V., Belyaev V.D., Semin G.L., Stadnichenko A.I., Sobyanin V.A., Selective oxidation of CO in H₂-rich gas over CuO-CeO₂ catalysts EuropaCat-VI, Innsbruck, Austria, 31. August-4 September, 2003, A3.088.

KINETIC MODEL OF α -METHYLSTYRENE OLIGOMERIZATION IN THE PRESENCE OF NaHY ZEOLITE

**N.G. Grigor'eva, A.N. Khazipova, I.M. Gubaidullin,
A.V. Balaev, B.I. Kutepov, R.R. Galyautdinova**

*Institute of Petrochemistry and Catalysis, Bashkortostan Republic Academy of Science and
Ufa Scientific Center, Russian Academy of Science
Bashkortostan, Ufa, Prospect Oktyabrya, 141 irekmars@mail.ru*

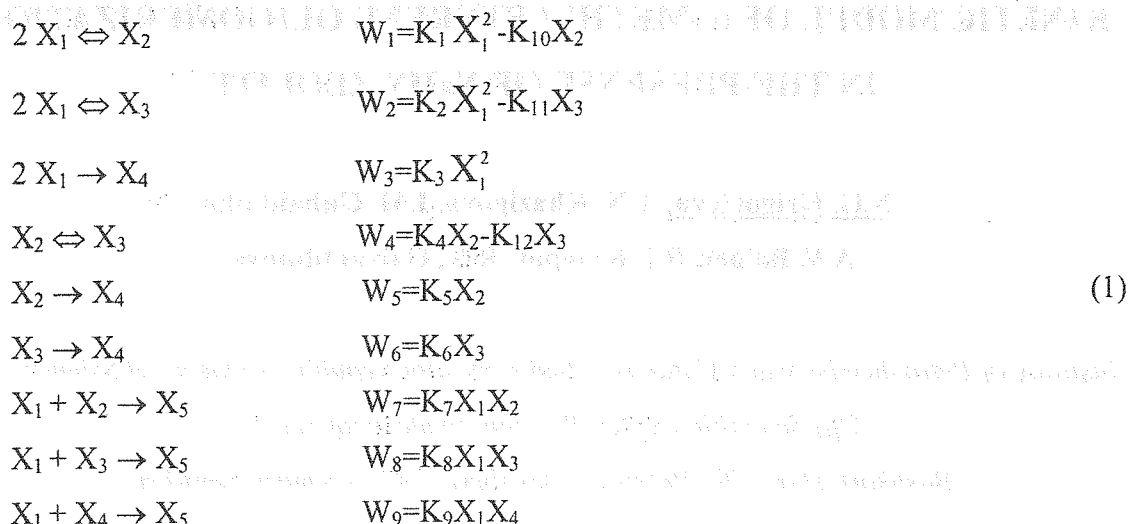
The α -methylstyrene dimers are known to be practically important and useful compounds. The linear dimers – 4-methyl-2,4-diphenylpenten-1 (α -dimer) and 4-methyl-2,4-diphenylpenten-2 (β -dimer) – are used as growth regulators of polymer chains in the production of polystyrene plastificators and as a base for synthetic oil lubricants. A cyclic dimer (1,1,3-trimethyl-3-phenylindan) is of interest as a reactive fuel, an organic glass plastificator and a scintillator component.

The paper presents the results of a study of α -methylstyrene oligomerization in the presence of zeolite of Y type. The reaction proceed at atmospheric pressure in temperature range of 40...120°C. Zeolite of Y type in NaH-form was used as a catalyst, an amount of the latter consists of 5...20% from that of a reagent. A quantitative analysis was carried out by gas-liquid chromatography method.

An effect of reaction conditions (temperature, catalyst amount, time) on yield and product composition of α -methylstyrene oligomerization was studied. In catalyst concentration of 5-15% mas. and at temperature of 70-100°C the reaction proceeds to give mainly linear dimers. A generation selectivity of the latter's consists of 90-92% mas. in α -methylstyrene conversion of 96-100% mas. With a rise of temperature and catalyst amount an yield of cyclic dimer sharply increases and gradually the latter is the main product.

A change in the dimer composition in time proceeds as follows: α -isomer is the first to be formed, in dependence on experiment temperature its concentration fast attains a maximum value and then gradually decreases. A concentration of β -isomer increases rather slower and proceeds via maximum. A cyclic dimer concentration sufficiently increases with temperature rise.

A following scheme of chemical transformations and the corresponding kinetic equations of step rates was made up on the basis of experiment analysis:



An indexation in (1): 1 – α -methylstyrene, 2 – α -dimer, 3 – β -dimer, 4 – cyclic dimer, 5 – trimer.

All experimental data were generated under isothermal conditions in periodic reactor with a mixer. The heterogeneous catalytic processes in the reactor may be correctly described in an approximation of ideal mixing. A mathematic description was developed with regard for the reactions proceeded with a marked decreasing of mole number of reaction gas mixture (or reaction volume).

Then, a mathematic description of the α -methylstyrene oligomerization process in isothermal reactor of ideal mixing is presented by equation system (2),(3).

$$\frac{dN}{dt} = \frac{G_k}{V_p} \sum_j \delta_j W_j = F_N, \quad \delta_j = \sum_i v_{ij}, \quad j=1\dots9 \quad (2)$$

$$\frac{dx_i}{dt} = \frac{F_i - x_i F_N}{N}, \quad F_i = \frac{G_k}{V_p} \sum_j v_{ij} W_j, \quad i=1\dots5 \quad (3)$$

bound conditions – $l=0$: $X_i = X_i^0$, $N=1$.

where x_i -component concentration, W_j – chemical reaction rates, $N=C/C_0$ – relative change in mole number of reaction mixture, v_{ij} – stoichiometric coefficients determined by transformation scheme (1), C and C_0 – mole density of reaction mixture and its initial value, G_k – catalyst weight, V_p – reactor volume, T – time.

The mathematic description (2), (3) with kinetic equations of a system of usual differential equations (2), (3) was carried out by the Kutt-Merson modified method.

A choice of kinetic parameters was carried out with the use of program complex developed in ICC AS BR and USC RAS. The calculations were carried out by an accidental choice with parabolic launching according to the chosen direction of constant choice.

Numerical values of kinetic parameters are listed in Table 1.

Table 1.

**Numerical values of Kinetic Parameters of α -Methylstyrene Oligomerization
Process in the Presence of 0,46 NaHY Catalyst**

No constant	$K_i (90^\circ\text{C}),$ $\text{m}^3/(\text{kg}_{\text{cat}}\cdot\text{hr})$	$E_i,$ kcal/mol	No constant	$K_i (90^\circ\text{C}),$ hr^{-1}	$E_i,$ kcal/mol
1	3,04	22,5	4	0,377	23,6
2	0,487	26,4	5	$2,1\cdot 10^{-2}$	27,9
3	0,339	28,7	6	0,101	8,8
7	$1,1\cdot 10^{-3}$	13,9	10	$2,0\cdot 10^{-2}$	23,1
8	2,574	9,1	11	$5,1\cdot 10^{-2}$	18,4
9	$3,1\cdot 10^{-3}$	11,5	12	$2,8\cdot 10^{-2}$	13,8

A comparison of calculated and experimental data is listed in Table 2 and Table 3.

Table 2.

**Comparison of Calculated and Experimental Values of Component
Concentration at 80°C and Catalyst Content 5% mas.**

Component	Time, hr							
	0,5		1,0		2,0		3,0	
	exper.	calcul.	exper.	calcul.	exper.	calcul.	exper.	calcul.
α -methylstyrene	58,6	68,7	51,1	52,2	41,0	35,0	31,1	26,2
α -dimer	33,1	25,9	39,5	39,3	48,0	52,6	56,1	59,1
β -dimer	2,4	2,4	2,7	3,1	3,1	3,4	3,5	3,5
cyclic dimer	2,0	2,0	2,4	3,0	3,1	4,1	3,3	5,1
trimers	3,9	1,0	4,3	2,4	4,8	4,8	6,1	6,6

Table 3.

**Comparison of Calculated and Experimental Values of Component
Concentration at 90°C and Catalyst Content 5% mas.**

Component	Time, hr							
	0,5		1,0		2,0		3,0	
	exper.	calcul.	exper.	calcul.	exper.	calcul.	exper.	calcul.
α -methylstyrene	38,7	43,3	27,5	55,7	14,4	63,4	5,6	8,3
α -dimer	44,0	44,0	54,1	55,7	63,8	63,4	67,5	66,5
β -dimer	5,8	6,5	6,0	8,0	9,4	9,2	11,7	10,6
cyclic dimer	6,5	5,0	6,6	6,3	7,1	7,4	8,8	8,2
trimers	5,0	1,2	5,8	2,5	5,3	4,2	6,4	6,4

An accuracy of a description of experimental data on a change in component concentration is error limits of an quantitative analysis.

PROCESS MODELING OF α -METHYLSTYRENE OLIGOMERIZATION IN TUBULAR REACTORS

N.G. Grigor'eva, A.N. Khazipova, I.M. Gubaidullin,

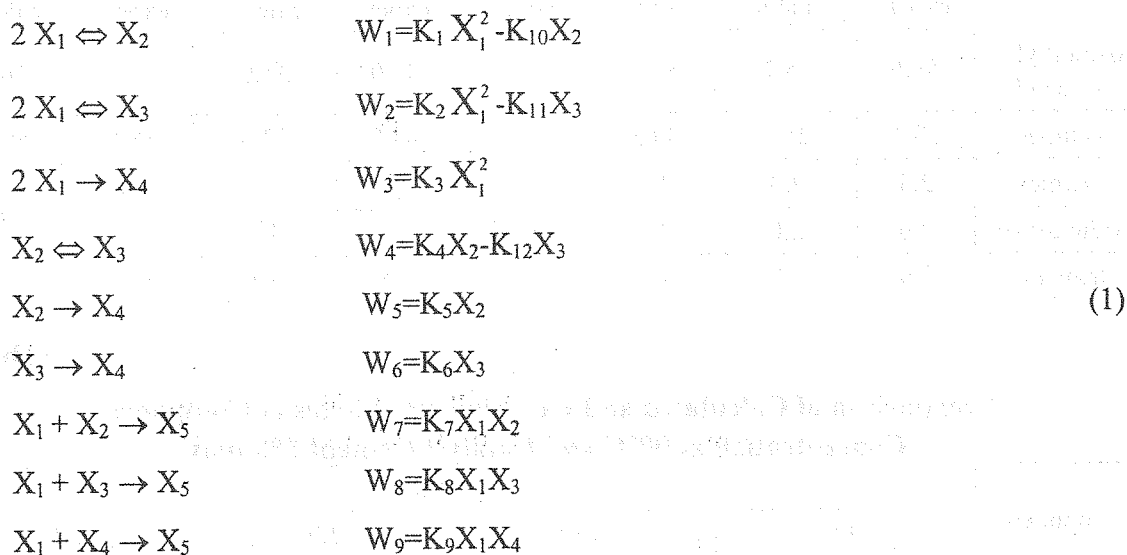
A.V. Balaev, B.I. Kutepov, R.R. Galvautdinova

*Institute of Petrochemistry and Catalysis, Bashkortostan Republic Academy of Science, and
Ufa Scientific Center, Russian Academy of Science.*

Bashkortostan, Ufa, Prospect Oktyabrya, 141 irekmars@mail.ru

To study regulations of a process proceeding in the liquid-solid catalyst reaction system a mathematic model was developed, the latter takes into account a sufficient decreasing in mole number in a reaction phase during chemical reaction proceeding.

A scheme of chemical transformations and corresponding kinetic equations of step is as follows :



Indexation in (1) : 1 - α -methylstyrene, 2 - α -dimer, 3 - β -dimer, 4 - cyclic dimer, 5 - trimer.

A mathematic description of non-isothermal process of α -methylstyrene oligomerization in a reactor with immovable catalyst layer is represented by an equation system of material and thermal balance (2)...(5) :

$$\frac{C_p N}{S} \frac{dT}{dl} = \gamma_k \sum Q_j W_j + \alpha_x S_x (T_x - T) \quad (2)$$

$$\frac{G_w C_w}{S} \frac{dT_x}{dl} = \alpha_x S_x (T - T_x) \quad (3)$$

$$\frac{1}{S} \frac{dN}{dl} = \gamma_k \sum_j \delta_j W_j, \quad \delta_j = \sum_i \nu_{ij} \quad (4)$$

$$\frac{1}{S} \frac{dx_i}{dl} = \frac{F_i - x_i F_N}{N}, \quad F_i = \gamma_k \sum_j \nu_{ij} W_j, \quad i=1\dots5 \quad (5)$$

bound conditions - 1=0: $X_i = X_i^0$, $N=N_0$, $T=T_0$,

where x_{ij} - component concentrations; W_j - chemical reaction rates; ν_{ij} - stoichiometric coefficients; N - mole consumption of a reaction mixture; T and T_x - temperatures of reaction medium and refrigerant; γ_k - bulk weight of a catalyst; C_p - mole heat capacity of a reaction mixture; Q_j - reaction heat effects; α_x - heat transfer coefficient via tube wall; S_x - specific surface of reaction tubes; S - tube cross-section; l - axial coordinate.

A calculation of a process for two technologic variants is possible with the use of a mathematic description (2)...(5) : in a reactor with heat removal and in adiabatic reactor (in this case in heat balance equation a heat transfer coefficient α_x corresponds to zero). A solution of a system of ordinary differential equation (2)...(5) was carried out by Cutt-Merson modified method.

The values of component enthalpies and of dependence of specific heat capacities on temperature were evaluated according to methods in /1/. The thermal physical parameters are listed in Table 1.

A semiempirical criterion equation (6) resulted from an analysis of processes in tubular heat exchangers /2/ was used for a calculation of heat transfer coefficient via a tube wall:

$$Nu = 0.037 * Re^{0.75} * Pr^{0.4} \left(\frac{\mu}{\mu_w} \right)^{0.11} \quad (6)$$

Where (Nu), (Re) and (Pr) criteria correspond to:

$$Nu = \frac{\alpha_x d_{tp}}{\lambda_w}, \quad Re = \frac{G_w d_{tp}}{S \mu_w}, \quad Pr = \frac{\mu_w c_w}{\lambda_w}$$

Where G_w and C_w - mixture consumption and heat capacity of refrigerant; λ_w and μ_w - heat transfer and viscosity of refrigerent.

When water is used as refrigerent , $\mu = \mu_w$ and the last cofactor in equation (6) correspond to 1.

Table 1

Values of Component Thermal Dynamic Parameters of Reaction Mixture of α -Methylstyrene Oligomerization Process

Parameter Names	Material Name				
	α -methylstyrene	α -dimer	β -dimer	Cyclic dimer	trimer
Gross-formulae	C_9H_{10}	$C_{18}H_{20}$	$C_{18}H_{20}$	$C_{18}H_{20}$	$C_{27}H_{30}$
Molecular weight, M (g/mole)	118,1	236,2	236,2	236,2	354,3
Standart heat of formation at 298 K, ΔH^0 (kcal/mole)	27,0	31,4	34,0	15,0	41,1
Constants in a series of heat capacity, C_p (cal/mole/K):					
A	-5,811	-21,98	-22,82	-26,72	-35,49
B	165,6	369,4	364,5	392,5	567,6
C	-108,2	-243,6	-236,0	-264,3	-378,5
D	28,2	60,03	57,27	66,1	93,97

Heat effects (kcal/mole) of chemical reactions (1) correspond to :

$$Q_1 = 22.6, Q_2 = 20.0, Q_3 = 39.0, Q_4 = -2.63, Q_5 = 16.4, Q_6 = 19.0, Q_7 = 17.3, Q_8 = 19.9, Q_9 = 0.92.$$

Component heat capacities and mole heat capacity of the reaction mixture according to Table 1 data are calculated by equation (7) :

$$C_{pi} = A_i + B_i(T/1000) + C_i(T/1000)^2 + D_i(T/1000)^3, \quad C_p = \sum C_{pi} X_i \quad (7)$$

At input temperature of 30°C the component heat capacities change in a range of 35...70 cal/mole K). Under adiabatic conditions a heating in the reactor is higher than 300°C due to the high exothermicity of α -methylstyrene oligomerization reactions. The above temperature is sufficiently higher than a limit value ($\sim 100^\circ\text{C}$) recommended by an experiment.

The main target of the process is to produce linear dimers and such a heating in a reactor is inadmissible either due to the loss of process control or to the preliminar formation of cyclic dimer.

Thus the modeling of α -methylstyrene oligomerization process in a tubular reactor was carried out. Results are given in Graf.1 and 2.

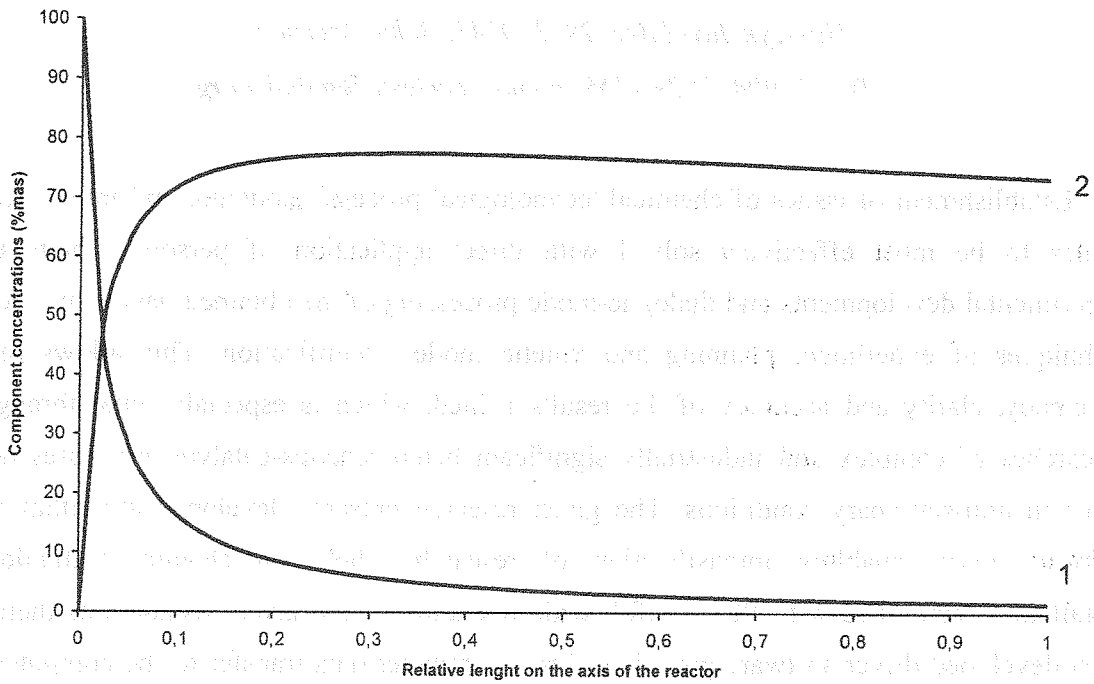
A calculating experiment for tubular reactor of $2,5 \text{ m}^3$ with a water as a refrigerant was carried out with the use of mathematic description (2)...(5). A choice of the catalyst amount was caused by the given output of linear dimers of 500 ton for 2-3 months.

The dependence of linear dimers output and maximum temperature on regime parameters were found : input temperature, α -methylstyrene, heat removal surface and diameter of reaction tubes.

The sensibility of regime parameters of α -methylstyrene oligomerization process to input temperature was calculated to be weak. Thus in the further calculations to choose optimal regimes the input temperature will be considered to be 30°C .

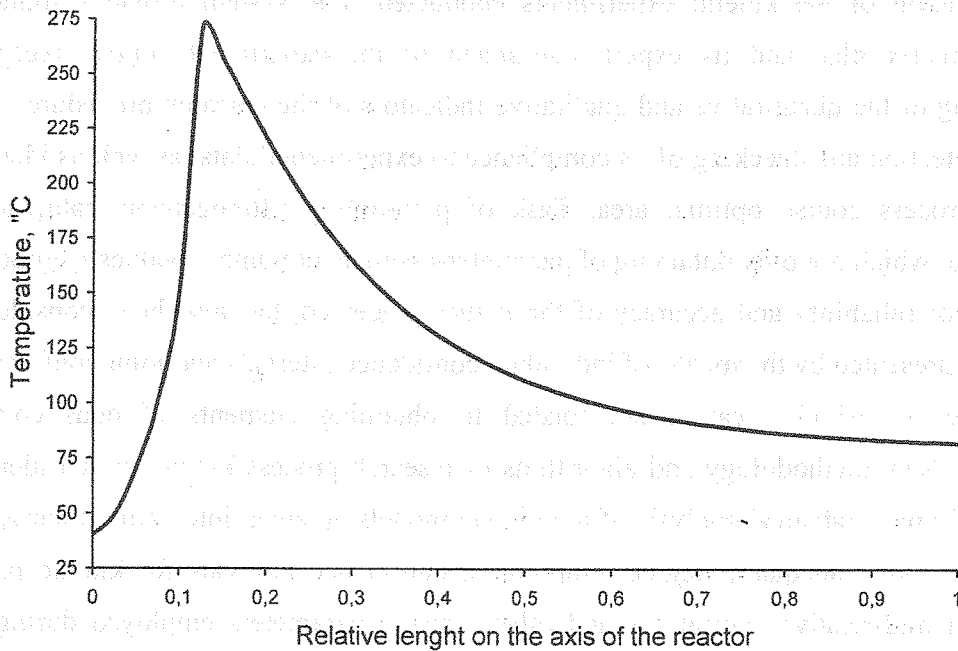
References

1. Reed R, Shervood T., Prausnitz J.M. Properties of gases and liquids. L. : Chemistry, 1982, 591 p.
2. Gukauskas A.A., Makaryavichus V.I., Shlangauskas A.A. Teplootdacha puchkov trub v poperechnom potoke gitkosti. M. : Energiya, 1975, 276 p.



Graf.1

The concentration change of α -MS (1) and linear dimers (2) on the length of



Graf.2

The temperature change of a reaction mixture on the length of tubes.

METHODOLOGY OF KINETIC MODEL IDENTIFICATION**I.Yu. Ibadzadeh, K.A. Guseynov, R.M. Kasimov, E.M. Mamedov***Institute of Chemical Problems National Academy of Sciences, Azerbaijan**Husseyn Javid Ave. 29, 370143, Baku, Azerbaijan**Tel.: (+99412) 39 4159, e-mail: ecclesia@ggbaku.org*

Establishment of issues of chemical/technological process' modeling and intensification comes to be most effectively solved with direct application of personal computer in experimental developments and dialogue-mode processing of the obtained data using modern techniques of experiment planning and kinetic model identification. This allows raising efficiency, clarity and accuracy of the results gained, which is especially vital throughout researches of complex and industrially significant heterogeneous-catalytic processes taking place in non-stationary conditions. The given research presents developed algorithmic and software tools, enabling intensification of researches held on chemical-technological installations combined with PC. For full-scale operation of the given installations there has been developed driver software providing direct parameter data transfer to the computer and output task codes onto the installation controls. Dialogue system, including software implementing various methods of optimal planning has been specifically developed for intensification of the kinetic experiments conducted. The system provides foundation of default matrix plan and its expert assessment of the experiment course, reception and processing of the quantitative and qualitative indicators of the research procedure, regressive model detection and checking of its compliance to experimental data, as well as identification of the process course optimal area. Task of pinpointing heterogeneous-catalytic process models, in which not only obtaining of parameter-assessment numeric values is important, but research of reliability and accuracy of the values perceived, has also been considered. This could be presented by the means of individual confidence intervals and joint confidence areas, difficulties of which creation are related to obtaining elements of quasi-covariational matrixes. New methodology and algorithms of research process kinetic model identification are based upon statistical analysis of the kinetic models obtained integrating their assessment nonlinearity and adequacy degree, pinpointing confidence intervals for kinetic parameters, values of mid-relative aberrations and other statistic parameters employed during the best model consecutive selection from the list. The given methodology has been used in studies of lower olefine acetoxylation reactions in particular, and several other chemical processes.

NEW PROCESS OF CATALYTIC DECOMPOSITION OF INORGANIC PEROXIDATES

E.G. Ippolitov, O.A. Kruglikova*, G.N. Kablutshaja*

Kurnakov Institute of General & Inorganic Chemistry, Moscow, Russia

**Moscow Pedagogical State University, Russia*

At study of catalytic decomposition of water solutions of perborates in at pH 8-13 the new catalyst is found. The reaction of decomposition пероксобората of sodium under certain conditions goes with this catalyst in an oscillatory mode.

It was revealed, that the accumulation of a peroxide product is possible at 295K. At 333K the reaction proceeds only with isolation of oxygen, similarly to decomposition of hydrogen peroxide solutions of the same concentration.

The carrying out of similar research for potassium hexahydroperoxostannate with this catalyst has shown, that the oscillatory process does not occur and does not depend on concentration of the catalyst.

Thus, the action of the detected catalyst is specific for peroxoborates. We can hope, that the determination of the mechanism of new oscillatory process will allow developing the new approach to catalytic oxidation by oxygen in reactors of a flowing type. With this purpose the opportunity of formation hydroxo- and hydroperoxoradicals by a method of inhibition [1, 2] was investigated. It was found, that the process is radical in interval pH that was investigated.

[1] V.A.Lunenok-Burmakina etc. Ukr.Chem.Journal, 1981, T.47, №10, with 1097

[2] N.I.Kusnetsova, L.G.Detusheva, Kinetics and catalysis, 1992, T.33, №.3, with 516.

PROCESSING OF LIQUID RADIOACTIVE WASTES CONTAINING ORGANOPHOSPHORUS COMPOUNDS

VI. Karpenko¹, O.A. Ozhereliev¹, A.N. Pestryakov²

¹*Seversk State Technological Institute, Seversk 636036, Russia,*

fax: 3822-77-95-29, e-mail: karpenko_vita@mail.ru

²*Fritz-Haber-Institut der MPG, Berlin 14195, Germany,*

fax: 49-30-8413-4405, e-mail: alex@fhi-berlin.mpg.de

Neutralization of liquid radioactive P-containing wastes of nuclear power using CaO powder as absorbent and catalyst has been studied in uniflow system. During the process all organophosphorus compounds were absorbed and converted to corrosion-inactive calcium phosphates. Radioactive elements were remained in the solid phase. Diluent hydrocarbons and organic fragments of P-containing molecules were oxidized by air to $\text{CO}_2 + \text{H}_2\text{O}$. In the case of applying the additional catalytic reactor containing honecomb supported Pt catalyst the degree of neutralization of gas emissions reached 95-98 %. On the base of thermodynamic calculations and laboratory tests a technological scheme of neutralization of the radioactive liquid P-containing wastes was suggested.

Introduction

Neutralization of radioactive wastes is one of the main problems of nuclear power [1]. Liquid wastes are the most dangerous because of their potential threat at long-term preservation (leakage of storage tanks, chemical reaction forming gaseous products, etc.). Conventional methods of the liquid wastes processing include hardening procedures – bitumization, cement, glazing, etc.

However, some of these problems are not solved till now. One of them is processing of the used liquid extraction compositions containing organophosphorus compounds and radioactive nuclides. Now this kind of the wastes is stored in tanks in liquid form and poses a threat for environment. Traditional methods of the neutralization of liquid wastes (incineration, plasma destruction, catalytic conversion [2-3]) can not be used because of the presence of phosphorus compounds. Phosphorus oxides are strong corroding agents for any kinds of steel; moreover, they fast deactivate all the catalysts [4-5].

The aim of the present study is development of the technology of liquid radioactive P-containing waste processing.

Experimental

The experiments were carried out in flow catalytic system under the following operating conditions: temperature 400-600°C; air flow rate 10 ml/s; consumption of tributylphosphate (TBP) was 1 g/s; composition of liquid organic waste - 45 % TBP, 40 % diluent (C₈-C₁₂ hydrocarbon mixture), 15 % H₂O. Reactor contained 5 g of CaO powder for neutralization of phosphorus oxides. The exhaust products were analyzed by chromatographic method.

Results and Discussion

Thermodynamic calculations revealed that for complete oxidation of 1 kg of the studied liquid waste the concentration of oxygen about 1500 mole/kg in air-vapor mixture is necessary. For total conversion of phosphorus oxides to corrosion-inactive phosphates consumption of CaO should be 450 mole/kg (Fig. 1)

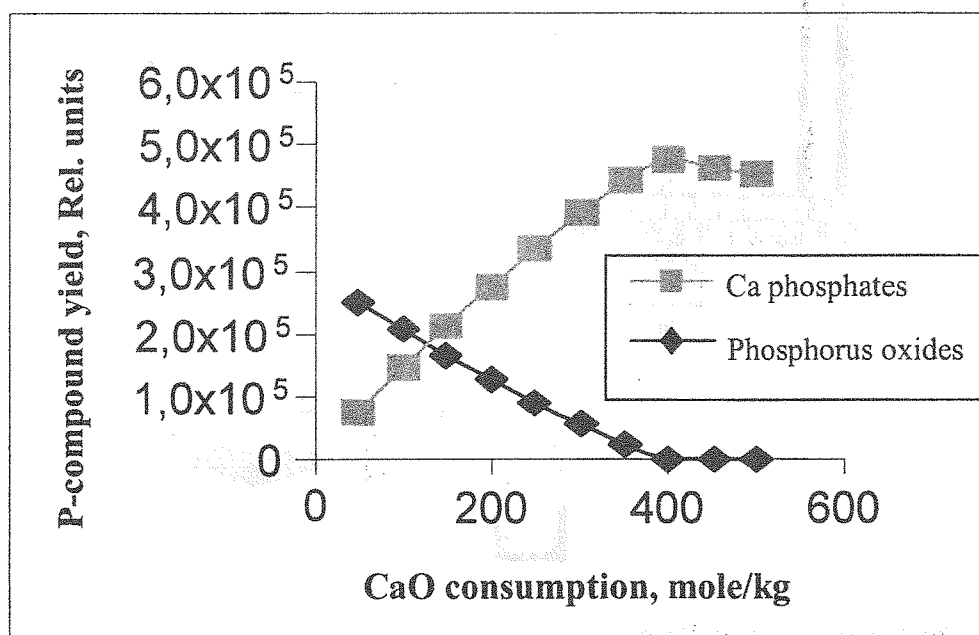


Figure 1. P-containing compounds yield versus CaO consumption

During the process TBP was oxidized in the reactor by oxygen in vapor-air mixture. Phosphorus oxides (products of oxidation) reacted with CaO powder forming grey friable powder of calcium phosphates. CaO partly catalyzed oxidation of hydrocarbons to CO₂, CO and other O-containing molecules. For total oxidation of HC to CO₂ and H₂O in the exhaust

gases the additional reactor contained honeycomb supported Pt catalyst was applied after P-absorbing system.

Usage of the calculated amounts of the reactants gave 100 % conversion of TBP to corrosion-inactive phosphates and 95-98 % conversion of hydrocarbons to $\text{CO}_2 + \text{H}_2\text{O}$. In the case of neutralization of radioactive TBP mixture the phosphate powder contains radioactive elements and may be utilized by standard methods.

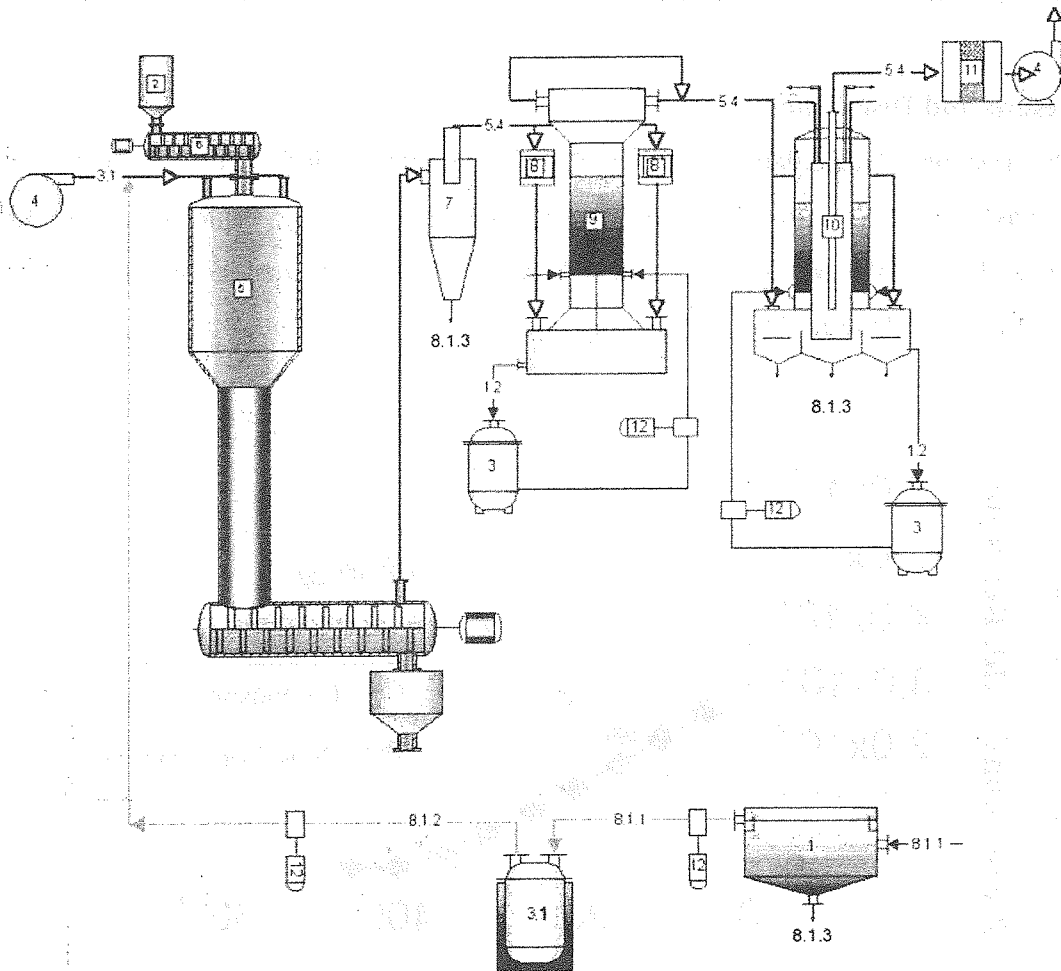


Figure 2. Technological scheme of the process.

- 1 – settling chamber; 2 – container with CaO; 3 – buffer containers; 4 – air pumps;
- 5 – neutralizer; 6 – CaO dosing screw; 7 – cyclone collector; 8 – catalytic reactor;
- 9 – foam scrubber; 10 – absorber; 11 – fine-fiber filter; 12 – rotary pumps;
- 1.2 – solutions; 5.4 – products of oxidation; 8.1.1 – organic wastes;
- 8.1.2 – heated organic wastes; 8.1.3 – mechanical impurities

On the base of results of thermodynamic calculations and laboratory experiments we suggest a technological scheme of neutralization of the radioactive liquid P-containing wastes (Fig. 2). The scheme consists in three main stages:

- pretreatment of the liquid wastes;
- neutralization of P-containing compounds with CaO powder;
- total oxidation of the exhaust gases.

Organic solution is extracted from the shipping container to the tank 3.1 through the coarse filter. Then it goes to the settling chamber 1 to remove mechanical impurities. Tank 3.1 has hot-water heater to decrease the waste viscosity. Then the solution is injected into the hot air flow and the gas mixture goes to the uniflow reactor 5 containing CaO powder. The process of P-compounds neutralization occurs at 600-700°C in autothermal mode forming calcium phosphates. The radioactive elements (mainly in the form of uranium nitrates) are decomposed to oxides and adsorbed on the powder surface. Hydrocarbons and organic fragments of the waste molecules are oxidized mainly to $\text{CO}_2 + \text{H}_2\text{O}$, as well as CO and other O-containing compounds. At accurate operating conditions the concentration of the products of partial oxidation does not exceed 100 mg/m^3 . Concentration of the nitrogen oxides is about $10\text{-}20 \text{ mg/m}^3$. Sulfur contained in the wastes is converted to calcium sulfates and remains in the powder. Then the exhaust gases come into the cyclone collector 7 to separate mechanical impurities and dust. After mechanical purification the exhaust gases are pumped into the catalytic reactor 8 for reburning CO and organic molecules. The neutralizer contains honeycomb supported Pt catalyst. To avoid emissions of the fine-dispersive particles to atmosphere the exhaust gases are washed with soda solution in the jet device 9 and film apparatus 10 and filtered on fine-fiber filter 11.

Solid products of the process consist in calcium phosphates, sulfates and contaminations of radioactive elements. They are transferred to standard treatment for extraction of uranium or to burial in the container for solid radioactive wastes.

References

1. Concept of development of nuclear power up to 2010, Moscow, Minatom, 2000, 29 p.
2. M.N.Bernadiner, A.P.Shurygin, Flame processing and neutralization of wastes, Moscow, Khimia, 1990.
3. O.L.Masanov, Nuclear power, 1995, Vol. 79, pp. 93-97.
4. V.V.Batratkov, V.P.Batratkov, L.N.Pivovarov, V.V.Sobol, Corrosion of construction materials. Gases and mineral acids, Moscow, Metallurgia, 1990.
5. N.M.Popova, Catalysts for purification of gas emissions, Moscow, Khimia, 1991.

IN SITU XPS CHARACTERISATION OF VPO CATALYST

**E. Kleimenov^{1*}, H. Bluhm¹, M. Hävecker¹, A. Knop-Gericke¹, A. Pestryakov¹,
D. Teschner¹, G.J. Hutchings², J.A. Lopez-Sanchez², J.K. Bartley², R. Schlögl¹**

**E-mail: kleimen@fhi-berlin.mpg.de*

¹*Fritz-Haber-Institut der Max-Planck-Gesellschaft, Department of Inorganic Chemistry,
Faradayweg 4-6, D-14195 Berlin, Germany; Fax +49 30 8413 4401*

²*Cardiff University, Department of Chemistry, P.O. Box 912, Cardiff, UK CF10 3TB*

Vanadium phosphorous oxides (VPO) are well-known as industrial catalysts for the selective oxidation of *n*-butane to maleic anhydride in the reaction



Numerous studies of the catalyst were performed in order to reveal structural peculiarities responsible for maleic anhydride formation ("active sites"). Vanadyl pyrophosphate ((VO)₂P₂O₇, V⁴⁺ phase) is generally accepted as a major phase of the active catalyst, but the presence of V⁵⁺ phases has also been found [1, 2]. A reaction mechanism with the participation of V⁵⁺ and V⁴⁺ was proposed [3], too. Thus, the nature of the active site is still under discussion.

X-ray photoelectron spectroscopy (XPS) is a well established technique for the determination of the surface oxidation state. Due to the short mean free path of electrons in a gas phase this technique generally must operate in high vacuum and can not be applied for catalyst characterisation during reaction. Our novel system overcomes this limitation. The experimental setup was developed for XPS investigations in gas atmosphere with pressure up to 5 mbar. General principles of the in-situ XPS system design can be found in [4]. The overall spectral resolution of the experimental system measured by the Ar 2p_{3/2} gas phase peak was set to better than 0.2 eV.

The VPO sample was prepared as described in [5] by heating the precursor (V₂O₄+H₃PO₄) at 145°C for 72 hours with a subsequent activation for 56 hours in 1.7% *n*-butane in air mixture at 400°C. Catalytic and structural characterization were done at standard conditions prior to the XPS measurements. The sample was investigated in a constant gas flow, regulated by mass-flow controllers. The temperature has been varied between 20°C and 400°C. Spectra were taken with two photon energies 730 eV and 1254 eV. This corresponds

to approximately 1 nm and 3 nm information depth ("surface" and "subsurface") for O1s-V2p spectral region [6]. The catalytic activity of the sample was registered by Proton Transfer Reaction –Mass Spectrometer simultaneously to the spectroscopic measurements.

The vanadium oxidation state of the catalyst was determined by two methods. Firstly, a deconvolution of V2p_{3/2} peak was performed. Two gauss components corresponding to V⁵⁺ and V⁴⁺ were used. O1s peak was used for binding energy calibration. Secondly, a formula derived by Coulston et al [7] was applied: $V_{ox}=13.82-0.68*[O(1s)-V(2p_{3/2})]$, where O(1s), V(2p_{3/2}) are the first momenta of O1s and V2p_{3/2} peaks after Shirley background subtraction. The mean oxidation state was calculated as an arithmetic average of the two results and half-difference between the results represents the error.

Table 1. Oxidation state of vanadium depending on conditions.

Gas mixture	T, °C	Oxidation state			
		Surface	Error	Subsurface	Error
<i>n</i> -butane/He+O ₂	150	4.24	0.12	4.33	0.12
<i>n</i> -butane/He+O ₂	400	4.15	0.07	4.30	0.04
<i>n</i> -butane/He	400	4.03	0.13	4.35	0.01
<i>n</i> -butane/He after 11 hours	400	3.95	0.12	4.28	0.03
<i>n</i> -butane/He	150	3.96	0.10	4.13	0.10
O ₂	400	4.42	0.10	4.47	0.01

XP spectra were taken in the reaction mixture (*n*-butane/He+O₂) at 150°C and 400°C, in anaerobic conditions (*n*-butane/He) at 400°C and 150°C and in O₂ at 400°C. Oxidation states at different conditions are shown in Table 1. The spectrum at 150°C in the reaction mixture reveals the presence of high amount of V⁵⁺. After heating to the usual reaction temperature of 400°C the V⁵⁺ amount was decreased both for surface and subsurface. The bulk oxidation state was higher and the surface oxidation state was lower than (4.22 ± 0.08) measured ex situ with X-ray tube (MgKα, 1254 eV photon energy).

After switching from aerobic to anaerobic conditions at 400°C the surface oxidation state increased and the subsurface oxidation state decreased. After cooling from 400°C to 150°C in *n*-butane/He the oxidation state developed the other way around. A decrease for the subsurface and increase for the surface was observed. This phenomenon can be explained by an oxygen redistribution and the formation of an oxygen-rich subsurface region at anaerobic

reaction conditions. The oxygen-rich region can be caused by oxygen diffusion towards the surface from deeper bulk layers or it indicates the presence of a structural phase which plays the role of a support for the active surface layer.

A decrease of the surface and subsurface oxidation state was observed after 11 hours in *n*-butane/He at 400°C. This decrease can be explained by a depletion of subsurface and surface oxygen because of the Mars-van-Krevelen mechanism which is generally accepted for this reaction. [8].

Our data represent the first XPS study of VPO under different reaction gas mixtures. The catalyst surface oxidation showed dynamic response on catalytic conditions in agreement with [9], [10]. The involvement of V^{5+} centres is supported by in situ X-ray absorption studies [2]. For the very first time our measurement give a hint to the depth location of this V^{5+} centres. A subsurface region with high oxidation state at anaerobic reaction conditions can be a sign for the subsurface location of V^{5+} centres present in the active VPO catalyst.

References

- 1 J.-C. Volta, Chemistry, 3 (2000), pp. 717-723
- 2 G. W. Coulston, S. R. Bare, H. Kung, K. Birkeland, G. K. Bethke, R. Harlow, N. Herron, P. L. Lee, Science, 275 (1997), pp 191-193
- 3 M. Abon, K. E. Bere, P. Delichere, Cat.Today, 33 (1997), p.15-23
- 4 D. F. Ogletree, H. Bluhm, G. Lebedev, C. S. Fadley, Z. Hussain, M. Salemon, Review of Sci. Instr., 73 (2002), pp. 3872-3877
- 5 J.A.Lopez-Sanchez, L. Griesel, J. K. Bartley, R. P.K. Wells, A. Liskowski, D. Su, R. Schlögl, J.-C. Volta, G. Hatchings, "High temperature preparation of vanadium phosphate catalysts using water as solvent", in print.
- 6 M. P.Seah, Surf. Interface Anal., 9 (1986), pp. 85-98
- 7 G. W. Coulston, E. A. Thompson, N. Herron, J.Catal. 163 (1996), 122
- 8 U. Rodemerck, B. Kubias, H.-W. Zanthoff, M. Baerns, Applied Catalysis A: General , 153 (1997), pp. 203-216
- 9 H. Bluhm, M. Hävecker, E. Kleimenov, A. Knop-Gericke, A. Liskowski, R. Schlögl, D. S. Su, Topics in catalysis, 23 (2003), pp. 99-107
- 10 M. Hävecker, R. W. Mayer, A. Knop-Gericke, H. Bluhm, E. Kleimenov, A. Liskowski, D. Su, R. Follath, F. G. Requejo, D. F. Ogletree, M. Salemon, J. A. Lopez-Sanchez, J. K. Bartley, G. J. Hatchings, R. Schlögl, J. Phys. Chem. B, 107, pp. 4587-4596

**STATISTICAL LATTICE MODELING
OF THE ADSORPTION AND REACTION PROCESSES
OVER THE SUPPORTED NANOPARTICLES**

E.V. Kovalyov, V.I. Elokhin, E.A. Cherezov, A.V. Myshlyavtsev

Boreskov Institute of Catalysis SB RAS

Prosp. Akad. Lavrentieva, 5, 630090, Novosibirsk, Russia

Fax: (+7-3832) 34 30 56, E-mail: elokhin@catalysis.nsk.su

The aim of the study is to reveal the mutual influence of the shape and of the surface morphology of the supported nanoparticles on the reaction kinetics. The analysis has been provided by means of the novel statistical lattice model, which imitates the physicochemical processes that proceed over the supported catalytic particles. To simulate the active metal particle the finite Kossel crystal located on the inert support has been chosen. The surface morphology of the particle is defined by distribution of heights of the metal atom columns. The metal atoms attract the nearest neighbor metal atom and the atoms of support. The attraction is characterized by interaction energies between the nearest neighbor metal atoms J_{mm} and between the metal atom and the support underneath J_{ms} . The change of morphology is caused by the thermal diffusion of the surface atoms. To simulate the diffusion of the metal atoms over the metal and support surfaces the standard the Metropolis algorithm [1] has been used. As a result the equilibrium shapes of the particle has been observed to depend on the temperature and the relative ratio of “metal-metal” and “metal-support” energies. At temperatures $\sim 700-900$ K the initial cubic shape of the metal crystal move to hemisphere. Increasing the temperature up to 1100 K result in dispersed shape of the particle, if such particles are located close enough, the coalescence of particles is possible.

The model reaction $A+B_2$ has been studied [2] (monomolecular adsorption of A , dissociative adsorption of B_2 and reaction between A_{ads} and B_{ads}) taking into account the roughening of the particle surface and the spillover phenomena of the adsorbed A_{ads} species over the support. The influence of the adsorption and the reaction processes on the equilibrium shape of the nm-sized particles was also investigated. The following propositions had been made to model the reaction proceeding on the supported catalyst particle: 1) the reaction starts on the equilibrium shape of the particle at a particular temperature; 2) B_2

molecule can adsorb with subsequent dissociation only on the two neighboring active sites of the catalyst particle situated at the same level; 3) A molecule can adsorb and diffuse both on the metal and support surface (spillover); 4) desorption of A_{ads} and B_{ads} is neglected; 5) the reaction between A_{ads} and B_{ads} proceeds immediately when they are brought into contact due to adsorption, or A_{ads} diffusion into the two neighboring active sites situated at the same level; 6) the probabilities of adsorbed species A_{ads} diffusion are governed by the above-mentioned Metropolis algorithm; 7) the simulation procedure makes provision for taking account of the lateral interactions both of A_{ads} and B_{ads} with each other and with near neighboring metal atoms with corresponding energies. After each attempt to adsorb A or B_2 molecule several attempts of diffusion of metal atoms and A_{ads} species were performed to equilibrate both the surface of the catalyst particle and the adsorbed layer.

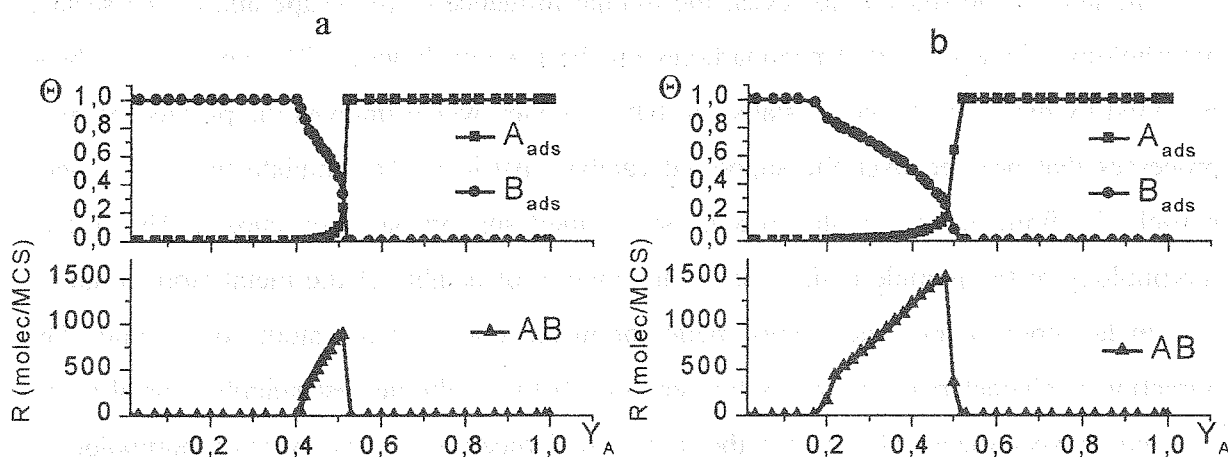


Fig. 1. The dependencies of A_{ads} and B_{ads} coverages (upper graph) and reaction rate (absolute value of formed AB molecules of product per one MCS - lower graph) versus molar ratio Y_A in the case of the flat surface of the particle. (a) The absence of A_{ads} diffusion; (b) A_{ads} diffusion over the support and the particle surfaces.

The kinetic dependencies of A_{ads} and B_{ads} coverages normalized on the number of the active sites of the catalyst particle versus molar ratio $Y_A = P_A/(P_A+P_{B_2})$ (P_i are the partial pressures of the reagents in the gas phase) obtained at different variants of the model reaction performance (with or without A_{ads} species and/or metal atoms diffusion, various ratios of interaction energies, etc.) has been compared with ones of the well-known Ziff-Gulari-Barshad model [3]. In our case ZGB-model corresponds to the performance of the reaction only on the initial flat uniform surface of the catalyst particle without any diffusion of adsorbates and metal atoms (Fig 1a). Introducing into the model the A_{ads} molecules diffusion over the metal and support surface leads to the considerable decrease of the unit B_{ads} coverage region observed in ZGB-model and to a minor shift (from 0.51 to 0.48) of the reaction rate maximum to the smaller values of Y_A [4,5] (Fig 1b) (in contrast to the behavior of ZGB-

model with A_{ads} diffusion). This effect is connected with additional source of A_{ads} molecules due to the spillover from the support to the active particle. In that way, the spillover effect leads to the effective increasing of the A reagent partial pressure.

When the reaction proceeds on the non-regular roughened surfaces all the regions with sharp stepwise changing of adsorbates coverage disappear (in this case the number of active sites convenient for B_2 adsorption is restricted) (Fig2 a-c). Introduction of the diffusion channel leads, as earlier, to the shift of the reaction window to the smaller values of Y_A . In this case (Fig. 2b) we can observe, again as earlier, the preferred occurrence of the reaction at the boundaries of the dense core of adsorbed B_{ads} island at low values of Y_A . Introduction into the model the diffusion of surface metal atoms results in the further change of the kinetic dependencies (Fig. 2c) which is connected with the dynamic change of the surface morphology determining the geometric impediments for B_2 adsorption.

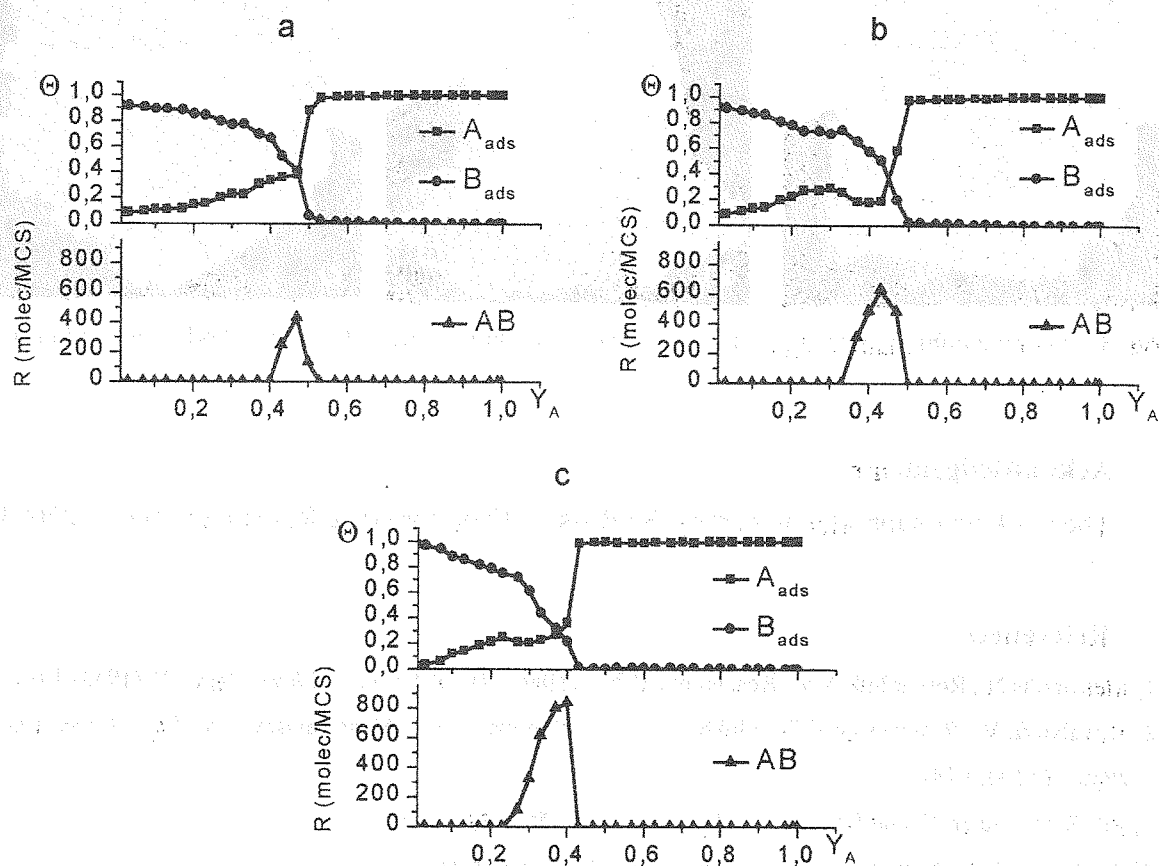


Fig. 2. The dependencies of A_{ads} and B_{ads} coverages (upper graph) and reaction rate (absolute value of formed AB molecules of product per one MCS - lower graph) versus molar ratio Y_A in the case of the roughened surface of the particle, $T = 500$ K. (a) - rigid surface, the absence of metal atoms and A_{ads} diffusion; (b) - rigid surface, A_{ads} diffusion over the support and the particle surfaces; (c) - dynamic surface, metal atoms and A_{ads} diffusion over the support and the particle surfaces.

Thus it has been shown (in the frames of the proposed model) that the shape of the active particle can change under the influence of the adsorbed layer, even in the absence of the “adsorbate-metal” interactions and that the kinetics on the nanometer-size particle can be remarkably different from those corresponding to the infinite surface. Introduction into the model the attractive interactions “adsorbate-metal” leads to the reversible adsorbate induced reshaping [6]. In this case the particles size determines the degree of reshaping, as in experiment [7].

Recently the software has been elaborated permitting the study of the 3D shapes of the equilibrated nanoparticles in the cases of the simple cubic lattice and of the body-centered metal crystal structures. Few examples of the simulated particles are shown in the Fig. 3.

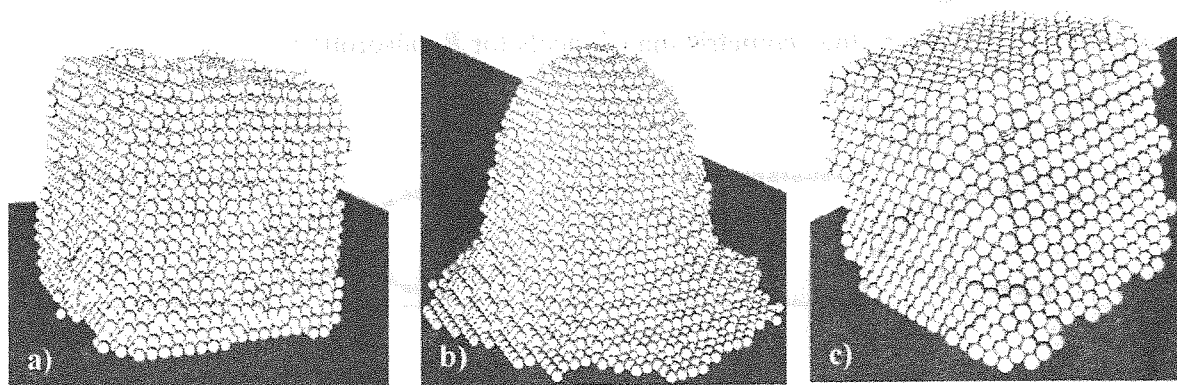


Fig. 3. a) simple cubic lattice, $J_{nm} = J_{ms}$; b) simple cubic lattice, $J_{nm} = 0.5 J_{ms}$; c) body-centered lattice, $J_{nm} = J_{ms}$.

Acknowledgements

The work was supported in part by the Russian Fund for Basic Research (# 00-03-22004).

References

- [1] Metropolis N., Rosenbluth A.V., Rosenbluth M.N., Teller A.H., Teller E., *J. Chem. Phys.*, **21** (1953) 1087.
- [2] Kovalyov E.V., Resnyanskii E.D., Elokhn V.I., Bal'zhinimaev B.S., Myshlyavtsev A.V. *Phys. Chem. Chem. Phys.*, **5** (2003) 784.
- [3] Ziff R.M., Gulari E. and Barshad Y., *Phys. Rev. Lett.*, **56** (1986) 2553.
- [4] Kaukonen H.-P., Nieminen R.M., *J. Chem. Phys.*, **91** (1989) 4380.
- [5] Ehsasi M., Matloch M., Frank O., Block J.H., Christmann K., Rys F.S., Hirschwald W., *J. Chem. Phys.*, **91** (1989) 4949.
- [6] Kovalyov E.V.; Elokhn V.I.; Myshlyavtsev A.V.; Bal'zhinimaev B.S. *Dokl. Phys. Chem.*, **381** (2001) 309.
- [7] Hansen P.L., Wagner J.B., Helveg S., Rostrup-Nielsen J.R., Clausen B.S., Topsøe H. *Science*, **295** (2002) 2053.

MATHEMATICAL MODELING OF REACTOR UNIT OF REFORMING SYSTEM TAKING INTO ACCOUNT DIFFERENT RADIAL DIRECTIONS OF ROW-GAS FLOW

A.V. Kravtsov, E.D. Ivanchina, S.A. Galushin, D.S. Poluboyartsev

Tomsk Polytechnic University, Chemical technological department,

Lenin ave. 30, Tomsk, 634034, Russia,

Fax: +7(3822)563435, E-mail: ied@zmail.ru

Experimental studies on industrial reactors with stationary catalyst layer and on stands showed the presence of the areas with essentially different velocities of row-gas flows causing hydro-dynamic non-uniformity.

Non-uniformity of coke deposits results in increasing non-homogeneity of concentration and temperature fields along with the width of reactor layer with radial input of row material. Linear velocity of the flow while moving from peripheral to central area has to be significantly increased due to decrease of cross-section square along the cone of movement of row-gas mixture. It leads to different intensity of mass-exchange processes in peripheral and central areas. While moving the row-gas mixture from the center to periphery the picture is reverse.

One of the possible methods to eliminate partially non-homogeneity of the concentration and temperature fields is to change the direction of row-gases flow from the center to periphery. In this case non-uniformity of temperature field (and hence the conversion of hydrocarbons) will be essentially lower while moving from the center to periphery because the decrease of volume velocity of the row-gases input will be compensated to some extent by the temperature decrease due to domination of endothermic reactions on the surface of catalyst.

Mathematical model of reactor with stationary grain layer and radial movement of row-gas flow is a system of equation of material and heat balance for multi-zone system with radial flow within each zone. The change of the components' concentration at the motion of gas flow in catalyst stationary layer within each zone is described as:

$$G_c \frac{\partial C_i}{\partial Z} + G_c \frac{\partial C_i}{\partial V} = \sum W_j$$

$$\text{at } Z = 0, C_i = 0,$$

$$V = 0, C_i = C_i^0 \text{ (at the entrance of the reactor),}$$

j – is the number of reaction, according the scheme of transformation of the row-material into the product; Z – is a reduced time or the whole amount of the processed row-material (m^3); G_C – is the gas expenditure; V – is the volume of catalyst; C_i – is the concentration of the substances.

In this model all zones maybe formed by cross-section of co-axial cylinders to count radial change of volume and linear velocity of row-gases flow. When the gas flows through a stationary grain catalyst layer, the input values of concentrations and temperatures of each next zone are the output values of those of the previous zone. Fig. 1 and 2 shows the coke concentration at catalyst, while the gas flows in the two possible directions.

Note that in the case of gas flow from the center to periphery the non-uniformity of coke deposition is essentially lower than that in the case of the opposite direction of the flow. The model calculation also showed that in the case of gas flow from the center to periphery the total output of aromatic hydrocarbons is 2-4% higher that can be explained by more uniform decreasing of catalyst activity.

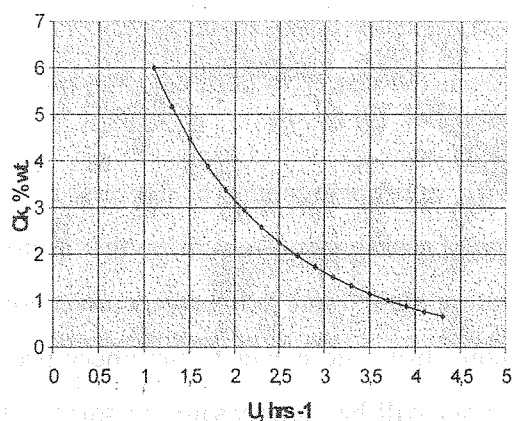


Fig. 1.

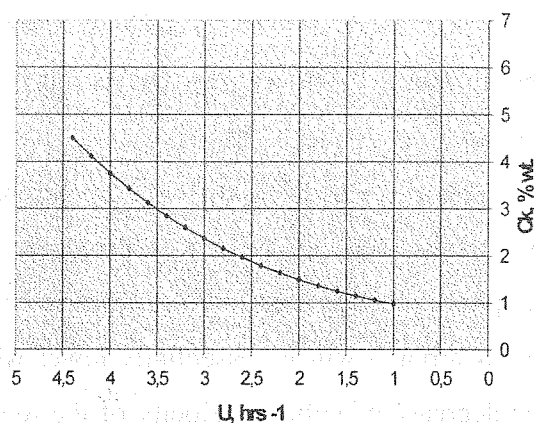


Fig. 2

Non-uniformity of coke deposits in catalyst layer is an important but not single factor to decrease the degree of transformation hydrocarbons at movement from periphery to the center.

Thermal effect of catalytic reforming is defined by the contents of cyclopentanes in row-materials as well as by depth of hydrocarbons transformation. This effect is high at the contact with peripheral layers of the catalyst and goes down while moving to the center in the direction shown in Fig. 3. To level the thermal loading and drops in reaction zone the volume

of the catalyst has to be increased along with the row-gas mixture. Moreover, the increase of the catalyst volume creates optimal conditions for ongoing the reaction of de-hydrolyzation of paraffin. For example, the change of the catalyst layout from increasing (1:2:4) to uniform one (1:1:1) decreases selectivity of the paraffin's transformation.

Table 1 presents the results of model calculation of output of aromatic hydrocarbons in the case of changing the row-gases flow. The catalyst volume was conventionally divided into 7 zones with equal radial interval.

The volume of each zone is increased at increasing the square of cross-section and the temperature is decreased as a result of endothermic process.

Table 1. Influence of the direction of row-gas flow on output of aromatic hydrocarbons.

Zone No.	Straight direction of the flow (Fig. 1)			Reverse direction of the flow (Fig. 2)			
	Volume velocity of the flow, V, hrs^{-1}	Temperature, $T, ^\circ\text{C}$	Aromatics, t/hrs	Volume velocity of the flow, V, hrs^{-1}	Temperature, $T, ^\circ\text{C}$	Aromatics, t/hrs	
1	0,6	481	16,00	0,6	430	15.06	
2	0,8	465	14,90	0,8	450	14.95	
3	1,0	450	12,69	1,0	460	14.60	
6	1,6	445	11,70	1,6	471	13.72	
7	2,5	440	8,89	2,5	481	12.98	
Average integral output			12,83	Average integral output			14,2

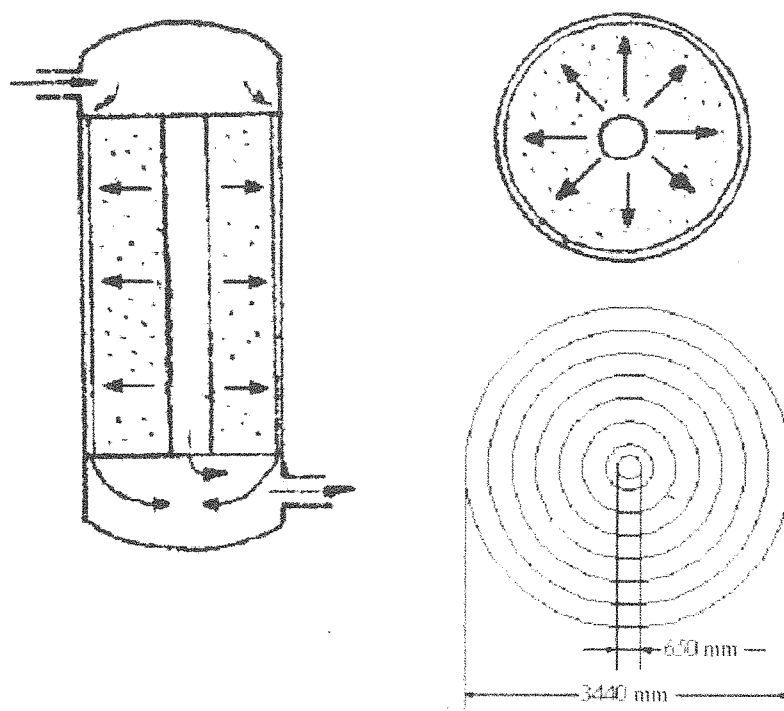


Fig. 3. Movement of the flow from the center to periphery.

The output of the aromatic hydrocarbons is the same while the row-gas mixture is moving from one conventional zone to another. Therefore the high values of volume velocities in initial zones and low output of aromatics are compensated by the higher temperatures. Table 1 shows that the output of aromatic hydrocarbons is increased due to the increasing of degree of transformation of paraffin and cyclopentanes.

Thus, non-uniformity of coke deposits on the catalyst's surface leads to hydro-dynamic non-uniformity of the row-gases flow from periphery to the center and non-uniformity of the temperature and concentration of hydrocarbons. Activity of the catalyst is changed lower while moving from the center to periphery. The output of the product is increased by 1-2% at the change of the flow direction from the center to periphery. The decrease of coke formation by 1-2% will allow to increase the inter-regeneration cycle by 1.2-1.3 times.

QUANTUM-CHEMICAL RESEARCH OF ELEMENTARY PROCESSES ON THE CATALYST SURFACE

Vitalina V. Kukueva

Fire Safety Institute, 18034, Ukraine, Cherkassy, Onoprienko, 8

The surfaces undergoes continuous changing during heterogeneous process by a such phenomena: formation and decomposition of intermediate surface compounds which have been caused by gas molecule adsorption; size and form changing of solid connected with transformation to gas products; formation the solid reaction products near the surface and so other. There are now an increasingly large number of quantum-chemical approaches in the area surface science because of its technological relevance in applied areas such as catalysis. They are convenient methods employed to solve the electronic structure problem at a surface.

Adsorption – more or less close cohesion of molecules on the solid surface, are appearing always as the first stage of chemical reaction. Although all atoms and molecules experience a van der Waals force on being brought near to a surface, those with open shells display far greater chemical interactions at close distances [1]. Theoretical treatments of this interaction assume that there is no overlap between the electrons on the atom and in the surface. The force arises from the interaction of the polarizable solid with dipolar quantum mechanical fluctuations of the atomic charge distribution. Chemisorption as against van der Waals, demands the sufficient activation energy. The formation heat can be comprised with chemical reaction formation heat. It goes through the activation complex formation between gas molecule and surface active center, and process velocity have been determined as velocity of the barrier overcoming of the potential energy curve at the molecules rapprochement.

The structure of surface's chemical compounds are defined not only the chemisorption peculiarities, but the modifying surface transformation too. It's refer not to many layer surface structure formation, but to the chemical and thermal transformations of the new functional groups immobilizing on the surface.

To investigate the chemical way to destruct of organic molecules immobilizing on the silica surface the quantum-chemical calculations have been provided by the MNDO method. The subject of reseach was threemethylphosphate $((\text{CH}_3\text{O})_3\text{P}=\text{O})$ as one of the representatives of phosphororganic compounds. Besides this substance demonstrates inhibiting properties on

the flame [2]. Hypothesis for the explanation of the negative catalyst behavior consist in the inhibitor possibility to connect the active centers of flame (H, OH, O and so oth.).

Calculations have been provided both for the isolated molecule and for the immobilized one on the silica surface. It was noted that the most energetic advantage destruction's way is radical decay in the both cases. This conclusion play clue role because the propagation of flame has chain nature. The calculation results you can see in the table.

The quantum-chemical calculation by the MNDO method of destruction ways of threemethylphosphate immobilized on the silica surface

No	The destruction's products of the three-methylphosphate on the silica surface	The formation heat ΔH_{298}^0 , kcal/mol
1	$\text{Si}[(\text{OH})_3\text{SiO}]_3\text{O}^\bullet + \text{OP}(\text{OCH}_3)_2^\bullet$	19,13
2	$\text{Si}[(\text{OH})_3\text{SiO}]_3\text{O}^- + \text{OP}(\text{OCH}_3)_2^+$	193,6
3	$\text{Si}[(\text{OH})_3\text{SiO}]_3\text{O}^+ + \text{OP}(\text{OCH}_3)_2^-$	226,19

It is worth noting that the enthalpy of isolated molecule $(\text{CH}_3\text{O})_3\text{P}=\text{O}$ ($\Delta H_{298}^0 = 143,45$ kcal/mol) almost in 7,5 times more than such values for the immobilizing one. Consequently the high-organized system (immobilization on the silica) is more predominant for the inhibiting properties of the threemethylphosphate.

For the next stage the collision complexes between destruction products and active centers of flame (H, OH, O) have been calculated to research scavenging effectiveness of these substances. The interaction probability has been estimated by the depth of minimum on the potential curves (dependence potential energy from distance between particles). The relative stability of the short living complexes have been determined by the comparative analysis of bind lengths and energies. The PO_2^\bullet have been find the most effective to connect active centers of flame among the all investigated destruction products. This result is in the good agreement with experimental works [2, 3].

References

1. A. Zangwill, Physics at surfaces (CUP, Cambridge, (1988)
2. Allen Twarowski, Combustion and flame 102: 41-54 (1995)
3. O. P. Korobejnichev, V. M. Shvarzberg, S.B. Il'in, Fisika gorenja i vzryva. 1997, т.33, № 3

PRODUCTION OF HIGH-OCTANE BLENDING FUEL BY REFORMING CATALYSATE FRACTIONATING

V.T. Liventsev, V.A. Karyakin, R.I. Kuzmina*,
G.M. Sidorov**, V.P. Sevostyanov*, V.R. Weinbender

JSC Saratov Petroleum Refinery, Saratov, Russia

**Saratov State University, Saratov, Russia*

***Ufa State Oil Technical University, Ufa, Russia*

Catalytic reforming remains principal technology of motor fuels production. Due to environmental requirements, mainstream of the modern oil reforming is production of unleaded gasoline with low benzene content.

Benzene percentage in marketable gasoline mainly depends on its content in reforming catalysate that is determined by raw materials quality and conditions of technological process. As a result, development of efficient technology of high-octane blending fuel production by reforming catalysate fractioning is an issue of the day.

Reforming catalysate is characterized by nonuniform distribution of octane units over fractions. High-boiling aromatized fractions have high values of octane unit, whereas light fractions of reformat are characterized by low octane units and considerable benzene content. Light and heavy fractions of reforming catalysate are used as high-octane blending fuel in production of unleaded gasoline, middle low-octane fraction is utilized as raw material for low-octane gasoline and aromatic hydrocarbons production. According to known technological schemes, reformat fractioning demands two or three fracking fractionators that implies complicated equipment and high power inputs.

Usually, reforming plant includes the only column of reformat stabilization therefore development of technology of reformat dividing directly in stabilization column into two parts – middle-octane and high-octane with lower benzene content – is of interest. It will permit to produce high-quality unleaded gasoline using catalysate of soft-regime reforming without expensive components, additional power inputs and capital investments.

The above problem is solved by dividing reformat into high- and middle-octane parts directly in column of reformat stabilization. It saves capital investments for additional column mounting and power inputs for fractioning.

There are three schemes of direct reformat dividing (fig. 1) developed. Unlike scheme 2, scheme 3 provides introduction of side-cut distillate from the 25th (from the bottom) plate of the first column into the top of the second column and return of distillate from the second

column in the plate of side-cut distillate output of the first column as well as middle-octane fraction withdrawal from the 2nd (from the top) plate of the second column.

It is necessary to note that schemes 1 (variant 1), 2 and 3 were figured out for the same temperature of raw material input (110 °C). However, in scheme 1 (variant 1) temperature of remainder (high-octane fraction) that is principal heat source for raw material amounts 255 °C whereas in schemes 2 and 3 – only 180 °C. Therefore in scheme 1 (variant 2), increase of remainder temperature up to 263 °C leads to raising of raw material input temperature up to 162 °C (table 1).

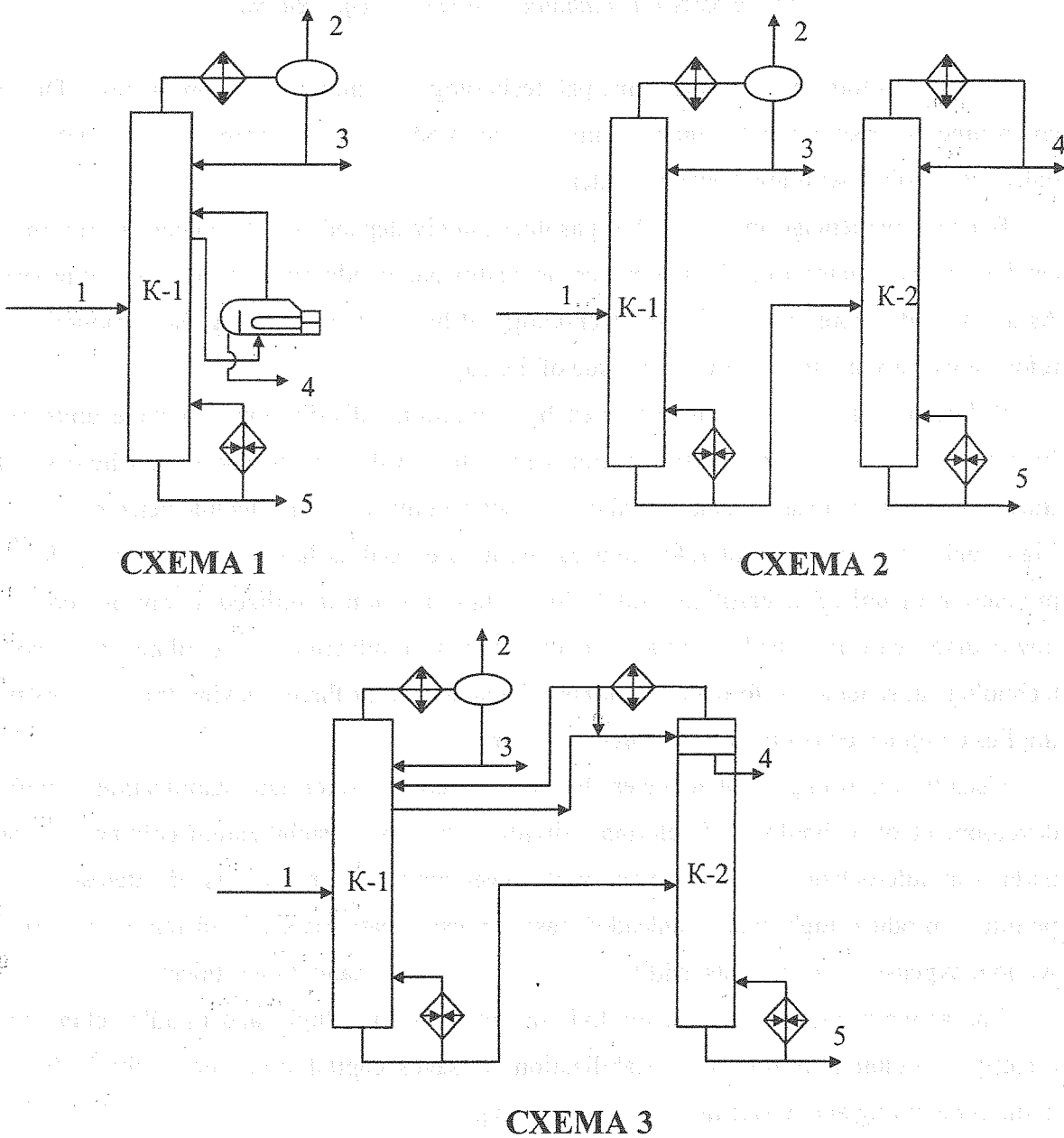


Fig. 1. Schemes of reformate dividing: 1 – raw materials; 2 – gas; 3 – top fraction of stabilization; 4 – middle-octane fraction; 5 – high-octane fraction

Optimization of reformat dividing schemes (octane unit c. 80 m.m.) with middle-octane fractions withdrawal by side-cut distillates is fulfilled. It is shown that scheme with middle-octane fractions withdrawal by side-cut distillate simultaneously both from corroborative and stripping sections is the most effective. Scheme with middle-octane fractions withdrawal by side-cut distillate from corroborative section is less effective than withdrawal from stripping section.

TABLE. Main characteristics of columns operation

Characteristics		Scheme 1		Scheme 2	Scheme 3
		Var. 1	Var. 2		
Consumption, % of raw material	side-cut distillate of the 1 st column into the 2 nd one	—	—	—	13.0
	distillate of the 2 nd column into the 1 st one	—	—	—	4.4
	hot stream of the 1 st column	247.8	260.9	200.0	204.4
	hot stream of the 2 nd column	—	—	87.0	173.9
	total consumption of hot stream	247.8	260.9	287.0	378.3
	irrigation of the 1 st column	56.9	90.4	5.4	13.0
	irrigation of the 2 nd column	—	—	62.8	93.9
	total consumption of irrigation	56.9	90.4	68.2	106.9
Temperature, °C	raw material input	110	162	110	110
	top of the 1 st column	71	70	68	68
	top of the 2 nd column	—	—	109	63
	bottom of the 1 st column	255	263	206	229
	bottom of the 2 nd column	—	—	180	180
Heat demand, MJ on 1 ton of raw material	condenser of the 1 st column	269.6	415.4	45.5	78.0
	condenser of the 2 nd column	—	—	433.6	371.6
	furnace for hot stream of the 1 st column	463.5	475.47	259.42	331.56
	hot stream of the 1 st column	263	269	225	244
	hot stream of the 2 nd column	—	—	200	185
	furnace for hot stream of the 2 nd column	—	—	277.63	205.85
	boiler	69.23	69.23	—	—

Characteristics		Scheme 1		Scheme 2	Scheme 3
		Var. 1	Var. 2		
total heat sink		269.62	415.36	479.11	449.61
total heat supply		532.6	544.70	537.05	537.41
Fractions content, % weight	iso-C ₅ – e.b. in top of stabilization*	4.69	2,76	11,5	4,97
	b.b. – C ₄ . in middle-octane fraction**	2.06	1.57	3.54	2.32
	toluene – e.b. in middle-octane fraction	13.75	1.75	1.78	3.52
	b.b. – 1,1,3-trimethylcyclopentane in high-octane fraction	6.87	1.74	1.75	2.43
	benzene in high-octane fraction	0.90	0.00	0.01	0.04
Pressure of the column top, MPa	first	1.2	1.2	1.2	1.2
	second	–	–	0.3	0.3
Octane unit, (m.m.)	middle-octane fraction	80.2	75.4	75.8	76.6
	high-octane fraction	95.6	97.8	97.7	94.4

*e.b. – end of boiling;

**b.b. – beginning of boiling.

By the example of reformatе dividing (octane unit c. 90), it is shown that scheme with middle-octane fractions withdrawal from corroborative section by side-cut distillate is more efficient than scheme of separation in two columns with successive withdrawal of stabilization top as the first column distillate whereas the last scheme is more effective than scheme with partially related streams. It is found that increase of number of plates in separation system from 40 to 100 (from 20 to 50 theoretical plates, correspondingly) does not proportionally raise quality of separation products. Thus, scheme 3 with simultaneous withdrawal of side-cut distillate from corroborative and stripping sections is the most flexible. It permits to withdraw side-cut distillate from either corroborative or stripping sections separately as well as simultaneous withdrawal from both sections. The last method is the most efficient, it greatly increases quality of motor fuels.

THE NEW METHOD OF SYNTHESIS OF TRANS-1,4-POLYISOPRENE (SYNTHETIC GUTTA PERCHA)

M.S. Chinova, O.V. Smetannikov, E.A. Mushina, Yu.Ya. Podolskiy,
E.M. Antipov, V.M. Frolov

The synthetic Gutta Percha (crystalline *trans*-1,4-polyisoprene) is used for obtaining thermoplastic materials for medical assigning, and for boot wear and tire industry.

A new catalytic system based on the titanium-magnesium catalysts has been elaborated for manufacturing of Gutta Percha. Polymerization of isoprene is performed in aliphatic solvents in the presence of titanium tetrachloride, deposited on finely dispersed magnesium dichloride, or in the presence of the same system immobilized on silica gel. Trialkylaluminum is used as co-catalyst. Polymerization proceed at 30 - 60°C at a molar ratio co-catalyst/catalyst 20 - 100 mol/mol; the concentration of isoprene in a reaction zone can be in the range from 1 to 4,8 mol/l.

According to the data of IR-spectroscopy polyisoprene obtained is characterized by a following microstructure: *trans*-1,4-units 97-98%, 3,4-units 2-3%. It was established, that the process of the isoprene polymerization proceeds via the "living chain" mechanism.

As contrasted with the natural Gutta Percha, whose crystalline phase contains both α - and β -modifications, the synthetic polymer crystallizes only in α -monocline form with melting point close to 75°C. Such unusually perfect constitution of polymer is characteristic only for a sample with nascent structure extracted directly from the chemical reactor. The melting and the subsequent crystallization results in formation of an usual β -crystalline phase.

The synthesized polyisoprene is easily processed by the melt technique and has good mechanical properties (relative elongation and the tensile strength are equal to 250-300% and 20 MPa respectively).

The financial support of the Russian Foundation for Basic Research (Grants No 02-03-32975 and 02-03-08117-inno) is gratefully acknowledged.

TITANIUM-MAGNESIUM CATALYSTS – UNIVERSAL CATALYSTS FOR POLYMERIZATION OF OLEFINS AND DIENES

O.V. Smetannikov, M.S. Chinova, E.A. Mushina, Yu.Ya. Podolskiy,

E.A. Antipov, V.M. Frolov

The new catalytic systems for olefine and diene polymerization have been created and studied. These systems are the titanium-magnesium catalysts (TMC) prepared according to the special procedure. It was established for the first time that TMC in combination with trialkylaluminum are very effective in a *trans*-polymerization of butadiene and isoprene. It was shown also that usage of these catalysts in copolymerization of butadiene and isoprene leads to formation of random copolymers. According to IR-spectroscopy, X-ray diffraction, and DSC data these catalysts allow to prepare both the crystalline and amorphous *trans*-copolymers depending on the composition of the monomer blends.

In the case of styrene polymerization the formation of isotactic polymer was observed. Some investigations were performed using TMC, modified with oligodienyl metal-aluminum complexes (metals – Ni, Zr, Ti). Oligodienyl complexes were synthesized by exchange reaction between the corresponding metal chloride and $\text{Al}(\text{i-C}_4\text{H}_9)_3$ in presense of 1,2- or 1,3-dienes.

It was found that using the modified TMC the linear low and middle density polyethylene (PE) can be obtained by homopolymerization of ethylene without the comonomers insertion. There are some evidences that these catalysts copolymerize ethylene with butene –1 (or hexene-1) with formation of high density high strength PE, whose properties are close to that of so-called PE-100.

In case of dienes these catalysts allow to prepare both *cis*- and *trans*-polydienes as well as their uniform blends.

The financial support of the Russian Foundation for Basic Research (Grants No 02-03-32975 and 02-03-08117-inno) is gratefully acknowledged.

SYNTHESIS OF OXIDE CATALYSTS $\text{CuO}+\text{ZrO}_2$ FOR METHANE COMBUSTION USING MOLTEN NH_4NO_3

I.V. Morozov¹, A.A. Fedorova¹, M.A. Novozhilov¹, V.F. Anufrienko², E. Kemnitz³

¹ 119992, Moscow, Lomonosov Moscow State University, Chemistry Department
morozov@inorg.chem.msu.ru, fedorova@inorg.chem.msu.ru

² Novosibirsk, Boreskov Institute of Catalysis

³ Berlin, Humboldt University, Chemistry Institute

In the last several decades dangerous waste of methane in atmosphere became a great problem in connection with rapid growth of industry. Methane is inert hydrocarbon and therefore it is difficult to oxidize it at relatively low temperatures ($< 600\text{ }^\circ\text{C}$). Catalysts on the base of noble metals are used to decrease methane oxidation temperature. But the application of these catalysts is limited because they are too expensive. Therefore attempts are undertaken to substitute mixed oxide catalysts for them. From this point of view transitional metal oxides and ZrO_2 modified by 3d-metal oxides are very interesting [1]. There are many articles about system $\text{CuO}+\text{ZrO}_2$ [2], but most of authors carefully investigated only samples with relatively low copper content (up to 20 mol. %). Our work deals with samples with copper content from 0.5 to 100 mol. %.

There are many methods of oxides synthesis. One of them is decomposition of metal salts in the molten alkali metals nitrates media [3]. The disadvantage of this method is the need of washing out the alkali metal salts in order to obtain pure mixed metal oxides. This stage can be avoided when NH_4NO_3 is used instead of alkali metal nitrates since an excess of ammonium nitrate can be simply eliminated from the system by sublimation/decomposition at moderate temperature. Small amounts of reaction mixture, low heating rate and high ratio of vessel volume to volume of sample are the conditions in which decomposition of ammonium nitrate melt occur without explosion.

Oxide samples ZrO_2 with CuO were synthesised by thermal decomposition ($170\text{-}300\text{ }^\circ\text{C}$) of mixtures of zirconium and copper nitrates with five molar excess of NH_4NO_3 . One sample (12 mol. % CuO) was also synthesised in molten potassium nitrate at $450\text{ }^\circ\text{C}$ (3 h). Then samples were calcinated at $500\text{ }^\circ\text{C}$ (1 h). Synthesised samples were green (copper content < 25 mol. %) or black (copper content > 25 mol. %).

All samples were investigated by XRD. Only lines of c-ZrO₂ were observed for samples with copper content from 5 to 20 mol. % and lines of c-ZrO₂ and CuO for samples with > 20 mol. % CuO. On the base of received results it can be assume that solid solution of CuO in ZrO₂ forms under this conditions with maximum copper content 20-25 mol. %. Samples 12 mol. % CuO/ZrO₂ synthesised in molten NH₄NO₃ and in molten KNO₃ had the same XRD – patterns.

Series of samples CuO/ZrO₂ (5-40 mol. % Cu) was investigated by electron microscopy and X-ray spectra element microanalysis. According obtained results samples consisted of high-porous particles with diameter 10-100 μm. These particles are metastable solid solution of CuO in c-ZrO₂. The crystal phase of CuO appeared in samples containing more than 20 mol. % CuO. Content of CuO on the surface of particles was about 17-33 % higher than its average volume content (Table 1). This fact indicates the formation of thin copper oxide film on the surface. Sample with 40 mol. % Cu was treated with concentrated HNO₃ for elimination bulk CuO from the surface. Content of copper in sample was about 25 mol. % after this process. Apparently this is maximum copper concentration in this solid solution. Calcination at 700 °C led to decomposition of metastable solid solution, as a result crystal phases m-ZrO₂ and CuO were formed. At the same time copper content on the surface increased and specific surface area (SA) strongly decreased.

Table 1.

copper content in sample, % (a)	surface copper content, % (b)	b/a	XRD	SA, m ² /g
10	11,7	1,17	c-ZrO ₂	1,5
15	17,7	1,18	c-ZrO ₂	56,6
15*	22,95	1,53	m-ZrO ₂ , c-ZrO ₂ , CuO	0,9
25	33,25	1,33	c-ZrO ₂ , CuO	74
40	52,0	1,30	c-ZrO ₂ , CuO	70,4
< 40**	25,3		c-ZrO ₂	91

* – sample 15 mol. % CuO calcinated at 700 °C for 1 h;

** – sample 40 mol. % CuO treated with concentrated (60 %) HNO₃ (3 h, with stirring) and then calcinated at 500 °C (2 h).

Measurements of pores were carried out for samples with 60 and 80 mol. % CuO. It was found that these samples have narrow distribution function of pore size (average pore diameter was 7 and 10 nm correspondingly).

Obtained samples were studied by EPR and ESDR methods. It was found that they differ from samples with analogous compositions synthesised by another method (coprecipitation). Results are presented in report.

Catalytic activity of the samples was investigated in the total methane oxidation reaction. Samples (430-775 mg) were preheated for 1 h at 400°C in a nitrogen gas flow. After cooling down to 200-250 °C the samples were exposed to the reaction gas mixture of 2,4 ml CH₄ + 9,6 ml O₂ (V_{CH₄}:V_{O₂} = 1:4) at atmospheric pressure and exposure time of 2 s (gas velocity 12 ml/min). The conversion of methane was calculated in terms of CO₂ formed.

Temperatures of 50% (T_{50%}) and 95% (T_{95%}) conversion are presented in table 2. Plot showing the conversion of methane as a function of temperature are presented in Fig. 1. Catalytic activities of samples are shown in table 2 as relative speeds referred to sample weight (R). They were calculated by following equation: $R = \frac{v \cdot \eta}{V \cdot m}$, where v = 2.4 ml/min – is speed of methane current, η – is conversion degree at 300 °C (η < 6 %), V – is molar volume of methane, m – is catalyst weight (g). Graph of dependencies T_{50%}, T_{95%} and R on copper content is presented in Fig. 1. It is interesting to mention that all these dependencies correlate with each other.

Table 2.

Sample	T _{50%} , °C	T _{95%} , °C	R, mmol·g ⁻¹ ·min ⁻¹
12Cu (KNO ₃)	400	470	0,0023
12Cu (NH ₄ NO ₃)	440	510	0,0014
20Cu	363	425	0,0073
30Cu	360	415	0,0112
60Cu	360	395	0,0114
70Cu	360	415	0,0114
80Cu	380	420	0,0104
90Cu	360	395	0,0093
95Cu	385	430	0,0069
CuO	415	490	0,0034

All catalysts are active for complete CH₄ oxidation to CO₂ (without CO) and H₂O in the temperature range 250 – 500 °C. Sample with 12 mol. % CuO produced in molten KNO₃ possesses better catalytic activity than sample with the same CuO content synthesised in molten NH₄NO₃. Catalytic activity increases with increasing of copper content to 30 mol. %, then it almost does not change up to 90 mol. % and then it decreases. So it was shown than pure CuO performs less specific catalytic activity than samples CuO+ZrO₂ with more than 20 mol. % Cu. Optimum composition is 30 mol. % CuO.

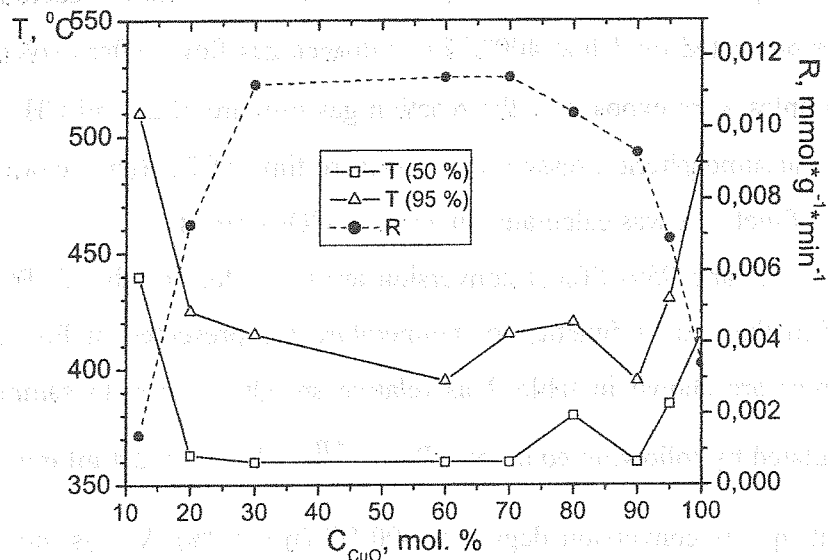


Fig. 1. Dependence of temperatures of 50 % and 95 % and catalytic activity methane conversion on copper content in samples $CuO + ZrO_2$.

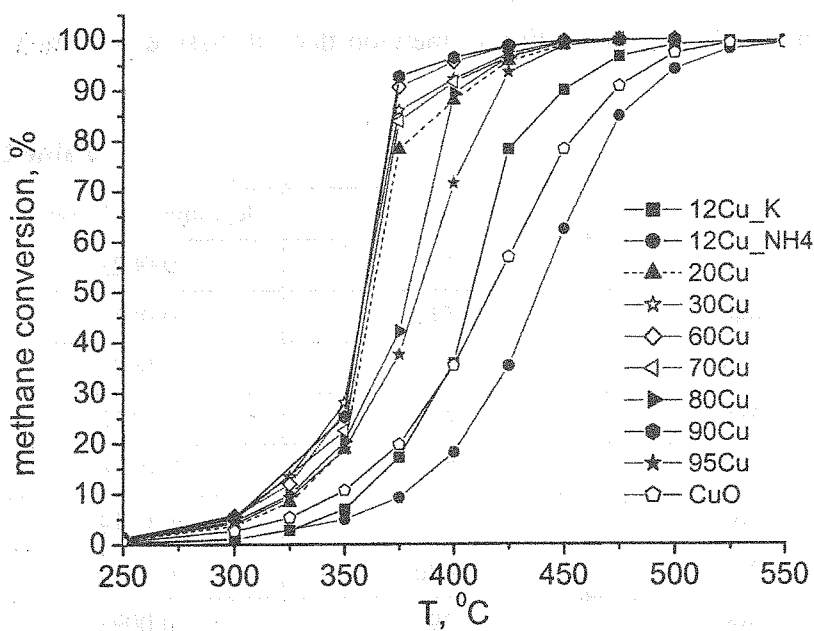


Fig. 2. Dependence of methane conversion on temperature in samples $CuO+ZrO_2$ (copper content 12-100 mol. %) presence.

The work was supported by the Russian Foundation for Basic Research (grant 01-03-33306a).

References

1. Choudhary V.R. et al. // *Angew. Chem.* 1996. V. 108. P. 20.
2. Dongare M.K. et al. // *Journal of Catalysis* 2001. V. 199. P. 209-216.
3. Kundakovic Lj., Flytzani-Stephanopoulos M. // *Applied Catalysis A: General* 1998. V. 171. P. 13-29.
4. Zhou Ren-xian et al. // *Applied Surface Science* 1999. V. 148. P. 263-270.
5. Afanasiev P., Geantet C. // *Coord. Chem. Rev.* 1998. V. 178-180. P. 1725-1752.

DEVELOPMENT OF THE IMPROVED NUMERICAL MODEL OF EXTRACTIVE DEAROMATIZATION OF A STRAIGHT-RUN DIESEL FRACTION 270-360 °C

D.E. Khalikov, S.A. Obukhova, E.G. Telyashev

*The Institute of Petroleum Refining and Petrochemistry
of Bashkortostan Republic Academy of Sciences*

Ufa 450065, Inicativnaya Str., 12, phone/fax: (3472) 42-24-71, vezirov@anrb.ru

Increasing severity of ecological requirements to diesel fuels quality that is to polycyclic hydrocarbons and in future to total aromatic hydrocarbons (AH) evokes necessity of development and introduction in industry of the technologies of diesel fractions dearomatization. One of the technologies permitting decrease of AH content in diesel fuels is extractive dearomatization [1].

Traditional extragents of industrial extraction processes such as glycols, sulfolane, N-methylpyrrolidon, phenol and others can't be used in this quality for extractive dearomatization of diesel fractions due to several reasons.

The heavy diesel fraction 270-360°C was chosen as an object of this study which is characterized [2] by increased content of the most undesirable bi- and polycyclic AH as compared to the broad diesel fraction.

Laboratory study [3] of the influence of such parameters of extraction as ratio extragent/feed, water content in extragent and temperature on properties of raffinates and extracts produced as a result of extractive dearomatization has been conducted. Extraction was conducted in one stage in a thermostatic extractor. The extragent was separated from the raffinate and extract phase by distillation. The experiments have shown that in the range studied the best results were obtained at the temperature of 20 °C and when ratio extragent/feed was equal to 3. Under these conditions study of the relation between water content in extragent (4-10% vol) and yield and quality parameters of raffinate and extract was conducted.

The research work performed has shown that when water content increases yield of raffinate (a dearomatized diesel fraction), which is the target product, also grows and reaches 87.5 %.

Significant redistribution of AH between raffinate and extract takes place during this process which is confirmed by the results of determination of AH content by chemical groups content analysis as well as by the results of determination of refractive index. Decrease of water content leads to decrease of AH content in raffinate and amounts to 20.2 %.

The basic features of the one-stage extraction of AH from a straight-run diesel fraction 270-360 °C using the extragent studied have been determined.

The results of laboratory study were used for correction of the model of the initial feed [4] and the coefficients of binary interactions in the equation of liquid/liquid phase equilibrium.

The model of diesel fraction was presented as a mixture of basic chemical groups of hydrocarbons and sulfur compounds. The model was improved by the method of selection of structure and content of components in order to guarantee maximum correspondence to the real diesel fraction used in the experiments according to chemical composition and physical-chemical properties.

Real experiments were reproduced in numerical experiments (fig. 1-2) using this improved model and its adequacy has been shown.

So on the basis of the laboratory and numerical experiments the improved model of one-stage extractive dearomatization of diesel fraction has been developed which can be used of optimization of multi-stage extraction parameters in numerical experiments and technological calculation of extractive equipment.

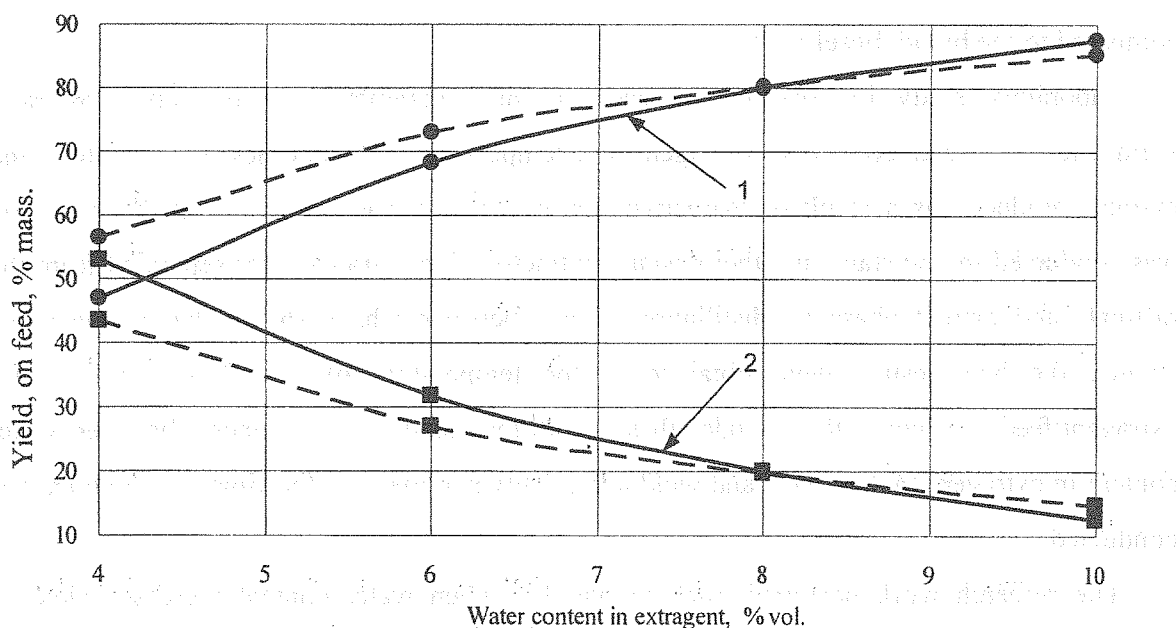


Fig. 1. Relation between water content in extragent and yield: 1 – raffinate, 2 – extract

- Results of numerical experiments
- Results of laboratory experiments

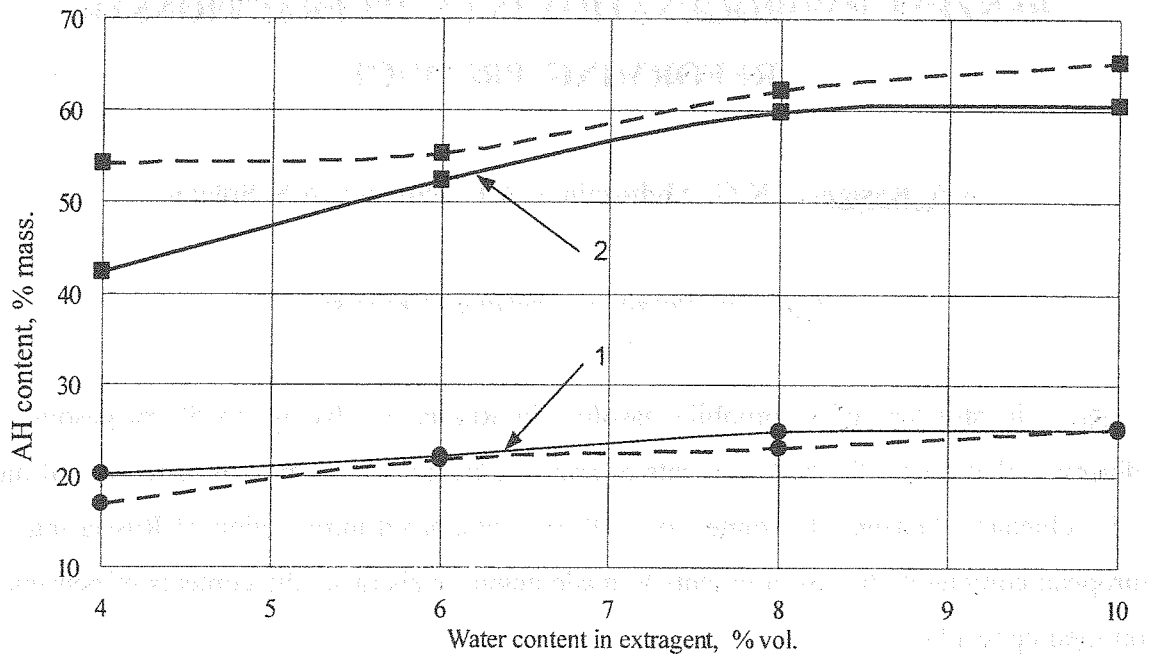


Fig. 2. Relation between water content in extragent and content of total AH in:

1 – raffinate, 2 – extract

●●●●●● Results of numerical experiments

———— Results of laboratory experiments

References

1. Khalikov D.E., Obukhova S.A., Vezirov R.R. Optimization of the process of diesel fuels extractive dearomatization using the method of numerical experiment / *Neftekhimiya i Neftepererabotka*, 2000 yr., № 1.
2. Khalikov D.E., Kulik A.A., Obukhova S.A. et al. Technology of production of diesel fuels with low aromatic hydrocarbons content / *Neftepererabotka i Neftekhimiya – 2002.* : Materials of scientific-practical conference. – Ufa: INKhP, 2002.
3. Khalikov D.E., Obukhova S.A. et al. Experimental study of extractive dearomatization of a straight-run diesel fraction 270-360 °C / *Neftepererabotka i Neftekhimiya – 2003.* : Materials of scientific-practical conference. – Ufa: INKhP, 2003.
4. Khalikov D.E., Obukhova S.A., Vezirov R.R. et al. Features of a straight-run diesel fraction simulation / *Material of the III Congress of petrorefiners of Russia.* – Ufa. –2001.

BENZENE HYDROGENATION IN LIGHT FRACTIONS OF REFORMING PRODUCT

A.A. Kasianov, K.G. Abdulminev, A.F. Ahmetov, A.S. Soloviev

Ufa State Petroleum Technical University

Now in structure of automobile gasoline in Russia involve up to 50 % gasoline of reforming, that causes the high contents of aromatic hydrocarbons and, in particular, of most toxic reluctant - benzene. In connection with the anticipated introduction of Russia into the European community the requirements to made engine fuels raise, the contents of benzene is confined up to 1 %.

Some alternatives of know-hows of drop of the contents of benzene at present are designed: extraction, alkylation, drop of stress and increase of bubble point of feed reforming. However specified methods have essential lacks precluding widespread occurrence - high capital and operational expenses, complementary quantity of scarce not limiting gases, drop of octane number or output of gasoline.

One of most effective and economically justified is the technology of reduction of concentration of benzene in reforming's gasoline by a method hydrogenation. The essence of process is encompass byed distillation of a gasoline with emanating head IBP – 85°C and residual 85°C - FBP of fractions. The fraction IBP - 85°C, containing up to 25 % of benzene, is exposed hydrogenation on platinum contents catalyst.

As features of process it is necessary to note, that on thermodynamic indexs the benzene is better hydrogenated at low temperature and heightened stress [1]. However at low temperature the speed of process is poor for industrial production, and the increase of temperature and stress augments a fraction of reactions hydrocracking paraffin and naphthenes hydrocarbons and, as the consequent, causes drop of yields of liquid products.

As a result of the held studies the optimum technological arguments of process allowing to receive a product of hydrogenation containing less the 0.1 % benzene and to minimize of loss from reactions hydrocracking at observance of conditions of industrial production were picked up.

The mixture hydrogenation of a head fraction with the rest 85°C - FBP allows to receive a component of high-octane gasoline containing less 1 % of benzene (tab. 1).

The table 1 - Performance of feedstock and products of process hydrogenation

Properties	Gasoline of reforming	Gasoline's fraction		Hydrogenated product (3)	Blend of (2) and (3)
		IBP – 85°C (1)	85°C – FBP (2)		
Yields, % wt.	100.0	33.0	67.0	33.1	100.1
RON	96.6	78.9	More 100	78.3	98.0
MON	87.0	76.5	92.3	75.9	88.2
ASTM distillation, °C					
IBP	40	39	86	38	42
10 % vol.	63	50	95	49	65
50 % vol.	108	60	116	58	112
90 % vol.	160	74	168	73	162
FBP	193	86	205	82	200
Aromatics hydrocarbons, % wt.	67.2	19.6	90.5	-	60.1
Benzene	5.5	16.0	0.3	Less 0.1	Less 1.0
Toluene	17.2	3.6	23.8	Less 0.1	15.9

References

1. Vvedenski A.A. Thermodynamic accounts petrochemical process.- L: GOSTOPTEXIZDAT, 1960.- 576 p.

OPTIMIZATION OF FEEDSTOCK COMPOSITION OF CATALYTIC REFORMER'S LAST REACTOR

A.A. Kasianov, A.F. Ahmetov

Ufa State Petroleum Technical University

For today of an opportunity of increase of performance catalytic reforming with a stationary catalyst bed in traditional technological execution practically are exhausted. Further increase of temperature and the drop of stress conducts to an intensive poisoning of the catalyst and drop of its activity. Applying of the advanced catalyst and optimization of a technological mode do not result in significant meliorating of index of process, since it has reached thermodynamics of a possible limit. The consideration of processes proceeding at each stage reforming demonstrates, that in the first and second reactors to the greatest degree proceed dehydrogenation of naphthenes and isomerization of paraffines, the fraction of reactions dehydrocyclization and hydrocracking is low owing to small time of contact of feed with the catalyst and significant temperature drop on a catalyst bed [1]. On the given indexes the third reactor considerably differs from head. Here there is more half of all catalyst of process, hence, time of contact - greatest; temperature of a stream on a catalyst bed, though and it is insignificant, but grows. All this promotes ascending of a fraction of reactions dehydrocyclization and hydrocracking.

The involvement in reactions hydrocracking of paraffines with number of carbon atoms 7 also is more desirable, since allows essentially to increase octane number of a product. On the other hand, hydrocracking of hydrocarbons with quantity of atoms of carbon less than seven results in formation of extremely gases and attracts drop of an yield of gasoline and hydrogen. Therefore for optimization of process last reactor was chosen.

The held analysis of a reactionary mixture of process reforming testifies that the reactionary mixture on a going into last reactor has up to 28 % of fractions boiling away at temperature up to 85 C . Hydrocarbons introduced in this fraction are not exposed reforming, moreover, at hydrocracking of these reductants the unvaluable gas is formed. Hence, it is desirable to remove easy hydrocarbons from a reactionary mix before third reactor.

For skilled endorsement of performance of the tendered schema of realization of process reforming the experiments on laboratory installation of a flowing type working under pressure of hydrogen were held. The installation modeled work of last reactor of installation catalytic reforming. The contents of aromatic hydrocarbons in source feed was 48 % wt.

As variable arguments of optimization were chosen temperature in a reactor and bubble point of a fraction routed to a reactor. By yardstick of optimization the yield of liquid product (balance sum of a head fraction and product of reforming) acted.

Source feed have distilled with production of fractions of feed (tab. 1).

The table 1 - Yields of residual fractions from source feed

Fraction	Yields, % wt.
85°C – FBP	72,0
95°C – FBP	65,6
105°C – FBP	60,2

The results of experiments (fig. 1) demonstrate, that the yields of products from source feed is lower than for alternatives with the deduction of a head fraction and with increase of temperature the difference is augmented.

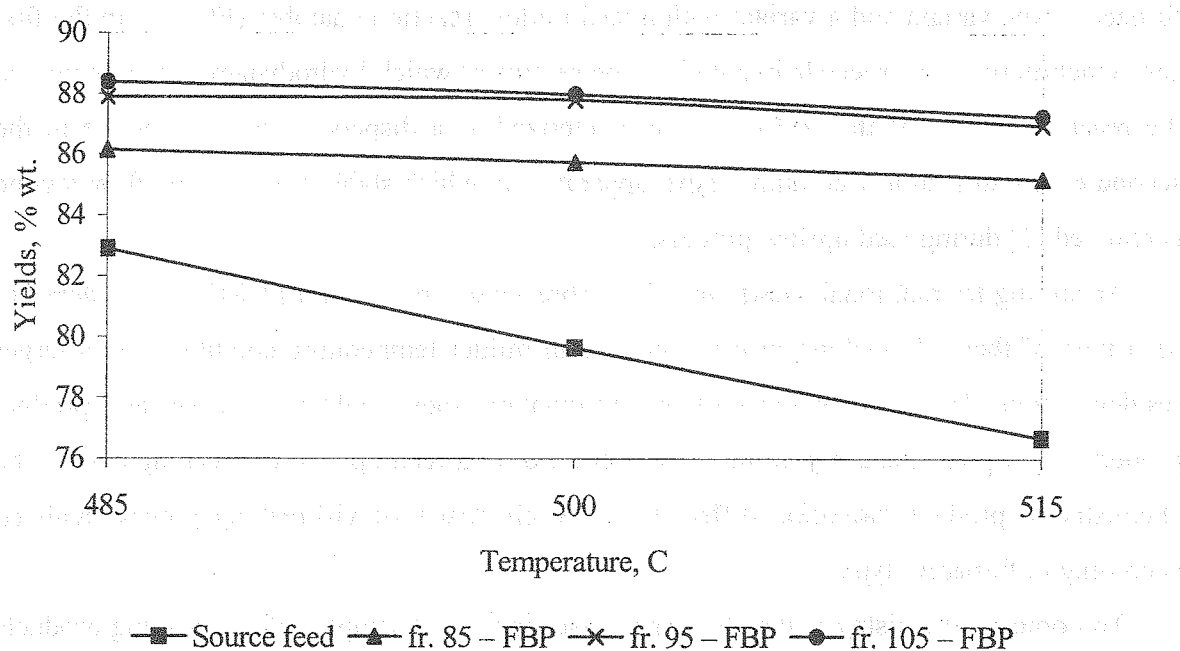


Figure 1. Dependence of an yields of gasoline on temperature and beginning of boiling of feed.

With increase of bubble point of a feed fraction the yield of liquid products raises, and the influence of temperature is reduced.

Thus, carried out researches is shown, that the removal from feed of last reactor of a head fraction allows to gain complementary quantity of a target reforming's product – high-octane reductant of gasoline or to augment temperature of process in the given reactor for increase of octane number of this product.

References

1. Geits B. etc. Chemistry of catalytic processes. M.: World, 1981. 551 p.

EFFECT OF THERMOLYSIS CONDITIONS AND TYPE OF VISBREAKING REACTOR ON STRUCTURE AND POLYDISPERSE STATE OF CRACKING RESIDUES

S.A. Obukhova, R.R. Vezirov, A.R. Davletshin, E.G. Telyashev

*The Institute of Petroleum Refining and Petrochemistry
of Bashkortostan Republic Academy of Sciences*

Ufa 450065, Initsiativnaya Str., 12, phone/fax: (3472) 42-24-71, vezirov@anrb.ru

At present the most widely used alternatives of visbreaking process realization are a furnace – type variant and a variant with a feed upflow reaction chamber (FURC). In the first case reaction process proceeds in a coil – type reactor in which hydrodynamic flow regime at the reaction section of the coil can be characterized as a disperse – ring one while in the second case – in a hollow column – type apparatus, in which stable churn – type flow regime is realized [1] during feed upflow process.

According to traditional viewpoints the visbreaking process with FURC is considered to be a type of thermal cracking process realized in milder temperature conditions with larger residence time. However, analysis of the information about yield distribution and product properties [1,2] has made it possible to suppose that in a feed upflow visbreaking reactor the chemistry of product formation differs from the chemistry of visbreaking process realized according to furnace – type.

To compare chemistry of the above processes industrial samples of visbreaking products realized according to furnace – type (485°C) and with FURC (448°C) using comparable feed – a tar of West – Siberian crude oil have been selected and analyzed.

In the given below X-ray diagrams of the samples (fig.) the small maximum (A) characterizes a packing of straight and brached paraffin chains, the maximum (B) – degree of structure order, the maximum (C) – distance in aliphatic chains packing [2] and saturated polymethylene chains [3].

Analysis of the result of X-ray investigations (table) has shown that during petroleum residues visbreaking process interplane distance d_{002} and degree of condensability f_k increase while these changes are less aident for the sample produced with FURC. Number of layers in a crystallite (m) increases for the sample of furnace – type cracking residue which is

explained by appearance of condensed structure of secondary origin. For the sample produced with FURC this parameter doesn't change indicative of insignificant proceeding of packing reactions.

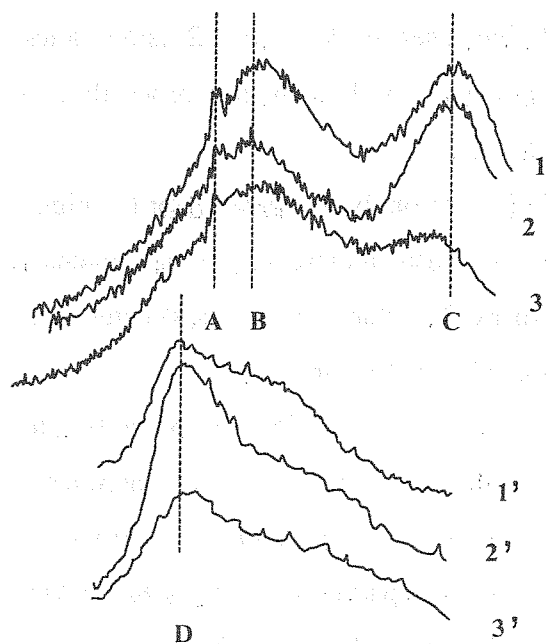


Fig. X-ray diagrams of feed and product of visbreaking process realized in different types.

1. Visbreaking feed
2. Cracking residue (furnace – type)
3. Cracking residue (with FURC)
- 1' Asphaltenes extracted from the visbreaking feed
- 2' Asphaltenes extracted from the cracking residue 2.
- 3' Asphaltenes extracted from the cracking residue 3

Intensity of the peak C for the sample produced with FURC almost disappears as compared to the initial feed indicative of active proceeding of dealkylation processes and breakage of methylene chains connecting base planes of undermolecular structures [4].

Table. X-ray crystal characteristics of visbreaking feed and products.

Sample	X-ray crystal characteristics					
	f_k	$d_{002}, \text{Å}$	$d_{11}, \text{Å}$	$L_C, \text{Å}$	m	$f_{\text{алиф}}$
Thermolysis feed and products						
1	0,13	3,678	4,599	13,1	3,6	0,23
2	0,18	3,634	4,576	15,2	4,2	0,23
3	0,16	3,648	5,515	13,1	3,6	0,13
Asphaltenes extracted from thermolysis feed and product						
1'	0,3	3,534	4,647	16,5	4,7	0,08
2'	0,5	3,480	4,576	24,7	7,0	0,08
3'	0,4	3,493	4,576	18,9	5,4	0,07

Accordingly the asphaltenes extracted from the samples 1, 2, 3 were analyzed. The results of X-ray crystal analysis have shown that interplane distance d_{002} decreases for both samples of cracking residues but for the sample produced with FURC it is closer to initial feed. Number of layers in crystallite (m) significantly increases for the sample 2' and to a less extent – for the sample, produced with FURC, indicative of less intense proceeding of polycondensation and packing reactions in the variant studied.

Intensity of reflection of asphaltene signal (peak D) is strongly pronounced for the high – temperature sample 2' and characterizes it as a high - condensated close to coke one. Intensity of asphaltene signal of the sample 3', produced with FURC, characterizes its structure as a more amorphous close to asphaltenes of initial feed one (1' – native origin).

Study of the samples by the method of low-angle X-ray diffusion [5] has shown that for tars and cracking residues four basic types of undermolecular compounds with a number of particles with inertia radius (R) within 13 – 449 Å are determined. Besides, the number of particles of minimum sizes is much larger than the number of particles of large sizes making it possible to consider particles of small sizes to be the basic element of heavy petroleum residues [6].

It has been shown that during high – temperature regime of tar cracking the largest particles of cracking residue increase with simultaneous increase of its total content (V) by 1.3%.

When the process is realized with FURC decrease of content of the largest particles by 1.9% is observed with simultaneous decrease of inertia radius of these particles and their mean diameter D indicative of proceeding of cracking reactions of undermolecular structures with formation of particles of smaller sizes.

Analysis of the residues by gel chromatography [7,8] and balance characteristics of visbreaking process have made it possible to determine molecular – mass distribution of the feed and the products. It has been shown that the furnace – type products are represented mainly by low – molecular compounds corresponding according to boiling points to gas and gasoline, while the FURC – type products – by mean molecular mass corresponding to light gasoil fractions.

So, the performed study has shown that when the process is realized in coil tube furnace under high temperature and low residence time reactions of liquid phase condensation proceed to a great extent accompanied by increased coke formation especially at the surface of reaction coil at the expense of local overheating of liquid phase.

When the process is realized with FURC at the expense of decrease of temperature, increase of residence time and uniformity of vapour – phase flow rate cracking of high – molecular compounds takes place with formation of mean molecular mass hydrocarbons providing high selective conversion of the process [1,9] with insignificant proceeding of packing reactions.

References

1. Obukhova S.A., Davletshin A.R., Khalikov D.E., Vezirov R.R. Features of petroleum residues thermolyses in an upward flow reaction chamber / Abstracts of XV International Conference on Chemical Reactors "Chemreactor- 15".- Helsinki, 2001.- P. 301- 304.
2. Davletshin A.R., Obukhova S.A., Vezirov R.R., Kalimullin M. M., Sukhorukov A.M. Effect of reaction device on efficiency of visbreaking process. Materials of the 2nd International symposium "Science and technology of hydrocarbon disperse systems", - Ufa, 2000, p.p. 44-45
3. Shishalov N.A. Basic concepts of structural analysis. M. ASUSSR, 1961, p.p. 366
4. Svergun D. I., Feygin L.A. X-ray and neutron low-angle diffusion. M.: Nauka,1986. - p.279
5. Syunyaev Z.I. Petroleum carbon. M.: Khimiya, 1980. – p.32-34
6. Poray – Koshits E.A. Diffuse scattering of X-rays at low angles. VFN, 1949, 4ed. – p.p.573-611
7. Safiyeva R.Z. Physical chemistry of petroleum. Physical – chemical basis of petroleum processing technology. M., Khimiya, 1998. – p.448
8. Determan G. Gel – chromatography. M., Mir, 1970. – p. 252
9. Vezirov R.R., Davletshin A.R., Obukhova S.A., Sukhorukov A.M. Visbreaking of petroleum residues in an upflow reaction chamber. Collection of scientific works of IP NKhP. XXXIIIed., Ufa, 2001. – p.p.62-64

FEATURES OF HYDROUPGRADING OF HIGH-AROMATIC PETROLEUM DISTILLATES

S.A. Obukhova, R.R. Vezirov, A.A. Kulik, E.G. Telyashev

*The Institute of Petroleum Refining and Petrochemistry
of Bashkortostan Republic Academy of Sciences*

Ufa 450065, Initsiativnaya Str., 12, phone/fax: (3472) 42-24-71, vezirov@anrb.ru

Modern worldwide and European ecological requirements strictly specify content of aromatic hydrocarbons (especially polycyclic ones) in diesel fuels. Introduction of similar requirements is expected in Russia. In this respect the problem of use of high-aromatic secondary distillates such as light catalytic cracking gasoil (LCCGO) as components of marketable diesel fuels is becoming more urgent. One of the methods of petroleum distillates dearomatization is their hydroupgrading. The scientific bases of the technology of hydroupgrading of LCCGO in mixture with a straight-run vacuum gasoil (SRVGO) have been developed.

The research works performed on laboratory and pilot scales with variation of pressure and catalytic systems have shown efficiency of the given technology. The laws of hydrogenation of sulfur compounds and different classes of aromatic hydrocarbons in the process of simultaneous hydroupgrading of SRVGO and LCCGO have been found out [1]. Study of the catalysts ГИИ-497Т (a catalyst of vacuum gasoil hydrotreatment), PK-442 (mild hydrocracking) and their layered loading has shown that the catalyst PK-442 is superior to the catalyst ГИИ-497Т and to the variant of their layered loading in practically all parameters including hydrogenation of aromatic hydrocarbons [2]. It has been shown that selective hydrogenation (above 70%) of carbon atoms in polycyclic aromatic structures of LCCGO can be efficiently conducted under the conditions of existing industrial vacuum gasoil hydrotreatment units on the catalyst PK-442 and during layed loading of the catalysts ГИИ-497Т and PK-442.

It is known that the reactions of hydrogenation of unsaturated and aromatic hydrocarbons, sulfur compounds contained in LCCGO and SRVGO, proceed with heat release, as a result the temperature of the product gas flow at the exit of the reactor increases. Temperature gradient can vary within broad limits (5 - 140°C) and depends on many factors [3]. To design

new hydrotreatment units and to convert existing ones to processing of the feed with high unsaturated and aromatic hydrocarbons content it is necessary to know the quantity of excess heat released in the reactor.

To calculate heat effect of a reaction the Hess law is usually used based on determination of the heat of feed and product formation. Calculation of heat effects and temperature gradients was conducted using typical techniques of petroleum and gas processing processes [4].

The heat effect of hydrogenation on one carbon atom included in aromatic structures was determined from the literature data [5]. Determination of the content of carbon atoms in aromatic structures with different ring numbers was conducted according the IR and UV – spectrophotometry data (see the table). The experimental data obtained on the catalyst PK-442 guaranteeing maximum degree of hydrogenation of sulfur compounds and aromatic and unsaturated hydrocarbons were used in calculation.

Distribution of sulfur compounds according to the groups in LCCGO was taken from the literature data [6].

Table – Basic data for calculation of the heat effect during simultaneous hydrougrading of SRVGO and LCCGO

	Pressure, MPa			
	4,0	6,0	8,0	10,0
Light catalytic cracking gas oil (fr. 200-350 °C)				
Degree of hydrogenation of the atoms of carbon:				
benzol	-	9,6	20,4	30,4
naphthalene	91,3	91,3	88,7	84,1
polycyclic	67,5	73,3	80,4	83,8
Degree of desulfurization, %	90,7	92,1	93,6	94,3
Degree of unsaturated removal, %	86,0	90,5	93,8	96,3
Straight-run vacuum gasoil (fr. 350 °C-KK)				
Degree of hydrogenation of the atoms of carbon:				
benzol	-	-	6,58	21,87
naphthalene	-	7,7	24,79	45,73
polycyclic	39,23	46,2	54,5	65,25
Degree of desulfurization, %	86,9	88,7	90,6	91,8

Calculation of the heat effect and the temperature gradient in the reactor for the degrees of hydrogenation obtained on the catalyst PK-442 in the pressure interval studied has shown that for the ratio SRVGO:LCCGO (85:15) during increase of pressure from 4.0 to 10.0 MPa temperature gradient in the reactor increases from 17 to 30°C and doesn't exceed the arbitrary permissible gradient 50°C.

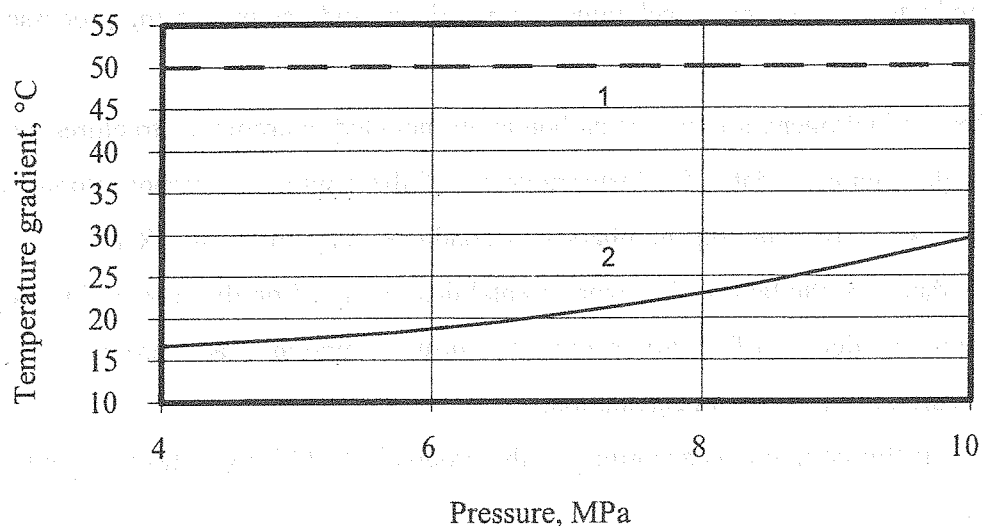


Fig.1 – Effect of pressure on temperature gradient in the reactor during simultaneous hydrougrading of SRVGO and LCCGO (relation 85:15) on the catalyst PK-442

1 – limitation on temperature gradient, 2 - temperature gradient in the reactor.

Calculation of the effect of LCCGO quantity in mixture with SRVGO (fig. 2) on temperature gradient in the reactor has shown that excess of temperature gradient in the reactor is above 50°C during inclusion of more than 50% of LCCGO.

Calculation of the consumption of hydrogen and fresh hydrogen-bearing gas (HBG) for maintaining partial pressure has shown that during simultaneous hydrougrading for every additional 10% mass of LCCGO it is necessary to increase consumption of fresh HBG by 0.4-0.45% mass on feed, and during increase of pressure from 4.0 to 10.0 MPa consumption of fresh HBG is 1.5-2.0 times more.

On the basis of our experimental, literature and industrial data calculation of heat effects and temperature gradients during simultaneous hydrougrading of SRVGO in mixture with LCCGO has been performed, the relation between temperature gradient and content of SRVGO in mixture has been found out, the general technological solutions for processing of the mixtures with different content of LCCGO have been proposed. The principle two-reactor technological scheme of hydrougrading of SRVGO in mixture with LCCGO is offered permitting to use different variants of catalytic loading and realize intermediate heat removal and supply of fresh HBG allowing to increase hydrogen partial pressure in the second reactor.

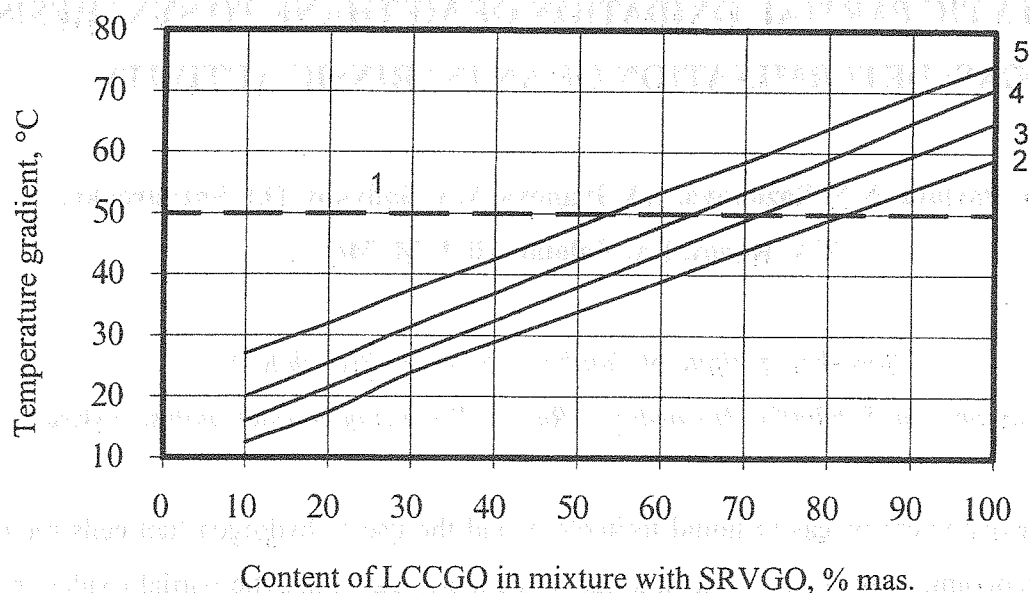


Fig.2 – Relation between temperature gradient in the reactor and LCCGO content in mixture with SRVGO under different pressures

1 – limit on temperature gradient;

2 – 4.0 MPa; 3 – 6.0 MPa; 4 – 8.0 MPa; 5 – 10.0 MPa.

References

1. Kulik A.A., Obukhova S.A., Vezirov R.R. et. al. Hydrogenation of aromatic hydrocarbons of light catalytic cracking gasoil during simultaneous hydrogenation with vacuum gasoil. Materials of the scientific – practical conference: Neftepererabotka i neftekhmiya – 2002. – Ufa, 2002. – p.p. 71-74.
2. Kulik A.A., Obukhova S.A., Vezirov R.R., Telyashev E.G. Effect of catalyst and pressure on results of simultaneous hydrotreatment of light catalytic cracking gasoil and vacuum gasoil. Neft' i gas. -2003, №1, p.p. 51-57.
3. Brayzer A.A., Volpin L.Sh., Fomin V.F., Yakimenko E.V., Neftepererabotka i neftekhmiya. 1978, №3, p. 3
4. Tanatarov M.A., Akhmetshina M.N., Fashutdinov R.A. et. al. Technological design of petroleum treatment units. M. Khimiya, 1987, p. 151.
5. Berg G.A., Khabibullin S.G. Catalytic hydrougrading of petroleum residues. Leningrad., "Kimiya", 1987, p. 151.
6. Lebedev B.L., Knyaz'kov A.L., Osipov L.N. et. al. Neftepererabotka i neftekhmiya. 2001, №2, p. 13.

CATALYTIC PARTIAL OXIDATION OF METHANE TO SYNTHESIS GAS: DETERMINATION OF AN INTRINSIC ACTIVITY

S.N. Pavlova, N.N. Sazonova, J.A. Ivanova, V.A. Sadykov, O.I. Snegurenko,
V.A. Rogov, I.A. Zolotarskii, E.M. Moroz

Boreskov Institute of Catalysis, Siberian Branch RAS

Pr. Lavrentieva, 5, 630090, Novosibirsk, Russia. E-mail: pavlova@catalysis.nsk.su

The development of gas-to-liquid technology and the use of hydrogen fuel cells require safe and economic conversion of natural gas to synthesis gas. Catalytic partial oxidation of methane (CPO) at short contact times is now considered as a low capital expenditure alternative to steam reforming of methane, in particular, for production of synthesis gas in compact reactors [1-3]. To determine the intrinsic activity of the catalysts in CPO at relevant experimental conditions, some difficulties have to be overcome. CPO is mildly exothermic, and severe heat transport limitations offer a major challenge. Furthermore, mass transport limitations as well as homogeneous gas-phase reactions may be also important [2-4].

In this work, to study the intrinsic activity of corundum supported mixed oxides in CPO at high temperatures and short contact times, highly diluted gas mixture, diluted catalyst bed and small catalyst grains have been used. The effect of the reactor diameter, the catalyst dilution and the catalyst bed length on the methane conversion and syngas selectivity have been studied. The intrinsic activity of lanthanum nickelate promoted by Pt and supported onto alumina of two types precovered by ceria-zirconia solid solution has been compared.

Experimental

As supports, microspheric α -Al₂O₃ (designed as A₀, 16 m²/g; 100 μ m mean diameter) containing an admixture of θ -Al₂O₃ and pure α -Al₂O₃ (designed as A, 4 m²/g, a fraction of 0.2-0.25 mm) were used. The oxide layer of Zr_{0.8}Ce_{0.2}O₂ (ZC) and the active components LaNi_{0.9}Pt_{0.1}O_x (LNP) or LaNiO₃+0.2 wt. % Pt (LNP0.2) were successively supported as described in [5]. The ZC content in the catalysts was 5-10 wt.%, LNP content was 3-7 wt.%. The phase composition and reducibility of catalysts were characterized with XRD and TPR [5].

The catalysts were tested in the POM at atmospheric pressure in a plug-flow quartz reactor with 5-10 mm inner diameter. The catalyst weight of 0.01 g was diluted with a quartz powder of particle sizes varied in the range of 0.5-0.074 mm. The catalyst bed length was 3-20

mm. Before a catalyst, the reactor space was filled with quartz sand. The position of the catalyst bed was aligned with the constant axial temperature profile of the furnace. Before testing, the catalysts were oxidized or reduced *in situ*. The flow rate of the reaction feed (1 vol.% CH₄, 0.5% O₂, He –balance) was 300 cm³/min. The reaction products were analyzed by the GC. The conversion of methane and product selectivities were calculated on the basis of carbon numbers of the reacted methane. Carbon balances were closed to within $\pm 5\%$.

Results and discussion

Catalyst phase composition and reducibility. According to XRD, the CeO₂-ZrO₂ oxide loaded onto both type of supports is a solid solution of the cubic structure. Supported lanthanum nickelate phase containing Pt corresponds to a perovskite structure which predominates in all catalysts. Some amounts of small NiO particles are also presented. The diffraction lines of Pt were not usually observed probably as a result of its incorporation into the perovskite structure.

The redox properties of the catalysts depend on the support nature, the perovskite stoichiometry and the presence of Ce-Zr solid solution. The catalysts based on the support A are easier reduced by H₂ as compared to samples based on A₀. In the latter case, more difficult reduction of perovskites as well as Ce-Zr solid solution assumes their stronger interaction with the θ -Al₂O₃ admixture. Another factor strongly influencing the perovskite reduction behavior is a stoichiometric ratio of La/Ni and the presence of Pt. [5].

Table 1. The effect of the catalyst bed arrangement on methane conversion and CO selectivity over reduced LNP-A₀

Quartz fraction, mm	Catalyst bed length, mm	Pressure drop, atm	Conversion, %		CO selectivity, %	H ₂ /CO
			CH ₄	O ₂		
0.5-0.25*	3	0	23	78	60	0.5
0.5-0.25	3	0	40	99	60	3
0.5-0.25	10	0	67	99	89	2.1
0.15-0.25	10	0.005	63	99	83	2
0.08-0.07	10	0.0075	77	99	90	2.2

* - the reactor diameter 10 mm

The effect of the catalyst dilution, the reactor diameter and the catalyst bed length on the activity. To minimize the temperature gradient along the catalyst bed, the catalyst was diluted with quartz. The quartz fraction 0.2-0.25 mm was chosen here to prevent a significant

pressure drop along the catalyst bed (Table 1). The methane conversion in the reactor filled with quartz and alumina is low and not presented here for brevity. For LNP-A₀, the methane conversions and syngas selectivities obtained for different arrangement of the catalyst bed are presented in Table 1. The low values of methane conversions and selectivities are observed for the 3 mm catalyst bed length and 10 mm reactor diameter. To prevent the longitudinal interdiffusion, the catalyst bed length must be 10-20 mm. The catalyst bed arrangement also affects the CPO reaction dynamics as shown in Fig. 1.

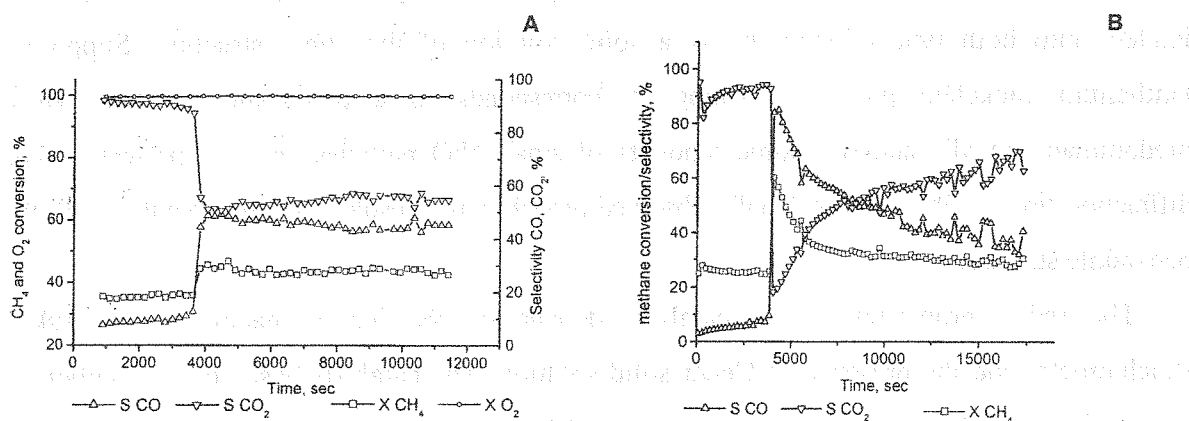


Fig. 1. The effect of the catalysts bed arrangement on the CPO reaction dynamics. LNP-ZC-A₀ catalyst. A – 5 mm reactor diameter, 20 mm catalyst bed length; B – 10 mm reactor diameter, 3 mm catalyst bed

The effect of the catalyst pretreatment and composition on an intrinsic activity

The activity of catalysts depends both on their composition and pretreatment. In general, methane conversion and selectivity to syngas on oxidized catalysts are lower as compared to reduced ones. In most cases, conversions are rather low and the products of deep oxidation mainly form. This appears to be determined by difficult reduction of lanthanum nickelate to metal Ni in highly diluted reactant mixture.

Reduced catalysts except LNP(0.2)-ZCA₀ sample (Fig.1A), are characterized by a high methane conversion and syngas selectivity due to Ni⁰ formation. All highly active catalysts contain LaNi_{0.9}Pt_{0.1}O₃ perovskite as a precursor, and the catalysts based on the support A are more effective. Fig. 1A and 2 show methane conversion and syngas selectivity for reduced LNP(0.2)-ZCA₀ and LNP-ZC-A catalysts as a function of the reaction time. Though for these samples the mode of activity variation in the course of induction period is quite different, in both cases it is followed by a sharp increase in the methane conversion and syngas selectivity.

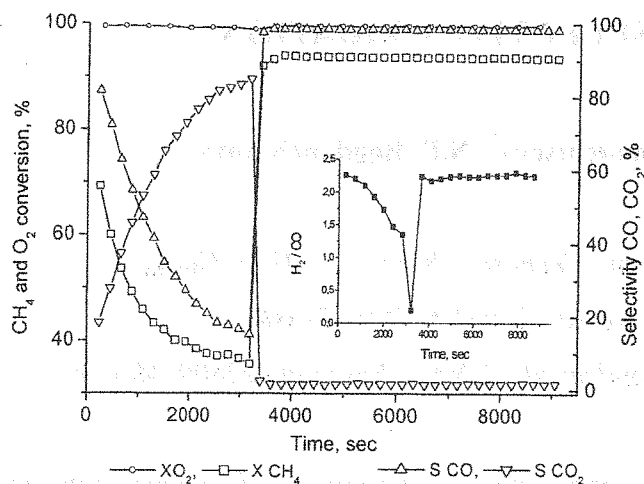


Fig. 2. CH₄, O₂ conversions, H₂/CO ratio and CO, CO₂ selectivities of reduced LNP-ZCA. 5 mm reactor diameter, 20 mm catalyst bed length.

The initial methane conversion and syngas selectivity are higher for LNP-ZC-A, while for LNP(0.2)-ZCA₀ sample deep oxidation products are mainly formed during the induction period.

The induction period was observed only for catalysts containing Ce-Zr solid solution. It is well known that prolonged relaxations of catalyst activity could not be caused by simple variation of the surface coverage by oxygen. They are usually observed when such side processes as phase transition, diffusion, and structural transformations caused by a change of a sample stoichiometry occur. The prolonged relaxations observed on reduced samples can be assigned to slowly proceeding oxidation of a reduced Ce-Zr solid solution followed by its structure rearrangement [6] and carbonization of its surface. Different dynamics in the course of the induction period as well as a different steady-state activity of the LNP-ZC-A and LNP(0.2)-ZCA₀ appear to be caused by a specificity of the components distribution on the surface of those reduced catalysts arising from their distinct perovskite stoichiometry.

References

- [1] P. M. Tornaiainen, X. Chu, L. D. Schmidt, *J.Catal.*, 1994, 146, 1
- [2] M.-F. Reyniers, C.R.H. Smet, P.G. Menon, G.B. Marin, *CATTECH* 6 (2002) 140
- [3] L. D. Schmidt, *Stud. Surf. Sci. Catal.*, Ed. E. Iglesia, J. J. Spivey, T. H. Fleisch, 2001, v.136, p.1
- [4] J. C. Sllaa, R. J. Berger and G. B. Marin, *Cat. Lett.*, 1997, 43, 63
- [5] A.V. Simakov, S.N. Pavlova, N.N. Sazonova, V.A. Sadykov, O.I. Snegurenko, V.A. Rogov, V.N. Parmon, *Chemistry in Sustainable Developm.* 11 (2003) 263.
- [6] V.A. Sadykov, T.G. Kuznetsova, et al, *React. Kinet. Catal. Lett.* 76 (2002) 83.

SUPPORTED FOAM COPPER CATALYSTS FOR METHANOL SELECTIVE OXIDATION

A.N. Pestryakov^{a, b}, E.V. Smolentseva^b, N.E. Bogdanchikova^c

^a *Fritz-Haber-Institut, Dept. Inorganic Chemistry, Berlin, D-14195, Germany*

^b *Tomsk Polytechnic University, Tomsk 634050, Russia*

^c *Centro de Ciencias de la Materia Condensada, UNAM, Ensenada 22800, Mexico*

Structural, mechanical, gas-dynamic and catalytic properties of copper catalysts supported on foam ceramics have been studied. Due to the three-dimensional open-porous cellular structure the foam catalysts have high gas permeability, mechanical strength, and low density. Catalytic activity and selectivity of the foam catalysts in the process of oxidation of methanol to formaldehyde exceed the characteristics of the conventional crystalline and granulated catalysts of the same composition. Different electronic states (ions, charged cluster, crystals) of copper on the catalyst surface have been studied by the method of UV-visible spectroscopy.

Introduction

Silver and copper catalysts are widely used in the processes of selective oxidation of alcohols to aldehydes and ketones [1-5]. Our previous studies revealed that catalysts based on the foam materials are very promising for usage in the processes of partial oxidation of alcohols to aldehydes [6-11]. Thus, bulk foam silver and foam copper catalysts have physicochemical and catalytic properties exceeding the characteristics of the traditional crystalline and granulated catalysts in alcohol partial oxidation. Foam materials have uniform cellular structure with anisotropy of mechanical and gas-dynamic properties. Geometric parameters of the elementary cell are set by the preparation conditions and can be varied within 0.5-5.0 mm diameter. Physical properties of the whole block change depending on the cell average diameter: porosity - 80-98 %, volume density - 0.1-0.5 g/cm³.

However, using the bulk metal catalysts leads to high consumption of the metals. This one can be reduced by applying the supported samples based on foam ceramics. The aim of the present study is investigation of the mechanical, gas-dynamic and catalytic properties of copper catalysts supported on foam ceramics in the methanol partial oxidation.

Experimental

The catalyst samples were prepared by supporting copper (10-20 %-wt.) on foam ceramics from aqueous solution of the metal nitrates by chemical reduction with hydrazine sulphate. The catalysts were tested in the catalytic methanol oxidation system under operating conditions close to the industrial ones:

- ◆ "soft" - $T = 500-600^{\circ}\text{C}$, methanol concentration 100 %, ratio $\text{O}_2/\text{CH}_3\text{OH} = 0.25$, methanol load on the reactor $180 \text{ g}/(\text{cm}^2 \cdot \text{h})$, air flow rate 2.8 ml/s, composition of vapor-air reaction mixture 45 % CH_3OH , 11 % O_2 , 44 % N_2 ;
- ◆ "hard" - $T = 600-700^{\circ}\text{C}$, methanol concentration 70 %, ratio $\text{O}_2/\text{CH}_3\text{OH} = 0.35$, methanol load $100 \text{ g}/(\text{cm}^2 \cdot \text{h})$, air flow rate 2.8 ml/s, composition of air-vapor mixture 37.5 % CH_3OH , 13.5 % O_2 , 49 % N_2 .

For comparison, traditional catalysts were also tested: crystalline copper under "soft" conditions and samples 40 % Cu/pumice under "hard" conditions. Gaseous products and formaldehyde were analyzed using chromatographic and titrimetric methods, respectively.

The specific surface area of the foam ceramics was $0.5 \text{ m}^2/\text{g}$, (catalyst volume 4 cm^3); of the Cu/pumice - $0.8 \text{ m}^2/\text{g}$, (12 cm^3); of the crystalline copper - $0.07 \text{ m}^2/\text{g}$, (4 cm^3). The difference in the specific surface of the samples does not influence significantly their catalytic properties, because the process occurs in an outward diffusion mode.

Diffuse reflectance UV-Visible spectra were taken on a Varian Cary 300 spectrometer equipped with a standard sphere using BaSO_4 as a reference.

Results and Discussion

Gas-dynamic measurements showed that the specific pressure losses in gas filtration through foam catalysts are much lower as compared to characteristics of granulated and crystalline catalysts (Fig. 1). However, at the same cell diameter the gas permeability of the ceramic supported sample is lower than compared to bulk foam copper. It is caused by thicker bridges (and, accordingly, higher density) in the cellular frames of the foam ceramics. The similar correlation we observed when studying supported foam-silver catalysts [6-7].

The strength towards compression of the foam materials depends strongly on the sample density and porosity and is determined by the strength of the cell bridges. Failure of brittle foam materials (such as ceramics) under compression takes place in steps, through layers of the frame cells. Supporting a metal increases the strength of the sample due to hardening of the frame bridges.

The catalytic experiments showed that the selectivity of foam Cu catalysts in the "hard" mode is much higher than that of Cu/pumice sample (Table 1). This is explained by better gas-dynamic properties of the foam catalysts. The characteristics of bulk foam copper and Cu/ceramics samples do not significantly differ. Catalyst with 20 % Cu on the ceramics and bulk foam copper showed stable activity during the prolonged performance. Less percentage of copper on the support leads to acceleration of the catalyst carbonization and deactivation of Cu/ceramics sample.

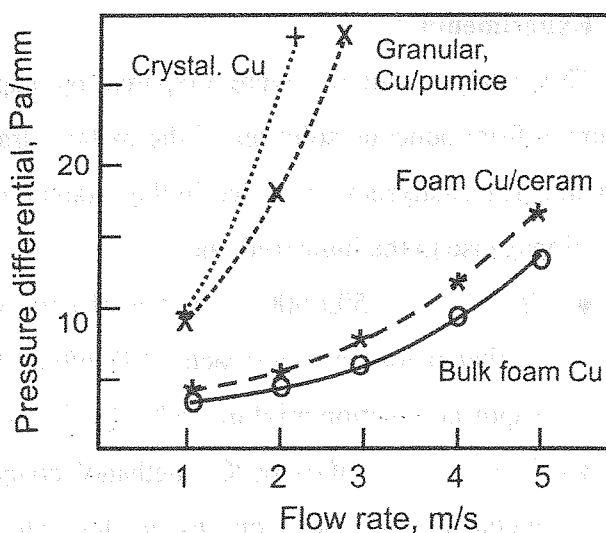


Figure 1. Pressure differential of the gas flow on copper catalysts.

Table 1. Catalytic properties of the copper samples in methanol oxidation

Catalyst	T, °C	CH ₂ O yield, %	Selectivity, %
Foam 20 % Cu/ceramics	550	51.8	72.3
	650	58.6	69.6
Bulk foam Cu	550	52.1	72.9
	650	58.0	70.5
40 % Cu/pumice	650	56.4	68.5
Crystalline Cu	550	48.9	71.1

UV-visible diffuse reflectance spectra of fresh Cu/pumice and foam Cu/ceramics samples display only unstructured absorption corresponding to large metal particles. After long-term work in catalytic reactor in the spectrum of Cu/ceramics catalyst noticeable signals at 390, 470, 580 nm and wide absorption in 600–650 nm range are observed (Fig. 2). Used Cu/pumice sample has similar pattern in UV-vis. range, but its signals are less pronounced and shifted to high-energy region. The same results we observed for Cu/pumice in the previous studies [7, 12]. According to literature data [13-17] the signals at 350-400 and 450-480 nm belong to O-Cu-O and Cu-O-Cu complexes (charge transfer bands). Absorption at 600–650 nm is attributed to electron d-d transitions in Cu²⁺ in octahedral surrounding by oxygen in CuO particles. Absorption bands in the range of 520–550 nm some authors attribute to CuAl₂O₃

[13-16]. However, formation of aluminate structures is not typical for corundum and pumice, so this signal can belong to plasmon resonance in Cu_n particles. According to our previous studies [7, 12], in the spectra of exhaust bulk foam-copper catalyst only two pronounced signals are observed: 365 nm (O-Cu-O) and 550 nm (Cu_n plasmon resonance). Thus, the prolonged run of the sample in catalytic reactor favors the formation of some amount of Cu^{2+} states and small metal particles, analogously to silver ones. It is one of the reasons of lower selectivity of copper in alcohol oxidation as compared with silver, as CuO is well-known catalyst for deep oxidation of organic compounds.

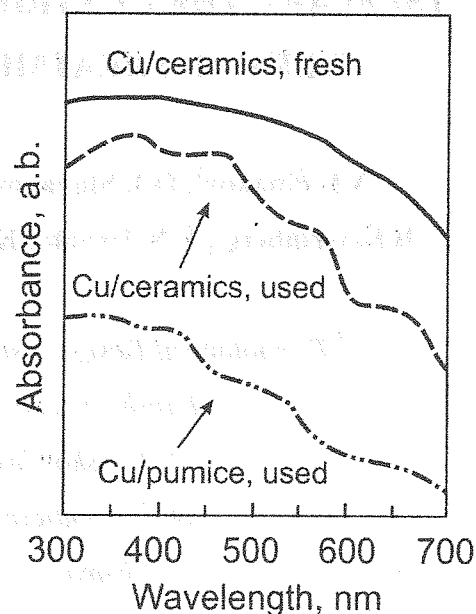


Figure 2. UV-visible spectra of copper catalysts

References

1. A.C. van Veen, O. Hinrichsen, M. Muhler, *J. Catal.*, 210 (2002) 53.
2. A. Nagy, G. Mestl, T. Rühle, G. Weinberg, R. Schlögl, *J. Catal.*, 179 (1998) 548.
3. Th. Schedel-Niedrig, M. Hävecker, A. Knop-Gericke, R. Schlögl, *Phys. Chem. Chem. Phys.* 2 (2000) 3473.
4. A. Knop-Gericke, M. Hävecker, T. Schedel-Niedrig, R. Schlögl, *Topics in Catalysis*, 15 (2001) 27.
5. A. Nagy, G. Mestl, *Appl. Catal. A: General*, 188 (1999) 337.
6. A.N. Pestryakov, V.V. Lunin, N.E. Bogdanchikova, V.P. Petranovskii, A. Knop-Gericke, *Catal. Commun.*, 4 (2003) 327.
7. A.N. Pestryakov, V.V. Lunin, A.N. Devochkin, L.A. Petrov, N.E. Bogdanchikova, V.P. Petranovskii, *Appl. Catal. A*, 227 (2002) 127.
8. A.N. Pestryakov, A.N. Devochkin, *React. Kinet. Catal. Lett.* 52 (1994) 429.
9. A.N. Devochkin, A.N. Pestryakov, L.N. Kurina, *React. Kinet. Catal. Lett.* 47 (1992) 13.
10. A.N. Pestryakov, A.A. Davydov, *J. Electron Spectr.* 74 (1995) 195.
11. A.N. Pestryakov, A.A. Fyodorov, A.N. Devochkin, *J. Advanced Materials* 5 (1994) 471.
12. V.S. Gurin, V.P. Petranovskii, A.N. Pestryakov, A. Kryazhov, O. Ozhereliev, M.A. Hernandez, A.A. Alexeenko, *European Physical J. D*, 24 (2003) 381.
13. O.V. Komova, A.V. Simakov, V.A. Rogov, D.I. Kochubei, G.V. Odegova, V.V. Kriventsov, E.A. Paukshtis, V.A. Ushakov, N.N. Sazonova, T.A. Nikoro, *J. Mol. Catal. A*, 161 (2000) 191.
14. V. Indovina, D. Pietrogioacomi and M.C. Campa, *Appl. Catal. B*, 39 (2002) 115.
15. M.C. Marion, E. Garbovski, M. Primet, *J. Chem. Soc. Faraday Trans.*, 86 (1990) 3027.
16. V.A. Markel, V.M. Shalaev, P. Zhang, W. Huynh L. Tay, T.L. Haslett, M. Moskovits, *Phys. Rev. B* 59 (1999) 10903.
17. V. Petranovskii, V. Gurin, N. Bogdanchikova, A. Licea-Claverie, Y. Sugi, E. Stoyanov, *Mat. Sci. Eng. A332* (2002) 174.

TSEFLAR – THE CENTRIFUGAL FLASH REACTOR FOR RAPID THERMAL TREATMENT OF POWDERED MATERIALS

V.I. Pinakov¹, O.I. Stoyanovsky¹, Yu.Yu. Tanashev², A.A. Pikarevsky¹,
B.E. Grinberg¹, V.N. Dryab¹, K.V. Kulik¹, V.V. Danilevich² and V.N. Parmon²

¹ *Technological Design Institute of Hydro-Pulse Techniques of SB RAS,*

Tereshkovoi str. 29, Novosibirsk 630090, Russia

² *Boreskov Institute of Catalysis of SB RAS,*

pr. Lavrentieva 5, Novosibirsk 630090, Russia

E-mail: tanashev@catalysis.nsk.su

Rapid heating of powders followed by their quenching is important in many fields of chemical engineering. For instance, the first stage of preparation of alumina based supports and catalysts is often performed through the so called “thermochemical activation (TCA)”, i.e. a short-time thermal treatment, of aluminum hydroxide at dehydration temperature, about 580 K, resulting in the formation of a substance with a high reactivity. Phase changes of solid oxygen containing compounds (hydroxides, salts, basic salts, clays, etc.) under heating are mainly determined by the dynamics of two physico-chemical processes. The first one is the removal of functional groups (OH^- , NO_3^- , CO_3^- and others), the second is the transformation of an initial crystal structure to that of oxide. Under slow heating these processes are conjugated, therefore an inactive raw material transforms into an other substance, crystal oxide mainly, which possesses, as a rule, a low reactivity. Otherwise, when heating is non-equilibrium, with the rate of hundreds degrees per second, the formation of a novel quasi-stable amorphous phase can occur [1]. This intermediate is characterized by stored energy and high reactivity.

The commercialized method of TCA is based on a dynamic contact of powder particles with hot exhaust gases [1] or hot granules of support or catalyst [2]. However, there are some disadvantages of this way of rapid thermal treatment, namely: bad ecology, pollution of the powder by products of the fuel combustion, instability in heating conditions, low efficiency of heat power application resulting in high energy consumption.

As an alternative, we have developed the concept of thermal impact in a so called Centrifugal Flash Reactor (the Russian abbreviation is “TSEFLAR”). This set-up is simple,

compact, environmental friendly and provides the more effective heat transfer to particles of reagent with a high rate of heating and quenching. The operation of the reactor is based on the regulated supply of a powder into the central part of the hot rotating plate which is profiled with a broadening to upwards. The centrifugal force ensures the reagent movement on the plate surface with the steady contact and following feed of the activated product into the cooling zone.

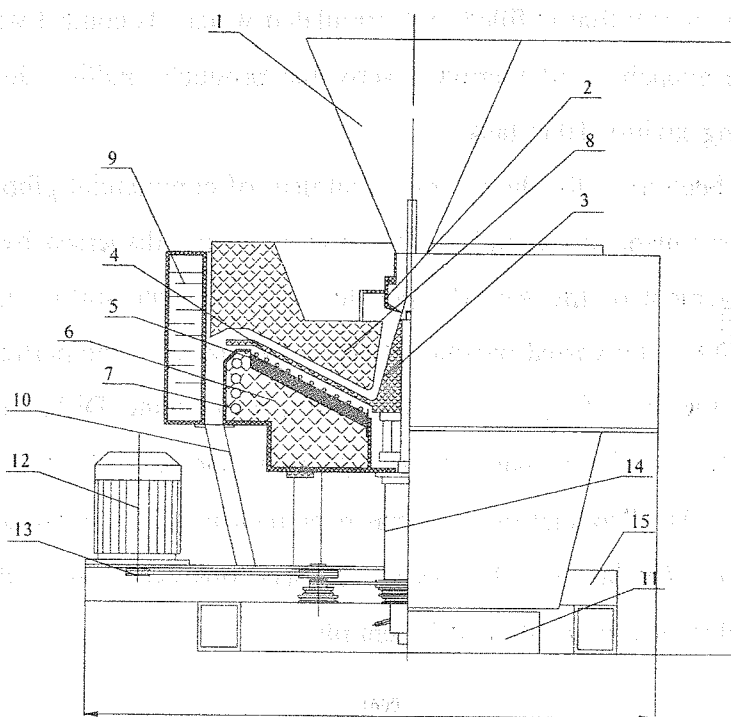


Fig. 1. The scheme of the TSEFLAR set-up. 1 – tank for raw material, 2 – metering unit, 3 – receiving cone of plate, 4 – plate, 5 – heaters, 6 – body, 7 – conduit for water, 8 – cover, 9 – cooling unit, 10 – turning cavity, 11 – tank for product, 12 – electric drive, 13 – belt drive, 14 – bearings body, 15 – frame.

A prototype of TSEFLAR has been designed and tested. Fig. 1 illustrates the scheme of the set-up. A raw material is falling down from tank 1 through metering unit 2 to hot receiving cone 3 of plate 4. While moving along plate on spiral-like trajectory, the heating of a powder is in progress. The electrical heating units 5 are disposed in insulated body 6 under the plate. The temperature over plate is controlled by set of thermocouples. The cylindrical lateral surface of body 6 is cooled by water through conduits 7. The powder under heating is moving in narrow cavity between the plate and insulated cover 8.

The time of the reagent residence on the plate, i.e. “contact time”, is regulated by the speed of the plate rotation. Centrifugal forces press the powder to the plate surface thus providing the heat transfer under direct contact of the particles with hot metal. In our opinion, this way of thermal treatment is more efficient than the common TCA-process under the

contact with hot gas. We have estimated the rate of heating of $\text{Al}(\text{OH})_3$ particle from $T_0 = 293$ K to $T_d = 583$ K after the contact with the hot medium. If the temperature of a solid surface is 773 K and the size of the particle is 100μ , the time for the temperature in the particle center to be rose up to T_d is no more than 0.1-0.2 s. On the contrary, the rate of heating by a hot gas is almost an order of magnitude lower.

Coming off the plate, the powder continues a spiral movement down the inner cylindrical surface of the cooling unit 9 that is filled with circulated water. Its contact with the cold wall ensures an effective quenching of thermally activated products. Falling down, the powder passes through turning cavities 10 to tanks 11.

This set-up has been used for the thermal treatment of commercial gibbsite produced in Russia. Before the treatment, the initial powder was dried and dispersed by a set of sieves. First of all, the movement of the $\text{Al}(\text{OH})_3$ powder over the plate surface has been studied using a video technique. The varied parameters were: the size d of the particles; the speed N of the plate rotation; the type of a plate; the temperature of the plate. Different versions of the plate were manufactured, with a plane, conic, spherical and special curvilinear ("constant acceleration") surface. The "contact time", τ , has been measured. The increase in τ from 0.25 to 1.50 s while N and d values are decreasing has been observed. Fig. 2 demonstrates the features of the particles movement along different plates.

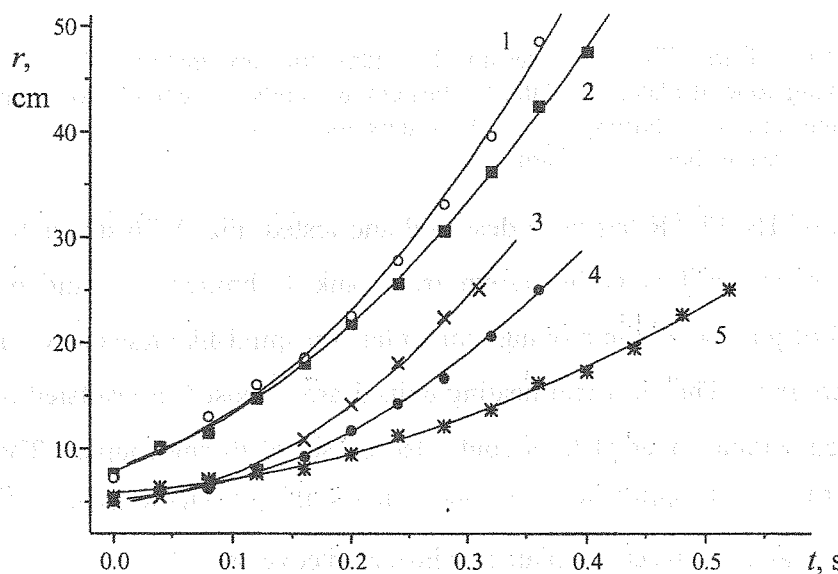


Fig. 2. Movement of gibbsite particles along different plates. r – distance between the particles and the center of the plate, t – time. $N = 220$ turns per minute, $d = 45 \mu$ (average). 1 – conic plate (with diameter $D = 1$ m), 2 – spherical plate ($D = 1$ m), 3 – plane plate ($D = 0.5$ m), 4 – conic plate ($D = 0.5$ m), 5 – plate of "constant acceleration" ($D = 0.5$ m).

The thermal treatment of gibbsite has been performed under temperature $T = 600 - 900$ K and $\tau = 0.5 - 1.4$ s. The products obtained are investigated by BET, X-ray and thermal analysis, electron microscopy, IR and NMR spectroscopy. It has been found that the initial substance transforms into a quasi-stable state, so called "centrifugally thermally activated" (CTA) product. The phase composition of the product under $T > 700$ K and $\tau \sim 1.4$ s includes gibbsite $\text{Al}(\text{OH})_3$ (0–20%), boehmite AlOOH (0–10%), pseudoboehmite AlOOH (0–20%) and X-ray amorphous phase $\text{Al}_2\text{O}_3 \cdot n\text{H}_2\text{O}$, where $n = 0.4 - 1.0$ (up to 100%). The thermal treatment results in the decrease of the water content from 34.6% to 5–15%, the decrease of dehydration temperature from 300–310 to 150–180°C and the increase of the surface area from 2–5 to 100–300 m^2/g because of the formation of microporous system. These parameters depend on the conditions of the activation such as the temperature of the plate, the contact time, the size of the particles, the rate of the powder feed, the initial temperature of the powder, the pressure of the mixture "steam + air" in the unit for the steam removal. The energy consumption under $T = 800$ K is about 7 kJ/g of $\text{Al}(\text{OH})_3$.

The main parameters of the CTA process can be easily controlled and the physico-chemical properties of the products are well reproduced. The CTA product has a high reactivity and is shown to be a promising starting material for the preparation of various alumina-based compounds including catalysts and catalyst carriers.

Acknowledgements. The work is financially supported by Presidium of SB RAS, the Ministry of Science and Technology of the Russian Federation and the Ministry of Education of the Russian Federation.

References

1. B. P. Zolotovskii, R. A. Buyanov, G. A. Bukhtiyarova, V. V. Demin and A. M. Tsybulevskii. // *React. Kinet. Catal. Lett.* 1995. V.55, No.2. Pp.523-535.
2. Patent application 517564, USSR, 1975.

MODERN CATALYSTS OF CLAUS PROCESS

A.V. Podshivalin

*The Institute of Petroleum Refining and Petrochemistry
of Bashkortostan Republic Academy of Sciences*

Ufa 450065, Iniciativnaya Str., 12, phone/fax: (3472) 42-24-71, vezirov@anrb.ru

The total degree of hydrogen sulphide into sulfur conversion according to Claus method usually amounts to 93 -96% and depends on operation efficiency of the heating device of high – temperature stage as well as of the catalysts of low – temperature stage [1,2].

The Claus catalysts used at present are made on the basis of active alumina ($\gamma\text{-Al}_2\text{O}_3$) [3]. Composition of the catalyst depends on feed quality, composition, presence of impurities and length and conditions of treatment [2]. Such qualities of $\gamma\text{-Al}_2\text{O}_3$ as high specific surface (up to $350\text{ m}^2/\text{g}$), large pores (200-5000 nm) which size can be regulated at shaping stage by crystallite size of the initial aluminium hydroxide. High mechanical strength and refractoriness ($T_p > 2000^\circ\text{C}$) make $\gamma\text{-Al}_2\text{O}_3$ one the best carrier for Claus catalysts [4].

Another parameter influencing choice of catalysts is their operation period. As a rule this parameter for the catalysts on the basis of alumina amounts to 3 – 5 years depending on operation conditions, composition of sour gases and many other factors.

Further role in catalysts deactivation play such factors as decrease of specific surface, crystal changes (due to hydrothermal and thermal destruction), sulfation of alumina and chemisorption of SO_2 . The process of decrease of activity of alumina catalysts at the expense of sulfation strongly is pronounced in low – temperature processes used for conducting reaction at the temperatures below sulfur dew point (Sulfren, SBA, Maxisulf) [2, 5]

Experimental study of the kinetics of alumina samples sulfation used as Claus reaction catalysts has been performed and quantitative correlation between sulfation and specific surface and catalyst iron content has been determined [6].

So, in spite of all its merits as a carrier for Claus process catalyst $\gamma\text{-Al}_2\text{O}_3$ has one essential drawback – sharp decrease of activity in the process of operation in unstable conditions.

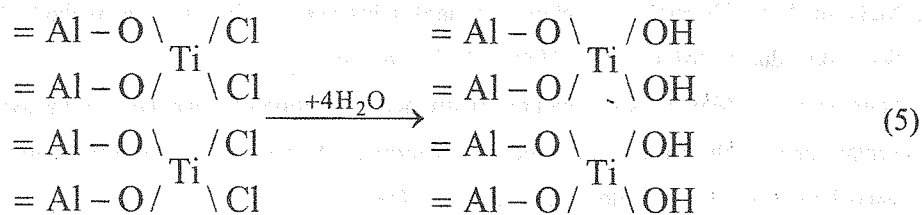
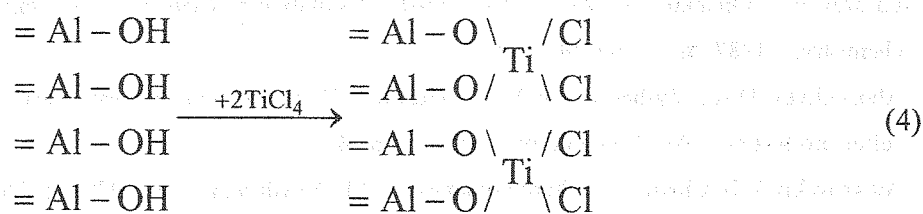
Lately the prospect of development of the technology of production of the catalyst on the basis of anatase form of titanium dioxide (TiO_2) is viewed. The catalysts on the basis of titanium dioxide have very high stability to sulfation and high activity in COS and CS_2 , hydrolysis reactor even in the presence of oxygen [7].

But usage of titanium dioxide as a catalyst becomes complicated by the fact that the catalysts on the basis of TiO_2 are very expensive and their mechanical strength is low which decreases their operation parameters.

The problem of synthesis of a high – active and mechanically strong catalyst for the process of elemental sulfur production can be solved by the method of molecular layering, that is application of a layer of TiO_2 on the surface of alumina.

One of the basic features of the method of molecular layering developed by Aleskovskiy V.B. et. al. [8-10] is possibility of successive build up of monolayers of structural units with known and given chemical composition and representing hard substances surface layer. Usage of molecular layering of reagents of different chemical composition in successive stage of the reaction makes it possible to synthesize hard substances with multizone surface structure with the given arrangement in the forming matter of the layers of different atoms connected with each other by covalent bonds. Structural – chemical changes connected with variation of chemical composition of surroundings of the central atom of the forming structural unit as well as change of its coordination number proceed during this process. This in its turn influence the character of the forming interatomic bonds. Coordination numbers of the matrix unit and of the matter of the synthesized layer can also vary. As a result in the process of molecular layering during build up of chemically bound into a common system monolayers of the structural units transformation of their parameters and formation of a number of transition structures with regulary varying characteristics will take place.

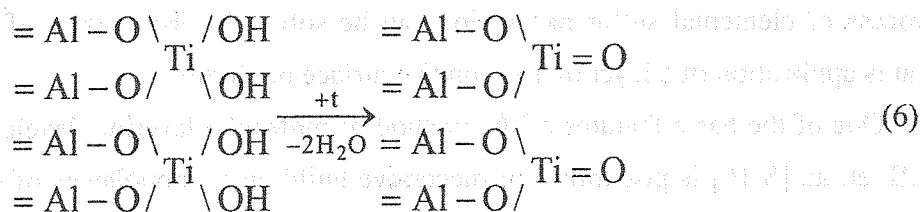
Synthesis of titanium dioxide on alumina surface is based on two successive reactions: interaction of titanium tetrachloride with preliminary hydroxysized aluminium surface and subsequent hydrolysis of chlorine-groups by steam which leads to renewal of hydroxide groups.



As a result of this reaction the titanium atoms which were formly included in composition of low-molecular chloride join to the surface of alumina. These atoms are supplied by water

molecules during hydrolysis. The result of each cycle of reaction consists in final build up of aluminium lattice by a monolayer of titanium – oxygen structural units.

The final stage of synthesis is calcinating of the catalyst with split out of water from the formed titanium dioxide monolayer:



Synthesis of such structures [11] has shown that a mixture of deformed rutile and anatase structures is formed at the surface of $\gamma\text{-Al}_2\text{O}_3$. Presence of only one silicon monolayer leads to a sharp decrease of $\gamma\text{-Al}_2\text{O}_3$ surface influence on phase formation. During subsequent cycles of the reaction of molecular layering only the anatase form of titanium dioxide is formed.

So it is possible to obtain the catalyst with strength properties and pores geometry of $\gamma\text{-Al}_2\text{O}_3$ and with chemical stability and catalytic activity of TiO_2 . The cost of this catalyst will be little higher than the cost of alumina carrier and much lower than the cost of massive titanium oxide catalyst.

References

1. Avdeyeva A.V. Production of sulfur and gases. – M.: Metallurgiya, 1977. – p.175
2. Grunvald V.R. The technology of gas sulfur. – M.: Khimiya, 1992. – p.272
3. Chemical encyclopaedia. T. 1. – M.: Sov. entsiklopediya, 1961. – p.118
4. Elvin B. Styles. Carriers and applied catalysts. Theory and practice. M.: Khimiya, 1991. – p.240
5. Abrosimov A.A. Encyclopaedical aspects of production and usage of petroleum products. – M.: BARS, 1999. – p.732
6. Lazarev V.I., Onopko T.V., Motyl' D.H. Study of sulfation of Claus process catalysts. Journal of applied chemistry. – 1987, № 7, – p.p.1465-1469
7. Abuskuliyev D.A., Vysheslavtsev Yu.F., Guseynov N.M. Modern processes and catalysts for elemental sulfur production. – M.: VNIIEgasprom, 1988. – p.64
8. Aleskovskiy V.B. Chemistry of hard substances. – M.: Vysshaya shkola, 1978. – p.256
9. Koltsov S.I. The reaction of molecular layering. – SPb.: SPbTI, 1992. – p.63
10. Malygin A.A. Chemical assembling of hard substances surface by the method of molecular layering. / Sorovsky educational journal. – 1998. – № 7, – p.p.58-64
11. Ishutina Zh.N., Malkov A.A. Features of structure formation of a nanolayer in the system $\text{Al}_2\text{O}_3\text{-SiO}_2\text{-TiO}_2$, synthesized by the method of molecular layering. / Materials of all-Russian seminar "Nanoparticles and nanochemistry". Chernogolovka 2-5 October 2000

<http://www.icp.ac.ru/Conference/Nanochem/I/Ishutina.html>

APPLICATIONS OF MSE-ARRAYS AT ATMOSPHERIC PRESSURE: “NON-THERMAL PLASMAS AS STERILISATION AND COATING TECHNIQUE”

**Christian Schrader¹, Philipp Sichler², Thorben Cordes¹, Lutz Baars-Hibbe¹,
Siegfried Draeger³, Stephanus Büttgenbach² and Karl-Heinz Gericke¹**

¹*Institut f. Physikal. und Theoret. Chemie, TU Braunschweig, Hans-Sommer-Straße 10,
D-38106 Braunschweig; E-Mail: K.Gericke@tu-bs.de*

²*Institut für Mikrotechnik, TU Braunschweig, Alte Salzdahlumer Str. 203,
D-38124 Braunschweig,*

³*Institut für Mikrobiologie, TU Braunschweig, Spielmannstrasse 7,
D-38106 Braunschweig*

Introduction

Non-thermal plasma processing techniques optimized for atmospheric pressure applications are the subject of a recent growing interest due to their significant industrial advantages. At atmospheric pressure thin film deposition with very high rates are possible and cost-intensive vacuum technology is avoided. There are many approaches published recently to overcome the problems to generate and sustain a stable uniform non-thermal atmospheric plasma^[1,2].

Recently, micro-structured electrode (MSE) arrays were introduced as alternative atmospheric pressure plasma sources^[3, 4]. They consist of a system of planar and parallel electrodes (comb structure) arranged on an insulating substrate and manufactured by means of modern micro machining and galvanic techniques. The electrode dimensions in the μm -range are small enough to generate sufficiently high electric field strengths to ignite gas discharges applying only moderate radio frequency voltages (13.56 MHz, less than 400 V in Ne, He, Ar and N₂).

Companies dealing with medical-, food-packaging-, air-conditioning- and military scopes constantly search for new technologies to improve sterilisation and functional coating techniques. The upcoming threat of terroristic usage of bioweapons also shift the focus of scientific work on new sterilisation techniques into an area of national interest. To absolutely decontaminate any material it is needed to deactivate thermo- and UV-resistant spores.

Conventional sterilisation techniques achieve this aim through damp heat (autoclave), dry heat, filtration, radiation or antibacterial agents. The disadvantages of damp- and dry- heat methods, filtration and also antibacterial agents are long process duration and the missing applicability on thermosensitive materials and “solution-free” conditions. The destruction of cellular macromolecules (DNA) by radiation as a further sterilisation technique is only efficient at wavelengths down to 200 nm because of the atmospheric absorption.

The plasma source as a new sterilisation tool produces hot electrons with kinetic energies around 5 eV. This energy correlates with electron temperatures up to 10.000 K. Gas molecules, ions and radicals approximately retain room temperature (300 K – 400 K). These facts lead us to the idea to utilize the non-thermal plasma as a source for adequate reactive particles applicable with substrate conserving requirements.

Observed microorganisms

In our sterilisation experiments the thermo resistant spores of the vegetative bacteria *Bacillus cereus* pertaining to the sporulating genus *Bacillus*, *Clostridium* and *Desulfotomaculum* were chosen because of their easy recognizability in growth and their less harmful properties compared to the other well-known example *Bacillus anthracis* (Anthrax). The UV-resistant spores of the fungus *Aspergillus niger* endure radiation with wavelengths < 200nm and therefore, they are used as a reference for the total deactivation under the influence of UV-radiation.

Experimental setup

The sterilisation and deposition setup consists of a RF generator using 13.56 MHz (ENI ACG-3B) equipped with a matching network (ENI MW-5D). Between the matching network and the MSE a special probe (ENI VI-Probe®) is inserted in order to measure voltage, current and phase angle of the system. An additional electrode plate is coplanary installed to the MSE array at a distance of 2 mm. A substrate (Si, Cu or different plastic films) is mounted on this electrode, which is biased with different AC frequencies (8.0 kHz – 10.5 kHz) leading to voltages from 500 Vpp to 1300 Vpp.

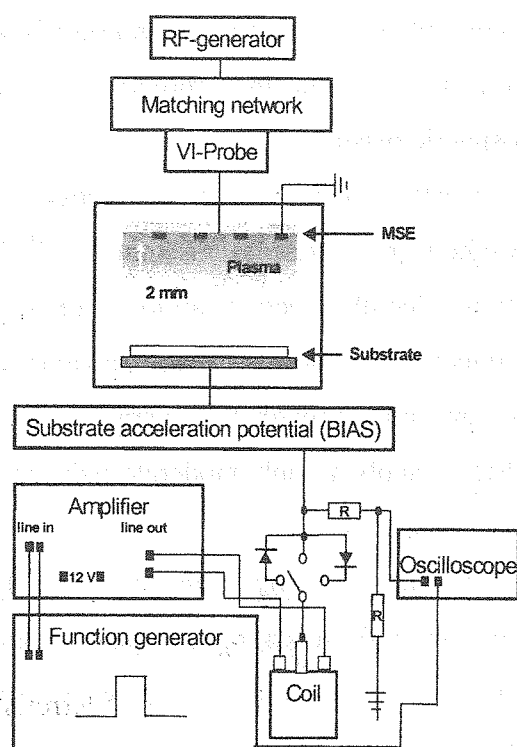


Figure 1: Sterilisation and deposition setup

The applied sine potential is monitored with an oscilloscope. If it is needed a high voltage diode can rectify the AC bias to a pulsed positive or negative DC(+/-) bias. The difference between the sterilisation and coating setup can be found in the maintenance of precursor molecules or atoms for the desired application. In order to supply sterilising agents helium, argon and oxygen were used. The applied precursor to functionalise surfaces is tetraethoxysilane-saturated helium. A conventional ice cooled bubbler transfers TEOS (vapor pressure: 2 mbar) into the buffer gas^[5,6].

Results

Using the sterilisation and deposition setup we successfully deposited SiO_2 -layers on various substrates (Si, Cu, polymer films) with a deposition rate of 30 nm/min (9.5 kHz AC bias up to 1000 Vpp). A gas stream of 1 % oxygen in helium (100 sccm, working pressure up to 100 mbar) was bubbled through TEOS at 0°C. We also successfully sterilised polymer films in helium (PET, PS and PP) inoculated with 10^6 thermo-resistant spores of the vegetative bacteria *Bacillus cereus* suspended in 50 μL probe suspension. Furthermore, we totally deactivated the same quantity of spores of the fungus *Aspergillus niger* in argon.

The MSE plasma source provides the reactive species at atmospheric pressure in He or Ar. The AC bias potential accelerates the charged particles, ions and electrons to the substrate. Figure 2 shows that the AC bias rectified to a pulsed DC-(+) bias not only accelerates the electrons resulting in an electron bombardement of the microorganisms on the substrate surface but also lowers the plasma sustaining voltage applied to the MSE array supporting the ignition.

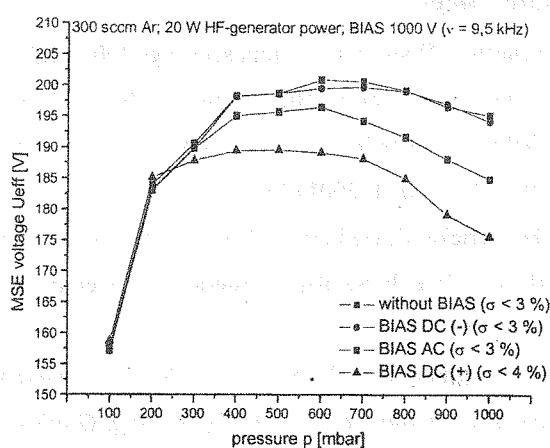


Figure 2: VI-Probe dependencies^[7]

The ions also are accelerated towards the substrate, but ion bombardement is not the exclusive sterilising agent. UV-radiation has to be considered as well. With the bias potential switched off we did not obtain a total deactivation of the spores. A mixture of UV-radiation, charged particle bombardement and the presence of radicals and meta-stables originating

from the residual gases oxygen or water always present in the vacuum chamber is responsible for the total deactivation of the spores.

Recently completed measurements show that we can associate accelerated reactive species with obtained sterilisation results. In the case of an applied DC(-) bias (10.4 kHz, -700 V) in helium (300 sccm) we predicted He^+ -Ions as sterilising agents and received good sterilisation results. The experiment with helium (300 sccm) and oxygen (3 sccm) linked with a DC (-) bias (10.4 kHz, -700 V) showed similar results like the experiment before. Thus, oxygen as a dominating source for reactive species in form of O_2^+ or metastables can be excluded in this special bias variation. The best sterilisation performance showed the gas discharge in a mixture of 300 sccm helium with 3 sccm oxygen with a DC-(+) acceleration potential (10.4 kHz, +700 V). In this case electrons and negatively charged oxygen ions were responsible for the total deactivation of the spores. The measurement with a DC-(+) bias (10.4 kHz, +700 V) in helium (300 sccm) showed an insufficient sterilisation performance. This fact could be interpreted that only electrons as sterilising agents cannot fulfill the demand of a total deactivation.

References

- [1] P. Scheffler, Dissertation, Braunschweig (2001), ISBN 3-89873-239-8.
- [2] C. Geßner, Dissertation, Braunschweig (2001), ISBN 3-89873-325-4.
- [3] C. Geßner, P. Scheffler, K.-H. Gericke, *Proceed. of the Intern. Conf. on Phenomena in Ionized Gases (XXV ICPIG), Nagoya, 4* (2001) 151-152.
- [4] K.-H. Gericke, C. Geßner, P. Scheffler, *Vacuum* **65** (2002) 291-297.
- [5] L. Baars-Hibbe, P. Sichler, C. Schrader, C. Geßner, K.-H. Gericke, S. Büttgenbach, *Surf. Coatings Technol.* (in press 2003)
- [6] L. Baars-Hibbe, C. Schrader, P. Sichler, K.-H. Gericke, S. Büttgenbach, *Proceed. of the Intern. Conf. on Phenomena in Ionized Gases (XXVI ICPIG), Greifswald, 3* (2003) 231-232.
- [7] L. Baars-Hibbe, C. Schrader, P. Sichler, K.-H. Gericke, and S. Büttgenbach, Micro-structured Electrode Arrays: High Frequency Discharges at Atmospheric Pressure: Characterization and new Applications, *Contrib. Papers Inter-national Symposium on Applied Plasma Science (ISAPS '03), Japan 2003*.

HYPERBOLIC CONCEPT OF LONGITUDINAL DISPERSION AND THE MODELING OF STRUCTURED CATALYST UNITS

N.M. Voskresenskii, S.I. Serdyukov, M.S. Safonov

Chemistry Department, Moscow State University, Leninskie gory, 110992 Moscow

Various physicochemical processes in apparatuses with a fixed bed of an active material (a sorbent or a catalyst) are most often calculated using one-dimensional continuous mathematical models. Wide use is made of the so-called standard dispersion model (SDM). In this model, convection–dispersion models for concentrations averaged over an apparatus cross section are described using an analog of well-known Fick's law, which leads to a parabolic differential equation. However, the "diffusion" mass transfer in this form cannot have anything in common with molecular diffusion. In this case, the diffusion term models the deviation of the longitudinal convective transfer from the average-velocity plug flow.

In the further development of one-dimensional models, attempts were made to take into account the nonuniform flow pattern. Its description in terms of a single parameter (longitudinal dispersion coefficient) involves uncertainty in boundary conditions [1,2]. A composite (combined) model was proposed [1,3], in which the flow was divided into parts with different average velocities. In this case, the differential equation of mass transfer in the flow is hyperbolic and has one or several parameters more than SDM.

The mass transfer in a flow was also proposed to be described using a wave model [4-6], in which the dispersion transfer is characterized by an equation containing a second time derivative. In this case, the equation is also hyperbolic and has three parameters.

In this communication, comparison was made between the wave and composite models of mass dispersion in a flow consisting of two parts with different flow patterns, in which there is a first-order reaction. It was shown that there is a unique correspondence between the parameters of the wave and composite models. The substantiation of these equations in terms of extended irreversible thermodynamics was considered.

1. M.S.Safonov, N.M.Voskresenskii. In the collection "Modern problems of physical chemistry", v.10, M., Publ. MSU, 1978, p.72-106.
2. K.R.Westerterp, A.E.Kronberg, A.H.Benneker, V.V.Dil'man. Trans. IChemE, v.74, Part A, N 11, 1996, p.944-951.
3. A.K.Jagota, E.Rhodes, D.S.Scott. Can. J. Chem. Engng, v.51, N 1, 1973, p.139-145.
4. K.R.Westerterp, V.V.Dil'man, A.E.Kronberg. AIChE Journal, v.41, N 9, 1995, p.2013-2028.
5. K.R.Westerterp, V.V.Dil'man, A.E.Kronberg, A.H.Benneker. AIChE Journal, v.41, N 9, 1995, p.2029-2039.
6. A.E.Kronberg, K.R.Westerterp. Chem. Engng. Sci., v.54, 1999, p. 3977-3993.

ELECTROCHEMISTRY IN WASTE WATER TREATMENT**A.M. Skundin and T.L. Kulova***A.N.Frumkin Institute of Electrochemistry of the Russian Academy of Sciences**31 Leninsky prospect, 119071 Moscow, Russia**fax: +7 (095) 952 0846; e-mails: skundin@gol.ru; tkulova@mail.ru*

There are at least two points, in which electrochemistry intersects with waste water treatment. Firstly, a number of electrochemical devices for waste water monitoring exist and are under development. Secondly, some electrochemical techniques for waste water detoxication treatment have certain advantages in comparison with chemical ones.

There is large diversity of electrochemical instruments for waste water analysis. First of all various polarographs must be mentioned. Secondly, many various ion-selective electrodes were developed in the last decades, so potentiometric method of analysis became very widespread together with traditional pH-metric analysis. Thirdly, there are many ammetric methods are used in waste water analysis, for example, ammetric determination of dissolved oxygen. Further, conductometric measurements are used for estimation of total ionic content.

The most interesting example of the devices for water purity checking is "Electrochemical water quality analyzer". It is automatic device for quantitative determination of organic impurities as well as traces of heavy metals in various types of water including natural, drinking, industrial, waste waters, and sewage. The analyzer functioning is based on electrochemical measurements of hydrogen adsorption on a platinum electrode. All organic substances and ions of heavy metals are capable to adsorb on a platinum surface lowering the hydrogen adsorption. Relative decrease of amount of adsorbed hydrogen is the measure of adsorbed impurities and can be recalculated to concentration of the impurity. The hydrogen adsorption at platinum is known to be very sensitive to presence of organic impurities and heavy metal ions, so the minimum detectable concentration of total organic carbon is about 0.01 ppm. Sensitivity to heavy metals is yet higher and is amounted to as low values as 0.0005 ppm.

The Electrochemical water analyzer is not able to determine the nature of organic impurity (i.e. it is not instrument for qualitative analyses of organics), it can discriminate only such classes of organic substances as easily oxidizable substances (e.g., aliphatic alcohols,

aldehydes, low-molecular acids such as formic acid and oxalic acid, etc.), moderately oxidizable substances (e.g., aromatic alcohols and acids, including phenols, surface-active substances, etc.), and hardly oxidizable substances (e.g. aromatic hydrocarbons and other cyclic compounds). In the overwhelming majority of cases it is sufficient for practical goals. In any case the analyzer can be used for monitoring of effectiveness of waste water treatment.

There are diverse electrochemical methods of waste water treatment. The simplest technique is usual plating of metals from waste water of surface finishing plants. This method can be effective only for rather high concentration of metal ions in the waste water. More widespread methods are various membrane technologies. Such technologies are sooner electro dialysis ones than truly electrochemical. Very effective are various sorption methods of waste water purification. There are some electrochemical methods of sorbents production directly in the course of water treatment. In these cases steel or aluminium anodes are used with yield of solid iron hydroxide or alumina with very high surface area.

Electrochemical oxidation of organic impurities is of great interest for waste water detoxication. Indeed, majority of organic substances can be anodic oxidized. However some problems can arise in the course of waste water anodic treatment. Firstly, the waste water must be electroconductive, i.e. it must contain sufficient amount of ionic species. Secondly, anodes must be made from stable materials because they are subjected to strong corrosive action. Thirdly, the products of anodic oxidation must be harmless.

The second requirement can be met by such stable metals as Ti, Ta, Nb etc. Unfortunately all these metals have very poor electrocatalytic activity. Their activity can be sufficiently enhanced with deposition of small amounts of platinum or composition from ruthenium and titanium oxides ("dimension stable anodes", DSA). Of late, the electrodes from boron-doped diamonds are considered as very promising for waste water treatment. They are very stable at the range of high anodic potentials.

The third requirement is very serious. Only low-molecular simple aliphatic compounds are oxidized directly to carbon dioxide and water. The primary products of oxidation of aromatic compounds are quinones, which can be even more harmful than initial impurities. Such problems must be solved by more deep oxidation. The interesting example of such a process is purification of hospitals and farms waste water from acetylsalicylic acid (Aspirin).

CIRCULATION REACTOR FOR AQUEOUS ALKALI OXIDATION OF ALCOHOLS

D.V. Staroverov, E.V. Varlamova, N.A. Kornakova, V.F. Shvets

D. Mendeleev University of Chemical Technology of Russia,

Miusskaya Sq. 9, 125047 Moscow, Russia

stardv@muctr.edu.ru

Oxidation of alcohols and aldehydes with oxygen in aqueous alkali solutions on supported noble metals has attracted attention as a method of preparation of valuable products and intermediates for fine chemistry [1, 2, 3] and surface-active amido and ether carboxylates [4, 5]. These reactions are environmentally friendly and can be performed with high selectivity under mild operating conditions. One of the main bottleneck for commercialization consists in reversible and/or irreversible catalyst deactivation.

Reversible is the result of noble metal over-oxidation and poisoning due to strongly adsorbed species. Irreversible deactivation is caused by noble metal crystallite agglomeration on carrier surface and growth due to Ostwald ripening as well as metal transfer deep into catalyst pores and leaching from catalyst into solution. The other problem is high-velocity heat-evolution during the oxidation of compounds with high reactivity.

Minimization of irreversible palladium catalyst over-oxidation and temperature conditions keeping can be easily achieved by using of circulation semi-periodical apparatus with remote trickle-bed reactor. We investigated the oxidation of some primary alcohols differed in chemical structure and physicochemical properties in circulation reactor and proposed concept of mathematical modelling of these processes. Ethylene glycol, isoamyl alcohol and isononylphenol adduct with ethoxylation degree of 12 (Neonol AF9-12) as starting alcohols and palladium-on-carbon catalysts were used. Influence of liquid and gas flow rates, liquid-phase reagents and oxidation products concentrations, oxygen partial pressure, and temperature was investigated.

It was established for all alcohols the mathematical model may be based on kinetic description including equations of rates of catalyst over-oxidation and reactivation under reaction mixture reducing power influence besides oxidation rate equation. The common

feature of all studied processes is proportionality of oxidation rate with balanced catalyst activity resulted from equality of over-oxidation and reactivation rates.

The model features for different starting alcohols are caused by their reactivity and physicochemical properties. For example, in case of high reactive ethylene glycol it is necessary to take into account the limiting influence of oxygen transfer 'gas-catalyst' on oxidation rate. In case of micellar Neonol AF9-12 the model is adequate at temperature below cloud point.

Irreversible deactivation of Pd/C-catalyst fixed bed during long run of Neonol AF9-12 oxidation was investigated. The assumption has been made that during one oxidation cycle catalyst activity varies weakly and can be considered as a constant and in each new oxidation cycle the activity decreases owing to irreversible deactivation. Observed reaction rate coefficient calculated by means of above mentioned mathematical model was used as the current catalyst activity index. The catalyst activity decreasing in consecutive oxidation cycles was determined. Effects of carbon carrier properties, palladium percentage, and oxidation temperature on irreversible deactivation rate and time life of Pd/C-catalyst was studied.

This work was financially supported by Ministry for Education of Russian Federation in terms of Research Program "New Investigations of the Higher School in the Field of Chemistry and Chemical Products". The authors wish to express their gratitude to V. Semikolenov (Boreskov Institute of Catalysis) for preparation of catalyst samples.

References:

1. T. Mallat and A. Baiker. *Catal. Today*, 19 (1994) 247.
2. M. Besson and P. Gallezot, *Catal. Today*, 57 (2000) 127.
3. J.H.J. Kluytmans et al. *Catal. Today*, 57 (2000) 143.
4. *Nonionic Surfactants (Surf. Sci. Ser., V. 72)*, N.M. Van Os ed. New York – Basel – Hong-Kong: M. Dekker, 1998. 291.
5. Староверов Д.В. и др., *Хим. пром. №1* (2000) 58.

DEVELOPMENT OF C₇-C₁₀ (C₁₁) PARAFFINIC HYDROCARBONS ISOMERIZATION PROCESS

N.R. Vezirova, R.R. Vezirov, S.A. Oboukhova, O.V. Arkhipova

*The Institute of Petroleum Refining and Petrochemistry
of Bashkortostan Republic Academy of Sciences*

Ufa 450065, Initsiativnaya Str., 12, phone/fax: (3472) 42-24-71, vezirov@anrb.ru

As a result of analysis of C₅-C₁₁ hydrocarbons processing schemes development for obtaining gasoline blends the trend for increasing of feed hydrocarbons processing selectivity was ascertained. Based on the trend ascertained the perspective scheme of selective conversion of C₅-C₁₁ naphthenic, aromatic and paraffinic hydrocarbons was developed permitting production of high-octane low-aromatics containing gasoline component corresponding to perspective environment protection requirements [1,2].

The selective processing scheme is based on the adsorptional separation of normal paraffins from the C₇-C₁₀ petroleum cut (containing C₁₁ hydrocarbons impurities) and their conversion in the catalytic isomerization process. Conversion of n-paraffins to components having branched structure allows obtaining from them high-octane non-aromatic gasoline components, due to what aromatic hydrocarbons content in the gasoline pool obtained from straight-run naphtha is lowered to 24-28 % [2]. Dependently from the correlation at blending with other high-octane compounds aromatics content in commercial grade fuels can be lowered to 10-15 %.

The main task of this scheme realization is development of the industrial technology of C₇-C₁₀ (C₁₁) paraffins isomerization.

On the base of the octane numbers data we can make the decision that among the C₇-C₈ paraffins the most desirable gasoline components are di- and three-alkyl-substituted, having in average octane numbers of 75 to 100. From among the C₉-C₁₀ (C₁₁) paraffins the most desirable components are three- and more alkyl-substituted isoparaffins. From the point of view of thermodynamic equilibrium displacement towards high-branched isomers formation it is more profitable to carry out the process at lower temperatures [3,4].

Conversion of C₇+ paraffins at platinum-containing alumina-based isomerization catalysts, or metal-aluminosilicate catalysts, being effective only at high temperatures (about

350-400 °C), is in sufficient degree accompanied by hydrocracking reactions, while among the obtained isocomponents a lowered outlet of di-branched isomers in comparison with those being thermodynamically probable [5] takes place – not more than 10-15 % to isomerize (see fig.1). Actually during C₇₊ paraffins isomerization in the high-temperature process the most desirable components are not formed, or formed in very little quantities, while at low temperatures the kinetic parameters of the process are very inferior. Consequently given type of catalysts is not very effective for using in the isomerization process of light naphtha paraffins. In recent years the announcements arose about development of the catalysts on the oxide base having high isomerizing activity at rather low temperatures [6].

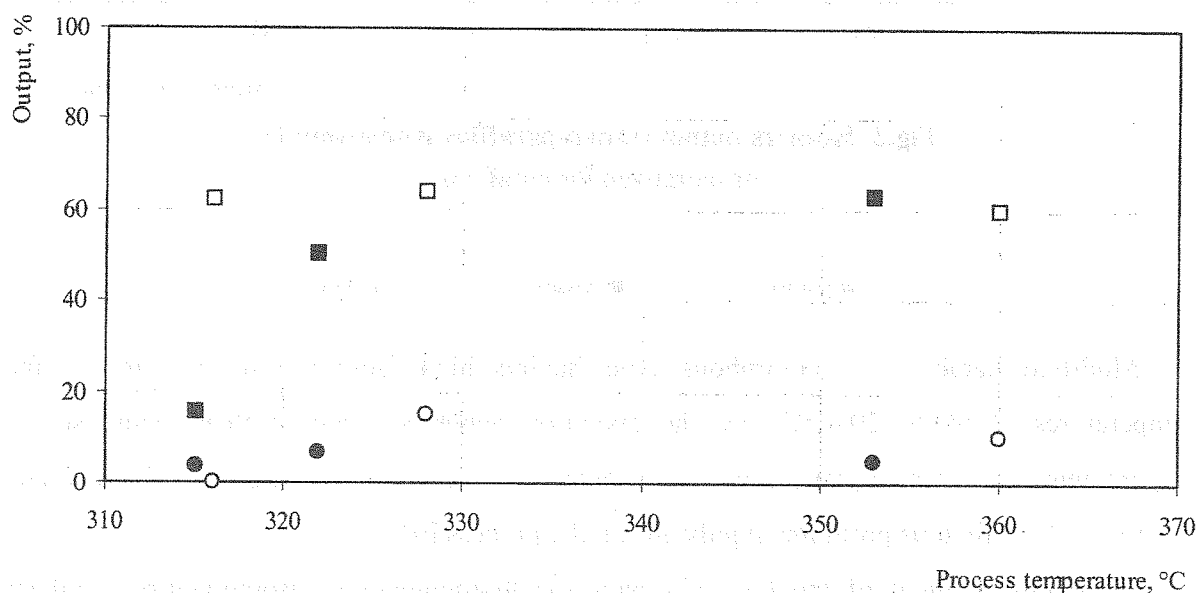


Fig.1. Isomers content in the products of isomerization of n-heptane and n-octane at metal-aluminosilicate catalyst

- methyl-hexanes output at n-heptane conversion
- 2,4-di-methyl-hexanes output at n-heptane conversion
- methyl-heptanes output at n-octane conversion
- di-methyl-heptanes output at n-octane conversion

Data of isoparaffins yield in isomerization reactions of n-paraffinic hydrocarbons at metal-zeolite catalysts (fig.2) show, that from the point of view of increase of conversion degree and selectivity while hydrocarbon chain increasing low temperatures (at the level of 200 °C) of the process are more optimal too [7,8].

Among the metal-zeolite isomerization catalysts more selective in formation of high-branched isomers are those obtained from relatively wide-porous high-silica and super-high-silica zeolites (for example zeolites type Pt-H β , dealuminated Pt-mazzit, ZSM-5 and others) [7].

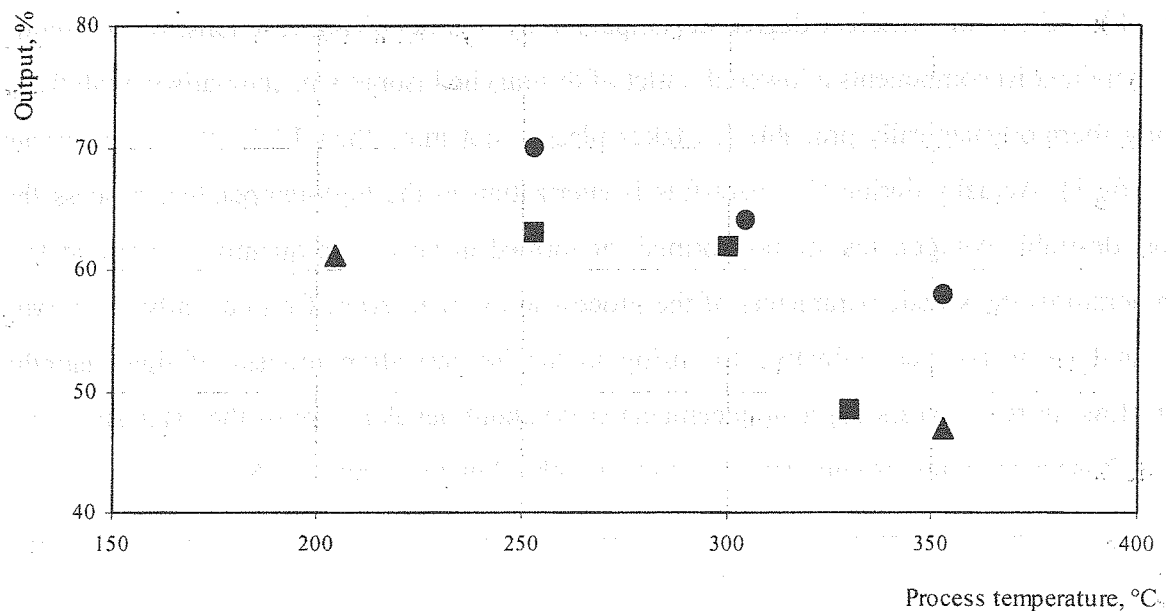


Fig.2. Isomers output from n-paraffins isomerization at metal-zeolite catalysts

● pentane ■ hexane ▲ heptane

Modified catalysts of amorphous type having high isomerizing activity at the temperatures of 90 to 200 °C, has the operation demerits, main of them being severe requirements to hetero-organic impurities content in the feed, regeneration difficulty and necessity of continuous promoter supply during the process [9].

Thus, development of the $C_7 - C_{10}$ paraffins low-temperature isomerization catalysts (based on either oxide or zeolite carrier) having high selectivity of di- and three-branched isomers formation.

One of the tasks to be solved at industrial realization of naphtha cut selective procession technology, is realization of combined conversion of C_7-C_{10} (C_{11}) paraffins. So, during the isomerization of the mixture of paraffins having different molecular weight the prior adsorption of hydrocarbons having higher chain length takes place that results in decreasing of isomerization degree of lower-molecular-weight hydrocarbons in comparison with their 'clear' conversion [7]. In order to increase selectivity and conversion degree of the paraffins is desired to carry out their separate isomerization, but from the economical point of view development of the catalytic systems providing for selective isomerization of paraffins having different chain length without their fractionation is more cost effective and feasible.

Isomerization is a multi-stage process, where equilibrium reactions of di-substituted, isomers formation go through equilibrium reactions of mono-substituted isomers formation

from normal paraffins, which rate being in average some higher. That is why isomerization of 'clear' mono-methyl-substituted paraffins is not feasible, because although it is accompanied by increase of high-branched components yield to the feed by 1,5-2,0 times than from n-paraffins, but during this process in a large degree formation of normal paraffins takes place. Consequently, increase of n-paraffins concentration in the feed must promote for the equilibrium displacement towards formation of the desired components – high-branched hydrocarbons. That is the precondition for feasibility of n-paraffins recycle from catalysate to the second stage of the isomerization reaction.

Thus, the principal approaches to industrial realization C_7-C_{10} (C_{11}) paraffinic fraction isomerization technology are developed and perspective directions of working out in this field are determined.

References

1. Vezirov R.R., Vezirova N.R., Telyashev I.R. //Neftepererabotka i neftekhimiya. – Moscow, 1997. – No. 8. – pp. 30 - 31.
2. Vezirov R.R., Vezirova N.R. //Abstracts of the International conference "Chemreactor-15". – Helsinki, 2001. – pp. 285-288.
3. Brooks B.T. and others. Oil chemistry. – Part 3. – Moscow-, 1958.
4. Smidovich Ye.V. Oil and gas processing technology. – Part 2. – Moscow, 1980.
5. Petrov A.A. Catalytic isomerization of hydrocarbons. – Moscow, 1960.
6. Shakun A.N., Fedorova M.L. //Materials of the conference «Petroleum refining and petrochemistry-2003», – Ufa, 2003. – pp. 106-107.
7. Vasilyev A.N., Galich P.N. //Neftepererabotka i neftekhimiya. – Moscow, 1996. – No. 4. – pp. 44-49.
8. Minachev Kh.M., Isakov Ya.I. Metal-containing zeolites in catalysis. – Moscow, 1976.
9. Bursian N.R. and others. Isomerization of paraffinic hydrocarbons. Subjective review. – Moscow, 1979.

SOLID ACIDS IN HALIDE-FREE CARBONYLATION OF DIMETHYL ETHER AND ISOMERIZATION OF ALKANES

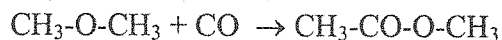
G.G. Volkova, Yu.R. Pak, A.A. Budneva, E.A. Paukshtis, A.N. Salanov

Boreskov Institute of Catalysis, Pr. Akademika Lavrentieva 5, Novosibirsk, 630090, Russia

The manufacture of acetic acid by the rhodium-catalyzed carbonylation of methanol is one of the most important industrial processes. Main disadvantages of this process are: homogeneous catalyst and halide promoter. Halides are highly corrosive and are poisons for many types of catalysts, so their use may limit the further chemistry which can be performed after carbonylation step. There are also difficulties in separation of the products from the catalyst. These problems can be overcome by design heterogeneous catalyst that can operate effectively without halide promoter.

The first step in methanol carbonylation is activation of C-I bond ($E = 240 \text{ kJ mol}^{-1}$) in methyl iodide. In order to exclude CH_3I it is necessary to activate C-O bond ($E = 350 \text{ kJ mol}^{-1}$) in methanol or in dimethyl ether (DME). DME is more favorable for carbonylation than methanol because it can be produced from syn-gas more effectively [1-2].

Solid acid catalysts are widely used in a number of industrially important reactions including isomerisation, alkylations, catalytic reforming of alkanes and cracking. The energy of the C-C bond in alkanes ($E = 344 \text{ kJ mol}^{-1}$) closely matches with the energy of the C-O bond (350 kJ mol^{-1}) in DME that is why we examine solid acids SO_4/ZrO_2 , WO_x/ZrO_2 and $\text{Cs}_x\text{H}_{3-x}\text{PW}_{12}\text{O}_{40}$ in the iodide-free carbonylation of the DME to methyl acetate:



Rhodium was added to catalysts in some specific state that can produce rhodium carbonyl complexes *in situ* on the surface of catalyst at high pressure of CO.

The RhCsPW_{12} catalysts were synthesized as described in [3]. $\text{Rh}/\text{SO}_4/\text{ZrO}_2$, $\text{Rh}/\text{WO}_x/\text{ZrO}_2$ samples were prepared from sulfated zirconium hydroxide XZO1077/01(1), XZO999/01(2) and tungstate doped zirconium hydroxide XZO861/02(3) from MEL by calcination at $650\text{-}800^\circ\text{C}$ and impregnation with 1%Rh using solution of rhodium chloride.

Activity and selectivity of the $\text{Rh}/\text{Cs}_x\text{H}_{3-x}\text{PW}_{12}\text{O}_{40}$ catalysts in iodide-free carbonylation of DME to methyl acetate are much higher than those of the $\text{Rh}/\text{SO}_4/\text{ZrO}_2$ and $\text{Rh}/\text{WO}_x/\text{ZrO}_2$ catalysts (Table 1) [3,4].

Table 1. Surface area and performance of catalysts in halide-free DME carbonylation at 473K and 10 bar after 120 min on stream

Samples	S BET m^2g^{-1}	Rate of methyl acetate formation		Selectivity %
		$\text{g l}^{-1}\text{h}^{-1}$	$10^{-8}\text{ mol g}^{-1}\text{s}^{-1}$	
1%Rh/Cs ₁ H ₂ PW ₁₂ O ₄₀	37	60	15	91
1%Rh/Cs _{1.5} H _{1.5} PW ₁₂ O ₄₀	57	180	45	94
1%Rh/Cs ₂ HPW ₁₂ O ₄₀	103	170	43	95
1%Rh/Cs _{2.5} H _{0.5} PW ₁₂ O ₄₀	216	35	9	96
1%Rh/SO ₄ /ZrO ₂ (1)	115	8	3	10
1%Rh/SO ₄ /ZrO ₂ (2)	127	12	5	15
1%Rh/WO _x /ZrO ₂	75	15	6	50

FTIR spectroscopy was applied to determine the acidity of the samples by monitoring the adsorption of pyridine, adsorbance band at 1540 cm^{-1} for Bronsted and 1450 cm^{-1} for Lewis acid sites.

Table 2. Acidity of the catalysts from FTIR spectra of pyridine adsorption

Samples	Bronsted acid sites		Lewis acid sites
	N, $\mu\text{mol g}^{-1}$	PA, kJ mol^{-1}	N, $\mu\text{mol g}^{-1}$
Rh/Cs ₁ H ₂ PW ₁₂ O ₄₀	139	1120	25
Rh/Cs _{1.5} H _{1.5} PW ₁₂ O ₄₀	128	1120	32
Rh/Cs ₂ HPW ₁₂ O ₄₀	118	1150	57
Rh/Cs _{2.5} H _{0.5} PW ₁₂ O ₄₀	48	1150	63
Rh/SO ₄ /ZrO ₂ (1)	38	1160	105
Rh/SO ₄ /ZrO ₂ (2)	70	1160	110
Rh/WO _x /ZrO ₂	38	1180	37

A threefold variation in Bronsted and Lewis sites was apparent across the range of samples (Table 2). The maximum of Bronsted acid sites ($139\text{-}118\ \mu\text{mol g}^{-1}$) was detected on Cs₁₋₂PW₁₂ samples, maximum of Lewis acid sites ($105\text{-}110\ \mu\text{mol g}^{-1}$) on sulfated zirconia. Proton affinities provide relative scale for Bronsted acid strength. Cs₁₋₂PW₁₂ catalysts are more acidic than SO₄/ZrO₂, WO_x/ZrO₂.

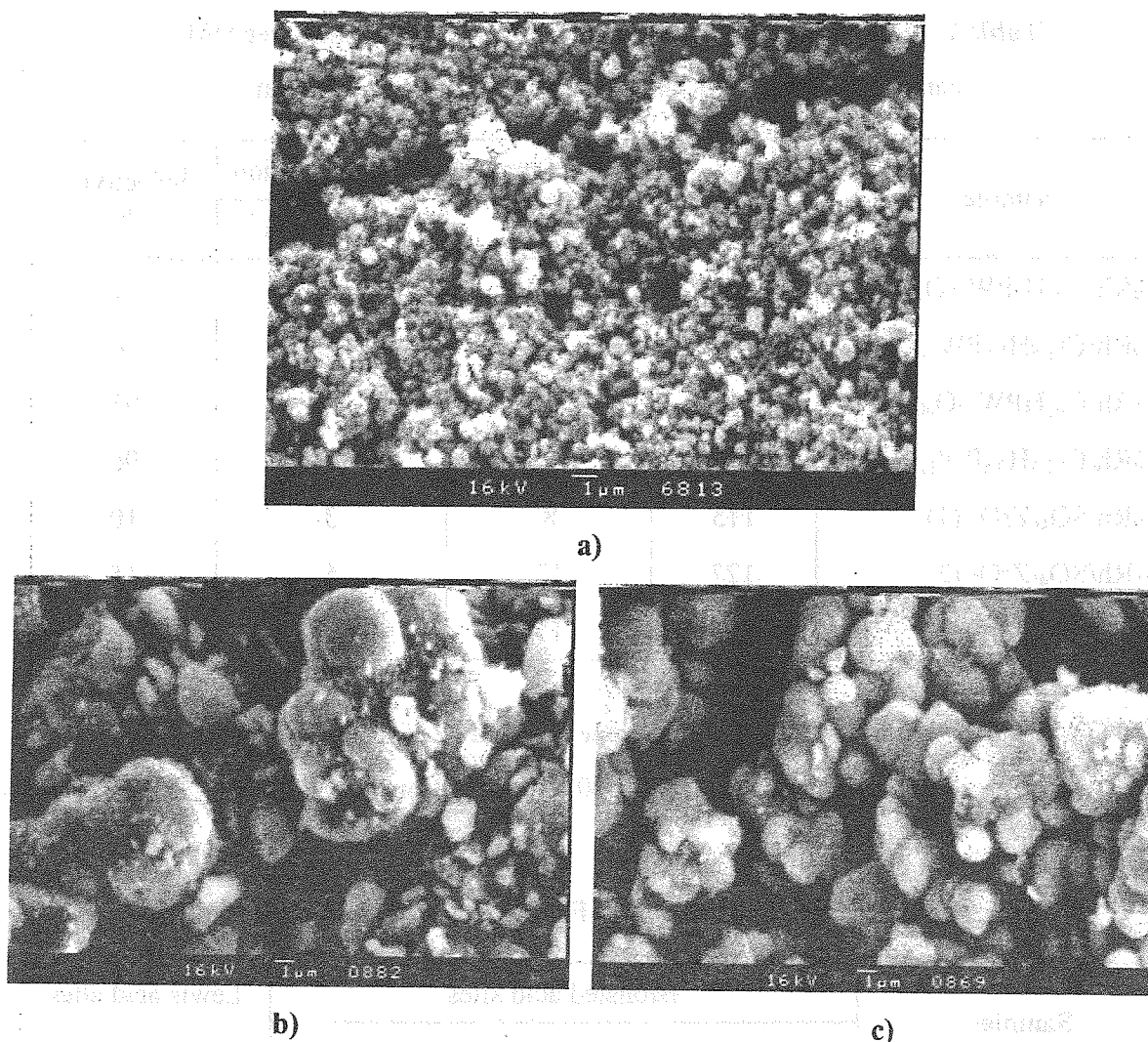


Figure 1. SEM photographs of the catalysts: a) Rh/Cs₂HPW₁₂O₄₀, b) Rh/SO₄/ZrO₂(1), c) Rh/WO_x/ZrO₂

Direct comparison of the rates of DME carbonylation and alkanes isomerization over Cs_xPW₁₂ catalysts (Figure 2) has shown that DME carbonylation in the absence of iodide promoter requires the presence of very strong Bronsted acid sites similar to those for skeletal isomerisation of n-paraffins on acidic cesium salts of 12-tangstophosphoric acid.

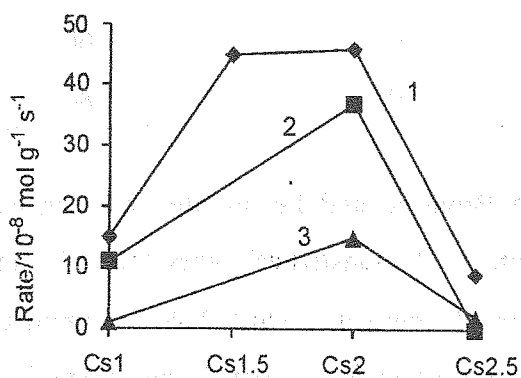


Figure 2. Comparison of the rates (1) of methyl acetate formation, (2) isopentane formation [5], (3) isobutane formation [6] over Cs_xPW₁₂ catalysts versus cesium content.

Low activity of sulfated and tungstated zirconia in DME carbonylation comparing with alkanes isomerization [7-8] may be connected with 1) lower concentration and strength of the Bronsted acid sites which are responsible for DME activation, and 2) the difference of CO and H₂ chemisorption on its surface. Irreversible chemisorption uptake of CO on Pt/WO_x/ZrO₂ was near two times lower than H₂ uptakes [9].

Destruction of DME molecules on the surface of Rh/SO₄/ZrO₂ is caused by Lewis acidity so high concentration of Lewis acid sites is the reason for poor selectivity of the sulfated zirconia catalysts in the halide-free carbonylation of DME.

Conclusion

It was shown that Rh/Cs_xH_{3-x}PW₁₂O₄₀ (1.5 ≤ x ≤ 2) are the best catalysts for halide-free DME carbonylation. Their behavior can be rationalized qualitatively by assuming that 1) activation of C-O bond in DME molecule and formation of metal-alkyl bond occurs in the presence of the strong Bronsted acid sites, and 2) these acid sites act in conjunction with Rh carbonyl complexes, which are responsible for CO insertion and acetates formation.

Acknowledgements

The authors thank MEL Chemicals Ltd. for providing the commercial XZO1077/01, XZO999/01 and XZO861/02 zirconia samples.

References

- [1] T. Shikada, Y. Ohno, T. Ogawa, M. Ono, M. Mizuguchi, K. Tomura, K. Fugimoto, *Stud. Sur. Sci. Catal.*, 119 (1998) 515.
- [2] T.H. Fleisch, R.A. Sills, M.D. Briscoe, *J. Natural Gas Chem.*, 11 (2002) 1.
- [3] G.G. Volkova, L.M. Plyasova, A.N. Salanov, G.N. Kustova, T.M. Yurieva, V.A. Likholobov, *Catal.Lett.* 80 (2002) 175.
- [4] G.G. Volkova, L.E. Pindyurina, L.S. Egorova, T.M. Yurieva, V.A. Likholobov, *Russian Patent* 2170724 (2001).
- [5] B.B. Bardin, R.J. Davis, *Topics in Catalysis*, 6 (1998) 77.
- [6] N. Essayem, G. Coudurier, M. Fournier, J.C. Vedrine, *Catal.Lett.*, 34 (1995) 223.
- [7] K. Arata, H. Matsushashi, M. Hino, H. Nakamura, *Catal. Today*, 81 (2003) 17.
- [8] T.Lei, J.S.Xu, W.M. Hua, Z.Gao, *Appl.Catal. A:General* 192 (2000) 181.
- [9] D.G. Barton, S.L. Soled, G.D. Meitzner, G.A. Fuentes and E. Iglesia, *J.Catal.*, 181 (1999) 57.

SKELETAL ISOMERIZATION OF N-PARAFFINS ON HETEROGENEOUS CATALYSTS WITH HIGHEST LEWIS ACIDITY

G.G. Volkova, L.N. Shkuratova, A.A. Budneva, E.A. Paukshtis, S.I. Reshetnikov

Boreshkov Institute of Catalysis, Pr. Akademika Lavrentieva 5,

Novosibirsk, 630090, Russia, g.g.volkova@catalysis.nsk.su

Naphtha isomerization is a simple and cost effective technology for increasing octane number of gasoline. Isomerization of naphtha is composed mainly of conversion of n-pentane and n-hexane into iso-pentane, mono-methyl and di-methyl hexane. Di-methyl hexane has higher octane number than mono-methyl hexane, and is preferentially produced at low temperature subject to chemical equilibrium. Recently new acid catalyst based on sulfated zirconia have been developed and successfully commercialized by UOP LLC [1-2]. This catalyst revealed higher activity for light naphtha isomerization at lower temperature and is less sensitive to the amount of water in feed oil than conventional catalysts.

By the large demand of desired isomerization products development of new more active catalysts have been continued [3]. There are several ideas about what is the main characteristic of active surface for isomerization: Bronsted or Lewis acidity or both of them [4-6]. Maximum densities of Lewis acid sites on sulfated zirconia catalysts determined by FTIR spectroscopy of pyridine or CO adsorption are 90 -121 $\mu\text{mol g}^{-1}$ [4-6].

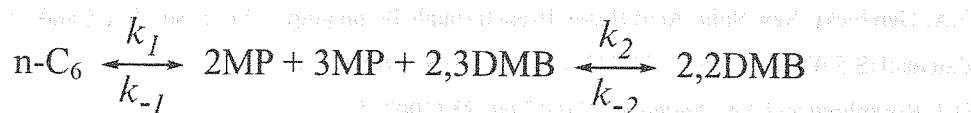
Studies at the Boreshkov Institute of Catalysis have shown that the number of catalyst $\text{Pt}/\text{SO}_4/\text{ZrO}_2$ with the Lewis acid sites in the range from 50 to 250 $\mu\text{mol g}^{-1}$ can be obtained depending on the preparation conditions (Table 1) [7]. The density of Lewis acid sites up to 250 $\mu\text{mol g}^{-1}$ is more than twice that earlier known one for sulfated zirconia [4-6].

Table 1. FTIR spectroscopy data of CO adsorption

Catalysts	νCO (cm^{-1})	Lewis acid sites $\text{N } \mu\text{mol g}^{-1}$	Bronsted acid sites $\text{N } \mu\text{mol g}^{-1}$
№ 1	2190-2185 2175 2150	50	85 140
№ 2	2200-2190 2175-2165	150	140
№ 3	2200-2190 2175-2165	250	170

Catalysts 2 and 3 were evaluated in isomerization of n-hexane in flow reactor. The study of the kinetics of isomerization of the n-hexane on solid superacids [8] has shown that it is possible to divide process into three stages. The first, most fast stage, is formation of 3-methyl pentane (3MP) from 2-methyl pentane (2MP), and then, 2,3-methyl butane (2,3DMB) formation up to thermodynamic equilibrium. The reactions of the isomerization of n-hexane and the formation of 2,2-methyl butane (2,2DMB) has the comparable rates. Third stage is the side products formation.

For the kinetic analysis the following reaction network was used:



The calculation of the rate constants, characterizing the catalyst activity and selectivity was performed on the base of mathematical model of plug flow reactor. It is assumed that the reactions are pseudo-first order in reagents.

The kinetic constants and activation energies were determined. The results of mathematical modeling are in good a agreement with experimental data (Table 2).

Table 2. Experimental and calculated kinetic data for catalysts 2 and 3 in n-hexane skeletal isomerization at the pressure 3 atm and temperature 200 °C

Parameters	Catalyst 2 Lewis acid sites 150 $\mu\text{mol g}^{-1}$		Catalyst 3 Lewis acid sites 250 $\mu\text{mol g}^{-1}$	
	Experiment	Calculation	Experiment	Calculation
2,2DMB. % wt.	1.5	1.5	4.6	4.5
2MP+3MP+2.3DMB	35.1	34.8	59.86	60.0
n-C ₆ conversion	40.3	40.2	69.2	69.3
Rate constants:				
k_1		0.224		0.909
k_{-1}		0.048		0.20
k_2		0.033		0.073
k_{-2}		0.053		0.12
n-hexane, h ⁻¹	2.79		4.68	
H ₂ : n-C ₆	2.09		1.87	

The data presented in Table 2 show that rate constant of n-hexane isomerization (k_1) for Catalyst 3 is fourfold as those for Catalyst 2, and k_2 which characterized the rate of desired

product (2,2DMB) formation for Catalyst 3 (Lewis acidity 250 $\mu\text{mol g}^{-1}$) is also twice as high as that for Catalyst 2 (Lewis acid sites 150 $\mu\text{mol g}^{-1}$).

From these data it may be concluded that the rate of hexane isomerization is mainly determined by the density of Lewis acid sites on the surface of Pt/SO₄/ZrO₂ catalysts.

References:

1. T. Kimura, Development of Pt/SO₄²⁻/ZrO₂ catalyst for isomerization of light naphtha, Catal.Today, 81 (2003) 57.
2. S.A. Gembicki, New Solid Acid Based Breakthrough Technologies, Stud. Sur. Sci. Catal., 130 (2000) 147.
3. Patents:US 5,036,035, US 6,495,733, US 6,448,198, US 5,629,257.
4. D.J. Rosenberg and J.A. Anderson, Catal.Lett. 83 (2002) 59.
5. E.A. Paukshitis, V.K. Duplyakin, V.P. Finevich, A.V. Lavrenov, V.L. Kirillov, L.I. Kuznetsova, V.A. Likholobov, B.S.Bal'zhinimaev, Stud. Sur. Sci. Catal., 130 (2000) 2543.
6. L. Zanibelli, A.Carati, C.Flego, R. Millini, Stud. Sur. Sci. Catal., 143 (2002) 813.
7. G.G. Volkova, L.N. Shkuratova, L.S. Egorova, E.A. Paukshitis, A.A. Budneva, S.I. Reshetnikov, V.K. Duplyakin, V.A. Likholobov, Patent Application (2003).
8. D.M. Brouwer, J.M. Olderek, Reac. Trav. Chim. 1968, 87, 721.

Catalyst	Catalytic activity		Lewis acid sites ($\mu\text{mol g}^{-1}$)	2,2DMB formation (%)
	Conversion (%)	2,2DMB selectivity (%)		
1	100	100	150	100
2	100	100	150	100
3	100	100	250	200
4	100	100	250	200
5	100	100	250	200
6	100	100	250	200
7	100	100	250	200
8	100	100	250	200

CATALYTIC SYNTHESIS OF AROMATIC HYDROCARBONS FROM LOW ALKANES

A.V. Vosmerikov, L.N. Vosmerikova, L.L. Korobitsyna, Ya.Ye. Barbashin

Institute of Petroleum Chemistry, Siberian Branch of the Russian Academy

of Sciences, 634021, 3, Akademichesky Avenue, Tomsk, Russia

fax: (3822)25-84-57, e-mail: pika@ipc.tsc.ru

High-silica zeolites of pentasil type are promising catalysts of a whole range of important chemical processes. Fixed structure of the crystal lattice and the presence of acidic sites of different types on its surface allows applying the zeolites in different chemical reactions, including the conversion of light alkanes into aromatic hydrocarbons. Nevertheless, at the application of an unmodified zeolite of ZSM-5 type the selectivity of aromatic hydrocarbons formation does not exceed 30% (Table 1). That is why, to improve the formation of aromatic hydrocarbons, promoting additives, preferentially Pt, Zn or Ga, are introduced into the zeolite composition. At the same time, the catalysts produced, despite of their high activity and selectivity, may not be used under commercial conditions because the sample properties do not meet the requirements of interlaminar and wear strengths. Mechanical strength of the catalysts may be improved by introducing a binder into the composition of a zeolite. Moreover, the existing zeolite catalysts are characterised by a short life between regenerations, which requires the simultaneous application of several reactors in the process scheme and the modification of the design and the regeneration system. In this connection the development and creation of a high-stability catalyst to be used in the conversion of light alkanes, which preserves a high activity and stability for aromatic hydrocarbons is an urgent task. This work presents the results of investigations of catalytic properties of galloaluminosilicates (GAS) in the process of conversion of C₃-C₄ light alkanes mixture into aromatic hydrocarbons.

Aluminosilicate (AS) modification by gallium was carried out via isomorphic replacement of Si⁴⁺ ions by Ga³⁺ ions in the zeolite crystal lattice at the stage of hydrothermal synthesis by a partial replacement of aluminium by gallium in the initial aluminosilicagel SiO₂/(Al₂O₃+Ga₂O₃). Gallium oxide content in the reaction mixture – 2.2 wt%. GAS produced in the synthesis process was converted into an active H-form via double decationization by 25% NH₄Cl solution at 90°C for 2 h followed by drying at 100°C and air calcination at 550°C for 6 h. To prepare a catalyst with a binder, a catalytic mass was obtained

by mixing galloaluminosilicate, pseudobeumite (PB) and water, nitric acid (0.1-0.15 mol/mol Al_2O_3) was added for plastification. The plastic mass obtained was subjected to extrusion. Catalyst grains ($d=2$ mm) were dried for 24 h on air, then in an air drier at 110°C for 24 h and calcined at 600°C for 6 h. The amount of a binder in a galloaluminosilicate was changed from 10 to 30 wt%. To carry out the test, a catalyst fraction of 0.25-0.50 mm was taken.

Aromatization of a mixture of light alkanes (propane – 73.7; *i*- and *n*-butane – 24.1 wt%) was performed on a flight type installation with the reactor volume of 5 cm^3 at atmospheric pressure, reaction temperature was $400\text{-}600^\circ\text{C}$, the feedstock space velocity was 100 h^{-1} . Before the tests galloaluminosilicates were treated by air at 300°C for 2 h and at 520°C for 3 h, then they were reduced in hydrogen flight at 520°C for 2 h, the space velocity of air and hydrogen was $1\text{ dm}^3/\text{h}$. The reaction products were analyzed by gas chromatography. When determining the period of a stable catalyst operation, the tests were run continuously for several days, the reaction products were analyzed at certain intervals that were equal for all the samples. The stability of catalyst operation was assessed by the changes both in the degree of feedstock conversion and in the selectivity of aromatic hydrocarbons formation.

DTA-DTG patterns of coked catalysts were recorded on "C" DTA-DTG instrument (MOM, Hungary) within $20\text{-}1000^\circ\text{C}$. The sample (400-500 mg) was heated in a platinum crucible on air at the rate of $10\text{ deg}/\text{min}$.

Table 1 shows the results of the study of the influence of the process temperature and period of operation of GAS containing different amounts of the binder on the composition of the products of the propane-butane fraction conversion. Galloaluminosilicates perform the aromatization of light alkanes more effectively than aluminosilicates. In this case a high yield of aromatic hydrocarbons over GAS is observed at 450°C already, and at 500°C the selectivity of arenes formation reaches more than 55% at the conversion degree of 98%. The main direction of the process over the initial GAS for more than 200 hours is $\text{C}_3\text{-C}_4$ alkanes aromatization, the selectivity of the aromatic hydrocarbons formation at 500°C and 100 h^{-1} for 216 hours surpassing 45%. With the increase in GAS operation the initial feedstock conversion gradually decreases and the selectivity of $\text{C}_1\text{-C}_2$ alkanes and $\text{C}_2\text{-C}_4$ alkenes increases. The rise of the process temperature to 550°C results in the increase in the feedstock conversion degree and yield of aromatic hydrocarbons.

An insignificant decrease in the feedstock conversion degree and selectivity of aromatic hydrocarbons conversion is observed at the binder introduction into GAS. At the same time, as seen from the data of the Table 1, the yield of aromatic hydrocarbons over GAS containing 10 and 20% PB decreases, respectively, by 1.7 and 3.8% after 216 hours of operation, while over the initial GAS- by 16.3%. Over GAS containing 30% of PB the selectivity of aromatic hydrocarbons conversion remains high, nevertheless, the degree of the feedstock conversion

decreases with time more abruptly than over another samples. Thus, within 144 hours of operation the conversion is only 84% at 500°C, whereas over GAS/20%-PB it was 85% after 216 h of operation. Over GAS/30%-PB the selectivity of aromatic hydrocarbons conversion decreases rapidly, and the selectivity of alkenes formation increases with operation period at 550°C.

Table 1. The influence of the temperature and operation period (t) of the catalysts on the conversion and composition of C₃-C₄ low alkanes conversion products (W=100 h⁻¹)*

Catalyst	t (h)	T _{reaction} (°C)	X (%)	A (%)	S ₁ (%)	S ₂ (%)	S ₃ (%)
AS	1	400	35	—	—	90.7	8.1
	1	450	60	8.8	14.7	76.6	7.4
	1	500	86	16.7	19.4	75.5	3.3
	1	550	96	27.4	28.5	67.4	2.1
	1	600	99	28.0	28.3	68.1	1.4
GAS	1	400	45	—	—	91.0	2.5
	1	450	77	22.9	29.7	63.7	0.8
	1	500	98	54.8	55.9	39.6	0.3
GAS	1	500	98	54.8	55.9	39.6	0.3
	96	500	98	51.7	52.8	42.2	0.6
	192	500	90	40.2	44.7	47.7	2.2
	216	500	84	38.5	45.8	43.5	3.9
	217	550	98	53.3	54.4	37.0	1.7
	240	550	91	49.8	54.8	33.9	4.9
GAS/10%-PB	1	500	93	45.5	48.9	44.8	0.8
	96	500	93	44.1	47.4	45.9	1.6
	192	500	87	44.1	50.7	41.2	2.4
	216	500	84	43.8	52.1	38.6	3.1
	217	550	98	57.4	58.6	33.2	1.5
	240	550	95	50.8	53.5	36.3	3.0
GAS/20%-PB	1	500	93	44.3	47.6	46.1	0.8
	96	500	90	43.7	48.5	42.8	2.2
	192	500	86	42.3	49.2	41.8	2.9
	216	500	85	40.5	47.6	43.4	2.9
	240	500	81	38.8	47.9	42.1	3.7
	241	550	98	53.5	54.6	37.2	1.0
	288	550	92	45.0	48.9	39.2	4.2
	312	550	82	42.6	52.0	33.4	8.0
	316	600	98	54.0	55.1	34.2	3.7
	340	600	74	29.1	39.3	34.9	20.6
GAS/30%-PB	1	500	94	42.4	45.1	48.5	1.0
	96	500	89	41.5	46.6	46.2	2.1
	144	500	84	41.2	49.0	42.7	3.1
	146	550	99	55.0	55.6	36.7	1.4
	192	550	79	37.1	47.0	38.0	8.5

Note. X is conversion degree; A is yield of aromatic hydrocarbons; S₁, S₂ and S₃ are selectivities of the formation aromatic hydrocarbons, C₁-C₂ alkanes and C₂-C₃ alkenes, respectively.

Thus, on the basis of the research performed it has been established that the process of C_3 - C_4 low alkanes conversion into aromatic hydrocarbons occurs over a gallium-containing catalyst at a high selectivity. When a binder is introduced into GAS, not only its mechanical strength improves, but the period of its stable operation during one service life also increases, which is very important for a commercial process.

Among the catalysts mixed with a binder, GAS/20%-PB contains the highest coke amount, which is explained by a longer operation time (Table 2).

Table 2. Characteristics of coked catalysts*

Catalyst (operation period, h)	T_{max} , forms of the coke burn-out ($^{\circ}C$)			T_b ($^{\circ}C$)	Coke amount (%)
	I	II	III		
GAS (240)	600	690	760	800	11.9
GAS/10%-PB (240)	550	610	-	a shoulder to 770	12.0
GAS/20%-PB (340)	580	700	-	a shoulder to 1020	19.6
GAS/30%-PB (200)	540	640	-	a shoulder to 925	16.4

Note. T_b is the temperature of the coke burnout.

On DTA curve for GAS/20%-PB one may allocate two exothermal peaks in the region 400-640 and 640-740 $^{\circ}C$ with respective maximums at 580 и 700 $^{\circ}C$ and a wide shoulder to 1020 $^{\circ}C$. The temperature of the coke burnout (1020 $^{\circ}C$) evidences a high polycondensation degree. The nature of the coke deposits formed on GAS/20%-PB and GAS/30%-PB is very close. The initial GAS and GAS/10%-PB contain significantly lower amounts of coke, and the condensed products formed are less condensed which is confirmed by a lower temperature of the coke burnout. Thus, the data of differential thermal analysis demonstrate that the increase in the period of a continuous catalyst operation above 240 h leads to a slight formation of highly condensed products, as a result, its regeneration will be very problematic. A prolonged life between regenerations of a galloaluminosilicate catalyst followed by a slight decrease in activity, leads to its irreversible deactivation, an excess accumulation of highly condensed coke deposits leads to catalyst overheating during the regeneration process. That is why the service life of GAS/20%-PB should not exceed 240-250 h, then it is necessary to perform an oxidative regeneration.

Thus, the most efficient catalyst among all the studied catalysts of C_3 - C_4 light alkanes aromatization is a zeolite containing 2.2% of gallium oxide introduced at the stage of the hydrothermal synthesis and mixed with 20% of pseudobeumite used as a binder. The application of this catalyst allows one to obtain the desired product at a selectivity of about 50% for all the service life of no less than 240 h. At the same time it is worth noticing that the service life of GAS/20%-PB is more than 350 h.

GLASS FIBER CATALYSTS FOR SO₂ OXIDATION: PILOT TESTS AT REAL GASES OF SULPHURIC ACID PLANT

A.N. Zagoruiko, V.D. Glotov**, N.N. Menailov*,
Yu.N. Zhukov**, V.M. Yankilevich**, B.S. Balzhinimaev, L.G. Simonova

Boreshkov Institute of Catalysis, Novosibirsk, Russia

**Katalyzator Company, Novosibirsk, Russia*

***Byisk Oleum Plant, Byisk, Russia*

Glass-fiber catalysts (GFC) represent itself the noble metals introduced in very small amounts (0.01-0.05 % mass) into silica-glass matrix [1]. The research investigations [2] showed that such catalysts demonstrate unique catalytic properties and may be used for performance of a wide range of catalytic reactions. Moreover, original geometry, high flexibility and high mechanical strength of such catalysts give the way to develop really new catalytic processes. In particular, the very promising way of Pt-containing GFC application is oxidation of sulfur dioxide [3] (instead of conventional vanadia catalysts). The most important question in this case is stability of catalyst operation in the media of real gases of sulfuric acid plants.

The pilot plant for resource testing of GFC was created at the Byisk Oleum Plant. The nominal gas loading of the pilot unit was equal to 200 st.m³/hour. The unit was installed in bypass to basic industrial SO₂-oxidation reactor. Hot inlet gas was collected from the real gaseous stream, fed to the first bed of the basic reactor. Outlet gas from the pilot unit was discharged into outlet pipeline of the basic plant. The pilot unit was provided with control system for measurement of gas temperatures in the pilot reactor, catalyst pressure drop and gas compositions of inlet and outlet gases.

GFC with platinum content of 0.02-0.03% for pilot tests was produced by Katalyzator Company. The catalyst was placed in layers (10-30 layers) in the bottom part of the cylindrical pilot reactor (Fig. 1) with inner diameter of 0.5 m. Catalyst glass-fiber support (Fig. 2) was woven in form of bunches, each of them consisting of 3 threads and, in turn, each thread was twisted from elementary glass microfibers with typical size of 7-9 microns [2]. The thickness of each thread was equal to ~ 1 mm, thickness of bunch – ~ 3 mm, the windows between bunches represented the squares with a side size of ~ 1 mm.



Fig. 1. Pilot reactor

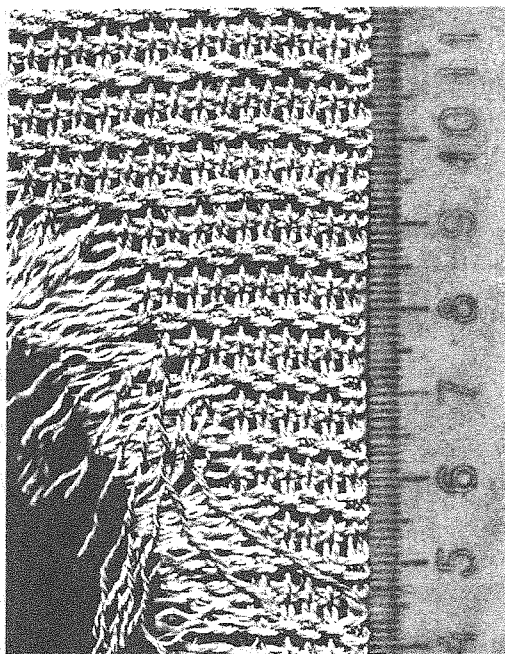


Fig. 2. View of the catalyst structure

The overall pilot tests duration was equal to 600 hours. The main pilot process parameters are shown in Table 1.

Table 1. Range of pilot tests parameters

No.	Parameter	Meas.unit	Range
1	Gas flow rate	st.m ³ /hour	20 - 150
2	Gas temperature at the catalyst bed inlet	°C	340 - 450
3	Gas temperature at the catalyst bed outlet	°C	320 - 536
4	SO ₂ concentration in inlet gases	% vol.	6,85 - 9,7
5	SO ₂ conversion	%	2 - 50
6	Catalyst bed pressure drop	mm WC	6 - 55

It should be noted that all main process operation parameters (gas flow rate and temperature of inlet gas, initial SO₂ concentration) were oscillating in time quite significantly. Therefore, for correct interpretation of experimental data it was necessary to perform more detailed analysis of results.

To estimate kinetic parameters of catalyst operation we used CSTR approximation both for mass and heat with application of 1st-order kinetic equation (in relation to SO₂). Processing of experimental data showed significant influence of diffusion limitations on observed rate of reaction. Kinetic region of reaction performance was observed only at relatively high gas flow rates (more than 100 m³/h) with activation energy equal to ~ 15 Kcal/mol.

Analysis of observed values of mass transfer coefficient showed quite unusual results. Relation between gas velocity and mass transfer coefficient was described by an order of ~ 0.93 in average. This value is significantly higher than that for conventional packed beds of granular catalysts (0.5-0.6). Moreover, visible rise of this order (up to values exceeding 1) was observed in the area of high gas velocities. From theoretical point of view it means, that in definite range of gas velocities the rise of gas flow rate (and, therefore, decrease of residence time) may lead to the increase of conversion, which looks quite impossible for conventional packed beds.

The most reasonable explanation of this fact is dynamic changing of gas fluid structure in the GFC layers with changing of gas velocities. While in the area of low gas velocities the gas fluids are mostly flowing around the outer surface of bunches, then with the rise of gas flow rate the fluids start to flow between threads and afterwards – between fibers inside the threads. The latter leads to increase of catalyst surface availability and intensification of mass exchange.

Unusual phenomena were also observed in analysis of experimental data in relation to pressure drop (ΔP) in catalyst layers. In particular, the average dependence order of ΔP from gas velocity was found to be unexpectedly low (0.3-0.5). Probably, it is also connected with dynamic changing of fluid flow structure, as well as changing of the structure of the catalyst packing itself. Analysis of start-up regimes (after catalyst charging) showed, that in initial period the observed pressure drop exceeds the value obtained in a long-term run by a factor of 1.7-2. This difference is gradually decreasing and becomes zero after 15-20 hours from reactor start-up. Possibly, in start-up regimes there occurs restructuring of the catalyst packing, caused by action of the gas flow and resulting in formation of channels for gas filtration. This hypothesis is confirmed by the experimental fact that no unusual pressure drop values were observed after reactor start-ups, which were not connected with catalyst charging and recharging.

The key point question of pilot tests at real industrial gases was analysis of catalyst operation stability and deactivation. Unfortunately, direct comparison of catalyst activity in the beginning and end of pilot tests was impossible (because of process parameters oscillations, leading to incomparable external conditions), so we used estimation procedure based on elaborated correlations related to observed kinetics with account of mass transfer. As soon as such correlations were based on time-averaged experimental array, any changing of catalyst activity would be easily seen in changing of ratio $K_{\text{exp}}/K_{\text{theor}}$ (experimentally defined and theoretically calculated for given experimental conditions observed kinetic constants,

respectively) in time. The results are demonstrated at Fig. 3. Though the data deviation is rather wide, it may be stated that no visible deactivation of the catalyst was detected during all pilot tests.

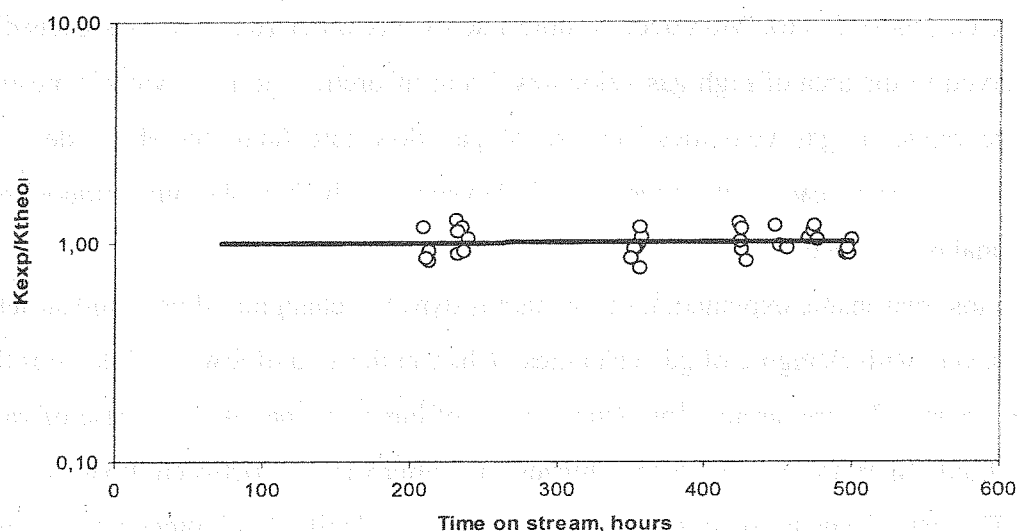


Fig. 3. Changing of relative catalyst activity during pilot tests.

The performed pilot test provided the ground for the following conclusions:

- ◆ Pt-containing glass-fiber catalyst (GFC) provides stable operation in the media of real industrial gases of sulfuric acid plant and shows no visible deactivation within 500 hours on-stream;
- ◆ the observed activity of GFCs is at least 4 times higher than that for conventional vanadia catalysts;
- ◆ GFCs provide stable operation at inlet gas temperature as low as 330-340 °C (compared with 370-410 °C for vanadia systems), thus giving the way for increase of achievable equilibrium conversion in adiabatic beds;
- ◆ GFCs packings are characterised with relatively low pressure drops;
- ◆ flexible mechanical structure of GFCs open the way for development of novel reactor designs.

In general it may be stated that obtained results confirmed high attractiveness of GFCs for development of new generation of catalytic processes for SO₂ oxidation in sulfuric acid plants.

References

1. L.G.Simonova, V.V.Barelko, A.V.Toktarev, V.I.Zaikovskii, V.I.Bukhtiarov, V.V.Kaichev, B.S.Balzhinimaev. *Kinetics and Catalysis*, 2001, v.42, No.6, pp.917-927.
2. B.S. Balzhinimaev, L.G. Simonova, V.V. Barelko, A.V. Toktarev, V.I. Zaikovskii and V.A.Chumachenko. *Chemical Engineering Journal*, 2003, v.91, No 2-3, pp.181-185.
3. B.S.Balzhinimaev, L.G.Simonova, V.V.Barelko, A.V.Toktarev, D.A.Arendarskii, E.A.Paukshtis, V.A.Chumachenko. *Catalysis in Industry*, 2002, v.5, pp.33-39.

NON-STEADY-STATE APPROACH TO STEADY-STATE KINETICS: CASE STUDY OF H₂S OXIDATION BY OXYGEN

Andrey N. Zagoruiko*, Vladimir V. Mokrinskii

Boriskov Institute of Catalysis

Pr. Lavrentieva, 5, 630090, Novosibirsk, Russia, e-mail: zagor@catalysis.nsk.su

Introduction

The research work described was initially aimed to study steady-state kinetics of catalytic oxidation of hydrogen sulfide by oxygen into elemental sulfur over vanadia-titania catalyst.

Oxidation of H₂S into elemental sulfur may be represented by reaction



where n – number of sulfur atoms in allotrope molecule. This reaction of selective oxidation is practically always accompanied by reaction of deep oxidation:



The reaction system is accomplished by Claus reaction:



Thermodynamic analysis shows that reaction (1) and (2) are practically irreversible, while Claus reaction may be significantly equilibrium limited, especially at elevated temperature and reaction gas moisture.

The steady-state kinetics of reaction system (1-3) was studied experimentally using direct-flow lab setup. Kinetic experiments included variation of reaction temperature (in range 230-300⁰C) and reagents concentrations. Special tests with different catalyst pellets size confirmed the achievement of pure kinetic area (with no diffusion limitations). Additional experiments proved the ideal mixing regime in the reactor.

Reaction mechanism and kinetic model

Characterization of commercial vanadia-titania IC-27-40 catalyst showed that the main catalytic activity is provided by vanadia. Though pure titania was also found to be very active in reactions (1-3) in this case it serves as a support only and is practically absent from the active surface. Further investigations demonstrated that in presence of hydrogen sulfide V₂O₅

* Corresponding author

is quickly reduced to V_2O_4 and the latter becomes the main active compound of the catalyst. Together with other research results it gave the way to formulate the hypothesis for reaction mechanisms able to describe the regularities observed in kinetic experiments. The most successful mechanism obtained in result of discrimination may be presented as follows:



where ZO corresponds to oxidized active site (surface V_2O_4), ZS – sulfided site (surface V_2O_3S) and Z – reduced site (surface V_2O_3). Such mechanism qualitatively describes aim reactions and, furthermore, it is thermodynamically consistent, being able to describe reversibility of Claus reaction, using usual equilibrium constant approach.

The rates of stages (4-7) may be expressed in terms of mass-action law as given below:

$$r_1 = k_1 C_{H_2S} \theta_O - \frac{k_1}{k_{p1}} \theta_S C_{H_2O} \quad (8)$$

$$r_2 = k_2 \theta_S - \frac{k_2}{k_{p2}} \theta C_{S_6}^{1/6} \quad (9)$$

$$r_3 = k_3 \theta_S \theta_O^2 - \frac{k_3}{k_{p3}} \theta^3 C_{SO_2} \quad (10)$$

$$r_4 = k_4 C_{O_2}^{1/2} \theta \quad (11)$$

where θ_O , θ_S and θ - surface concentrations (surface fractions) of ZO, ZS и Z respectively, k_i – rate constants, k_{pi} – equilibrium constants. The rate equation system is accomplished with rates for reaction mixture gaseous and surface components:

$$\begin{aligned} W_{H_2S} &= -r_1 \\ W_{S_6} &= r_2 \\ W_{SO_2} &= r_3 \\ W_{O_2} &= -1/2 r_4 \\ W_{H_2O} &= r_1 \end{aligned} \quad (12)$$

$$\begin{aligned} W_{\theta O} &= \partial \theta_O / \partial \tau = -r_1 - 2 r_3 + r_4 \\ W_{\theta S} &= \partial \theta_S / \partial \tau = r_1 - r_2 - r_3 \\ W_{\theta} &= \partial \theta / \partial \tau = r_2 + 3 r_3 - r_4 \end{aligned} \quad (13)$$

It may be easily seen that general thermodynamic consistence of a model is provided by evident relationship

$$K_{P3} = \frac{k_{P1}^2 k_{P2}^3}{K_p^2} \quad (14)$$

where K_p – equilibrium constant for Claus reaction.

Elaboration of steady-state kinetic equations

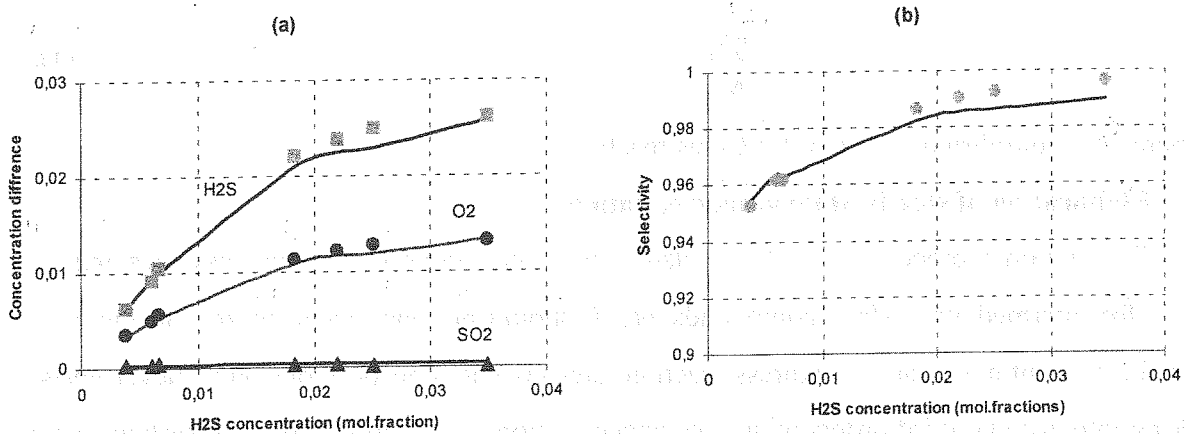
Conventional procedure of steady-state kinetic equations elaboration assumes that all rates for intermediate surface compounds $\partial\theta_i/\partial\tau$ should be made equal to zero to eliminate surface concentrations and to express reaction rates via gas concentrations only. Nevertheless, taking into account third orders of surface concentrations in equation (10) such system cannot be resolved algebraically.

Moreover, the individual rates of reactions (1-3) cannot be separated because this reaction system contains intersection of participating substances. For example, it is impossible to distinguish the H_2S consumption in reactions (1) and (3) (concentration of sulfur vapors was impossible to measure). Separate investigation of Claus reaction kinetics (in absence of oxygen) is possible but it was found that oxygen strongly influences the catalyst surface state and, evidently, in presence of oxygen Claus reaction rate will be significantly different. All this made elaboration of usual steady-state kinetic equations impossible.

Earlier authors tried to propose the kinetic steady-state equations for the given reaction system [1]. Though the description results were relatively good, the proposed equations were physically and thermodynamically inconsistent, so the achieved results look as successful empirical fitting only. The most important problem was inadequate (or “incorrect”) temperature dependence of model parameters – it was found impossible to fit the defined kinetic parameters into Arrhenius dependence.

Non-steady-state approach

The idea of non-steady-state approach here is to use equations (8-14) as a transient kinetic model to describe reaction rates. To obtain the steady-state solution it is necessary to numerically integrate surface rate expressions (13) starting from zero time to infinite time until the moment when all transient equations (13) become equal to zero. Such procedure gives the steady-state values of θ_i corresponding to given set of gas concentrations and, therefore, gives the way to calculate reaction rates for individual components (equations (12)). The optimal values of rate and equilibrium constants may be then be defined by application of conventional minimization procedure using whole experimental array. Application of this approach made possible to create kinetic model, providing good description of experimental data. The examples of such description are given in the figures below.



Results of experimental steady-state data description by non-steady-state model under variation of H₂S inlet concentration: (a) - reaction rates (in terms of difference between inlet and outlet concentrations), (b) - selectivity of oxidation into sulfur. Lines – model, points – experiments.

Notably, the proposed model provides adequate description both for cases of complete reaction system and Claus reaction performance only. It also has good predictive force for such sophisticated and important reaction parameters as selectivity in a wide concentration and temperature range and reflects many observed reaction regularities like slight decrease of reaction rate and selectivity with rise of water vapors content etc. It is also important to note that obtained values of model parameters show “correct” behavior with variation of reaction temperature: rate constants are increasing and adsorption equilibrium constants are decreasing under temperature rise with character of changing closed to Arrhenius type. This is a good proof for physical consistency of a proposed model.

Conclusions

Non-steady-state kinetic models may be used for treatment of steady-state kinetic data in case when algebraic elaboration of steady-state kinetic equations is impossible or complicated. The proposed approach includes numerical integration of time-dependent differential equations until achievement of steady-state, resulting in possibility to numerically obtain the rate values for separate reaction stages for given composition of reaction mixture. The obtained non-steady-state model may be then applied in simulation of catalyst pellets and catalyst beds in research and engineering purposes.

The case study demonstrates application of such approach for steady-state kinetic description of complicated reaction system of hydrogen sulfide oxidation by oxygen. The performed study provided good qualitative and quantitative description of experimental data in wide concentration and temperature range.

Reference

- [1] A.N.Zagoruko, V.V.Mokrinskii. Kinetics of the hydrogen sulfide direct oxidation into sulfur over V-Ti catalyst IC-27-40. – in Proc. Of Chemreactor-14 Int. Conference, June 23-26, 1998, Tomsk, Russia, pp.133-134.

STUDY OF PHYSICAL-CHEMICAL CHARACTERISTICS OF THE CATALYST FOR DIRECT OXIDATION OF HYDROGEN SULFIDE

T.R. Zhdanov, A.V. Podshivalin, O.V. Arkhipova

*The Institute of Petroleum Refining and Petrochemistry
of Bashkortostan Republic Academy of Sciences*

Ufa 450065, Inicativnaya Str., 12, phone/fax: (3472) 42-24-71, vezirov@anrb.ru

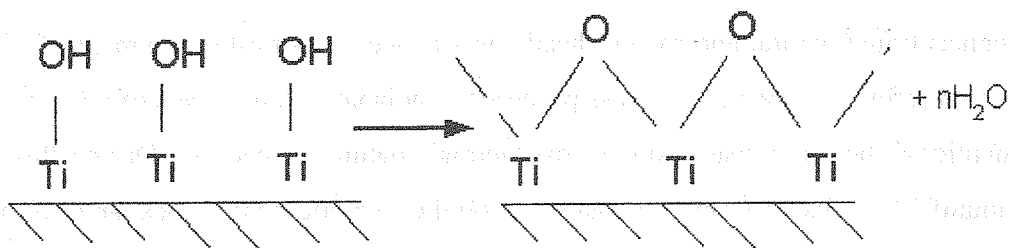
Direct oxidation of hydrogen sulfide is a perspective catalytic process used for treatment of low-concentrated natural and casing- head gases as well as for after-treatment of off- gases of petroleum refining. When the process proceeds in adiabatic static layers of a grainy catalyst large quantity of heat is released due to exothermal nature of reaction. During this process due to ununiformal distribution of the gas flow on the catalytic surface local areas of overheat appear which temperature is much higher than the mean temperature in the catalyst layer. Besides, during oxidative annealing aimed at desorption of sulfur from catalyst pores local areas of sulfur ignition appear also leading to sharp increase of temperatures which are much higher permissible ones [1]. So study of the effect of temperature on physical – chemical characteristics of the catalyst for direct oxidation and determination of its thermostability threshold is an important problem.

Pilot- industrial samples of the titanoxide catalyst TOK-3 presented by Bashneftekhimi company which had been calcined in laboratory conditions (muffle furnace, atmosphere of air) at 200-900 °C were used as objects of our study. The calcined samples were investigated by X-ray crystal analysis, low- angle X-ray scattering and thermography analysis. Specific surface was determined by the method of low temperature desorption of gases. Mechanical strength was determined by the method of granule pressing.

The results of X-ray crystal analysis have shown that initial catalyst consists of TiO_2 in the form of anatase (fig.1, peak a) and in the form of rutile in negligible quantity in (fig. 1, peak r). A part of the catalyst is in the form of fine-dispersed x-ray amorphous state, a part in the fine – dispersed crystal form. Sizes of crystallites in the initial catalyst are about 50 Å on the average. During thermal treatment intensity of anatase lines increases which is explained by increase of the share of crystal phase. Heating up to 400°C does not lead to any change of phase composition. Further heating up to 600°C leads to insignificant increase of the rutile phase. During thermal treatment at 700-800°C the phase composition sharply changes: the

anatase phase decreases while the rutile phase increases. This change of phase composition can evoke decrease of catalyst activity because activity of tetragonic rutile is much below than activity of face- aligned anatase [2].

Change of phase composition and transition of the catalyst from amorphous into crystal state is confirmed by the results of thermography analysis. (fig. 2). Endothermal effect is observed at 120°C, corresponding to removal of adsorbed moisture, and at 700-750°C which is probably explained by polymorphous transformation of active anatase phase in unactive rutile phase. During this process removal of hydroxyl group OH with formation of water takes place [3]. The mechanism of dehydration of chemically bound water is given below:



The results of the X-ray crystal analysis were compatible with the results of the analysis by low-angle X-ray scattering method. If volume of structural porosity of initial catalyst is recognized as a '1' the volume is not changed at 400-600°C and amounts to 0.14 at 700°C and to 0.04 at 800°C. Sizes of pores determined by the method of Ginye vary to a great extent, especially sizes of small large pores (table 2). Increase of temperature leads to decrease of the share of small pores and increase of the share of large pores (above 100 Å).

Table 2. Relation between of sizes of pores (R) and relative volume of catalyst pores (u) and thermotreatment temperature.

initial catalyst		200°C		400°C		600°C		700°C		900°C	
R, Å	u	R, Å	u	R, Å	u	R, Å	u	R, Å	u	R, Å	U
21,7	0,27	20	0,25	-	-	-	-	-	-	-	-
-	-	45	0,2	35	0,2	39	0,17	-	-	-	-
59	0,21	-	-	78	0,14	-	-	52	0,25	64	0,48
108	0,24	85	0,33	-	-	89	0,18	110	0,016	-	-
144	0,08	95	0,07	145	0,32	144	0,21	160	0,14	163	0,15
196	0,2	210	0,15	204	0,15	231	0,29	224	0,18	238	0,14
-	-	-	-	268	0,19	306	0,15	345	0,36	340	0,24

The result of the study of the effect of thermotreatment on specific surface (S_{sp}) of and strength of the catalyst (S) are given in fig.3. A little increase of S_{sp} at temperatures of 400-

600°C is observed, that is possibly connected with removal of the adsorbed sulfur from catalyst pores, while S_{sp} being abruptly decreased during increase of temperature above 600°C due to increase of the degree of crystallinity. Strength of the catalyst increases with raise of temperature at the expense of densification of crystal lattice packing. Decrease of strength is observed at 700-750°C which can be explained by decompaction of crystal structure induced by chemically bound water which is in accordance with the results thermography analysis.

The research works performed made it possible to find out the temperature interval within which no phase changes in the volume of the titanoxide catalyst, decrease of its specific surface, changes of its pore characteristics and decrease of catalytic activity are observed. The limiting temperature determining the threshold of catalyst thermostability is 600°C. At the basis of the study performed the recommendations for usage of the catalyst in the technology of off-gases after-treatment at Ufimsky NPZ have been developed.

References

1. Grunvald V.R. The technology of gas sulfur. Moscow. Khimiya, 1992, p. 272.
2. Alkhasov T.G., Bagirov R.M. et al. Transport, processing and usage of gas. Moscow. VNIIEgasprom, 1985, №86 p. 24.
3. Meyer K. Physical-chemical crystallography. Moscow. Metallurgiya, 1972, p. 480.

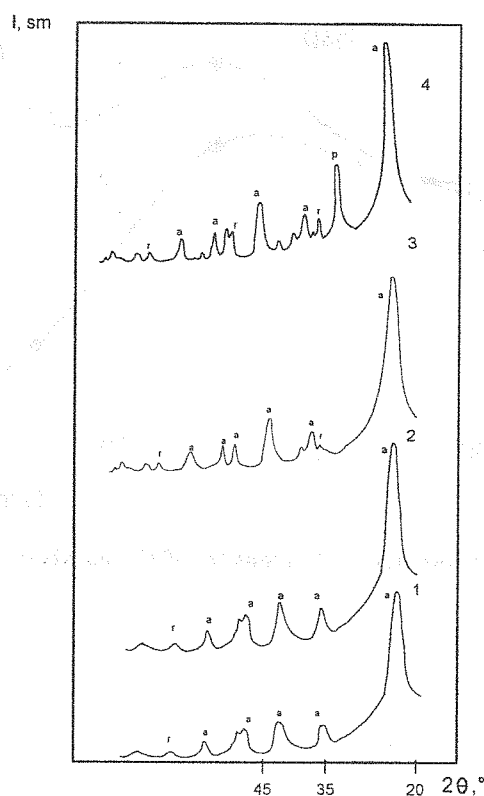


Fig. 1. X-ray diagrams of the catalyst

1 – initial; 2 – calcined at 200-400°C; 3 – calcined at 400-600°C; 4 – calcined at 600-800°C.

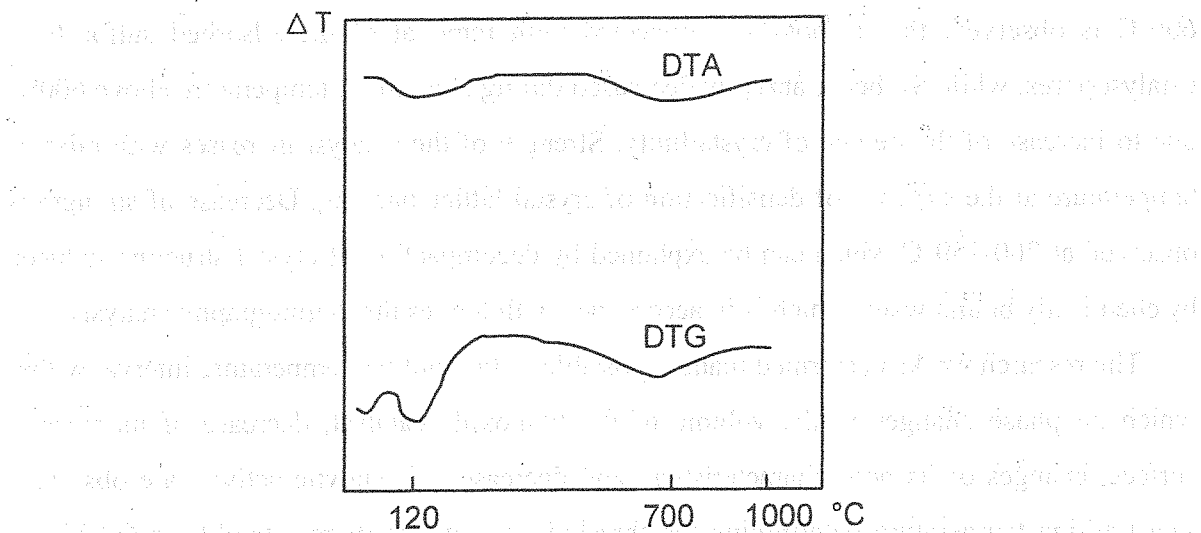


Fig. 2. Thermogram (DTA) and thermogravigram (DTG) of the catalyst

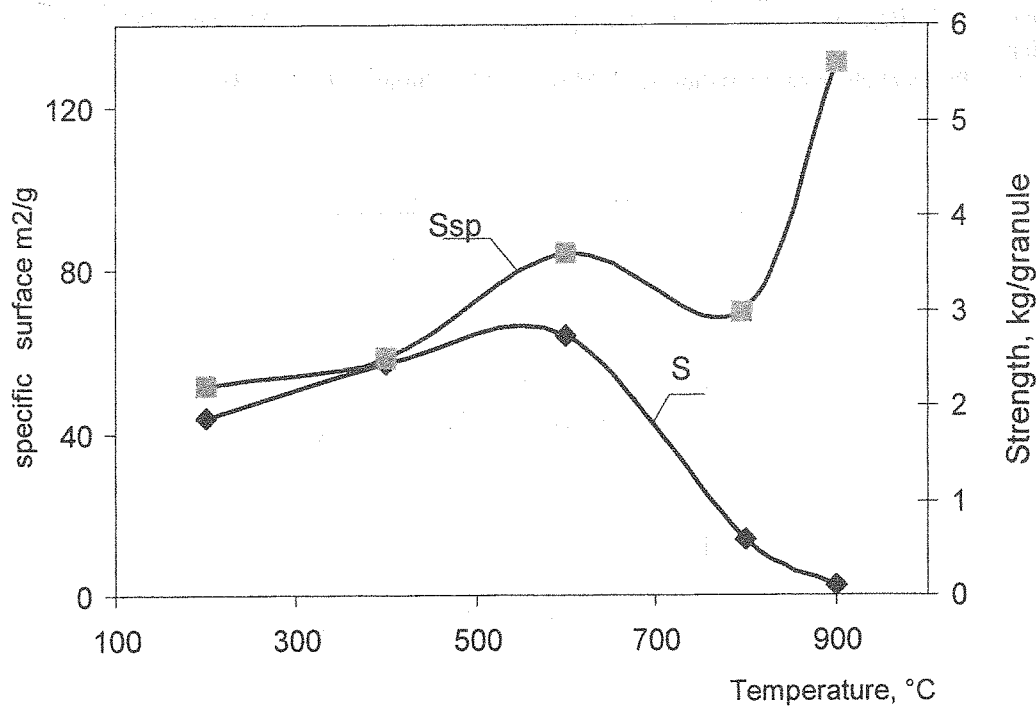


Fig. 3. Relation of specific surface and strength of the catalyst from thermotreatment

CATALYTIC AND HOMOGENEOUS HIGH-TEMPERATURE OXIDATION OF METHANE

A.A. Slepterev, V.S. Salnikov, P.G. Tsyrunnikov,

A.S. Noskov*, V.N. Tomilov*, N.A. Chumakova*, A.N. Zagoruiko*

Omsk department of Boreskov Institute of Catalysis, Omsk, Russia

**Boreskov Institute of Catalysis, Novosibirsk, Russia*

Catalytic burning of natural gas (methane) is more environmentally clean than usual flame combustion. Catalytic oxidation of methane is of great interest for went exhausts of coal mines. Though in this case the methane concentrations are relatively low (not exceeding 2% vol.) its combustion in reverse-process may give the way to concentrate reaction heat in the reactor up to 800° – 1000°C. This heat may be easily utilized. At such temperatures the methane homogeneous oxidation becomes possible in the free volume between large catalyst pellets, in the inert bed of Raschig rings and at their surface, as well as in the void space of reactors. The aim of this study was to obtain initial experimental data on catalytic (up to 600°C) and homogeneous (700° – 1100°C) oxidation of lean methane-air mixtures, modeling the mine exhausts.

Catalytic oxidation

Table 1. Kinetic data on catalytic methane oxidation.

No.	Catalyst	Conditions	Kinetic equation
1	2% mass. Pd/ γ -Al ₂ O ₃ , incinerated at 600°C, 4 hours	T = 450° – 500°; C _{CH₄} = 5 – 15 st.ml/l	W = 6,03 • 10 ⁴ • e ^{-84200/(R • T)} • C, [st.cm ³ CH ₄ /(g•s)].
2	0.5% mass. Pd/ γ -Al ₂ O ₃ , incinerated at 600°C, 6 hours	T = 400° – 500°; C _{CH₄} = 5 – 15 st.ml/l	W = 3,07 • 10 ⁴ • e ^{-94000/(R • T)} • C, [st.cm ³ CH ₄ /(g•s)].
3	12% mass. MnO _x / Al ₂ O ₃ incinerated at 950°C, 4 hours	T = 400° – 500°; C _{CH₄} = 5 – 15 st.ml/l	W = 2,59 • 10 ⁴ • e ^{-106800/(R • T)} • C, [st.cm ³ CH ₄ /(g•s)].

Data in table 1 were detected in kinetic region with catalyst pellets fraction of 0.4 – 0.8 mm, activation energies are given in J/(mole•°K).

Homogeneous oxidation

The special design of flow reactors on the base of small-diameter ceramic tubes was created for fast high-temperature heating of reaction mixture without methane oxidation. The gas was fed via two-channel ceramic tube (external diameter of 3 mm and channels diameter of 0.5 mm), providing efficient gas heating up to 1000°C (with the tube length up to 300 mm)

in practically complete absence of methane oxidation. We used ceramic tubes with external diameters 3.0, 5.2 and 8.1 mm (internal diameters were 2, 3 and 5.2 mm, respectively) as reactors. It was possible to densely fit the tubes into each other, thus changing the length of reaction zone from 20 to 160 mm. Temperature control was provided by thermocouples, situated directly at the external surface of tubes.

Initial methane content in the reaction mixture was fixed at the level 0.2, 0.5, 1.0 and 2.0 % vol. (2 – 20 st.ml CH₄/l). The range of gas flow velocity was 4 - 220 l/hour, corresponding to variation of residence time in the range of 0.006 -1.5 sec. Temperature in experiments was varied from 700 to 1100°C. Gas composition after reactor was analyzed chromatographically.

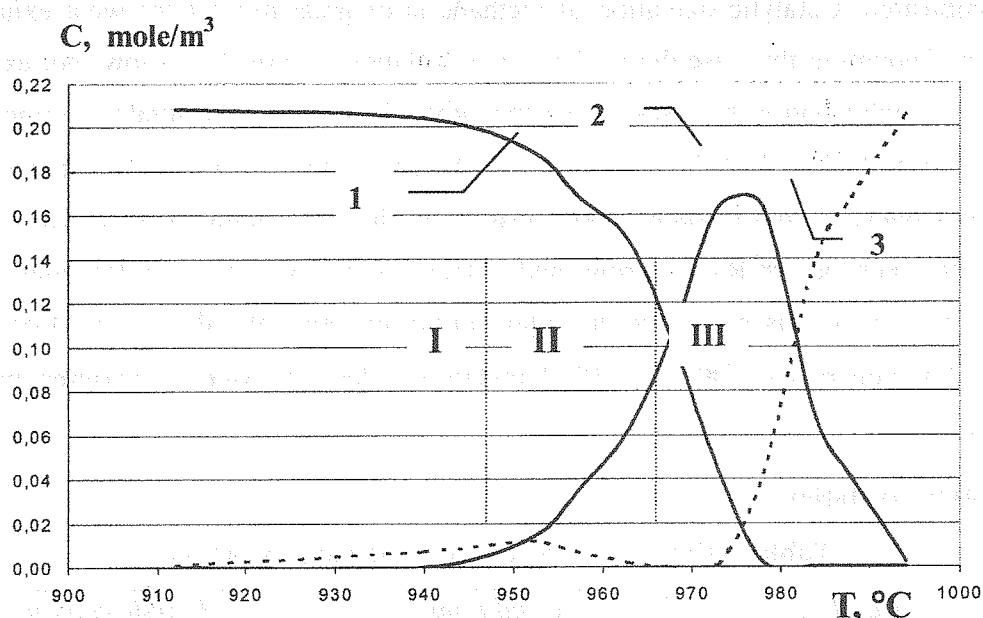


Fig. 1. Example temperature dependence of methane conversion (1), formation and consumption of CO (2), formation of CO₂ (3).

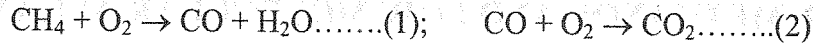
Fig.1 demonstrate the typical temperature dependence of methane conversion and formation of products (CO and CO₂). It is seen, that carbon monoxide is formed in significant quantities with maximum on the CO concentration curve at methane conversion range 0.7-0.9. CO₂ formation curve is even more complicated: maximum, minimum and then sharp rise. Minimum CO₂ concentration corresponds to methane conversion of 0.40-0.65, where selectivity of CO formation reaches 80-98%. Such dependencies are typical for all reactors practically in all regimes of kinetic experiments.

Studies of reactor temperature influence at constant residence time and residence time influence at constant temperature on conversion data C_{CH_4} (CO)-T и X - τ showed that:

- with decrease of residence time "concentration-temperature" curves are shifting to the area of higher temperatures;

- with decrease of temperature "conversion-residence time" curves are shifting to the region of higher residence time.

As soon as direct conversion of methane into CO₂ is insignificant (region I, curve 3) it is possible to use consecutive scheme for process description:



with corresponding first-order reaction rates: $W_1 = k_1 C_{\text{CH}_4} \dots\dots(3); \quad W_2 = k_2 C_{\text{CO}} \dots\dots(4)$, where k_1, k_2 – rate constants for reactions (1) and (2) respectively.

Search of k_1 and k_2 values, providing the most adequate process description, showed that both pre-exponential factors and activation energies depend upon reactor diameter (Table 2).

Table 2. Pre-exponential factors and activation energies for constants k_1 and k_2 . Values are given without temperature correction.

Reactor diameter	k_{10}	E_{a1}/R	K_{20}	E_{a2}/R
8.1 mm	$4.27 \cdot 10^{11}$	$2.76 \cdot 10^4$	$6.92 \cdot 10^9$	$2.32 \cdot 10^4$
5.2 mm	$1.43 \cdot 10^{13}$	$3.26 \cdot 10^4$	$7.80 \cdot 10^9$	$3.64 \cdot 10^4$
3 mm	$5.09 \cdot 10^{14}$	$3.78 \cdot 10^4$	$1.86 \cdot 10^{10}$	$3.95 \cdot 10^4$

Correction of systematic error in temperature measurements provided more accurate description of the process (see fig.2).

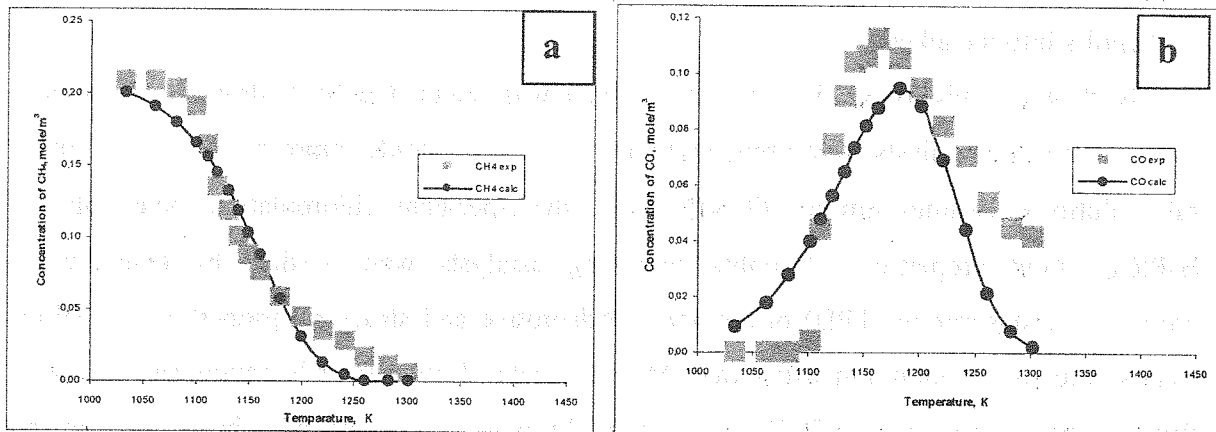


Fig. 2. Comparison of experimental and simulation data with account of systematic temperature correction (+13 °C) for methane (a) and carbon monoxide (b) concentrations. Reactor diameter: 8.1 mm.

Finally, the reaction rates equations may be represented in the following form:

$$W_1(d, T) = e^{-1.3797d + 37.808} e^{\frac{-1985.7d + 43456}{T}} C_{\text{CH}_4} \quad (11)$$

$$W_2(d, T) = e^{-0.1859d + 24.038} e^{\frac{-3266.2d + 50780}{T}} C_{\text{CO}} \quad (12)$$

where W – reaction rates (sec⁻¹), d – equivalent channel diameter (mm), T – temperature (°K), C – concentrations (molar fractions).

**PHYSICOCHEMICAL PROPERTIES OF MODIFIED
ZEOLITE-CONTAINING CATALYSTS AND THEIR CATALYTIC
ACTIVITY IN THE PROCESS OF COUPLED CONVERSION
OF METHANOL AND LOW MOLECULAR ALKANES**

S.S. Safronova, L.M. Koval

36, Lenina Av, Tomsk, Russia, 634050, Tomsk State University, Sweta_SS@freemail.ru

For the last years the essential meaning of the processing of conversion of cheap hydrocarbon raw materials is becoming of great interest as in Russia as well in the abroad the conversion of oil and other associated gases, fraction C₃-C₄ of hydrocarbon into valuable organic connections such as alkenes and aromatic hydrocarbons, components of car petrol. New advanced method of processing of alkenes and arenes is the process of combined conversion of methanol and low molecular alkanes C₃-C₄. The actual realization of this method is connected mainly with the processing of modern thermostabl catalysts: such as high silica zeolites of type ZSM-5, catalyzing as splitting hydrocarbons as the conversion of methanol's into the alkenes.

Synthesis of highly silicious zeolites (HSZ) was conducted by hydrothermal method. Modified zeolite catalysts were prepared by the method of zeolite impregnation in H-form by salt solutions: gallium nitrates GaNO₃·8H₂O, three-per-cent chloroplatinic acid solution H₂PtCl₆. Acid properties of zeolite-containing catalysts were studied by temperature-programmed desorption (TPD) of ammonia. Adsorptive and structural properties of zeolites were studied on vacuum unit with quartz MacBen scales. Before the adsorption, samples were fired at the temperature of 723K in vacuum during 4 hours. As adsorbates, benzol and methanol were used. Studies of coupled conversion process of methanol and wide fraction of light hydrocardons into hydrocarbons on zeolite-containing catalysts were carried out on circulating unit with a stationary catalyst layer, with the volume of 4cm³, at weight hour space raw material conveying velocities of 1h⁻¹ by methanol and 240h⁻¹ by wide fraction of light hydrocardons within the temperature range from 673 to 823 K under atmospheric pressure. Analysis of gaseous and liquid reaction products was conducted by chromatographic method in the mode of temperature programming from 323 to 493 K. The degree of methanol

and propane-butane conversion was taken for catalyst activity measure, selectivity of alkenes and arenes was estimated on the basis of their content in reaction products.

The researched samples of zeolites are characterized by biporous structure, i.e. which contain micro- and mesopore. The evaluation of microporous structure given catalysts according to the theory of volumetric filling microporous, showed that all researched zeolites have two types of micropores with different sizes. The implementation of optimal methods of Hooek-Javis, Rossenbroak, isotherms of an adsorption of methanol to the researched samples on an equation Dubinin-Astachov with two exponents proves that the result of porous structure to adsorption of molecules of bensol, as the result of experimental adsorption method. It is clear that zeolite HSZ – 30 with more volume and size of micropores has more adsorption volume according to the methanol. The analysis of dates according to adsorption of molecules of methanol for modified HS-zeolites, showed that the narrow pores of zeolites lead to more active interaction of molecules of methanol on the surface of catalyst. For further evaluation of the adsorption - power characteristics, we need to deduct isosteric heat of adsorptions of methanol for zeolite-bearing catalysts. It is showed that the heat of adsorption for these samples has extreme character, which is important for non-localized adsorption on the energetically non-surfaces and it is regard by the interaction adsorbate - adsorbate. The structure and adsorption volume of modified zeolite-bearing catalysts depends on the nature and quantity of introduced modifying agents. The research of the acid properties HSZ by the method TPD of ammonia, showed, that for all samples is characterized the presence of two types of acid centers of (L- and B-centers). There is maximum of concentration in the results of zeolite. The introduction of modifiers, which leads to the change of his acid spectrum, which reflexes on his behavior in catalysis. On this base of the research of physicochemical properties of the samples of catalysts, it is identified, that the main catalytic activity in the synthesis of alkenes in the process of combined conversion of methanol and low alkanes C₃-C₄, which is outlined the result of zeolite (SiO₂/Al₂O₃=30) with the greater pores and maximum of concentration of acid centers on the surface. The introduction of Ga and Pt by zeolite impregnation leads to changes of physicochemical catalytic properties in the process of coupled methanol and propane-butane fraction conversion: their activity and arene formation selectivity increases, number of strong acid centers, pore dimensions are reduced, but adsorptive capacity increases. This is probably determined by the fact, that particles neutralize strong acid centers of zeolite matrix, situated near the canal entrances or in their intersection places, creating new centers with a greater interaction energy.

HOMOGENEOUS LIGHT-INDUCED DEGRADATION OF METHYLPHENOLS IN THE AQUEOUS MEDIA

Tatiana V. Sokolova¹, Olga N. Chaikovskaya¹, Irina V. Sokolova¹, Edvard A. Sosnin²

¹*Siberian Physical-Technical Institute at Tomsk State University,*

1, Novo-Sobornaya, Sq., Tomsk, 634050, Russia, 7(3822)533034, sokolova@phys.tsu.ru

²*High Current Electronics Institute of the Siberian Branch of Russian Academy of Sciences,*

4, Akademicheskoy Av., Tomsk, 634050, Russia, badik@loi.hcei.tsc.ru

Solvated phenols have attracted many workers because of their participation in the proton-transfer and oxidation reactions. On the other side, phenols are the most widespread pollutants in the environment [1]. Water chlorination as a means of its disinfection is most widely used in practice, even though it gives rise to the formation of chlorine phenols of varying composition. Their biological action is more dangerous than phenol itself [2]. The use of UV radiation of varying power is one of modern techniques for water purification from organic molecular contamination. This is ecologically safe technique. Using lasers significantly extends the possibilities of studying phototransformation mechanisms and photolysis control [3]. The narrow spectral range of laser radiation produced a selective effect on individual molecular electron states. The low laser-beam divergence allows laser light to be transported with a minimum loss to any point of interest and the energy deposited in the solution to be determined. An increase in the power density of exciting radiation in a narrow spectral range may cause nonlinear laser – matter interactions. Along with the above advantages, laser sources have some defects, such as complex equipment, which requires high operating costs and highly skilled maintenance personnel. Simple and reliable radiation sources with a long service life are necessary for both scientific research and industrial applications. In particular exciplex lamps [4] belong to such sources. Like exciplex lasers, these lamps producing a narrow emission spectrum can selectively excite molecules.

The methyl-substituted phenols (cresols) are widely distributed in atmosphere and hydrosphere and absorb in UV range of spectra. Methylphenols, used in wood preservative industry, can behave as a major pollutants [5]. In this work, we studied the photolysis of aqueous methyl-substituted phenols (*o*- and *p*-cresol) solutions under spontaneous irradiation, with pulsed KrCl* ($\lambda_{exc} = 222$ nm) and XeBr* excilamps ($\lambda_{exc} = 283$ nm) and under irradiation

with a mercury lamp. The efficiency of phototransformations and photodegradation behavior were determined by measuring the spectral and luminescence characteristics of irradiated solutions.

Experimental

An OKN-11M high-pressure mercury-vapor lamp and pulsed *U*-barrier-discharge KrCl* ($\lambda_{\text{exc}} = 222 \text{ nm}$) and XeBr* excilamps ($\lambda_{\text{exc}} = 283 \text{ nm}$) with the parameters $\Delta\lambda = 5\text{--}10 \text{ nm}$, $W_{\text{peak}} = 18 \text{ MW/cm}^2$, $f = 200 \text{ kHz}$, and a pulse duration of $1 \mu\text{s}$, developed under the supervision of Prof. V. F. Tarasenko were used for photochemical investigations as UV-radiation sources [6]. The examined compounds were put in a rectangular quartz cell. To avoid heating of the solution under irradiation with the excilamp and to provide stable operation, the setup was air-cooled using a ventilator. The exposure time was 1–40 min. During this time, the energy from 0.5 to 20 J/cm^2 was deposited into the solution. The radiation sources were chosen due to the fact that 283-nm radiation falls within the long-wavelength absorption band of cresols (formed by the $S_0 \rightarrow S_1$ transition), whereas 222-nm radiation falls within the intermediate absorption band (formed by $S_0 \rightarrow S_2$ and $S_0 \rightarrow S_3$ transitions). Light of the mercury lamp is only weakly absorbed by neutral forms of the examined molecules and is absorbed more intensively by anionic forms of molecules present in the alkaline medium. The pH of the medium was changed by addition of an alkali (KOH) to the solution. The concentration of the examined molecules in solutions was $5 \cdot 10^{-4} \text{ mol/L}$.

Conclusions

1. The photolysis of aqueous solutions of *p*-cresol is more efficient than that of analogous solutions of *o*-cresol irrespective of the radiation source and the pH of the medium.
2. The efficiency of cresol phototransformations in the alkaline medium is higher under spontaneous irradiation with the XeBr* lamp ($\lambda_{\text{exc}} = 283 \text{ nm}$). In the neutral medium, it is higher under irradiation with the KrCl* lamp ($\lambda_{\text{exc}} = 222 \text{ nm}$).

This work was supported by the Ministry of Education of the Russian Federation (Project No. E 02-12.2-63).

References

1. Legrini O., Oliveros E., Braun A.M., Chem. Rev. 1993, vol. 84, p. 891.
2. Goncharuk V.V., Potapenko N.P., Chemistry and technology of water. (Russ.), 1998, vol. 20, p. 190.
3. Tchaikovskaya O.N., Sokolova I.V., Bazyl' O.K. et al., Intern. J. of Photoenergy, 2002, , vol. 4, p. 79.
4. Lomaev M.I., Skakun V.S., Sosnin E.A. et al., Techn. Phys. Letters. 1999, vol. 20, p. 27.
5. Mazellier P., Bolte M., J. Photochem. photobiol. A.Chem., 2000, vol. 132, p. 129.
6. Tarasenko V. F., Chernov E. B., Erofeev M. V. et al., 1999, Appl. Phys. A, vol. 69, Suppl., p. 327.

REDUCTION METHOD FOR NONLINEAR SYSTEMS OF DIFFERENTIAL EQUATIONS OF CHEMICAL KINETICS

B.V. Alexeev and N.I. Koltsov

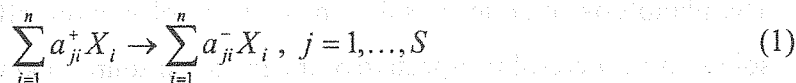
Department of Physical Chemistry of Chuvash State University,

Moskovskii prospect 15, 428015 Cheboksary, RUSSIA

E-mail: koltsov@chuvsu.ru, Fax: +78352 428090

One of approaches to lower the dimension of kinetic models of chemical reactions is reduction of dimension of the system ordinary differential equations describing these reactions. This approach consists in division of the whole time interval into subintervals, on each of them only the part of the complex mechanism of reaction is realized. The method described in [1,2] achieves reduction of the systems on time subintervals by omitting small monoms in polynomials of differential model. The drawback of this method is that reduced differential model may loss chemical consistency (corrupts conservation laws etc.). Our method differs in that we omit stages rates (instead of monoms) when and while they are small. This permits to reduce the models of wider class of reactions, described by complex kinetic behaviour, yet preserving the chemical sense.

Mathematical model of the chemical reaction proceeding through stages



(convertible stages are written separately as two irreversible ones) looks like

$$\dot{x}_i = \sum_j r_j (a_{ji}^- - a_{ji}^+), \quad (2)$$

where rates of stages r_j are defined according to the acting masses law

$$r_j = k_j \prod_{i=1}^n x_i^{a_{ji}^+} \quad (3)$$

through kinetic parameters (constants of stages rates) k_j , concentrations x_i of substances X_i and stoichiometric coefficients of stages a_{ji}^+ . We shall consider, that the total number of atoms of each kind remains constant during reaction. As each of substances participates at least in one law of conservation of the number of atoms, concentrations of all substances

during reaction are limited to some constant: $|x_i| \leq R$. The basic idea of our method of a reduction is that process of reduction should keep laws of conservation valid. This idea realized in the following rule of a reduction: change of system occurs only during those moments of time when the value of some stage rate (3) achieves some level ε (level of significance). If stage rate achieves this value, while increasing, then since this moment of time this particular stage is included in the mechanism and if stage rate decreases to level of significance then this stage is excluded from the mechanism. By this way of reduction at each time interval the system of differential equations of a kind (2) remains chemically intelligent as corresponds to the initial mechanism with exception of some stages. The solutions of reduced system will be limited since laws of conservation of atoms are determined by the list of substances and their chemical formulas and do not affected by exception or addition of any stages.

Let's note, that the method of reduction in [1] contains another rule of reduction at which monoms of the polynomial system of differential equations (2) of the model (instead of stages rates) are compared with the level of significance. However, comparison of monoms, followed by their exception or addition, leads to the loss of the "chemical sensibility" of the system (2). It can lead also to essential change of properties of the reduced system in relation to initial model.

Let's estimate in a general view an error of a suggested method of a reduction, i.e. an error of replacement of a vector of solutions $x_i(t)$ of initial system by the vector of solutions $y_i(t)$ of the reduced system according to the level of significance ε . Let t_0, t_1, t_2, \dots be the moments of change of the list of active stages (the moments of switching). During the initial moment of time t_0 , generally speaking, the list also can be changed (in a case when one or several stages rates is less than level of significance). On each interval of time between the consecutive moments of switching $t = t_{k-1}$ and $t = t_k$ the vectors of solutions of the initial and reduced systems satisfy to systems of polynomial differential equations $\dot{x}_i = \sum_j r_j(x)(a_{ji}^- - a_{ji}^+)$ and $y_i' = \sum_{J_+} r_j(y)(a_{ji}^- - a_{ji}^+)$, where sum on J_+ corresponds to "significant" stages (i.e. stages with rate, which is greater than the level of significance on an interval $t_{k-1} \leq t < t_k$) and to the stages reaching the significance at $t = t_{k-1}$. Behaviour in time of an error $\Delta = \sqrt{\sum (x_i - y_i)^2}$ of replacement of the exact solution with reduced one is determined by equation

$$\Delta' = \frac{1}{\Delta} \sum_i (x_i - y_i) \left(\sum_j (r_j(x) - r_j(y))(a_{ji}^- - a_{ji}^+) + \sum_{J_-} r_j(y)(a_{ji}^- - a_{ji}^+) \right), \quad (4)$$

where the sum on J_- corresponds to insignificant stages on an interval $t_{k-1} \leq t < t_k$ and to the stages losing the significance at $t = t_{k-1}$. If M is maximal molecularity of the mechanism

stages, and K is a maximal constant of stages rates, then the derivative $\frac{\partial r_j}{\partial x_i}$ under condition

$|x_i| \leq R$ has upper estimation $L = KMR^{M-1}$. By the theorem of mean value

$r_j(x) - r_j(y) = \sum_i \frac{\partial r_j}{\partial x_i}(\xi)(x_i - y_i)$. Values $r_j(y)$ in the sum on J_- do not exceed the level of

significance $r_j(y) \leq \varepsilon$. In view of it the error Δ is estimated by differential inequality

$\Delta' \leq nLMS\Delta + \sqrt{n}MS\varepsilon$. The solution of an inequality results in the following estimation of the value of Δ

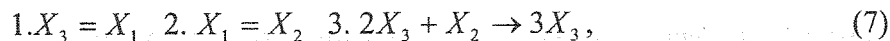
$$\ln \frac{\varepsilon + L\sqrt{n}\Delta(t_k)}{\varepsilon + L\sqrt{n}\Delta(t_{k-1})} \leq nLMS(t_k - t_{k-1}). \quad (5)$$

As $\Delta(t_0) = 0$, recursive application of (5) allows to find an estimation Δ at any moment of time $t \geq t_0$

$$\Delta(t) \leq \frac{\varepsilon}{L\sqrt{n}} (e^{nLMS(t-t_0)} - 1). \quad (6)$$

Thus, the error arising at transition from exact system to reduced one, is estimated by the function linear on the level of significance ε and can be made arbitrary small at a corresponding choice of the level of significance, although the multiplier may be big in real examples. Obviously, more detailed analysis will allow to receive more exact estimation of this multiplier.

Let's consider three-stage reaction



which is characterized by a self-oscillatory behaviour at the values of constants of stages rates

$k_1 = 2.89, k_{-1} = 0.01, k_2 = 0.034, k_{-2} = 0.1, k_3 = 2000c^{-1}$ and initial conditions

$x_1(0) = 0.2, x_2(0) = 0.8, x_3(0) = 0$ (see fig. 1a). On fig. 1b the dependence $x_1(t)$ for the

reduced system is represented at level of significance $\varepsilon = 0.001$ is represented, and also

intervals of the significance of stages 1,-1,2,-2,3 are shown, designated accordingly by the

values 0.1,0.2,0.3,0.4,0.5. Thus the second stage, characterized in the opposite direction by

the rate $k_{-2}x_2$, has intervals of insignificance not only in an initial period, but also during all the time of reaction. It can be explained by the fact, that the limiting cycle arising in the given reaction is characterized by small values of x_2 , which leads to the existence of an interval of insignificance of the second stage rate in the opposite direction during each period of self-oscillations. The difference of the exact and reduced solutions $x_1(t)$ on an interval from 0 up to $40c$ varies in the range from -0.0078 up to 0.0522 . As mentioned above, this error can be lowered to any value by the choosing the small enough level of significance.

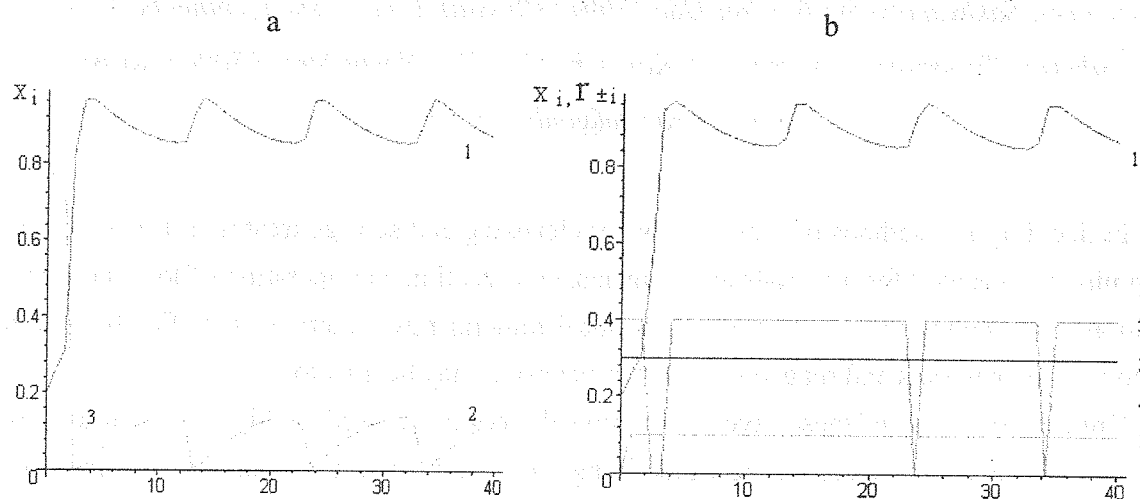


Fig. 1. Dependences $x_i(t)$ and $r_i(t)$, $i=1,2,3$ for the reaction (7): a - values of $x_i(t)$ calculated by exact model; b - 1' $x_1(t)$, 1-3 $r_i(t)$, 4-5 $r_{-i}(t)$, calculated by the reduction method.

Thus, we have developed an effective method of reduction of systems of the differential equations of chemical kinetics. The essence of a method consists in taking into the account during each moment of time only those stages of process which rate is bigger than some chosen level of significance. The method can be applied for research of dynamics of the chemical reactions described by complex nonmonotonic kinetic behaviour.

References

1. Tropin A.V., Maslennikov S.I. and Spivak S.I., *Kinetika i Kataliz*, 1995, 36(5), 658. (in Russian).
2. Galina G.K., Spivak S.I., Vajman A.M. and Commissarov V.D., *Doklady Akademii Nauk*, 1998, 362(1), P.57. (in Russian).

WET OXIDATION OF ORGANIC IMPURITIES BY HYDROGEN PEROXIDE IN THE PRESENCE OF Fe-PILLARED CLAYS

**S.Ts. Khankhasaeva¹, L.V. Brizgalova¹, E.Ts. Dashinamzhilova¹,
A. Ryazantsev², S.V. Badmaeva¹**

¹*Baikal Institute of Nature Management, Siberian Branch of the Russian Academy of Sciences, Sakhyanova Str. 6, Ulan-Ude 670047 (Russia), E-mail: shan@binm.baikal.net*

²*Siberian Transport University, D. Kovalchuk Str. 191, Novosibirsk 630049 (Russia)*

E-mail: raastu@online.sinor.ru

In deciding on methods of recycling water cleansing and sewage treatment it is necessary to minimize expenses for materials and reagents, construction and operation of local cleansing installations. Maximum use of inexpensive local mineral raw materials, specifically, natural bentonites as materials and reagents for water cleansing may be a factor.

Unique properties of these layered aluminosilicates are caused by high value of specific surface of particles dispersed in the water along with the existence of trade cations, hydroxyl groups and adsorbed water molecules in their structure [1]. Modification of bentonites makes it possible to expand substantially area of their application [2–5]. Modification is performed through incorporation of metall hydroxypolycations into interlayer space followed by calcining of samples at 200–500 °C. Thus obtained layer-pillar pore structured samples, referred to as pillar-clays, possess well-developed specific surface and are in routine applicable as sorbents for sewage freeing from flotation agents, pesticides, dyes and others. There are practically no works on their application as oxidation catalysts for organic impurities in the sewage.

The purpose of the present work is obtaining of layer-pillar structured materials on the basis of montmorillonite modified by iron (III) and examination of their catalytic properties in wet oxidation of toxic organic impurities (phenol and dyes).

To produce layer-pillar structured material the bentonite has been used from Tuldon site (Buryatia) represented mostly by montmorillonite (65 %) and kaolinite (5 %). Naturally occurring mineral (composition, mass fraction, %: 69.0 SiO₂, 16.7 Al₂O₃, 2.6 Fe₂O₃, 1.5 CaO, 1.3 MgO, 2.8 K₂O, 2.2 Na₂O, 5.6 H₂O) was suspended in distilled water, solution was clarified, and finely dispersed fractions were separated by centrifugation. Fe-pillared clay (Fe-PC) has been obtained through modifying of bentonite by mono- and binuclear iron (III) hydroxocomplexes as in [6]. Quantitative determination of Fe was performed by sulfosalicylic acid photometry according to [7]. Iron content, recalculated to Fe₂O₃, corresponded to 5.9 % in Fe-PC, with consideration of iron content in naturally occurring clay. Concentration of

dyes and phenol in solution were determined by photometric evaluation using KFK-2 and Specord UV-VIS instruments. Texture parameters of Fe-PC were measured at ASAP-2400 Micromeritics setup by nitrogen adsorption at 77 K: specific surface was 99,3 m²/g; mean diameter of pores - 8,4 nm; total pore volume - 0,202 cm³/g; micropores volume - 0,003 cm³/g. The testings of catalytic properties were carried out in the reaction of phenol and anionic dyes Acid chrom dark-blue (AC), Direct black (DB) oxidation by hydrogen peroxide. The oxidation experiments were carried out in a well-stirred glass reactor with a reflux condenser at atmospheric pressure and temperature 50 °C (phenol), 40, 25 °C (dyes).

Initial concentration of phenol was varied from 94 up to 300 mg/l, molar ratio H₂O₂: phenol from 7,5:1 up to 25:1, concentration of catalyst from 5,0 up to 28,8 g/l, pH of a reaction mixture from 1,3 up to 5,4. The intermediate products of phenol oxidation - hydroquinone, p-benzoquinone and carboxylic acids- were detected by HPLC (Milichrom A-02 chromatograph with an UV detector). The kinetics of phenol consumption was studied. On kinetic curves of phenol consumption the induction period was watched. The rate of phenol oxidation increased at increase of initial concentrations of phenol and of hydrogen peroxide. The maximum reaction rate was watched at pH 2,3, the further increase pH resulted to decreasing of reaction rate. A time of phenol complete conversion varied from 20 up to 120 min depending on initial conditions of reaction.

Initial concentration of dye in solutions varied in limits from 100 up to 500 mg/l, hydrogen peroxide concentration - from 2*10⁻³ up to 0,05 M; pH - from 2,0 up to 5,0; catalyst concentration - from 0,5 up to 5,0 g/l. Influencing initial concentrations of reactants, temperature and pH on the rate of decrease of AC concentration was studied. The catalyst a Fe-PC was active in range pH from 2,0 up to 6,2, thus the noticeable slowing down of oxidation of dyes was watched at pH above 4,0. The optimum conditions of reactions permitting to achieve a high conversion of a dye (99 %) were determined. At reuse of catalyst the decreasing of a rate of AC oxidation was insignificant. The results on oxidation of phenol and organic dyes demonstrate prospects of practical use of catalyst a Fe-PC during oxidation of organic pollutants of sewages.

This work was supported by the Russian Foundation for Basic Research (№ 01-05-97254).

References

1. Yu. I. Tarasevich. Prirodnye sorbenty v protsessakh ochistki vody. Naukova dumka, Kiev. 1981.
2. A/ Vaccari. App. Clay Sci. 14 (1999) 161.
3. S. L. Jons. Catal. Today. 2 (1988) 209.
4. C.I. Warburton. Ibid. 2 (1988) 271.
5. A. S. Panasyugin, A. S. Rat'ko, N. P. Masherova. Russian journal of inorganic chemistry. 43 (1998) 1437.
6. M. A. Shchapova, S. Ts. Khankhasaeva, A. A. Ryazantsev, A. A. Batoeva, S.V. Badmaeva. Chemistry for Sustainable Development. 10 (2002) 375.
7. Yu. Yu. Lurie. Analiticheskaya khimiya promyshlennykh i stochnykh vod. Khimiya, Moscow, 1984.

THE METHOD OF DETERMINATION NUMBER OF STATIONARY STATES AT THE DECISION OF THE REVERSE TASK OF CHEMICAL KINETICS

E.S. Patmar, N.I. Koltsov

The Chuvash State University, Cheboksary, Russia

E-mail: edi@chuvsu.ru

A step of reverse problem decision is discrimination of mechanisms of reactions on number of internal stationary states (ISS) - stationary states, in which intermediate substances concentrations is nonzero. In the work [1] the criterion of multiplicity of stationary states (MSS) has been developed. This criterion allows to hold on discrimination of mechanisms on the basis of a realization two ISS. However this method does not give an opportunity to determine a realization of three and more ISS. In [2] it is shown, that ISS number can grow without limited all bounds with growth intermediate substances number. In [3] the opportunity of exponential increases in ISS number is established with growth of quantity of intermediate substances: for the mechanisms with three intermediate substances probably up to 9 ISS, for the mechanisms with four intermediate substances – 27 ISS's and in general for mechanisms with n intermediate substances are possible 3^{n-1} ISS. The estimations resulted in [2,3] have a theoretical nature and show only potential opportunity of big number ISS occurrence. In works [4-5] the general methods are given. These methods allow to determine ISS number. In [4] the consecutive exceptions method is considered. Its basic drawback is a fast growth of necessary calculations number at increase in number of intermediate substances and lock basic impossibility over of all possible values of constants of rates. That is why this can not establish set ISS number realization (that is necessary for discrimination). Other method [5] (based on cylindrical splittings constructions) allows to determine a realization of this or that ISS number, but the necessity for such calculation grows twice exponentially on n (to quantity of intermediate substances). Necessary calculations number growth rate with growth n is a common drawback of both methods.

We have developed a new method of definition given ISS number realizability. It is as following:

1) researched system stages rates constants (instead of intermediate substances concentration) are determined;

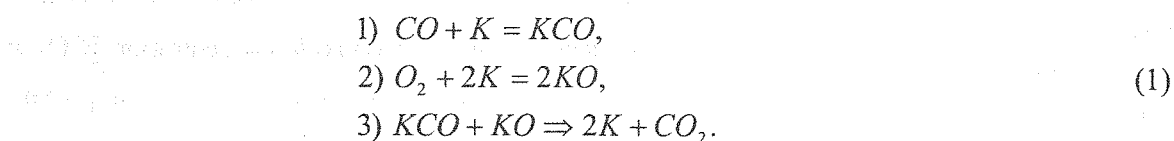
2) the set of all possible values of concentration is broken on n-dimensional (as a rule rectangular) "areas";

3) for each of these areas possible values stages rates constants ("constants values area") are counted up;

4) then maximum ISS number is determined on the a condition, that it does not surpass number of "areas" for which the values stages rates constants can be the same identical.

The difference of the given method from a method [4] is that of determination of stages rates constants, instead of intermediate substances concentration. That is why the linear algebraic equations are solved instead of nonlinear ones. Concrete values of constants of rates of stages, and ranges of their changes due to that number ISS can be determined not only at the given values of constants of rates of stages are considered not, but also to determine a basic opportunity of a realizability of set number ISS. The given method also allows to establish a realization of certain ISS number and to construct the areas described by set ISS number. Therefore it is applied both at a discrimination stage and at a stage a conditions finding at which concrete ISS number for researched reaction is realized.

Let's consider the given method application for the reaction $2CO + O_2 \rightarrow 2CO_2$ proceeding under the three-stage scheme:



It is known that, this scheme is characterized by 3 ISS and described by the following system of equations stationary:

$$k_1[CO]x_1 - k_{-1}x_2 = r, \quad 2k_2[O_2]x_1^2 - 2k_{-2}x_3^2 = r, \quad k_3x_2x_3 = r, \quad x_1 + x_2 + x_3 = 1$$

or after transformation

$$k_{-1}x_2 + r = k_1[CO]x_1, \quad 2k_{-2}x_3^2 + r = 2k_2[O_2]x_1^2, \quad r = k_3x_2x_3, \quad x_1 + x_2 = x_4, \quad x_4 + x_3 = 1, \quad (2)$$

where x_1, x_2, x_3 , $[CO]$ and $[O_2]$ - concentration of intermediate substances, K, KCO, KO and the basic reagents CO and O_2 , k_{i} - constants of rates of stages. After introduction of new variables

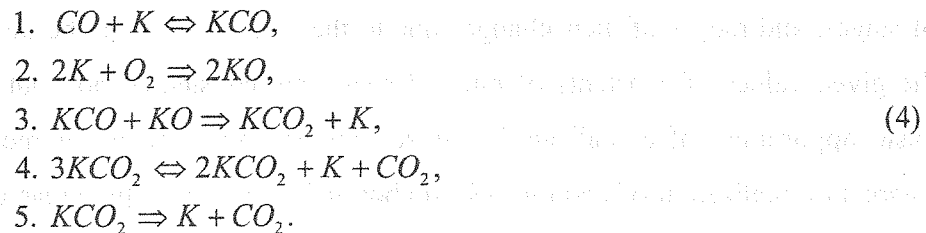
$$y_1 = r/(k_1[CO]x_1), \quad y_2 = r/(2k_2[O_2]x_1^2), \quad y_3 = r/k_3x_2x_3, \quad y_4 = x_2/x_4, \quad y_5 = x_3$$

the system (2) will become

$$\begin{aligned} y_1 + k'_1 \cdot y_1 / y_5 = 1, & \quad y_2 + k'_2 \cdot y_2^2 \cdot y_3^2 / y_1^2 = 1, \quad y_3 = 1, \\ y_4 + k'_4 \cdot y_4 y_5 / y_1 = 1, & \quad y_5 + k'_5 \cdot y_1^2 / (y_2 y_4 y_5) = 1, \end{aligned} \quad (3)$$

where $0 \leq y_1, y_2, y_4, y_5 \leq 1$, $y_3 = 1$. Values of all variables y_i , except for y_3 , were broken into 5 intervals ($a_i^j < y_i \leq b_i^j$), the general areas number was equal $5^4=625$. Unambiguity of areas was checked on the basis linearization the equations of system (3). The number the crossed "areas of values of constants" at the given stage was equal 4. The further splitting of areas with crossed values has allowed to establish a realization of no more than 3 crossings. This means that the realization is no more, than 3 ISS.

As a result of applying the above-described method, for example, for a reaction of carbon monoxide catalytic oxidation, the mechanism of six ISS is constructed:



In fig. 1 the kinetic dependence is depicted. It proved that there are six ISS in the reaction proceeding via mechanism (4).

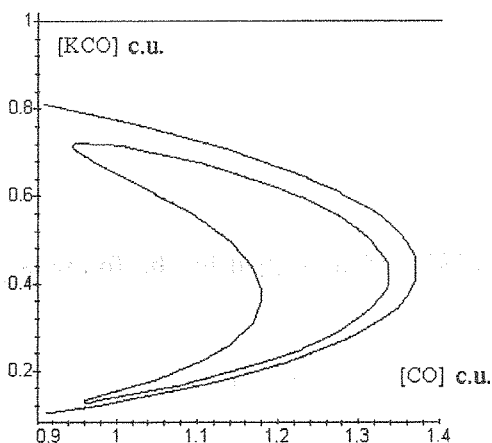


Fig.1 Dependence of concentration [KCO] of carbon monoxide oxidation reaction is proceeding via scheme (4) on monoxide concentration [CO] at: $k_1 = 1$; $k_{-1} = 0.001$; $k_2 = 5$; $k_3 = 1.01$; $k_4 = 37500$; $k_{-4} = 25000$; $k_5 = 125$ (s^{-1})

The given method is realized as the program in language Delphi 6 and allows to investigate number ISS different catalytic the reactions proceeding on one-routing five - and six-stages mechanisms.

References

1. Koltsov N.I., Fedotov V.H., Alekseev B.V. // Reports of the Russian Academy of Science. 1988. V. 302. №1. P. 126.
2. Alekseev B.V. and Koltsov N.I. // Mendeleev Communications. 1998. V.8. №3. P.116.
3. Patmar E.S., Alekseev B.V., Koltsov N.I. // Reports of the Russian Academy of Science. 2000. V.371. №5. P. 638.
4. Bykov V. I., Kytmanov A.M., Lazman M. Z. Method of Exception in Computer Algebra of Multinomials. Novosibirsk: Science, 1991. 232 p.
5. Buhberg B., Colinz D., Loos R. Computer Algebra. Symbolical and Algebraic Calculations. M.: World, 1986. 392 p.

MECHANISMS OF PLASTICIZATION AND MODIFICATION OF PETROLEUM RESIDUES WITH PARTICIPATION OF ELEMENTAL SULFUR CLUSTERS

I.R. Telyashev, R.R. Vezirov, E.G. Telyashev

The Institute of Petroleum Refining and Petrochemistry

of Bashkortostan Republic Academy of Sciences

Ufa 450065, Inicativnaya Str., 12, phone/fax: (3472) 42-24-71, vezirov@anrb.ru

Study aimed at investigation of the features of the process of interaction of elemental sulfur with petroleum residues is an urgent problem and represents practical interest from the point of view of sulfur – bitumen binders production.

The investigations performed before have shown that at relatively low temperatures (in conditions of physical-chemical treatment) clusters of sulfur and plasticity and elasticity to petroleum residues [1]. Depending on conditions of physical-chemical action quantity of entrained sulfur amounts to 5 – 15 %.

Study by X-ray crystal analysis has shown that addition of sulfur to petroleum residues strongly changes its structure towards amorphous state.

Disordering and loss of strength of gel pseudo-crystal lattices of asphaltenes and destruction of crystal structures of normal paraffins [2, 3] take place accompanied by increase of interplane distance d_{002} determined by reflection of hexagon layers of carbon atoms arranged into graphite – like packs and characterizing density of condensed aromatic structures package. Analysis of the asphaltenes released from petroleum residues compositions with different quantities of sulfur added has shown that addition of elemental sulfur increases its content in asphaltenes as compared to the initial one. During this process a part of sulfur is in crystal form depending on intensity of treatment (thermal or mechanical-active) [3,4]. Interaction with sulfur also leads to decrease of molecular mass of asphaltene structures [5].

The experimental data obtained permit to represent the mechanisms of plasticization and modification of petroleum residues in the form of successive physical – chemical and chemical processes proceeding with participation of sulfur clusters.

When sulfur is added to petroleum residue its interaction with hydrocarbons of dispersive medium and resins takes place at first. Besides, there is a level of saturation of dispersive medium by sulfur which depends on its chemical composition and quantity. The main influence on interaction of sulfur with asphaltenes is exerted by possibility of penetration of clusters into nucleus of dispersed system where asphaltenes are situated. When dispersed system is saturated by sulfur and diffusion difficulties have been overcome interaction of sulfur with a dispersed phase – asphaltenes is possible.

As result of interaction sulfur is introduced into interlayer space of asphaltene crystallites hexagon layers (discs) of carbon atoms arranged into graphite-like packs (nucleus of the dispersed system) which is confirmed by increase of interplane distance d_{002} . The introduced sulfur at first exists in asphaltenes in the form of crystal formations of different sizes which gives a signal of crystal sulfur on X-ray diagram. Additional energy action leads, from one point of view, to release from asphaltenes of the largest crystal sulfur formations connected to asphaltene framework by rather weak forces of intermolecular interaction. From the other point of view, a stronger intermolecular bond is formed between separate clusters of sulfur and graphite – like matrix of asphaltene nucleus. Mutual action of those factors leads to decrease of interplane distance during mechanical - active and thermal treatments. As a result of increase of the quantity of introduced sulfur weakening of the bond between separate layers of asphaltene crystallites (that is inside disperse system nucleus and solvent shell takes place. This leads to destruction of large asphaltene associations, decrease of its molecular mass and transition of the system into a less ordered amorphous state decreasing the role of asphaltene framework in formation of viscous – plastic properties of the system.

When a certain limit of sulfur in asphaltene is achieved its introduction into their crystal structure is stopped and its excess quantity has practically no increasing effect even during strong energetic actions. Further increase of the quantity of sulfur added doesn't lead to its interaction with petroleum residue hydrocarbons, besides unbound sulfur will exist in a disperse state in the system.

So, interaction with elemental sulfur leads to the change of quantitative and qualitative characteristics of dispersive medium as well as of dispersed phase of petroleum residues explaining plastizing action of sulfur on them.

Independently of molecular state of sulfur in the moment of introduction further interaction takes place practically in a homogeneous (liquid) medium with formation of three forms of sulfur – dissolved, chemically bound and disperse. Quantitative distribution among them is determined by the quantity of sulfur introduced, chemical composition and nature of

petroleum residue as well as parameters of introduction regime. The character of distribution plays a decisive role on forming properties of sulfur – bitumen compositions and determine the technology of their preparing and usage to a great extent.

The features found out permit to select the technology and regimes of physical-chemical treatment of petroleum residues aimed at obtaining compositions with the characteristics needed.

References

1. Telyashev I.R., Obukhova S.A., Larionov S.L. Influence of elemental sulfur introduction on reological characteristics of petroleum residues. / Materials of the Congress of petroleum and gas refiners of Russia, section II: – Ufa, 2000. – P. 71-72.
2. Telyashev I.R., Davletshin A.R., Obukhova S.A. Study of interaction of heavy petroleum residues with elemental sulfur. / Neftepererabotka i neftekhimiya. – 2000. – №1. – P. 31-34.
3. Telyashev I.R., Obukhova S.A., Vezirov R.R., Telyashev E.G. Optimization of the process of elemental sulfur introduction in asphaltene structures of heavy petroleum residues. // Bashkirskii Khimicheskii Zhurnal. – 2000. – Vol. 7. – № 5. – P. 62-63.
4. Telyashev I.R., Obukhova S.A., Kut'in Ju.M., Telyashev E.G. Impact of interaction parameters on sulfur distribution in compositions with petroleum residues / Abstracts of XV International Conference on Chemical Reactors “Chemreactor-15”. – Helsinki, 2001. – P. 293-295.
5. Telyashev I.R., Obukhova S.A., Vezirov R.R., Telyashev E.G. Interaction Between Oil Dispersed System and Elemental Sulfur / Dynamics of Multiphase Systems. Proceedings of International Conference on Multiphase Systems. – Ufa, 2000. – P. 475-478.

DYNAMICS OF WATER SORPTION ON CONSOLIDATED LAYER “CaCl₂ IN ALUMINA”: NMR MICROSCOPY AND MODELLING

E.A. Ivanov¹, I.S. Glaznev¹, I.V. Koptug², Yu.I. Aristov¹

¹*Boriskov Institute of Catalysis, Pr. Lavrentieva 5, Novosibirsk, 630090 Russia*

²*International Tomography Centre, Novosibirsk, 630090 Russia*

Introduction

It is well known that diffusion in porous media strongly depends on pore configuration. For biporous solids the relative contribution of inter- and intraparticle diffusion resistances dictates the adsorption kinetics. Here we present the experimental results on kinetics of water sorption by consolidated layer (prepared with a binder) when water vapour is the only component in the gas phase that is typical, for instance, for adsorption heat pumps. The water transport and sorption were studied using ¹H NMR microimaging experiments on sorbed water spatial distribution in the sorbent layer and its temporal evolution. A crossover from the water transport limited by intraparticle (or bed) diffusion to that limited by the interparticle diffusion was found when the amount of the binder decreased from 20 wt.% to 2.5 wt.%. For quantitative description of the experimental data a mathematical model of the water transport and adsorption was developed.

Experimental

Consolidated SWS layers were prepared using Al₂O₃ powder (particle size between 0.25 and 0.5 mm) together with a binder (pseudoboehmite). In order to analyse the relative importance of the diffusional resistance in *macropores* between the adsorbent particles and in *mesopores* inside the particles (average size 7 nm), we varied the amount of the binder (2.5-20 wt.%). The alumina were moulded with the binder as a cylindrical tablet of 16 mm diameter and 6 mm thickness and then impregnated with an aqueous solution of CaCl₂. Salt content in the dry samples was 21.5 wt.%. Porous structure of the layer was determined by SEM, BET and mercury porosimetry.

¹H NMR microimaging experiments were performed at 300 MHz on an Avance NMR spectrometer equipped with the microimaging accessory. A sample was placed in the rf coil of the NMR probe with its axis oriented along the magnetic field of the superconducting

magnet, pumped down and connected to an evaporator to maintain a fixed vapour pressure over the sample during the water sorption process.

The sample holder allows the water adsorption only through the upper flat surface of the tablet.

Results and discussion

Mercury porosimetry experiments show that the volume of *macropores* or transport pores ($\geq 0.1 \mu\text{m}$) in the SWS layer decreases from $0.25 \text{ cm}^3/\text{g}$ down to $0.1 \text{ cm}^3/\text{g}$ with the binder content increase (Fig. 1). These pores correspond to the space between the primary adsorbent particles.

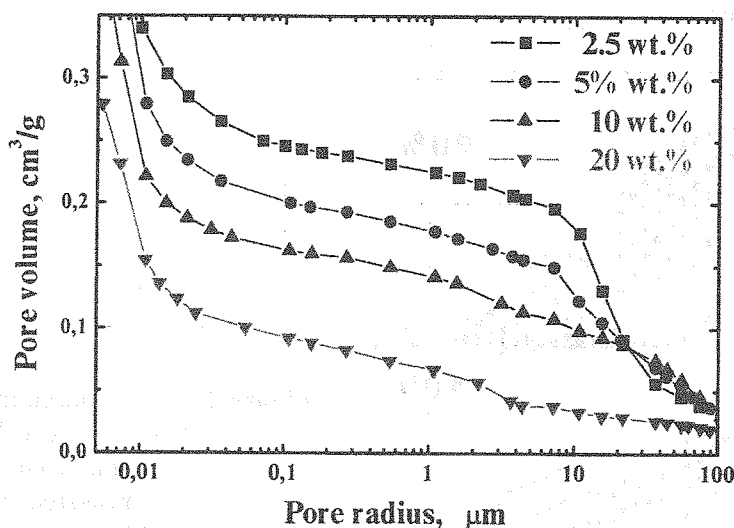


Figure 1. The total pore volume obtained by mercury porosimetry at various binder contents (2.5 – 20 wt.%).

The water distribution profiles at various binder contents (2.5, 10 and 20 wt.%) are presented in Fig. 2. The water adsorption becomes faster if the binder amount decreases due to the reduction of intraparticle diffusional resistance. Moreover, the crossover from the water transport limited by intraparticle (or bed) diffusion (at 20 wt.% of the binder) to that limited by the interparticle diffusion (at 2.5 wt.%) is clearly seen (Fig. 2). Intermediate behaviour was observed at 10 wt.% of the binder.

For quantitative description of the experimental data the following equations were used:

$$\varepsilon \frac{\partial C}{\partial t} = \varepsilon \frac{D}{L^2} \frac{\partial^2 C}{\partial x^2} - \rho R(C, Z), \quad C|_{t=0} = 0, \quad C|_{x=0} = C^f, \quad \left. \frac{\partial C}{\partial x} \right|_{x=L} = 0,$$

$$G \frac{\partial Z}{\partial t} = GR(C, Z), \quad Z|_{t=0} = 0,$$

where C is the water concentration in gas phase, Z is the sorbate concentration, ϵ is the layer voidage, L is the layer depth, D is the macropore diffusivity, ρ is the adsorbent density.

It is convenient to present the mass transfer rates in term of an effective mass transfer coefficient k , defined according to a linear driving force equation [1]:

$$R(C, Z) = ka(Z^* - Z),$$

where a is the external surface area per unit particle volume and Z^* is the equilibrium value of Z .

The appropriate dimensionless parameter characterizing the mass transfer is the Sherwood number, defined as $Sh = 2R_p k / D_p$, where R_p is the pellet radius, D_p is the diffusivity. It is known that the limiting value of Sherwood number for low Reynolds number flow is 2, and we have $k = D_p / R_p$.

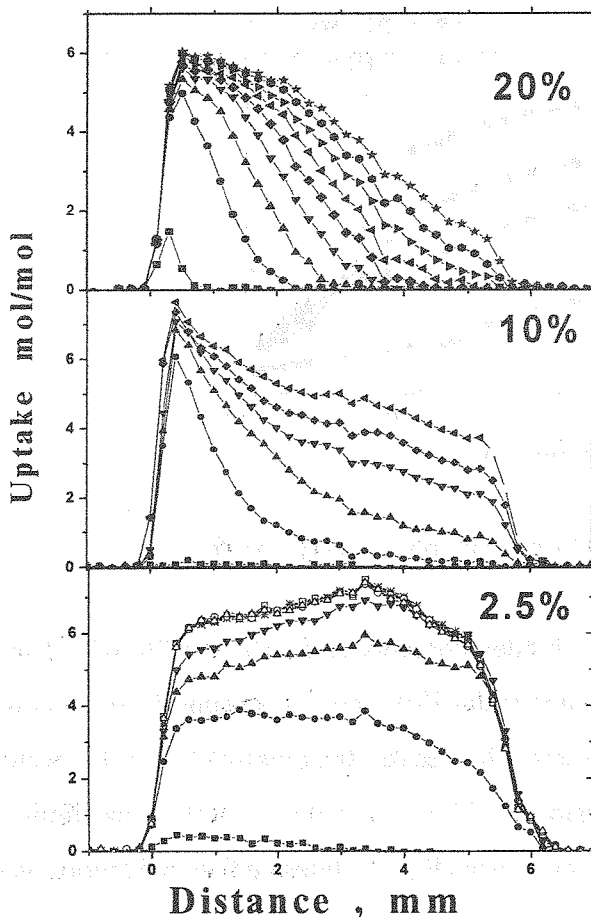


Figure 2. Water concentration profiles in the SWS layers at binder content 2.5, 10.0 and 20.0 wt.%. The profiles are measured every 86 min. First profile () is recorded at time 11 min. Water vapour pressure is 7.2 mbar.

The model described leads to a set of partial differential equations. The system was solved numerically with the method of lines, which reduces system to a set of ordinary differential equations (ODEs) with initial conditions. These ODEs were then solved using the numerical integration routine [2]. We used the semi-implicit Runge-Kutta methods for

integration of set of stiff equations with an integration step adaptation. Solving the model yields values for the water concentration at each bed grid point.

The model proposed appears to describe satisfactory our experimental data obtained for the interparticle diffusion regime, so that the experimental and calculated profiles of water spatial distribution are close (Fig. 3).

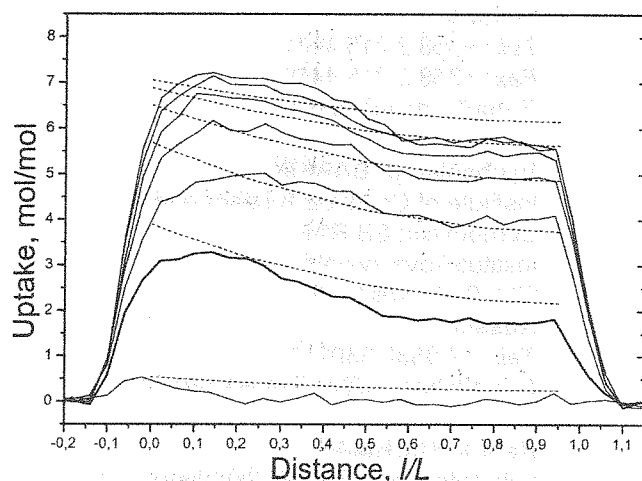


Figure 3. Experimental (solid) and calculated (dashed) water concentration profiles in the SWS layer with the binder content 5 wt.%. The profiles are measured every 86 min. Vapour pressure is 7.2 mbar. Modeling parameters: $D = 4 \text{ cm}^2/\text{s}$, $k = 1.5 \cdot 10^{-4} \text{ s}^{-1}$.

The model proposed can be used for further simulation of the kinetics of water sorption inside the SWS consolidated layer prepared with a binder under vacuum conditions. There are no mathematical simplifications needed, since numerical techniques have been used. It is further possible to increase the complexity of the diffusivity and equilibrium terms and still use numerical analysis. Comparison of simulations with experiments for the different SWS allows us to obtain the parameters of the model with various binder contents.

Acknowledgments. The authors thank the Russian Foundation for Basic Research (projects N 02-03-32304 and 02-03-32770), the Netherlands Organisation for Scientific Research (project 03-03-89014-NWO), the Integration Grant Program of the SB RAS (project N 166) and the NATO (grant PST.CLG.979051) for partial financial support of this work.

References

1. D.M. Ruthven: *Principles of Adsorption and Adsorption processes*. John Wiley & Sons, Inc, 1984.
2. J. Villadsen, M.L. Michelsen: *Solution of Differential Equation Models by Polynomial Approximation*. Prentice-Hall, Englewood Cliffs 1978.

List of participants (conference and exhibition)

Ruben ALDACO

Departamento de Ingenieria Quimica y
Quimica Inorganica, Universidad de Cantabria
Avda. Los Castros, s/n
39005 Santander
Spain
Tel.: 34 942 201588
Fax: 34 942 201590
E-mail: gareaa@unican.es

Tatiana N. ALEKSANDROVA

BIC Europe B.V.
Zijdweg 5a
2244 BC, Wassenaar
The Netherlands
Tel.: +31 70 514 49 26
Fax: +31 70 514 64 80
E-mail: taleksandrova@biceurope.com

Ekaterina ANANIEVA

Institute of Chemical Process Engineering
(CVT), University of Karlsruhe
Kaiserstr., 12
76131 Karlsruhe
Germany
Tel.: +49 721 608 4266
Fax: +49 721 6086118
E-mail: Ekaterina.Ananieva@ciw.uni-
karlsruhe.de

Vladimir I. ANIKEEV

Boreskov Institute of Catalysis SB RAS
pr. Akad. Lavrentieva, 5
630090 Novosibirsk
Russia
Tel.: +7 3832 397447
Fax: +7 3832 397447
E-mail: anik@catalysis.nsk.su

Alexander G. ANSHITS

Institute of Chemistry and Chemical
Technology SB RAS
Akademgorodok
660036 Krasnoyarsk
Russia
Tel.: +7 3912 439431
Fax: +7 3912 439342
E-mail: anshits@icct.ru

Oxana V. ARKHIPOVA

Institute of Petroleum Refining and
Petrochemistry AN RB
Iniciativnaya str., 12
450065 Ufa
Russia
Tel.: +7 3472 422471
Fax: +7 3472 422471
E-mail: vezirov@anrb.ru

Kalle ARVE

Laboratory of Industrial Chemistry
Åbo Akademi University
Biskopsgatan 8
20500 Turku
Finland
Tel.: +358 2 215 4431
Fax: +358 2 215 4479
E-mail: karve@abo.fi

Vyacheslav S. BABKIN

Institute of Chemical Kinetics and
Combustion SB RAS
Institutskaya avenue, 3
630090 Novosibirsk
Russia
Tel.: +7 3832 330217
E-mail: babkin@ns.kinetics.nsc.ru

Henrik BACKMAN

Laboratory of Industrial Chemistry
Åbo Akademi University
Biskopsgatan 8
20500 Turku
Finland
Fax: +358 2 215 4479
E-mail: Henrik.Backman@abo.fi

Alexander V. BALAEV

Institute of Petrochemistry and Catalysis
of Bashkir Academy of Science
pr. Oktaybrya, 141
450068 Ufa
Russia
Tel.: +7 3472 313544
Fax: +7 3472 312750
E-mail: irekmars@mail.ru

Viktor V. BARELKO

Institute of Problems of Chemical Physics RAS
142432 Chernogolovka
Russia
Tel.: +7 096 522 1817
Fax: +7 096 522 1260
E-mail: barelko@icp.ac.ru

Larissa V. BARYSHEVA

Boreskov Institute of Catalysis SB RAS
pr. Akad. Lavrentieva, 5
630090 Novosibirsk
Russia
Tel.: +7 3832 344901
Fax: +7 3832 341878
E-mail: barysheva@catalysis.nsk.su

Vadim V. BOGATOV
Institute of Chemical Problems
29, Husein Javid aven.
370143 Baku
Azerbaijan
Tel.: +994 12 39 4159
E-mail: vbogatov@yahoo.com

Anatoliy A. BOGUSHEVSKII
Russian Center of Science and Culture
Friedrichstrabe 176-179
10117 Berlin
Germany
Tel.: +49 30 20 30 2 250
Fax: +49 30 20 44 05 8
E-mail: info@russisches-haus.de

Hartmut BUCKA
Agrolinz Melamin International
St. Peter Str., 25
4021 Linz
Austria
Tel.: 0043 732 6914 3914
Fax: 0043 732 6914 6 3914
E-mail: hartmut.bucka@agrolinz.com

Valerii I. BYKOV
Krasnoyarsk State Technical University
Kirenskogo str., 26
660074 Krasnoyarsk
Russia
Tel.: +7 3912 497638
Fax: +7 3912 430692
E-mail: bykov@fivt.krasn.ru

Leonid A. BYKOV
JSC "Chemphys", IPChPh RAS
142432 Chernogolovka
Russia
Tel.: +7 096 522 1817
Fax: +7 096 522 1260
E-mail: lbik@chgnet.ru

Jean-Claude CHARPENTIER
Department of Chemical Engineering/CNRS
BP 2077 Villeurbanne cedex
France
Tel.: +33 4 72 43 1670
Fax: +33 4 72 43 1702
E-mail: charpentier@cpe.fr

Boris N. CHETVERUSHKIN
Institute of Mathematical Modelling RAS
Miusskaya pl., 4, build. A
125047 Moscow
Russia
Tel.: +7 095 972 1159
Fax: +7 095 250 7986
E-mail: chetver@imamod.ru

Maria S. CHINOVA
Topchiev Institute of Petrochemical Synthesis
RAS
Leninsky pr., 29
119991 Moscow
Russia
Tel.: +7 095 955 4176
Fax: +7 095 230 2224
E-mail: mushina@ips.ac.ru

Victor A. CHUMACHENKO
JSC "Katalizator"
Tikhaya str., 1
630052 Novosibirsk
Russia
Tel.: +7 3832 329445
Fax: +7 3832 332252
E-mail: vic@katcom.ru

Nataliya A. CHUMAKOVA
Borekov Institute of Catalysis SB RAS
pr. Akad. Lavrentieva, 5
630090 Novosibirsk
Russia
Tel.: +7 3832 341278
Fax: +7 3832 343056
E-mail: chum@catalysis.nsk.su

Natalia G. CHURBANOVA
Institute for Mathematical Modeling RAS
Miusskaya Sq., 4
125047 Moscow
Russia
Tel.: +7 095 973 0385
Fax: +7 095 972 0723
E-mail: nata@imamod.ru

Leonid B. DATSEVICH
University of Bayreuth
Universitätsstr. 30
D-95447 Bayreuth
Germany
Tel.: +49 921 55 7432
Fax: +49 921 55 74 35
E-mail: datsevich@uni-bayreuth.de

Wulf DIETRICH
University of Dortmund
Department of Biochemical and Chemical
Engineering
Emil-Figge-Str., 66
44227 Dortmund
Germany
Tel.: +49 231 755 2582
Fax: +49 231 755 2698
E-mail: wulf.dietrich@bci.uni-dortmund.de

Andrey V. DIMAKI
Institute of Strength Physics and Materials
Science SB RAS
Academicheskii pr., 2/1
634021 Tomsk
Russia
Tel.: +7 3822 258881
Fax: +7 3822 259576
E-mail: dav@usgroups.com

Nikolay M. DOBRYNKIN
Borekov Institute of Catalysis SB RAS
pr. Akad. Lavrentieva, 5
630090 Novosibirsk
Russia
Tel.: +7 3832 344491
Fax: +7 3832 341878
E-mail: dbn@catalysis.nsk.su

Victor G. DOROKHOV
Institute of Problems of Chemical Physics RAS
142432 Chernogolovka
Russia
Tel.: +7 096 522 1817
Fax: +7 096 522 1260
E-mail: vicd@icp.ac.ru

Viatcheslav G. DZYUBENKO
JSC STC "VLADIPOR"
Bolshaya Nizhegorodskaya, 77
600016 Vladimir
Russia
Tel.: +7 0922 276439
E-mail: Vladimir@memb.elcom.ru

Elmahboub Amer EDREDER
Petroleum Research Center - Tripoli-Libya
Gergarech - Tripoli
20 Tripoli
Libya
Tel.: +218 218 36821
Fax: +218 218 36820
E-mail: mahdred@hotmail.com

Gerhart EIGENBERGER
Stuttgart University
Boblinger Strabe, 72
70199 Stuttgart
Germany
Fax: +49 711 641 2242
E-mail: eigenberger@icvt.uni-stuttgart.de

Vladimir I. ELOKHIN
Borekov Institute of Catalysis SB RAS
pr. Akad. Lavrentieva, 5
630090 Novosibirsk
Russia
Tel.: +7 3832 344770
Fax: +7 3832 331055
E-mail: elokhin@catalysis.nsk.su

Anna A. FEDOROVA
Lomonosov Moscow State University
Lenynskie Gory
119899 Moscow
Russia
Tel.: +7 095 939 2870
Fax: +7 095 195 1224
E-mail: fedorova@inorg.chem.msu.ru

Pavel A. FOMIN
Lavrentiev Institute of Hydrodynamics SB RAS
pr. Akad. Lavrentieva, 15
630090 Novosibirsk
Russia
Tel.: +49 308 104 3456 (Germany)
Fax: +49 308 104 1227
E-mail: pavel_fomin@mail.ru

Sergei I. GALANOV
Tomsk State University
Lenin Ave., 36
634050 Tomsk
Russia
Tel.: +7 3832 420386
E-mail: galanov@xf.tsu.tomsk.su

Sergey A. GALUSHIN
Tomsk Politechnic University
Lenin ave., 30
634006 Tomsk
Russia
Tel.: +7 3822 563443
Fax: +7 3822 563435
E-mail: bird@tpu.ru

Vladimir V. GALVITA
Max-Planck-Institute Magdeburg
Sandtorstr. 1
39104 Magdeburg
Germany
E-mail: galvita@mpi-magdeburg.mpg.de

Regina R. GALYAUTDINOVA
Institute of Petrochemistry and Catalysis
of Bashkir Academy of Science
pr. Oktaybrya, 141
450068 Ufa
Russia
Tel.: +7 3472 313544
Fax: +7 3472 312750
E-mail: irekmars@mail.ru

Aurora GAREA
Departamento de Ingenieria Quimica y
Quimica Inorganica, Universidad de Cantabria
Avda. Los Castros, s/n
39005 Santander
Spain
Tel.: 34 942 201588
Fax: 34 942 201590
E-mail: gareaa@unican.es

Viktor GJELAJ

University of Tirana, Faculty of Natural
Sciences, Department of Chemistry
Str." Don Bosko", P.no. 326, Sh. no.1, Ap.no 9
Tirana

Albania

Tel.: + 355 4 378092/378093

Fax: + 355 4 261249/270753

E-mail: faculty_nat_scienc@hotmail.com

Alexei Yu. GLADKY

Boreskov Institute of Catalysis SB RAS
pr. Akad. Lavrentieva, 5
630090 Novosibirsk

Russia

Tel.: +7 3832 341771

Fax: +7 3832 343056

E-mail: gladky@catalysis.nsk.su

Irina M. GLIKINA

Eastern-Ukrainian National University,
Severodonetsk Technological Institute
Sovetskiy pr., 59-A
93400 Severodonetsk, Lugansk region

Ukraine

Tel.: 380 6452 34028

Fax: 380 6452 34028

E-mail: prin@ixt.lg.ua

Krzysztof Jan GOSIEWSKI

Pedagogical University of Czestochowa
ul. Klodnicka 14/37
44-100 Gliwice

Poland

Tel.: +48 32 2322835

Fax: +48 32 4010124

E-mail: gosiew@cidg.net.pl

Nellya G. GRIGORIEVA

Institute of Petrochemistry and Catalysis
of Bashkir Academy of Science
pr. Oktaybrya, 141
450068 Ufa

Russia

Tel.: +7 3472 313544

Fax: +7 3472 312750

E-mail: irekmars@mail.ru

Achim GRITSCH

Institute Für Chemische Verfahrenstechnik,
Universität Stuttgart
Böblinger Str. 72
70199 Stuttgart

Germany

Tel.: +49 711 641 2270

Fax: +49 711 641 2242

E-mail: gritsch@icvt.uni-stuttgart.de

Irek M. GUBAIDULIN

Institute of Petrochemistry and Catalysis
of Bashkir Academy of Science
pr. Oktaybrya, 141
450068 Ufa

Russia

Tel.: +7 3472 313544

Fax: +7 3472 312750

E-mail: irekmars@mail.ru

Valentin V. GUZEEV

FSUE "Kargin Institute of Polymer
Technologies"

606000 Dzerzhinsk

Russia

Tel.: +7 8313 255000

Fax: +7 8313 331318

E-mail: niip@kis.ru

Dashuri HADAJ

University of Tirana, Faculty of Natural
Sciences, Department of Chemistry
Str." Don Bosko", P.no. 326, Sh. no.1, Ap.no 9
Tirana

Albania

Tel.: + 355 4 378092/378093

Fax: + 355 4 261249/270753

E-mail: faculty_nat_scienc@hotmail.com

Ahmad HANIF

PERTAMINA UPSTREAM
Jl. Merdeka Timur No.6
14th Fl. Jakarta

Indonesia

Tel.: 62 21 352 1564

Fax: 62 21 350 8029

E-mail: ahanif@pertamina.com

Vladimir L. HARTMANN

JSC Novomoskovsk Institute of Nitrogen
Industry

Kirova str., 11

301650 Novomoskovsk

Russia

Tel.: +7 087 62 51 027

Fax: +7 087 62 34 364

E-mail: vhart@yandex.ru

Iraida IBADZADEH

Institute of Chemical Problems
Husseyyn Javid Ave., 29
370143 Baku

Azerbaijan

Tel.: +994 12 39 4159

E-mail: godsgivn@heart.baku.az

Valerij K. IKONNIKOV
FSUE Russian Scientific Center "Applied
Chemistry"
pr. Dobroljubova, 14
197198 St. Petersburg
Russia
Tel.: +7 812 238 9345
Fax: +7 812 238 9251
E-mail: ikon@smart.spb.ru

Abdul Jelil ILIYAS
King Fahd University of Petroleum & Minerals
966 Dhahran
Saudi Arabia
Tel.: +966 3 860 1924
Fax: +966 3 860 4234
E-mail: ajiliyas@kfupm.edu.sa

Evgueni G. IPPOLITOV
Kurnakov Institute of General & Inorganic
Chemistry RAS
Leninski pr., 31
119991 Moscow
Russia
Tel.: +7 095 236 3522
Fax: +7 095 954 1279
E-mail: ippolitov@igic.ras.ru

Zinfer R. ISMAGILOV
Boreskov Institute of Catalysis SB RAS
pr. Akad. Lavrentieva, 5
630090 Novosibirsk
Russia
Tel.: +7 3832 341219
Fax: +7 3832 397352
E-mail: zri@catalysis.nsk.su

Lyubov A. ISUPOVA
Boreskov Institute of Catalysis SB RAS
pr. Akad. Lavrentieva, 5
630090 Novosibirsk
Russia
Tel.: +7 3832 343763
Fax: +7 3832 343056
E-mail: isupova@catalysis.nsk.su

Sergey S. IVANCHEV
St. Petersburg Department of
the Boreskov Institute of
Catalysis SB RAS
pr. Dobroljubova, 14
197198 St. Petersburg
Russia
Tel.: +7 812 238 0890
Fax: +7 812 233 0002
E-mail: ivanchev@SM2270.spb.edu

Eugene A. IVANOV
Boreskov Institute of Catalysis SB RAS
pr. Akad. Lavrentieva, 5
630090 Novosibirsk
Russia
Tel.: +7 3832 397308
Fax: +7 3832 343056
E-mail: eugene@catalysis.nsk.su

Yuliya A. IVANOVA
Boreskov Institute of Catalysis SB RAS
pr. Akad. Lavrentieva, 5
630090 Novosibirsk
Russia
Tel.: +7 3832 341681
Fax: +7 3832 343056
E-mail: ivanova@catalysis.nsk.su

Viatcheslav V. KAFAROV
Universidad Industrial de Santander
Chemical Engineering Department
A.A. 678 Bucaramanga
Colombia
Fax: 57 76 350540
E-mail: kafarov@uis.edu.co

Vitaliy I. KARPENKO
Seversk State Technological Institute
Communisticheskii pr., 65
636036 Seversk
Russia
Fax: +7 382 779529
E-mail: karpenko_vita@mail.ru

Alexei KASIANOV
Institute of Petroleum Refining and
Petrochemistry AN RB
Iniciativnaya str., 12
450065 Ufa
Russia
E-mail: Vezirov@anrb.ru

Vladimir B. KAZANSKII
Zelinskii Institute of Organic Chemistry RAS
Lenin ave., 47
117913 Moscow
Russia
Tel.: +7 095 137 7400
Fax: +7 095 135 5328
E-mail: vbk@ioc.ac.ru

Sesegma T. KHANKHASAEVA
Baikal Institute of Nature Management
SB RAS
Sakhyanova str., 6
670047 Ulan-Ude
Russia
Tel.: +7 3012 433068
Fax: +7 3012 434753
E-mail: shan@binm.baikal.net

Vladimir D. KITLER
Tomsk Research Center, Department of
Structural Macrokinetics SB RAS
Akademicheskii pr., 10/3
634021 Tomsk
Russia
Tel.: +7 3822 259838
Fax: +7 3822 259838
E-mail: yurkova@fisman.tomsk.ru

Lioubov KIWI-MINSKER
Swiss Federal Institute of Technology,
Institute of Chemical Engineering LGRC /
EPFL
CH-1015 Lausanne
Switzerland
Tel.: +41 21 693 3182
Fax: +41 21 693 3190
E-mail: Lioubov.Kiwi-Minsker@epfl.ch

Evgueni KLEIMENOV
Fritz-Haber-Institut der Max-Planck-
Gesellschaft
Faradayweg 4-6
D-14195 Berlin
Germany
Tel.: +49 30 8413 4522
Fax: +49 30 8413 4401
E-mail: kleimen@fhi-berlin.mpg.de

Frank KLOSE
Max-Planck-Institute for Dynamics of Complex
Technical Systems Magdeburg
Sandtorstraße 1
D-39106 Magdeburg
Germany
Tel.: +49 391 6110 321
Fax: +49 391 6110 532
E-mail: klose@mpi-magdeburg.mpg.de

Alexey S. KNYAZEV
Institute of Petroleum Chemistry SB RAS
Akademicheskii pr., 3
634050 Tomsk
Russia
Tel.: +7 3822 258623
Fax: +7 3822 258350
E-mail: kas854@mail.ru

Nikolay I. KOLTSOV
Chuvash State University
Moskovskii pr., 15
428015 Cheboksary
Russia
Tel.: +7 8352 498792
Fax: +7 8352 428090
E-mail: koltsov@chuvsu.ru

Igor V. KOPTYUG
International Tomography Center SB RAS
Institutskaya str., 3A
630090 Novosibirsk
Russia
Tel.: +7 3832 333561
Fax: +7 3832 331399
E-mail: koptuyug@tomo.nsc.ru

Bashkim KORRIKU
University of Tirana, Faculty of Natural
Sciences, Department of Chemistry
Str." Don Bosko", P.no. 326, Sh. no.1,
Ap.no 9 Tirana
Albania
Tel.: + 355 4 378092/378093
Fax: + 355 4 261249/270753
E-mail: faculty_nat_scienc@hotmail.com

Tatiana L. KOULOVA
Frumkin Institute of Electrochemistry RAS
Leninsky pr., 31
119071 Moscow
Russia
Tel.: +7 095 955 4593
Fax: +7 095 952 0846
E-mail: tkulova@mail.ru

Roman A. KOZLOVSKIY
Mendeleev University of Chemical
Technology of Russia
Miusskaya sq., 9
125047 Moscow
Russia
Tel.: +7 095 978 9554
Fax: +7 095 978 9554
E-mail: kra@muctr.edu.ru

Anatoliy V. KRAVTSOV
Tomsk Politechnic University
Lenin ave., 30
634034 Tomsk
Russia
Tel.: +7 3822 563443
Fax: +7 3822 563435
E-mail: kravtsov@tpu.ru

Alexander KRONBERG
Twente University
P.O. Box 217
7500 AE Enschede
The Netherlands
Tel.: +31 53 489 1088
Fax: +31 53 489 2882
E-mail: a.e.kronberg@ct.utwente.nl

Igor V. KUCHIN
Institute of Coal and Coal Chemistry
SB RAS
Rukavishnikova str., 21
650099 Kemerovo
Russia
Tel.: +7 3842 365561
Fax: +7 3842 281838
E-mail: Stefoglo@yandex.ru

J.A.M. KUIPERS
University of Twente
P.O. box 217
7500 AE Enschede
The Netherlands
Tel.: +31 53 489 3039
Fax: +31 53 489 2882
E-mail: J.A.M.Kuipers@utwente.nl

Vitalina V. KUKUEVA
Fire Safety Institute
Onoprienko str., 8
18034 Cherkassy
Ukraine
Tel.: 380 472 456157
Fax: 380 472 456157
E-mail: kukueva@yahoo.com

Sergey M. KULIKOV
Karl Winnacker Institut der DECHEMA
Theodor-Heuss-Allee 25
60486 Frankfurt/M
Germany
Tel.: +49 069 7564 309
E-mail: smkulikov@hotmail.com

Irina A. KURZINA
Tomsk State University of Architecture
and Building,
Department of Chemistry
Solyanaya sq., 2
634003 Tomsk
Russia
Tel.: +7 382 2 65 42 65
Fax: +7 382 2 75 33 62
E-mail: kurzina99@mail.ru

Andrey V. KUSTOV
Mendeleev University of Chemical
Technology of Russia
Miusskaya sq., 9
125047 Moscow
Russia
Tel.: +7 095 978 9589
Fax: +7 095 973 3136
E-mail: shvets@muctr.edu.ru

Raisa I. KUZMINA
Saratov State University
Astrakhanskaya, 83, bldg 1
410026 Saratov
Russia
Tel.: +7 8452 525007
Fax: +7 8452 271491
E-mail: kuzminaraisa@mail.ru

Evgenii E. LEVCHENKO
Russian Center of International Scientific and
Cultural Cooperation of Ministry
of Foreign Affairs RF
Vozdvizhenka, 14
101999 Moscow
Russia
Tel.: +7 095 290 1550
Fax: +7 095 200 1209

Oleg I. LOMOVSKII
Institute of Solid State Chemistry and
Mechanochemistry SB RAS
Kutateladze str., 18
630128 Novosibirsk
Russia
Tel.: +7 3832 320657
Fax: +7 3832 320657
E-mail: lomov@solid.nsc.ru

Boris N. LUKYANOV
Borekov Institute of Catalysis SB RAS
pr. Akad. Lavrentieva, 5
630090 Novosibirsk
Russia
Tel.: +7 3832 343210
Fax: +7 3832 341187
E-mail: lukjanov@catalysis.nsk.su

Oktyabrina A. LUZHETSKAYA
Exhibition Center SB RAS
pr. Akad. Lavrentieva, 17
630090 Novosibirsk
Russia
Tel.: +7 3832 303740
Fax: +7 3832 303740
E-mail: expo@ad-sbras.nsc.ru

Lev L. MAKARSHIN
Borekov Institute of Catalysis SB RAS
pr. Akad. Lavrentieva 5
630090 Novosibirsk
Russia
Tel.: +7 3832 342831
Fax: +7 3832 343056
E-mail: makarshin@catalysis.nsk.su

Michael MANGOLD

Max-Planck-Institut fuer Dynamik komplexer
technischer Systeme
Sandtorstrasse 1
39106 Magdeburg

Germany

Tel.: +49 391 6110 361

Fax: +49 391 6110 513

E-mail: mangold@mpi-magdeburg.mpg.de

Alexander V. MISCHENKO

Institute on Inorganic Chemistry SB RAS
pr. Akad. Lavrentieva, 3
630090 Novosibirsk

Russia

Tel.: +7 3832 344877

Fax: +7 3832 344489

E-mail: am@che.nsk.su

Ilya I. MOISEEV

Kurnakov Institute of General and
Inorganic Chemistry RAS
Lenin ave., 31
117907 Moscow

Russia

Tel.: +7 095 952 1203

Fax: +7 095 954 1279

E-mail: iimois@igic.ras.ru

Vladimir A. MOZGUNOV

Mendeleev University of Chemical
Technology of Russia
Miuskaya sq., 9
125047 Moscow

Russia

Tel.: +7 095 978 6589

Fax: +7 095 200 4204

E-mail: v-mozgunov@yandex.ru

Andreas MUELLER

Institut fur Mikrotechnik Mainz GmbH
Carl-Zeiss-Str. 18-20
D-55129 Mainz

Germany

Tel.: +49 6131 990 377

Fax: +49 6131 990 205

E-mail: muellera@imm-mainz.de

Dmitriy A. MUKHORTOV

FSUE Russian Scientific Center "Applied
Chemistry"
pr. Dobrolubova, 14
197198 St. Petersburg

Russia

Tel.: +7 812 103 0406

Fax: +7 812 103 0406

E-mail: pdsac@peterlink.ru

Dmitry Yu. MURZIN

Laboratory of Industrial Chemistry
Åbo Akademi University
Biskopsgatan 8
20500 Turku

Finland

Tel.: +358 22 154985

Fax: +358 22 154479

E-mail: dmurzin@abo.fi

Vladislav M. MYSOV

Scientific-Engineering Center "Zeosit" SB RAS
pr. Akad. Lavrentieva, 5
630090 Novosibirsk

Russia

Tel.: +7 3832 396251

Fax: +7 3832 396251

E-mail: mysov@batman.sm.nsk.ru

Gernot NELL

Frankfurt/Main (Parr Instrument
(Deutschland) GmbH)
Rosskopfstrasse 25
60489 Frankfurt

Germany

Tel.: +49 69 571058

Fax: +49 69 5870300

E-mail: gernot@parrinst.de

Olga V. NETSKINA

Boreskov Institute of Catalysis SB RAS
pr. Akad. Lavrentieva, 5
630090 Novosibirsk

Russia

Tel.: +7 3832 342691

Fax: +7 3832 342336

E-mail: netskina@catalysis.nsk.su

Alexander S. NOSKOV

Boreskov Institute of Catalysis SB RAS
pr. Akad. Lavrentieva, 5
630090 Novosibirsk

Russia

Tel.: +7 3832 341878

Fax: +7 3832 341878

E-mail: noskov@catalysis.nsk.su

Svetlana A. OBUKHOVA

Institute of Petroleum Refining and
Petrochemistry AN RB
Iniciativnaya str., 12
450065 Ufa

Russia

Tel.: +7 3472 422471

Fax: +7 3472 422471

E-mail: vezirov@anrb.ru

Ammar Almaraid OMER

High Technical Institute

Main Street

733 Sirte

Libya

Tel.: 00218 54 66210**Fax:** 00218 54 64790**E-mail:** abany2003@hotmail.com**Nickolay M. OSTROVSKII**

AD Hemijska Industrija HIPOL

Industrijska zona

25250 Odzaci

Jugoslavija

Tel.: 381 25 743 221**Fax:** 381 25 743 191**E-mail:** ostrovski@hipol.com**Zinaida P. PAI**

Boreskov Institute of Catalysis SB RAS

pr. Akad. Lavrentieva, 5

630090 Novosibirsk

Russia

Tel.: +7 3832 397264**Fax:** +7 3832 343056**E-mail:** zpai@catalysis.nsk.su**Yulya R. PAK**

Novosibirsk State University,

Boreskov Institute of Catalysis SB RAS

pr. Akad. Lavrentieva 5

630090 Novosibirsk

Russia

Fax: +7 3832 343056**E-mail:** g.g.volkova@catalysis.nsk.su**Valentin N. PARMON**

Boreskov Institute of Catalysis SB RAS

pr. Akad. Lavrentieva, 5

630090 Novosibirsk

Russia

Tel.: +7 3832 343269**Fax:** +7 3832 343269**E-mail:** parmon@catalysis.nsk.su**Dmitry S. PASHKEVICH**FSUE Russian Scientific Center "Applied
Chemistry"

14, Dobrolubov ave.

197198 St. Petersburg

Russia

Tel.: +7 812 103 0406**Fax:** +7 812 103 0406**E-mail:** pdsac@peterlink.ru**Edison S. PATMAR**

Chuvash State University

Moskovskii pr., 15

429900 Cheboksary

Russia

Tel.: +7 835 2 49 87 38**Fax:** +7 835 2 42 80 90**E-mail:** edi@chuvsu.ru**Ivan E. PENNER**

Institute of Optics of Atmosphere SB RAS

pr. Akademicheskii, 10/3

634055 Tomsk

Russia

Tel.: +7 3822 259875**E-mail:** penner@iao.ru**Ludmila N. PEREPECHKO**

Kutateladze Institute of Thermophysics

SB RAS

pr. Akad. Lavrentieva, 1

630090 Novosibirsk

Russia

Tel.: +7 3832 396572**Fax:** +7 3832 343480**E-mail:** io@itp.nsc.ru**Alexey N. PESTRYAKOV**

Tomsk Polytechnic University

Lenin ave., 30

634050 Tomsk

Russia

Tel.: +7 3822 415861**Fax:** +7 3822 520808**E-mail:** anp@tspace.ru**Igor F. PIMENOV**

Chemical-Technological Center

Efremova str., 10

119048 Moscow

Russia

Tel.: +7 095 242 9949**Fax:** +7 095 248 8779**E-mail:** info@chemcenter.ru**Vitaly N. PISARENKO**Mendeleev University of Chemical
Technology of Russia

Miusskaya sq., 9

125047 Moscow

Russia

Tel.: +7 095 978 6589**Fax:** +7 095 200 4204**E-mail:** pvn@muctr.edu.ru

Elena V. PISARENKO
Mendeleyev University of Chemical
Technology of Russia
Miuskaya sq., 9
125047 Moscow
Russia
Tel.: +7 095 978 6589
Fax: +7 095 200 4204
E-mail: evpisarenko@mail.ru

Irina V. PIVOVAROVA
Boreskov Institute of Catalysis SB RAS
pr. Akad. Lavrentieva, 5
630090 Novosibirsk
Russia
Tel.: +7 3832 341878
Fax: +7 3832 341878
E-mail: noskov@catalysis.nsk.su

Alexei V. PODSHIVALIN
Institute of Petroleum Refining and
Petrochemistry AN RB
Iniciativnaya str., 12
450065 Ufa
Russia
Tel.: +7 3472 422471
Fax: +7 3472 422471
E-mail: podshivalin@anrb.ru

Svetlana A. POKROVSKAYA
Boreskov Institute of Catalysis SB RAS
pr. Akad. Lavrentieva, 5
630090 Novosibirsk
Russia
Tel.: +7 3832 341278
Fax: +7 3832 343056
E-mail: pokrov@catalysis.nsk.su

Oleg I. POTATURKIN
Institute of Automatics and Electrometry
SB RAS
pr. Akad. Koptiyuga, 1
630090 Novosibirsk
Russia
Tel.: +7 3832 344033
Fax: +7 3832 333863
E-mail: potaturkin@iae.nsk.su

Mohammad RAHMANI
School of Bioscience and Process Technology,
Vaxjo University
Vejdes Plat 6
SE - 351 9 Vaxjo
Sweden
Tel.: +46 470 70 8831
Fax: +46 470 70 8756
E-mail: Mohammad.Rahmani@ibp.vxu.se

Medisetti Venkata RAMAKRISHNA
Ranbaxy Research Laboratories Ltd
122001 Gurgaon
India
Tel.: 91 124 2342001 10
Fax: 91 124 234 3545
E-mail: ramakrishna.venkata@ranbaxy.com

Andreas REITZMANN
Institute of Chemical Process Engineering
(CVT), University of Karlsruhe
Kaiserstr., 12
76131 Karlsruhe
Germany
Tel.: +49 721 608 4266
Fax: +49 721 608 6118
E-mail: andreas.reitzmann@ciw.uni-
karlsruhe.de

Vladimir A. REMNYEV
Boreskov Institute of Catalysis SB RAS
pr. Akad. Lavrentieva, 5
630090 Novosibirsk
Russia
Tel.: +7 3832 343846
Fax: +7 3832 343056
E-mail: remnyov@catalysis.nsk.su

Sergey I. RESHETNIKOV
Boreskov Institute of Catalysis SB RAS
pr. Akad. Lavrentieva, 5
630090 Novosibirsk
Russia
Tel.: +7 3832 331618
Fax: +7 3832 343056
E-mail: resh@catalysis.nsk.su

Liisa RIHKO-STRUCKMANN
Max Planck Institute for Dynamics of Complex
Technical Systems
Sandtorstrasse, 1
D-39106 Magdeburg
Germany
Tel.: +49 391 611 0318
Fax: +49 391 611 0353
E-mail: rihko@mpi-magdeburg.mpg.de

Natalia Yu. ROMANYUKHA
Institute for Mathematical Modeling RAS
Miuskaya Sq., 4
125047 Moscow
Russia
Tel.: +7 095 250 7910
Fax: +7 095 972 0723
E-mail: rona@imamod.ru

Gunther RUPPRECHTER

Fritz Haber Institute of MPG
Faradayweg 4-6
14195 Berlin

Germany

Tel.: +49 30 8413 4132

Fax: +49 30 8413 4105

E-mail: ruppachter@fhi-berlin.mpg.de

Vladimir Yu. RYZHKIN

FSUE Russian Scientific Center "Applied
Chemistry"

pr. Dobroljubova, 14
197198 St. Petersburg

Russia

Tel.: +7 812 238 9345

Fax: +7 812 238 9251

E-mail: ikon@smart.spb.ru

Svetlana S. SAFRONOVA

Tomsk State University

Lenin Ave., 36
634050 Tomsk

Russia

Tel.: +7 3822 423944

E-mail: sweta_ss@freemail.ru

Matoi SAKAMOTO

ISTC

Luganskaya str., 9
115516 Moscow

Russia

Tel.: +7 095 797 6045

Fax: +7 095 797 6014

E-mail: sakamoto@istc.ru

Alexei A. SALAMACHIN

Russian Center of Science and Culture

Friedrichstrabe 176-179
10117 Berlin

Germany

Tel.: +49 30 20 30 2 250

Fax: +49 30 20 44 05 8

E-mail: info@russisches-haus.de

Elhadi Eidabah SALEM MOHAMED

Petroleum Research Center - Tripoli-Libya

Gergarech -Tripoli
20 Tripoli

Libya

Tel.: +218 218 36821

Fax: +218 218 36820

E-mail: mahdred@hotmail.com

Steffen SCHIRRMEISTER

Research&Development,
Technology Management
Friedrich-Uhde-Strasse 15
44141 Dortmund

Germany

Tel.: +49 231 547 3265

Fax: +49 231 547 2938

E-mail: SchirrmeisterS@tkf-

uhde.thyssenkrupp.com

Klaus SCHÖFFEL

Norsk Hydro ASA Research Ctr Porsgrunn

N-3901 Porsgrunn

P.O. Box 2560

N-3901 PORSGRUNN

NORWAY

Tel.: +47 3592 4076

Fax: +47 3592 4738

E-mail: Klaus.Schoffel@hydro.com

Christian SCHRADER

Institut fuer Physikalische und Theoretische
Chemie -Abteilung Laserchemie

Hans-Sommer-Strasse 10

38106 Braunschweig

Germany

Tel.: +49 531 391 5345

Fax: +49 531 391 5396

E-mail: Ch.Schrader@tu-bs.de

Nataliya L. SEMENDYAEVA

Lomonosov Moscow State University

Lenynskie Gory

119899 Moscow

Russia

Tel.: +7 095 939 4079

Fax: +7 095 939 2596

E-mail: NatalyS@cs.msu.su

Sergey I. SERDYUKOV

Moscow State University

Leninskie Gory

119899 Moscow

Russia

Tel.: +7 095 939 4649

Fax: +7 095 939 2158

E-mail: serdkv@tech.chem.msu.ru

Fakhry SEYEDEYN-AZAD

University of Isfahan

Hezar Jerib Ave.

81744 Isfahan

Iran

Tel.: 0098 311 7932688

Fax: 0098 311 6682887

E-mail: fsazad@eng.ui.ac.ir

Valeriy F. SHVETS
Mendeleyev University of Chemical
Technology of Russia
Miusskaya Sq., 9
125047 Moscow
Russia
Tel.: +7 095 978 9589
Fax: +7 095 978 9554
E-mail: shvets@muctr.edu.ru

Georgii M. SIDOROV
Ufa State Oil Technical University
Kosmonavtov str., 1
450062 Ufa
Russia
Tel.: +7 3472 529742
Fax: +7 3472 529742

Valentina I. SIMAGINA
Borekov Institute of Catalysis SB RAS
pr. Akad. Lavrentieva, 5
630090 Novosibirsk
Russia
Tel.: +7 3832 342336
Fax: +7 3832 342336
E-mail: simagina@catalysis.nsk.su

Alexandre M. SKUNDIN
Frumkin Institute of Electrochemistry RAS
Leninsky prosp., 31
119071 Moscow
Russia
Tel.: +7 095 955 4020
Fax: +7 095 952 0846
E-mail: skundin@gol.ru

Artyom A. SLEPTEREV
Omsk Department of the Borekov Institute of
Catalysis SB RAS
Neftezavodskaya str., 54
644040 Omsk
Russia
Tel.: +7 3812 662275
Fax: +7 3812 646156
E-mail: tsyr@mail.ru

Oleg V. SMETANNIKOV
Topchiev Institute of Petrochemical
Synthesis RAS
Leninsky pr., 29
119991 Moscow
Russia
Tel.: +7 095 955 4176
Fax: +7 095 230 2224
E-mail: mushina@ips.ac.ru

Galina P. SNYTIKOVA
Scientific-Engineering Center "Zeosil" SB RAS
pr. Akad. Lavrentieva, 5
630090 Novosibirsk
Russia
Tel.: +7 3832 396251
Fax: +7 3832 396251
E-mail: galas@batman.sm.nsc.ru

Tatiana V. SOKOLOVA
Tomsk State University
Novo-Sobornaya Sq., 1
634050 Tomsk
Russia
Tel.: +7 3822 533426
Fax: +7 3822 533034
E-mail: sokolova@phys.tsu.ru

Alexander A. SOLOVYANOV
JSC GAZPROM
Nametkina str., 16
117997 Moscow
Russia
Tel.: +7 095 719 4681
Fax: +7 095 719 2751
E-mail: A.Solovianov@adm.gazprom.ru

Alexey A. SPIRIDONOV
Borekov Institute of Catalysis SB RAS
pr. Akad. Lavrentieva, 5
630090 Novosibirsk
Russia
Tel.: +7 3832 397309
Fax: +7 3832 343056
E-mail: spiridonov@catalysis.nsk.su

Semyen I. SPIVAK
Bashkir State University
Frunze str., 32
450074 Ufa
Russia
Tel.: +7 3472 236162
Fax: +7 3472 236680
E-mail: s.spivak@bashnet.ru

Dmitry V. STAROVEROV
Mendeleyev University of Chemical
Technology of Russia
Miusskaya Sq., 9
125047 Moscow
Russia
Tel.: +7 095 978 9554
Fax: +7 095 973 3136
E-mail: stardv@ppty.ru

Evgeni F. STEFOGLO
Institute of Coal and Coal Chemistry SB RAS
Rukavishnikova str., 21
650099 Kemerovo
Russia
Tel.: +7 3842 365561
Fax: +7 3842 281838
E-mail: Stefoglo@yandex.ru

Pavel A. STOROZHENKO
Institute of Chemistry and Technology of
Elemento-Organic Compounds
Vavilova str., 28
117813 Moscow
Russia
Tel.: +7 095 273 1136
E-mail: ecos@ecos.incitrade.ru

Thomas SUHARTANTO
PERTAMINA UPSTREAM
Jl. Merdeka Timur No.6
14th Fl. Jakarta
Indonesia
Fax: 62 21 3508021
E-mail: tsuhartanto@pertamina.com

Valentina I. SUKHODOLOVA
Samoilov Institute of Fertilizers and
Insectofungicides
Leninskii pr., 55
117919 Moscow
Russia
Tel.: +7 095 312 0025
E-mail: niuif@fertilizers.ru

Yury Yu. TANASHEV
Borekov Institute of Catalysis SB RAS
pr. Akad. Lavrentieva, 5
630090 Novosibirsk
Russia
Tel.: +7 3832 342831
Fax: +7 3832 343056
E-mail: tanashev@catalysis.nsk.su

Lumturie TEP SHI
University of Tirana, Faculty of Natural
Sciences, Department of Chemistry
Str. "Don Bosko", P.no. 326, Sh. no.1, Ap.no 9
Tirana
Albania
Tel.: + 355 4 378092/378093
Fax: + 355 4 261249/270753
E-mail: faculty_nat_scienc@hotmail.com

Johan H. TERWEL
BIC Europe B.V.
Zijde weg 5a
2244 BC, Wassenaar
The Netherlands
Tel.: +31 70 514 4926
Fax: +31 70 514 6480
E-mail: info@biceurope.com

Oleg A. TRUBACHEV
JSC Rikom SPb
Piskarjevskij pr., 63, of.308
195273 St.Petersburg
Russia
Tel.: +7 812 320 1626
Fax: +7 812 249 7833
E-mail: trubachev@ricomspb.ru

Said F. URMANCHEEV
Institute of Mechanics,
Ufa Scientific Center RAS
Karl Marx Str., 12, building 6
450000 Ufa
Russia
Tel.: +7 3472 230878
Fax: +7 3472 230878
E-mail: said@anrb.ru

Hubert J. VERINGA
ECN/BIC Europe B.V.
ECN, Westërduinweg 3
1755 LE Petten
The Netherlands
Tel.: +31 224 564628
Fax: +31 224 568487
E-mail: veringa@ecn.nl

Rustem R. VEZIROV
Institute of Petroleum Refining and
Petrochemistry AN RB
Iniciativnaya str., 12
450062 Ufa
Russia
Tel.: +7 3472 422471
Fax: +7 3472 422471
E-mail: vezirov@anrb.ru

Alexander V. VOSMERIKOV
Institute of Petroleum Chemistry SB RAS
Akademicheskii pr., 3
634021 Tomsk
Russia
Tel.: +7 3822 258021
Fax: +7 3822 258457
E-mail: pika@ipc.tsc.ru

Krzysztof WARMUZINSKI

Institute of Chemical Engineering, Polish
Academy of Sciences
ul. Bałtycka, 5
44-100 Gliwice

Poland

Tel.: +48 32 231 0318

Fax: +48 32 231 0318

E-mail: kwarmuz@iich.gliwice.pl

Gregor F. W. WILLE

CPC-Systems GmbH
Hanauer Landstr. 526, G 58 III
60434 Frankfurt/Main

Germany

Tel.: +49 69 4109 2749

Fax: +49 69 4109 2322

E-mail: wille@cpc-net.com

Ilguzar A. YAKUSHEV

JSC TATNEFTEKHIMINVEST-HOLDING
Ershova str., 29

420045 Kazan, Tatarstan

Russia

Tel.: +7 843 2 724305

Fax: +7 843 2 764304

E-mail: jakushev@tnhi.bancorp.ru

Andrey N. ZAGORUIKO

Boreskov Institute of Catalysis SB RAS
pr. Akad. Lavrentieva, 5
630090 Novosibirsk

Russia

Tel.: +7 3832 344491

Fax: +7 3832 341878

E-mail: zagor@catalysis.nsk.su

Sergey P. ZAKOVRYASHIN

Presidium SB RAS
pr. Akad. Lavrentyeva, 17
630090 Novosibirsk

Russia

Tel.: +7 3832 301956

Fax: +7 3832 342852

E-mail: zakov@sbras.nsc.ru

Tatiana V. ZAMULINA

Boreskov Institute of Catalysis SB RAS
pr. Akad. Lavrentieva, 5
630090 Novosibirsk

Russia

Tel.: +7 3832 341297

Fax: +7 3832 343056

E-mail: zam@catalysis.nsk.su

Xiaohui ZHANG

University of Dortmund
Department of Biochemical and
Chemical Engineering
Emil-Figge-Str., 66
44227 Dortmund

Germany

Tel.: +49 231 755 2582

Fax: +49 231 755 2698

E-mail: xiaohui.zhang@bci.uni-dortmund.de

Tatiana E. ZHUKOVA

Ministry of Industry,
Science and Technologies
Tverskaya str., 11

103906 Moscow

Russia

Tel.: +7 095229 75 87

Ilya A. ZOLOTARSKII

Boreskov Institute of Catalysis SB RAS
pr. Akad. Lavrentieva, 5
630090 Novosibirsk

Russia

Tel.: +7 3832 344491

Fax: +7 3832 341878

E-mail: zol@catalysis.nsk.su

AUTHOR INDEX*

Ruben ALDACO	241	Irina M. GLIKINA	171
Ekaterina ANANIEVA	97	Krzysztof Jan GOSIEWSKI	235
Vladimir I. ANIKEEV	133	Nellya G. GRIGORIEVA	305, 308
Oxana V. ARKHIPOVA	403	Irek M. GUBAIDULIN	305, 308
Kalle ARVE	39	Ahmad HANIF	250
Vyacheslav S. BABKIN	260	Vladimir L. HARTMANN	253
Henrik BACKMAN	257	Iraida IBADZADEH	284, 312
Alexander V. BALAEV	305, 308	Valerij K. IKONNIKOV	225
Viktor V. BARELKO	274, 275, 279	Abdul Jelil ILIJAS	58
Larissa V. BARYSHEVA	173	Evgueni G. IPPOLITOV	313
Vadim V. BOGATOV	284	Zinfer R. ISMAGILOV	175
Hartmut BUCKA	253	Lyubov A. ISUPOVA	74
Valerii I. BYKOV	286	Sergey S. IVANCHEV	111
Leonid A. BYKOV	274	Eugene A. IVANOV	426
Jean-Claude CHARPENTIER	23	Yuliya A. IVANOVA	356
Boris N. CHETVERUSHKIN	184, 294	Viatcheslav V. KAFAROV	104, 129
Maria S. CHINOVA	335, 336	Vitaliy I. KARPENKO	314
Nataliya A. CHUMAKOVA	266, 290	Alexei KASIANOV	344, 345
Natalia G. CHURBANOVA	184, 294	Vladimir B. KAZANSKII	90
Leonid B. DATSEVICH	35, 101	Sesegma T. KHANKHASAEVA	418
Wulf DIETRICH	43	Liubov KIWI-MINSKER	29, 47
Andrey V. DIMAKI	159	Evgueni KLEIMENOV	318
Nikolay M. DOBRYNKIN	262	Frank KLOSE	151
Victor G. DOROKHOV	279	Alexey S. KNYAZEV	86
Elmahboub Amer EDREDER	103	Nikolay I. KOLTSOV	414, 420
Gerhart EIGENBERGER	8	Igor V. KOPTYUG	15
Vladimir I. ELOKHIN	54, 321	Tatiana L. KOULOVA	376
Anna A. FEDOROVA	337	Roman A. KOZLOVSKIY	118
Pavel A. FOMIN	188	Anatoliy V. KRAVTSOV	229, 325
Sergei I. GALANOV	298	Alexander KRONBERG	147
Sergey A. GALUSHIN	229, 325	Igor V. KUCHIN	137, 141
Vladimir V. GALVITA	302	J.A.M. KUIPERS	10, 147
Regina R. GALYAUTDINOVA	305, 308	Vitalina V. KUKUEVA	329
Aurora GAREA	239	Sergey M. KULIKOV	209
Alexei Yu. GLADKY	80	Irina A. KURZINA	70

Andrey V. KUSTOV	118	Sergey I. SERDYUKOV	375
Raisa I. KUZMINA	331	Fakhry SEYEDEYN-AZAD	245
Boris N. LUKYANOV	218	Valeriy F. SHVETS	118, 378
Lev L. MAKARSHIN	271	Georgii M. SIDOROV	331
Michael MANGOLD	107	Valentina I. SIMAGINA	113
Ilya I. MOISEEV	33	Alexandre M. SKUNDIN	376
Andreas MUELLER	179	Artyom A. SLEPTEREV	407
Dmitriy A. MUKHORTOV	35, 125	Oleg V. SMETANNIKOV	335, 336
Dmitry Yu. MURZIN	39, 257	Tatiana V. SOKOLOVA	412
Vladislav M. MYSOV	221	Semyen I. SPIVAK	210
Olga V. NETSKINA	113	Dmitry V. STAROVEROV	378
Alexander S. NOSKOV	262, 266	Evgeni F. STEFOGLO	137, 141
Svetlana A. OBUKHOVA	341, 348, 352	Thomas SUHARTANTO	250
Ammar Almaraid OMER	217	Yury Yu. TANASHEV	364
Nickolay M. OSTROVSKII	62, 82	Oleg A. TRUBACHEV	225
Zinaida P. PAI	117	Said F. URMANCHEEV	66
Yulya R. PAK	384	Rustem R. VEZIROV	348, 352, 380, 423
Valentin N. PARMON	7, 271, 364	Alexander V. VOSMERIKOV	391
Dmitry S. PASHKEVICH	121, 125	Gregor F. W. WILLE	192
Edison S. PATMAR	420	Andrey N. ZAGORUIKO	202, 395, 399
Alexey N. PESTRYAKOV	360, 318	Xiaohui ZHANG	51
Vitaly N. PISARENKO	166, 168	Ilya A. ZOLOTARSKII	198, 356
Elena V. PISARENKO	156, 166, 168		
Alexei V. PODSHIVALIN	66, 368, 403		
Svetlana A. POKROVSKAYA	198		
Mohammad RAHMANI	246		
Andreas REITZMANN	97		
Sergey I. RESHETNIKOV	47, 82, 221, 388		
Liisa RIHKO-STRUCKMANN	162		
Natalia Yu. ROMANYUKHA	184		
Gunther RUPPRECHTER	205		
Vladimir Yu. RYZHKIN	225		
Svetlana S. SAFRONOVA	410		
Elhadi Eldabah SALEM MOHAMED	103		
Christian SCHRADER	371		
Nataliya L. SEMENDYAEVA	112		

* Only conference participants are included into this index.

CONTENT

Plenary lectures

PL-1

Valentin N. Parmon

NEW WAYS OF PRODUCTION AND UTILIZATION OF N_2O 7

PL-2

Grigorios Kolios, Gerhart Eigenberger

AUTOTHERMAL REACTOR CONCEPTS FOR THE ENERGY-EFFICIENT
COUPLING OF ENDO- AND EXOTHERMIC REACTIONS..... 8

PL-3

M. van Sint Annaland, J. Smit, U. Kuerten, S.A.R.K. Deshmukh, J.A.M. Kuipers

DEVELOPMENT AND MODELLING OF MEMBRANE REACTORS..... 10

PL-4

Igor V. Koptug

NMR IMAGING: A POWERFUL TOOLKIT FOR CATALYTIC RESEARCH..... 15

PL-5

Jean-Claude Charpentier

4 MAIN OBJECTIVES FOR THE FUTURE OF CHEMICAL AND PROCESS
ENGINEERING MAINLY CONCERNED BY THE SCIENCE AND
TECHNOLOGIES OF NEW MATERIALS PRODUCTION..... 23

Key-note lectures

KN-1

Kiwi-Minsker L.

HYDROGEN PRODUCTION FOR THE FUEL CELLS IN MOBILE APPLICATIONS 29

KN-2

Tsodikov M.V., Moiseev I.I.

AN APPROACH TOWARD THE UTILIZATION OF RENEWABLE FEEDSTOCKS:
 CO_2 SELECTIVE REDUCTION; ALCOHOLS INTO MOTOR FUEL CONVERSION 33

KN-3

Datsevich L.B., Mukhortov D.A.

NEW MULTIPHASE FIXED-BED TECHNOLOGIES. COMPARATIVE ANALYSIS OF
INDUSTRIAL PROCESSES (EXPERIENCE OF DEVELOPMENT AND
INDUSTRIAL IMPLEMENTATION)..... 35

Oral presentations

SECTION I. PHYSICO-CHEMICAL AND MATHEMATICAL BASES OF PROCESSES OCCURRING ON CATALYSTS SURFACE

OP-I-1

Klingstedt F., Eränen K., Arve K., Wärnå J., Lindfors L.-E., Murzin D.Y.

KINETICS OF NO_x REDUCTION OVER Ag/ALUMINA BY A HIGHER HYDROCARBON IN EXCESS OF OXYGEN 39

OP-I-2

Dietrich W., Grünewald M., Agar D.W.

THEORETICAL STUDIES ON MULTIFUNCTIONAL CATALYSTS WITH INTEGRATED ADSORPTION SITES 43

OP-I-3

Bulushev D.A., Ivanov E.A., Reshetnikov S.I., Kiwi-Minsker L., Renken A.

TRANSIENT KINETICS OF V/Ti-OXIDES REDUCTION BY TOLUENE 47

OP-I-4

Zhang X., Schubert S., Grünewald M., Agar D.W.

STUDIES ON THE KINETICS OF CARBON DIOXIDE ABSORPTION WITH IMMOBILISED AMINES 51

OP-I-5

Elokhin V.I., Latkin E.I., Matveev A.V., Gorodetskii V.V.

TURBULENT AND STRIPES WAVE PATTERNS CAUSED BY LIMITED CO_{ADS} DIFFUSION DURING CO OXIDATION OVER Pd(110) and Pt(100): STATISTICAL LATTICE MODELS 54

OP-I-6

Iliyas A.J., Sulaiman S.

KINETIC MODELLING OF META-XYLENE ISOMERIZATION OVER USY ZEOLITE IN A RISER SIMULATOR 58

OP-I-7

Ostrovskii N.M., Kenig F.

ABOUT MECHANISM AND MODEL OF DEACTIVATION OF ZIEGLER-NATTA POLYMERIZATION CATALYSTS 62

OP-I-8

Urmancheev S.F., Podshivalin A.V., Kireev V.N.

MATHEMATICAL MODELING OF HYDROGEN SULFIDE OXIDATION PROCESSES IN CELL-TYPE THERMOCATALYTIC REACTORS: HYDRODYNAMIC ASPECTS 66

OP-I-9

Kurzina I.A., Cadete Santos Aires F.J., Bergeret G., Bertolini J.C.

TOTAL OXIDATION OF METHANE OVER Pd CATALYSTS SUPPORTED ON SILICON NITRIDE. INFLUENCE OF THE SUPPORT NATURE 70

OP-I-10 <u>Isupova L.A., Tanashev Yu.Yu., Kharina I.V., Moroz E.M., Litvak G.S., Boldyreva N.N., Paukshtis E.A., Burgina E.B., Budneva A.A., Shmakov A.N., Rudina N.A., Kruglyakov V.Yu., Parmon V.N.</u> REACTIVITY OF TSEFLAR™-TREATED GIBBSITE IN THE REHYDRATION PROCESS UNDER MILD CONDITIONS	74
OP-I-11 <u>Gladky A.Yu., Ustugov V.V., Nizovskii A.I., Parmon V.N., Bukhtiyarov V.I.</u> <i>IN-SITU</i> THERMOGRAPHY TO STUDY SURFACE TEMPERATURE OF NICKEL CATALYST DURING CATALYTIC REACTION OF PROPANE OXIDATION	80
OP-I-12 <u>Ostrovskii N.M., Reshetnikov S.I.</u> THE INFLUENCE OF OXYGEN MOBILITY IN SOLID CATALYST ON TRANSIENT REGIMES OF CATALYTIC REACTION	82
OP-I-13 <u>Knyazev A.S., Magaev O.V., Vodyankina O.V., Koscheev S.V., Boronin A.I., Titkov A.I., Salanov A.N., Kurina L.N.</u> PHOSPHATE-PROMOTED SILVER CATALYSTS FOR THE ETHYLENE GLYCOL OXIDATION	86
OP-I-14 <u>Kazanskii V.B., Sokolova N.A.</u> A NOVEL SPECTRAL APPROACH TO THE STUDY OF DIFFUSION OF INDIVIDUAL COMPONENTS IN GASEOUS MIXTURES INVOLVED IN CATALYTIC REACTIONS OR GAS SEPARATION ON ZEOLITES	90

SECTION II. PROCESSES IN CHEMICAL REACTORS

OP-II-1 <u>Ananieva E., Reitzmann A., Kraushaar-Czarnetzki B.</u> DIRECT GAS-PHASE EPOXIDATION OF PROPENE WITH NITROUS OXIDE OVER MODIFIED SILICA-SUPPORTED FeO _x CATALYST	97
OP-II-2 <u>Datsevich L.B.</u> OSCILLATION THEORY: EXPERIMENTAL CONFIRMATION AND CONTRADICTIONS BETWEEN THE THIELE / ZELDOVICH MODEL AND EXPERIMENTAL DATA IN LIQUID-PHASE REACTIONS	101
OP-II-3 <u>Edreder E.A., Eldabah. S.M.</u> STUDY OF VISBREAKING OF ATMOSPHERIC RESIDUE DERIVED FROM WAXY CRUDE OIL	103

OP-II-4	
<u>Kafarov V.V., Dallos C.</u>	
A MODEL OF MULTIFUNCTIONAL REACTOR FOR PARTIAL OXIDATION OF METHANE TO METHANOL.....	104
OP-II-5	
<u>Mangold M., Zhang F., Kienle A.</u>	
SYSTEMATIC MODELLING AND NONLINEAR ANALYSIS OF MEMBRANE REACTORS.....	107
OP-II-6	
<u>Kondratiev Ju.N., Ivanchev S.S.</u>	
POSSIBILITIES FOR OPTIMIZATION OF TECHNOLOGICAL MODES FOR ETHYLENE POLYMERIZATION IN AUTOCLAVE AND TUBULAR REACTORS.....	111
OP-II-7	
<u>Kurkina E.S., Semendyaeva N.L.</u>	
MATHEMATICAL MODELING OF NONLINEAR PHENOMENA DURING THE REACTION OF CO OXIDATION OVER Pt-GROUP CATALYSTS.....	112
OP-II-8	
<u>Simagina V.I., Stoyanova I.V., Gentsler A.G., Tayban E.S., Netskina O.V.</u>	
HYDROGENOLYSIS OF ORGANOHALOGEN COMPOUNDS OVER BIMETALLIC SUPPORTED CATALYSTS.....	113
OP-II-9	
<u>Pai Z.P.</u>	
PHASE-TRANSFER CATALYSIS: SPECIFICITY OF CONDUCTING OF HYDROCARBONS OXIDATION REACTIONS.....	117
OP-II-10	
<u>Shvets V.F., Kozlovskiy R.A., Kozlovskiy I.A., Makarov M.G., Suchkov J.P., Koustov A.V.</u>	
THE CAUSE AND QUANTITATIVE DESCRIPTION OF CATALYST DEACTIVATION IN THE ETHYLENE OXIDE HYDRATION PROCESS.....	118
OP-II-11	
<u>Pashkevich D.S.</u>	
APPLICATION OF NON-STATIONARY HEAT CONDITIONS FOR RUNNING HIGH-EXOTHERMICAL CHEMICAL SYNTHESIS IN DEVELOPMENT OF INDUSTRIAL-SCALE REACTORS.....	121
OP-II-12	
<u>Pashkevich D.S., Alekseev Yu.I., Mukhortov D.A., Petrov V.B., Asovich V.S., Shelopin G.G.</u>	
APPLICATION OF NON-STATIONARY BED OF SOLID PHASE FOR A REACTOR DEVELOPMENT FOR HIGH-EXOTHERMAL PROCESSES USING ELEMENTAL FLUORINE IN A GAS-SOLID SYSTEM.....	125

OP-II-13

Jiménez F.Y., Kafarov V.V., Núñez M.

NEURAL NETWORKS AND FUZZY LOGIC FOR PREDICTION OF CATALYSTS DEACTIVATION DURING HYDROTREATMENT OF DEASPHALTED VACUUM BOTTOMS IN INDUSTRIAL REACTOR..... 129

OP-II-14

Anikeev V.I., Yermakova A.

FUNDAMENTALS OF CHEMICAL REACTIONS IN SUPERCRITICAL WATER AND THEIRS PRINCIPAL APPLICATIONS..... 133

OP-II-15

Kuchin I.V., Kravtsov A.V., Stefoglo E.F.

MODELING OF GAS-LIQUID REACTORS TAKING INTO ACCOUNT THE LIMITATION OF LIQUID REACTANT DIFFUSION TO THE INTERPHASE IN PROCESSES OF MASS-TRANSFER WITH CHEMICAL REACTION 137

OP-II-16

Stefoglo E.F., Kuchin I.V., Zhukova O.P.

FUNDAMENTALS OF THE INFLUENCE OF GAS DISSOLVED CONCENTRATION IN REACTION MEDIUM ON PERFORMANCE OF GAS-LIQUID PROCESSES ON SUSPENDED CATALYST..... 141

SECTION III. NEW TYPES OF CHEMICAL PROCESSES AND REACTORS

OP-III-1

Glouchenkov M., Kronberg A., M. van Sint Annaland, Kuipers J.A.M.

PULSED COMPRESSION REACTOR CONCEPT FOR SYNTHESIS GAS PRODUCTION..... 147

OP-III-2

Klose F., Hamel Ch., Joshi M., Tota A., Seidel-Morgenstern A.

OPTIMIZED OXIDANT DOSING IN PACKED-BED MEMBRANE REACTORS FOR THE CATALYTIC OXIDATION OF HYDROCARBONS..... 151

OP-III-3

Minigulov R.M., Ban A.G., Pisarenko E.V.

NOVEL INDUSTRIAL PROCESS OF METHANOL PRODUCTION FROM NATURAL GAS OF NORTH GAS FIELDS 156

OP-III-4

Dimaki A.V., Shilko E.V., Psakhie S.G.

CELLULAR AUTOMATA METHOD AS A TOOL FOR COMPUTER-AIDED STUDY OF PROCESSES IN CHEMICAL REACTORS 159

OP-III-5

Ye Y., Rihko-Struckmann L., Munder B., Sundmacher K.

EXPERIMENTAL STUDY ON ELECTROCHEMICAL MEMBRANE REACTOR FOR n-BUTANE PARTIAL OXIDATION..... 162

OP-III-6

Minigulov R.M., Ban A.G., Pisarenko E.V., Pisarenko V.N.
NOVEL INDUSTRIAL PROCESS OF HIGH-OCTANE OXYGENATED MOTOR FUEL PRODUCTION FROM NATURAL GAS..... 166

OP-III-7

Minigulov R.M., Ban A.G., Pisarenko E.V., Pisarenko V.N.
NOVEL PROCESS OF COMPLEX PROCESSING OF PRODUCED WATER OF GAS FIELDS 168

OP-III-8

Glikina I.M.
CHEMICAL PROCESSES INVESTIGATION BY AEROSOL NANOCATALYSIS TECHNOLOGY 171

OP-III-9

Barysheva L.V., Chumakova N.A., Stepanov D.A., Khanaev V.M.
SIMULATION OF CATALYTIC DEHYDROGENATION PROCESS IN A FIXED BED CONTAINING MOVING FINE SOLID PARTICLES..... 173

OP-III-10

Ismagilov Z.R., Kerzhentsev M.A., Sazonov V.A., Tsykoza L.T., Shikina N.V., Kuznetsov V.V., Ushakov V.A., Mishanin S.V., Kozhukhar N.G., Russo G., Deutschmann O.
DESIGN OF CATALYSTS AND CATALYTIC BURNERS FOR FUEL CELL POWER PLANT REFORMER 175

OP-III-11

Müller A., Cominos V., Hessel V., Horn B., Schürer J., Ziogas A., Jähnisch K., Grosser V., Hillmann V., Jam K.A., Rinke G., Kraut M., Bazzanella A.
FLUIDIC BUS SYSTEM FOR CHEMICAL PROCESS ENGINEERING IN THE LABORATORY AND FOR SMALL-SCALE PRODUCTION..... 179

OP-III-12

Romanyukha N.Y., Churbanov A.G., Churbanova N.G., Chetverushkin B.N.
NUMERICAL SIMULATION OF FLOW DISTURBANCES INDUCED BY BOUNCY FORCE IN A HORIZONTAL REACTOR 184

OP-III-13

Mitropetros K., Fomin P.A., Hieronymus H.
SOME SAFETY ASPECTS OF A BUBBLY MEDIUM INSIDE CHEMICAL REACTOR 188

OP-III-14

Schwalbe Th., Wille G.
MICROREACTORS AS TOOLS FOR BETTER CHEMISTRY AND THEIR INTEGRATION INTO PROCESS OPTIMISATION AND INTENSIFICATION..... 192

OP-III-16
Noskov A.S., Zolotarskii I.A., Pokrovskaya S.A., Kashkin V.N., Korotkikh V.N.
 AMMONIA OXIDATION INTO NITROUS OXIDE OVER Mn/Bi/Al CATALYST.
 FLUIDIZED BED REACTOR APPLICATION 198

OP-III-17
Zagoruiko A.N.
 PERFORMANCE OF SELECTIVE CATALYTIC EXOTHERMIC REACTIONS IN THE
 "REVERSED HEAT WAVE" MODE: A WAY TO IMPROVE SELECTIVITY 202

OP-III-18
**Rupprechter G., Morkel M., Borasio M., Freund H.-J., Kaichev V.V.,
 Prosvirin I.P., Bukhtiyarov V.I.**
 METHANOL DECOMPOSITION ON Pd(111) STUDIED BY HIGH-PRESSURE
 SFG AND XPS SPECTROSCOPY 205

OP-III-19
Kulikov S.M.
 DETOXICATION OF A CHLORINATED ORGANIC COMPOUNDS IN A
 MEMBRANE SEPARATED REACTOR IN AN AQUEOUS MEDIA 209

OP-III-20
Mustafina S.A., Spivak S.I.
 THE COMPUTING EXPERIMENT AND OPTIMIZATION
 OF CATALYTIC PROCESSES 210

**SECTION IV. CHEMICAL REACTORS FOR SOLVING THE FUEL AND
 ENERGY PRODUCTION PROBLEMS**

OP-IV-1
Omer A.A.
 THE FORMATION AND CONTROL OF NO_x EMISSIONS 217

OP-IV-2
Kulikov A.V., Lukyanov B.N., Kuzin N.A., Simonova L.G., Kirillov V.A.
 CATALYTIC HEATING ELEMENTS OF 0.75 kW POWER 218

OP-IV-3
Mysov V.M., Reshetnikov S.I., Stepanov V.G., Ione K.G.
 SYNTHESIS GAS CONVERSION INTO HYDROCARBONS (GASOLINE RANGE)
 OVER BIFUNCTIONAL ZEOLITE-CONTAINING CATALYST: EXPERIMENTAL
 STUDY AND MATHEMATICAL MODELLING 221

OP-IV-4
Ikonnikov V.K., Bersh A.V., Ryzhkin V.Yu., Zhukov N.N., Trubacjev O.A.
 OPTIMIZATION OF THE REACTOR INTENDED FOR HYDROGEN AND BOEHMITE
 PRODUCTION FROM WATER-SUSPENDED ALUMINIUM POWDER 225

OP-IV-5

Kravtsov A.V., Ivanchina E.D., Galushin S.A., Poluboyartsev D.S.
APPRAISAL OF Pt-CATALYSTS AND PREDICTION OF DEVELOPMENT WORK
DUTY IN INDUSTRIAL TECHNOLOGY OF REFORMING OF BENZINE
USING NON-STATIONARY KINETIC MODEL 229

SECTION V. WASTE DETOXICATION AND PROCESSING

OP-V-1

Gosiewski K.J.
EFFICIENCY OF HEAT RECOVERY VERSUS MAXIMUM CATALYST
TEMPERATURE IN A REVERSE-FLOW COMBUSTION OF METHANE 235

OP-V-2

Irabien A., Garea A.
MODELLING OF IN DUCT DESULFURIZATION REACTORS 239

OP-V-3

Irabien A., Aldaco R.
FLUIDIZED BED REACTOR FOR FLUORIDE REMOVAL 241

OP-V-4

Seyedeyn-Azad F., Zhang Dong-ke
KINETIC STUDY OF DIRECT DECOMPOSITION OF NITRIC OXIDE
OVER COPPER ION-EXCHANGED ZSM-5 ZEOLITE 245

OP-V-5

Rahmani M., Cruise N., Sohrabi M., Augustsson O., Sanati M.
ORANGO SILICON POISONING OF Pt/ γ -Al₂O₃ CATALYST IN TOTAL
OXIDATION OF VOC 246

OP-V-6

Hanif A., Suhartanto T., Green M.L.H.
CO₂ REFORMING OF CH₄ TO SYNGAS (CO/H₂) USING Ni-WC/Al₂O₃ &
Ni-CaO/Al₂O₃ CATALYSTS FOR JAMBI GAS FIELD UTILISATION 250

OP-V-7

Hartmann V.L.
EFFECT OF SULFUR REMOVAL CATALYST GRANULES PROPERTIES ON
THE COMMERCIAL-SCALE BED MACROKINETICS 253

OP-V-8

Backman H., Rahkamaa-Tolonen K., Wärnä J., Salmi T., Murzin D.Yu.
MODELLING OF H₂/D₂ EXCHANGE OVER Pd 257

OP-V-9

Babkin V.S., Bunev V.A., Kakutkina N.A., Laevsky Yu.M., Namyatov I.G.
ASPECTS OF REVERSE-PROCESS WITH GAS-PHASE REACTION
FOR METHANE OXIDATION 260

OP-V-10

Dobrynkin N.M., Batygina M.V., Noskov A.S.

COMPLETE ABATEMENT OF ANILINE AND PHENOL IN WASTEWATER IN THE PRESENCE OF CARBON CATALYSTS BY AIR OXIDATION AND ADSORPTIVE-CATALYTIC OXIDATION IN LIQUID PHASE 262

OP-V-11

Noskov A.S., Chumakova N.A., Klenov O.P., Tsyrunikov P.G., Korotkikh V.N., Drobyshevich V.I., Yausheva L.V.

THEORETICAL AND EXPERIMENTAL STUDY OF METHANE VENT-GASES UTILIZATION FOR HIGH-TEMPERATURE HEAT PRODUCTION IN UNSTEADY-STATE OPERATION 266

Poster Presentations

PP-1 Andreev D.V., Makarshin L.L., Parmon V.N.

METHANOL DECOMPOSITION IN THE MICROREACTOR WITH DIRECT RESISTANCE HEATING AND A MASSIVE COPPER CATALYST 271

PP-2 Barelko V.V., Prudnikov A.A., Bykov L.A., Khromov V.A., Bubnov K.I., Manukovsky Yu.D.

CASSETTE REACTOR DESIGN WITH SILICA FIBER GLASS WOVEN CATALYSTS FOR PURIFICATION OF INDUSTRIAL GAS EXHAUSTS FROM ORGANIC IMPURITIES (THREE YEARS EXPERIENCE OF INDUSTRIAL EXPLOITATION) 274

PP-3 Syropiatov V.Ya., Barelko V.V.

CATALYTIC ACTIVATION OF FURNACE ATMOSPHERE FOR METALS AND ALLOYS GAS NITRIDING PROCESS (8 years of development and exploitation of "catalytic nitriding") 275

PP-4 Chuntian Wu, Dorokhov V.G., Suknev A.P., Balzhinimaev B.S., Barelko V.V.

HIGH SELECTIVE FIBER GLASS WOVEN CATALYSTS DOPED BY NOBLE METALS IN THE REACTIONS OF AROMATIC NITRO-COMPOUNDS REDUCTION 279

PP-5 Bogatov V.V., Kasimov R.M., Mamedov E.M., Guseynov K.A., Ibadzadeh I.U.

FLEXIBLE AUTOMATED PILOT PLANT FOR RESEARCH OF CHEMICAL-TECHNOLOGICAL PROCESSES 284

PP-6 Bykov V.I., Tsybenova S.B.

THE PARAMETRICAL ANALYSIS OF TURING'S TWO-DIMENSIONAL MODEL 286

PP-7 Ivanova E.A., Chumakova N.A., Chumakov G.A., Boronin A.I.

MODELING OF RELAXATION OSCILLATIONS IN CO OXIDATION OVER METALLIC CATALYSTS WITH CONSIDERATION OF RECONSTRUCTIVE HETEROGENEITY OF THE SURFACE 290

PP-8	<u>Churbanova N.G.</u> , <u>Chetverushkin B.N.</u> , <u>Trapeznikova M.A.</u> SIMULATION OF GAS FLOWS AT LOW MACH NUMBER.....	294
PP-9	<u>Galanov S.I.</u> , <u>Sidorova O.I.</u> , <u>Kurina L.N.</u> , <u>Golovko A.K.</u> THE CATALYTIC SYNTHESIS OF ACETONITRILE.....	298
PP-10	<u>Galvita V.</u> , <u>Sobyanin V.</u> , <u>Sundmacher K.</u> THE USE OF ETHANOL FOR COMBINED HEAT AND POWER STATIONS ON THE BASIS OF POLYMER ELECTROLYTE FUEL CELLS	302
PP-11	<u>Grigor'eva N.G.</u> , <u>Khazipova A.N.</u> , <u>Gubaidullin I.M.</u> , <u>Balaev A.V.</u> , <u>Kutepov B.I.</u> , <u>Galyautdinova R.R.</u> KINETIC MODEL OF α -METHYLSTYRENE OLIGOMERIZATION IN THE PRESENCE OF NaHY ZEOLITE	305
PP-12	<u>Grigor'eva N.G.</u> , <u>Khazipova A.N.</u> , <u>Gubaidullin I.M.</u> , <u>Balaev A.V.</u> , <u>Kutepov B.I.</u> , <u>Galyautdinova R.R.</u> PROCESS MODELING OF α -METHYLSTYRENE OLIGOMERIZATION IN TUBULAR REACTORS.....	308
PP-13	<u>Ibadzadeh I.Yu.</u> , <u>Guseynov Kamran A.</u> , <u>Kasimov Rasim M.</u> , <u>Mamedov Eldar M.</u> METHODOLOGY OF KINETIC MODEL IDENTIFICATION	312
PP-14	<u>Ippolitov E.G.</u> , <u>Kruglikova O.A.</u> , <u>Kablutshaja G.N.</u> NEW PROCESS OF CATALYTIC DECOMPOSITION OF INORGANIC PEROXIDATES.....	313
PP-15	<u>Karpenko V.I.</u> , <u>Ozhereliev O.A.</u> , <u>Pestryakov A.N.</u> PROCESSING OF LIQUID RADIOACTIVE WASTES CONTAINING ORGANOPHOSPHORUS COMPOUNDS.....	314
PP-16	<u>Kleimenov E.</u> , <u>Bluhm H.</u> , <u>Hävecker M.</u> , <u>Knop-Gericke A.</u> , <u>Pestryakov A.</u> , <u>Teschner D.</u> , <u>Hutchings G.J.</u> , <u>Lopez-Sanchez J.A.</u> , <u>Bartley J.K.</u> , <u>Schlögl R.</u> <i>IN SITU</i> XPS CHARACTERISATION OF VPO CATALYST.....	318
PP-17	<u>Kovalyov E.V.</u> , <u>Elokhin V.I.</u> , <u>Cherezov E.A.</u> , <u>Myshlyavtsev A.V.</u> STATISTICAL LATTICE MODELING OF THE ADSORPTION AND REACTION PROCESSES OVER THE SUPPORTED NANOPARTICLES	321
PP-18	<u>Kravtsov A.V.</u> , <u>Ivanchina E.D.</u> , <u>Galushin S.A.</u> , <u>Poluboyartsev D.S.</u> MATHEMATICAL MODELING OF REACTOR UNIT OF REFORMING SYSTEM TAKING INTO ACCOUNT DIFFERENT RADIAL DIRECTIONS OF ROW-GAS FLOW	325
PP-19	<u>Kukueva V.V.</u> QUANTUM-CHEMICAL RESEARCH OF ELEMENTARY PROCESSES ON THE CATALYST SURFACE	329
PP-20	<u>Liventsev V.T.</u> , <u>Karyakin V.A.</u> , <u>Kuzmina R.I.</u> , <u>Sidorov G.M.</u> , <u>Sevostyanov V.P.</u> , <u>Weinbender V.R.</u> PRODUCTION OF HIGH-OCTANE BLENDING FUEL BY REFORMING CATALYSATE FRACTIONATING	331

PP-21	<u>Chinova M.S.</u>, Smetannikov O.V., Mushina E.A., Podolskiy Yu.Ya., Antipov E.M., Frolov V.M. THE NEW METHOD OF SYNTHESIS OF TRANS-1,4-POLYISOPRENE (SYNTHETIC GUTTA PERCHA).....	335
PP-22	<u>Smetannikov O.V.</u>, Chinova M.S., Mushina E.A., Podolskiy Yu.Ya., Antipov E.A., Frolov V.M. TITANIUM-MAGNESIUM CATALYSTS – UNIVERSAL CATALYSTS FOR POLYMERIZATION OF OLEFINS AND DIENES	336
PP-23	Morozov I.V., <u>Fedorova A.A.</u>, Novozhilov M.A., Anufrienko V.F., Kemnitz E. SYNTHESIS OF OXIDE CATALYSTS $\text{CuO}+\text{ZrO}_2$ FOR METHANE COMBUSTION USING MOLTEN NH_4NO_3	337
PP-24	Khalikov D.E., <u>Obukhova S.A.</u>, Telyashev E.G. DEVELOPMENT OF THE IMPROVED NUMERICAL MODEL OF EXTRACTIVE DEAROMATIZATION OF A STRAIGHT-RUN DIESEL FRACTION 270-360°C	341
PP-25	<u>Kasianov A.A.</u>, Abdulminev K.G., Ahmetov A.F., Soloviev A.S. BENZENE HYDROGENATION IN LIGHT FRACTIONS OF REFORMING PRODUCT	344
PP-26	<u>Kasianov A.A.</u>, Ahmetov A.F. OPTIMIZATION OF FEEDSTOCK COMPOSITION OF CATALYTIC REFORMER'S LAST REACTOR.....	346
PP-27	Obukhova S.A., <u>Vezirov R.R.</u>, Davletshin A.R., Telyashev E.G. EFFECT OF THERMOLYSIS CONDITIONS AND TYPE OF VIBREAKING REACTOR ON STRUCTURE AND POLYDISPERSE STATE OF CRACKING RESIDUES	348
PP-28	Obukhova S.A., <u>Vezirov R.R.</u>, Kulik A.A., Telyashev E.G. FEATURES OF HYDROUPGRADING OF HIGH-AROMATIC PETROLEUM DISTILLATES.....	352
PP-29	Pavlova S.N., Sazonova N.N., <u>Ivanova J.A.</u>, Sadykov V.A., Snegurenko O.I., Rogov V.A., Zolotarskii I.A., Moroz E.M. CATALYTIC PARTIAL OXIDATION OF METHANE TO SYNTHESIS GAS: DETERMINATION OF AN INTRINSIC ACTIVITY	356
PP-30	<u>Pestryakov A.N.</u>, Smolentseva E.V., Bogdanchikova N.E. SUPPORTED FOAM COPPER CATALYSTS FOR METHANOL SELECTIVE OXIDATION	360
PP-31	Pinakov V.I., Stoyanovsky O.I., <u>Tanashev Yu.Yu.</u>, Pikarevsky A.A., Grinberg B.E., Dryab V.N., Kulik K.V., Danilevich V.V., Parmon V.N. TSEFLAR – THE CENTRIFUGAL FLASH REACTOR FOR RAPID THERMAL TREATMENT OF POWDERED MATERIALS	364
PP-32	Podshivalin A.V. MODERN CATALYSTS OF CLAUS PROCESS.....	368

- PP-33 Schrader C., Baars-Hibbe L., Cordes T., Draeger S., Sichler P.,
Büttgenbach S., Gericke K.-H.
APPLICATIONS OF MSE-ARRAYS AT ATMOSPHERIC PRESSURE:
"NON-THERMAL PLASMAS AS STERILISATION AND COATING
TECHNIQUE" 371
- PP-34 Voskresenskii N.M., Serdyukov S.I., Safonov M.S.
HYPERBOLIC CONCEPT OF LONGITUDINAL DISPERSION AND
THE MODELING OF STRUCTURED CATALYST UNITS 375
- PP-35 Skundin A.M., Kulova T.L.
ELECTROCHEMISTRY IN WASTE WATER TREATMENT 376
- PP-36 Staroverov D.V., Varlamova E.V., Kornakova N.A., Shvets V.F.
CIRCULATION REACTOR FOR AQUEOUS ALKALI
OXIDATION OF ALCOHOLS 378
- PP-37 Vezirova N.R., Vezirov R.R., Obukhova S.A., Arhipova O.V.
DEVELOPMENT OF THE C₇-C₁₀ (C₁₁) PARAFFINIC HYDROCARBONS
ISOMERIZATION PROCESS 380
- PP-38 Volkova G.G., Pak Yu.R., Budneva A.A., Paukshtis E.A., Salanov A.N.
SOLID ACIDS IN HALIDE-FREE CARBONYLATION OF DIMETHYL
ETHER AND ISOMERIZATION OF ALKANES 384
- PP-39 Volkova G.G., Shkuratova L.N., Budneva A.A., Paukshtis E.A., Reshetnikov S.I.
SKELETAL ISOMERIZATION OF N-PARAFFINS ON HETEROGENEOUS
CATALYSTS WITH HIGH LEWIS ACIDITY 388
- PP-40 Vosmerikov A.V., Vosmerikova L.N., Korobitsyna L.L., Barbashin Ya.Ye.
CATALYTIC SYNTHESIS OF AROMATIC HYDROCARBONS FROM
LOW ALKANES 391
- PP-41 Zagoruiko A.N., Glotov V.D., Menailov N.N., Zhukov Yu.N., Yankilevich V.M.,
Balzhinimaev B.S., Simonova L.G.
GLASS FIBER CATALYSTS FOR SO₂ OXIDATION: PILOT TESTS
AT REAL GASES OF SULPHURIC ACID PLANT 395
- PP-42 Zagoruiko A.N., Mokrinskii V.V.
NON-STEADY-STATE APPROACH TO STEADY-STATE KINETICS:
CASE STUDY OF H₂S OXIDATION BY OXYGEN 399
- PP-43 Zhdanov T.R., Podshivalin A.V., Arhipova O.V.
STUDY OF PHYSICAL -CHEMICAL CHARACTERISTICS OF THE
CATALYST FOR DIRECT OXIDATION OF HYDROGEN-SULFIDE 403
- PP-44 Slepterev A.A., Salnikov V.S., Tsyruльников P.G., Noskov A.S., Tomilov V.N.,
Chumakova N.A., Zagoruiko A.N.
CATALYTIC AND HOMOGENEOUS HIGH-TEMPERATURE
OXIDATION OF METHANE 407

PP-45	<u>Safronova S.S., Koval L.M.</u> PHYSICOCHEMICAL PROPERTIES OF MODIFIED ZEOLITE-CONTAINING CATALYSTS AND THEIR CATALYTIC ACTIVITY IN THE PROCESS OF COUPLED CONVERSION OF METHANOL AND LOW MOLECULAR ALKANES	410
PP-46	<u>Sokolova T.V., Chaikovskaya O.N., Sokolova I.V., Sosnin E.A.</u> HOMOGENEOUS LIGHT-INDUCED DEGRADATION OF METHYLPHENOLS IN THE AQUEOUS MEDIA	412
PP-47	<u>Alexeev B.V., Koltsov N.I.</u> REDUCTION METHOD FOR NONLINEAR SYSTEMS OF DIFFERENTIAL EQUATIONS OF CHEMICAL KINETICS.....	414
PP-48	<u>Khankhasaeva S.T., Brizgalova L.V., Dashinamzhilova E.Ts., Ryazantsev A.A., Badmaeva S.V.</u> WET OXIDATION OF ORGANIC IMPURITIES BY HYDROGEN PEROXIDE IN THE PRESENCE OF Fe-PILLARED CLAYS	418
PP-49	<u>Patmar E.S., Koltsov N.I.</u> THE METHOD OF DETERMINATION NUMBER OF STATIONARY STATES AT THE DECISION OF THE REVERSE TASK OF CHEMICAL KINETICS.....	420
PP-50	<u>Telyashev I.R., Vezirov R.R., Telyashev E.G.</u> MECHANISMS OF PLASTICIZATION AND MODIFICATION OF PETROLEUM RESIDUES WITH PARTICIPATION OF ELEMENTAL SULFUR CLUSTERS.....	423
PP-51	<u>Ivanov E.A., Glaznev I.S., Koptuyug I.V., Aristov Yu.I.</u> DYNAMICS OF WATER SORPTION ON CONSOLIDATED LAYER "CaCl ₂ IN ALUMINA": NMR MICROSCOPY AND MODELLING	426
	LIST OF PARTICIPANTS	430
	AUTHOR INDEX.....	444
	CONTENT	446

B.I.C. Europe B.V., The Netherlands



Advanced Catalysts
and Processes



BIC Europe BV as the Representative of Boreskov Institute of Catalysis (BIC) in Novosibirsk, Russia operates as a Liaison between BIC and European Institutes, Universities and Companies.

The purpose of BIC Europe BV is to spread knowledge and skills on advanced catalytic technologies.

Our services include:
research, marketing and advertisement assistants, partner identification, communications, etc.

Boreskov Institute of Catalysis is one of the largest research institutes on advanced catalysis in the world and comprises a wealth of knowledge, both fundamental and application oriented, for a broad scale of processes in the chemical, petrochemical and environmentally related industries.

BIC is specialized in solving problems of catalysis and making use of all aspects from fundamental and theoretical to industrial mastering of new catalysts.

BIC Europe BV is providing a unique platform for commercial synergy of Boreskov Institute of Catalysis in Novosibirsk, Russia and European Institutes, Universities and Companies.

BIC Europe BV has a broad network of engineers and scientists specialized in chemistry, reactor engineering, environmental protection and sustainable development.

We can offer adequate solutions and services for your problems of catalyst selectivity, efficiency, reprocessing and connected reactor engineering at low costs and with short lead time.

Present activities comprise:

- Food processing
- Environmental protection and emission control
- Water and air purification
- Gas to liquid conversion
- Biomass gasification and syngas processing
- Catalysts production, upgrading and optimization
- Catalysts characterization and testing.

XVI International Conference on Chemical Reactors

CHEMREACTOR-16

Editor: Professor Alexander S. Noskov

The abstracts are printed as presented, and all responsibilities we address to the authors. Some abstracts underwent a correction of misprints and rather mild editing procedure.

Compilers: Tatiana V. Zamulina
Elena L. Mikhailenko

Computer processing of text: Natalia A. Tsygankova

Cover design: Nina F. Poteryaeva

Подписано в печать 13.11.2003
Печ.л. 57,5

Заказ N

Формат 60x84/8
Тираж 250

Отпечатано на полиграфическом участке издательского отдела
Института катализа СО РАН
630090, Новосибирск, пр. Академика Лаврентьева, 5